CANADIAN

JOURNAL OF

RESEARCH

SPECIAL PROBLEMS CONNECTED WITH THE TAKE-OFF AND LANDING OF AIRCRAFT[1]

BY J. J. GREEN[2]

Abstract

A theoretical analysis has been made of the effect of gradient, wind, and com-
binations thereof, on the take-off and landing of aeroplanes. Formulas and
charts are given which permit the determination of the length of the ground run
for any given conditions providing that the performance on a level surface in
still air is known.
The effect of wind and current on the take-off of seaplanes has also been
investigated. Formulas and charts have been derived for the determination
of take-off time and distance under any given conditions from a knowledge of the
take-off speed, time, and distance in still air and still water. This analysis
indicates that in the take-off of seaplanes the wind is in general of more im-
portance than the current, and, in consequence, take-off should always be carried
out upwind.

A few aerodromes are in existence on which there is a gradient in the
direction of take-off and landing. As this feature may in general be a dis-
advantage, an investigation has been made on the effect of varying wind and
gradient on the take-off run and landing run of aeroplanes. This investiga-
tion is carried out in Part I of this paper. In Part II a somewhat similar
problem has been analyzed, viz., the effect of wind and current on the take-
off of seaplanes.

PART I
THE EFFECT OF WIND AND GRADIENT ON THE TAKE-OFF AND LANDING OF AEROPLANES

In analyzing the effect of wind and gradient on the take-off and landing
runs of aeroplanes, three cases have been considered: (1) the effect of gradient
in the absence of wind; (2) the effect of wind in the absence of a gradient;
(3) the combined effect of wind and gradient. The analysis is based on
uniform gradients, and, since the results are referred to the performance on
a level aerodrome, the type of surface on the gradient is assumed to be the
same as on the level surface for which take-off and landing characteristics of
any particular aeroplane are known. The wind is assumed to be blowing
either directly up or down the gradient. Theoretical formulas have been
developed giving the effect of gradient, wind, and combined wind and gradient
on the take-off time and distance, and the landing run.

The effect of gradient in the absence of wind is capable of almost exact solution. The theoretical treatment of the effect of wind on take-off leads to a formula that differs slightly, in its predictions, from the results of measured take-offs. By slight modification the formula has been made to agree closely with the results of tests. Charts have been prepared showing the effect of wind and gradient on the take-off and landing runs of aeroplanes of which the take-off and landing speeds in still air are included in the range 35 to 75 m.p.h.

Symbols Used

m = Mass of aircraft,

g = Acceleration due to gravity, taken as 32.2 ft. per sec.^{2},

θ = Angle of gradient (radians),

x = Gradient defined as $\dfrac{\text{rise per 100 ft.}}{100}$; for small slopes $\theta = x$,

V_T = Take-off speed (still air), in feet per second when used in the formulas but given in miles per hour on the charts,

V_L = Landing speed (still air), in feet per second in the formulas but given in miles per hour on the charts,

t_1 = Take-off time or duration of landing run in seconds on a level surface in still air,

t_2 = Take-off time or duration of landing run in seconds resulting from the effect of grade or wind or both,

D_1 = Take-off run or landing run in feet on a level surface in still air,

D_2 = Take-off run or landing run in feet resulting from the effect of grade or wind or both,

f = Mean acceleration during take-off or mean deceleration during landing in feet per sec.^{2},

v_w = Wind speed, in feet per second when used in the formulas.

(1) Effect of Gradient in the Absence of a Wind

A. Take-off Upgrade

The retarding force due to the gradient will be $mg \sin \theta$, hence the deceleration will be $g \sin \theta$, and since θ will in general be small this can be written $g\theta$ or xg. If V_T and t_1 are the take-off speed and time on the level, then after a time t_1 on the gradient the velocity will be $V_T - xgt_1$. If t_2 is the take-off time up the gradient, then on the level after time t_2 the velocity would have been $V_T \cdot \dfrac{t_2}{t_1}$, but owing to the gradient this is reduced to

$$V_T \cdot \frac{t_2}{t_1} - x \cdot g \cdot t_2 = V_T ,$$

from which we obtain

$$\frac{t_2}{t_1} = \frac{1}{1 - \dfrac{x \cdot g \cdot t_1}{V_T}} . \tag{1}$$

This equation gives the take-off time up the gradient in terms of the take-off speed, the take-off time on the level, and x, the gradient. Equation (1) gives

immediately the conditions under which take-off is impossible, for when $1 - \dfrac{x \cdot g \cdot t_1}{V_T} = 0$, t_2 becomes infinite. Hence take-off becomes impossible when

$$\frac{x \cdot g \cdot t_1}{V_T} = 1, \text{ or } x = \frac{V_T}{g \cdot t_1} \cdot$$

Since x is now likely to be large this should be written

$$\sin \theta = \frac{V_T}{g \cdot t_1} \cdot \tag{2}$$

From which the value of θ for which take-off is impossible is given in terms of g and the take-off speed in feet per second and take-off time on the level.

For take-off on the level we have,

$$D_1 = \frac{V_T^2}{2f} \text{ or } f = \frac{V_T^2}{2D_1} \cdot$$

Similarly up the gradient

$$D_2 = \frac{V_T^2}{2(f - x \cdot g)} = \frac{V_T^2}{2\left(\dfrac{V_T^2}{2D_1} - x \cdot g\right)} \cdot$$

Hence

$$\frac{D_2}{D_1} = 1 - \frac{2x \cdot g \cdot D_1}{V_T^2} \tag{3}$$

gives the take-off distance up the gradient in terms of take-off characteristics on the level.
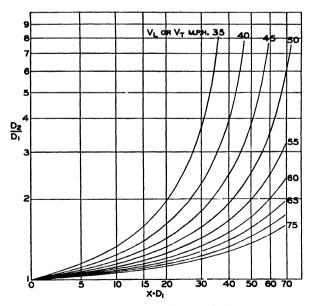

FIG 1. *Effect of gradient in the absence of wind on the length of the take-off run up the gradient or the landing run down the gradient.*

Equation (3) could be derived directly from Equation (1) by substituting

$$D_1 = \frac{V_T \cdot t_1}{2} \quad \text{and} \quad D_2 = \frac{V_T \cdot t_2}{2}.$$

Fig. 1. contains curves from which the ratio $\frac{D_2}{D_1}$ can be read off for the appropriate value of $x \cdot D_1$ and the take-off speed V_T of the aeroplane under consideration.

B. Take-off Downgrade

By similar treatment the equations for take-off time and distance down the gradient are found to be:—

$$\frac{t_2}{t_1} \qquad \frac{1}{1 + \dfrac{x \cdot g \cdot t_1}{V_T}} \tag{4}$$

$$\frac{D_2}{D_1} - \frac{1}{1 + \dfrac{2x \cdot g \cdot D_1}{V_T^2}} \tag{5}$$

Fig. 2. contains curves from which the ratio $\frac{D_2}{D_1}$ can be read off for the appropriate value of $x \cdot D_1$ and the take-off speed of the aeroplane under consideration.

C. Landing Run Upgrade

On the level surface with no wind, the time t_1 for the landing run is given by the equation

$$t_1 = \frac{V_L}{f},$$

where V_L = landing speed in feet per second, and f = mean deceleration in feet per sec.[2]

The length of the landing run is given by

$$D_1 = V_L \cdot t_1 - \frac{1}{2} \cdot f \cdot t_1^2,$$

and substituting for t_1, we obtain

$$D_1 = \frac{1}{2} \frac{V_L^2}{f},$$

from which

$$f = \frac{V_L^2}{2D_1}.$$

The equations for time and distance of the upgrade landing run will be

$$t_2 = \frac{V_L}{f + x \cdot g} \qquad \text{and} \qquad D_2 = \frac{1}{2} \cdot \frac{V_L^2}{f + x \cdot g},$$
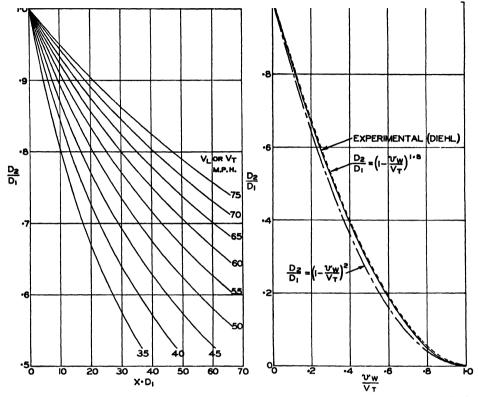
FIG. 2. *Effect of gradient in the absence of wind on the length of the take-off run down the gradient or the landing run up the gradient.*

FIG. 3. *Effect of wind on the length of the take-off run from a level surface.*

and by substituting for f we obtain,

$$D_2 = \frac{1}{2} \cdot \frac{V_L^2}{\frac{V_L^2}{2D_1} + x \cdot g}$$

or

$$\frac{D_2}{D_1} = \frac{1}{1 + \frac{2x \cdot g \cdot D_1}{V_L^2}}, \qquad (6)$$

which is an equation identical with that for the take-off run downgrade except for the substitution of V_L for V_T.

From the curves of Fig. 2 the ratio of the upgrade landing run to the level surface landing run can be read off at the appropriate value of $x \cdot D_1$ and the landing speed V_L of the aeroplane under consideration.

D. Landing Run Downgrade

The equations for the time and distance of the landing run downgrade follow from the foregoing treatment,

$$t_2 = \frac{V_L}{f - x \cdot g} \qquad \text{and} \qquad \frac{D_2}{D_1} = \frac{1}{1 - \dfrac{2x \cdot g \cdot D_1}{V_L^2}}, \qquad (7)$$

which is an equation similar to that for the take-off run upgrade, except that V_T is replaced by V_L.

The curves of Fig. 1 enable the landing run downgrade to be evaluated at the appropriate values of x, D_1, and V_L.

(2) Effect of Wind in the Absence of a Gradient

A. Take-off Upwind

With the notation used before and assuming that the mean acceleration f remains the same in a wind, we have

$$V_T - v_w = f \cdot t_2 ,$$

where v_w is the wind velocity and t_2 the new take-off time.   By substituting for f we obtain,

$$V_T - v_w = V_T \cdot \frac{t_2}{t_1} ,$$

therefore,

$$\frac{t_2}{t_1} = \left(1 - \frac{v_w}{V_T} \right) . \qquad (8)$$

If D_1 and D_2 are the corresponding take-off runs then

$$\frac{D_2}{D_1} = \left(\frac{t_2}{t_1} \right)^2 = \left(1 - \frac{v_w}{V_T} \right)^2 . \qquad (9)$$

Diehl's curve (1, p. 440) of measured take-off runs plotted for various wind speeds has been replotted in Fig. 3 together with Equation 9.   It is obvious that Equation 9 leads to smaller take-off runs than are achieved in actual practice.   It follows, therefore, that the assumption of the same mean acceleration against a wind as in still air does not agree exactly with actual behavior during take-off, and that the mean acceleration against a wind must be less than that in still air.   The equation:—

$$\frac{D_2}{D_1} = \left(1 - \frac{v_w}{V_T} \right)^{1\cdot8} \qquad (10)$$

agrees very closely with the measured effect of wind on take-off run (Fig. 3).

B. Take-off Downwind

For this condition we have,

$$V_T + v_w = f \cdot t_2$$

(on the assumption that the mean acceleration down wind is the same as in still air), and therefore,

$$\frac{t_2}{t_1} = \left(1 + \frac{v_w}{V_T} \right) . \qquad (11)$$

The distance is given by

$$\frac{D_2}{D_1} = \left(1 + \frac{v_w}{V_T}\right)^2 . \qquad (12)$$

It is apparent from the upwind treatment that in actual practice the mean downwind acceleration is likely to be greater than the mean acceleration in still air, and that the take-off distances will probably be more accurately given by

$$\frac{D_2}{D_1} = \left(1 + \frac{v_w}{V_T}\right)^{1\cdot8}, \qquad (13)$$

which is obtained by giving v_w a negative sign in the formula for upwind take-off.

C. Landing Run Upwind

For the no wind case we have

$$V_L = f \cdot t_1 ,$$

where f is the mean deceleration, and for the upwind case

$$V_L - v_w = f \cdot t_2 ,$$

the same deceleration being assumed.

Hence

$$\frac{t_2}{t_1} = \left(1 - \frac{v_w}{V_L}\right) . \qquad (14)$$

If D_1 and D_2 are the corresponding landing runs then,

$$D_1 = \frac{1}{2} \cdot \frac{V_L^2}{f} \qquad \text{and} \qquad D_2 = \frac{1}{2} \cdot \frac{(V_L - v_w)^2}{f} .$$

Therefore

$$\frac{D_2}{D_1} = \left(1 - \frac{v_w}{V_L}\right)^2 . \qquad (15)$$

D. Landing Run Downwind

By similar treatment the downwind times and distances will be given by

$$\frac{t_2}{t_1} = \left(1 + \frac{v_w}{V_L}\right) \qquad (16)$$

and

$$\frac{D_2}{D_1} = \left(1 + \frac{v_w}{V_L}\right)^2 . \qquad (17)$$

(3) Combined Effect of Gradient and Wind

When the wind is blowing up the gradient, take-off will be made down the gradient since both the slope and the wind will be effective in reducing the take-off time and run. Similarly when the wind is blowing down the gradient, landing will be made up the gradient since both the slope and the wind will be effective in reducing the landing run. Since these cases present no difficulty, charts have not been prepared for them.

Two cases are now considered: (1) take-off with the wind blowing down the gradient; (2) landing with the wind blowing up the gradient. In both, the effects of wind and gradient are acting against each other. It is obvious that for winds whose velocities are below a certain critical velocity the effect of the gradient will predominate, and for winds stronger than the "critical wind" the effect of the gradient will be less than the effect of the wind. For winds whose velocities are below the critical wind velocity, take-off must be carried out down the slope (downwind) and landings made up the slope (downwind), but, for winds whose velocities are above the critical velocity, take-offs and landings must be made into wind.

Take-off with the Wind Blowing Down the Gradient

From the preceding treatment it follows that for the upgrade take-off the length of run will be given by

$$\frac{D_2}{D_1} = \left\{\frac{1}{1 - \dfrac{2x \cdot g \cdot D_1}{V_T^2}}\right\} \left\{1 - \frac{v_w}{V_T}\right\}^{1\cdot 8}, \tag{18}$$

where the first term gives the unfavorable effect of slope and the second term gives the favorable effect of wind.

The downgrade take-off run will be given by

$$\frac{D_2}{D_1} = \left\{\frac{1}{1 + \dfrac{2x \cdot g \cdot D_1}{V_T^2}}\right\} \left\{1 + \frac{v_w}{V_T}\right\}^{1\cdot 8}. \tag{19}$$

The ratio

$$\frac{\text{upgrade run}}{\text{downgrade run}} = \left\{\frac{V_T^2 + 2x \cdot g \cdot D_1}{V_T^2 - 2x \cdot g \cdot D_1}\right\} \left\{\frac{V_T - v_w}{V_T + v_w}\right\}^{1\cdot 8},$$

and for the critical wind velocity this ratio must be unity, which leads to

$$x \cdot D_1 = \frac{V_T^2}{2g} \left\{\frac{\left(1 + \dfrac{v_w}{V_T}\right)^{1\cdot 8} - \left(1 - \dfrac{v_w}{V_T}\right)^{1\cdot 8}}{\left(1 + \dfrac{v_w}{V_T}\right)^{1\cdot 8} + \left(1 - \dfrac{v_w}{V_T}\right)^{1\cdot 8}}\right\} \tag{20}$$

which for any particular aeroplane gives the critical take-off wind velocity for a given gradient.

Equation (20) has been used to prepare the curves of Fig. 4 for the determination of the critical take-off wind velocity for any given gradient. From the appropriate values of $x \cdot D_1$ and V_T the take-off speed, the value of v_w/V_T can be read off and hence the value of v_w, the critical wind velocity for take-off.

Landing with the Wind Blowing up the Gradient

From the foregoing treatment it follows that the upgrade landing run will be given by

$$\frac{D_2}{D_1} = \left\{\frac{1}{1 + \dfrac{2x \cdot g \cdot D_1}{V^2}}\right\} \left\{1 + \frac{v_w}{V_L}\right\}^2, \tag{21}$$
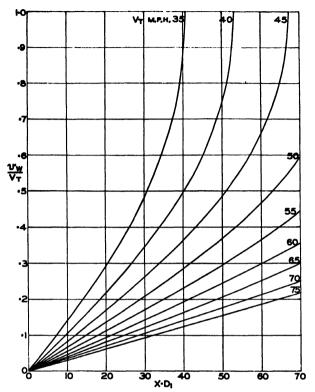
FIG. 4.   *Curves for the determination of the critical wind velocity for take-off on a gradient.*

and the downgrade landing run will be given by

$$\frac{D_2}{D_1} = \left\{ \frac{1}{1 - \dfrac{2x \cdot g \cdot D_1}{V_L^2}} \right\} \left\{ 1 - \frac{v_w}{V_L} \right\}^2 , \tag{22}$$

by equating these for the critical wind velocity we have,

$$x \cdot D_1 = \frac{V_L^2}{2g} \left\{ \frac{\left(1 + \dfrac{v_w}{V_L}\right)^2 - \left(1 - \dfrac{v_w}{V_L}\right)^2}{\left(1 + \dfrac{v_w}{V_L}\right)^2 + \left(1 - \dfrac{v_w}{V_L}\right)^2} \right\}$$

$$= \frac{V_L^2}{2g} \left\{ \frac{2 v_w V_L}{V_L^2 + v_w^2} \right\}$$

$$= \frac{V_L^2}{g} \left\{ \frac{\dfrac{v_w}{V_L}}{1 + \left(\dfrac{v_w}{V_L}\right)^2} \right\} . \tag{23}$$

The curves of Fig. 5 have been prepared from Equation (23) for the determination of the critical landing wind velocity for any given gradient, and are used in the same manner as the curves of Fig. 4.
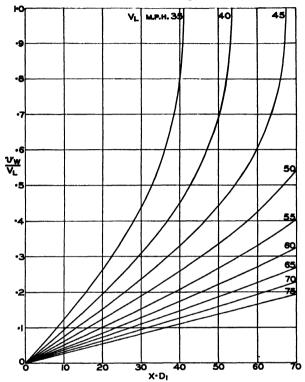

FIG. 5.   *Curves for the determination of the critical wind velocity for landing on a gradient.*

Equations (21) and (22) must be used for the determination of the length of run under any given conditions of wind and grade.   It must be remembered that all speeds used in the formulas must be in feet per second.

Although curves are not given for the length of run in the two favorable cases where gradient and wind effects are working together, the formulas for the length of run in these cases are as follows:

Wind Blowing up the Gradient for Take-off

The length of run, if the take-off is down the gradient, will be given by,

$$\frac{D_2}{D_1} = \left\{\frac{1}{1 + \dfrac{2x \cdot g \cdot D_1}{V_T^2}}\right\} \left\{1 - \frac{v_w}{V_T}\right\}^{1\cdot8}. \tag{24}$$

Wind Blowing Down the Gradient for Landing

The length of run, if the landing is up the gradient, will be given by,

$$\frac{D_2}{D_1} = \left\{\frac{1}{1 + \dfrac{2x \cdot g \cdot D_1}{V_L^2}}\right\} \left\{1 - \frac{v_w}{V_L}\right\}^{2}. \tag{25}$$

PART II
THE EFFECT OF WIND AND CURRENT ON THE TAKE-OFF OF SEAPLANES

The effect of wind and current on the take-off of seaplanes has been analyzed by using the simplifying assumption that the mean acceleration during take-off is independent of wind or current. Approximate expressions have been derived for the take-off time and distance in a wind with no current, in a current with no wind, and for the case where both wind and current are present. Curves have been prepared from which time and distance can be rapidly derived for any particular case. The following conclusions have been drawn.

The effect of wind alone on take-off distance is more marked than its effect on take-off time.

The effect of current alone on take-off distance is less marked than its effect on take-off time.

The effect of current on take-off time is closely analogous to the effect of wind on take-off time but is of opposite sign. In taking-off against a current the over-all take-off distance (referred to shore) is exactly the same as the distance for take-off in still water. In taking-off with a current there is a very small saving in take-off distance over that in still water.

In general, irrespective of the direction of the current, there will be a saving in take-off distance if the take-off is made into wind. The time of take-off will also be reduced except for that case in which the velocity of the current exceeds that of the wind, and both are in the same direction.

Symbols Used

V_T = Take-off speed of seaplane (still air),
t_1 = Take-off time in seconds in the absence of wind and current,
t_2 = Take-off time in seconds resulting from the effect of wind or current or both,
D_1 = Take-off run in the absence of wind and current,
D_2 = Take-off run resulting from the effect of wind or current or both,
f = Mean acceleration during take-off,
v_w = Wind speed,
v_c = Speed of current.

(1) Effect of Wind in the Absence of Current

The effect of wind alone on take-off time and distance has already been analyzed in Part I for landplanes. For a seaplane, identical expressions are obtained.

Upwind

Take-off time

$$\frac{t_2}{t_1} = \left(1 - \frac{v_w}{V_T}\right). \tag{26}$$

Take-off distance

$$\frac{D_2}{D_1} = \left(1 - \frac{v_w}{V_T}\right)^2. \tag{27}$$

In the case of landplanes it was noted that Equation (27) did not agree with the results of actual take-off tests.

In the case of seaplanes it has been found (2) that the actual take-off times in a wind are given very closely by Equation (26), and hence, Equation (27) for the take-off distance, derived from Equation (26), is considered to hold with reasonable accuracy.

Downwind

The equations for downwind take-off time and distance will be,

$$\frac{t_2}{t_1} = \left(1 + \frac{v_w}{V_T}\right) \tag{28}$$

and

$$\frac{D_2}{D_1} = \left(1 + \frac{v_w}{V_T}\right)^2. \tag{29}$$

These four equations have been plotted on the charts as the special case

$$v_c/V_T = 0$$

(2) Effect of Current in the Absence of Wind

Take-off with the Current

For the case of zero current

$$V_T = f \cdot t_1 ,$$

and taking-off with the current

$$V_T = v_c + f \cdot t_2$$

(the same mean acceleration as in still water is assumed).

By substituting for f and rearranging, we obtain

$$\frac{t_2}{t_1} = \left(1 - \frac{v_c}{V_T}\right) . \tag{30}$$

Again, for zero current

$$V_T^2 = 0 + 2f \cdot D_1 ,$$

with the current

$$V_T^2 = v_c^2 + 2f \cdot D_2$$

$$= v_c^2 + V_T^2 \cdot \frac{D_2}{D_1}$$

Therefore

$$\frac{D_2}{D_1} = 1 - \left(\frac{v_c}{V_T}\right)^2 . \tag{31}$$

The values of t_2/t_1 and D_2/D_1 can be read from Figs. 6 and 7 for any particular value of the ratio v_c/V_T.

The take-off distance given by Equation (31) refers, of course, to distance relative to the shore. The take-off distance measured along the surface of the water is given by,

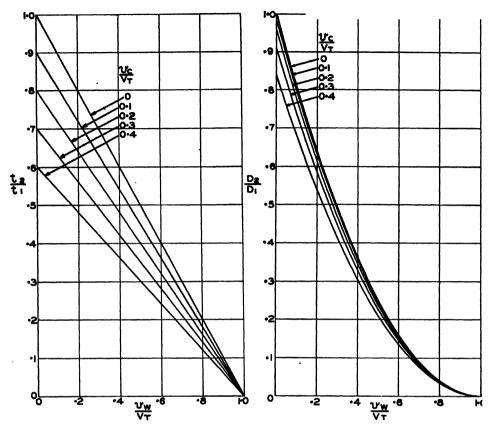$$(V_T - v_c)^2 = 0 + 2f \cdot D_2$$

$$= V_T^2 \cdot \frac{D_2}{D_1} .$$

FIG 6. *Take-off time upwind with the current.*

FIG. 7. *Take-off distance upwind with the current.*

Therefore

$$\frac{D_2}{D_1} = \left(1 - \frac{v_c}{V_T}\right)^2 \tag{31 A}$$

It is considered that distance measured along the water surface is less important than distance referred to shore. Equation (31) and Fig. 7 show that the effect of current on take-off distance referred to the shore is very small indeed.

Take-off Against the Current

In still water

$$V_T = f \cdot t_1 ,$$

and against a current

$$V_T + v_c = f \cdot t_2$$

$$= V_T \cdot \frac{t_2}{t_1} .$$

Therefore

$$\frac{t_2}{t_1} = \left(1 + \frac{v_c}{V_T}\right). \qquad (32)$$

Again, the over-all distance required to take off against the current reckoned from the point at which the backward drift with the current ceases to the take-off point is given by,

$$V_T^2 = 0 + 2f \cdot D_2 ,$$

but in still water,

$$V_T^2 = 0 + 2f \cdot D_1 .$$

Therefore

$$D_2 = D_1 \qquad (33)$$

The value of t_2/t_1 given by Equation (32) can be read from Fig. 8 for the case $v_w/V_T = 0$.
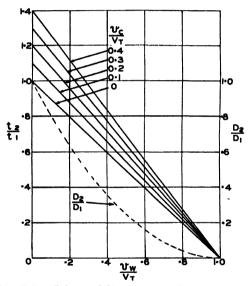

FIG. 8.   *Take-off time and distance upwind against the current.*

The take-off distance given by Equation (33) is again referred to shore, and is the same as the take-off run in still water and still air.

The take-off distance measured along the surface of the water will be given by

$$(V_T + v_c)^2 = 0 + 2f \cdot D_2$$

$$= V_T^2 \cdot \frac{D_2}{D_1} .$$

Therefore

$$\frac{D_2}{D_1} = \left(1 + \frac{v_c}{V_T}\right)^2 . \qquad (33\,A)$$

Again, this distance is unimportant unless the question arises of clearing obstacles on the surface that are moving with the current.

(3) Combined Effect of Wind and Current

It is obvious from the foregoing treatment that the equations for take-off times and distances will be as follows:—

1. Wind and Current in Opposite Directions

Case A.   Take-off with the current (upwind)

$$\frac{t_2}{t_1} = \left(1 - \frac{v_c}{V_T}\right)\left(1 - \frac{v_w}{V_T}\right) \qquad \frac{D_2}{D_1} = \left(1 - \frac{v_c^2}{V_T^2}\right)\left(1 - \frac{v_w}{V_T}\right)^2$$

Case B.   Take-off against the current (downwind)

$$\frac{t_2}{t_1} = \left(1 + \frac{v_c}{V_T}\right)\left(1 + \frac{v_w}{V_T}\right) \qquad \frac{D_2}{D_1} = \left(1 + \frac{v_w}{V_T}\right)^2$$

2. Wind and Current in the Same Direction

Case C.   Take-off with the current (downwind)

$$\frac{t_2}{t_1} = \left(1 - \frac{v_c}{V_T}\right)\left(1 + \frac{v_w}{V_T}\right) \qquad \frac{D_2}{D_1} = \left(1 - \frac{v_c^2}{V_T^2}\right)\left(1 + \frac{v_w}{V_T}\right)^2$$

Case D.   Take-off against the current (upwind)

$$\frac{t_2}{t_1} = \left(1 + \frac{v_c}{V_T}\right)\left(1 - \frac{v_w}{V_T}\right) \qquad \frac{D_2}{D_1} = \left(1 - \frac{v_w}{V_T}\right)^2$$
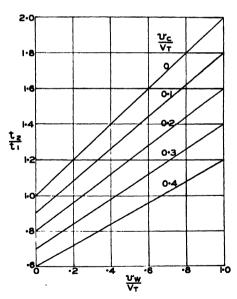

FIG. 9.   *Take-off time downwind with the current.*

Obviously Case A (*i.e.*, upwind) is the correct way to take off for *Condition 1*, since there is a saving both in time and distance over the still water, no wind, take-off.   Case B causes a loss in both time and distance.

As regards *Condition 2*, even for the very lightest winds there will be a saving in distance by taking-off into wind (Case D), since even for large values of v_c, the value of v_c^2 / V_T^2 is small, and the effect of the current in reducing take-off run in Case C is consequently almost negligible in comparison with the unfavorable effect of even moderate winds. The time of take-off will also be reduced by taking-off upwind, providing that the velocity of the wind is greater than that of the current. If this is not the case the take-off time will be increased.

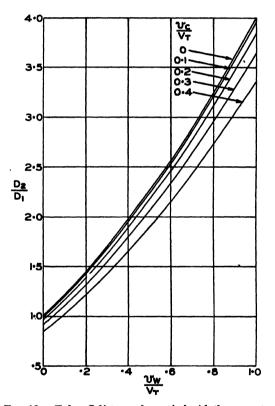Cases A, C, and D are given in the curves of Figs. 6, 7; 9, 10; and 8.

FIG. 10. *Take-off distance downwind with the current.*

Acknowledgment

References

1. DIEHL, W. S. Engineering aerodynamics. The Ronald Press Company, New York. 1936.
2. JONES, E. T. Effect of wind on the take-off of seaplanes. British Aeronautical Research Committee R. and M. No. 1593. 1934.

EXCITATION IN SOURCES FOR SPECTROSCOPIC ANALYSIS[1]

By G. O. LANGSTROTH[2] AND D. R. McRAE[2]

Abstract

From the viewpoint of the spectroscopic analyst, it is desirable to obtain some knowledge concerning the phenomena that result in the emission of radiation from certain types of sources. Results of intensity measurements on the vibration bands of the violet cyanogen system, and on certain lines in the tin spectrum, indicate that in the condensed d-c. and a-c. spark discharges the excitation is predominantly thermal in character, just as in the freely burning carbon arc. The values for the maximum temperature in the discharge columns of these three sources were found to be very nearly 9500°, 7800°, and 7000° K., respectively. It was observed, however, that the Boltzmann character of the distribution over various energy states was lost when the usual inductance was removed from the d-c. spark circuit.

One of the five investigated tin levels exhibited an abnormal behavior, which may possibly be accounted for by the occurrence of collisions of the second kind. There is also evidence to show that the emitting column is surrounded by a relatively cold layer of atoms originating in the material placed on the electrode. This layer absorbs some of the intensity of the lines ending on the ground level.

Quantitative methods of spectroscopic analysis depend on the determination of the relative intensities of appropriate spectral lines as emitted by a source containing the sample to be analyzed. It is highly desirable to investigate the phenomena that result in the emission of these radiations. There are at least three important mechanisms in operation in the source; these are responsible for *(a)* the release of material from the electrode, *(b)* the diffusion of the material after its release, and *(c)* the excitation of the material in the discharge column. This paper is concerned with a study of the excitation mechanism, *(c)*, in condensed d-c. and a-c. spark discharges, as well as in the freely burning carbon arc.

A considerable number of investigators have studied the excitation in the discharge column of freely burning arcs. It has been shown from intensity measurements that the distribution of cyanogen molecules over the higher rotational states (4, 9), and over the vibrational states (7), may be expressed by an equation of the Boltzmann form with a distribution temperature of approximately 7000° K. for the normal arc. This value was found to be little affected by changes in arc length, current strength, or applied voltage, nor did it vary appreciably for different regions along the axis of the discharge (9). It agrees essentially with the distribution temperature found from measurements on the rotational structure of the C_2 bands (3). Moreover, intensity data for the gold spectrum suggested that the distribution of atoms over the various energy states might be represented by a similar equation, using the same distribution temperature (10). Support for this view has been obtained from a comparison of relative intensities in the potassium spectrum as radiated from arcs and from flames (1). Indeed an atomic distribution of the Boltzmann form has been found in sources in which the

conditions must be thought to be less favorable to it than in the arc (*e.g.* the caesium discharge tube (6)).

These and similar investigations indicate that in the arc column the distribution of the component atoms and molecules over the various energy states may be represented by a Boltzmann equation with a single value of the distribution modulus, and the appropriate values for the energies and statistical weights of the states. Ornstein and Brinkman (8) consider that the excitation is predominantly thermal in character, and that the value of the distribution modulus at any point in the discharge is given by the temperature of the arc gases at that point. It may be shown (see Section 1), that the distribution modulus as determined, say, from the cyanogen vibration bands, corresponds to a temperature only slightly lower than the maximum temperature existing in the discharge column. It is significant that it agrees with temperatures determined by other methods (2, 5).

In the present investigation, measurements were made of the relative intensities of the 0-0, 1-1, and 2-2, violet cyanogen bands, as radiated by the condensed d-c. and a-c. sparks, and by the freely burning carbon arc. Measurements were also made of the intensity ratios of the tin lines $\lambda3262/\lambda3175$, $\lambda3262/\lambda3034$, $\lambda2850/\lambda3009$, $\lambda2850/\lambda3034$, $\lambda2840/\lambda3034$, $\lambda2840/\lambda2706$, and $\lambda2863/\lambda3009$, as radiated by the d-c. spark and by the carbon arc. These ratios involve transitions from five different initial levels whose maximum energy separation is about 9000 cm^{-1}.

The data indicate that the excitation is thermal in character in d-c. and a-c. spark discharges, just as in the freely burning arc. The relative population of one ($^3P_2^0$) of the five investigated tin levels, however, exhibits an abnormal behavior which may possibly be accounted for by the occurrence of collisions of the second kind.

It was found that the distribution in the d-c. spark preserves its Boltzmann character when the inductance in the circuit is markedly increased, and that the distribution temperature is little affected. There is, however, a change in the relative population of the abnormal $^3P_2^0$ level. On the other hand, when the inductance is removed from the circuit, the distribution loses its Boltzmann character, the populations of high levels being relatively greater than expected. This behavior is perhaps not surprising, since the duration of the discharge is very considerably shortened, and the fields are probably relatively high as indicated by the diffuse broadening of many of the lines.

There is no evidence of appreciable self-absorption in the discharge column itself under the conditions of these experiments. There is evidence to show, however, that the discharge is surrounded by a relatively cold layer of the atoms originating in the material placed on the electrode. This layer absorbs an appreciable fraction of the intensity of lines ending on the ground level, but does not noticeably affect the intensity of lines ending on somewhat higher levels. In choosing lines to be used in spectroscopic analysis, it appears to be desirable to avoid when possible those which end on the ground level as well as those which originate in abnormal levels (*e.g.* $^3P_2^0$, tin, in these experiments).

1. Theoretical Foundation of the Experiments

In this section it is shown that if the excitation in a source be predominantly thermal in character, the observed intensity ratio (I_i/I_n) of two transitions arising from different initial levels of an atom or molecule, should be closely described by,

$$I_i/I_n \;=\; P_{in}e^{-\Delta E_{in}/kT}; \quad P_{in} \;=\; \left(\frac{\nu_i}{\nu_n}\right)^4 \cdot p_i g_i/p_n g_n \;, \tag{1}$$

where ν represents the wave number of the transition, P the transition probability, and ΔE the energy separation of the initial levels of statistical weights g_i and g_n; k is Boltzmann's constant. The significance of the distribution modulus, T, depends somewhat on the conditions existing in the source, and will be referred to below.

(a) Thermal Excitation under a Constant, Uniform, Temperature. The relative intensities of lines or bands radiated from a body of vapor at a uniform temperature which does not vary with time are given by Equation (1). The distribution modulus, T, corresponds to the temperature of the vapor.

(b) Thermal Excitation under a Constant Temperature which is not Uniform over the Emitting Volume. In actual sources the temperature is lower at the boundaries of the discharge column than it is on the axis. If the temperatures are constant with time, Equation (1) is replaced by,

$$I_i/I_n \;=\; P_{in} \frac{\displaystyle\int_{-r_o}^{r_o} e^{-E_i/kf(r)}\,dr}{\displaystyle\int_{-r_o}^{r_o} e^{-E_n/kf(r)}\,dr} \tag{2}$$

where r denotes the radial distance from the axis of the discharge, and r_0 the radius of the emitting column. E represents the energy of the initial state above the ground level, and the temperature is given by some function $f(r)$. It is to be ascertained how well the intensities calculated from Equation (2) may be expressed by Equation (1), and what relation the distribution modulus found from Equation (1) bears to the actual discharge temperatures. It may be pointed out that Equation (2) is developed for the case in which the image of the source is focused on the spectrograph slit.

Let the temperature at a distance r from the axis of a thermally excited discharge be given by,

$$T \;=\; T_m e^{-\beta r^2} \;, \tag{3}$$

where β is a constant. The boundary of the emitting column (at r_o) is to be associated with a temperature T_o, which is not sufficiently great to cause appreciable excitation as compared with that in the axial region. If the axial temperature is 7500° K. (cf. the arc) the intensity of the 0-0 cyanogen band radiated from a region at 4000° K. is calculated to be only about 1% of the axial intensity. Hence for this case T_o may be taken as approximately 4000° K. A value for r_o may be obtained from the observed radius of the

emitting column in the arc, *i.e.*, approximately 1.6 mm. These values for T_m, T_o, and r_o, give a value for β in Equation (3) of 0.25 per sq. mm. Suppose in another thermal discharge the axial temperature is 10,000° K. (cf. the d.-c. spark). T_o is approximately 5000° K. The observed radius of the d.-c. spark discharge is about 1.6 mm., *i.e.*, r_o is 1.6 mm. Hence, β for this discharge is 0.27 per sq. mm.

Substitution of Equation (3) with these β-values in Equation (2), and graphical integration, permits the calculation of relative intensities as radiated from the two hypothetical sources, in terms of the appropriate P factors. The ratios of the integrated exponentials in Equation (2) (which replace the simple exponential term of Equation (1)), have been calculated for chosen cyanogen and tin transitions. They are given in Table I, along with the corresponding values of the distribution modulus for which Equation (1) gives the same ratios.

<div align="center">TABLE I</div>

Source	Axial temp., °K.	Boundary temp., °K.	$\left(I_i/I_n \cdot \dfrac{1}{P_{in}}\right)$				Equivalent modulus for Equation (1)			
			Cyanogen		Tin		Cyanogen		Tin	
			$\dfrac{1-1}{0-0}$	$\dfrac{2-2}{0-0}$	$\dfrac{3262}{3175}$	$\dfrac{2850}{3009}$	$\dfrac{1-1}{0-0}$	$\dfrac{2-2}{0-0}$	$\dfrac{3262}{3175}$	$\dfrac{2850}{3009}$
I	7500	4000	0.658	0.430	0.398	0.164	7140	7100	6720	7000
II	10000	5000	0.713	0.521	0.509	0.267	9100	9110	9270	9550

The average value of the equivalent modulus is 6990° K. for Source I, and 9260° K. for Source II.

It is apparent that the relative intensities radiated by Sources I and II may be closely represented by Equation (1) with values of the distribution modulus of 6990° and 9260° K. respectively. These values for the modulus correspond to temperatures somewhat lower than the maximum temperatures in the discharge columns.

It was assumed in these calculations that the density of atoms and molecules was uniform throughout a section of the discharge column. If it is greater near the axis, as may well be so in an actual source, the values required for the modulus of Equation (1) approximate more nearly to the maximum temperatures.

(c) Thermal Excitation under a Variable Temperature which is not Uniform over the Emitting Volume. A more complicated situation is encountered in thermal excitation in which the temperatures, and the density of atoms and molecules over a section of the discharge, are not constant with time. The integrated exponentials of Equation (2) must be further integrated over time, consideration being taken of the variations in temperature and in particle density. Calculations have been made of the relative intensities for chosen cyanogen and tin transitions in three specific cases. In all three it is assumed

that the axial temperature is initially 10,000° K., but changes abruptly after a time to 7500° K. In Case I, the duration of the initial period multiplied by the density of particles present is taken as equal to the corresponding product for the second period; in Case II this ratio is taken as 1 : 3; in Case III, it is taken as 1 : 6. Table II contains the values required for the distribution modulus in Equation (1), if this equation is to describe the calculated intensity ratios.

Table II indicates that under these conditions, also, the relative intensities may be closely represented by Equation (1), using values of 8710°, 8130°, and 7860° K. for the distribution modulus in the three cases. If the density of the particles remains essentially constant with time, the value of the modulus of Equation (1) corresponds

TABLE II

Source	Equivalent modulus for Equation (1)			
	Cyanogen		Tin	
	$\dfrac{1-1}{0-0}$	$\dfrac{2-2}{0-0}$	$\dfrac{3262}{3175}$	$\dfrac{2850}{3009}$
I	8560	8600	8800	8880
II	8000	8020	8160	8350
III	7890	7780	7780	7980

very nearly to the time average axial temperature of the source, (*i.e.*, to 8750°, 8100°, and 7860°K.).

2. Experimental Procedure

Method of Attack. The transition probabilities of the violet cyanogen bands are known (7). Hence application of Equation (1) of the last section to intensity measurements on three or more bands arising from different initial levels permits one to determine, *(a)* whether a Boltzmann distribution holds for the cyanogen molecules in the source emitting the radiation, and *(b)* if it does, what the value of the distribution modulus is. This procedure has been employed in the study of all the sources investigated.

The distribution of atoms over the various energy states, and its relation to the molecular distribution, were investigated as follows. The *P* factors of Equation (1) were experimentally determined for certain lines in the tin spectrum (energy diagram, Fig. 1) from the observed relative intensities radiated by a chosen source. This involved the assumption that the excitation was thermal, and that the distribution modulus had the same value as that determined from the cyanogen bands. The intensities of the tin lines were then measured for a second source which had a considerably different distribution temperature as determined from the cyanogen bands. These were compared with the values calculated from Equation (1), using the determined *P* factors and the new value of the cyanogen distribution modulus. Agreement of calculation with observation was taken to indicate that in both sources the excitation was thermal. This procedure was employed in a study of the d-c. spark and the d-c. arc.
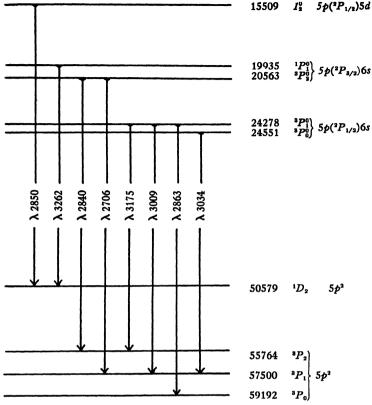
15509 $I_{\frac{0}{2}}$ $5p(^2P_{1/2})5d$

19935 $^1P^0_1$ \
20563 $^3P^0_2$ $\Big\}$ $5p(^2P_{3/2})6s$

24278 $^3P^0_1$ \
24551 $^3P^0_0$ $\Big\}$ $5p(^2P_{1/2})6s$

$\lambda\,2850$ $\lambda\,3262$ $\lambda\,2840$ $\lambda\,2706$ $\lambda\,3175$ $\lambda\,3009$ $\lambda\,2863$ $\lambda\,3034$

50579 $^1D_2$ $5p^2$

55764 $^3P_2$ \
57500 $^3P_1$ $\Big\}$ $5p^2$ \
59192 $^3P_0$

FIG. 1. *Energy diagram for tin.*

Apparatus and Technique. The d-c. and a-c. spark discharges were produced by the circuits shown in Fig. 2. These circuits are used in this laboratory in making spectroscopic analyses. Special experiments were also carried out with the d-c. circuit containing an inductance of 100 H; others were made with the inductance removed.

High Resist.   2000 μH   2000 μH

$\sim$4Kv. d-c.   0·1 μF $\sim$3Kv. a-c.   0·02 μF

(a)   (b)
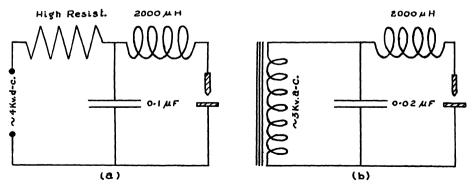
FIG. 2. *Circuits for, (a) d-c., and (b) a-c. spark discharge.*

In experiments with the d-c. spark, the plane electrode of a copper point-plane pair (separation, 3 mm.), was covered by a deposit containing tin, and lithium tartrate to furnish carbon for the cyanogen bands. Six separate sparks, each striking a fresh surface, constituted an exposure. It is estimated that the amount of tin in the area of the deposit affected by a single spark was about 3×10^{-8} gm. In experiments with the a-c. spark, various loads of Rochelle salt were placed on the plane electrode, and exposures of from 30 to 120 sec. were made. In experiments with the arc, a deposit similar to that used with the d-c. spark was placed in a shallow depression in one of the purified graphite electrodes. The arc was operated with an electrode separation of about 3 mm., and a direct current of about 8 amp.

The image of the source was focused by means of a quartz condensing lens on the slit of a Hilger E2 quartz spectrograph; in a few experiments a larger instrument was used. Calibration marks were put on each plate by means of a step-slit and quartz band lamp. Intensities were measured by the standard method employing a Moll microphotometer. Corrections for background intensity were made when necessary. The cyanogen band intensities were determined from the maximum blackening near the head of the bands; corrections were made for tails of preceding bands.

The intensities of the tin lines and the cyanogen bands were measured from the same exposures in experiments with the d-c. spark; in experiments with the arc, they were determined from different exposures, owing to the high intensity of the cyanogen bands. The conditions of operation of the arc were kept constant for all exposures.

3. Results

Relative Intensities of the Cyanogen Bands as Radiated from the d-c. Spark, the a-c. Spark, and the d-c. Arc. Observed values of the intensity ratios 1-1/0-0, and 2-2/0-0, and those calculated from Equation (1), using the stated value of the distribution temperature, are given for the three sources in Table III.

TABLE III

The d-c. spark		The a-c. spark		The d-c. arc	
$\frac{1-1}{0-0}$	$\frac{2-2}{0-0}$	$\frac{1-1}{0-0}$	$\frac{2-2}{0-0}$	$\frac{1-1}{0-0}$	$\frac{2-2}{0-0}$
0.628	0.420	0.603	0.360	0.558	0.333
0.640	0.437	0.595	0.365	0.572	0.305
0.650	0.416	0.581	0.374	0.550	0.357
0.645	0.430	0.578	0.354	0.600	0.317
0.642	0.391	0.612	0.383	0.589	0.346
0.630	0.430	0.602	0.367		
0.635	0.430				
0.647	0.431				
Av. 0.640	0.423	0.596	0.367	0.574	0.332
Calc. 0.647	0.421	0.600	0.366	0.576	0.336
T, °K. 9500		7800		7000	

Relative Intensities of the Tin Lines as Radiated from the d-c. Spark, and the d-c. Carbon Arc. The tables give the observed intensity ratios, and the ratios calculated from the following equations, using the stated value of the distribution modulus T (cf. Equation (1)).

$$\frac{3262}{3175} = 2.04e^{-6200/T} \qquad \frac{2850}{3034} = 0.95e^{-12900/T}$$

$$\frac{3262}{3034} = 3.06e^{-6600/T} \qquad \frac{2840}{3034} = 1.65e^{-5700/T}$$

$$\frac{2850}{3009} = 1.25e^{-12600/T} \qquad \frac{2840}{2706} = 1.90 \qquad \frac{2863}{3009} = 0.93$$

The P factors for these equations were determined from measurements on the d-c. spark rather than on the arc, since with the former source both the tin and the cyanogen intensities could be determined from the same exposure. The last two equations are concerned with intensity ratios of lines that come from the same initial level (*i.e.*, $\Delta E = 0$).

TABLE IV

THE ORDINARY D-C. SPARK.   CYANOGEN MODULUS 9000° TO 9700° K.; AVERAGE 9500° K.
(TABLE III)

T, °K.	3262/3175		3262/3034		2850/3009		2850/3034		2840/3034		2840/2706		2863/3009	
	Obs.	Calc.	Obs.	Calc.	Obs	Calc.	Obs	Calc.	Obs.	Calc.	Obs.	Calc.	Obs.	Calc.
9000	1.04	1.03	1.37	1.47	0.321	0.310	0.236	0.225	0.87	0.88	2.00	1.90	0.92	0.93
9900	1.08	1.10	1.58	1.57	—	—	—	—	0.89	0.93	—	—	0.93	—
9400	1.10	1.06	1.53	1.51	0.307	0.326	0.232	0.240	0.93	0.91	1.92	—	0.94	—
9600	1.03	1.07	1.60	1.53	—	—	—	—	0.94	0.92	1.86	—	0.94	—
9400	1.04	1.06	1.51	1.51	0.316	0.326	0.245	0.240	0.88	0.91	1.81	—	0.93	—
9700	1.10	1.08	1.53	1.54	—	—	—	—	0.95	0.92	—	—	0.90	—
Av. 9500	1.07	1.07	1.52	1.52	0.315	0.321	0.238	0.235	0.91	0.91	1.90	1.90	0.93	0.93

TABLE V

THE D-C. ARC.   CYANOGEN MODULUS 6700° TO 7300° K.; AVERAGE 7000° K.
(TABLE III)

T, °K.	3262/3175		3262/3034		2850/3009		2850/3034		2840/3034		2840/2706		2863/3009	
	Obs.	Calc.	Obs.	Calc.	Obs.	Calc.	Obs.	Calc.	Obs.	Calc.	Obs.	Calc.	Obs.	Calc.
7500	0.90	0.89	1.29	1.27	0.251	0.232	0.155	0.170	1.07	0.77	1.95	1.90	1.18	0.93
7400	0.89	0.88	1.20	1.26	0.249	0.229	0.163	0.168	1.09	0.76	2.04	—	1.18	—
7700	0.90	0.91	1.32	1.30	—	—	—	—	1.07	0.79	1.80	—	1.10	—
6800	0.78	0.82	1.20	1.16	—	—	—	—	—	—	—	—	—	—
6800	0.84	0.82	1.10	1.16	—	—	—	—	—	—	—	—	—	—
6700	0.79	0.81	1.14	1.15	—	—	—	—	—	—	1.98	—	1.29	—
7000	0.88	0.84	1.12	1.20	—	—	—	—	—	—	—	—	—	—
Av. 7100	0.85	0.85	1.20	1.21	0.250	0.230	0.159	0.169	1.08	0.77	1.94	1.90	1.19	0.93

4. Discussion

Examination of Table III shows that the observed relative intensities of the 0-0, 1-1, and 2-2 violet cyanogen bands radiated by the d-c. spark agree closely with those calculated on the assumption that the cyanogen molecules are distributed over the initial states in a Boltzmann distribution. The distribution modulus has a value of 9500° K. There is likewise good agreement in the data for the a-c. spark, and for the arc, the values of the distribution modulus being respectively 7800° and 7000° K.

A comparison of Tables IV and V indicates that the observed tin intensity ratios 3262/3175, 3262/3034, 2850/3009, and 2850/3034 for the d-c. spark and for the arc, agree with those calculated on the assumption that the tin atoms are distributed over the initial levels in a Boltzmann distribution, with a modulus equal to that determined from the cyanogen bands. The ratios involve transitions from the 1_2^0, $^1P_1^0$, $^3P_1^0$, and $^3P_0^0$ levels (Fig. 1). These levels are considered to exhibit "normal" behavior as contrasted with that of $^3P_2^0$. The behavior of λ2840 and λ2706, which arise from the $^3P_2^0$ level, and of λ2863, which ends on the ground level, will be referred to later.

TABLE VI

THE D-C. SPARK WITH A CIRCUIT INDUCTANCE OF 100 HENRIES

T, °K.	3262/3175		3262/3034		2850/3009		2850/3034		2840/3034		2840/2706		2863/3009	
	Obs.	Calc.	Obs.	Calc.	Obs.	Calc.	Obs.	Calc.	Obs.	Calc.	Obs.	Calc.	Obs.	Calc.
9400	1 08	1.06	1.49	1.51	—	—	—	—	0.79	0.91	—	1.90	0.89	0.93
9900	1.06	1.10	1.52	1.58	0.346	0.350	0.276	0.259	0.82	0.93	1.99	—	0.81	—
9100	1.04	1.04	1.52	1.48	0.295	0.312	0.230	0.230	0.76	0.89	2.01	—	0.80	—
8500	1.03	0.99	1 35	1.41	0.273	0.281	0.205	0 208	0.68	0.85	2.03	—	0.75	—
9500	1.07	1.07	1.49	1.52	0.315	0.330	0.257	0.242	0.81	0.91	2.08	—	0.78	—
9200	1.06	1.04	1.46	1.49	—	—	—	—	0.80	0.89	—	—	0.82	—
Av. 9300	1.06	1.05	1.47	1.50	0.307	0.318	0.242	0.235	0.78	0.90	2.03	1.90	0.81	0.93

On this evidence it is believed that the excitation in the condensed d-c. spark discharge is normally thermal in character, just as in the arc. The same is probably true of the condensed a-c. spark, whose general characteristics lie between those of the d-c. spark and the arc. The distribution modulus as found for spark discharge probably approximates rather closely (see Section 1) to the

TABLE VII

THE D-C. SPARK WITH THE INDUCTANCE REMOVED FROM THE CIRCUIT—OBSERVED INTENSITY RATIOS

	$\frac{3262}{3175}$	$\frac{3262}{3034}$	$\frac{2850}{3009}$	$\frac{2850}{3034}$	$\frac{2840}{3034}$	$\frac{2863}{3009}$
	1.05	1.45	- -	—	1.44	0.96
	0.96	1.39	0.366	0.310	1.43	0.93
	1.05	1.44	—	—	1.33	0.90
	1.06	1.43	0.391	0.307	1.37	0.98
Av.	1.03	1.43	0.379	0.309	1.39	0.94
Equiv. T, °K.*	9000	8700	10600	11400	—	—

It is to be noted that different intensity ratios require different values of the distribution modulus. Hence Equation (1) does not apply.

average axial temperature during the arc-like phase which follows the ignition period. Otherwise it is difficult to understand why extension of this phase by introduction of high inductance does not appreciably alter the value of the distribution modulus (compare Tables IV and VI). The excitation in the condensed d-c. spark with the inductance removed from the circuit is apparently not thermal in character, the populations of high states being relatively greater than those expected (Table VII). This is perhaps not surprising in view of the fact that *(a)* the duration of the discharge is relatively very short, and *(b)* the fields present during emission are probably relatively high, as suggested by the observed diffuse broadening of many of the lines.

While the above description of the excitation holds for four of the five initial levels investigated, it does not lead to correct results for the intensities of transitions from the $^3P_2^0$ level. Tables IV and V show that when the P factor for $\lambda2840/\lambda3034$ is determined from the observed intensity ratio for spark discharge the calculated ratio for the arc is nearly 30% too small. On the other hand, the ratio of $\lambda2840$ to $\lambda2706$, which originates in the same level, is essentially constant for all types of discharge. The explanation of the behavior of $\lambda2840$ is therefore to be sought in some anomalous behavior of the $^3P_2^0$ level. As shown by Tables IV, V, and VI, its population in the ordinary d-c. spark, and in the d-c. spark with high inductance, is 30% and 40% smaller than that expected on the basis of its population in the arc. The anomalous character of this level is possibly to be accounted for by the occurrence of collisions of the second kind.

An interesting feature of the data of Tables IV to VII is the observed difference in the ratio $\lambda2863/\lambda3009$ for different sources. Since $\lambda2863$, $\lambda3009$, and $\lambda3175$ originate in the same level ($^3P_1^0$), and since $\lambda3009$ and $\lambda3175$ behave normally, the differences in the ratio cannot be due to an abnormality in the $^3P_1^0$ level, but must arise from phenomena connected with the $\lambda2863$ transition. $\lambda2863$ ends on the lowest level of the ground state. Its anomalous behavior can hardly result from absorption by other atoms in the discharge itself, since, if this were so, self-absorption should play an even more important part for lines ending on the $^3P_1$ and $^3P_2$ levels (*e.g.* the "normal" lines $\lambda3009$, $\lambda3034$, $\lambda3175$), *i.e.*, the relative populations of the $^3P_0$, $^3P_1$, and $^3P_2$ levels at 8000° K. are respectively 100, 222, and 270. If however there is a relatively cold layer of tin atoms surrounding the emitting column, $\lambda2863$ will be the only radiation to be appreciably absorbed by it, *i.e.*, the relative populations of $^3P_0$, $^3P_1$, and $^3P_2$ at, say, 500° K., are respectively 100, 2.5, and 0.03. Changes in the thickness of this layer are sufficient to account for changes in the observed intensity of $\lambda2863$.

In choosing lines for use in quantitative spectroscopic analysis it is obviously desirable to avoid those lines which end on the lowest level of the ground state, as well as those which originate in abnormal levels such as $^3P_2^0$. Whether any particular level exhibits normal behavior might be shown by obtaining data analogous to that given for $\lambda2840/\lambda3034$ in the tables of this paper.

Since the excitation in these sources is thermal in character, the populations of the various states as compared with the populations of the ground state may be calculated for the different elements of the periodic table. Such calculations furnish a rough guide for the sensitivity of spectroscopic methods as applied in the analysis of any element. The figures in Table VIII give the ratio of the population in the *raie ultime* initial state to that in the ground state (per unit statistical weight) for most of the elements as excited in a source with a discharge temperature of 7000° K.

TABLE VIII

$N_r g_o / N_o g_r$	Elements
$>10^{-2}$	Li, Na, K, Rb, Cs, Ca, Sr, Ba, Y, La, In, Tl.
$10^{-2} - 10^{-3}$	Cu, Ag, Al, Bi, Cr, Mn, Fe, Co, Ni, Sc, Ga, Ti, V, Cb, Ru, Rh, Pt.
$10^{-3} - 10^{-4}$	Au, Be, Mg, Cd, B, Si*, Sn.
$10^{-4} - 10^{-5}$	Zn, Hg, Pb, P*, As*, Sb*, S*, Se, Te*.
$10^{-5} - 10^{-7}$	C*, O*, Cl*, Br*.
$10^{-7} - 10^{-15}$	N*, H, Xe, Kr, A, Ne, He.

The figures for these elements are upper limits of the ratio, either because the raie ultime is not well defined, or because the energy diagram is not well known to the authors.

The intensity of the *raie ultime* depends on several factors in addition to the population of the initial level per unit statistical weight, *viz.*, the statistical weights of initial and ground levels, the transition probability, the number of transitions from the initial level and their transition probabilities, and, for a given total amount of the element present, on the degree of ionization of the element. The above figures give only a rough idea, therefore, of the sensitivity of spectroscopic methods for the different elements.

It is to be noted that the relative population of the initial level is large for elements that are readily detected by spectroscopic analysis with ordinary sources (*e.g.*, most metals), but that it is small for those which are not (*e.g.*, the rare gases and the halogens). It is suggested that development of sources having considerably higher discharge temperatures would permit spectroscopic analysis for the latter group of elements.

Acknowledgments

References

1. VAN DER HELD, E. F. M. and HEIËRMAN, J. H. Physica, 2 : 71-74. 1935.
2. HÖRMANN, H. Z. Physik, 97 : 539-560. 1935.
3. TER HORST, D. TH. J. and KRYGSMAN, C. Physica, 1 : 114-118. 1933.
4. LOCHTE-HOLTGREVEN, W. and MAECKER, H. Z. Physik, 105 : 1-15. 1937.
5. MANNKOPFF, R. Z. Physik, 86 : 161-184. 1933.
6. MOHLER, F. L. J. Research Natl. Bur. Standards, 16 : 227-231. 1936.
7. ORNSTEIN, L. S. and BRINKMAN, H. Proc. Roy. Acad. Amsterdam, 34 : 33-41. 1931.
8. ORNSTEIN, L. S. and BRINKMAN, H. Physica, 1 : 797-824. 1934.
9. ORNSTEIN, L. S. and BRINKMAN, H. Proc. Roy. Acad. Amsterdam, 34 : 498-504. 1931.
10. ORNSTEIN, L. S. and SAMBURSKY, S. Proc. Roy. Acad. Amsterdam, 34 : 1-2. 1931.

THE ALTITUDE EFFECT ON THE SPECIFIC IONIZING POWER AND ZENITH ANGLE DISTRIBUTION OF COSMIC RAYS[1]

By DAROL K. FROMAN[2] AND J. C. STEARNS[3]

Abstract

Measurements made with a quadruple-coincidence Geiger-Müller counting system at altitudes of 120 and 14,160 ft. give the intensity, J, of cosmic ray ionizing particles at various zenith angles, ψ. The distribution, $J_{(\psi)} = J_0 e^{-0.175\psi} \cos^2 \psi$, does not differ significantly from any measured values, and agrees with all observations within 0.5 and 3.0% of the vertical intensities at the lower and higher altitudes respectively. The total number of rays incident per unit area per unit time was found, and the specific ionization was determined by comparison with ionization chamber measurements. The results are given below.

Altitude, ft.	120	14,160
Mean specific ionization in ion pairs per centimetre in air at one atmosphere, i.	†54.8 ± 1.8 *82.0 ± 2.6	*87.5 ± 6
Total number of rays incident per hour per square centimetre of level surface, N_1.	78.3 ± 2.5	306 ± 22
Total number of rays incident per hour per square centimetre of surface normal to the rays, N_2.	109 ± 3.5	425 ± 30
Number of vertical rays incident per hour per square centimetre per unit solid angle, J_0.	58.4 ± 1.9	228 ± 15

† Ionization chamber data from Clay and Jongen (4).
* Ionization chamber data from Millikan and Cameron (18).

Introduction

The variation of cosmic ray intensity with zenith angle has been measured at single altitudes by Tuwim (23), Bernardini (2), Medicus (15), Skobelzyn (20), and others. Johnson (7) has made these measurements at altitudes of 620 and 6280 ft. in northern United States, and at sea level and at 14,200 ft. in Peru (8). Street and Woodward (21) have made an absolute measurement of the vertical intensity at sea level. With the aid of Johnson's measurements and Millikan's (17) ionization chamber values, Street and Woodward calculated the average specific ionization of the cosmic rays. General agreement has not been obtained on the value of the specific ionization, nor on

the variation of the zenith angle distribution with altitude.   For these reasons it was decided to redetermine the zenith angle distribution and specific ionization near sea level and at a high altitude.   Observations were made at Ste. Anne de Bellevue, Que., and at the High Altitude Laboratory on Mount Evans, Colorado.

Experimental Arrangement

The apparatus consisted of a quadruple-coincidence Geiger-Müller "telescope" with the counters arranged as shown in Fig. 1.   The counters were mounted so that the central, or direction, line (dotted in Fig. 1) could be held at any desired zenith angle, the long axes of the counters remaining horizontal. The distance, L, between the axes of extreme counters was 30.48 cm., and the inside diameter of the cylindrical electrodes in the counters was 2.54 cm.
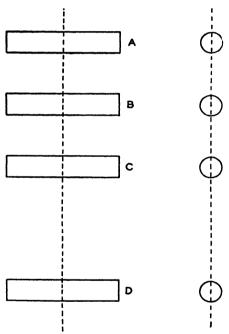
FIG. 1.   *Arrangement of Geiger-Müller counters.*

The quadruple-coincidence counting rate, *i.e.*, the frequency with which the four counters were excited simultaneously, was determined at each 15° interval in zenith angle from the vertical to 75° inclusive.   The readings were taken in the magnetic southern azimuth so as to average out the east-west asymmetry of about 2%.   The north-south asymmetry is negligible at the latitudes at which this work was done.   At the low altitude station, where the variations in barometric pressure were appreciable, a second quadruple-coincidence telescope was operated always in the vertical position.   This set furnished data for direct comparison of the intensity at any angle with the vertical intensity determined under identical meteorological conditions.

The efficiency of each counter was determined by the ratio of the quadruple to the triple counting rate with the particular counter disconnected.   In this case the counter occupied either position B or C in Fig. 1, these two positions giving the same results.   Both triple and quadruple rates were corrected for the accidental rates.   These accidental rates were determined by taking counting rates with the counters out of line.

The absorption of a counter and its shield was found by a comparison of the triple counting rates of the other three counters with the fourth counter in, and out of, line with the other counters of the telescope.

The recording circuit used was a modification of that described by Johnson and Street (10).

Theory for Determining the Absolute Intensity

Let $J_{(\psi)}$, the absolute intensity of the radiation, be the number of rays incident per unit time per unit solid angle per unit area normal to the rays at zenith angle ψ. In Fig. 2 let the z-axis be vertical and let the direction line of the counters (dotted in Fig. 2) lie in the xz-plane. The rotation of the

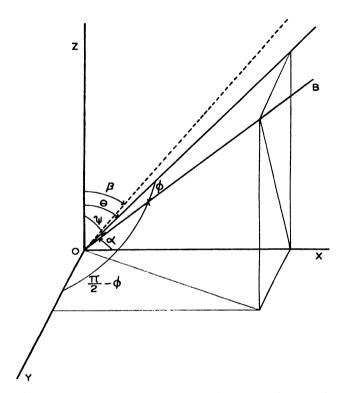Fig. 2. *Diagram showing angular relations to aid in integration over the counters.*

system takes place about the y-axis which is parallel to the long axes of the counters. β is the zenith angle of the direction line of the counters, and the direction angles of any ray, BO, incident at the origin are α, $(\pi/2 - \phi)$, ψ, θ is the angle between the z-axis and the plane defined by the y-axis and the incident ray, BO.

Then, from Fig. 2,

$$\cos \psi = \cos \theta \cos \phi . \tag{1}$$

The side and end views of the outside pair of counters are shown in Fig. 3. From this diagram it is seen that, if we neglect for the moment the half ellipses on the ends of one extreme counter as seen from the other, the exposed

area of the counter system, projected normally to BO, is

$$A = (d - L \tan \phi)\{w - L \tan |\theta - \beta|\} \cos \phi \cos |\theta - \beta|$$
$$= L^2 (\tan b - \tan \phi)\{\tan a - \tan |\theta - \beta|\} \cos \phi \cos |\theta - \beta| . \qquad (2)$$
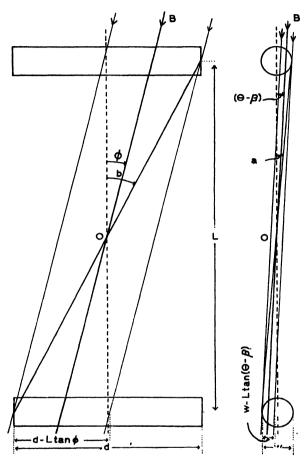

FIG. 3. *Diagram showing rays through extreme counters.*

The area is projected normally to the ray BO since the intensity, J, is defined in terms of the number of rays incident upon unit area measured normal to the rays.

Now it is known from the work of Skobelzyn (20), Johnson (7), and others that, approximately,

$$J_{(\psi)} = J_0 \cos^2 \psi = J_0 \cos^2 \theta \cos^2 \phi, \qquad (3)$$

and this function can be used for integration over the small solid angle of the counter system for any value of β. Let $R_{(\beta)}$ be the counting rate when

the zenith angle of the direction line of the telescope is β. The solid angle contained between θ and $\theta + d\theta$, ϕ and $\phi + d\phi$ is $\cos \phi \, d\theta d\phi$. Then

$$R_{(\beta)} = \int_{\phi=-b}^{+b} \int_{\theta=-a}^{+a} J_0 \cos^2 \theta \cos^2 \phi \cdot L^2 (\tan b - \tan \phi)\{\tan a$$
$$- \tan |\theta - \beta|\} \cos |\theta - \beta| \cos^2 \phi \, d\theta d\phi .$$

Since the east-west asymmetry is small for the range of azimuth angle included by the counters, the ϕ-function in the integrand may be considered as even between the limits $-b$ and $+b$, and we may write,

$$R_{(\beta)} = 2J_0 L^2 \int_0^b (\cos^4 \phi \tan b - \cos^3 \phi \sin \phi) d\phi \int_{\beta-a}^{\beta+a} \cos^2 \theta \cos |\beta - \theta|$$
$$\{\tan a - \tan |\beta - \theta|\} \, d\theta$$

$$= \frac{2J_0 L^2}{\cos a \cos b} \int_0^b (\cos^4 \phi \sin b - \cos^3 \phi \sin \phi \cos b) d\phi$$

$$\times \left[\int_{\beta-a}^{\beta} \{\sin a \cos^2 \theta \cos (\beta - \theta) - \cos a \cos^2 \theta \sin (\beta - \theta)\} d\theta \right.$$

$$\left. + \int_{\beta}^{\beta+a} \{\sin a \cos^2 \theta \cos (\theta - \beta) - \cos a \cos^2 \theta \sin (\theta - \beta)\} d\theta \right]$$

$$= \frac{2J_0 L^2}{3 \cos a \cos b} \left[\frac{3}{8} b \sin b + \frac{1}{4} \sin b \sin 2b + \frac{1}{32} \sin b \sin 4b + \frac{1}{4} \cos^5 b \right.$$

$$\left. - \frac{1}{4} \cos b \right] \left[2 (1 - \cos a)^2 + 2 (\cos a - \cos 2a)\cos^2 \beta \right], \quad (4)$$

where
$$b = \tan^{-1} d/L \quad \text{and} \quad a = \sin^{-1} w/L . \quad (5)$$

Street and Woodward (21) have shown the effective diameter, w, of a counter to be the inside diameter of the cylindrical copper electrode. The effective axial length, d_1, was determined by taking counting rates for various displacements of one of the middle pair of counters parallel to its long axis. Then $\frac{1}{2}d_1$ is the displacement necessary to reduce the counting rate to one-half its maximum value. However, it can be seen from Fig. 4 that, for a ray incident at an angle α to the direction line of the telescope, the effective area of an extreme counter is increased at each end by an amount

$$A = \frac{\pi r^2 \tan \alpha}{2} ,$$

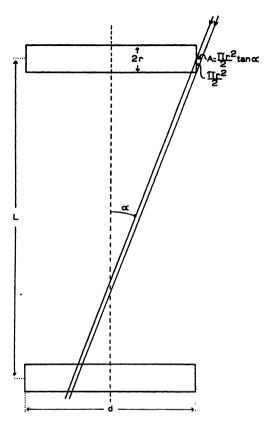or the effective half-length by

$$\frac{\pi r \tan \alpha}{2} .$$

FIG. 4. *Diagram showing end correction for extreme counters.*

Hence the mean correction to be added to the value of the effective axial half-length is

$$s = \frac{1}{\tan^{-1} d_1/L} \int_0^{\tan^{-1} d_1/L} \frac{\pi r}{2} \tan \alpha \, d\alpha$$

$$= - \frac{\pi r}{2 \tan^{-1} d_1/L} (\log_e \cos \tan^{-1} d_1/L) , \qquad (6)$$

and the corrected effective length becomes

$$d = 2(d_1 + s) . \qquad (7)$$

Values of $\dfrac{R_{(\beta)}}{J_0}$, calculated by means of Equations (4) and (5) from experimentally determined values of d, L, and w, are shown in the third column of Table I. The use of Equation (4) means that we are assuming a $\cos^2\psi$ distribution of intensities.

TABLE I

$\beta°$	$\cos^2 \beta$	$R_{(\beta)}/J_0$	$R_{(\beta)}/J_0 \cos^2 \beta$	$R_{(\beta)}/J_0$, corrected
0	1	1.0470	1.047	1.0470
15	0.93300	0.9769	1.047	0.9332
30	0.75000	0.7853	1.047	0.7166
45	0.50000	0.5241	1.047	0.4568
60	0.25000	0.2627	1.050	0.2187
75	0.06699	0.07122	1.062	0.05664

It will be seen from column four of Table I that $R_{(\beta)}$ is closely proportional to $\cos^2\beta$, there being only a slight deviation from proportionality at large zenith angles where the intensity is low. Hence, even if the actual intensity distribution differs slightly from a $\cos^2\psi$ distribution, β can be interchanged with ψ in any experimentally determined intensity function of β.

Let the true intensity function be

$$J_{(\psi)} = J_0 f_{(\psi)} = J_0 f_{(\beta)} . \tag{8}$$

The proportionality constants in column four of Table I are found on the assumption that $f_{(\psi)} = \cos^2\psi$. In order to find J_0 accurately from measured values of $R_{(\beta)}$, these constants must be corrected by multiplying them by $\frac{f_{(\beta)}}{\cos^2 \beta}$, where $f_{(\beta)}$ is the function found by experiment. The corrected values of this ratio, $R_{(\beta)}/J_0$, are given in the last column of Table I for the function

$$J_{(\psi)} = J_0 e^{-0.176\psi} \cos^2\psi,$$

which is shown later to fit the data. Thus a value of J_0 can be found from the counting rate taken at any zenith angle.

If E is the efficiency of the counting system, then the values of $J_{(\psi)}$ found by the above method must be multiplied by $\frac{1}{E}$ to give absolute values.

Moreover, there is a correction for the absorption of the counters themselves and their shields.

The total number of rays incident per unit time per unit area of level surface will be

$$N_1 = 2\pi \int_0^{\pi/2} J_{(\psi)} \sin \psi \cos \psi \, d\psi , \tag{9}$$

and the total number of rays incident per unit time per unit area of surface normal to the rays will be

$$N_2 = 2\pi \int_0^{\pi/2} J_{(\psi)} \sin \psi \, d\psi . \tag{10}$$

If these cosmic ray ionizing particles form Q pairs of ions per unit volume per unit time in air at one atmosphere pressure, the mean specific ionization is given by

$$i = Q/N_2 \text{ ion pairs per cm.} \tag{11}$$

In calculating i by means of this relation, Q is found by ionization chamber measurements, and it is assumed that only the ionizing rays which actuate counters are responsible for the ionization.

Experimental Results

Observations of the cosmic ray intensities were made continuously from September 28, 1936 until June 3, 1937, at Ste. Anne de Bellevue, and from July 1 until July 15, 1937, at the Mount Evans High Altitude Laboratory.

The efficiency of each counter was measured at each station. The efficiency, E, of the system is the product of the separate efficiencies of the four counters. Table II gives the accidental counting rates and efficiencies. The efficiencies of all four counters were nearly the same.

TABLE II

Altitude, ft.	120	14,160
Triple accidental rate per hr.	0.6 ± 0.1	3.3 ± 1.0
Quadruple accidental rate per hr.	0.3 ± 0.08	0.7 ± 0.3
Efficiency of quadruple set, E	0.833 ± 0.021	0.515 ± 0.036

The effective axial length, d_1, was found by taking counting rates for various displacements of one of the middle counters. These rates, less accidentals, at an altitude of 120 ft. are given in Table III, and are plotted against displacement in Fig. 5. From Fig. 5, the value of half of the effective axial length is found to be 5.96 cm., *i.e.*, $d_1 = 11.92 \pm 0.05$ cm. The probable error given for d_1 is estimated from the probable errors given in Table III.
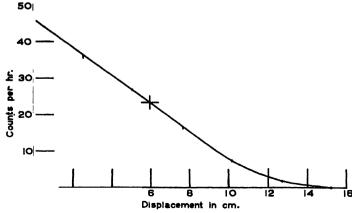

FIG. 5. *The variation of counting rate with lengthwise displacement of a middle counter.*

The observed counting rates, $R_{(\beta)}$, at the two stations are given in Table IV. These values are corrected for accidentals, but are not corrected for efficiencies and absorption of the counters. The values for altitude 120 ft. have been corrected to a barometric pressure of 76.0 cm., and those for altitude 14,160 ft. to a pressure of 46.7 cm. These pressures are very near the means at the two stations and the corrections are small.

TABLE III

Displacement in cm.	Counting rate per hr.
0.00	46.5 ± 0.38
2.54	35.9 ± 0.42
5.08	26.9 ± 0.36
7.62	16.44 ± 0.28
10.16	7.73 ± 0.18
12.70	1.82 ± 0.11
15.24	0.00 ± 0.08

TABLE IV

$\beta°$	Altitude 120 ft.		Altitude 14,160 ft.	
	Total counts	$R_{(\beta)}$ per hr.	Total counts	$R_{(\beta)}$ per hr.
0	48360	44.4 ± 0.14	4706	106.6 ± 1.0
15	20605	39.9 ± 0.19	2058	92.3 ± 1.5
30	15743	30.7 ± 0.16	1359	76.0 ± 1.3
45	9742	19.0 ± 0.14	1109	43.9 ± 0.9
60	4573	8.90 ± 0.09	506	24.3 ± 0.6
75	1579	2.51 ± 0.05	255	7.6 ± 0.4

The counting rates given in Table IV are plotted against zenith angle in Fig. 6. The probable errors are represented by the vertical lines. The curves drawn are both of the form

$$R_{(\beta)} = R_0 e^{-0.175\beta} \cos^2 \beta , \qquad (12)$$

and the agreement with experimental values seems sufficiently good for us to use

$$f_{(\psi)} = f_{(\beta)} = e^{-0.175\beta} \cos^2 \beta = e^{-0.175\psi} \cos^2 \psi$$

for our intensity distribution function. This has been done in calculating the values in the last column of Table I.

The absorption of the counters and their shields was found to reduce the counting rate to $(87.1 \pm 1.7)\%$ of the incident value. This value omits the absorption of the thin wooden roof above the system and the top covering of the upper counter, since our experience, and that of Street and Woodward (21), shows that the number of detectable secondaries produced in this thin layer above the system very nearly cancels its absorption.

J_0 was calculated for each zenith angle, at the two altitudes, and mean values were found by weighting in proportion to the number of rays counted at each angle. These mean values were then corrected for efficiencies and absorption, and the final values are given in Table V. Also N_1 and N_2, calculated by means of Equations (9) and (10), are given in Table V.
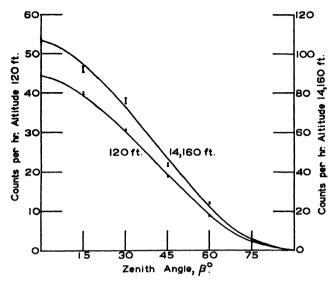
FIG. 6. *The quadruple-coincidence counting rate as a function of zenith angle for altitudes of 120 and 14,160 ft. The values are not corrected for absorptions or for efficiencies.*

Specific Ionization

Many observers have measured the ionization produced by cosmic rays. Millikan and Cameron (18), however, give absolute values taken at very nearly the same altitudes and latitudes as those of our stations, and we shall use their values for calculating the specific ionization. From the table of values given by Millikan and Cameron, we find the number of ion pairs produced per cubic centimetre per second by cosmic rays in air at one atmosphere to be 2.48 and 10.31 at our lesser and greater altitudes respectively. The specific ionizations, i, calculated from these values by means of Equation (11) are given in Table V. The calculation of the probable errors quoted for the

TABLE V

Altitude, ft.	120	14,160
Mean specific ionization in ion pairs per centimetre in air at one atmosphere, i.	†54.8 ± 1.8 *82.0 ± 2.6	*87.5 ± 6
Total number of rays incident per hour per square centimetre of level surface, N_1.	78.3 ± 2.5	306 ± 22
Total number of rays incident per hour per square centimetre of surface normal to the rays, N_2.	109 ± 3.5	425 ± 30
Number of vertical rays incident per hour per square centimetre per unit solid angle, J_0.	58.4 ± 1.9	228 ± 15

† *Ionization chamber data from Clay and Jongen (4).*
* *Ionization chamber data from Millikan and Cameron (18).*

values of i involves an estimate of the probable errors in the results given by Millikan and Cameron. This estimate has been made from data given by them as an example of a typical run.

Discussion of Results

Measurements of the specific ionization produced by cosmic rays at sea level have been made by various observers using several different methods. Some of the results previously obtained are given below for comparison with the value obtained here, *viz.*, 82.0 ± 2.6 ion pairs per cm. at sea level. Bothe and Kolhörster (3) found $i = 90$ per cm., and Messerschmidt (16), 110 per cm. Kolhörster and Tuwim (12) found $i = 135 ± 13$ per cm. by taking counting rates with a single counter held with its axis at various orientations. Swann (22) found $i = 60$ per cm. by a direct ionization measurement with a linear amplifier. Evans and Neher (6) set an upper limit of 70 ± 10 per cm. from fluctuation measurements in an ionization chamber. Anderson (1) gives a value of 31 per cm., Locher (14) 36 per cm., and Kunze (13) 19 per cm., found by counting droplets along tracks in cloud chambers. It is obvious that the last method must lead to a lower limit. Anderson (1) estimates 122 per cm. from considerations of the energy loss of cosmic ray particles in passing through matter. Street and Woodward (21) give a value of 100 ± 3.7 per cm., and Kolhörster and Jánossy (11), 106 per cm., found by essentially the same method as that described here. Regener and Pfotzer (19) give $i = 103$ per cm. between altitudes 18 and 20 km. Danforth and Ramsey (5) obtain a value of 21 per cm. from considerations involving the efficiency of a single counter, but it seems that this must be a lower limit since they neglect wall effects. The arithmetic mean of all these values is in good agreement with our result.

Clay and Jongen (4) have recently given a value of 1.66 ions per cc. per sec. formed by cosmic rays at sea level in air at one atmosphere. This result has been corrected to a free air basis by taking the effects of the walls of the ionization chamber into account. Using this value we obtain for the specific ionization at sea level 54.8 ± 1.8 ion pairs per cm. which agrees well with values found by other methods. It is possible that all previous estimates of i, determined by the method described here, are too high because of the high value of the total ionization used.

The method used here for integration over the counter system gives a value differing by less than 1% from the value obtained by applying the equation given by Street and Woodward (21) to the system for $\beta = 0°$. The value quoted here for J_0, 58.4 ± 1.9 per sq. cm. per hr. per unit solid angle, at sea level is somewhat higher than that of Street and Woodward, *viz.*, 48.0 ± 1.7 per sq. cm. per hr. per unit solid angle. The zenith angle distributions found for both altitudes were the same within experimental error. This result is in agreement with the work of Regener and Pfotzer (19). The distribution is definitely broader than that found by Johnson (7) at an altitude of 620 ft., but it is in good quantitative agreement with his result for an altitude of

6,280 ft.   In Peru, Johnson (8) finds the distribution to be slightly broader at sea level than at 14,200 ft.

The ratio of the total number of rays effective in ionization, N_2, at the higher station to that at the lower is 3.9 ± 0.3, and the ratio of the specific ionizations is 1.07 ± 0.08.   Johnson (8) finds 3.78 and 1.20 for these ratios for altitudes nearly the same in Peru.   Although the differences are not significant, the values found in Peru might be expected to be smaller than the others, since Johnson and Read (9) have shown that for a given altitude a lesser fraction of the shower-producing radiation than of the total is excluded, near the equator, by the earth's magnetic field.   The fact that the frequency of showers increases more rapidly with altitude than does the total radiation, causes the intensity, as determined by ionization chambers, to increase more rapidly than the coincidence counting rates, since only one count is registered for any number of particles passing through the counters simultaneously.   The ratio of specific ionizations given by Johnson (7) as 1.3 for altitudes of 6,280 and 620 ft. seems very high.   However, there is either a numerical or typographical error in this result*.   A correction reduces this value to about 1.2. This value would be still further reduced if it is found, as is expected from our work and Johnson's work in Peru, that the angular distribution is not broader at 6,280 ft. than at sea level.

References

 1. ANDERSON, C. D.   Phys. Rev. 44 : 406-416.   1933.
 2. BERNARDINI, G.   Nature, 129 : 578-579.   1932.
 3. BOTHE, W. and KOLHÖRSTER, W.   Z. Physik, 56 : 751-777.   1929.
 4. CLAY, J. and JONGEN, H. F.   Physica, 4 : 245-255.   1937.
 5. DANFORTH, W. E. and RAMSEY, W. E.   Phys. Rev. 49 : 854.   1936.
 6. EVANS, R. D. and NEHER, H. V.   Phys. Rev. 45 : 144.   1934.
 7. JOHNSON, T. H.   Phys. Rev. 43 : 307-310.   1933.
 8. JOHNSON, T. H.   Phys. Rev. 45 : 569-585.   1934.
 9. JOHNSON, T. H. and READ, D. N.   Phys. Rev. 51 : 557-564.   1937.
10. JOHNSON, T. H. and STREET, J. C.   J. Franklin Inst. 215 : 239-246.   1933.
11. KOLHÖRSTER, W. and JÁNOSSY, L.   Z. Physik, 93 : 111-122.   1934.
12. KOLHÖRSTER, W. and TUWIM, L.   Z. Physik, 81 : 435-439.   1933.
13. KUNZE, P.   Z. Physik, 83 : 1-18.   1933.
14. LOCHER, G. L.   Phys. Rev. 39 : 883-888.   1932.
15. MEDICUS, G.   Z. Physik, 74 : 350-378.   1932.
16. MESSERSCHMIDT, W.   Z. Physik, 78 : 668-688.   1932.
17. MILLIKAN, R. A.   Phys. Rev. 39 : 397-402.   1932.
18. MILLIKAN, R. A. and CAMERON, G. H.   Phys. Rev. 37 : 235-252.   1931.
19. REGENER, E. and PFOTZER, G.   Physik. Z. 35 : 779-784.   1934.
20. SKOBELZYN, D.   Compt. rend. 194 : 118-121.   1932.
21. STREET, J. C. and WOODWARD, R. H.   Phys. Rev. 46 : 1029-1034.   1934.
22. SWANN, W. F. G.   Phys. Rev. 44 : 961-968.   1933.
23. TUWIM, L.   Berlin Berichte, 19: 91-106, 360-373.   1931.

* *The existence of this error has been confirmed by private communication with Dr. Johnson.*

A STUDY OF THE JOULE AND JOULE-THOMSON EFFECTS[1]

BY A. L. CLARK[2] AND L. KATZ[3]

Abstract

This paper contains material not treated in a previous paper on the same subject. It deals particularly with the Joule and Joule-Thomson effects at low and at high pressures and also near the critical point. These effects have been calculated by various methods from available data. The value of the internal pressure (Joule effect) has been calculated (for the first time) for the two-phase, liquid-vapor state, and compared with values obtained from the equation of state. This internal pressure is nearly a linear function of the external pressure. The values of the internal pressure have also been calculated for low pressure where values have been in doubt. The behavior of the specific heat at constant volume as a function of the temperature has also been studied and related to the behavior of the internal pressure. The inversion of the Joule and Joule-Thomson effects is examined. The internal pressure evidently rises to a maximum as the pressure is increased at constant temperature, and probably falls off to zero and becomes negative. For helium the pressure for inversion is relatively low. The inversion curve for the Joule-Thomson effect has also been studied, and it is shown that even for carbon dioxide an inversion of the effect may be expected. When the values of the two effects are small we must have recourse to experimental methods because the calculations cannot be made with accuracy. When however these values are large, calculations yield results of good accuracy, probably better than may be obtained by experiment.

In an earlier paper (3) one of the authors discussed the general relations for the perfect gas and the functions that may be used to measure the departure of real gases from the ideal gas. These expansion functions were given and their interrelations deduced. In particular, the Joule and Joule-Thomson effects were studied, and some calculated values of the magnitudes of these effects were given. The Joule effect is the change in temperature experienced by a gas when it expands into a vacuum, or expands without doing external work. The Joule-Thomson or Joule-Kelvin effect is the change in temperature experienced by a gas when it expands through a porous plug, or medium, or through a valve against an external pressure. The discussion of their values at low pressures and at temperatures below the critical temperature was reserved for a later paper. In the meantime new measurements and calculations have appeared, and there have been contributions to the general subject by several observers. During the past few months the work has been taken up anew, and the present paper gives the results of the investigation of points not discussed in the earlier paper.

As in the earlier paper

$$\lambda = \left(\frac{\partial U}{\partial v}\right)_T = T\left(\frac{\partial P}{\partial T}\right)_v - P \tag{1}$$

has been taken as the measure of the Joule effect, and

$$\mu = \left(\frac{\partial T}{\partial P}\right)_{W^*} = \frac{T\left(\frac{\partial v}{\partial T}\right)_P - v}{c_P} \tag{2}$$

as the measure of the Joule-Thomson effect.   Roebuck (20) has taken

$$\eta = \left(\frac{\partial T}{\partial P}\right)_U, \tag{3}$$

which he calls the Joule coefficient, to measure the Joule effect.   This is related to λ through the equation

$$\lambda = \left\{c_P\left(\frac{\partial P}{\partial v}\right)_T - P\left(\frac{\partial P}{\partial T}\right)_v\right\}\eta. \tag{4}$$

λ as defined by Equation (1) may be interpreted either as the amount of energy required to maintain the temperature constant when unit mass of the gas expands by unit volume without doing external work, or as the internal or cohesion pressure. η is the ratio of the change of temperature to the change of pressure in the same expansion when there is no change in the internal energy. μ is the Joule-Thomson coefficient, or the ratio of the change in temperature to the change in pressure when the gas expands through the porous plug, or in any manner so as to emerge after expansion with negligible kinetic energy of flow.   The only external work is that done against the pressure existing on the exit side of the plug or orifice.   In other words the enthalpy remains constant.

The early experiments of Gay-Lussac, of Joule, and of Hirn, showed that λ is very small, so small that they were unable to detect its existence.   Indeed it is so small that it still is almost impossible to measure this quantity experimentally with any degree of accuracy.   In a paper by Keyes and Sears (10) some measurements of the Joule effect for carbon dioxide are given.   The temperature changes were of the order to be expected.   Roebuck (15), in a paper on the Joule-Thomson effect in air, has mentioned some unpublished work on the measurement of λ by one of his students.   The results again are of the proper order.

The senior author of the present paper has worked intermittently for some years with an apparatus for the direct measurement of both λ and η.   The experimental set-up is much like that used by Joule nearly 100 years ago. Compressed gas is allowed to expand suddenly into an evacuated chamber. The entire apparatus (tanks and valve) is immersed in a constant temperature bath.   A differential manometer is arranged so as to measure the change in pressure throughout the system immediately after expansion and later when the temperature has returned to that of the bath.   Values of λ and η are determined from measurements easily made, even with hydrogen.   None of the results have been published.

* *W is the enthalpy ($U + Pv$) per unit mass.*

The values for the internal pressure, λ, for carbon dioxide near the critical temperature and for nitrogen at temperatures between 0° and 150° C., have been calculated recently by Michels (11, 12, 13) and co-workers from their own $Pv - P$ data. The method of calculation will appear later in this paper. Roebuck has calculated both λ and η for a number of gases from his experimental values of μ. He has shown that η for helium is independent of the pressure but is positive at low temperatures (cooling), zero at $-70°$ C., and negative (heating) at high temperatures. To explain this unexpected result he takes into account the change in the number of collisions per unit time, per molecule, due to change in volume. Expansion brings about a change in the energy distribution. If the forces between the molecules are attractive, the speeding up of those taking part in the collisions represents an increase of kinetic energy. If the volume is increased, the number of collisions is decreased and the mean kinetic energy is lowered. Jeans (8, p. 190) is of the opinion that the amount of work obtainable from the change in the number of collisions on expansion is nil.

An excellent summary of the earlier work on the experimental determination of the Joule-Thomson coefficient will be found in a paper by Hoxton (7). For more recent data the bibliographies found in Roebuck's papers (15–20) should be consulted. μ for steam, and a bibliography of works on this substance, will be found in Report IV of the Steam Research Program, by F. G. Keyes, L. B. Smith, and H. T. Gerry. The most outstanding and painstaking work on the experimental determination of μ in recent years is that carried out by Roebuck and by Roebuck and Osterberg, using porous plugs of the radial flow type. The gases investigated were: air, helium, argon, nitrogen, and their mixtures.

Internal Pressure—Joule Effect

The free expansion coefficient, λ, as defined in Equation (1), may be interpreted either as the change in internal energy when unit mass of the gas expands by unit volume at constant temperature, or as the internal pressure. To show that λ *is* the internal pressure we use the general relation

$$dQ = dU + P\,dv,$$

from which

$$\left(\frac{\partial Q}{\partial v}\right)_T = \left(\frac{\partial U}{\partial v}\right)_T + P = \lambda + P, \tag{5}$$

and also

$$dQ = c_v dT + l_v dv, \tag{6}$$

where l_v may be regarded as either the total amount of energy required per unit mass per unit change of volume, the so-called latent heat of expansion, or as a pressure, such that an amount of energy $l_v dv$ is required to change a unit mass of gas through the volume dv against the pressure l_v, which is called the total or thermal pressure. From Equation (6) we obtain

$$l_v \quad \left(\frac{\partial Q}{\partial v}\right)_T. \tag{7}$$

Hence
$$l_v = \lambda + P, \qquad \qquad (8)$$

i.e., the total pressure is the sum of the internal and external pressures.

Method of Calculation

Values of λ may be calculated by the graphical method used by Amagat, as was done by the senior author (3). This involves plotting the $Pv - P$ isotherms on a large scale. Then since the isometrics on such a diagram are straight lines through the origin, the corresponding values of P and T at constant volume may be obtained by means of a straight edge or a stretched thread. The $P - T$ isometrics are then drawn, and the values of the slope $\left(\dfrac{\Delta P}{\Delta T}\right)_v$ may be found for any pair of values of P and T, and the value of λ may be calculated by means of Equation (1).

The following method is a modification of the foregoing. The $Pv - P$ data may be interpolated to obtain the values of P and T at constant volume, so that the slope $\left(\dfrac{\Delta P}{\Delta T}\right)_v$ may be calculated. The accuracy with which λ can be determined by either method varies considerably over the range of available data, since it depends on the numerical difference between the values of $T\left(\dfrac{\Delta P}{\Delta T}\right)_v$ and P. When λ is large (high pressures and low temperatures) the accuracy is about the same as for P and T. When λ is small, however, the accuracy is determined by the position of the first significant figure in the difference. For example, if $T\left(\dfrac{\Delta P}{\Delta T}\right)_v - P = 13.247 - 13.157 = 0.090$, and if P and T are known to one part in 10,000, λ will be correct to about 5%.

The calculation may also be carried out as follows. Suppose the isometrics in terms of P and T have been drawn or the values tabulated. Then at any point P, T, where λ is to be calculated, a second point $P + \Delta P$, $T + \Delta T$ is taken. It is easily seen that

$$\lambda = T\left(\frac{P_{T+\Delta T} - P_T}{\Delta T}\right) - P_T = (T + \Delta T)\left(\frac{P_{T+\Delta T} - P_T}{\Delta T}\right) - P_{T+\Delta T}, \qquad (9)$$

which gives the value of λ at a point approximately at the middle of the interval between the two points, or at $T + \dfrac{\Delta T}{2}$, $P + \dfrac{\Delta P}{2}$.

Again the average values of the derivatives on both sides of the point P, T may be taken so that

$$\lambda = T\frac{1}{2}\left(\frac{P_T - P_{T-(\Delta T)_1}}{(\Delta T)_1} + \frac{P_{T+(\Delta T)_2} - P_T}{(\Delta T)_2}\right) - P_T, \qquad (10)$$

which is in some respects preferable. If $(\Delta T)_1 = (\Delta T)_2$, this reduces to Equation (9). Michels used Equation (9) for his calculations, while for

most of the work of this paper Equation (10) was used. Table I shows the method and accuracy of a sample calculation, using Michel's (12) data for carbon dioxide, where the density of the gas was 28.1756 times the normal density.

TABLE I

SAMPLE CALCULATION OF λ BY MEANS OF EQUATION (10)

T, °C.	P, atm.	$\left(\dfrac{\Delta P}{\Delta T}\right)_v$	$\left(\dfrac{\Delta P}{\Delta T}\right)_v$, average	λ, atm.	Estimated accuracy, %
25.053	26.3707				
		0.12318			
49.712	29.3972		0.12165	9.879	0·1
		0.12013			
75.260	32.4664				

Saturated Two-phase Region

Within the saturated two-phase region

$$l_v = \frac{L}{v_1 - v_2},\tag{11}$$

where L is the ordinary latent heat per unit mass, v_1 is the specific volume of the higher phase (vapor), and v_2 that of the lower phase (liquid). Then by Equation (8)

$$\lambda = \frac{L}{v_1 - v_2} - P.\tag{12}$$

Since for pure fluids P is the same for all volumes at the same temperature, L, v_1, and v_2 are constant, so that λ is a constant; *i.e.*,

$$(\lambda)_T = \text{constant}\tag{13}$$

or

$$(\lambda)_P = \text{constant},\tag{14}$$

where Equations (13) and (14) refer to the saturated two-phase region only.

Equation (12) may be deduced easily from the Clapeyron-Clausius equation, *viz.*:

$$\frac{\partial P}{\partial T} = \frac{L}{T(v_1 - v_2)}\tag{15}$$

$$\lambda = T\left(\frac{\partial P}{\partial T}\right)_v - P = \frac{L}{v_1 - v_2} - P.\tag{16}$$

It will be seen that λ, like P, is independent of the volume. It remains constant from 100% liquid to 100% vapor, a fact that should be remembered when any theory of liquefaction is considered. If λ is interpreted as an energy function, then during the process of vaporization at constant temperature, the internal energy is a linear function of the volume. If, on the

other hand, λ is regarded as a pressure, the molecules are able to move apart during the process of evaporation without any change in the internal pressure. Further, from Equation (12) we obtain

$$L = (\lambda + P)(v_1 - v_2) = l_v(v_1 - v_2) . \tag{17}$$

$P(v_1 - v_2)$ is the external heat of vaporization, or the energy used in separating the molecules against the external pressure, while $\lambda(v_1 - v_2)$ is the internal heat of vaporization, or the energy used in separating the molecules against the internal pressure. The total heat of vaporization, L, is stored as potential energy, and is equal to the work done against the total pressure, l_v.

The reduced value of λ may be defined as

$$\Lambda = \theta\left(\frac{\partial \pi}{\partial \theta}\right)_\varphi - \pi , \tag{18}$$

where θ, π, and φ are the reduced values of temperature, pressure, and volume defined as in van der Waals' original use of derived magnitudes, *i.e.*, the reduced temperature, pressure, and volume are the ratios of the actual temperature, pressure, and volume to the critical values of these quantities. It follows that

$$\Lambda = \frac{\lambda}{P_c} . \tag{19}$$
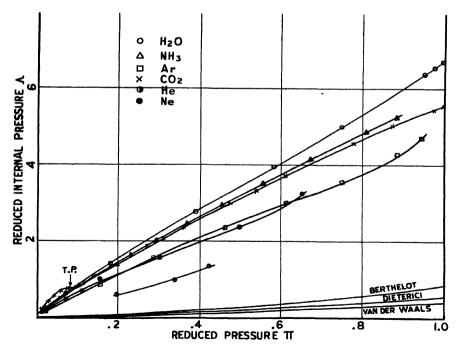
FIG. 1.   *Internal pressure—saturated two-phase region.   Water vapor pressure data of Keyes, Smith, and Gerry. All other data from Tables Annuelles Int. de Constants, Vol. 9, 1929. (T.P. = triple point of carbon dioxide).*

The reduced values for different gases may be calculated if the values of λ are determined by means of Equation (16), using saturated vapor pressure data. These values are shown in Fig. 1 plotted as a function of the reduced pressure. It will be seen that the internal pressure is nearly a linear function of the external pressure, the lines being slightly curved near each end. It follows that the internal pressure and the saturated vapor pressure expressed as functions of the temperature must be of nearly the same form.

Fig. 2 shows the values of λ along the critical isothermal plotted against the pressure, the results calculated by Michels (11) for carbon dioxide being used. Values of λ calculated from the saturated vapor data are also shown. The two curves intersect at the critical pressure. The curve calculated from the saturated vapor data is really the locus of the saturated vapor pressure points on a series of curves like that of Michels for various temperatures below the critical.
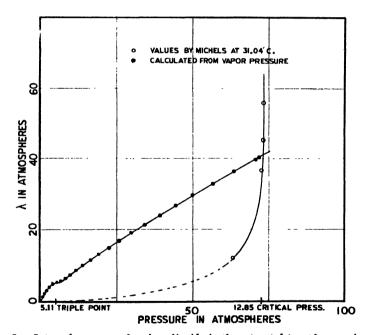
FIG. 2. *Internal pressure of carbon dioxide in the saturated two-phase region.*

Low Pressure Region—Equations of State

Since the first attempt by Hirn to correct the ideal gas equation, many equations of state have been proposed, each attempting to take into account the intermolecular forces and the actual total volume of molecules in order to obtain better agreement with the behavior of real gases. It seems evident that if such equations are to be applicable to the problems under discussion, they must yield values of the internal pressure comparable with those values calculated from $Pv - P$ data or observed directly. Conversely, the degree

of accuracy with which a certain equation of state may predict the magnitude of the internal pressure may be taken as a measure of its value in the application to problems involving internal energy, departure from the law of Joule, or any quantities depending on the variation of λ.

From van der Waals' reduced equation of state

$$\left(\pi + \frac{3}{\varphi^2}\right)\left(3\varphi - 1\right) = 8\theta$$

the value of Λ is

$$\Lambda = \frac{3}{\varphi^2} \tag{20}$$

or if $\pi\varphi = \frac{8}{3}\theta$ approximately,

$$\Lambda = \frac{27}{64}\frac{\pi^2}{\theta^2} . \tag{21}$$

The equation of state proposed by Dieterici in its reduced form is

$$\pi = \frac{\theta e^{2\left(1 - \frac{1}{\varphi\theta}\right)}}{2\varphi - 1} ,$$

which yields

$$\Lambda = \frac{2\pi}{\theta\varphi} . \tag{22}$$

If $\pi\varphi = \frac{e^2}{2}\theta$ (approximately), then

$$\Lambda = \frac{4}{e^2}\frac{\pi^2}{\theta^2} . \tag{23}$$

And finally the reduced equation of Berthelot, the empirical relations between T_c, P_c, and v_c, and the modified constants, a, b, and R suggested by him, being used, is

$$\left(\pi + \frac{16}{3}\frac{1}{\theta\varphi^2}\right)\left(\varphi - \frac{1}{4}\right) = \frac{32}{9}\theta .$$

Hence

$$\Lambda = \frac{32}{3}\frac{1}{\theta\varphi^2} . \tag{24}$$

If the approximate relation $\pi\varphi = \frac{32}{9}\theta$ is assumed, then

$$\Lambda = \frac{27}{32}\frac{\pi^2}{\theta^3} . \tag{25}$$

Values of Λ calculated from the equations of van der Waals and Dieterici differ only by a constant factor of 1.28316, the equation of van der Waals giving the lower value. Theoretically both equations have the same validity (9, p. 174), being true for the first order of quantities only. Figs. 3 and 4 show the reduced internal pressure as calculated by means of the above three equations of state and actual values for various substances calculated from $Pv - P$ data.

A few points for ether, calculated from the data of Keyes and Felsing (9), the semi-empirical equation of state of Hildebrand (6) being used, are also shown. This equation is of particular interest because it was developed from a consideration of attractive and repulsive molecular forces varying inversely with some powers of the distance.

λ is given by

$$\lambda = \left(\frac{\partial U}{\partial v}\right)_T = \frac{ma}{v^{m+1}}\left\{ 1 - \left(\frac{v_0}{v}\right)^{n-m}\right\} , \qquad (26)$$

where v is the molal volume at any temperature and pressure, and v_0 is the molal volume at zero pressure and at absolute zero. If λ is zero, then $v_0 = v$, which enables one to calculate the value of v_0, a value that is independent of the values of m and n. Hildebrand used the data of Keyes and Felsing and arrived at the equation for ether

$$\lambda = \frac{3180 \times 10^4}{v^2}\left\{ 1 - \left(\frac{79}{v}\right)^8\right\} , \qquad (27)$$

where $a = 3180 \times 10^4$, $m = 1$, $v_0 = 79$, and n is chosen empirically equal to 9. It will be remembered that the equation of van der Waals gives $\lambda = \frac{a}{v^2}$.
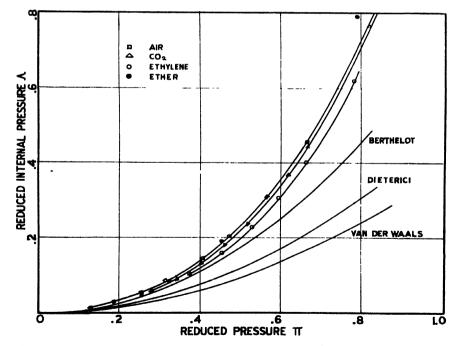
FIG. 3. *Reduced internal pressure at constant temperature* $\theta = 1 \cdot 061$. *Curves for air, carbon dioxide, and ethylene calculated by means of Equation (10). Curves for ether calculated by means of Equation (27). Data: Air—Witkowski, Penning and of Holborne and Otto. Carbon dioxide—A. Michels and C. Michels. Ethylene—A. Michels, J. de Gruyter, and F. Niessen. Ether—Keyes and Felsing.*
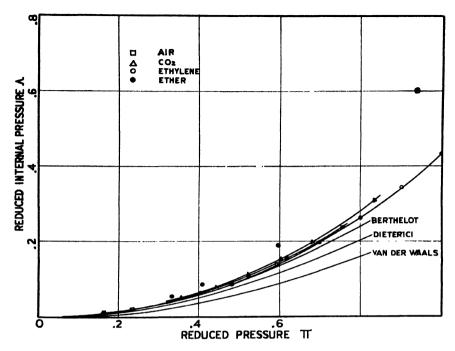
FIG. 4.   *Reduced internal pressure at constant temperature* $\theta = 1 \cdot 309$.   *Same as Fig. 3, only at a higher temperature.*

The graphs of Figs. 3 and 4 show that the equation of Berthelot gives results that are in fair agreement with the values calculated from P, v, T data even at pressures of $\pi = 0.5$, whereas the equations of van der Waals and of Dieterici give results that depart widely from these calculated results. As P approaches zero, $\left(\dfrac{\partial P}{\partial T}\right)_v$ also approaches zero, and therefore $\lambda = T\left(\dfrac{\partial P}{\partial T}\right)_v - P$ approaches zero.   The agreement with the values calculated from P, v, T data shown by all three equations is better at low than at high pressures.   Also the agreement at high temperatures is better than at low.

In general the equation of Berthelot shows best agreement with the calculated values.   None of the equations however show λ increasing as rapidly with either temperature or pressure as is required by the graphs giving the calculated results.

In the two-phase, liquid-vapor region the values of λ obtained from the equations of state are low compared with those obtained from P, v, T data. Thus in Fig. 1, the three lower graphs were obtained by substituting the reduced value of P and the corresponding reduced values of T for water in Equations (21), (23), and (25).   The resulting values of Λ were then plotted against π.   These curves should be compared with the more accurate curve obtained by substituting the same saturated vapor data in Equation (16).

It is to be noted that the equations themselves do not yield unique internal pressure values for this region, but give the values of λ if the proper values of P and T (found experimentally) are used.

High Pressure

For all substances investigated, calculation shows that at low pressure the internal energy decreases upon isothermal compression, i.e., $\left(\dfrac{\partial U}{\partial P}\right)_T$ is negative. At a certain pressure, depending on the temperature, it reaches a minimum value and further compression causes it to increase. Eventually $\left(\dfrac{\partial U}{\partial P}\right)_T$ becomes positive.

Now

$$\lambda = \left(\frac{\partial U}{\partial P}\right)_T \left(\frac{\partial P}{\partial v}\right)_T . \tag{28}$$

Since $\left(\dfrac{\partial P}{\partial v}\right)_T$ is always negative*, λ is positive at low pressure, zero when $\left(\dfrac{\partial U}{\partial P}\right)_T = 0$, and negative at high pressure. From Equations (8) and (11) the pressure at which λ is zero is given by

$$P = T\left(\frac{\partial P}{\partial T}\right)_v = l_v \tag{29}$$

(when the external pressure is the total pressure).

The pressure at which the internal energy is a minimum, $\left(\dfrac{\partial U}{\partial P}\right)_T = 0$ and $\lambda = 0$, varies greatly even with gases. It varies from a few atmospheres with helium to thousands of atmospheres with other gases.†

Bridgman (2) finds that with liquids the pressure at which $\left(\dfrac{\partial U}{\partial P}\right)_T = 0$ is about 7000 atm. or higher. For solids he gives values ranging from 5800 atm. for sodium at 30° C. to 21,000 atm. for iridium at the same temperature.

The curves of Figs. 5, 6, and 7 illustrate the general character of λ as a function of the external pressure at constant temperature. The curves of Fig. 8 are plotted from values taken from Fig. 5 and show the variation of λ with temperature at constant pressure. The agreement at 20 atm. with values given by Roebuck is seen to be very good.

---

* The completely unstable region required by the equation of van der Waals is excluded.

† Bridgman (1) assigns a negative value to $\left(\dfrac{\partial U}{\partial P}\right)_T$ for helium at room temperatures up to pressures more than 15,000 atm., whereas Roebuck's calculations show λ to be negative even at atmospheric pressure and 0° C. This would indicate that $\left(\dfrac{\partial U}{\partial P}\right)_T$ has already become positive at this low pressure. The results obtained in this investigation, while not conclusive, show that λ is very small and certainly negative at even fairly low pressure. This is in agreement with Roebuck's work.
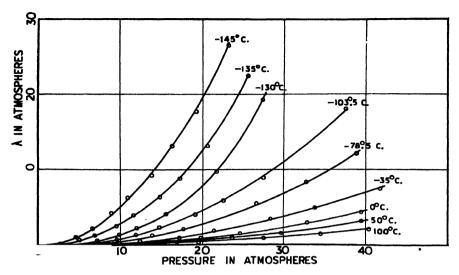
FIG. 5.   *Variation of* λ *with pressure at constant temperature.   Air.   Calculated by means of Equation (10) from Pv−P data of Witkowski, Penning, and of Holborne and Schultze.*
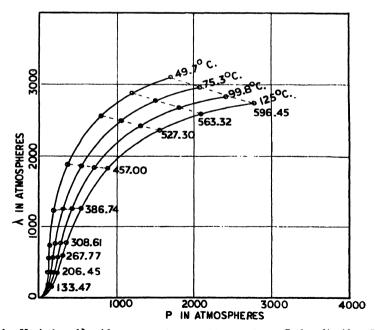

FIG. 6.   *Variation of* λ *with pressure at constant temperature.   Carbon dioxide.   Calculated by means of Equation (10) from Pv−P data of A. and C. Michels.   Points joined by dotted lines are at the same volume or density (numbers indicate density relative to that at N.T.P. as unit).*
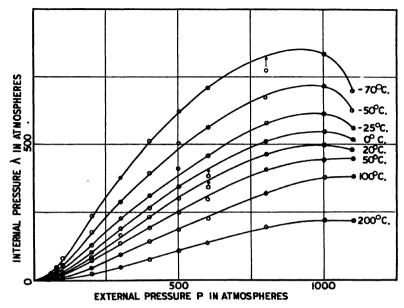
FIG. 7.   *Variation of λ with pressure at constant temperature.   Nitrogen.*

$$\lambda = T\left(\frac{\partial P}{\partial T}\right)_v - P = -\left\{\frac{\frac{T}{v}\left(\frac{\partial v}{\partial T}\right)_P}{\frac{P}{v}\left(\frac{\partial v}{\partial P}\right)_T} + 1\right\} P$$

Values of $\frac{P}{v}\left(\frac{\partial v}{\partial P}\right)_T$, $\frac{T}{v}\left(\frac{\partial v}{\partial T}\right)_P$, *and P are from data of W. E. Deming and L. E. Shupe.*

Note: *The values of* λ *calculated for 1200 atm. pressure are extremely erratic; no doubt extrapolated values given by Deming and Shupe are not sufficiently accurate.*

Specific Heat at Constant Volume

A study of the curves, Fig. 9, which show λ as a function of the temperature at constant volume, leads to interesting results.   From Equation (1)

$$\left(\frac{\partial \lambda}{\partial T}\right)_v = T\left(\frac{\partial^2 P}{\partial T^2}\right)_v = \left(\frac{\partial c_v}{\partial v}\right)_T. \tag{30}$$

Since the slope of these curves is given by $\left(\frac{\partial \lambda}{\partial T}\right)_v = \left(\frac{\partial c_v}{\partial v}\right)_T$, it is seen that as one goes from curve to curve at constant temperature the slope becomes greater as the critical volume is approached, and the change in λ, and therefore c_v, is seen to become greater as the critical temperature is approached. Similarly, along any one of the curves (isometric) the slope increases as the critical temperature is approached, so c_v is an increasing function of the temperature.
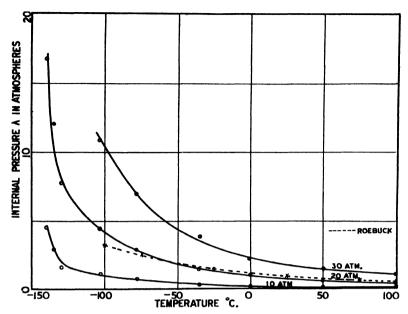
FIG. 8.   *Variation of* λ *with temperature at constant pressure. Air. Full lines were obtained by taking values off graphs in Fig. 5 at 10, 20, and 30 atm. pressure.   Dotted line shows values of* λ *calculated by Roebuck from his experimental values of* μ *for air at 20 atm. pressure.*

Young (21) has shown that $\left(\frac{\partial^2 P}{\partial T^2}\right)_v = 0$ for isopentane near the critical point.   This leads one to expect that the curves do not continue to rise indefinitely but pass through a maximum.   Recently Michels *et al.* (11) has calculated c_v for carbon dioxide, and has shown that it passes through a maximum near the critical point.   Where the value of c_v is a maximum, the following must hold—

$$\left(\frac{\partial c_v}{\partial v}\right)_T = T\left(\frac{\partial^2 P}{\partial T^2}\right)_v = \left(\frac{\partial \lambda}{\partial T}\right)_v = 0 . \tag{31}$$

There is thus complete agreement between the behavior of c_v and that of λ studied as functions of the temperature at constant volume.

Joule-Thomson Effect

The Joule-Thomson coefficient defined by Equation (2) is the change in temperature per unit-change of pressure experienced by a gas while expanding through a porous plug.   This effect is due to the departure of the gas from the laws of Boyle and Joule.   It may be shown that

$$\mu = -\frac{1}{c_P}\left(\frac{\partial W}{\partial P}\right)_T = -\frac{1}{c_P}\left(\frac{\partial (U + Pv)}{\partial P}\right)_T$$

$$= -\frac{1}{c_P}\left\{\lambda\left(\frac{\partial v}{\partial P}\right)_T + \left(\frac{\partial (Pv)}{\partial P}\right)_T\right\} . \tag{32}$$

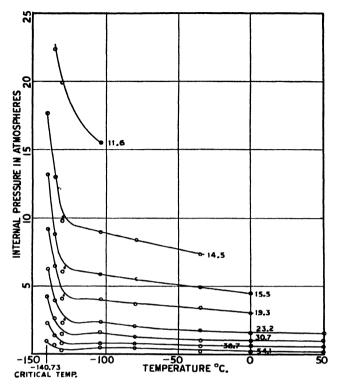Fig. 9.   *Variation of* λ *with temperatre at constant volume.   Air.   Calculated by means of Equation (10) from Pv — P data of Witkowski, Penning, and of Holborne and Schultze (see Fig. 5).   Figures on graphs indicate the specific volume in cc. per gm., the critical specific volume being 2.86 cc. per gm. (not shown).*

If the gas obeyed the laws of Boyle and Joule, λ and $\left(\dfrac{\partial(Pv)}{\partial P}\right)_T$ would be zero, and so μ would be zero.

At low temperature and pressure, as has been noted, λ is generally positive (cooling on expansion), and since $\left(\dfrac{\partial v}{\partial P}\right)_T$ is always negative, the contribution of $\lambda\left(\dfrac{\partial v}{\partial P}\right)_T$ to μ is positive.   Also, as Amagat has shown, $\left(\dfrac{\partial(Pv)}{\partial P}\right)_T$ is negative at sufficiently low temperature and pressure, and its contribution to μ is also positive.   Thus μ, being the results of two effects, may be larger in magnitude than either and may be measurable when λ is not.   If either the temperature or pressure is changed sufficiently, one or both effects may change sign, so that the value of μ may pass through zero and become negative, as experiment shows is true.

From the discussion in the first part of this paper, it is evident that λ is of greater theoretical importance than either μ or η, but because of the greater ease with which μ is measured and because of its application to the liquefaction of gases, it has received most attention.

Inversion Curve

Through an examination of the signs and magnitude of λ, $\left(\dfrac{\partial v}{\partial P}\right)_T$, and $\left(\dfrac{\partial (Pv)}{\partial P}\right)_T$, it may be shown that the points for which μ is zero trace out a curve on the $Pv - P$ diagram essentially as shown in Fig. 10. This is known as the inversion curve. Expansion of a gas between any two states represented by points within the area enclosed by the inversion curve results in cooling of the gas. Expansion between any two states represented by points on the diagram which are outside the curve will result in a heating of the gas. Finally, expansion across the curve will result in heating, cooling, or no effect, depending on the position of the initial and final states.
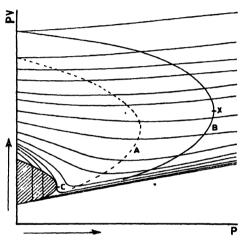
FIG. 10.   *Inversion curve for μ.   Dotted line, A, is the locus of points on the isothermals for which $\left(\dfrac{\partial (Pv)}{\partial P}\right)_T = 0$.   Solid line, B, is the locus of points for which $\mu = 0$.   Shaded area is the two-phase equilibrium region, and point C is the critical point.   Expansion between any two pressures greater than X results in heating only.*

It is seen from the diagram that there is a pressure above which expansion between any two states (for all temperatures) results in heating only. This is to be expected, since, as the pressure increases, $\left(\dfrac{\partial (Pv)}{\partial P}\right)_T$ increases and is positive, whereas $\left(\dfrac{\partial v}{\partial P}\right)_T$ decreases rapidly. This explains why the first attempts of Kamerlingh Onnes to liquefy helium failed. The pressure before expansion was too high. Such a maximum pressure and, as a matter of fact, the whole inversion curve, was predicted by Porter (14) from the equations of van der Waals and Dieterici, and has been confirmed experimentally by a number of investigators. Fig. 11 shows the inversion curve calculated from van der Waals' equation of state, with the reduced temperature and pressure as co-ordinates. On the same diagram the experimentally determined values of θ and π, for $\mu = 0$, for air and nitrogen given by Roebuck, and the calculated values for carbon dioxide from Fig. 12 are shown. Roebuck brought
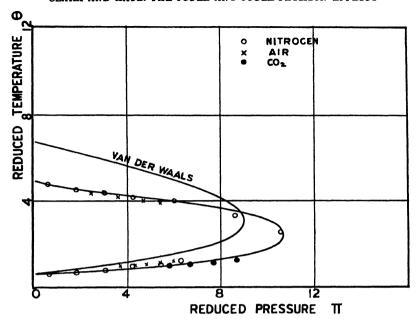
FIG. 11. *Inversion curves for μ from van der Walls' equation and from experimental results. Nitrogen and air, from data by Roebuck; carbon dioxide, from our calculated curves, see Fig. 12.*

the upper and lower halves of the air inversion curve together at a maximum pressure somewhat lower than that given by van der Waals' equation. If the law of corresponding states holds, the calculated maximum inversion pressure is greater than that given by van der Waals' equation as shown. It should also be noted that there is better agreement between the equation and experimental data in the low pressure, low temperature region.

Method of Calculation

Though μ has been measured experimentally by a number of investigators, the range is still very limited, and indirect methods of calculation have to be resorted to for extremely low or high temperatures.

One method is essentially the same as that described for λ, only in this case the isothermals on the $Pv - P$ diagram are cut by isopiestics to obtain values of Pv at T and $T + \Delta T$.

μ is calculated by means of the following relation:

$$
\mu = \frac{1}{c_P P}\left\{ T\left(\frac{(Pv)_{T+\Delta T} - (Pv)_T}{\Delta T}\right) - (Pv)_T \right\}
$$

$$
= \frac{1}{c_P P}\left\{ (T + \Delta T)\left(\frac{(Pv)_{T+\Delta T} - (Pv)_T}{\Delta T}\right) - (Pv)_{T+\Delta T} \right\}, \tag{33}
$$

which gives μ at approximately the middle of the interval between the two points.
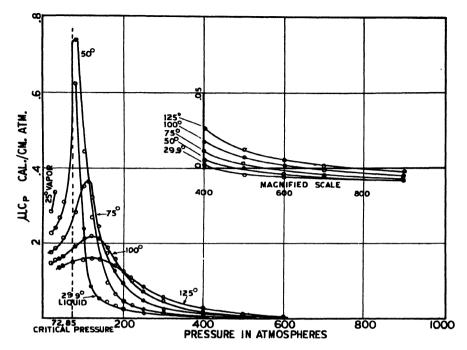
FIG. 12.   *μ_{C_P} for carbon dioxide.   Calculated by means of Equation (31) from Pv — P data of Michels.*

Deming and Shupe (4) used graphs of the residual quantity α to determine the derivative $\left(\dfrac{\partial \alpha}{\partial T}\right)_P$, and calculated μ from the equation:

$$\mu = \frac{T\left(\dfrac{\partial v}{\partial T}\right)_P - v}{c_P} = \frac{\alpha - T\left(\dfrac{\partial \alpha}{\partial T}\right)_P}{c_P} , \qquad (34)$$

where α is defined by:

$$\alpha = \frac{RT}{P} - v . \qquad (35)$$

The residual quantity method is more accurate for temperatures removed from the critical, since, at such temperatures, the $Pv - P$ isothermals are nearly straight lines, whereas the $\alpha - T$ isopiestics are quite curved and the slope $\left(\dfrac{\partial \alpha}{\partial T}\right)_P$ is measured with greater precision.

.More recently Edmister (5) employed the residual quantity method to calculate μ for methane; the derivative $\left(\dfrac{\partial \alpha}{\partial T}\right)_P$ was determined by the chord area method of graphical differentiation on a large-scale plot.

TABLE II
Critical constants used

Substance	Critical pressure, atm.	Critical temperature, °K.	Substance	Critical pressure, atm.	Critical temperature, °K.
He	2.261	55.19	Ethylene	49.98	282.65
Ne	26.86	44.38	CO$_2$	72.85	304.19
Air	37.25	132.42	NH$_3$	111.50	405.55
Ar	47.996	150.65	H$_2$O	217.88	647.85
Ether	36.7	467.7			

References

1. BRIDGMAN, P. W. Modern Physics, 7 : 1-33. 1935.
2. BRIDGMAN, P. W. The physics of high pressure. G. Bell and Sons, Ltd., London. 1931.
3. CLARK, A. L. Trans. Roy. Soc. Can. 18, III : 293-311. 1924.
4. DEMING, W. E. and SHUPE, L. E. Phys. Rev. 37 : 638-654. 1931.
5. EDMISTER, W. C. Ind. Eng. Chem. 28 : 1112-1116. 1936.
6. HILDEBRAND, J. II. Phys. Rev. 34 : 984-993. 1929.
7. HOXTON, L. G. Phys. Rev. 13 : 438-479. 1919.
8. JEANS, J. J. The dynamical theory of gases. Second edition. Cambridge University Press, London. 1916.
9. KEYES, F. G. and FELSING, W. A. J. Am. Chem. Soc. 41 : 589-619. 1919.
10. KEYES, F. G. and SEARS, F. W. Proc. Natl. Acad. Sci. U.S. 11 : 38-41. 1925.
11. MICHELS, A., BIJL, A., and MICHELS, C. Proc. Roy. Soc. London, A, 160 : 376-384. 1937.
12. MICHELS, A. and MICHELS, C. Proc. Roy. Soc. London, A, 153 : 201-214. 1935.
13. MICHELS, A., WOUTERS, H., and DE BOER. Physica, 1 : 587-594. 1934.
14. PORTER, A. W. Phil. Mag. 111 : 554-568. 1906.
15. ROEBUCK, J. R. Proc. Natl. Acad. Arts Sci. 60 : 537-596. 1925.
16. ROEBUCK, J. R. Proc. Natl. Acad. Arts Sci. 64 : 287-334. 1930.
17. ROEBUCK, J. R. and OSTERBERG, H. Phys. Rev. 43 : 60-69. 1933.
18. ROEBUCK, J. R. and OSTERBERG, H. Phys. Rev. 45 : 332-340. 1934.
19. ROEBUCK, J. R. and OSTERBERG, H. Phys. Rev. 46 : 786-790. 1934.
20. ROEBUCK, J. R. and OSTERBERG, H. Phys. Rev. 48 : 450-457. 1935.
21. YOUNG, S. Proc. Phys. Soc. London, 13 : 602-657. 1895.

TRANSPORT OF MATERIAL IN SOURCES FOR SPECTROSCOPIC ANALYSIS[1]

BY G. O. LANGSTROTH[2] AND D. R. McRAE[2]

Abstract

A study of the transport of material in the condensed d-c. spark discharge has been made, with the object of placing quantitative spectroscopic methods of analysis on a less empirical basis and thus permitting, *(a)* the recognition of certain conditions of source operation which lead to unreliable determinations, and *(b)* the determination of some of the criteria to be fulfilled for maximum precision in analytic measurements.

Variations in the transport phenomena, as indicated by variations in the relative distributions of emitting atoms of various elements along the discharge axis on the addition of certain substances to a sample, appear to be closely connected with the ionization potentials and masses of the elements, and with the ionization potentials of other particles present in the discharge. The data indicate the necessity for the use of a spectroscopic buffer, and provide certain criteria for the choice of the buffer and of the internal standard element.

The exact nature of the mechanism of transport is uncertain, but various considerations indicate that neither the motion of ions under the influence of the field nor diffusion in the ordinary sense is sufficient to account for observed features.

The increasing use of quantitative spectroscopic methods of analysis in various fields of research and in industry makes it highly desirable to obtain some understanding of the basic phenomena on which the methods depend. Studies of the mechanisms of sources serve to place the methods on a well understood, rather than on a purely empirical, basis. As a result, those conditions of source operation which lead to unreliable results may be recognized and avoided, and considerable information is made available concerning the appropriate method of attack on special analytic problems.

Previous investigations (4) have indicated that the excitation in condensed spark discharges produced by circuits having a fairly long oscillation period (10^{-4} sec.) may be considered as thermal in character, just as in the freely burning arc. The present article is concerned with a study of the second of the important source mechanisms, *viz.*, the transport of material through the discharge gap after it has been released from the electrode. The investigations have been limited to a study of the d-c. spark discharge, but there can be little doubt that the inferences drawn from it apply in some degree to any of the ordinary forms of spark discharge. In the authors' experience, condensed spark sources have been found to be capable of more reliable deter-

minations than the less commonly used arc sources; hence they merit more detailed study.

There is some evidence that the transport phenomena in arc sources involve an equilibrium between ordinary thermal diffusion of material from the region of the electrode and movement of ions of the material under the influence of the electric field (5). As is indicated in Section 3 of the present article, transport of material in spark sources involves more complex phenomena.

For the most part the investigations consisted of a study of the relative distribution of intensity along the lengths of spectral lines of various elements. Under the conditions employed, the intensity distribution for an element corresponded closely to the time integrated distribution of the emitting atoms of the element along the axis of the discharge.

In general, the intensity ratio of two lines due to different elements was found to be different at different points along their length. The relation between the ratio at a point near the loaded electrode, and that, say, at the centre of the discharge gap, was not constant, but could be altered by the addition of certain substances to the material placed on the electrode. The extent to which it was altered appeared to depend on the ionization potentials and masses of the two elements, and on the ionization potentials associated with the added substance. The observed variations are undoubtedly due to variations in the transport phenomena.

From the viewpoint of practical analysis, it is important to recognize that such variations may occur. *Unless appropriate precautions are taken*, the intensity ratios—and hence the determined concentrations—may vary with variations in the extraneous composition of the samples, even though the amounts of the internal standard and the investigated element present remain constant. Such variations lead to unreliable results. It should be emphasized that this statement is made purely on the basis of observed variations in the transport phenomena, and does not take into consideration variations which may occur in the mechanism responsible for the release of material from the electrode. The latter factor may be expected to introduce further complications.

On the basis of the present results, the precautions which should be taken to minimize the effects of variations in transport phenomena are; *(a)* the use of an appropriate "spectroscopic buffer", and *(b)* the choice of an appropriate internal standard element.

Section 1 deals with a description of the experimental procedure; the experimental results are given in Section 2. Section 3 is concerned with some considerations of the mechanism of spark discharge from the viewpoint of spectroscopic analysis. Section 4 deals mainly with the practical problem of the effects produced by variations in the transport phenomena, and with the means of minimizing them.

1. Experimental Procedure

The spark discharge was produced by the d-c. circuit (4) used for making analyses. A switch inserted in the circuit permitted single sparks to be

taken at any desired intervals. The calculated oscillation period of the circuit ($C = 0.12 \mu F$, $L = 2000 \mu H$, $R \sim 3\Omega$) was about 10^{-4} sec.; this value may be expected to approach the actual value closely (7, p. 83; 9, p. 342).

For the most part the electrodes consisted of a copper point-plane pair (separation, 2.5 mm.) as previously described (4). An image of the discharge (magnification, $\sim 5 \times$) was focused on the slit of a quartz Hilger E2 spectrograph, the axis of the discharge being parallel to the slit. Since this was done with a quartz-fluorite achromatic lens, the distribution of intensity along the length of a spectral line corresponded closely to the time integrated axial distribution in the discharge of atoms emitting the particular wavelength of light.

A portion (1/50 cc.) of a special solution (see Table I) was dried on the plane electrode (9 × 10 mm.). The electrodes were placed in position, and an exposure consisting of six single sparks, each of which was made to strike a fresh surface on the plane, was taken. The procedure was repeated with the addition of various chosen substances to the standard solution. The intensities at three or four points along the lengths of chosen lines of the various elements were determined for each exposure, and the intensity ratios at the various axial points calculated. Intensity measurements were made by the standard method employing a Moll microphotometer, calibration marks being put on each plate with the aid of a step-slit and quartz band lamp.

There was no evidence of appreciable self-reversal or self-absorption in the lines chosen for the investigation. As is indicated in Table III, all the examined transitions, except those for boron, aluminium, and possibly manganese, are associated with final levels which lie at some distance above the ground level. Moreover the amounts of the elements present in the discharge were small. The amount of tin present on the electrode, for example, was only 2×10^{-7} gm. per sq. mm., and the amount removed by a single spark was less than 8×10^{-8} gm.

The standard solutions, to which the additions were made, contained two or more of the elements given in Table I. The water of crystallization has been omitted from the chemical formulas. V, M, and b.p. denote respectively the ionization potential, atomic mass, and boiling point. The last named

TABLE I
ELEMENTS FOR STANDARD SOLUTIONS

Element	Conc., gm. per cc. × 10^5	V, volts	M	B.p., °C.	Compound	Characteristics
Hg	2	10.34	200.6	357	HgCl$_2$	B.p. 301° C.
Zn	1	9.36	65.4	907	ZnCl$_2$	B.p. 732° C.
Cd	2	8.96	112.4	—	CdCl$_2$	B.p. 960° C.
B	0.5	8.29	10.8	2250	H$_3$BO$_3$	Decomp. 185° C.
Mg	1	7.61	24.3	1110	Mg(NO$_3$)$_2$	—
Mn	0.8	7.41	54.9	1900	MnCl$_2$	B.p. 1190° C.
Pb	1	7.38	207.2	1613	Pb(NO$_3$)$_2$	Decomp. 357° C.
Sn	1	7.30	118.7	2270	SnCl$_2$	Decomp.
Al	1	5.96	27.0	1800	Al$_2$(SO$_4$)$_3$	Decomp. < 770° C.

value is given in order to suggest the range covered in the investigations, and to indicate that stability and ease of evaporation play little part in the phenomena to be discussed later. Some of the substances change their form in solution and so are not present on the electrode in the stated compound; moreover, many of them, at least, may be changed during the passage of a single spark.

TABLE II

SUBSTANCES FOR ADDITION TO STANDARD SOLUTIONS

Substance	Conc., gm. per cc. $\times 10^2$	Lowest V, volts	Characteristics
Sugar	4	11.22 (C)	Decomp. easily
NH$_4$Cl	0.5–5	12.96 (Cl)	Decomp. 350° C.
H$_3$BO$_3$	4	8.29 (B)	Decomp. 185° C.
CaCl$_2$	4	6.09 (Ca)	B.p. 1600° C.
Li tartrate	4	5.37 (Li)	Decomp. easily
KNO$_3$	4	4.32 (K)	Decomp. 400° C.
NaK tartrate	4	4.32 (K)	Decomp. easily
KCl	0.5–5	4.32 (K)	Sublimes 1500° C.

While the intensity distributions were usually determined for the lines given in Table III, other lines were sometimes examined as well. They gave essentially the same results. Table III gives the initial and final levels (with their energies in cm.$^{-1}$) of the commonly examined transitions, as well as the energies of the ground levels of the atoms (1, 3).

TABLE III

LINES COMMONLY INVESTIGATED

Element	λ, Å	Initial state		Final state		Ground state
Hg	3131	$\begin{cases} {}^3D_1 & (6s3d) \\ {}^1D_2 & (6s6d) \end{cases}$	$\begin{matrix} 12845 \\ 12848 \end{matrix}$	$\begin{matrix} {}^3P_2^o & (6s6p) \\ {}^3P_1^o & (6s6p) \end{matrix}$	$\begin{matrix} 44769 \\ 44769 \end{matrix}\Big\}$	84179
Hg$^+$	2847	${}^2S_{1/2}(5d^{10}7s)$	55566	${}^2P_{1/2}^o(5d^{10}6p)$	90672	151280
Zn	3302	${}^3D_2$ (4d)	12994	${}^3P_1^o$ (4s4p)	43265	75769
Cd	3403	${}^3D_1$ (5s5d)	13052	${}^3P_0^o$ (5s5p)	42425	72539
Cd$^+$	2748	${}^2S_{1/2}(4d^{10}6s)$	53386	${}^2P_{3/2}^o(5p)$	89758	136377
B	2497	${}^2S_{1/2}$ (3s)	40039	${}^2P_{3/2}^o(2s^22p)$	15	0
Mg	2780	${}^3P_{1,2}(3p^2)$	$\begin{cases} 3840 \\ 3799 \end{cases}$	${}^3P_{2,1}^o(3s3p)$	$\begin{cases} 39801 \\ 39761 \end{cases}$	61672
Mg$^+$	2791	${}^2D_{3/2}(3d)$	49777	${}^2P_{1/2}^o(3p)$	85598	121267
Mn	4034	—	—	—	—	—
Pb	3639	$2_2^o[6p({}^2P_{1/2})7s]$ 24536		${}^3P_1$ (6p^2)	52004	59821
Sn	3175	${}^3P_2^o[5p({}^2P_{1/2})6s]$ 24278		${}^3P_2$ (5p^2)	55764	59192
Al	3082	${}^2D_{3/2}(3d)$	15846	${}^2P_{1/2}^o(3s^23p)$	48281	48281

2. Results

It became apparent early in the investigation that any description of the changes in the relative distribution of intensity for two elements, brought about by addition of substances to a standard sample, must involve a con-

sideration of the masses and the ionization potentials of the elements. In order to separate effects due to mass difference from effects due to ionization potential difference, experiments were carried out with *(a)* a series of elements having different masses but comparable ionization potentials, and *(b)* a series having different ionization potentials but comparable masses. Since the occurrence of such series is not common in the periodic table, these data must be somewhat limited. Results of typical experiments are given in Tables IV and V.

The tabulated values are the intensity ratios for various pairs of elements at different distances, *D*, from the loaded plane electrode. For the purposes of comparison of the relative distributions of intensity, the ratios at the point nearest the plane have been set equal to 1.00. This is permissible since the relative distributions are not appreciably affected by such changes in the concentrations as would be required to give an observed value of 1.00 at

TABLE IV

CHANGES IN THE RELATIVE DISTRIBUTION OF INTENSITY FOR ELEMENTS HAVING COMPARABLE IONIZATION POTENTIALS BUT DIFFERENT MASSES

		Sn–Pb			Mn–Pb			Mg–Pb	
M, ratio =		119/207			54.9/207			24.3/207	
V, ratio =		7.30/7.38			7.41/7.38			7.61/7.38	
Addition		*D*, mm.			*D*, mm.			*D*, mm.	
	0.4	1.2	1.9	0.4	1.2	1.9	0.4	1.2	1.9
None	1.00	0.96	1.20	1.00	1.20	1.36	1.00	0.98	1.31
Sugar	1.00	0.96	1.02	1.00	1.39	1.52	1.00	1.21	1.34
H_2BO_3	1.00	1.00	1.24	1.00	1.27	1.46	1.00	1.26	1.46
Li tart.	—	—	—	1.00	1.27	1.37	1.00	0.93	0.81
KCl	1.00	1.12	1.10	1.00	1.10	1.15	1.00	0.69	0.74

TABLE V

CHANGES IN THE RELATIVE DISTRIBUTION OF INTENSITY FOR ELEMENTS HAVING COMPARABLE MASSES BUT DIFFERENT IONIZATION POTENTIALS

		Hg–Pb			Cd–Sn			Mg–Al	
M, ratio =		201/207			112/119			24.3/27.0	
V, ratio =		10.3/7.38			8.96/7.30			7.61/5.96	
Addition		*D*, mm.			*D*, mm.			*D*, mm.	
	0.4	1.2	1.9	0.4	1.2	1.9	0.4	1.2	1.9
None		1.00	0.78	0.94	1.00	0.91	0.90	1.00	0.98	0.93
Sugar		1.00	0.85	0.91	1.00	1.07	1.07	1.00	0.85	0.85
H_2BO_3		1.00	0.84	0.87	1.00	0.95	0.92	1.00	0.96	0.99
Li tart.		1.00	0.51	0.38	1.00	0.79	0.69	1.00	0.60	0.54
KCl	1.00*	0.88	0.39	0.38	1.00	0.49	0.49	1.00	0.54	0.58

* *This ratio had a maximum slightly closer than 0.4 mm. to the plane electrode when potassium chloride was added to the solution.*

this point.   It is equivalent to changing the concentrations of some elements by small factors.   In view of this procedure, the results reflect only the variations in the transport phenomena, and are not directly concerned with variations in the mechanism responsible for the release of material from the electrode.

Table VI contains data for a series of elements chosen for their ionization potential differences without respect to their mass differences.   The relative distribution for any two of the elements may of course be obtained from the given data.   The mode of representation is the same as that for Tables IV and V.

The results of all the experiments may be generalized as follows:

(a) Lines of different elements have, in general, different intensity distributions along their length.

(b) The relative distributions depend on the ionization potentials and masses of the elements, and on the ionization potentials of other atoms present in the discharge.

(c) When easily ionized atoms (*e.g.*, potassium) are present in the discharge, the distribution of an element relative to that of a more easily ionized element of comparable mass falls off more sharply toward the unloaded electrode than it does when easily ionized atoms are absent (cf. Table V). A similar statement may be made concerning the distribution of a light element relative to that of a heavy element of comparable ionization potential.   The effect of mass difference is, however, marked only for very light elements (*e.g.*, magnesium).   It has only a small influence in the case of manganese with a mass of 54.9 (cf. Table IV)..

The following remarks may be made concerning particular points brought out by the data.

(1) Since the discharge contains a considerable number of copper atoms liberated from the electrodes, *marked* changes in the relative distributions of intensity are to be expected only on addition of atoms having an ionization potential lower than that of copper (7.68 v.) *i.e.*, the presence of the copper atoms tends to "stabilize" the discharge.   This point is illustrated by the curves of Fig. 1 and the data of Tables IV, V, and VI.

(2) If the number of copper atoms released from the electrodes is decreased, as it might reasonably be by the presence of an appreciable layer of salts over the electrode, the relative distributions should be changed somewhat owing to the partial substitution of some other atoms for copper in the discharge.   It may be seen from Table VI, for example, that addition of a substance associated with high ionization potentials to a standard solution tends to change the relative distributions in the direction expected for a partial substitution of difficultly ionized atoms for copper.

(3) The relative distribution of two elements depends on the composition of the standard solution, since other elements present may be considered as

TABLE VI

CHANGES IN THE RELATIVE DISTRIBUTION OF INTENSITY FOR VARIOUS ELEMENTS ON ADDITION OF DIFFERENT SUBSTANCES

Elements in std. solution	Addition	Hg–Sn D, mm			Cd–Sn D, mm			Zn–Sn D, mm			B–Sn D, mm		
		0.4	1.2	1.9	0.4	1.2	1.9	0.4	1.2	1.9	0.4	1.2	1.9
Hg, Cd, Sn	None	1.00	0.80	0.78	1.00	0.84	0.84	—	—	—	—	—	—
Mg, Pb, Al	Sugar	1.00	0.88	0.88	1.00	1.07	1.07	—	—	—	—	—	—
Mn	H₃BO₃	1.00	0.92	0.78	1.00	0.95	0.92	—	—	—	—	—	—
	KCl	0.90	0.35	0.35	1.00	0.49	0.49	—	—	—	—	—	—
Hg, Zn, Sn	None	1.00*	0.87	0.97	—	—	—	1.00	1.11	1.04	1.00	1.12	1.48
B	KCl	0.88	0.41	0.35	—	—	—	1.00	0.61	0.56	1.00	0.63	0.65

Elements in std. solution	Addition	Mg–Sn D, mm			Mn–Sn D, mm			Pb–Sn D, mm			Al–Sn D, mm		
		0.4	1.2	1.9	0.4	1.2	1.9	0.4	1.2	1.9	0.4	1.2	1.9
Hg, Cd, Sn	None	1.00	1.00	1.02	1.00	1.24	1.14	1.00	1.03	0.83	1.00	1.04	1.12
Mg, Pb, Al	Sugar	1.00	1.27	1.32	1.00	1.44	1.47	1.00	1.04	0.96	1.00	1.48	1.55
Mn	H₃BO₃	1.00	1.27	1.18	1.00	1.27	1.19	1.00	0.99	0.81	1.00	1.31	1.20
	KCl	1.00	0.63	0.70	1.00	0.99	1.06	1.00	0.91	0.93	1.00	1.16	1.18
Hg, Zn, Sn	None	1.—	—	—	—	—	—	—	—	—	—	—	—
B	KCl	—	—	—	—	—	—	—	—	—	—	—	—

* These ratios had a maximum slightly closer than 0.4 mm. to the plane electrode on the addition of potassium chloride to the solution.

additions. The observed differences between the distributions for simple and for complex standard solutions are always in the expected direction.

(4) The data of Table VI, unlike those of Tables IV and V, include in many cases the resultant effect of mass difference and ionization potential difference. The behavior of the mercury-tin, cadmium-tin, and lead-tin ratios is almost entirely due to the latter factor, since all are fairly heavy elements. It is to be noted that the distribution lead-tin is little affected by additions, as expected from the fact that lead and tin have comparable ionization potentials. For the zinc-tin and manganese-tin ratios the mass difference effect begins to be felt (cf. Table IV, manganese-lead), but is still relatively small. For the magnesium-tin ratios, the behavior is due almost entirely to the mass difference effect, since magnesium and tin have comparable ionization potentials. For the aluminium-tin ratios both effects are present, but operate in opposite directions and so tend to compensate each other. As a result, the distribution does not change markedly on additions, although the mass difference effect appears to be somewhat the stronger with potassium chloride additions (cf. Fig. 1, aluminium-lead). For the boron-tin ratios both effects are present and operate in the same direction. The changes in the relative distribution
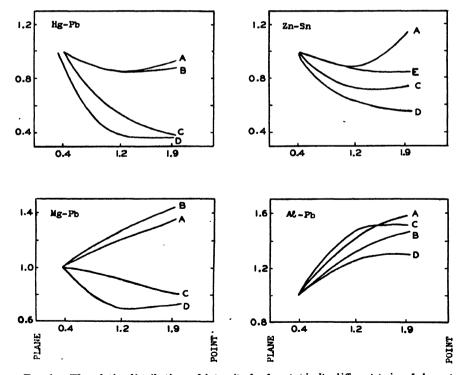
FIG. 1. *The relative distributions of intensity for four typically different pairs of elements on addition of various substances to standard samples. The ordinates represent intensity ratios; the abscissas, distances from the loaded electrode in millimetres. Additions: A = sugar, B = H₃BO₃, C = Li. tart., D = KCl, E = CaCl₂.*

are comparable to those for the mercury-tin ratios although the ionization potential difference is much less.

The changes which occur in the relative distributions on the addition of substances with successively lower ionization potentials are shown in Fig. 1 for four typical pairs of elements. These are, *(a)* mercury-lead, ionization potential difference effect alone, *(b)* magnesium-lead, mass difference effect alone, *(c)* zinc-tin, both effects with the ionization potential effect predominating, *(d)* aluminium-lead, both effects operating in opposite directions.

The results of certain other experiments deserve some mention since they support the interpretations already given.

(a) Experiments in which graphite rather than copper electrodes were used, but otherwise similar to those described, gave results consistent with the data of this section.

(b) Experiments in which potassium nitrate or sodium potassium tartrate, instead of potassium chloride, was added to the standard solutions, showed that the effect of the potassium salt addition was not connected with the stability or ease of evaporation of the salt on the electrode.

(c) Experiments in which the amount of the added salt (ammonium chloride or potassium chloride) was varied, showed that the observed relative distributions are not dependent on the amount of the salt added within the limits of the investigation. The limiting values of the added concentrations were 0.5×10^{-2} and 5×10^{-2} gm. per cc. of potassium chloride or ammonium chloride.

In several experiments the temperatures at different points along the discharge axis were determined from the intensity ratio of 3262/3175, tin, in the way previously described (4). The results, given in Table VII, indicate that the temperature of neutral atoms is essentially constant along the axis, although there is a suggestion that with ammonium chloride addition the temperature is slightly higher near the loaded electrode.

TABLE VII

TEMPERATURE MEASUREMENTS ALONG THE DISCHARGE AXIS

Addition	Observa-tions	Average intensity ratio 3262/3175, tin					
		0.4 mm.	T, °K.	1.2 mm.	T, °K.	1.9 mm.	T, °K.
None	1	1.06	9400	1.09	9800	1.02	8900
NH₄Cl	7	1.11	10100	1.07	9500	1.07	9500
KCl	3	1.04	9200	1.05	9300	1.04	9200

On the other hand, the intensity ratio of 2791 Mg^+/2780 Mg decreased more or less regularly toward the unloaded electrode under all conditions. The observed values for various distances from the plane electrode are given in Table VIII. It is clear from these figures that the ionization process is not

in an equilibrium state throughout the spark gap. A possible explanation is indicated in the following section.

TABLE VIII
CHANGES IN THE RELATIVE DISTRIBUTIONS OF SPECTRAL LINES OF THE IONIZED AND NEUTRAL ATOM (Mg)

Addition	Distance from plane electrode, mm.		
	0.4	1.2	1.9
None	4.5	2.9	3.0
Li. tart.	1.9	0.7	0.8
KCl	2.0	0.9	0.8

The Hg^+ line $\lambda 2847$, and the Cd^+ line $\lambda 2748$, were quite strong in the neighborhood of the loaded electrode, but decreased so rapidly in intensity that measurements could not be made near the centre of the gap. The decrease in intensity is more marked relative to the atomic lines, than is the case with magnesium.
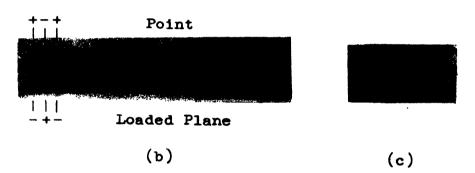
3. The Mechanism of Spark Discharge from the Viewpoint of Spectroscopic Analysis

If the persistence of temperature excitation is neglected, each single spark produced by the commonly used circuit containing the gap, a capacity, and an inductance may be considered to consist of several separate discharges, each of which is associated with a half oscillation of the circuit. There may be from 20 to 30 such discharges per spark (see Plate I, and also the excellent reproductions in Reference 7). The oscillation period of the circuit is little affected by changes in the nature of the spark gap (7, 9), and may be quite closely calculated from a knowledge of the circuit constants (7). If the inductance in the circuit described in Section 1 be reduced to that of the leads, the oscillation period decreases from about 10^{-4} to 10^{-6} sec.

The potential difference across the spark gap during these discharges is not high (8). On each half oscillation except the first, it has an initial value of about 300 volts, but falls rapidly and reaches a value of about 35 volts in a small fraction of a half period; it remains at this value for the duration of the half oscillation. Neither the time relations nor the magnitudes of these voltages are markedly affected by changes in the gap length or in the oscillation period. In view of the magnitudes of the voltages, it is probable that each of the discharges which constitute a single spark begins as a glow discharge, but rapidly changes to an arc-like form as the cathode becomes locally heated by positive ion impact.

The spectroscopic analyst is primarily interested in the spread of the vapor of the electrode material through the gap, and with its excitation and the subsequent emission of light. When a spark is viewed with the aid of a rotating mirror, characteristic luminous streamers may be seen to start off from both electrodes at each half oscillation, and to proceed with diminishing velocity toward the centre of the gap (7, 9, 10, 11). The streamers are associated in some way with the vapor of the electrode material, since they radiate its spectrum exclusively.

PLATE I

+ – +

– + –

(a)

+ – +   Point

– + –   Loaded Plane

(b)

(c)

Rotating mirror photographs of single sparks produced by a circuit having a period of approximately 10^{-4} sec., showing the separate discharges which take place at each half oscillation. Owing to the small rotational speed of the mirror, the streamers are not so strongly curved as they appear with higher speeds, i.e., when shorter period sparks are examined. (a) Photograph of a single spark between copper point electrodes. (b) Photograph of a single spark between a copper point and a copper plane electrode loaded with sodium potassium tartrate as for analysis. Note the progress of a characteristic luminosity arising from the plane electrode; this luminosity is probably to be associated with emission of light from the atoms of the load material. (c) Photograph taken with the mirror stationary, in order to indicate the width of the image of the slit which was placed immediately before the spark gap in (a) and (b). The speed of rotation of the mirror was not the same in (a) and (b): in both, the discharges occurred at intervals of 5 × 10^{-5} sec.

It is difficult to see how the streamers could result from the motion of electrons through a more or less stationary cloud of vapor. The passage of electrons from the cathode takes place during the greater part of the half oscillation, and should produce a streamer having a time width in the rotating mirror photograph, of approximately half a period at the cathode. The streamers may be obtained, however, as quite sharp curved lines of a time width of only a small fraction of a half period. Furthermore, the streamers start from *both* electrodes, although those from the cathode are usually the more prominent. A consideration of the velocity of the streamers leads to a similar conclusion. The velocity with which the envelope of the streamers advances depends on the metal used for the electrodes and on the constants of the circuit, but may be as low as 20,000 cm. per sec. If the field in the arc-like phase of the discharge is 20 v. per cm. (cf. fields in metal arcs (12, p. 587 *ff*)), and if the mobility of an electron be taken as 24,000 cm. per sec. per v. per cm. (12, p. 526), the electron drift velocity is 500,000 cm. per sec.; *i.e.*, it is higher than the minimum velocity of the streamers, and in view of what has been said concerning the constancy of the gap voltages, should not change very much when the conditions are changed.

The motion of positive ions under the influence of the field can play little part in transport of material through the gap, or in the development of the streamers. The ions, with a mobility of about 1.4 cm. per sec. per v. per cm. (14), have a drift velocity of about 28 cm. per sec. in a field of 20 v. per cm. Hence, in 5×10^{-6} sec., the distance traveled under the influence of the field is only about 0.001 mm. Well developed streamers have been observed, however, with circuits having a half period of only 2×10^{-6} sec. Furthermore, streamers start from *both* electrodes, so that some ions move with, and some against, the field.

It is difficult to see how diffusion of vapor, in the ordinary sense, from the region of the electrodes can play the leading role in the production of streamers in sparks produced by short period circuits. That the diffusion is too slow is shown by the following consideration. Suppose the most favorable condition for rapid diffusion exists, *i.e.*, that all the material vaporized from the electrode during a half oscillation be concentrated in a small region at the electrode surface at the beginning of the half oscillation. The diffusion equations are similar to the equations for the flow of heat from an instantaneous point source (2, p. 149 *ff*). At a time t after the formation of the source, the concentration, C, at a distance, r, from the electrode, is,

$$C = Q/(2\sqrt{\pi D t})^3 \cdot e^{-r^2/4Dt} , \tag{1}$$

where Q is the amount of vapor originally in the source, and D is the diffusion coefficient. The maximum concentration at a distance r from the electrode is attained in a time t_m, given by,

$$t_m = r^2/6D \tag{2}$$

and is,

$$C_m = 0.196Q/r^3 \tag{3}$$

The value of D for fairly heavy atoms at a temperature of 2000° K. may be taken to be about 4.5 (13).   If the temperature in the gap be 10,000° K. (4), D should, from kinetic theory considerations ($D \propto \sqrt{T}$), be about 10.1, but might be as high as 22 ($D \propto T$).   Using 10.1 for D, it is calculated that the maximum concentration at a point 1 mm. distant from the electrode is attained only after 1.7×10^{-4} sec.   The concentrations at this point calculated in terms of the maximum concentration have the following values at the stated times.

t(sec. $\times 10^6$)	=	1	2	4	100
C/C_m	=	4×10^{-105}	10^{-51}	5×10^{-25}	0.29

The figures show that if the concentration at the point is to be detectable after say, 4×10^{-6} sec., the maximum concentration attained has to be many powers of 10; this is of course out of the question.   Furthermore, even if D be taken to have the unreasonably large value of 300 in order to account for an appreciable concentration at 1 mm. from the electrode after 4×10^{-6} sec., the diffusion equations can hardly account for a comparable concentration at 3 mm. from the electrode after, say, 12×10^{-6} sec.

In view of the above considerations, it is highly probable that neither the motion of electrons or ions under the influence of the field, nor the diffusion of particles in the ordinary sense, can account for the characteristic features of the streamers produced in sparks with very small oscillation periods. The explanation must be sought in some other phenomenon.   An interpretation of many of the observed features may be made on the basis of the existence of a pressure wave which moves out from the electrodes at each half oscillation. While reasonable inferences leading to the description of a possible transport mechanism may be drawn concerning the origin of the disturbances, such deductions are too speculative to justify detailed discussion in the present article.   The exact nature of the transport mechanism in sparks requires further experiments for its elucidation.

Calculations from the previously given diffusion equations indicate that diffusion of material in the ordinary sense is sufficiently rapid to play a considerable part in the transport phenomena in sparks having a period of the order of 10^{-4} sec.   Since the mechanism referred to above must also enter, however, the resulting phenomena are undoubtedly of a complex nature.

Whatever the nature of the transport mechanism may be, it involves collisional processes.   Hence the rate of transport of an element along the discharge axis depends on the characteristics of the element, and on the characteristics of other particles present in the gap, *i.e.*, any damping of the translational motion of particles along the axis must depend on such factors as the number of elastic and inelastic collisions, the collisional cross section and hence the velocity, the ease of ionization, and the masses of the particles. It is undoubtedly on this basis that the results of Section 2 are to be explained.

4. Significance of the Data for Practical Analysis

Quantitative spectroscopic methods of analysis are based on the assumption that the intensity ratio of two lines due to the internal standard and investigated element is a constant function of the amounts of the elements present in the samples. It is clear from the data of Section 2 that when an image of the source is focused on the spectrograph slit, this ratio depends in general on the point in the source from which the examined light is radiated. Furthermore, the ratio for light radiated from a given point in the discharge may depend so strongly on the character of the extraneous material present in the samples as to make determinations based on it worthless as precision measurements (cf. Fig. 1). The variations that may occur in the ratio when no condensing lens is used, or when an image of the source is focused, say, on the collimator lens, reflect in addition any variations that may occur in the mechanism responsible for the release of material from the electrode, and so lie outside the scope of the present article. It is unquestionably important, however, that the operation of the various source mechanisms be kept as constant as possible, no matter what the optical set-up may be.

On the basis of the present results, the following precautions appear to be sufficient to minimize the effects of variations in the transport mechanism in the spark discharge: *(a)* addition to the sample of a "large" excess of some suitable salt (the spectroscopic buffer), and *(b)* the choice of an appropriate internal standard element.

(a) The spectroscopic buffer. For the present purpose the buffer should contain an element of low ionization potential. If such an element is present in sufficient amount, reasonable variations in the extraneous composition of the samples are not expected to materially alter the transport phenomena, since it was found that the relative distributions of intensity were independent of the amount of salt added within stated limits. The buffer should be capable of drying on the electrode in a closely adhering, uniform layer which is not flaked off by the action of the spark, and should not give rise to a complicated spectrum.

Organic salts are usually to be preferred to inorganic salts, since they form more suitable layers on the electrode. Sodium potassium tartrate has been found to be satisfactory, but cannot be used in analyses for sodium or potassium. Lithium tartrate has been used in such analyses, but it is possible that the precision of the determinations might be increased by the use of a buffer containing a more easily ionized element. The probable error was about 4% when lithium tartrate was used (6).

(b) The choice of an internal standard element. It is obviously desirable that the investigated and internal standard elements should behave in nearly the same way in the discharge. So far as the question of transport is concerned, they should have as nearly as possible the same ionization potential. Moreover, if the investigated element has an atomic mass of less than, say, 50, an internal standard element having as nearly as possible the same

mass should be chosen. With the heavier elements, however, the mass becomes unimportant.

For other reasons, the following characteristics are important in an internal standard element. It should give rise to suitable lines in convenient spectral regions, and should not interfere with the lines to be examined; the excitation potentials of the investigated element and internal standard lines examined should be as nearly as possible the same.

The relative importance of fulfilling any one of these different criteria depends on the characteristics of the investigated element; in many cases it may be necessary to partially disregard some of them in order to fulfil the most important. It may be pointed out that further experiments on the mechanism responsible for the release of material from the electrode may indicate other desirable qualities in both internal standard elements and spectroscopic buffers.

Acknowledgments

References

1. BACHER, R. F. and GOUDSMIT, S. Atomic energy states. 1st ed. McGraw-Hill Book Co., New York. 1932.
2. CARSLAW, H. S. The conduction of heat. 2nd ed. Macmillan and Co., London. 1921.
3. GROTRIAN, W. Graphische Darstellung der Spektren, II. 1st ed. Springer, Berlin. 1928.
4. LANGSTROTH, G. O. and McRAE, D. R. Can. J. Research, A, 16 : 17-27. 1938.
5. MANNKOPFF, R. Z. Physik, 76 : 396-406. 1932.
6. McRAE, D R., LANGSTROTH, G. O., and FOSTER, J. S. Proc. Roy. Soc. London. In press.
7. MILNER, S. R. Phil. Trans. A, 209 : 71-88. 1909.
8. MILNER, S. R. Phil. Mag. 24 : 709-721. 1912.
9. ROYDS, T. Phil. Trans. A, 208 : 333-347. 1908.
10. ROYDS, T. Phil. Mag. 19 : 285-290. 1910.
11. SCHENCK, C. C. Astrophys. J. 14 : 116-135. 1901.
12. THOMSON, J. J. and THOMSON, G. P. Conduction of electricity through gases. 3rd ed. Cambridge University Press. 1933.
13. WILSON, H. A. Phil. Mag. 24 : 118-125. 1912.
14. WILSON, H. A. Rev. Modern Phys. 3 : 156-189. 1931.

NOTE ON THE ANALYSIS OF THE γ-RAYS OF RADIUM E[1]

By J. A. Gray[2] and J. F. Hinds[3]

It is assumed that the energy in a beam of ionizing rays is proportional to the ratio of the ionization produced by the beam in a thin layer of gas, carbon dioxide in the present work, to the mass absorption coefficient of the rays in the gas. The relative numbers of particles (photons) in different beams can then be found by dividing relative energies by the energy of a single particle.

There is little doubt that the γ-rays of radium E form a continuous spectrum. The absorption curve of these γ-rays in aluminium has been obtained by the writers, who have shown also that, under the conditions of the experiment, this absorption is closely fitted by the equation

$$I = 26.3e^{-130m} + 32.5e^{-29m} + 13.9e^{-7.03m} + 7.7e^{-2.79m} + 19.6e^{-0.19m},$$

where I is the ionization produced by the rays in the ionization chamber, after the rays have passed through an aluminium sheet of mass m per sq. cm. This equation holds only up to a value of m of 2.45 gm. A separate experiment showed that the soft γ-rays of radium D, which are "L" rays from an element of atomic number 83, give under the same conditions an initial ionization of 2660.

The γ-rays of radium E were considered to consist of a number of component beams, of relative mass absorption coefficients 130, 29, 7.03, and the other values. The respective energies in electron volts of single photons in these components are 5800, 9700, 15,800, 21,600, and 63,000, these figures being obtained from the wave-lengths corresponding to the respective absorption coefficients.

Before the relative numbers of photons in the various components can be calculated, correction has to be made for the absorption of the rays in the air traversed by them before reaching the window of the ionization chamber, for absorption in this window, and for absorption in the gas filling the chamber. There is a further correction for the effect of the walls of the chamber, which were of steel. When all these corrections are made, the relative numbers of photons are 5 of 5800, 5.7 of 9700, 3.8 of 15,800, 2.1 of 21,600, and 20 of 60,000 volts and greater, respectively. For radium D soft γ-rays, the corresponding number is 630.

Previous experiments by the senior author showed that approximately 25% of radium D atoms emit a soft γ-ray, so that the effect of the γ-rays of radium E, as far as absorption in aluminium is concerned, is the same as if on disintegration 0.2% of the atoms emitted photons of energy 5800 volts, 0.23% photons of energy 9700 volts, 0.15% photons of energy 15,800 volts, 0.08% photons of energy 21,600 volts, and 0.8% photons of energy 60,000 volts and greater.
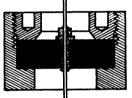
If 40,000 volts is taken as midway between 21,600 and 60,000, then about 0.7% of the disintegrating atoms emit photons with energies less than 40,000 volts, and about 0.8%, photons with energies greater than this. There will be, of course, some atoms emitting photons with energies less than 5000 volts.

It is difficult to see how one can express the properties of the γ-rays of radium E in a more suitable manner. Analysis of the rays in the hardest component will be attempted in the near future.

NOTE ON A VACUUM TIGHT SEAL FOR ELECTRODES WITH HIGH INSULATION

The method described was used after it had been found that hard sealing wax plugs have a tendency to flow when subjected to pressure differences of the order of one atmosphere, particularly when the room temperature exceeds 70° F.

A permanent high insulation seal can easily be made from materials available in almost any workshop. The accompanying figure is drawn to scale, but the dimensions may be varied over a wide range to suit requirements.

FIG. 1. *Diagram of vacuum tight seal with high insulation.*

An ebonite plug is made so as to fit freely in a brass tube, and is pressed against a shoulder by a threaded brass ring, which has two holes drilled in it to take a face pin wrench. The shoulder has a small annular V-shaped groove cut in it to facilitate making the joint.

A standard brass screw, faced smooth under the head and with two small flats filed at right angles to the slot, is drilled to take the electrode which is soldered at the outer end. The screw is tightened in the plug by using a wrench on the flats, after which the faces of the ebonite are carefully scraped. It is important that these surfaces should not be touched with the fingers after this operation. The plug is immersed in melted paraffin for a sufficient length of time to heat it so that the wax runs off freely when it is removed. A thin coating is desirable, and is all that is necessary to protect the ebonite from the action of the atmosphere. Rapid rotation of the plug is effective in removing excess wax.

After cooling, the plug is inserted in the tube and the ring screwed down. No gasket is necessary. Joints of this type have been in use for years and have given complete satisfaction.

Note by J. A. Gray

Other people may know of the insulator, the preparation of which has been described above by Mr. Bradfield, but a great many do not. We are using it in electrometers, ionization amplifiers, and ordinary electroscopes, and find it very satisfactory indeed; so much so, that we do not bother about other insulators. The only disadvantage that we have noticed so far about its use, is that it is not suitable in the presence of methyl iodide.

R. D. BRADFIELD.

DEPARTMENT OF PHYSICS,
QUEEN'S UNIVERSITY, KINGSTON, ONTARIO.

APPLICATION OF QUARTZ CRYSTALS TO THE MODULATION OF LIGHT[1]

BY D. W. R. McKINLEY[2]

Abstract

The resonating X-cut quartz crystal has been used as a self-compensator for white light modulation.

The properties of the 49° cut quartz crystal are described. This crystal combines low power input and stable high frequency with a wide light aperture and improved light output. For many purposes a convergent beam of light may be used, without the need of a compensating device.

Vibrating quartz crystals have the property of dynamically rotating the plane of polarization of a plane polarized beam of light passing along the optic axis. The light emerging from a polarizer-quartz, plate-analyzer system is transmitted in flashes of twice the crystal frequency.

1. The X-cut Quartz Crystal Light Modulator

A plane parallel beam of white light is polarized by the polaroid P_1 (or by a Nicol prism) and passes through the quartz crystal C, making a small angle of 2° or 3° with the Z (optic) axis, Fig. 1. It is reflected from the mirror M_1 and passes back through the crystal to the mirror M_2, which reflects the light
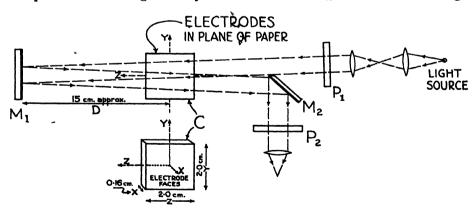
FIG. 1.

to one side. The light is then passed through the analyzing polaroid P_2, and may be focused as desired. The polaroids are so arranged that the light cut-off is complete when the crystal is not oscillating, provided that the beam is parallel.

When the output from a vacuum tube oscillator is applied to the crystal at its fundamental resonant frequency, light appears uniformly over that part of the crystal seen through P_2. As the oscillator voltage is increased, the intensity of the transmitted light increases. The optimum effect occurs with inputs of the order of 20 to 25 watts.

The principle of this quartz cell is not the same as that of the Kerr cell, in which the observed light depends not only on the applied voltage but also on the distance D, reaching a maximum when D is one-eighth of the electrical wave-length of the alternating voltage. The intensity of light transmitted through quartz does not vary in the same manner with the distance D, by virtue of the complex rotation pattern of the vibrating crystal. Rotation pattern is an expression used to describe the appearance of the vibrating crystal when placed between polaroids and viewed directly in monochromatic light. The bright spots represent the vibration loops of the standing waves in the crystal.

Light that passes through the more active portions of the quartz on its first transmission will, in general, pass through parts of lesser activity on its return, and is consequently no longer polarized perpendicular to the polarization plane of P_2. On the other hand, light going through the least active portions of the crystal on its initial passage will be returned through a more active part, and therefore also suffers a net change of polarization. So the whole observed crystal surface appears strongly illuminated, and all trace of pattern disappears.

The usual arrangement up to the present has been to pass the light once through the active quartz plate and then through a quartz slab of opposite rotatory power; this annuls the static light rotation of the first plate and permits white light cut-off. Because the above-mentioned reflection method utilizes every portion of the crystal, the light efficiency is greater than it is in the latter method where the light passes but once through the quartz and compensator, because in this arrangement only the active portions of the excited crystal transmit light.

The upper limit of useful frequencies seems to be about 2.5 megacycles, since beyond this the crystal becomes too thin to admit the beam of light. If the frequency in kilocycles per second is f and the thickness in centimetres is d, then $f = \dfrac{287}{d}$.

It is possible to modulate the oscillator voltage at audio frequencies and therefore to modulate the light beam at these frequencies, when the high frequency light interruptions are used as a carrier. The high value of Q of the quartz resonator $\left(Q = \dfrac{\omega L}{R} \right)$ may be reduced considerably by tightly clamping the crystal and thus increasing the sideband range. In a test, the

driving frequency could be varied 5 kc. from the mean of 2000 kc. without appreciably affecting the light output.   This frequency range would be useful for speech frequencies.   However, it is unlikely that this quartz light cell would compare favorably with the usual moving metal ribbon, glow lamp, and other types of light cells for audio frequencies.   The quartz cell will respond to a small band of very high frequencies.

A suggested application is its use as a high frequency chronograph to put a time base on high speed film.   It has been used in this laboratory in conjunction with a tuned photocell in measurements on the velocity of light, though the crystal described in the second part of this paper has been more satisfactory for the purpose.

2. The 49° Cut Quartz Crystal Light Modulator
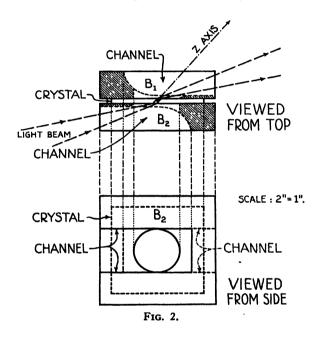
To obtain the most pronounced electro-optical effect, the light should pass along or close to the optic axis.   This condition is satisfied in the X-cut type.   However, to secure higher fundamental frequencies it is necessary to reduce the crystal thickness; this unavoidably narrows the light aperture.

A thick crystal may be driven at higher harmonics to obtain higher frequencies of interrupted light, but there are three disadvantages to this procedure.   First, the power required to excite the crystal harmonically is much greater than that needed to excite the fundamental frequency, if the same resultant light intensity is assumed.   Second, the line grating formed in the crystal by the nodes and loops of harmonic vibrations causes much of the light to be deviated from the main beam, and for some applications this is undesirable.   Third, increased power input results in increased heating of the crystal, and, owing to the large temperature coefficient of frequency for the X-cut type (20 to 35 cycles per megacycle per °C.), the frequency will vary rapidly unless elaborate precautions are taken to maintain a constant temperature.

The light aperture may be made independent of the fundamental frequency by so orientating the cut that the Z-axis is inclined at an angle to the faces of the plate.   However, as the angle of inclination is increased the piezoelectric effect decreases and becomes zero when the Z-axis is perpendicular to the faces.   The angles should be at least 49° in order that light entering at a small angle to the faces will be refracted through the crystal in the same, or nearly the same, direction as the Z-axis.

Lack and co-workers (1) showed that the unwanted coupling between the x_y and z_z strains is zero at $+31°$ and $-60°$; consequently, there is less danger of fracturing crystals when the orientations have these values.   These writers have also calculated the temperature coefficient of frequency in terms of the inclination of the Z-axis, and have shown that at $+35°$ and $-49°$ the desired shear vibration has zero temperature coefficient.   Of these, the 49° cut is useful for optical purposes, and the angle is also sufficiently close to that of the 60° cut to minimize undesired couplings and permit greater power inputs than does either the X or Y cuts.

The 49° cuts used in this work have an average thickness of about 0.063 cm. and are 2.54 cm. square, with frequencies between 3725 and 4050 kc. The crystal is mounted between two brass blocks, B_1 and B_2 (of dimensions 3.2 by 3.2 by 0.67 cm.), which serve as electrodes. A hole, 1.3 cm. in diameter, is drilled in the centre of each electrode. The blocks are channelled, Fig. 2, to enable light to enter at a small angle to the crystal faces. The crystal is properly orientated between the electrodes, the two plates are clamped together in an insulated holder, and pressure is applied by means of two set screws. The amount of clamping is not usually critical.

FIG. 2.

Owing to the thinness of the crystal, it is no longer necessary to pass light through in a parallel beam. Light may be focused through it, provided that the angle of the light cone is not too large.

The effective maximum thickness of the optical path is about 0.082 cm., and in general is less because the light does not enter at grazing incidence. This thickness corresponds to a rotatory dispersion of the visible spectrum of eight to ten degrees. This means that in practice good cut-off of white light may be obtained for many purposes without the use of either compensator plate or the reflection method described in the first part of this paper.

In fact, for operation with a tuned photocell, best results are obtained without any compensating medium between the polaroids; this is probably due to reflection and absorption losses of the compensator. However, if absolute panchromatic cut-off is desired, a solution of a sugar of the opposite rotatory power is quite effective with crystals of this thickness.

Very little exciting power is necessary for these crystals. Two to five watts of radio frequency input will drive them to strong light output. Owing to their design, the crystals have withstood, without fracture, voltages as high as the flashover voltage between the electrodes. Normally they are operated far below this breakdown voltage, since increasing the input beyond about ten watts does not proportionately increase the output.

As the power consumption is small, the crystals do not heat excessively and require no cooling system, even for several hours of operation. This fact, together with the zero temperature coefficient, ensures a very stable oscillation frequency. Tight coupling is used between the driving oscillator and the crystal circuit; consequently, the oscillator locks with the crystal frequency.

For the past year these 49° cut crystals have been used at the McLennan Laboratory in a method for measuring the velocity of light, and have given satisfactory results. Measurements are as yet incomplete, but at present the indicated accuracy of the method is of the order of that obtained in the Kerr cell and rotating mirror experiments. Many more observations will be made before an account of this work is published.

Reference

1. LACK, F. R., WILLARD, G. W., and FAIR, I. E. Bell System Tech J. 13 : 453-463. 1934.

THE INFLUENCE OF THICKNESS ON THE MEASURED THERMAL CONDUCTIVITY OF FIBREBOARD AND ROCK WOOL[1]

By J. D. Babbitt[2]

Abstract

The thermal conductivity of samples of rock wool and fibreboard of various thicknesses (0.5 to 2.0 in.) was measured by means of a hot-plate apparatus. It was found that when surface effects were eliminated the conductivity obeyed Fourier's law.

It has been found recently, (1, 2, 3) that there is a considerable change in the measured thermal conductivity of a material when the test is made on samples of different thicknesses. Corkboard, fibreboard, and rock wool were tested, and although practically no change was found in the value of k for corkboard as the thickness was increased from $1\frac{1}{2}$ to 4 in., yet the results indicated that "the conductivity of a 2-inch fibreboard is approximately 23% greater than that of a $\frac{1}{2}$-inch board of the same material. In matted materials, consisting of grasses or other fibres stretched between layers of papers, the difference is about 50%". These figures are so large that they are of importance not only for purposes of practical insulation but also for theoretical considerations.

It has always been implicitly assumed that Fourier's law,

$$Q = kA \frac{dt}{dx},$$ (1)

holds for the transmission of heat through solid materials, and that the quantity of heat transmitted is inversely proportional to the thickness of the material. In Equation (1), Q is the quantity of heat transmitted, k is the coefficient of conductivity, A is the area, and $\frac{dt}{dx}$ is the temperature gradient. It has been assumed that this law holds for the flow of heat through fibreboards, where the insulating property is due to the entrapped air cells, and it is even applied to fibrous materials such as rock wool, where the air cells constitute a much greater proportion of the volume. It was supposed that as long as the dimensions of the air cells were small in comparison with the thickness of the material, the thermal resistance of the various cells would be additive; thus the total resistance would be proportional to the thickness. When the density of a material such as rock wool becomes so low that convection currents can flow through the sample as a whole and are not confined to the individual air spaces, then the conductance would be expected to approach that of an unfilled air space and to vary with the thickness in a similar manner. In practice, however, density

of packing of the mineral wools used is great enough to prevent the flow of such convection currents through the material, and therefore the conductance should vary inversely as the thickness, according to Fourier's law.

The suggestion has been made that the effect in fibreboards may be due to the decreasing effect of surface resistance as the thickness becomes greater. There are two effects that should be distinguished.

(a) In the first place, it is known that the conductivity of fibreboards is decreased if the fibres can be made to lie parallel to the surface, so that the heat has to flow across the fibres and from fibre to fibre instead of along the individual fibres. This result has been demonstrated experimentally by Finck (4). He showed that the conductivity of some materials can be more than doubled by arranging the fibres parallel to the direction of the heat flow. Now, owing to the method of manufacture of fibreboards, the fibres in those layers near the surface tend to lie parallel to the surface, while those in the body of the material are directed at random. The surface layers would thus have a greater thermal resistance than the material in the centre of the sample, and this would cause thin samples to show a conductivity lower than that of thick ones.

(b) The second surface effect that would change the measured value of the conductivity is purely experimental and is inherent in the method of testing. The standard method of measuring the thermal conductivity of homogeneous building materials is by means of a hot-plate apparatus, in which the quantity of heat flowing across a slab of the material placed between a hot and a cold plate maintained at definite temperatures is measured. In such an apparatus it is impossible to maintain perfect thermal contact between the plates and the samples, and this slight temperature drop is neglected. In effect, it is assumed that the slight difference between the conductance of the film of air separating the samples and the plates and that of a film of the material of the same thickness is negligible (6). This assumption is quite true for all samples having small conductance, but with poor insulators or with thin samples this surface effect becomes relatively greater and may become large enough to influence the value obtained for the conductivity. If this should occur it would cause the measured conductivity of thin samples to appear less than that of thicker samples, since the conductivity of air is less than that of the material.

When these two effects have been eliminated from the measurements on the conductivity of samples of a homogeneous material, the measured conductivity should be independent of thickness (Fourier's law). Since changes of 23 and 50% in the conductivity seemed to be larger than one would expect from either of the above-mentioned effects, and, since if they are to be found, they are much too large to be neglected, it seemed to be well worth while to investigate the problem further.

Method of Measurement

Since in all insulating materials such as fibreboards and corkboards there is a substantial variation in the conductivity of individual samples owing to

small local variations in material, density, arrangement of fibres, and other factors, it is important in testing for the effect of thickness to eliminate these variations if possible. The plan was therefore adopted of beginning a series of measurements with a thick sample and reducing the thickness for each subsequent measurement. This reduction in thickness of the fibreboards tested was effected by means of the sanding apparatus of the International Fibre Board Limited, Ottawa. Through any one series of tests, therefore, the measurements were made on the same identical sample.* The thickness of the sample of the rock wool in bat form was reduced by pulling off the outer layers of the wool until the sample was of requisite thickness; in each test the density of packing of the wool was the same. No provision was made to obtain an identical sample of granulated wool for each test, but great care was taken that the density remained the same, and that the wool was packed as nearly as possible in a similar manner.

The samples of fibreboards were always in a bone dry condition at the beginning of the test, and it was found that the increase in moisture during the test was very small. It was not considered necessary to dry the rock wool for the tests, since the absorption of moisture by this material is negligible.

The tests were all made in the hot-plate apparatus of the National Research Laboratories which has been described in detail elsewhere (5). It consists of a hot-plate, 1 ft. square, surrounded by a guard ring 3 in. wide. The dimensions of the face of the sample must therefore be 18 by 18 in. The rock wool was placed in wooden frames constructed of strips of wood ½ in. thick. The width of these strips varied according to the desired thickness of the sample. The two faces of the frames were covered with brown kraft paper 0.005 in. thick. The thickness of all samples was determined by measuring the distances between the outside surfaces of the plates, with and without the samples in place. The difference in the two measurements was taken as the thickness of the sample. Measurements were made at each of the four corners of the plates, and the mean value was taken as the thickness. The pressure on all samples was the same, being that of a large weight attached to the plates by means of pulleys.

Results

The results obtained in these measurements are tabulated in Table I. Two samples of fibreboard were tested, both being supplied by the International Fibre Board Limited. Fibreboard I was an old sample that had been in the laboratory for more than two years. Fibreboard II was manufactured recently, and was taken from a commercial batch. The two surfaces of this sample had already been smoothed by sanding when originally supplied. It is to be noticed that there is an increase in the conductivity of Fibreboard I when the thickness is reduced from 2 to 1.5 in. The changes in the conductivity as the thickness is reduced from 1.495 to 0.276 in. are about what

---

* *There would be, of course, small local variations in the nature of the material in different parts of the fibreboards; it is impossible to eliminate these variations.*

one might expect from observational errors and local changes in the sample.* The conductivity of Fibreboard II remained practically constant in all tests. The behavior of these fibreboards can be quite easily explained.   There was evidently in Fibreboard I a surface layer in which the fibres were arranged

TABLE I

Mean temp., °F.	Temp. diff., °F.	Thickness, in.	k, B.T.U., per hr. per sq. ft. per °F. per in.	C, B.T.U., per hr. per sq. ft. per °F.	$R = \dfrac{1}{C}$
Fibreboard I: density, 17.8 lb. per cu ft.					
59.1	61.7	2.081	0.409	0.197	5.09
58.7	62.4	1.495	0.429	0.287	3.48
55.0	54.0	0.995	0.436	0.438	2.28
56.7	58.5	0.759	0.432	0.569	1.76
54.7	54.4	0.486	0.424	0.870	1.15
53.6	52.3	0.276	0.416	1.506	0.66
Fibreboard II: density, 12.2 lb. per cu ft.					
56.8	58.6	1.970	0.357	0.181	5.53
56.6	58.1	1.512	0.359	0.237	4.21
56.5	58.1	1.018	0.350	0.344	2.91
55.4	55.9	0.751	0.355	0.473	2.11
56.6	58.2	0.495	0.344	0.694	1.44
Rock wool in bat form: density, 7.1 lb. per cu ft.					
59.0	58.1	2.012	0.225	0.112	8.98
56.2	57.5	2.002	0.228	0.114	8.83
56.7	58.3	1.527	0.236	0.155	6.47
58.5	62.0	1.073	0.235	0.219	4.57
56.1	57.3	0.517	0.233	0.450	2.22
55.6	56.3	0.276	0.231	0.838	1.19
Granulated rock wool: density, 7.9 lb. per cu. ft.					
55.0	55.0	2.005	0.283	0.141	7.08
56.9	58.8	2.007	0.276	0.138	7.27
54.2	53.5	1.535	0.266	0.173	5.77
53.6	52.2	1.004	0.271	0.270	3.71
53.7	52.5	0.523	0.266	0.509	1.96

parallel to the surface.   This was removed in the first sanding, with the result that the conductivity increased.   The 0.5 in. of fibreboard that was removed to reduce the thickness was taken off one surface of the sample.   In the second reduction of thickness the material was removed from the opposite surface, and there is another small increase of conductivity that may be due to the effect of fibre arrangement, but is not so large as the first reduction and may possibly be fortuitous.   This increase in conductivity with decreasing thick-

* *Too much reliance must not be placed on the results obtained with the ½ in. sample, since this is a rather thin fibreboard and the conductance is large.*

ness is just opposite to the effect that Allcut reports, but it is probably a similar effect.   Evidently Allcut tested samples in all of which the fibres in the surface layers were parallel to the surface; consequently, in the thinner samples the conductivity is smaller owing to increased influence of the surface layers.   In our work the surface layer was removed to reduce the thickness; this gave an
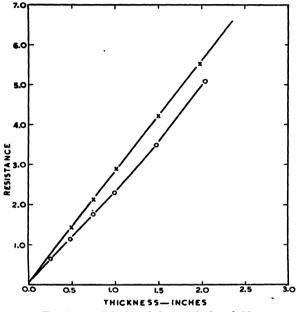
FIG 1.   o, *Fibreboard I;* x, *Fibreboard II.*
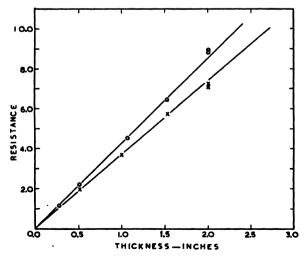
FIG. 2.   o, *Rock wool in bat form;* x, *rock wool granulated.*

increased conductivity. Fibreboard II shows no change in the conductivity with thickness, presumably because the surface layers were removed in the preliminary sanding during the manufacture of the sample. The two samples of rock wool also show no appreciable change in conductivity.

In Figs. 1 and 2 these results have been presented in a different manner. Here the resistance R of the samples has been plotted against the thickness. If the thermal conductivity of the material accurately obeyed Fourier's law, the points should give a straight line; any curvature denotes a departure from this law. The effect of the surface layers in Fibreboard I is plainly evident. This method of representing the results is also instructive in that it gives a method of determining the effect of the temperature drop from plate to sample, as explained above. If there were no errors due to this, the curve would pass through the origin; this would show that with no material between the plates the heat transfer would be infinite. When the surface effect is present, some resistance, even with no material between the plates, should be found; in other words, the curve would not pass through the origin but would cut the y-axis at a finite point. In our samples this effect, as shown above, is very small; in fact, in the rock wool it is too small to be distinguished. There is some evidence of such an effect in the fibreboards, but it is so small that it comes within the limits of the observational error. These results are extremely satisfactory in that they prove conclusively that we are justified in neglecting the resistance between sample and plate in our hot-plate tests, at least with fibreboards and rock wool. When this end effect is not negligible, the true conductivity of the material can be accurately determined from this type of graph by using the slope of the curve. This, of course, could be done only when the material obeys Fourier's law, and thus gives a linear relation between resistance and thickness.

These experiments show that when surface effects have been eliminated the transmission of heat through fibreboards and rock wool (of sufficient density) may be treated as a true conduction obeying Fourier's law. Thus, in the calculation of the resistance of a wall in which these materials are incorporated, the use of a formula that treats the resistance as the thickness divided by the conductivity is quite legitimate.

Acknowledgment

The author wishes to thank Mr. E. H. J. Barber of the International Fibre Board Limited, who kindly superintended the sanding of the fibreboard samples, for his co-operation.

References

1. ALLCUT, E. A. Proc. Inst. Mech. Engrs. 128 : 195-233. 1934.
2. ALLCUT, E. A. and EWENS, F. G. School of Engineering Research, University of Toronto, Bull. 149. 1937.
3. ALLCUT, E. A. and EWENS, F. G. Heating, Piping, Air Conditioning, 9 : 328-334. 1937.
4. FINCK, J. L. Bur. Standards J. Research, 5 : 973-984. 1930.
5. NIVEN, C. D. Can. J. Research, 7 : 115-130. 1932.
6. VAN DUSEN, M. S. J. Am. Soc. Heating Ventilating Engrs. 26 : 625-656. 1920.

DENSITY DIFFERENCES AT THE CRITICAL POINT ACCORDING TO R. PLANK'S EQUATION OF STATE[1]

By R. RUEDY[2]

Abstract

If R. Plank's equation of state is assumed to apply, the densities measured at two levels, 1 cm. apart, in a column of gas kept at the critical temperature, may differ by more than 5%. A large correction is therefore required for densities determined at the critical point unless the entire contents of the tube is vigorously stirred. Van der Waal's equation shows that the difference in level corresponding to a relative difference in density, $(\rho - \rho_c)/\rho_c$, is proportional to the third power of the relative difference; according to Wohl's equation it is proportional to the fourth, and according to Plank, to the fifth, power of the relative difference in density.

Introduction

The study of equations of state that apply alike to gases and to vapors reached its peak in the attempts to test van der Waal's equation, proposed in 1872, and to establish the range over which it applies. At the present time the success in separating isotopes opens the field to a renewed and more promising investigation with perfectly pure materials. Experiments for testing the equation of state of substances containing but one kind of molecule have not yet been undertaken, since only small volumes of such gases are available. The amount is nevertheless sufficient to permit a study of the behavior of gases at the critical point (3). The critical volume of heavy water is 2.74 cc. per gm. at a critical pressure, p_c, of 221.5 kg. per sq. cm. and a critical temperature, t_c, of 371.5° C., whereas the corresponding values for ordinary water are: $v_c = 3.066$ cc. per gm., $p_c = 225.5$ kg. per sq. cm., and $t_c = 374.23°$ C. (2).

The study of the critical point, or critical stage, as it might more properly be called, reduces in most cases to the determination of the critical temperature and the critical volume. The determination of the critical temperature is based on the disappearance of the meniscus between the liquid and its vapor, and the usual determination of the critical volume relies on the rule of the rectilinear diameter of the curve representing the densities of the liquid and the vapor as a function of the temperature.

The rule of the rectilinear diameter, enunciated by Cailletet and Mathias, states that when the density of the liquid and that of its saturated vapor are

plotted as a function of the temperature, the average values of the two densities fall on a virtually straight line sloping in the direction of the higher temperatures.   The density indicated by this line at the critical temperature is the critical density.   Figs. 1 and 2 show the rectilinear diameter of krypton and xenon, water and carbon dioxide, according to the most recent measurements (6, 9).   A remarkable feature of both curves is the rapid change in the densities of liquid and vapor as the critical region is approached; this almost sudden fall, or rise, to the common limit would alone justify the distinction of a critical point, where the slightest change in temperature produces a relatively large change in density.   Recent, more accurate work seems to show that at low temperatures, instead of falling upon a perfectly straight line, the real average values lie slightly below the straight line, whilst near the critical stage the values lie above the middle line.   The succession of average values represents a curve of the third degree with a pronounced point of inflection.
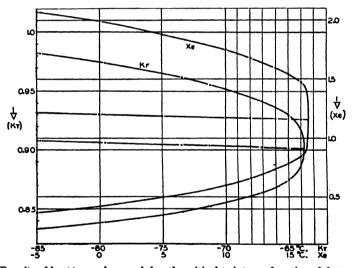
FIG. 1.   *Density of krypton and xenon below the critical point as a function of the temperature.*

In the short method of determining the density at the critical stage a series of closed tubes filled to various heights with the liquid substance is used (1). When heat is applied to a tube in which the ratio between the mass of the substance and the inner volume of the tube is smaller than the critical density of the liquid, the meniscus falls, and the last traces of liquid are found to disappear at a definite temperature.   At this temperature the computed average density is equal to the density of the saturated vapor.   When the ratio between the mass and the volume is larger than the critical density and the tube is heated, the meniscus rises, and the last trace of the vapor disappears as a bubble at the top of the tube.   At this stage the computed density of the contents must be equal to the density of the liquid boiling at constant volume

under the pressure of its own vapor. A series of these dew and boiling points is determined for various amounts of liquid in the tube, and the temperature is plotted as a function of the computed densities. At the critical temperature the rectilinear diameter intersects the curve at the critical density.
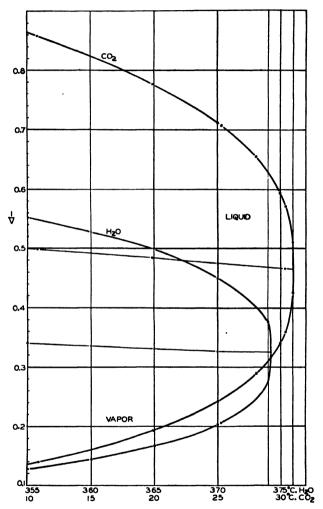
FIG. 2. *Density of carbon dioxide and water below the critical point as a function of the temperature (Michels, Eck).*

The critical temperature is deduced from the flat maximum of the curve obtained on plotting the temperature at which the meniscus disappears against the amount of liquid used.

Owing to the large changes in density caused by changes in temperature near the critical point, the meniscus always moves towards the top or the

bottom of the tube before disappearing, except in the quite unlikely case where the amount of substance present is such that the density is the true critical density. In practice the equilibrium is established so slowly in the range close to the critical point that when the temperature increases at a finite rate the system passes through the critical state before the boundary line between liquid and vapor has time to move. Even with slow heating, the influence of gravity causes the density in the tube to vary from level to level. The density differences to be expected on the basis of the equation of state at the critical point, and the corresponding changes in the optical and dielectric properties, are of interest for a better understanding of the behavior of liquid and vapor (8). A difficulty in this study is that the critical temperatures of only a few substances have been determined with a high degree of accuracy (ordinary water (2), 374.23° C.; krypton (6), −63.75° C. or 209.39° K.; carbon dioxide (7), −31.04° C.).

Equations of State of the Fifth Degree

The unequaled advantages of van der Waal's equation of state are its simple form and the wide range over which it gives a general explanation of the behavior of the properties of liquids and gases. It states that in place of the pressure $p = RT/v$ per unit area, computed for a gas with perfectly inert molecules, the pressure is for a real gas smaller by the amount a/v^2, because of the mutual attraction between molecules, which varies as a certain function of the distance, approximately as the inverse fourth power of the distance between molecules. More recent work suggests that the inverse sixth power would be more accurate. On the other hand the volume available for the free motion of the molecules is $(v - b)$ instead of v, owing to the finite size of the molecules; consequently,

$$p = \frac{RT}{v - b} - \frac{a}{v^2}.$$

The constants a and b are determined by the fact that at the critical stage the equation has a point of inflection at which the curve representing p as a function of v has three roots in common with the tangent. In reality the constant b also constitutes a correction for the repulsion between molecules at very close contact, forces which vary more nearly as the inverse twelfth power of the distance, and, therefore, affect the values at the highest pressure and smallest volumes. Wohl (13) takes them into account by adding the term $c/(v - b)^3$. The introduction of this term is justified also by the value of the ratio $RT_c/p_c v_c$ obtained on the assumption that the curve representing p and v has at the critical point four points in common with the tangent; the ratio $RT_c/p_c v_c$ is computed to be 3.75 instead of van der Waal's admittedly too small value of 2.67. The measured values for many organic compounds lie between 3.5 and 4.0, and no value as low as 3 is obtained for any gas. It would perhaps have been more correct to write the term that takes repulsion into account as c/v^4 or $c/(v - b)^4$ if the law of the inverse twelfth power is valid for the repulsive forces.

It is certain that the forces between molecules depend in a complicated way upon the distances between molecules, and upon the nature of the atomic forces, which vary from molecule to molecule. As long as the exact laws are but imperfectly known, the corrections to the pressure may be introduced by means of a series of terms according to descending powers of v or $(v - b)$, the number, n, of the terms depending on the accuracy desired and the numerical work thought to be justified. The difference between the molecular forces of different elements is considered by introducing so many constants that their number exceeds by at least one the number of terms in $(v - b)$ or v. R. Plank's recent equation can be used when five terms are involved (10):

$$p = \frac{RT}{(v - b)} - \frac{a_2}{(v - b)^2} + \frac{a_3}{(v - b)^3} - \frac{a_4}{(v - b)^4} + \frac{a_5}{(v - b)^5} .$$

On the assumption that at the critical stage the curve representing p as a function of v has five points in common with the tangent and that this tangent is parallel to the v-axis, the following relations are obtained:

$$\frac{RT_c}{p_c(v_c - b)} = n = 5$$

$$\frac{RT_c}{p_c v_c} = n(1 - b/v_c) = n(1 - 1/\alpha)$$

with

$$b = v_c/\alpha = M/\alpha\rho_c .$$

$$a_2 = (n - 1)(\alpha - 1)bRT_c/2 = 2b(\alpha - 1)RT_c \text{ for } n = 5$$
$$a_3 = (n - 1)(n - 2)(\alpha - 1)^2 b^2 RT_c/1 . 2 . 3n = 2b^2(\alpha - 1)^2 RT_c$$
$$a_4 = (\alpha - 1)^{n-2} b^{n-2} RT_c = b^3(\alpha - 1)^3 RT_c$$
$$a_5 = (\alpha - 1)^{n-1} b^{n-1} RT_c = b^4(\alpha - 1)^4 RT_c .$$

The constant $\alpha = v_c/b$ remains arbitrary and may be so chosen that $RT_c/p_c v_c$ agrees with the measured values (Table I).

TABLE I

VALUES OF $\alpha = v_c/b$ AND OF $RT_c/p_c v_c$

$RT_c/p_c v_c$	α	Examples of values of $RT_c/p_c v_c$
3.33	3	Oxygen, 3.34; neon, 3.25
3.44	$3\frac{1}{3}$	Argon, nitrogen, 3.43; krypton, 3.44
3.57	$3\frac{1}{2}$	Xenon, 3.6
3.66	$3\frac{3}{4}$	Carbon dioxide, 3.636
3.75	4	Benzene, 3.71; pentane, 3.77
4	5	Propyl alcohol, 4

An equation of state of the fifth degree was proposed by van der Waal who put

$$b = b_o - b_1/v + b_2/v^2$$

Such an equation enters into modern theories of the liquid state (4, 10, 11). That the value of b is a constant over the whole range of temperatures is not to be expected, since the molecular spectrum reveals an increase in the distance between the atoms when the excitation is increased by heat, while at the same time the higher energy at the higher temperatures produces a greater deformation of the molecules and causes closer approach of their centres during collisions. To a certain extent the two effects cancel each other.

The equation of the fifth degree will apply alike to liquids and gases only if there is no shift in the importance of the terms in $(v - b)$ during the transition from the liquid to the gaseous state. Such a shift, which is caused by a change in the laws of attraction and repulsion, might be expected when the molecules acquire or lose a certain amount of the orientation that exists in the solid state, often as the result of ionization (salts). There is of course no complete separation between liquid and solid state and, therefore, no sharp gap that would mark presence or absence of orientation, no more than there is, as regards viscosity, a sharp boundary between liquid and solid state. Glass as an undercooled liquid, and liquid crystals, in which patches of oriented molecules are merely due to the unusual length of the molecules, illustrate how the different states of matter shade one into the other. But any possible orientation in the liquefied noble gases, such as neon and argon, does not involve the functioning of forces not already present in the gas. The properties of solid neon and argon seem to be governed by exactly the same forces that cause the gases to deviate from the ideal law (5); consequently, there exists a certain continuity of the gaseous, the liquid, and even the solid states of neon and argon. The facts that throughout a wide range of corresponding temperatures, from the lowest to at least three-fourths of the critical temperature, the density of liquid xenon is equal to that of liquid oxygen, and that the densities of their vapors are also the same, despite the difference in their chemical properties, suggest that the effect of the orientation of oxygen molecules need not be included as a new and important factor in the equation of state.

The Barometric Formula According to R. Plank's Equation

When volumes are replaced by densities, Plank's equation may be written

$$p = RT \frac{\rho}{(M - b\rho)} - a_2 \frac{\rho^2}{(M - b\rho)^2} + a_3 \frac{\rho^3}{(M - b\rho)^3}$$

$$- a_4 \frac{\rho_4}{(M - b\rho)^4} + a_5 \frac{\rho^5}{(M - b\rho)^5} .$$

If the pressure at any point in the gas is due to the column of gas above it, then

$$dp = - \frac{\rho}{1033} dh ,$$

the height being expressed in centimetres and the pressure in atmospheres; consequently,

$$- \frac{dh}{1033 d\rho} = RT \frac{M}{(M - b\rho)^2} + \sum_{r=2}^{r=5} (-1)^{r+1} rM \frac{\rho^{r-2}}{(M - b\rho)^{r+1}} .$$

If $1/\alpha \rho_c$ is written in place of b/M, an integration gives for the height h, where the density is ρ,

$$\frac{h}{1033} = RT \ln \frac{M}{\rho} (1 - \rho/\alpha\rho_c) - \frac{RT}{M} (1 - \rho/\alpha\rho_c)^{-1}$$

$$+ \frac{RT_c}{2M} (\alpha^4 - 1)(1 - \rho/\alpha\rho_c)^{-2}$$

$$- \frac{RT_c}{3M} (1 + 2\alpha + 3\alpha^2)(\alpha - 1)^2 (1 - \rho/\alpha\rho_c)^{-3}$$

$$+ \frac{RT_c}{4M} (1 + 3\alpha)(\alpha - 1)^3 (1 - \rho/\alpha\rho_c)^{-4}$$

$$- \frac{RT_c}{5M} (\alpha - 1)^4 (1 - \rho/\alpha\rho_c)^{-5} ,$$

apart from an arbitrary constant. On introducing

$$1 - \frac{\rho}{\alpha\rho_c} = \frac{\alpha - 1}{\alpha} \left(1 - \frac{\rho_c - \rho}{(\alpha - 1)\rho_c} \right) = \frac{\alpha - 1}{\alpha} \left(1 - \frac{y}{\alpha - 1} \right)$$

this formula becomes

$$\frac{h}{1033} = \frac{RT}{M} \left(\ln \frac{\alpha - 1}{\alpha} \frac{M}{\rho_c} + \ln \left(1 - \frac{y}{\alpha - 1} \right) - \ln \left(1 + y \right) - \frac{\alpha}{\alpha - 1} \left(1 - \frac{y}{\alpha - 1} \right)^{-1} \right)$$

$$+ \frac{\alpha}{\alpha - 1} \frac{RT_c}{M} \left(\frac{\alpha}{2} \left(1 + \alpha + \alpha^2 + \alpha^3 \right) \left(1 - \frac{y}{\alpha - 1} \right)^{-2} \right.$$

$$- \frac{\alpha^2}{3} \left(1 + 2\alpha + 3\alpha^2 \right) \left(1 - \frac{y}{\alpha - 1} \right)^{-3} + \frac{\alpha^3}{4} \left(1 + 3\alpha \right) \left(1 - \frac{y}{\alpha - 1} \right)^{-4}$$

$$\left. - \frac{\alpha^4}{5} \left(1 - \frac{y}{\alpha - 1} \right)^{-5} \right) .$$

When the column of gas is at the critical temperature, T_c, the difference in height, Δh, between the layer where the density is ρ and that where the density is ρ_c, or where $y = (\rho - \rho_c)/\rho_c = 0$, is given by

$$\frac{M}{RT_c} \frac{\Delta h}{1033} = ln\left(1 - \frac{y}{\alpha - 1}\right) - ln\left(1 + y\right) - \frac{\alpha}{\alpha - 1}\left(1 - \frac{y}{\alpha - 1}\right)^{-1}$$

$$+ \frac{\alpha}{\alpha - 1}\left(\left(1 + \alpha + \alpha^2 + \alpha^3\right)\left(1 - \frac{y}{\alpha - 1}\right)^{-2}\right.$$

$$+ \frac{\alpha^2}{3}\left(1 + 2\alpha + 3\alpha^2\right)\left(1 - \frac{y}{\alpha - 1}\right)^{-3}$$

$$\left. + \frac{\alpha^3}{4}\left(1 + 3\alpha\right)\left(1 - \frac{y}{\alpha - 1}\right)^{-4} + \frac{\alpha^4}{5}\left(1 - \frac{y}{\alpha - 1}\right)^{-5}\right).$$

For short columns, y is small, not more than 5%, and after development of the powers of $(1 - y/(\alpha - 1))$ in series the expression can be reduced, in practice, to

$$\frac{\Delta h}{1033} = -\frac{\alpha^6}{(\alpha - 1)^6} \frac{RT_c}{M}\left(\frac{y^5}{5} - \frac{(\alpha - 7)}{6(\alpha - 1)} y^6\right)$$

This expression gives the difference in height above or below the level where the density is ρ_c and that where the relative density difference is y. For all substances, the height depends in the same way on the relative density difference y and on the value of $\alpha = v_c/b$. Thus with $R = 82.1$

$$\frac{M}{T_c} \Delta h = 9.66 \times 10^5\left(\frac{y^5}{5} + \frac{y^6}{3}\right), \quad \text{for} \quad \alpha = 3,$$

$$\frac{M}{T_c} \Delta h = 4.76 \times 10^5\left(\frac{y^5}{5} + \frac{y^6}{6}\right), \quad \text{for} \quad \alpha = 4,$$

$$\frac{M}{T_c} \Delta h = 3.23 \times 10^5\left(\frac{y^5}{5} + \frac{y^6}{12}\right), \quad \text{for} \quad \alpha = 5.$$

Apart from the ratio α, the nature of the gas enters into the factor M/T_c, which varies from 0.1 to 0.5 and higher.

The heights measured from the level with the critical density in question and computed by using various equations of state (11), are compared in Table II. For Plank's equation only the values for $\alpha = 3$ and $\alpha = 4$ are given; the heights for $\alpha = 5$ are a third of those obtained for $\alpha = 3$, and indicate therefore an even more pronounced variation in density with the height. When the column of gas is at the temperature $T = T_c (1 + t/T_c)$, the difference in height between the layer at which the density is ρ, and that

at which it is ρ_c, is equal to the height Δh_c computed for the critical temperature plus a correction such that

$$\frac{\Delta h}{1033} = \frac{\Delta h_c}{1033} + \frac{R}{M}\frac{t}{T_c}\left(ln\ \frac{1 - \dfrac{y}{\alpha - 1}}{1 + y} - \alpha\ \frac{y}{1 - \dfrac{y}{\alpha - 1}}\right).$$

Although Plank's equation has been applied to but a few substances, carbon dioxide and water among them, there is no doubt that with van der Waal's equation the contact between the p,v curve and the horizontal tangent at the critical point is not sharp enough to give agreement with the measured values.

TABLE II

DENSITY CHANGES IN A COLUMN OF GAS OF MOLECULAR WEIGHT M NEAR THE CRITICAL TEMPERATURE, T_c

Percentage change y	$\frac{M}{T_c}\Delta h$, cm.			
	van der Waal	A. Wohl	R. Plank	
			$\alpha = 3$	$\alpha = 4$
−0.5	0.006			
−1	0.05	0.0003		
−2	0.4	0.0044	0.0006	0.0003
−3	1.3	0.024	0.0046	0.0023
−4	3.2	0.078	0.019	0.010
−5	6.2	0.185	0.058	0.029
−6	10.7	0.389	0.141	0.070

On the Experimental Determination of the Density at the Critical Stage

The direct method of determining the density differences in a column of gas near the critical temperature by means of small floats of varying buoyancy is cumbersome, and is inaccurate when the density varies rapidly with the height. The use of floats suspended from a fine quartz spiral prevents stirring of the entire contents, and requires that corrections be applied for the suspension system when the float and a portion of the spring dip into the liquid. A closely wound spiral offers a considerable resistance to the passage of the material from the space enclosed by the spiral to the space between the spiral and the walls of the tube, or vice versa. Grids of thin wires from 0.5 to 3 mm. in diameter, spaced 2 to 20 mm. apart, are actually used as shields against strong air currents. Stirring of the contents of the tube outside the spiral is not likely to affect the material held inside the spiral since the gas between the wires is virtually at rest, and since the pressure differences near the critical point are much smaller than the forces causing

a strong air current.   The density may vary without an appreciable change in pressure, whereas, on the contrary, a change in temperature in the critical region produces a much larger variation in density than at any other temperature.   Thorough mixing in a reasonable time is obtained, therefore, only by heating the contents of the tube, and densities read while the temperature is decreasing are likely to be lower than the values found when the temperature is increasing.

The optical methods used for obtaining the density differences are disadvantageous owing to the turbidity of the fluid at the critical point.   The method developed by Töpler for studying streaks which depends directly upon the existence of a density gradient in the material, seems nevertheless to suit the purpose.   In this method the column of gas is placed between a projecting lens and an evenly illuminated surface that serves as a bright background.   The lens projects on a screen an image of the background, and by cutting off from one side all the rays of light but those in the very axis of the optical system each point on the screen is made to correspond to a point in the background.   Hence any deflection of the ray that might be caused by a region of varying density between background and lens causes the image point to lose brightness in favor of the region of uniform density.   The sensitivity of the method is greater, the narrower the space between the optical axis and the edge limiting the pencil of rays, and the greater the distance s between the lens and the edge used for reducing the cross section of the pencil of light.   The distance s may amount to a few metres, and the distance e from edge to axis to a few microns.   Experience shows that when an arc lamp is used a deflection corresponding to about one-eighth second, or about 0.6×10^{-6} radian, may be detected by this means.

In a column of gas, in which the density varies with the height, a beam of light arriving in a virtually horizontal direction is bent into arcs of radius

$$R = \frac{n}{\text{grad } n} = \frac{d}{e}$$

where d is the length of the path in the layer considered, and e is the small angle that the emerging ray forms with the incident ray.   In the general case, n and grad n vary slowly, and the values of R are so large that the path described is a single flat arc, or a straight line.   For gases and vapors

$$n = 1 + c\rho/\rho_o \; ; \quad \text{grad } n = \frac{c}{\rho_o} \text{grad } \rho ,$$

where ρ_o is the density at $0°$ C. and 760 mm. of mercury, and c is a small constant, equal to 0.000296 in the case of nitrogen ($\rho_o = 0.00125$, $\rho_c = 0.32$), 0.000335 for carbon dioxide ($\rho_o = 0.002$, $\rho_c = 0.46$), 0.000067 for neon ($\rho_o = 0.0009$, $\rho_c = 0.484$), 0.000428 for krypton ($\rho_o = 0.0058$, $\rho_c = 0.9085$). The value of n is not likely to exceed 1.1 at the critical stage; consequently, in practice,

$$e = \frac{d}{n} \text{ grad } n = \frac{cd}{\rho_o} \text{ grad } \rho .$$

When the average change of ρ over a distance of 1 cm. is about 5%, and the light traverses a column of gas 1 cm. thick in the section containing the axis of the tube, the angle of deflection e is at least 10^{-5}, and Töpler's method for detecting streaks should reveal at a glance the density differences in a column of gas kept at a temperature close to the critical.

In substances possessing strong molecular absorption bands in the near infra-red, such as the OH band, the position of the band may undergo a strong shift as the liquid or vapor approaches the critical point.   The influence of the approach to a common limit upon the refractive index in the visible spectrum remains to be investigated.

References

1. CENTNERSZWER, M.   Z. physik. Chem. 49 : 199-207.   1904.

2. ECK, H.   Physik. Z. 38 : 256.   1937.

3. HARAND, J.   Monatsh. 65 : 153-184.   1935.

4. HIRSCHFELDER, J., STEVENSON, D. and EYRING, H.   J. Chem. Phys. 5 : 896-912.   1937.

5. LONDON, F.   Z. physik. Chem. B11 : 222-251.   1931.

6. MATHIAS, E., CROMMELIN, C. A. and MEIHUIZEN, J. J.   Compt. rend. 204 : 630-633.   1937.

7. MICHELS, A., BLAISSE, B., and MICHELS, C.   Proc. Roy. Soc. A160 : 358-375.   1937.

8. NAHERNIAC, A.   Ann. phys. 7 : 528-597.   1937.

9. PATTERSON, H. S., CRIPPS, R. STAFF., and WHYTLAW-GRAY, R.   Proc. Roy. Soc. 86 : 579-590.   1912.

10. PLANK, R.   Forsch. Gebiete Ingenieurw. 7 : 161-173.   1936.

11. RUEDY, R.   Can. J. Research, 9 : 637-640.   1933.

12. TURNER, L. A.   Am. Physics Teacher, 5 : 241-243.   1937.

13. WOHL, A.   Z. physik. Chem. 99 : 207-225.   1921.

The articles in the van der Waal's Centenary number of Physica were received too late to be of use for the present paper.

A DEVICE FOR THE AUTOMATIC REGULATION OF THE CURRENT IN A SHEARER X-RAY TUBE[1]

By HUGH LE CAINE[2]

Abstract

A device for rendering automatic the operation of a Shearer X-ray tube is described. Its functions are: (i) to regulate the leak valve mechanically so as to maintain a constant current; (ii) to disconnect the high tension transformer and close the leak valve when a failure of any part of the vacuum system causes high pressure and excessive tube current, the tube restarting as soon as the pressure again becomes low enough.

Standard, inexpensive, radio parts, a small motor, and suitable gearing to connect motor and valve are all that are required. The limits within which the tube current can be held may be made very narrow.

In a Shearer X-ray tube, the current is regulated by adjustment of the amount of air which flows through a needle or leak valve into the tube. It is impossible to keep the tube current fixed over long periods without adjustment of the valve. The device described below has been used to make these adjustments automatic. Its action may be seen by reference to the circuit diagram. The tube current flowing through R_1 and R_2 produces a voltage drop, which, together with a fixed voltage B_1, is applied to the grid of the tube T_1. T_1 is operated close to the "cut-off point." In this region the curvature of the tube's characteristic surface is such that the "dynamic plate resistance", $\dfrac{\partial E_p}{\partial I_p}$, may be considered a function of the grid voltage. In this way the grid controls the fraction of the alternating voltage, E_1, which appears across the plate resistor R_4. In the grid circuit of the thyratrons, T_2 and T_3, this variable fraction of E_1 is combined with a second alternating voltage E_2 of the same frequency as E_1 and 180° out of phase with it. The magnitudes of E_1 and E_2 are so chosen that for a definite potential applied to the grid of T_1 the resultant alternating voltage in the grid circuit of T_2 and T_3 is zero. Above and below this critical potential, the resultant voltage has opposite phases. It may be seen from the diagram that the plates of T_2 and T_3 are at alternating voltages in phase with E_1 and E_2 respectively. With the bias battery, B_2, correctly adjusted, a resultant alternating voltage in the grid circuit of T_2 and T_3 may be made to fire either T_2 or T_3, depending upon its phase. A corresponding field of the motor is energized, and the motor turns in one direction or the other. If R_1 and B_1 are so adjusted that the desired X-ray tube current places the grid of T_1 at the critical potential mentioned, any change in tube current will cause the motor to turn. This motion may be transmitted to the valve through suitable gearing; thus the leak may be increased or decreased until the desired value of tube current is re-established.

To reduce the wear on the mechanism, the range of current values over which the thyratrons remain non-conducting should be made as wide as experimental conditions permit. The width of the range may be controlled by varying the thyratron bias. If R_1 is changed to maintain a different tube current, the relative sensitivity remains the same.
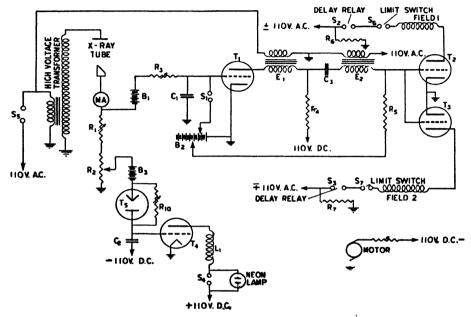
FIG. 1. *Device for regulating the current in a Shearer X-ray tube.*

B_1, 90 v.	R_3C_1, approx. 10 sec.	E_1, approx. 40 v. R.M.S.
B_2, 18 v., $1\frac{1}{2}$ v. taps provided.	$R_{10}C_2$, approx. 200 sec.	E_2, approx. 10 v. R.M.S.
B_3, 45 v.	R_4,R_5, approx. 20,000 ohms.	L_1S_8, circuit-closing relay.
R_1, R_2, determined by X-ray tube current.	C_3, 2 μf.	T_4, power triode; T_5, diode.

Neutrals of a-c. and d-c. supply grounded.

Overshooting must be avoided by allowing time for the pressure to become uniform over the vacuum system after an adjustment of the valve. A contact, S_1, on the motor, stops it after every revolution by bringing the grid momentarily to the proper potential. The grid circuit is then allowed to charge through R_3 to the difference in potential between B_1 and the tube current drop across R_1 and R_2. If the voltage necessary to cause firing of the thyratrons is E volts below the normal bias, the time, t, between revolutions of the motor can be expressed as a function of e, the resultant alternating voltage in the grid circuit.

$$t = C_1R_3 \log(1 - e/E) .$$

Thus, the rate at which the valve is adjusted becomes smaller as the operating value of current is reached, and is zero when $e = E$. The edge of the operating

range is approached asymptotically. Owing to random fluctuations in the tube current its mean value will be at the centre of the range. The factor C_1R_3 is the time constant of the grid circuit (neglecting $R_2 + R_1$), and can be adjusted to give the most rapid correction possible without overshooting. If desired, the speeds of increasing and decreasing the leak may be made unequal by shifting the potential on the battery side of S_1 from the centre of the operating range.

The contact at S_1 must be closed for a small part of the revolution, and must be made in such a way that the motor cannot stop with the contact closed. A small spring may be provided to rotate the armature past this point. An alternative scheme which positively avoids "dead spots" is to connect a double-pole, double-throw relay so that the circuit is closed only while the armature is between the energized and the non-energized positions. The latter method was used, as such a relay was available.

It is important that the tube T_1 be correctly chosen and operated on a suitable part of its characteristic surface. If ΔI is the greatest deviation of X-ray tube current from operating value which can occur without turning the motor, $I/\Delta I$ may be called the relative sensitivity of the device. It may be expressed as a function of ΔE_T, the excess of bias applied to the thyratrons over the firing point bias, according to the equation

$$\frac{I}{\Delta I} = E_{B_1} \frac{\partial E_{R_5}}{\partial E_g} \frac{1}{\Delta E_T},$$

where E_{B_1} is the voltage of the battery B_1, E_{R_5} is the alternating voltage developed in R_5, E_g is the potential of the grid of T_1. Firing is assumed to occur when the peak value of the resultant alternating voltage exceeds ΔE_T.

If operation is confined to a portion of the tube's characteristic surface where $\frac{\partial^2 E_p}{\partial I_p{}^2} = 0$, and it is assumed that the area of this region is not zero, then,

$$\frac{\partial E_{R_5}}{\partial E_g} = \frac{E_1 \dfrac{\partial^2 E_p}{\partial E_g\,\partial I_p} R_b}{\left(\dfrac{\partial E_p}{\partial I_p} + R_b\right)^2}.$$

R_b is the a-c. plate load, approximately R_4 and R_5 in parallel. To obtain the greatest sensitivity, the tube should be so chosen that $\dfrac{\partial E_{R_5}}{\partial E_g}$ is as great as possible. R_b is limited by the maximum resistance which may be introduced into the grid circuit of the thyratrons. Pentodes have very large values of $\dfrac{\partial^2 E_p}{\partial E_g\,\partial I_p}$, but are less suitable in other respects than triodes of the medium μ class. Types '27, '01A, or 6C5, operating on the negative side of the projected cut-off point, are satisfactory, although the condition $\dfrac{\partial^2 E_p}{\partial I_p{}^2} = 0$ is satisfied over a rather small range. The above expression for sensitivity,

$I/\Delta I$, has been verified experimentally, a '27 tube being used for T_1. The circuit will maintain its calibration during the life of T_1. When the tube is operated properly, the dynamic plate resistance is independent of plate voltage and heater voltage. Thus the circuit is not affected by changes in supply voltages. Owing to the use made of T_1, changes in the characteristics of the thyratrons do not cause a shifting of the value of current to be maintained, and affect only the sensitivity.

If the motor is connected as shown, it must be provided with a split field. This type of motor is now commercially available. Any thyratron capable of controlling sufficient power is satisfactory. Type 885, the least expensive thyratron, will control 20 watts, when the external impedance is suitably chosen. Type FG-17 was used, as it was available. Variations of the circuit will readily occur to those interested in the design. Between motor and valve, gearing from a discarded clock forms a convenient connection, providing a large number of ratios. Springs should be used to reduce the lost motion to a point at which the motor will pick up the valve in at least one revolution. A fine, closely wound helix of steel wire, about No. 28, is a very satisfactory belt. Limit switches, S_6, S_7, normally closed, are placed in the field circuit to limit the travel of the valve.

The thermal delay relays (S_2, S_3, R_6, R_7) are not required unless the a-c. supply is disconnected frequently, but are a convenience in any thyratron circuit. They can be made cheaply from a "blinker plug", or thermal interrupter. This is stripped down to the fibre disc supporting the compound bar and contacts, and the heating coil (R_6, R_7) is connected as shown. The time taken for the contacts to close may be adjusted by bending the fixed contact leaf.

Occasionally the pressure in the X-ray tube rises temporarily, owing to a failure of the power supply to the pump, or for other reasons. The tube current may then become too great. Overload protection which removes the voltage from the high tension transformer primary is therefore provided. The circuit then remains open for a period depending on the severity of the overload. The tube current drop through a part of R_2 is applied to the grid of a power tube T_4 through a bias battery B_3 and rectifier T_5. When the resultant grid potential drops to a certain value, the relay opens the transformer-primary circuit. The time constant involved in the opening action is small. The rectifier allows the grid to charge positively only through the shunt path R_{10}. The time constant, $R_{10}C_2$, is quite large. The duration of a severe load is approximately the opening time of the relay. The charge acquired by the grid condenser, and therefore the time for which the circuit is open, is proportional to the extent of the overload. Since E_1 is obtained from a transformer connected across the high tension transformer primary, the valve closes automatically at full speed whenever the tube is shut down. It was intended originally to provide for a limited number of automatic reclosures. This has been found unnecessary, since the rapidity of release of the circuit prevents any harm during the severest overload possible. This action allows the tube to restart as soon as conditions permit.

The cathode of T_5 should be heated from the d-c. line. Then a power interruption which causes the cathode to cool also allows C_3 to charge negatively; this prevents the relay L_1S_5 from closing before the circuit is operative.

None of the circuit constants are critical. R_1, R_2 should be wire wound; R_3, R_{10} may be carbon. R_1, R_3, R_{10} are more conveniently adjusted if suitably tapered. B_1 and B_3 may be replaced by separate power packs; B_1 must be stabilized by a 90 volt neon lamp in the conventional manner. B_3 may be replaced by a low resistance potentiometer between ground and -110 d.c. The highest permissible resistance is determined by the time during which the contact is closed. The neon lamp is required to absorb surges when a quick opening relay is used.

The device has been used for making long exposures and has operated without attention for periods of 200 hr. at a time. The same arrangement could be used for mechanically regulating any device for controlling a quantity having associated with it a continuously changing potential. The impedance of the circuit could be high. The circuit is not suited for use with low potentials such as those found in ordinary bridge circuits.

Acknowledgment

NOTE ON "THE ALTITUDE EFFECT ON THE SPECIFIC IONIZING POWER AND ZENITH ANGLE DISTRIBUTION OF COSMIC RAYS", BY DAROL K. FROMAN AND J. C. STEARNS

Dr. M. L. Rowles, Macdonald College, has kindly pointed out to the writers two errors in the paper of the above title appearing in the Canadian Journal of Research, A, 16 : 29-40.   1938.

On p. 33, the last line should read: $\dfrac{\pi r \tan \alpha}{4}$.

On p. 34, Equation (7) should read: $d = d_1 + 2s$.

A correction for the first error increases the values quoted for J_o, N_1 and N_2, and decreases the value quoted for i, by 7%.   In the original paper the calculations were made with Equation (7) in its correct form.

<div align="right">D. K. FROMAN.</div>

MACDONALD COLLEGE,
MACDONALD COLLEGE P.O., QUE.
Received April 22, 1938.

THE VARIATION OF THE ELECTRICAL CONDUCTIVITY OF THE ATMOSPHERE WITH HEIGHT[1]

By D. C. Rose[2]

Abstract

The conductivity of the atmosphere has been measured during flights in aeroplanes near ground level and up to about 16,000 ft. Seven flights were made during the autumn and winter of 1936–1937. The Gerdien type of conductivity apparatus was used. An attempt was also made to measure potential gradients by the radioactive collector method. This method was impractical, probably because of charges acquired by the aeroplane. It did, however, serve to indicate the presence of intense local space charges such as charged clouds. On one flight, observations were taken near a thunderstorm, but owing to difficulties in interpretation no conclusions regarding the exact nature or location of the charges could be drawn. The conductivity increased rapidly with height in a manner in general agreement with the data of other observers. Positive and negative conductivities were found to be equal, within the experimental error, at heights between about 1000 and 10,000 ft. At higher altitudes the negative conductivity was greater than the positive. The presence of clouds and frontal discontinuities usually caused a reduction in continuities.

Introduction

While a great deal is known about the quantities describing the electrical state of the atmosphere at the surface of the earth, relatively few investigations have been carried out on the variation with height of such quantities as conductivity, space charge, potential gradient. A review of early experimental work on the subject covering the years from the first experiments of Franklin in 1750 until about 1928 has been prepared by Gish (1, pp. 182-186). Observations were taken with the aid of kites, balloons, and aeroplanes. In general, the conductivity has been found to increase with altitude fairly uniformly except for departures that may be due to haze layers or clouds. The potential gradient is generally believed to decrease with altitude, though observations do not always agree in the amount of decrease. The potential gradient is very difficult to measure, and no doubt varies considerably; consequently, no great agreement among individual observations should be expected. The ionic density is also thought to increase somewhat with altitude, though measurements are relatively few, and, owing to the existence of different kinds of ions, there is often uncertainty in regard to the actual property that is being measured.

A valuable contribution to the knowledge of atmospheric electric phenomena was made in the flight of the stratosphere balloon "Explorer II" on November 11, 1935. The data obtained have been published by Gish and Sherman (2, pp. 94-116). Conductivity measurements were made at heights up to 72,000 ft., and, from these and comparison with cosmic ray data, deductions that were unexpected were made regarding the variation of mobility with height and the distribution of condensation nuclei.

The object of the present experiments was to investigate the possibilities of measuring atmospheric electric quantities during flights in aeroplanes, and to make further studies of their variation in different types of weather. It was also hoped that by taking observations near thunderstorms or cumulus clouds that might develop into thunderstorms, further information could be added to that already existing on the process of the building up of the electric charges that cause thunderstorms. Conductivity and potential gradient measurements were taken, and the results show that the potential gradient measurements are of little value, but the conductivity measurements were reasonably successful and in good agreement with previous work. Only once was it possible to observe effects near a thunderstorm.

The work is a continuation of work undertaken in 1931, in which conductivity observations were taken during four flights (4). In plotting the results of the 1931 flights the values for mobilities of positive and negative ions were assumed, and the results were plotted in terms of small ion density rather than of conductivity. As the values of the mobilities were very uncertain, and, as Gish and Sherman have pointed out, so little is known of the variation of mobility with height (2, p. 105), the method of expressing the results in the previous paper (4) is of little value. Therefore, the results of two of the early flights will be rediscussed here.

Apparatus

Conductivity Apparatus

The Gerdien type of conductivity apparatus was used. Fig. 1 is a schematic sketch of the tube, electrometer, and switch used to connect the electrometer to the conductivity apparatus or to the potential gradient apparatus. The design was somewhat different from that used in the 1931 flights, in that the tube was larger and the potential was applied to the cylindrical tube surrounding the collecting electrode instead of to the electrode itself. This cylinder, to which the potential was applied, was supported in an outer shielding tube as shown. The important dimensions of the apparatus were: inside diameter of tube, 7.60 cm.; length of tube, 33 cm.; diameter of collecting rod, 0.79 cm.; length of rod, 31.25 cm.

FIG. 1. *Schematic diagram of apparatus.*

The rod was supported on an amber insulator attached to the honeycomb at the entrance, and by a single insulated support that connected it to the electrometer at the other end. Amber insulation was used throughout. The conductivity was measured by observing the rate of movement of the electrometer fibre over a few divisions of the scale, and was given by

$$\frac{C_1 K \frac{dx}{dt}}{4\pi C V},$$

where C_1 is the capacity of the whole insulated system, collector and electrometer, and C is the capacity of the collector and its supports. K is the factor by means of which the electrometer deflection, X, is reduced to volts, and V is the voltage applied to the tube surrounding the collecting electrode. C_1 and C were measured by comparison with a standard variable condenser, and were found to be 71.9 $\mu\mu$f. and 9.6 $\mu\mu$f., respectively. The voltage applied to the tube was usually 229 volts, and, since the voltage of the collector was never allowed to change by more than a few volts from ground, the above differential expression, rather than its integrated form, was used to calculate conductivities.

A honeycomb about $\frac{3}{4}$ in. deep with $\frac{1}{8}$ in. square holes and kept at ground potential was placed at the entrance of the tube. The insulating ring between the flared entrance and the high potential cylinder was so fitted that there were no irregularities in the surface and no flow of air between the inner and outer tubes. The necessity for the honeycomb is discussed in the paper (4) describing the 1931 flights. It is shown that the air in the tube would be very turbulent if this honeycomb were not used. Since the velocity of the air through the honeycomb is very high, the number of ions lost to its metal surfaces by diffusion would be negligible. Hence the loss in conductivity due to its presence would be limited to the loss of ions brought into contact with the metal by the motion of the air through it. As only a small part of the total air passing through the honeycomb can come into contact with the metal, the loss due to its presence would not be expected to be appreciable. A reversing switch in the battery circuit made it possible to change the potential of the cylinder quickly from positive to negative.

The conditions under which this equipment will measure conductivity are also discussed in the previous paper (4). The velocity of the air in the tube, and the potential, dimensions, and other factors must be such that a radius r_0 given by the equation

$$r_0{}^2 \approx \frac{2MVL}{v \, \log \frac{b}{a}} \tag{1}$$

must be less than the radius of the inner tube b; V is the potential, M the mobility, L the length of the tube, v the velocity of the air stream, and a the radius of the collecting electrode. An air speed indicator was carried on one of the flights, and at various times during the flight the pilot tube was held in the rear end of the conductivity tube in order to obtain an approximate

measure of the air speed.   The speed indicated under observation conditions was about 90 miles per hr.   If the worst case at high altitudes be taken, with a mobility of say 3 cm. per sec. per volt per cm. and an air speed in the tube of 3000 cm. per sec. (about 67 m.p.h.), then the value of r_0 given by Equation (1) is 2.5.   This is sufficiently less than the radius of the tube (3.8 cm.) to ensure that a condition of saturation would not be reached.

In the 1931 flights the conductivity tube was mounted on the bottom of the plane a few inches below the fuselage, the apparatus being supported through the camera hole.   In the present apparatus the tube was mounted about a foot under one wing; the supports projected out through a window and held the tube 8 or 10 in. from the cabin fuselage.   A high wing, cabin monoplane was used.   Owing to the fact that the velocity of the ions is small compared with the speed of the aeroplane, any fields produced by charges on the aeroplane would have no effect on the conductivity.   The possibility of ionization due to the propeller motion, heat from the engine, or contamination by exhaust gases must also be considered.   It is doubtful whether temperatures high enough to cause any appreciable ionization would be encountered, and, in view of the relative speed of rotation of the propeller and its forward motion through the air, it is doubtful whether enough air would be ionized: to affect the conductivity seriously.   The exhaust manifold carried the gases well below and to the rear of the conductivity tube; hence, apart from the possibility of leaks in the manifold, no contamination would be expected.   As the probability of there being a leak small enough to affect the results without changing the order of magnitude of the conductivities was small, no special tests for such contamination were made.   A location for the conductivity tube well clear of the slip stream would have been preferable, but practical considerations made it impossible to mount it sufficiently far from the cabin to be completely out of the stream of air that passed close to the engine or propeller.

The Potential Gradient Apparatus

An attempt was made to measure the potential gradient near the plane by means of radioactive collector.   The radioactive material (radium DEF mixture) was located in a small shielded, but well ventilated, chamber on the end of a rod placed in the air stream.   This rod was used in two positions. In Flights 1 to 4 it extended vertically through the bottom of the cabin so that the radioactive head was about level with the bottom of the wheels during flight; it was about 2 ft. below the fuselage.   It was therefore necessary to draw it up during take-off and landing.   In Flights 5 to 7 the rod was placed through a side window and supported by a strut pointing downwards at an angle of about 45 degrees.   The end extended about 2 ft. beyond the wing struts, and was about $1\frac{1}{2}$ ft. off the ground, when the aeroplane was on land, and 6 ft. out from the bottom edge of the cabin fuselage.   The same electrometer was used for measuring the potential gradient and the conductivity.   Its suitability for both purposes will be discussed in the next paragraph.   That this method did not prove successful as a measure of

potential gradient was not entirely unexpected. Its failure is due to charges acquired by the aircraft or perhaps by the rod supporting the collector as it moves rapidly through the air. It did, however, prove useful in one flight near a thunderstorm, when sudden changes in potential could be observed readily.

The Electrometer

The electrometer employed in the 1931 flights was reconditioned and used in the present experiments. A single Wollastan wire fibre about one inch long, suspended between two knife edges, was used. The knife edges were charged to plus and minus 45 volts. The electrometer and galvanometer used in conjunction with resistance thermometers for relative humidity measurements were mounted on a vibration proof support. With some alterations in design, after the first flight, a very satisfactory method of support was achieved.
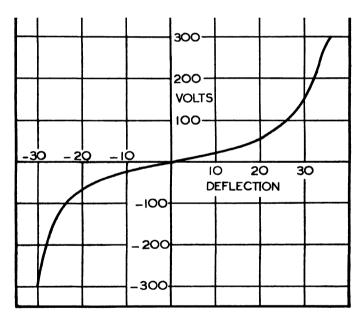
FIG. 2. *Typical calibration curve for the electrometer.*

The electrometer was particularly well adapted for the purpose, in view of the shape of its calibration curve. Fig. 2 shows a typical calibration curve. At low voltages the sensitivity was of the order of one division per volt and reasonably linear over a range of ± 10 volts. The conductivity measurements were always taken over a range of less than 10 divisions on each side of the zero positions. As the voltage was increased, the sensitivity decreased to such an extent that voltages as high as about 350 could be read as accurately as the conditions of the experiment required.

The electrometer did not retain its calibration as steadily as might have been desired. The sensitivity changed somewhat with temperature, particularly at the higher voltages. Calibration curves were prepared before and after each flight, and some points could be determined during flight. By comparing these points with the calibration curves, a curve could be obtained which was within 5% of the correct value over the range in which conductivities were measured. For conductivity measurements, the slowest rate of movement of the fibre measured was of the order of a division in two minutes. Rates up to several divisions per minute were observed as the conductivity increased at high altitudes. It is estimated that the probable error would be less than 10% for high altitudes but perhaps somewhat higher in the low conductivities at low altitudes, allowance being made for a slight zero shift with different altitudes of the plane.

Meteorological Instruments

In addition to conductivity and potential gradient, relative humidity, temperature, and pressure were measured. For relative humidity measurements, two resistance thermometers were used, one of which was wet periodically throughout the flight. These were connected to a bridge circuit (3) which gave a measure of the difference between wet and dry bulb temperatures. These thermometers were placed in the slip stream. By an alteration in the circuit one of them could be used to measure the dry bulb temperature. Since the thermometers were under one wing and well shielded from direct sunlight and well ventilated, no special radiation shields were provided. The temperature was also measured by a strut thermometer placed well out of the slip stream. The temperature in the slip stream was usually about two degrees higher than that of the surrounding air, owing to the fact that the air cooling the engine was mixed in the slip stream. Relative humidities were calculated by means of the partial water vapor pressure in the slip stream and the temperature of the surrounding air as measured by the strut thermometer. Smithsonian meteorological tables were used for the reductions.

A Tycos aneroid barometer was also carried. This was of a meteorological, aeroplane type, and had been calibrated against standards before the series of flights. Approximate altitudes were noted by observing the altimeter on the plane's instrument panel.

Experimental Procedure

The procedure adopted in each flight was as follows: After the apparatus had been mounted in the aeroplane and notes taken on the weather conditions on the ground, the flight was started. The first observations were usually taken at an altitude of 1000 ft., as read on the aircraft altimeter. After that, observations were taken at 2500 ft., 4000 ft., and at levels every 2000 ft. higher. Conductivity readings were taken while the aeroplane was flying level and as nearly as possible at constant speed. Usually four conductivity observations were taken at one level, two of each sign. The temperature readings were taken between conductivity observations; this ensured that the

plane had been flying at a constant level long enough for the thermometers to reach equilibrium. After the conductivity and temperature readings were recorded, a reading was taken of the potential indicated by the radioactive collector. The pressure also was noted, usually several times, at each level. During ascent between levels, potential gradient readings were taken, and water was sprayed on the linen covering of the wet thermometer.

Clouds were avoided as much as possible during ascent, but during descent, if clouds were within reach, conductivity and potential measurements were taken while the aeroplane was flying just over the top of the clouds. Potential measurements were made during the descent through the clouds, and another set of conductivity and potential measurements were taken just below the clouds. No consistent observations other than these were made on conductivity during descent. To avoid turning while readings were taken and during climbs, the plane was usually flown more or less in a straight line, usually starting from Ottawa towards Montreal, and returning over the same route, or perhaps turning southward and flying along the St. Lawrence river for a short distance before returning to Ottawa. The country covered is a relatively flat area between the Ottawa and St. Lawrence rivers, and, though the course varied, the flights usually covered a distance of from 50 to 100 miles east or southeast of Ottawa and return by a triangular route. The time required to complete the flight was about three hours. In Flights 1 to 3, owing to imperfect engine adjustment for high altitude, only 10,000 to 11,000 ft. was reached, but in Flights 4 to 7, 15,000 to 16,000 ft. was reached, this being about the ceiling for the plane used, unless unreasonably long times were taken to climb between levels.

As the planes used for these flights were also used for other purposes which took precedence over the atmospheric electric observations, and because the author had other work on hand, the flights had to be arranged at times convenient to the parties concerned rather than at the times of occurrence of chosen weather conditions.

Results

Variation of Conductivity with Altitude

The results of each flight will be discussed separately and then all results will be summarized, particular reference to the observations near clouds being left for a later section. The recent flights are numbered one to seven in the order in which they were made, and the two 1931 flights, which are rediscussed, are numbered 3A and 4A; these were Flights 3 and 4 mentioned in the previous paper.

Flight 1—September 1, 1936. Fig. 3

At the beginning of the flight the sky was mostly overcast with stratus clouds a few hundred feet thick and at a height of about 5000 ft. Towards the end of the flight the sky cleared slightly. Weather maps show a weak front passing over Ottawa on September 1. At 8 hours there was a centre of low pressure over the Gulf of St. Lawrence; a high, north of Hudson Bay;

and another low, west of Lake Michigan. This was the only flight during which the aeroplane flew through clouds on ascent. Fig. 3 shows the positive and negative conductivity, relative humidity, temperature, specific humidity, and partial potential temperature. The meteorological observations show a different air mass above about 6000 ft., or above the cloud level. The conductivity, instead of increasing continuously, shows a discontinuity at the cloud level and an excess of positive conductivity above the cloud. The potential gradient observations indicated that the cloud probably contained a considerable quantity of electric charge. However, as will be discussed
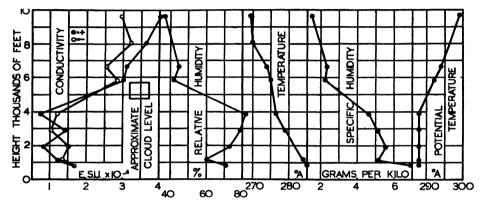
FIG. 3. *Flight 1.*

later, just what the potential gradient apparatus measured was not very certain; consequently, conclusions drawn from observations with it are somewhat speculative. As the air above the cloud layer was very stable (probably polar continental), it is unlikely that the excess of positive conductivity was due to a flow of ions or condensation nuclei from lower levels into this region. A possible explanation lies in the reduction of the negative ion density owing to a tendency to neutralize positive charge in the upper part of the cloud. This is also indicated by the fact that the negative conductivity is considerably below the average of that observed in all flights at the levels from 6000 to 10,000 ft., while the positive conductivity is about equal to the average (see Fig. 12).

During the summer of 1936, including the time at which Flights 1 to 4 were made, potential gradient observations were taken on the ground at a country station about seven miles northwest of Ottawa (5). The results showed a definite relation between the passage of fronts and disturbances in the potential gradient.

On September 1 a minor disturbance in the potential gradient that started shortly before noon was noted. As there was no precipitation, this was probably due to increased turbulence in the lower air. The conductivity record below cloud levels also showed virtually no increase of plus or minus

conductivity up to cloud levels, probably owing to an unusual distribution of condensation nuclei due to the turbulence near the frontal surface.

Flight 2—September 11, 1936.   Fig. 4

The sky was completely overcast, there being two definite cloud layers. The lower layer consisted of very irregular cumulus or stratocumulus clouds of varying heights lying between 2000 to 6000 ft. and covering about 40 to 60% of the sky.   A small local thunderstorm occurred during the latter part of the flight, and observations were taken near it.   These will be described later.   The upper layer of clouds (altostratus) was well above the
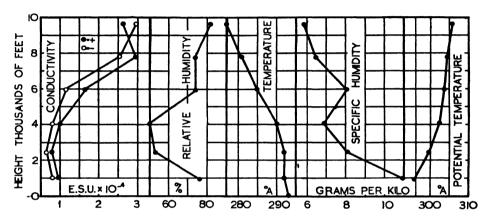
FIG. 4.   *Flight 2.*

highest level reached, probably at about 20,000 ft., and the sky was completely overcast.   The weather maps and barograph record show a system of two or more weak fronts moving across the continent from the west.   The conductivity measurements showed values much less than average up to 6000 ft., about the upper limit of the lower cloud level.   Then a rapid increase was noted at an altitude of 7800 ft. and no definite further increase at the highest level at which observations were made, 9620 ft.   The positive conductivity was higher than the negative except at the highest level.

Flight 3—September 22, 1936.   Fig. 5 .

On September 22, as on September 11, two cloud layers were noted.   The lower layer consisted of a few scattered fractocumulus clouds at about 4000 to 6000 ft.   The upper layer almost covered the sky and was quite thin and very high, probably altostratus.   The weather conditions are shown in detail in Fig. 7 of the paper (5) describing the potential gradient observations on the ground.   The 8 a.m. weather map for September 22 shows a weak cold front in an east-westerly direction just north of Ottawa.   On September 23 this had become a warm front and had receded some distance farther north. At the time of flight, while the aeroplane was flying at an altitude of 6100 ft., the temperature suddenly rose about 2° C.   The point is marked "X", in

Fig. 5. The specific humidity curve shows a discontinuity at this point. Apparently the aeroplane had entered a different air mass. The conductivity curves are abnormal. Very low values were noted at 1000 and 2800 ft., then after the usual increase up to about 6000 ft., abnormally low values were again noted at the higher altitudes. No doubt these abnormal values were the result of changes in the ionic equilibrium near the frontal surface, though there were no clouds near the line of flight.
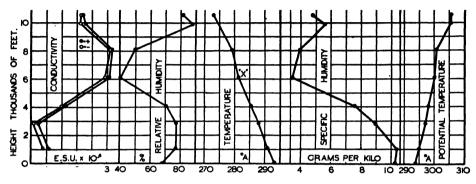
FIG. 5.   *Flight 3.*

Flight 4—October 9, 1936.   Fig. 6

At the beginning of this flight no clouds were visible, but when an altitude of a few thousand feet was reached a small bank of stratocumulus was noted some distance to the east, and a few scattered fractocumulus some distance to the south. A detailed description of the weather conditions is given in Fig. 8 of the report (5) on potential gradient observations on the ground. The weather map showed an anticyclonic condition with a depression west of Lake Superior. The barometer was falling slightly at the time of the flight; the centre of the anticyclone had therefore just passed. There was considerable haze and a light northeast wind typical of conditions just after the passing of a centre of high pressure. The conductivity shows a fairly steady increase with height up to the highest level reached, the values of the positive and negative conductivities being virtually the same.

Flight 5—November 16, 1936.   Fig. 7

The sky was almost covered with low broken stratocumulus or nimbocumulus clouds, and occasional light snow flurries were noted. The weather map shows a deep depression over the Labrador coast, a high over the Mississippi Valley, and another high over northwestern Hudson Bay. The barometer was rising rapidly owing to the anticyclone spreading over the southeastern United States. The low broken clouds, the shape of the potential temperature curve, and the fact that the air was quite bumpy at low levels indicate considerable turbulence at levels up to 5000 or 6000 ft. Above this level the air was quite clear and very cold, the temperature dropping to
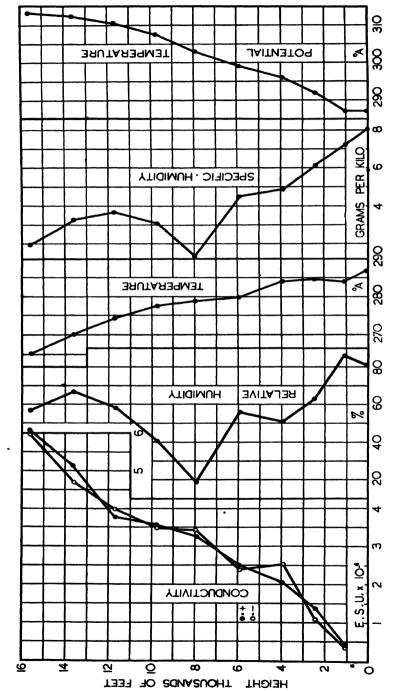
FIG. 6. *Flight 4.*

FIG. 7. *Flight 5.*
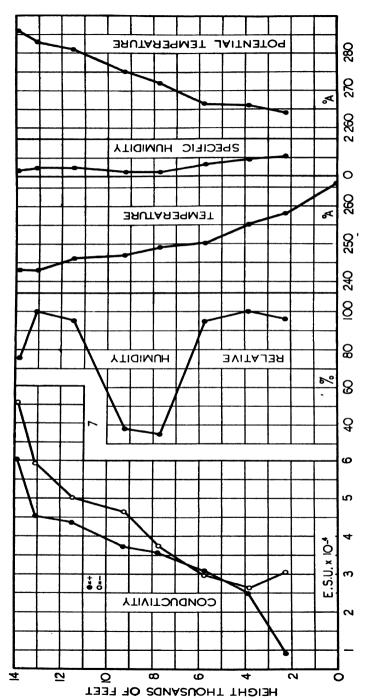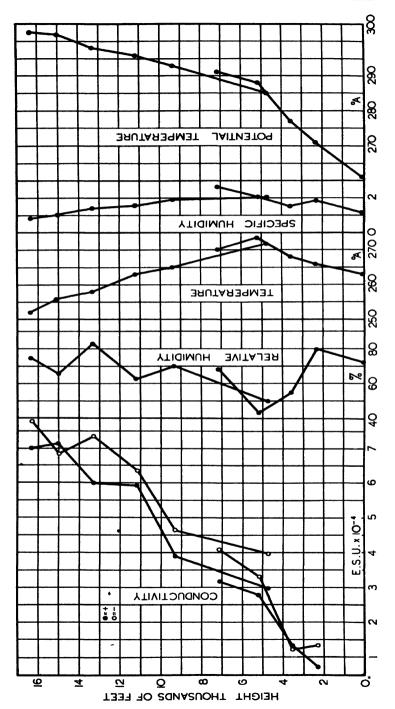
FIG. 8. *Flight 6.*
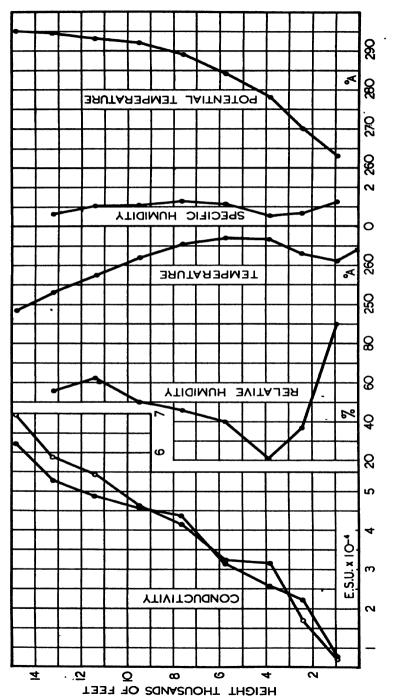
FIG. 9.   *Flight 7.*

$-30°$ C. at 13,000 ft. The conductivity increased fairly consistently with height, with the exception that an unusually high negative value was noted at the lowest point observed. No definite reason for the high negative conductivity at this point is apparent, though the cloud formation was such that local space charges might be expected and an unusually high potential gradient was recorded at the same level. Unfortunately the continuous recording of potential gradient at the ground station outside Ottawa had to be discontinued about November 1; the general behavior of the potential gradient at the time of this and subsequent flights was therefore not observed. The negative conductivity was considerably higher than the positive at levels of 9000 ft. and higher. It should be noted, however, that owing to the very low temperatures encountered in this flight, the calibration of the electrometer was not known as accurately as it was in other flights.

Flight 6—December 9, 1936.   Fig. 8

On the morning of December 9 the sky was clear, but at the time of the flight it was completely overcast, there being two definite layers. The lower layer, uniform stratus, covered about half the sky with a definite boundary, and was about 3000 ft. high. The upper layer, thin altostratus, was well above the highest point reached. The 8 a.m. weather map shows a centre of high pressure over the Gulf of St. Lawrence, and a series of lows over the middle western parts of the United States and the prairie provinces in Canada. The barometer was falling as a centre of low pressure was obviously approaching from the west. After the plane had reached a height of about 7000 ft. it was brought to the ground to permit a passenger to disembark, and the flight was then resumed. The curves in Fig. 8 are broken accordingly. The agreement in values found at overlapping levels is reasonably good. During ascent the observations at 3600 ft. were taken near the edge of the lower cloud bank, but no attempt was made to fly in the cloud. Throughout most of the flight the negative conductivity was higher than the positive.

Flight 7—February 16, 1937.   Fig. 9

The weather on February 16 was typical of an approaching anticyclone. The barometer was rising, the visibility very good, and the sky clear, except for scattered cirrus clouds forming cirrostratus. A light northwest wind was blowing. The weather map shows an elongated centre of high pressure running northward from the upper Great Lakes. Two fairly deep lows are shown on the Atlantic coast; one north of Newfoundland and one centered over the eastern United States just north of Florida.

The conductivity increased steadily with altitude, positive and negative values being nearly the same at low altitudes, and negative values being higher at heights above 10,000 ft. The conditions of this flight probably represent as nearly as possible those to be expected in fresh polar continental air coming over completely snow-covered and mostly uninhabited territory. It is interesting to note that the conductivity curves more closely resemble the average

of those for the seven flights (Fig. 12) than does any other, though the conductivity is higher at low altitudes.

Flight 3A—April 18, 1931.   Fig. 10

Flight 4A—June 7, 1931.   Fig. 11

Conductivity of one sign only was measured during ascent and of the other sign during descent in all the 1931 flights.   Hence Figs. 10 and 11 show the meteorological observations during both ascent and descent.   In Flight 3A there was but little difference in conditions, but in Flight 4A the humidity curves for ascent and descent are rather different.   The relative humidity observations, however, for descent are not very reliable at points where the temperature was below freezing, because the water supply was usually frozen after two or
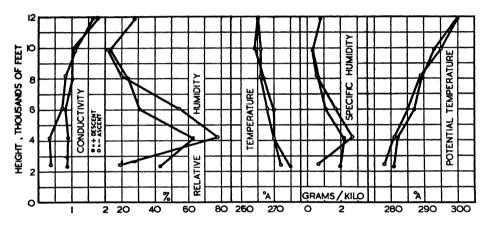
FIG. 10.   *Flight 3A.*
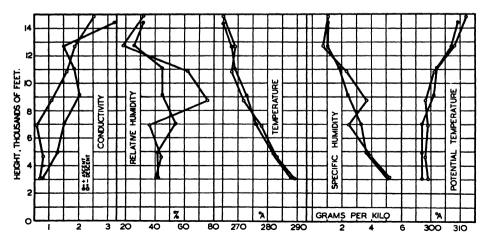
FIG. 11.   *Flight 4A.*

three hours' flying, and the wick could not be properly wetted between obser-
vations.   In the present work (Flights 1 to 7) precautions were taken to keep
the water supply from freezing; and, also, the thermometers were in a more
accessible position for wetting.

Weather notes on the days of Flights 3A and 4A are not as complete as
were those of the recent flights, though as the 1931 flights were all taken in
reasonably fine weather, the weather was anticyclonical and the sky was
clear or only few fractocumulus clouds were present.   As the reduction factor,
necessary to reduce to conductivity the readings taken with the 1931 apparatus
was not very accurately known, the conductivity units in Figs. 10 and 11 are
arbitrary.   In general, however, the conductivity increases with height, though
the amount of the increase seems considerably less than that in the seven
recent flights. .

Mean Variation in Conductivity

The mean curves for the variation of positive and negative conductivities
with height, as shown in Fig. 12, were obtained in the following way.   As
the conductivities on different flights were not all measured at exactly
the same altitudes, those at a height from, say, 500 to 1750 ft., were
averaged and the heights were averaged, and thus a mean value was obtained.
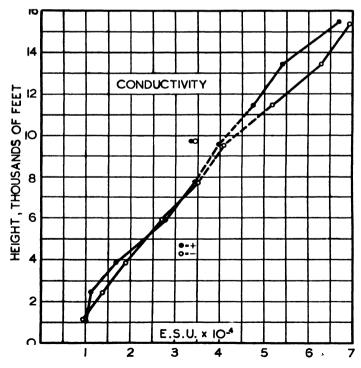
Fig. 12.   *Mean conductivity curves.*

A second point included observations at heights between 1750 and 3250 ft., another between 3250 and 5000 ft., another between 5000 to 7000 ft., and so on. As most of observations were taken at or near 1000, 2500, 4000, 6000 ft. etc., the averages represented closely the means of the conductivities taken at these levels. The data obtained in the 1931 flights are not included in the average. If all observations were included, the portion of the curves shown by the broken lines would include the points to the left of that part of the curve at conductivities of $+3.3$ and -3.4, and at a height of 9705 ft. instead of as shown. The points through which the curve was drawn at this level were obtained by excluding the observations at the highest altitudes on Flights 2 and 3, where there is an abnormal reduction in conductivity. In Flight 2 there was definite evidence of intense charges in nearby clouds; a thunderstorm was passed not very far from where the measurements were taken. In Flight 3, a frontal surface was encountered at an altitude of about 6000 ft. Certain points taken during Flight 1 might also have been excluded, as a front was encountered in that flight also. Their exclusion, however, would not have made very much difference in the shape of the mean curve.

Observations at ground levels have shown that on the average the potential gradient is positive, and a positive space charge is found. It is generally accepted that this falls off very rapidly with height; consequently, at the lowest point included in Fig. 12 no appreciable space charge would be expected. Once the space charge becomes negligibly small, the ratio of plus and minus conductivities must be equal to the ratio of the effective mobilities of the positive and negative ions present. In regions at low altitudes, in which the number of condensation nuclei is appreciable, the conductivity is reduced considerably by the presence of the nuclei, and it would be impossible to predict with any accuracy much about the ratio of positive to negative conductivities. Over a considerable range of much higher altitudes, in the stratosphere, where the density of nuclei is thought to be negligible, Gish and Sherman (2, pp. 94-116) found the ratio of the conductivities to be equal to that of the mobilities of positive and negative ions. In the present results (Fig. 12) the mean values of the positive and negative conductivities are almost equal at the lowest altitude. From about 1500 to about 5000 ft. the positive conductivity is slightly less than the negative, though in view of the small amount of data available, it is doubtful whether the difference is significant. Hence, from about 1000 to 10,000 ft. the curve indicates that the positive and negative conductivities are very nearly equal in magnitude. If one accepts the assumption that there is no space charge, then, in view of the fact that small negative ions are invariably found to have greater mobilities than small positive ions, equal conductivities would indicate that the loss of small negative ions, due to combination with condensation nuclei or with large positive ions, is greater than the corresponding loss of small positive ions. Scrase (6) has estimated the combination coefficient of the various types of ions, and finds that the combination coefficients of small negative ions with uncharged nuclei and

with large positive ions are greater than the corresponding coefficients for small positive ions with uncharged nuclei or with large negative ions. Though he expressed some doubt as to the validity of the equations used, the results here are at least in qualitative agreement with the relative values of the coefficients found.

At the higher levels, above 10,000 ft., the effect of nuclei becomes less and the value of the negative conductivity becomes greater than the positive. The ratio (mean of three highest points gives 0.92), however, is higher than the value (0.78) found by Gish and Sherman (2, pp. 94-116) at still higher levels on the stratosphere flight. The transition to a nuclear free state would not be expected to take place rapidly, and would probably not be complete until the stratosphere was reached; a close agreement in this ratio is therefore not to be expected. The actual magnitude of the conductivities at different heights agrees reasonably well with the values found by Gish and Sherman and with those of Wigand (9, 10).

In regard to the differences in the curves in Figs. 3 to 11, there is little further to be said. Where obvious explanations of differences between individual curves and the mean curves exist, these are noted in the individual discussions of the flights. It should be noted that these curves represent conductivity observed on ascent only, where clouds were avoided as much as possible, and the aeroplane flew through no clouds except in Flight 1.

Potential Gradient Observations

That the method used for measuring potential gradient is impracticable when applied to observations taken in aeroplanes is shown by the following. First, the position of the potential electrode in the bottom of the plane was such that, in the normal earth's field, that is, positive with height, if the aeroplane and the collector electrode took up the potentials of the air at their corresponding levels, the potential of the collector electrode should be negative with respect to the plane. In fact, virtually all readings taken while the aeroplane was flying level and the sky was free from clouds were positive. Second, the nature of the readings when the plane was climbing, flying level, and descending was such that some effect other than the atmospheric electric field must have been predominant in the potentials measured, except when high potentials were encountered near charged clouds.

That the potential measurements are not reliable can be seen when the measurements of Flight 3 are examined. At the lowest altitude, 1080 ft., a steady potential of +35 volts* was observed while the aeroplane was flying level. As soon as the plane was put in a climbing attitude and the engine throttle opened accordingly, the potential started to decrease, dropping to values as low as −10 volts. While the aeroplane was flying level at the next altitude at which conductivity measurements were taken, namely 2830 ft.,

* *It is difficult to estimate the gradient in volts per metre that this would represent, unless a model of the aircraft was constructed.*

the potential rose to +143 volts. During the next climb between levels it dropped again to 45 volts, and when the flying was level at 4050 ft. it rose to +177 volts. This drop in potential occurred more or less consistently during periods of climb at low altitudes. Once altitudes of 8000 or 10,000 ft. were reached, the drop would be only a few volts, and on a few occasions an increase in potential during ascent was noted. During descent, with the engine idling, irregular variations in potential would sometimes take place, and sometimes it would merely decrease regularly until levels near ground were reached.

In view of these observations, the results of the potential gradient measurements are not considered worth publishing in detail, and only those taken when the aeroplane was flying near a thunderstorm will be shown. It was not entirely unexpected that this method of measuring potential gradient would not be satisfactory, because of the highly ionized state of the engine exhaust gases. Wigand (8) has shown that these may bear a net charge, and therefore the plane will have an opposite charge. Further, the potential observations are nothing more than a measure of the potential between an insulated rod and the plane. The action of the radioactive collector and the rod supporting it in a very rapidly moving air stream is uncertain. As the plane is constantly acquiring a charge owing to the effect of the exhaust gases, or by other means, and the electrode is constantly losing a charge owing to removal by the field of more ions of one sign than of the other, it is the difference between these two effects that will be observed. Apparently these effects under normal cloud-free conditions are such that the earth's field is reversed, and, from the magnitude of the voltages measured, the spurious effects appear to be greater than the normal earth's field.

Observations Near Clouds

During flight through clouds, conditions were changing too rapidly to permit conductivity readings to be made. Only readings on the potential gradient electrode were taken. The aeroplane flew through clouds during descent on Flights 2, 3 and 5, and a cloud layer was penetrated during ascent on Flight 1. On the other flights, either no clouds were present or they could not be reached easily.

The positive potential measured in normal, cloud-free areas, though it varied considerably in no consistent manner, was usually between about 50 and 200 volts. During flight near or through clouds, if potentials no greater than about 200 volts were encountered, the results were considered to indicate that no great local charges were present. If the potential measuring apparatus indicated voltages of several hundred volts, it was considered a fair indication that local space charges existed nearby. As the potential electrode was on the bottom of the plane, positive potentials would normally be expected to indicate a negative field. This might be due to a large negative charge higher up, a positive charge below, or a combination of both. Reversals in the field might mean that the aeroplane was flying through a centre of space

charge, or that a point was passed at which there was a field reversal due to, say, a combination of nearby local volumes of positive and negative space charges. Such a reversal usually occurs at ground levels when a thunderstorm passes overhead. However, during flight through clouds in which there is considerable space charge due to charged water drops, the potential difference between the plane and the collector will more likely be fixed by the relative amounts of charge picked up and lost by both, as the result of the water drops wetting the surface and then being blown off as a fine spray. The resulting potential would give a measure, not of the potential gradient, but of other effects. The fine spray blown off the struts and other parts of the plane can easily be seen during flight through rain or heavy mist. If the temperature is at or below the freezing point, and the cloud particles consist wholly or partly of ice crystals, the resulting charges acquired by the plane and collector would again be expected to be different. Hence, though charges were observed in clouds on three flights, the details of which are described below, unfortunately no conclusions as to their exact polarity or location can be drawn until better methods of observation are obtained.

In Flight 1, while the aeroplane was ascending it was necessary to fly through a fairly uniform layer of stratus clouds. During ascent towards the clouds the potential rose rapidly to about 400 volts at an altitude a little higher than 4000 ft., then as the aeroplane passed through the cloud the potential reversed to a high negative value (about −250 volts). Just above the cloud while the aeroplane was flying level at 6000 ft. it remained negative (−65 volts), then at higher levels became positive again. How much of the negative potential observed was due to the change in attitude of the plane, as described in the previous section, and how much was due to space charges in the cloud is uncertain. However, just below the cloud an unusually high positive potential was observed, and just above, a negative value was recorded when the aeroplane was flying level. It might be noted that the conductivity observations are not inconsistent with the assumption of a positive charge in the cloud.

In Flight 2, during descent, a small thunderstorm was passed, the line of flight lying a mile or two to the north of the centre of the storm. It was not known until after landing that the storm had developed into a thunderstorm, as no lightning was seen during the flight. The potential measurements taken as the plane flew towards the storm, at an altitude about equal to that of the top of the clouds, and then as the plane descended through the clouds around the outer edge of the storm centre, are shown in Fig. 13. The storm was quite small, and the cumulus cloud at its centre extended only up to about 7000 ft. The largest cloud shown in the figure represents the storm centre, and, if the path of the aeroplane as shown is considered to be in a vertical plane, the direction of flight being west, the storm centre was estimated to be about two or three miles to the south. Though considerable rain and mist was encountered, the only part of the flight which penetrated clouds of sufficient density to limit visibility to such an extent that ground or cloud forms

were completely obscured is indicated by *CC* in Fig. 13. The horizontal axis represents very roughly the distance in miles. The sizes of the clouds as shown should not be considered in relation to this scale, as the cloud areas could be drawn only roughly from memory after the flight and the few notes taken on cloud formation. The line of flight was sufficiently far away from the storm centre that no great turbulence was noted.
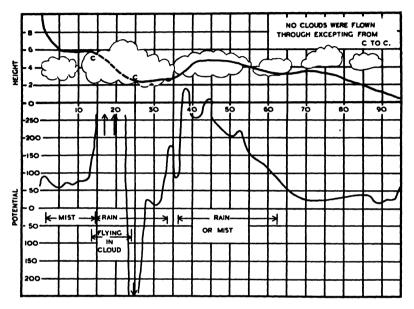
FIG. 13.   *Changes in potential during flight near a thunderstorm.*

If it could be assumed that the potential electrode was behaving in the normal way, and that the electric charges involved were in the cloud at the storm centre, then the polarity of the cloud would appear to be opposite to that found in the Wilson type of thunderstorm. If it is assumed that the potential of the collecting electrode is fixed by the effect of water drops striking it, then the polarity it will assume for a given type of space charge is still ambiguous. A few conductivity measurements were taken shortly before the cloud was entered. Conductivities from 5 to 45 E.S.U. were noted but they were changing too rapidly to permit a decision to be made as to whether positive or negative was higher.

The only other occasion on which excessive potentials were noted was during ascent in Flight 5. During flight at the lowest level observed, namely, 2270 ft., an unusually high potential (about 400 volts) was recorded. At the same level the negative conductivity was much greater than the positive (see Fig. 7). This level was considerably below the base of the clouds, and, though no precipitation was noted when the observations were made, there had been a slight snow flurry just before the take-off, and another during the landing. Under such circumstances local space charges would not be unexpected.

On Flights 3 and 5 the aeroplane flew through clouds during descent. Small isolated clouds of the fractocumulus or fractostratus type were chosen. No changes of sufficient magnitude were noted in the potential measurements to indicate any quantity of local space charge.

To investigate the effect of clouds on conductivity on some occasions during descent, conductivity measurements were taken during flight just above the tops of clouds, and another set immediately afterwards just below the clouds. In Table I these are compared with the mean values of conductivities as shown by the curve in Fig. 12. Most of the differences are negative; that is, the presence of the clouds appeared to reduce the conductivity. Exceptions are shown in Flights 1 and 5. In both cases there is some evidence of local space charge in the cloud, and in Flight 5 the differences are small. The two sets of observations recorded during Flight 3 were taken some distance apart, and there was considerable difference in cloud level.

In conclusion it may be stated that the use of aeroplanes in studying atmospheric electricity could give a great deal of information about atmospheric electric effects if extended to regular flights and flights under chosen conditions. Some other method of measuring potential gradients should be

TABLE I

Flight and sign		Conductivities		Differences* from mean		Altitude, ft.	
		Above clouds	Below clouds	Above clouds	Below clouds	Above clouds	Below clouds
1	+	3.02	0.73	+0.32	−0.92	5860	3870
	−	2.85	1.22	+0.20	−0.63		
3	+	1.55	0.73	−0.7	−0.8	4890	3520
	−	1.35	0.88	−1.0	−0.9		
3	±	1.73	1.36	−1.2	−0.7	6290	4700
	−	1.54	1.13	−1.3	−1.1		
5	+	3.00	2.01	−0.2	+0.35	7260	3850
	−	3.12	2.21	−0.08	+0.3		

* *Positive differences indicate conductivities higher than the mean value.*

developed. A generating voltmeter would possibly be satisfactory, or a doublet might be used which would give a measure of the difference in potential between similar electrodes above and below the plane.

At present it is generally accepted that the process of building up charges to produce thunderstorms involves the forming and the breaking up of water drops, or their motion in ionized air (11). In Flight 2, in which there was evidence of charged clouds, considerable precipitation was noted in regions where high potentials were encountered. In Flight 1 no precipitation was observed, and in Flight 5, though no precipitation was noted at the point at which the high potential gradient was recorded, local snow flurries were

noticed shortly before and after the flight. The physical state of the cloud must be important. During Flight 5 the temperature at cloud levels was well below the freezing point; the cloud, therefore, probably consisted of ice crystals. If further measurements were made with improved apparatus, and more detailed attention were given to the nature of the clouds, it should be possible to obtain strong evidence for or against present theories regarding the generation of electric charges in thunderstorms.

Acknowledgments

References

1. GISH, O. H.   Actual and potential results from electrical exploration of the atmosphere. Trans. Am. Geophys. Union, Seventeenth Annual Meeting.   1936.

2. GISH, O. H. and SHERMAN, K. L.   Stratosphere Series No. 2, National Geographic Society.   1936.

3. ROSE, D. C.   Can. J. Research, 5 : 156-161.   1931.

4. ROSE, D. C.   Can. J. Research, 5 : 625-635.   1931.

5. ROSE, D. C.   Can. J. Research, A, 15 : 119-148.   1937.

6. SCRASE, F. J.   The charged and uncharged nuclei in the atmosphere and their part in atmospheric ionization.   Air Ministry, Geophysical Memoirs, 64.   1935.

7. SIMPSON, SIR GEORGE and SCRASE, F. J.   Proc. Roy. Soc. London, 161 : 309-352.   1937.

8. WIGAND, A.   Ann. Physik, 85 : 333-361.   1928.

9. WIGAND, A.   Phys. Z. 22 : 36-46.   1921.

10. WIGAND, A.   Ann. Physik, 66 : 81-109.   1921.

11. WILSON, C. T. R.   J. Franklin Inst. 208 : 1-12.   1929.

THE REFRACTIVE INDICES OF LIQUID HELIUM I AND HELIUM II[1]

By H. E. JOHNS[2] AND J. O. WILHELM[3]

Abstract

The refractive indices of liquid Helium I and Helium II were measured by means of a Wollaston cell. The value obtained with $\lambda 5461$ Å for He I at 4.2° K was 1.0206 ± 0.0012; for He I at 2.26° K, 1.0269 ± 0.0004; and for He II at 2.18° K, 1.0269 ± 0.0004. It was also shown that the index changed by less than ± 0.00007 in passing from a point in He I to a point with the same density in He II. It was concluded, therefore, that there is no change in the molecular refractivity in passing from He I to He II.

Experimental

The apparatus employed was essentially the same as that used in the measurement of the refractive indices of liquid oxygen, nitrogen, and hydrogen, as described by the authors (1). In order to measure the very much smaller refractive index of liquid helium the optical arrangement was altered. Two vertical slits were used as a collimator; consequently, the light reached the cell in a very narrow parallel beam. When the cell was turned to large critical angles of approximately 80° it was found that the beam was deviated slightly. This was due to the fact that the cell was slightly prismatic at the edges and at such large angles, even with a narrow parallel beam, much of the light passed through the cell near its periphery. Because the rays were deviated, the telescope could not be used in a fixed position but had to be rotated to follow the image as the cell was turned. When the illumination suddenly disappeared the readings on the divided head were taken. Four settings were made in this manner, both sides of the cell being used. On account of the slight prismatic effect, readings on opposite sides of the cell did not differ by 180°, but the average of readings on opposite sides must give the correct critical angle very closely, unless the plates are badly distorted. Measurements made in this way with a telescope gave an estimated accuracy of 5′ in the critical angle, which corresponds to a variation of ± 0.0004 in the index. The measurements in He I at 4.22° K. were considerably more difficult to make owing to the larger critical angle and the vigorous boiling which took place. Since there is less interest in the refractive index in this case, the eye alone was used to determine the position at which the light was cut off,

and the setting was made only to the nearest tenth of a degree. With this method the critical angle was determined to within 20′ and the index to within ± 0.0012.

Results

The results obtained for λ 5461A° are given in Table I.

TABLE I

—	Temp., °K.	Critical angle	Refractive index	Density (2, 3)	$\dfrac{1}{\rho}\dfrac{\mu^2-1}{\mu^2+2}$
He I	4.22	78° 28′ ± 20′	1.0206 ± 0.0012	0.1255	0.109
He I	2.26	76° 51′ ± 5′	1.0269 ± 0.0004	0.1470	0.122
He II	2.18	76° 51′ ± 5′	1.0269 ± 0.0004	0.1470	0.122

In addition to making the above measurements, an effort was made to ascertain whether there was any measurable difference in the refractive indices of He I and He II at temperatures at which the liquids had the same density. For this purpose the telescope was set so that the last fringe of the interference pattern was placed in the middle of the image of the slit. Any very slight further turning of the cell would cause this last fringe to pass out of sight altogether, and thus the cell could be accurately set at the critical position. This was done with He II boiling under a pressure of 35 mm., corresponding to a temperature of 2.18° K, then the pressure was raised to 46 mm., corresponding to a temperature of 2.26° K, for which the helium had the same density. In this case the question of distortion by the plates of the cell does not enter and a change of 1′ could have been detected. The λ point was passed through several times in this way and no change in the position of the critical ray was observed. Therefore it is possible to state that the index changes by less than ± 0.00007 in passing from a point in He II to a point in He I which has the same density. We conclude, therefore, that He I and He II have the same molar refractivities.

The values obtained for the refractive indices agree with the preliminary value 1.028 $\pm$ 0.006 obtained by Wilhelm and Cove (4), as the index for He II. The refractive index was measured for one wave-length only, but the dispersion of liquid helium is plainly very small. The value of μ^2 at 2.18 ° K. is 1.0545, which corresponds closely to the dielectric constant, $K = 1.0558$ (5).

References

1. JOHNS, H. E. and WILHELM, J. O. Can. J. Research, A, 15 : 101-108. 1937.
2. MATHIAS, E., CROMMELIN, C. A. and ONNES, H. K. Leiden Comm. 172b. 1925.
3. ONNES, H. K. and BOKS, J. D. A. Leiden Comm. 170b. 1924.
4. SATTERLY, J. Rev. Modern Phys. 8 : 347-357. 1936.
5. WOLFKE, M. and KEESOM, W. H. Leiden Comm. 192a. 1927

A NEW FORM OF GAS THERMOMETER FOR USE AT VERY LOW TEMPERATURES[1]

By A. H. Woodcock[2]

Abstract

A new form of helium gas thermometer is described, which is designed for permanent installation in low temperature equipment in order to cover the difficult region between the temperatures of liquid hydrogen and of liquid helium. The device departs radically from the usual gas thermometer practice by having the volume of gas which remains at room temperature considerably larger than that of the thermometer bulb proper. It is shown theoretically that by this means the sensitivity, as compared with that of an ordinary gas thermometer with the same initial pressure and temperature, is greatly increased at the lowest temperatures. Thus it is possible to construct a thermometer which is sufficiently sensitive in the region below 20° K. to read temperatures to within 0.1° with the aid of an ordinary mercury manometer, and yet have a pressure only of the order of one atmosphere at room temperature. An experimental test has shown that the device is entirely practicable.

Introduction

The choice of suitable working thermometers for temperatures attainable with the aid of liquid hydrogen and liquid helium is a matter of some difficulty in practical low temperature work, and it is necessary to use different types of thermometer for different temperature ranges. From room temperature down to the boiling point of liquid hydrogen, 20° K, resistance thermometers are extensively used, being accurate, sensitive, and convenient. Between 20 and 14° K the vapor pressure of the hydrogen in the cryostat gives an entirely satisfactory measure of the temperature, and between 4.2 and 1.5° K the vapor pressure of helium is similarly used. The greatest difficulty arises in the range between 14 and 4° K. In this range the electrical thermometers become much less sensitive, requiring elaborate methods for the measurement of the small changes of resistance or thermal e.m.f., and it is frequently simpler to use a helium gas thermometer.

In the usual types of gas thermometer, care is taken to make the volume of gas in the connecting tubes leading to the manometer, the "dead space" which remains at room temperature, as small as possible. If it is desired to make a thermometer of this type a permanent part of the low temperature equipment, it would probably be filled to a pressure of the order of one atmosphere at room temperature. Its sensitivity is then inconveniently small for measurements of reasonable accuracy in the range desired. Sufficient sensitivity can be obtained by making the pressure approximately atmospheric at the hydrogen point, but this involves either refilling the thermometer every time it is used, or making the construction heavy enough to withstand a large pressure at room temperature.

The thermometer to be described in the present paper is designed to be sufficiently sensitive in the range from 14 to 4° K to make readings to within

0.1° with ease, and yet to have a sufficiently small pressure at room temperature that the thermometer can be permanently installed in a helium liquefier. This end is achieved by departing radically from the usual practice in the construction of gas thermometers, and making the volume of gas which remains at room temperature considerably larger than that of the thermometer bulb proper (see Fig. 1). It is still advisable to make the volume of the connecting tube, along which there is a temperature gradient, as small as is compatible with reasonably rapid action.
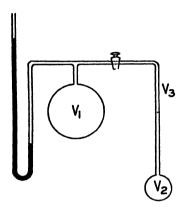
FIG. 1. *Double bulb gas thermometer.*

Although the field of usefulness of this type of thermometer is rather limited, the proposal aroused such argument that the author thought it would be of interest to construct one and test it, and that the possibility of its use might be of interest to others.

In appearance the construction is somewhat similar to the gas thermometer recently described by Mendelssohn and Pontius (1). However, the two devices are fundamentally different in their action, and in the function of the upper bulb. The thermometer designed by Mendelssohn and Pontius is intended for the measurement of small temperature changes, and, like an ordinary helium thermometer which has atmospheric pressure at liquid hydrogen temperature, has to be refilled every time it is used.

Theory

In considering the theoretical behavior of the thermometer in question, certain simplifying assumptions can be made, since it is not intended to be used when extreme accuracy is required. It will be assumed:

1. That the gas used can be treated as a perfect gas throughout the range. This will be very nearly true for pure helium from 14 to 4° K, since the pressure at the lower end of the range is considerably less than atmospheric.

2. That a steady state is reached in a reasonably short time, after which the gas in any part of the thermometer and connections is at the same temperature as the immediate surroundings in the cryostat equipment, and effects due to any further exchange of gas between the two bulbs can be neglected.

3. That thermomolecular pressure differences can be neglected in comparison with the pressures to be measured.

4. That changes in volume of the bulbs can be neglected.

Consider first a gas thermometer of the usual type, in which all volumes are negligible except that of the lower bulb. Let it be filled at room temperature

T_1 to a pressure π_1. Then at the low temperature T the pressure is given by

$$\pi = \pi_1 T / T_1 \tag{1}$$

and the sensitivity by

$$d\pi/dT = \pi_1/T_1 \tag{2}$$

which is constant over the whole temperature range.

Next consider a thermometer of the type shown in Fig. 1, in which a volume V_1 is kept at a temperature T_1, and only the volume V_2 is subjected to the low temperature T which it is required to measure. When the thermometer is first filled we have volume $V_1 + V_2$, all at pressure and temperature P_1, T_1. When it is in use we have a volume V_1 at pressure and temperature P, T_1, and a volume V_2 at the same pressure P but temperature T. Since the total mass of gas is constant.

$$P_1 V_1 / T_1 + P_1 V_2 / T_1 = P V_1 / T_1 + P V_2 / T$$

or

$$P = \frac{P_1 T (V_1 + V_2)}{(V_1 T + V_2 T_1)} = \frac{P_1 T}{T_1} \ \frac{1 + v}{1 + vT/T_1} , \tag{3}$$

where $v = V_1/V_2$ is the volume ratio.

Then the sensitivity is given by

$$\left(\frac{\partial P}{\partial T}\right)_{T_1 \ constant} = \frac{P_1}{T_1} \ \frac{1 + v}{(1 + vT/T_1)^2} \tag{4}$$

When T/T_1 is small this sensitivity becomes considerably greater than the sensitivity (Equation (2)) of an ordinary gas thermometer, supposing the initial pressure and temperature to be the same. It follows also from Equation (4) that, while an increase in the volume ratio v will increase the sensitivity at very low temperatures, it will decrease the range of temperature over which the gain in sensitivity occurs.

In operation, the upper bulb V_1 is supposed to be kept at a constant temperature T_1, and it is necessary to investigate the errors due to fluctuations in this temperature. Let the temperature of V_1 change to T_1', and the measured pressure to P', while the lower temperature remains equal to T. We now have

$$P_1 V_1 / T_1 + P_1 V_2 / T_1 = P V_1 / T_1 + P V_2 / T = P' V_1 / T_1' + P' V_2 / T ,$$

which gives

$$P' = \frac{P_1 T}{T_1} \ \frac{1 + v}{1 + vT/T_1'} ,$$

and

$$\left(\frac{\partial P'}{\partial T_1'}\right)_{T \ constant} = \frac{P_1}{T_1} \ \frac{T^2}{T_1'^2} \ \frac{v(1 + v)}{(1 + vT/T_1')^2}$$

If T_1' is approximately equal to T_1, i.e., $(T_1 - T_1')$ small compared with $(T_1 - T)$, this reduces to

$$\left(\frac{\partial P'}{\partial T_1'}\right)_T = v\left(\frac{T}{T_1}\right)^2 \left(\frac{\partial P}{\partial T}\right)_{T_1} \tag{5}$$

Therefore, when T is small, changes in temperature of the upper bulb have a very much smaller effect upon the pressure than changes in the temperature to be measured.

The effect of the finite volume of the connecting tube can be taken into account by considering an additional small volume V_3 at a temperature T_3, intermediate between T and T_1. An expression for the correction can easily be obtained if it can be assumed that the temperature gradient is uniform along the tube. However, this assumption may be far from correct in practice, and it is likely to be more satisfactory to take account of this, and other small errors, by calibrating the thermometer at two or three known temperatures, under actual working conditions.

Table I shows, for a thermometer with a volume ratio $V_1/V_2 = 10$, filled to a pressure of 100 cm. of mercury at 300° K, the calculated sensitivity at different temperatures, the calculated fluctuation due to changes in the temperature of the upper bulb, and the sensitivity as compared with an ordinary gas thermometer under the same initial conditions.

It will be seen that when

TABLE I

$V_1 = 10V_2, \; P_1 = 100 \text{ cm.}, \; T_1 = 300° \text{ K}$

T °K	$\left(\dfrac{\partial P}{\partial T}\right)_{T_1}$ cm./°K	$\left(\dfrac{\partial P}{\partial T_1}\right)_T$ cm./°K	Sensitivity as compared with ordinary thermometer
300	0.030	0.303	0.09
200	0.062	0.277	0.19
100	0.195	0.217	0.64
50	0.515	0.143	1.7
20	1.32	0.059	4.4
15	1.63	0.041	5.4
10	2.06	0.023	6.8
5	2.69	0.008	8.9

the lower bulb is at 15° K, a change of 4° in the temperature of the upper bulb has the same effect as a change of only 0.1° in the temperature to be measured. For accurate work the upper bulb ought to be kept in ice, or in a water bath at a known temperature, but for many purposes this refinement could be neglected.

Experimental Test

As a check on the calculations, a thermometer was made up as shown in Fig. 1, with volumes $V_1 = 320$ cc., $V_2 = 39.7$ cc., and V_3 about 6 cc. It was filled with pure helium to a pressure of 76.7 cm. at a temperature of 22.5° C. The gas was used first to determine the volume of the manometer connections, which form a part of the volume V_1. This was accomplished by shutting off V_2 with a tap, and then noting the change in pressure when V_1 was immersed in liquid air.

With the initial conditions stated above, the pressure to be expected at the boiling point of liquid hydrogen, 20.45° K, was calculated by Formula (3), and found to be 31.16 cm. The measured pressure with the bulb V_2 in hydrogen boiling at atmospheric pressure, and V_1 simply exposed to the room, was 30.7 cm.

The curve in Fig. 2 shows the calculated relation between pressure and the temperature. T of the lower bulb, for the thermometer used. The dotted

straight line shows the behavior of an ordinary gas thermometer, with V_1 negligible, under the same initial conditions. The circle marks the test reading made at hydrogen temperature. The agreement is close enough to show that the predicted gain in sensitivity is actually attained at temperatures below about 80° K, and that the device is entirely practicable. It ought, however, to be calibrated at two or three known temperatures, under actual working conditions, in order to allow for small errors due to the connecting tube, and other causes.
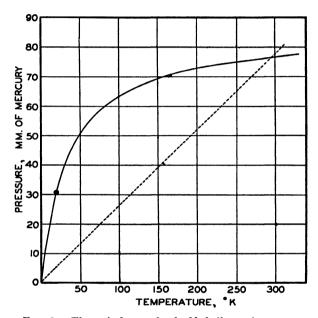
FIG. 2. *Theoretical curve for double bulb gas thermometer.*

Acknowledgments

The author wishes to express his thanks to Prof. E. F. Burton for his encouragement and interest, and to Prof. J. Satterly and Prof. H. Grayson Smith for many helpful discussions.

Reference

1. MENDELSSOHN, K. and PONTIUS, R. B. Phil. Mag. 24 : 777-787. 1937.

VIBRATION OF POWER LINES IN A STEADY WIND

IV. NATURAL FREQUENCIES OF VIBRATION OF STRINGS WITH STRENGTHENED ENDS[1]

By R. Ruedy[2]

Abstract

When the mass of unit length of a string of length $2L$, instead of being uniform, increases from the centre toward the ends according to the law $(1 + x/L)^m$, the natural frequencies of vibration are lower than those of the uniform string, but the ratios between the frequencies of successive overtones remain virtually unchanged, and with the exception of the first one or two overtones agree with those of a uniform string having a mass per unit length $(2(1 + \lambda)^{(m+2)/2} - 1)/\lambda(m + 2)$ times that at the centre of the strengthened string. The reduction in the natural frequencies of vibration is, of course, larger the greater the ratio between the masses at the two ends, whereas the value of m has a relatively small influence. The overtones form two distinct series: one, corresponding to the harmonics of even order, is always present; the other, corresponding to the harmonics of odd order, is suppressed when the density of the string increases from one end to the other (unsymmetrical span).

Introduction

Various measures are taken in order to suppress, or at least reduce, the vibrations invariably present when steady winds blow against the span of a transmission line strongly stretched by its own weight. Since in the course of time the vibrations injure the conductor near the point at which the wires are fastened to the insulating supports, special clamps and holders have been designed to relieve the strain; but as little is known about the stresses that arise when a transverse wave is reflected at the end of a string, an unfailing remedy in the nature of an improved clamp has yet to be found (5). Other devices, the vibration dampers, are intended to reduce the amplitudes of vibration to less than about one-tenth of the amplitude observed along the unprotected span (3, 4). Dampers are attached to the power line, at one or several points within the same span; as they partake of the vibrations of the conductor, they absorb energy inherent in the motion of the wire and reduce the amplitudes of the displacements. The construction of the dampers varies from simple weights at one end or both ends of a flexible bar (so-called torsion damper and Stockbridge dumbbell) to shock absorbers with spring suspension and oil or air damping (Holt damper), and from simple loops or festoons of wire, loosely or firmly tied to the first and last feet of the span, to the design in which the conductor is separated into an external hollow conductor resting on a supporting core (Preiswerk line). In view of the requirements in regard to design, material, and adjustment necessitated by the use of vibration dampers, the simple expedient of strengthening the ends of the string by merely adding to its thickness is remarkably successful in comparison. Various methods of stiffening the conductor near the clamps and increasing its resistance

to bending forces are in practical use: in one method, sleeves, slightly tapered on the inner side, are screwed around the conductor on both sides of the clamp; in another method, pieces several feet long, of the conductor used, are tied to the ends, or are strung along the conductor, by means of auxiliary clamps, an arrangement known as armor rods, or a piece of strong wire is wound around the ends. Flexible blades of metal are sometimes added in place of rods.

On the 220 kv. line, 125 miles long, from Beauharnois over Cumberland and South March (Ontario) to the Chats Falls on the Ottawa, a line built in 1932, a helix of round rods is twisted around the conductor in order to dampen the vibrations near the end of the wire. Festoon dampers are used on the 55 mile stretch of the 110 kv. line built in 1934 for carrying Gatineau power from Ottawa to Cornwall.

Strengthening devices are simpler in their construction than vibration dampers, but when they have to be added to a line already completed it becomes necessary to untie the conductor at the clamp. They reduce the amplitudes of vibration near the ends only in proportion to their mass. The effects to be expected when the strengthening member forms a constituent part of the wire, and is subject to the same tension as the conductor, have not hitherto been examined. A study of this problem, the string with strengthened ends, is of interest not only as regards the question of lessening vibrations and their injurious effects, but also as adding to our knowledge of non-harmonic vibrations in a field that lies particularly close at hand, since it embraces the problem of the uniform string as merely one particular case.

Equation of the Vibrating String of Finite Length L.

When the mass of unit length of a vibrating string of length L stretched by a constant tension S is a function $m(x)$ of the distance x from the origin, the transverse displacements y obey the differential equation

$$\frac{\partial^2 y}{\partial t^2} = \frac{S}{m(x)} \frac{\partial^2 y}{\partial x^2}.$$

The assumption that the solution is given by

$$y = Y(x)T(t)$$

leads to the relation

$$T(t) = A_t \sin \omega t + B_t \cos \omega t$$

for the time function, and to the relation

$$\frac{d^2 Y}{dx^2} + \frac{\omega^2}{S} m(x) Y = 0$$

for the curve described by the vibrating string. Strings of very different lengths will have to be considered; consequently, it is advisable to express distances and displacements in fractions of the length L of the string. In order that the equation for Y remain valid in the new units of length, the

function expressing the mass per unit length has to be multiplied by L, and the force or tension S divided by L, since forces have the dimension MLT^{-2}. At the same time, a function $\rho(x/L)$ takes the place of $m(x)$. With

$$\eta = Y/L \quad \text{and} \quad \xi = x/L$$

the equation giving the curve described by the vibrating string becomes

$$\frac{d^2\eta}{d\xi^2} + \frac{\omega^2}{S} L^2 \rho(\xi)\eta = 0 .$$

The string with constant density is readily included in the treatment if the mass of unit length of the string is assumed to obey the law

$$\rho(\xi) = \rho_0(1 + \lambda\xi)^m,$$
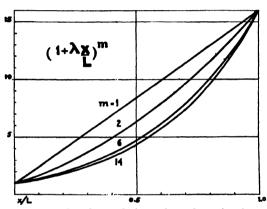
FIG. 1. *Density variations along the string for* $(1+\lambda)^m = 16$ *and various values of m.*

where m, as a general rule, is a whole number. The mass per unit length is equal to ρ_0 at that end of the string which is taken as the origin, and equal to $\rho_0(1 + \lambda)^m$ at the distant end of the string. When m is a large, and λ a small, number, the mass density increases gradually near the origin, and more and more abruptly as the other end is approached. In practice the mass of an element of a string or conductor that is strengthened at the end is at the farther end from 5 to 20 times as great as it is at the origin. Tables I and II and Fig. 1 show the rates at which the mass varies along the string for different values of m when $(1 + \lambda)^m$ = 4 (Table I), $(1 + \lambda)^m = 16$ (Fig. 1), and $(1 + \lambda)^m = 25$ (Table II).

On choosing, finally, under these conditions

$$\xi_1 = 1 + \lambda\xi$$

as the independent variable, the equation of the string changes to

$$\frac{d^2\eta}{d\xi_1^2} + \omega^2 \frac{L^2}{\lambda^2} \frac{\rho_0}{S} \xi_1{}^m \eta = 0 .$$

Its solution in Bessel functions of the order $1/(m + 2)$ is (2)

$$\eta = C_1\sqrt{\xi_1}J_{\frac{1}{m+2}}\left(\frac{2}{m + 2} \omega \frac{L}{\lambda}\sqrt{\frac{\rho_0}{S}} \xi_1^{\frac{m+2}{2}}\right)$$

$$+ C_2\sqrt{\xi_1}J_{-\frac{1}{m+2}}\left(\frac{2}{m + 2} \omega \frac{L}{\lambda}\sqrt{\frac{\rho_0}{S}} \xi_1^{\frac{m+2}{2}}\right)$$

TABLE I

VALUES CONNECTED WITH $(1 + \lambda)^m = 4$ FOR $m = 1, 2, 6$, AND 14, AND VARIOUS VALUES OF

$$\xi_1 = (1 + \lambda\xi)$$

$\xi = \dfrac{x}{L}$	$(1+\lambda)=4$, $\lambda=3$			$(1+\lambda)^2=4$, $\lambda=1$			$(1+\lambda)^6=4$, $\lambda=0.26$			$(1+\lambda)^{14}=4$, $\lambda=0.1041$		
	$\xi_1^{1/2}$	$\xi_1^{(m+2)/2}$	ξ_1^m	$\xi_1^{1/2}$	$\xi_1^{(m+2)/2}$	ξ_1^m	$\xi_1^{1/2}$	$\xi_1^{(m+2)/2}$	ξ_1^m	$\xi_1^{1/2}$	$\xi_1^{(m+2)/2}$	ξ_1^m
0	1.0			1.0			1.0			1.0		
0.1	1.14	1.48	1.3	1.049		1.21	1.013	1.108	1.166	1.005	1.086	1.156
0.2	1.27	2.02	1.6	1.095		1.44	1.023	1.225	1.355	1.010	1.179	1.334
0.3	1.38	2.62	1.9	1.140		1.69	1.038	1.350	1.562	1.016	1 279	1.537
0.4	1.48	3.24	2.2	1.183		1.96	1.051	1.486	1.811	1.021	1.386	1.769
0.5	1.58	3.94	2.5	1.224		2.25	1.063	1.631	2.082	1.026	1.501	2.035
0.6	1.67	4.65	2.8	1.265		2.56	1.075	1.786	2.386	1.031	1.624	2.337
0.7	1.76	5.45	3.1	1.304		2.89	1.087	1.950	2.727	1.036	1.756	2.678
0.8	1.84	6.22	3.4	1.342		3.24	1.099	2.130	3.108	1.041	1.897	3.070
0.9	1.92	7.07	3.7	1.378		3.61	1.111	2.319	3.531	1.046	2.046	3.500
1.0	2.0	8	4.0	1.414		4.0	1.123	2.520	4.001	1.051	2.208	4.000
γ	0.64			0.66			0.68			0.69		

The last complete line represents the values of $(1 + \lambda)^{1/2}$, $(1 + \lambda)^{(m+2)/2}$ and $(1 + \lambda)^m$, which are frequently required.   The expression γ is also listed for later use.

TABLE II

VALUES CONNECTED WITH THE DENSITY FUNCTION $\xi_1 = (1 + \lambda\xi)^m$ FOR $(1 + \lambda)^m = 25$ AND

$$m = 1, 2, 6, \text{ AND } 14$$

$\xi = \dfrac{x}{L}$	$(1+\lambda)=25$, $\lambda=24$			$(1+\lambda)^2=25$, $\lambda=4$			$(1+\lambda)^6=25$, $\lambda=0.71$			$(1+\lambda)^{14}=25$, $\lambda=0.2585$		
	$\xi_1^{1/2}$	$\xi_1^{(m+2)/2}$	ξ_1^m	$\xi_1^{1/2}$	$\xi_1^{(m+2)/2}$	ξ_1^m	$\xi_1^{1/2}$	$\xi_1^{(m+2)/2}$	ξ_1^m	$\xi_1^{1/2}$	$\xi_1^{(m+2)/2}$	ξ_1^m
0	1.0			1.0			1.0			1.0		
0.1	1.84	6.23	3.4	1.18		1.96	1.035	1.316	1.51	1.011	1.224	1.43
0.2	2.41	14	5.8	1.34		3.24	1.069	1.701	2.22	1.024	1.496	2.03
0.3	2.86	23.39	8.2	1.48		4.84	1.101	2.165	3.19	1.037	1.817	2.84
0.4	3.26	34.65	10.6	1.61		6.76	1.133	2.718	4.48	1.049	2.198	3.97
0.5	3.61	47.05	13	1.74		9.0	1.164	3.371	6.19	1.062	2.644	5.48
0.6	3.92	60.24	15.4	1.84		11.56	1.194	4.135	8.41	1.075	3.173	7.54
0.7	4.22	75.15	17.8	1.95		14.44	1.223	5.022	11.25	1.086	3.783	12.34
0.8	4.49	90.52	20.2	2.05		17.64	1.252	6.045	14.86	1.098	4.499	13.90
0.9	4.75	107.2	22.6	2.14		21.16	1.280	7.216	19.39	1.109	5.330	18.70
1.0	5.0	125.0	25	2.24		25	1.308	8.551	25	1.121	6.292	25.0
γ	0.29			0.33			0.376			0.39		

or a sum of such terms, since the principle of the superposition applies even to the string of variable density. The solutions are readily checked by differentiation. The two conditions that the displacements remain permanently zero at $\xi = 0$ and at $\xi = 1$ furnish two equations valid at the origin and at the end of the string, and elimination of C_1 and C_2 from these two relations gives for the natural frequencies of vibration of the string the equation

$$J_{\frac{1}{m+2}}\left(\frac{2}{m+2}\,\omega\frac{L}{\lambda}\sqrt{\frac{\rho_0}{S}}\right)J_{-\frac{1}{m+2}}\left(\frac{2}{m+2}\,\omega\frac{L}{\lambda}\sqrt{\frac{\rho_0}{S}}\,(1+\lambda)^{\frac{m+2}{2}}\right)$$
$$-\,J_{-\frac{1}{m+2}}\left(\frac{2}{m+2}\,\omega\frac{L}{\lambda}\sqrt{\frac{\rho_0}{S}}\right)J_{\frac{1}{m+2}}\left(\frac{2}{m+2}\,\omega\frac{L}{\lambda}\sqrt{\frac{\rho_0}{S}}\,(1+\lambda)^{\frac{m+2}{2}}\right) = 0\,,$$

or, with

$$z = \frac{2}{m+2}\,\omega\frac{L}{\lambda}\sqrt{\frac{\rho_0}{S}}$$

$$J_{\frac{1}{m+2}}(z)J_{-\frac{1}{m+2}}\left(z(1+\lambda)^{\frac{m+2}{2}}\right) - J_{-\frac{1}{m+2}}(z)J_{\frac{1}{m+2}}\left(z(1+\lambda)^{\frac{m+2}{2}}\right) = 0\,.$$

In view of the occurrence of various Bessel functions of any order between 0 and $\frac{1}{2}$, a survey of the field by experimental means alone, without at least a preliminary mathematical study, would lead to serious difficulties.

The Frequency Equation

When the mass of an element of the string taken at the distant end greatly exceeds the mass of an element of the same length taken at the origin, the density function $(1 + \lambda\xi)^m$ reduces to $\lambda\xi^m$. The equation for η is

$$\eta = C_1\sqrt{\lambda\xi}J_{\frac{1}{m+2}}\left(\frac{2}{m+2}\,\omega\frac{L}{\lambda}\sqrt{\frac{\rho_0}{S}}\,(\lambda\xi)^{\frac{m+2}{2}}\right)\,.$$

The constant C_2 is equal to zero since at the origin the value of $J_{1/(m+2)}$ is zero, and that of $J_{-1/(m+2)}$ is infinity. The frequencies are determined by the solutions, j_n, of the Bessel function $J_{1/(m+2)}$

$$J_{\frac{1}{m+2}}\left(\frac{2}{m+2}\,\omega L\sqrt{\frac{\rho_0}{S}}\lambda^{\frac{m}{2}}\right) = 0\,.$$

Hence only those frequencies are allowed for which

$$\omega = \frac{m+2}{2\lambda^{\frac{m}{2}}}\sqrt{\frac{S}{\rho_0}}\,\frac{j_n}{L}\,,$$

with $j_n = 2.9,\, 6.03,\, 9.2\,\ldots$ for $J_{\frac{1}{4}}$; or $j_n = 2.8,\, 5.91,\,\ldots$ for $J_{\frac{1}{3}}$, and the limits $2.404,\, 5.520,\, 8.654,\,\ldots$ set by J_0, whereas the equation for the uniform string is

$$\omega = n\frac{\pi}{L}\sqrt{\frac{S}{\rho_0}}\,.$$

In other words, when λ is assumed to be very large, the natural frequencies of vibration of the string strengthened at the end are very much lower than the frequencies of the stretched string with uniform mass per unit length.

In the more general case, the linear density of the string does not vanish at the origin, and the natural frequencies of vibration are determined by more complicated equations, such as, for instance, for $(1 + \lambda)^m = 4$,

$$J_{\frac{1}{3}}(z)J_{-\frac{1}{3}}(8z) - J_{-\frac{1}{3}}(z)\,J_{\frac{1}{3}}(8z) = 0, \text{ for } m = 1$$

with the solutions $z_1 = 0.44$, $z_2 = 0.90$, $z_3 = 1.35$.

$$J_{\frac{1}{4}}(z)J_{-\frac{1}{4}}(4z) - J_{-\frac{1}{4}}(z)J_{\frac{1}{4}}(4z) = 0, \text{ for } m = 2$$

with the solutions $z_1 = 1.025$, $z_2 = 2.10$.

$$J_{\frac{1}{8}}(z)J_{-\frac{1}{8}}(2.52z) - J_{-\frac{1}{8}}(z)J_{\frac{1}{8}}(2.52z) = 0, \text{ for } m = 6.$$

$$J_{\frac{1}{16}}(z)J_{-\frac{1}{16}}(2.208z) - J_{-\frac{1}{16}}(z)J_{\frac{1}{16}}(2.208z) = 0, \text{ for } m = 14.$$

For values of z less than 10, the solutions are determined by using the tables for $J_{\frac{1}{3}}$ and $J_{\frac{1}{4}}$ (2). It is known that when z is greater than about 10,

$$J_\nu(z) = \sqrt{\frac{2}{\pi z}}\Big(\zeta_\nu(z)\cos\psi_1 - \xi_\nu(z)\sin\psi_1\Big)$$

$$J_{-\nu}(z) = \sqrt{\frac{2}{\pi z}}\Big(\zeta_\nu(z)\cos\psi_{11} - \xi_\nu(z)\sin\psi_{11}\Big),$$

where

$$\psi_1 = z - \frac{\pi}{4} - \nu\frac{\pi}{2}$$

$$\psi_{11} = z - \frac{\pi}{4} + \nu\frac{\pi}{2}$$

$$\zeta_{+\gamma}(z) = 1 - \frac{(4\gamma^2 - 1)(4\gamma^2 - 3^2)}{1 \cdot 2(8z)^2}$$

$$+ \frac{(4\gamma^2 - 1)(4\gamma^2 - 3^2)(4\gamma^2 - 5^2)(4\gamma^2 - 7^2)}{1 \cdot 2 \cdot 3 \cdot 4(8z)^4} \cdots + R_p$$

$$\xi_{+\gamma}(z) = \frac{4\gamma^2 - 1}{8z} - \frac{(4\gamma^2 - 1)(4\gamma^2 - 3^2)(4\gamma^2 - 5^2)}{1 \cdot 2 \cdot 3(8z)^3} + \cdots R_p.$$

With the aid of these formulas it may be shown that for values of z greater than 10, that is, for vibrations of frequencies normally produced by a steady wind blowing against a power line:

$$J_\nu(z)J_{-\nu}\big(z(1 + \lambda)^{\frac{m+2}{2}}\big) - J_{-\nu}(z)J_\nu\big(z(1 + \lambda)^{\frac{m+2}{2}}\big) = J_\nu(z_1)J_{-\nu}(z_2) - J_{-\nu}(z_1)J_\nu(z_2)$$

$$= \frac{2}{\pi}\sin\nu\pi\sqrt{\frac{1}{z_1 z_2}}\Big(\sin(z_1 - z_2)\big(\zeta(z_1)\zeta(z_2) + \xi(z_1)\xi(z_2)\big)$$

$$- \cos(z_1 - z_2)\big(\zeta(z_1)\xi(z_2) - \xi(z_1)\zeta(z_2)\big)\Big)$$

This expression becomes equal to zero when

$$\tan z\,(1 - (1 + \lambda)^{\frac{m+2}{2}}) = \frac{\zeta(z)\xi\big(z(1 + \lambda)^{\frac{m+2}{2}}\big) - \xi(z)\zeta\big(z(1 + \lambda)^{\frac{m+2}{2}}\big)}{\zeta(z)\zeta\big(z(1 + \lambda)^{\frac{m+2}{2}}\big) + \xi(z)\xi\big(z(1 + \lambda)^{\frac{m+2}{2}}\big)}$$

The practical value of this formula is enhanced by the fact that for the values of ν and m here concerned, the ζ's reduce to unity and the ξ's to the first term of the series; consequently, for all the overtones excepting the second and perhaps the third the frequencies are given with an accuracy sufficient for all practical purposes by

$$\tan z\left((1+\lambda)^{\frac{m+2}{2}} - 1\right) = \xi\left(z(1+\lambda)^{\frac{m+2}{2}}\right) - \xi(z)$$

that is

$$\tan z\left((1+\lambda)^{\frac{m+2}{2}} - 1\right) = \frac{4\nu^2 - 1}{8z}\left(\frac{1}{(1+\lambda)^{\frac{m+2}{2}}} - 1\right)$$

or

$$z\tan z\left((1+\lambda)^{\frac{m+2}{2}} - 1\right) = \frac{4\nu^2 - 1}{8}\frac{(1+\lambda)^{\frac{m+2}{2}} - 1}{(1+\lambda)^{\frac{m+2}{2}}}$$

On writing

$$\left((1+\lambda)^{\frac{m+2}{2}} - 1\right)z\tan z\left((1+\lambda)^{\frac{m+2}{2}} - 1\right) = \frac{4\nu^2 - 1}{8}\frac{\left((1+\lambda)^{\frac{m+2}{2}} - 1\right)^2}{(1+\lambda)^{\frac{m+2}{2}}}$$

it is seen that after solving

$$x\tan x = c$$

where the value of the constant c depends on λ, ν, and m, the natural frequencies of vibration higher than the second or third overtone are found from the formula

$$2\pi f_n = \omega_n = x_n \frac{m+2}{2L}\frac{\lambda}{(1+\lambda)^{\frac{m+2}{2}} - 1}\sqrt{\frac{S}{\rho_0}},$$

while for a string with a constant density throughout the length

$$\omega_n = n\frac{\pi}{L}\sqrt{\frac{S}{\rho_0}}.$$

A comparison between the frequencies of the string with strengthened ends and those of the uniform string is readily made with the aid of Table III which lists the values of γx_n for the examples illustrated in Tables I and II, and Fig. 1. The lowest frequencies are computed from the solutions z of the original frequency equation, namely

$$\omega_n = \lambda z_n \frac{m+2}{2L}\sqrt{\frac{S}{\rho_0}}.$$

Fig. 2 represents the function $x\tan x$ used for the higher frequencies. In the range of the solutions of the equation $x\tan x = c$, from values of x near zero to very large values, it will, of course, be found that, as x increases, smaller and smaller values of $\tan x$ are sufficient to equal a given value c; in other words, the solutions x_n tend to lie closer to multiples of π. Hence the values of ω_n for the higher overtones follow at intervals that are only a fraction,

$$\gamma = \frac{m+2}{2}\frac{\lambda}{(1+\lambda)^{\frac{m+2}{2}} - 1},$$

of the interval π known to separate the natural pulsations of the uniform string, and a string with the uniform mass $\gamma^{-\frac{1}{2}}$ has the same higher resonance frequencies as the string along which the mass changes, although the shape of the waves differ in the two instances. As is to be expected, the frequencies are considerably reduced when the ratio $(1 + \lambda)^m$ between the mass at the distant end and the mass at the origin is high, whereas the exponent m exerts a relatively slight influence; consequently, a concentration of the added mass at or near the origin produces almost the same reduction in the resonance frequencies and the same advantages as a gradual increase in density along the entire length.

TABLE III

RESONANCE FREQUENCIES OF THE STRENGTHENED STRING IN MULTIPLES OF $\sqrt{S/\rho_0}/L$
(EVEN-NUMBERED OVERTONES)

	$(1 + \lambda)^m = 4$				$(1 + \lambda)^m = 16$				$(1 + \lambda)^m = 25$			
	3.14	6.28	9.43	12.57	3.14	6.28	9.43	12.57	3.14	6.28	9.43	12.57
$m = 0$	3.14	6.28	9.43	12.57	3.14	6.28	9.43	12.57	3.14	6.28	9.43	12.57
1	1.90	4 05		8.10								
		4.08	6.08	8.10		2.44	3.54	4.64		2	2.93	3.81
2	2.04	4.20			1.20	2.52						
		4.16	6.30	8.38		2.59	3.83	5.07		2.20	3.24	4.25
6		4.31	6.45	8.60		2.80	4.17	5.55		2.37	3.52	4.67
14		4.34	6.49	8.65		2.85	4.26	5.67		2.52	3.75	4.98

Where two slightly different results are given for the same value of m, the upper line refers to the solution obtained from the equation valid at all frequencies, the lower line to the solution valid at higher and higher frequencies, beginning, as a comparison shows, with the first overtone.
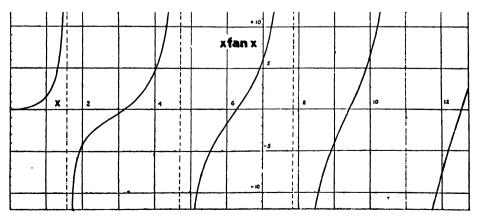
FIG. 2. *Values of $x \tan x$ for the determination of the overtones of the strengthened string with an even number of loops.*

Symmetrical String with Strengthened Ends

If a piece of wire is so attached to the string of length L that the density increases with the distance on the one as well as on the other side of the origin, while the centre is unconstrained, those natural frequencies of vibration which have a node at the centre and at the end, that is, the overtones with an even number of loops, remain unchanged and may simply be taken over from the unsymmetrical string. At the same time a new series of frequencies appears which show a loop at the centre of the span and nodes at both ends. If these boundary conditions are taken into account, the equation for the frequencies becomes

$$J_{\frac{m+1}{m+2}}\left(\frac{4}{m+2}\ \omega\ \frac{L}{\lambda}\sqrt{\frac{\rho_0}{S}}\right) J_{\frac{1}{m+2}}\left(\frac{4}{m+2}\ \omega\ \frac{L}{\lambda}\sqrt{\frac{\rho_0}{S}}\ (1+\lambda)^{\frac{m+2}{2}}\right)$$

$$+\ J_{-\frac{m+1}{m+2}}\left(\frac{4}{m+2}\ \omega\ \frac{L}{\lambda}\sqrt{\frac{\rho_0}{S}}\right) J_{-\frac{1}{m+2}}\left(\frac{4}{m+2}\ \omega\ \frac{L}{\lambda}\sqrt{\frac{\rho_0}{S}}\ (1+\lambda)^{\frac{m+2}{2}}\right)\ =\ 0\ .$$

For instance, for $(1+\lambda)^m = 4$,

$$J_{\frac{2}{3}}(2z)J_{\frac{1}{3}}(16z) + J_{-\frac{2}{3}}(2z)J_{-\frac{1}{3}}(16z)\ =\ 0,\quad \text{for}\quad m\ =\ 1$$

with the approximate solutions $2z_1\ =\ 0.26;\ 2z_2\ =\ 0.69\ \ldots$

$$J_{\frac{3}{4}}(2z)J_{\frac{1}{4}}(8z) + J_{-\frac{3}{4}}(2z)J_{-\frac{1}{4}}(8z)\ =\ 0,\quad \text{for}\quad m\ =\ 2$$

with the approximate solutions $2z_1\ =\ 0.59;\ 2z_2\ =\ 1.6$

$$J_{\frac{7}{8}}(2z)J_{\frac{1}{8}}(5.04z) + J_{-\frac{7}{8}}(2z)J_{-\frac{1}{8}}(5.04z)\ =\ 0,\quad \text{for}\quad m\ =\ 6\ .$$

By using the series for large values of z it is easy to show that when as in the present example

$$\nu_2\ =\ 1\ -\ \nu_1$$

then

$$J_{\nu_1}(z_1)J_{\nu_2}(z_2) + J_{-\nu_1}(z_1)J_{-\nu_2}(z_2)\ =$$

$$\sqrt{\frac{4}{\pi^2 z_1}}\ \cos\,(2\nu_1 - 1)\,\frac{\pi}{2}\Big(\cos\,(z_1 - z_2)\Big(\zeta_{\nu_1}(z_1)\zeta_{\nu_2}(z_2) + \xi_{\nu_1}(z_1)\xi_{\nu_2}(z_2)\Big)$$

$$-\ \sin\,(z_1 - z_2)\Big(\zeta_{\nu_1}(z_1)\xi_{\nu_2}(z_2) - \xi_{\nu_1}(z_1)\zeta_{\nu_2}(z_2)\Big)\Big)\ =\ 0\ .$$

The roots larger than $z\ =\ 10$ are given by

$$\tan\,(z_1 - z_2)\ =\ \frac{\zeta_{\nu_1}(z_1)\,\zeta_{\nu_2}(z_2) + \xi_{\nu_1}(z_1)\,\xi_{\nu_2}(z_2)}{\zeta_{\nu_1}(z_1)\,\xi_{\nu_2}(z_2) - \xi_{\nu_1}(z_1)\,\zeta_{\nu_2}(z_2)}\ .$$

For frequencies higher than that of the second or third overtone the expression reduces to

$$\tan z\left((1+\lambda)^{\frac{m+2}{2}} - 1\right)\ =\ \cfrac{8z}{4\left(\cfrac{m+1}{m+2}\right)^2 - 1 - \cfrac{\cfrac{4}{(m+2)^2} - 1}{(1+\lambda)^{\frac{m+2}{2}}}}$$

an equation that can be written in the standard form

$$\frac{\tan x}{x}\ =\ c\ .$$

For instance, when $(1 + \lambda)^m = 4$, and where now $z = \dfrac{4}{m+2}\, \omega \dfrac{L}{\lambda}\sqrt{\dfrac{\rho_0}{S}}$,

$\dfrac{\tan 7z}{7z} = 1.35$, for $m = 1$, with the solutions $7z$
$$= 0.87; 4.55; 7.76; 10.92$$

$\dfrac{\tan 3z}{3z} = 1.855$, for $m = 2$, with the solutions $3z$
$$= 1.12; 4.6; 7.785$$

$\dfrac{\tan 1.52z}{1.52z} = 1.7$, for $m = 6$

$\dfrac{\tan 1.208z}{1.208z} = 2.24$, for $m = 14$.

FIG. 3.   *Values of tan x/x for the determination of the overtones of odd orders.*

It is known that when x lies between 0 and $\pi/2$ the ratio $\tan x/x$ is always larger than unity.   As x begins to increase beyond the value π the ratio $\tan x/x$ increases from zero to very large values.   The same growth is repeated each time that x has increased by the amount π, but, with each step, larger values of $\tan x$ are required in order to obtain a given ratio c (Fig. 3).   In other words, at the higher frequencies the solutions x tend more and more toward the values $n\pi/2$.   The higher overtones follow, therefore, from the equation

$$x_n = \left((1 + \lambda)^{\frac{m+2}{2}} - 1\right) z = \frac{4}{m+2}\left((1 + \lambda)^{\frac{m+2}{2}} - 1\right)\frac{\omega L}{\lambda}\sqrt{\frac{\rho_0}{S}}$$

or

$$\omega_n = x_n \frac{m+2}{4L}\frac{\lambda}{(1 + \lambda)^{\frac{m+2}{2}} - 1}\sqrt{\frac{S}{\rho_0}} = \frac{\gamma}{2}\frac{x_n}{L}\sqrt{\frac{S}{\rho_0}} ,$$

whereas for the string of length $2L$ and constant mass ρ_0 per unit length

$$\bar{\omega}_n = n\frac{\pi}{2L}\sqrt{\frac{S}{\rho_0}}.$$

When the solutions x_n lie sufficiently close to $n\pi/2$, the correction factor γ, as before, reduces the natural frequencies of the uniform string to the resonance frequencies of the string strengthened at the ends.

References

1. CARROLL, J. S. and KOONTZ, J. A.   Elec. Eng. 55 : 490-493.   1936.
2. KARAS, K.   Sitzber. Akad. Wiss. Wien, 145 : 797-826.   1936.
3. PIPES, L. A.   Elec. Eng. 55 : 600-614.   1936.
4. RUEDY, R.   Can. J. Research, 13A : 99-110.   1935.
5. STURM, R. G.   Elec. Eng. 55 : 455-465; 673-388.   1936.

WATER AND WATER-ALCOHOL INJECTION IN A SUPER-CHARGED JAGUAR AIRCRAFT ENGINE[1]

By M. S. Kuhring[2]

Abstract

Tests have been carried out in order to determine the effect of water injection on the operation of a full-scale aircraft engine. A Jaguar Mk IV supercharged aircraft engine was used and quantities of water as great as 83 lb. per 100 lb. of fuel were injected. As would be expected, the use of water permitted large gains in power without increase in cylinder temperature and apparent detonation. An increase of approximately 90 b.hp. was obtained. Quite appreciable cooling of the air-fuel charge was noted. The specific fuel consumption remained the same or slightly better with injection. From the results it would appear that alcohol does not improve the operation of the engine appreciably, although tests were conducted only at full rich mixtures.

Introduction

The take-off power of modern, high performance aircraft engines is to a very large extent limited by the octane rating of the fuel used. Should it be required to increase the take-off power of a specific engine, it will be necessary, owing to the tendency towards detonation, to use a fuel of higher octane value in order that there will not be a dangerous increase in engine temperatures.

To avoid the use of higher octane fuels or to increase the take-off power beyond that permitted by fuels at present available, the injection of certain substances such as aniline has been tried. Water injection, though tested in small laboratory and automotive engines, did not appear, from a review of the literature, to have been tried in full-scale aircraft engines, and it was considered that the subject was worthy of investigation.

Experimental

The engine used was a supercharged Armstrong Siddeley Jaguar Mark IV aircraft engine. It had been employed for a recently completed program of detonation tests, and thermocouples were fitted in the temperature plug, cylinder head, and cylinder base.

Time did not permit overhauling the engine after the detonation tests, during which the engine had operated for long periods under extremely severe conditions of detonation and during which wear had doubtless occurred, and

deposits of oil had been baked on some of the cooling fins, and thus prevented adequate cooling.   Consequently, there will be noted an unduly large spread in temperature of the different cylinders.

Method of Injection

The water was fed from the main under city pressure, passed through a calibrated orifice plate, and thence through copper tubing into a distance piece between the carburettor and the supercharger.   The distance piece was drilled to permit the insertion of two small copper tubes which were sealed at one end and drilled in such a manner as to direct fine jets of water at the acorn nut which covers the rear end of the supercharger spindle.   The water, traveling at high speed, was atomized at this point and drawn into the super-charger impeller.   This arrangement is shown in Figs. 1, 2, and 3.
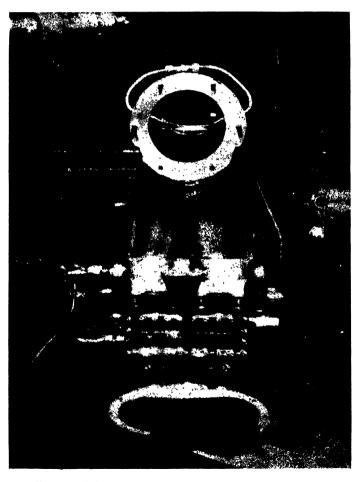
FIG. 1.   Injector unit.   View looking towards injector from supercharger.   Four outlet holes may be seen.

The alcohol-water mixture was drawn from a tank and forced into the injection system by means of an electrically driven gear pump.

Measurements

Power was measured by means of a Heenan and Froude hydraulic dynamometer (DPRX6).   (Fig. 4).

FIG. 2.   *Jets being directed against piece of round bar to show degree of atomization.*

FIG. 3.   *Showing water being passed from injector.   The unit has been removed from the supercharger flange and turned away from the engine.   The acorn nut against which the water impinges may be seen directly behind the injector unit.*

Fuel consumption was measured by means of B & B Mk IX flowmeters calibrated in Imperial pints per hour.   The fuel consisted of 87 octane aviation gasoline having a specific gravity of 0.710.

The temperatures of the cylinder head, cylinder base, temperature plug, and charge were measured by means of thermocouples.   Cylinder head

thermocouples were of the spark plug washer type and were fitted to the rear plug of each cylinder. Cylinder base thermocouples were screwed into the cylinder clamping ring. The Jaguar cylinders are provided with two pairs of spark plug holes so that plugs can be fitted at the front when the engine is used as either a pusher or tractor engine. During the tests, spark plugs were fitted one in front and the other at the rear of each cylinder, and temperature plugs of monel metal and stainless steel were screwed in the spare spark plug opening at the rear of each cylinder. These plugs are similar to the temperature plugs used to indicate detonation in the U.S. Army Air Corps method of octane rating of gasoline.
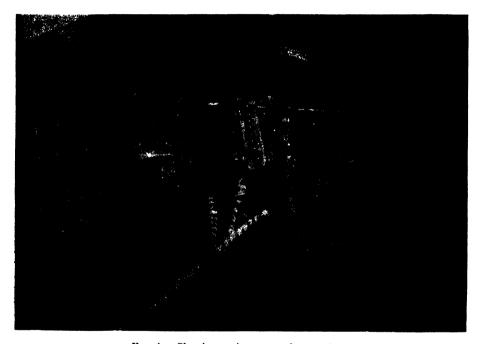
FIG. 4.   *Showing engine mounted on test bed.*

The charge temperature was determined by means of a thermocouple at the tip of a stainless steel plug screwed into the induction pipe near the intake port of No. 4 cylinder, the opening normally intended for priming being used. The tip of this plug was projected well into the cylinder port in order that an accurate indication of the temperature of the charge entering the port would be obtained. Figs. 5, 6, and 7 show the thermocouples and their arrangement.

Air and oil temperatures were measured with distant reading dial thermometers.

Engine speed was determined by means of an electrical timing device which indicates the time required for 1000 revolutions of the crankshaft.

Cooling Air

The air speed used in each experiment is given in the tables. Cowling was provided as shown in Fig. 4.

Carburettor Air

To avoid recirculation of exhaust gases and to maintain intake air temperatures at the desired point, all air passing to the carburettor was taken from the blower duct and passed through a steam radiator. From the radiator the air was passed through a pipe into a surge box. It is in this box that temperatures were taken.

FIG. 5.   *Thermocouples as fitted to engine.*

Details of Engine

The engine used was an Armstrong Siddeley Jaguar Mk IV, fitted with a type E Supercharger.

Air-cooled twin row radial
Dry weight, 897 lb.
Number of cylinders, 14
Bore, 5 in.
Stroke, $5\frac{1}{2}$ in.
Displacement, 1512 cu. in.
Normal r.p.m., 1700
Maximum r.p.m., 1870

Rated b.hp. at 11,500 ft. with a manifold pressure of 28.42 in. of mercury, absolute.
Compression ratio, 5 : 1
Carburettor, Claudel Hobson A.V.T. 70E.
Oil pressure, 65/100 lb.
Supercharger ratio, 12.9 : 1

Lubricating oil, Castrol R

The lubricating oil after leaving the scavenge pump passed through the carburettor and induction pipe jacket and heated the charge. This heating occurred after the air left the intake air thermometer and may have had a slight effect on the temperature of the charge entering the ports. It is considered that the effect would not be large.

Results

First Test

Results of the first test are shown in Table I and in Figs. 8, 9, and 10. The engine was operated on gasoline only, and readings were taken. Following this, water was injected in increasing amounts, and readings were taken until

the quantity of water injected was 60.9 lb. for each 100 lb. of fuel consumed. This was the maximum water flow possible through the equipment with the pressure then available. Following the test the engine was again operated without injection of water; the readings taken were very similar to those obtained at the start of the test.

FIG. 6.   *Showing thermocouples on engine.*

The manifold pressure at which this test was carried out was 32.0 in. of mercury, absolute, but later tests were conducted at a manifold pressure of 35.0 in. of mercury, absolute.

In Figs. 8, 9, and 10, the results of this test are represented by triangles. It will be noted that the temperatures of the temperature plugs, cylinder head, and base are slightly lower than the corresponding figures for later tests. This is due to the lower manifold pressure at which the engine was operated.

FIG. 7.   *Thermocouple junction box.*

Second Test

A second test was conducted to extend the range so that the optimum value could be determined. To permit more water to reach the engine the number of holes in the injection tubes was increased from four to eight and these were enlarged. Data for this test are shown in Table II and in Figs. 8, 9, and 10. In the curves the results are represented by crosses. The results are very similar to those of the first test. The ratio of water to fuel injected was less than the maximum obtained during the first test although the actual quantity of water was greater. This was due to the fact that the manifold pressure was greater and more fuel was being used.

It may be observed from the results of these two tests that the benefits obtained by water injection were still increasing at the maximum rate of injection obtained.
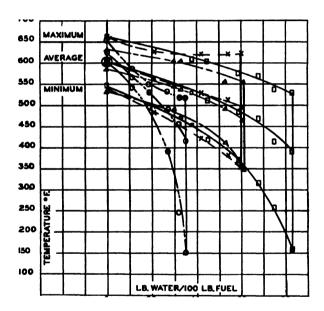
FIG. 8. *Effect of varying amounts of injected water on temperature plugs.* △, *First test;* ✕, *second test;* ☐, *fourth test;* ○, *fifth test.*

Third Test

It was considered that advantage should be taken of the opportunity to determine the effect of a definite rate of injection of water at progressively greater throttle openings or manifold pressures.

The engine was operated without water injection at a manifold pressure of 35.0 in. of mercury. Readings were taken and water was then injected at a rate of flow which it was considered possible to maintain over quite a wide range of throttle opening. This rate of flow was maintained constant except

at one point at which it was increased for a sufficient length of time to take a set of readings (at a manifold pressure of 38.0 in. of mercury); it was then adjusted to the original rate for the remainder of the test. This point at which the rate of water flow was increased is plotted in Figs. 11, 12, and 13 as a circle, and the other points are indicated by crosses.
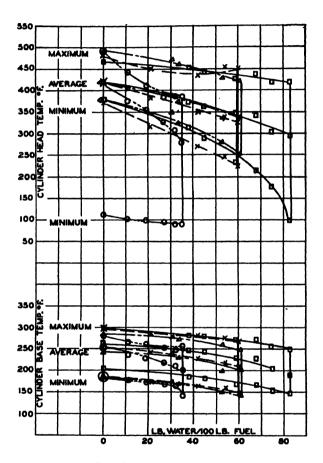
FIG. 9.   *Effect of varying amounts of injected water on temperatures of cylinder base and cylinder head.   △, First test; ✕, second test; □, fourth test; ○, fifth test.*

The throttle was opened progressively until the manifold pressure was 39.4 in. of mercury, absolute. This was as high a pressure as the supercharger would develop at full throttle opening.

Results of this test are given in Table III and Figs. 11, 12, and 13, and will be discussed later.

Fourth Test

In order to carry the water injection curve to a point at which the benefits secured by injection would cease, or until power would fall off, another source of water supply at a higher pressure was arranged.

The engine was operated at a manifold pressure of 35.0 in. of mercury and with increasing rates of water injection.
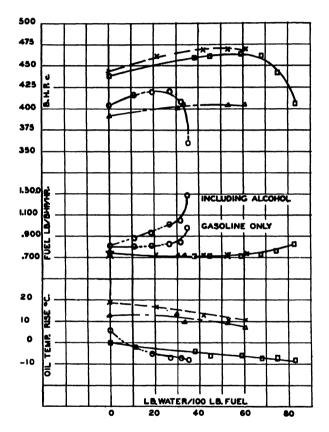
FIG. 10. *Effect of varying amounts of injected water on power, fuel consumption, and heat rejected to lubricating oil.*
△, *First test;* ✕, *second test;* □, *fourth test;* ○, *fifth test.*

At a flow of 83 lb. of water per 100 lb. of fuel it was definitely established that the point of maximum gain had been passed for the particular engine conditions.

Results of this test will be found in Table IV and in Figs. 8, 9, and 10. In the figures, readings are represented by squares.

Fifth Test

Obviously if water for injection is carried in a tank in the aircraft it is subject to freezing in the winter unless some antifreeze such as alcohol is added.

On take-off at the present time, high performance aircraft engines are operating with virtually as rich a mixture as is possible, and the addition of alcohol to the injection water, in sufficient quantities to prevent freezing, is
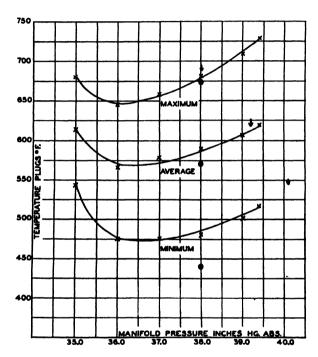
FIG. 11.   *Effect of constant rate of water injection on permissible manifold pressure (temperature plugs).*

apt to make the mixture over rich.   However, it was decided to try a mixture of water-alcohol which would be satisfactory as an antifreeze.   Tests were made with a mixture containing 46.25% of alcohol by weight.   The results are given in Table V and plotted, as circles in Figs. 8, 9, and 10.   The specific fuel consumption is shown for gasoline alone and for both gasoline and alcohol.

Discussions and Conclusions

The temperatures of temperature plug, cylinder head, and cylinder base tended with one exception to drop with water injection.   The maximum temperatures of cylinder head and temperature plug in the second test dropped at first and then rose slightly.   This is due probably to a local cylinder condition and might be ignored.

The specific fuel consumption was slightly lower with water injection up to the point at which power dropped off. All tests were conducted with the mixture control in the full rich position, including that with the alcohol-water injection. It had been hoped to obtain mixture control curves with the various degrees of water injection and particularly with the alcohol mixture, but this was not possible at the time.
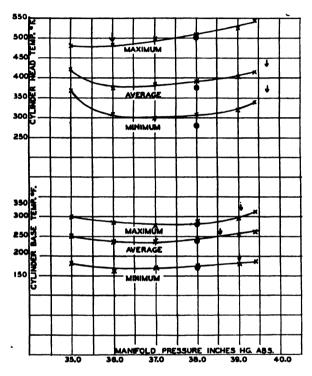
FIG. 12. *Effect of constant rate of water injection on permissible manifold pressure (cylinder base and cylinder head temperatures).*

The engine heat transferred to the lubricating oil, as shown by the oil temperature rise, tended to drop as water was injected, and the engine temperature decreased, in spite of the fact that power output increased.

Supercharger cooling was obviously one of the advantages of the water injection, as indicated by the charge temperature in the tables. When the engine was operating at a given manifold pressure without the water injection, and the water was then turned on, the manifold pressure, owing to the cooling effect, dropped, and the throttle had to be opened appreciably in order to maintain the given manifold pressure. This was repeated at each increase in rate of water injection. The power increase as shown in Fig. 10 gives about

25 hp. gain with water injection when the manifold pressure is maintained constant.

Figs. 11, 12, and 13 show more clearly the advantage to be derived. As stated previously, in these tests water was injected at the rate of only 35 to 37 lb. per 100 lb. of fuel. The power curve (Fig. 10) indicates that best results are obtained at a rate of flow of between 60 and 65 lb. of water per 100 lb. of fuel. This is confirmed by the better performance indicated by the single point readings taken at a manifold pressure of 38 in. with a rate of flow of
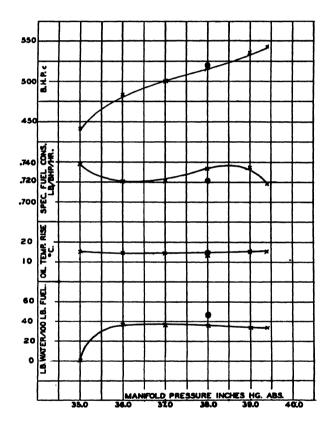
FIG. 13. *Effect of constant rate of water injection on permissible manifold pressure (power, fuel consumption, and heat rejected to lubricating oil).*

approximately 47 lb. per 100 lb. of fuel. Evidently the advantages gained, as shown in Figs. 11, 12, and 13 are not the maximum obtainable. Arrows placed above the curves in Figs. 11 and 12 indicate the point at which the temperatures, after dropping, increased to the values at the start, and would therefore indicate the increase in manifold pressure permissible to maintain the engine at a given temperature.

With the exception of the maximum readings, which as stated before were probably local, it would appear that with a similar rate of water injection the manifold pressure may be increased from 35.0 to 38.5 or 39.0 in. of mercury, or, expressed in horsepower, increased from 441 to 523 or 535 b.hp., a gain of 82 or 94 b.hp.

Though water injection offers an attractive method of increasing the performance of an engine at take-off and possibly even at cruising power, certain points must not be overlooked. Although sufficient water could easily be carried for take-off, a sufficient supply for cruising presents difficulties both in regard to weight and the possibility of freezing in cold weather.

From the small amount of work done in this series of tests it would appear that the use of alcohol as an antifreeze does not give the same improvement in performance as that given by water injection, although the question has not been fully examined as only one gasoline mixture strength was used.

Water recovery from the exhaust if feasible would appear to be a solution of this difficulty. There is in the exhaust an amount of water vapor roughly equal to that of the fuel consumed. In the exhaust of an engine into which water is injected at the rate of 50 lb. per 100 lb. of fuel there would be an additional 50% of water. It would then be necessary to recover from the exhaust approximately 33% of the water vapor for injection. The exhaust temperature, though not measured, is probably considerably lower with water injection, and this would favor water recovery. Water recovery from the exhaust has been used on airships but the necessary equipment might be too cumbersome for aeroplanes.

As pointed out previously, the fuel used was 87 octane gasoline containing lead tetraethyl, and it was found, at the end of virtually all the test runs, that the spark plugs were on the verge of failure. Some of the spark plugs failed before the end of the tests owing to the building up of a deposit on the insulator. It would appear from this that the lead, instead of being carried out of the combustion chamber in the form of a vapor, was being deposited in the combustion chamber and thus fouled the plugs. Hotter running plugs might improve operation but would not prevent the deposit from covering the combusion chamber.

Heavy deposits were found on the tops of the pistons. Over large areas of the piston, carbon had flaked off, and it is quite possible that this carbon caused pre-ignition at times, particularly during the last run, when the tests were concluded owing to irregular operation of one and possibly more of the cylinders.

Examination of the engine after the test showed cylinders and pistons to be in exceptionally good condition. Further tests with a non-leaded fuel should be carried out to determine whether it was the deposition of lead which caused the spark plugs to fail, or whether carbon alone would cause failure. Such tests would also indicate to what extent water injection in the engine could be used to replace at least some of the lead in a fuel.

TABLE I

WATER INJECTION TESTS

Engine started 11.23 a.m., off 11.53 a.m.; started 3.20 p.m., off 5.22 p.m.   Velocity of cooling air, 123 m.p.h. past cylinder heads
Cold junction, 62° F.   Barometer, 29.85 in. of mercury.   Sp. gr. of fuel, 0.710.

Time	4.20*	4.40**	4.44	4.49	4.52	4.55	4.58	5.02	5.05	5.08	5.10	5.13
Water flow												
in. of Hg	—	—	1.56	1.81	1.88	4.75	4.75	6.25	6.25	—	—	—
lb./hr.	—	—	88	96	98	156	156	179	179	—	—	—
lb./100 lb. fuel	—	—	30.5	32.9	33.6	52.9	53.0	60.9	60.9	—	—	—
Fuel												
pints/hr.(FM)	—	323	325	329	329	332	331	331	331	—	324	322
lb./b.hp./hr.(FM)	—	0.746	0.732	0.732	0.732	0.739	0.737	0.737	0.735	—	0.745	0.746
R.p.m.	—	1702	1710	1702	1704	1699	1699	1697	1699	—	1694	1701
B.hp.	—	384	394	398	399	399	399	399	400	—	386	383
B.hp.	—	391	401	404	405	405	405	404	404	—	390	390
Manifold press., in. of Hg	32.0	32.1	31.8	32.0	31.9	31.9	32.0	32.0	31.9	—	32.0	32.0
Intake air, °F.	—	80	78	77	77	76	75	73	70	—	70	70
Charge temp., °C.	—	142	112	107	107	103	98	94	94	—	129	133
Cooling air, °F.	—	46	46	46	47	47	47	47	47	—	47	47
Oil												
Press.	—	75	75	75	75	75	75	75	74	—	75	75
Inlet press.	—	61	61	62	62	62	62	62	61	—	61	61
Outlet press.	—	73	74	73	72	72	71	70	69	—	69	71
Temp. rise, °F.	—	12	13	11	10	10	9	8	8	—	8	10
Cylinder head, °F.												
1‡	—	371	364	326	322	307	281	270	258	—	364	382
2	—	378	368	357	354	343	329	326	314	—	368	375
3	—	382	368	361	354	333	322	311	300	—	378	385
4	—	430	406	392	389	371	361	347	336	—	420	433
5	—	413	382	364	361	329	314	304	292	—	403	410
6	—	464	447	444	433	410	403	399	399	—	457	460
7	—	403	382	382	375	361	354	354	354	—	385	385

TABLE I—*Continued*

WATER INJECTION TESTS

Engine started 11.23 a.m., off 11.53 a.m.; started 3.20 p.m., off 5.22 p.m.   Velocity of cooling air, 123 m.p.h. past cylinder heads

Cold junction, 62° F.   Barometer, 29.85 in. of mercury.   Sp. gr. of fuel, 0.710.

Time	4.20°	4.40°°	4.44	4.49	4.52	4.55	4.58	5.02	5.05	5.08	5.10	5.13
Cylinder head, °F.—Conc.												
8	—	490	471	460	460	444	430	430	420	—	477	487
9	—	406	389	385	385	368	361	350	347	—	406	406
10	—	447	392	385	385	350	343	329	326	—	433	437
11	—	396	350	343	340	314	307	300	296	—	389	389
12	—	430	389	364	361	289	285	262	251	—	423	430
13	—	406	368	347	343	285	281	262	258	—	399	399
14	—	413	375	368	368	333	329	311	307	—	406	406
1	—	378	340	326	326	281	281	258	258	—	382	382
Av.	—	416	389	377	374	346	336	325	337	—	408	413
Max.	—	490	471	460	460	444	430	430	420	—	477	487
Min.	—	371	350	326	322	281	281	258	251	—	364	375
Cylinder base, °F.												
1	—	225	225	211	211	201	193	186	176	—	208	220
2	—	251	248	243	241	239	232	229	220	—	237	245
3	—	239	235	227	225	220	211	208	201	—	222	232
4	—	263	263	253	253	243	248	235	227	—	251	265
5	—	243	239	229	229	211	201	196	183	—	235	241
6	—	248	253	243	243	239	235	239	235	—	243	251
7	—	211	211	211	211	203	201	201	201	—	211	211
8	—	243	235	229	227	225	218	216	211	—	227	235
9	—	286	277	277	272	263	260	253	248	—	277	283
10	—	263	253	248	243	235	227	216	208	—	201	258
11	—	186	171	166	166	153	150	142	140	—	171	176
12	—	263	253	243	243	211	206	191	181	—	251	263
13	—	243	235	222	220	186	183	176	168	—	235	239
14	—	258	243	241	239	225	220	211	203	—	248	255
Av.	—	244	241	232	230	218	199	207	200	—	230	241
Max.	—	286	277	277	272	263	260	253	248	—	277	283
Min.	—	186	171	166	166	153	150	142	140	—	171	176

TABLE I—*Concluded*
WATER INJECTION TESTS

Engine started 11.23 a.m., off 11.53 a.m.; started 3.20 p.m., off 5.22 p.m.
Cold junction, 62° F. Barometer, 29.85 in. of mercury. Sp. gr. of fuel, 0.710. Velocity of cooling air, 123 m.p.h. past cylinder heads

Time	4.20*	4.40**	4.44	4.49	4.52	4.55	4.58	5.02	5.05	5.08	5.10	5.13
Temperature plugs, °F.												
1	—	531	490	471	467	450	413	399	378	—	528	538
2	—	563	528	525	519	503	490	477	467	—	554	557
3	—	585	547	541	538	506	490	474	457	—	585	591
4	—	585	550	541	538	509	500	480	471	—	588	591
5	—	544	500	474	471	450	413	392	371	—	538	538
6	—	630	603	603	597	566	557	557	554	—	627	627
7	—	621	575	575	575	554	547	544	547	—	606	603
8	—	618	588	588	588	560	554	547	541	—	612	618
9	—	585	560	557	554	525	516	503	503	—	585	585
10	—	603	550	541	538	497	484	460	460	—	603	603
11†												
12	—	585	538	516	516	440	413	357	347	—	579	588
13†												
14	—	582	538	535	535	497	490	467	464	—	582	582
Av.	—	586	547	539	536	505	489	471	463	—	582	585
Max.	—	630	603	603	597	566	557	557	554	—	627	627
Min.	—	531	490	471	467	440	413	357	347	—	528	538

*No water. **Water turned on after readings were taken. ‡Cylinder number. † Out of order.

TABLE II
WATER INJECTION TESTS

Engine started 3.00 p.m., off 5.37 p.m.; restarted 6.03 p.m., off 6.41 p.m.
Cold junction, 52° F. Barometer, 30.25 in. Hg. Sp. gr. of fuel, 0.710. Velocity of cooling air, 119 m.p.h. (at 32° F.).

Time	3.42*	3.45*	3.48**	3.49	3.53	3.56	4.00	4.05	4.09	4.13	4.16	4.21
Water flow												
in. Hg.	—	—	—	1	1	3.69	3.75	6.13	6.50	7.88	7.94	7.75
lb./hr.	—	—	—	70	70	139	140	177	182	202	203	201
lb./100 lb. fuel	—	—	—	21.6	21.3	42.0	41.9	52.8	54.3	59.9	60.4	59.6
Fuel												
pints/hr.(FM)	355	357	—	365	370	373	376	377	377	380	378	379
lb./b.hp./hr.(FM)	0.728	0.729	—	0.717	0.720	0.718	0.724	0.723	0.723	0.727	0.722	0.722
R.p.m.	1692	1700	—	1701	1694	1702	1696	1689	1700	1702	1701	1701
B.hp.	433	435	—	452	455	461	461	463	463	464	465	465
B.hp.	441	443	—	459	462	468	468	470	469	470	470	470
Manifold press., in. of Hg	35.0	35.0	—	34.8	35.0	34.9	35.0	34.9	35.0	35.0	35.0	35.0
Intake air, °F.	79	78	—	77	76	75	75	75	74	74	72	72
Charge temp., °F.	123	123	—	97	93	88	88	88	88	84	84	84
Oil												
Press.	76.5	76.5	—	76.5	76.5	76.5	76.5	76.5	76.5	76.5	76.5	77
Inlet press.	37	38	—	37	40	43	43	43	43	43	43	43
Outlet press.	56	57	—	57	57	56	56	55	54	54	54	53
Temp. rise, °F.	19	19	—	20	17	13	13	12	11	11	11	10
Cylinder head, °F.												
1	372	372	—	361	316	280	271	248	248	233	225	241
2	382	382	—	372	358	344	330	319	319	312	304	308
3	379	379	—	372	354	333	326	308	308	297	290	290
4	443	443	—	42i	410	396	389	379	379	372	368	361
5	416	416	—	396	365	337	326	308	308	301	290	297
6	483	483	—	457	450	434	434	430	434	434	434	437
7	389	396	—	379	375	368	365	361	354	358	354	351
8	454	454	—	416	413	407	400	447	454	454	450	443

TABLE II—*Continued*
WATER INJECTION TESTS

Engine started 3.00 p.m., off 5.37 p.m.; restarted 6.03 p.m., off 6.41 p.m.
Cold junction, 52° F.   Barometer, 30.25 in. Hg.   Sp. gr. of fuel, 0.710.   Velocity of cooling air, 119 m.p.h. (at 32° F.).

Time	3.42*	3.45*	3.48**	3.49	3.53	3.56	4.00	4.05	4.09	4.13	4.16	4.21
Cylinder head, °F.—*Conc.*												
9	400	403	—	393	389	372	368	354	354	354	351	347
10	440	443	—	416	416	389	389	368	368	375	358	361
11	396	400	—	358	358	333	340	323	326	323	308	312
12	443	440	—	400	389	319	312	282	290	267	271	271
13	393	396	—	358	347	282	282	248	260	241	244	248
14	410	416	—	386	389	354	347	323	326	308	301	316
1	372	372	—	319	319	271	271	241	248	225	229	241
Av.	414	416	—	392	381	354	349	336	338	331	325	320
Max.	483	483	—	457	450	434	434	447	454	454	450	443
Min.	372	372	—	361	316	282	271	248	248	233	225	241
Cylinder base, °F.												
1	235	235	—	235	241	206	197	181	178	176	171	171
2	258	258	—	255	253	241	237	229	227	227	220	220
3	237	239	—	239	229	220	218	208	206	206	201	198
4	269	272	—	272	260	258	253	248	245	243	243	248
5	258	248	—	243	232	216	216	203	203	193	191	191
6	274	295	—	272	272	274	269	277	265	263	265	263
7	220	220	—	220	216	211	206	208	208	206	206	†
8	239	239	—	235	229	235	225	225	225	225	222	220
9	279	286	—	291	286	281	281	269	274	274	269	267
10	267	263	—	255	258	251	248	237	241	235	232	232
11	186	186	—	173	173	166	163	150	158	156	147	147
12	267	267	—	260	253	251	225	198	203	186	186	188
13	243	245	—	245	225	220	191	173	173	168	168	168
14	265	267	—	255	251	237	235	216	218	206	201	211
Av.	250	251	—	246	241	233	226	216	216	212	209	210
Max.	279	295	—	291	286	281	281	277	274	274	269	267
Min	186	186	—	173	173	166	163	150	158	156	147	147

TABLE II—*Concluded*

WATER INJECTION TESTS

Engine started 3.00 p.m., off 5.37 p.m.; restarted 6.03 p.m., off 6.41 p.m.
Cold junction, 52° F. Barometer, 30.25 in. Hg. Sp. gr. of fuel, 0.710. Velocity of cooling air, 119 m.p.h. (at 32° F.).

Time	3.42*	3.45*	3.48**	3.49	3 53	3.56	4.00	4.05	4.09	4.13	4.16	4.21
Temperature plugs. °F.												
1	540	540	—	502	480	437	420	379	382	354	354	368
2	581	584	—	553	547	521	512	493	496	483	487	487
3	584	590	—	559	556	534	521	493	499	474	474	474
4	587	605	—	572	569	556	544	534	534	525	521	518
5	562	562	—!	499	496	450	440	416	420	400	396	396
6	656	662	—	626	626	611	620	620	620	626	623	626
7	605	605	—	575	575	569	565	562	559	559	559	559
8	623	626	—	596	596	590	590	605	611	602	596	593
9	602	602	—	575	578	553	553	540	540	528	525	525
10	623	626	—	587	590	562	562	544	547	537	521	531
11†												
12	608	611	—	559	559	470	470	423	430	372	400	407
13†												
14	602	605	—	565	575	534	537	499	509	487	483	490
Av.	598	602	—	564	562	532	528	509	512	496	495	498
Max.	656	662	—	626	626	611	620	620	620	626	623	626
Min.	540	540	—	499	480	437	420	379	382	354	354	368

* No water.   ** Water turned on after readings were taken.   † Out of order.

TABLE III
WATER INJECTION TESTS

Engine started, 3.00 p.m., off, 5.37 p.m.; restarted, 6.03 p.m., off, 6.41 p.m.
Cold junction, 52° F.   Barometer, 30.25 in. of mercury.   Sp. gr. of fuel, 0.710.   Velocity of cooling air, 119 m.p.h. (at 32° F.)

Time	4.30*	4.33**	4.55	4.58	5.02	5.05	5.09	5.13	5.16	5.20	5.23	5.26	5.29
Water flow													
in. of Hg	—	—	3.25	3.13	3.13	3.25	6.0	3.13	3.44	3.38	3.19	3.19	3.13
lb./hr.	—	—	131	128	128	131	175	128	134	133	129	129	128
lb./100 lb. fuel	—	—	37.8	37.1	36.3	36.7	47.4	34.4	35.9	34.7	33.5	34.1	33.5
Fuel													
pints/hr.(FM)	364	362	391	388	398	402	416	419	420	431	434	426	430
lb./b.hp./hr.(FM)	0.740	0.738	0.728	0.721	0.711	0.721	0.721	0.730	0.733	0.732	0.734	0.716	0.718
R.p.m.	1701	1696	1707	1708	1706	1702	1697	1702	1701	1691	1700	1689	1701
B.hp.	437	436	477	478	497	495	512	510	509	523	525	528	532
B.hp.	442	441	482	483	502	501	520	518	518	533	535	539	543
Manifold press., in. of Hg	35.0	35.0	36.0	36.0	37.0	37.0	38.0	33.0	38.0	39.0	39.0	39.4	39.4
Intake air, °F.	72	71	72	71	71	73	76	77	78	79	80	82	83
Charge temp., °F.	119	123	88	88	88	93	93	97	97	97	97	97	97
Oil													
Press.	77	77	77	77	77	77	77	77	77	77	77	76	76
Inlet press.	42	41	39	41	43	44	45	45	47	47	46	47	47
Outlet press.	55	56	52	55	58	58	59	60	60	61	61	62	62
Temp. rise, °F.	13	15	13	14	15	14	14	15	13	14	15	15	15
Cylinder Head, °F.													
1	368	368	308	308	316	308	297	308	308	319	319	333	337
2	386	386	344	347	351	351	347	354	361	361	365	375	382
3	382	389	344	344	351	347	340	351	358	358	361	372	379
4	447	450	389	393	416	420	423	437	427	430	434	437	440
5	423	423	344	344	361	365	368	389	386	393	396	396	400
6	477	480	447	447	464	461	464	477	477	483	487	496	502
7	382	386	358	358	361	361	358	361	368	372	379	379	382

TABLE III—Continued
WATER INJECTION TESTS

Engine started 3.00 p.m., off, 5.37 p.m.; restarted, 6.03 p.m., off, 6.41 p.m.   Velocity of cooling air, 119 m.p.h. (at 32° F.).
Cold junction, 52° F.   Barometer, 30.25 in. of mercury.   Sp. gr. of fuel, 0.710.

Time	4.30°	4.33**	4.55	4.58	5.02	5.05	5.09	5.13	5.16	5.30	5.23	5.26	5.29
Cylinder Head, °F.—Conc.													
8	499	502	477	483	496	496	502	512	509	525	525	537	544
9	403	403	375	379	396	393	379	393	396	400	403	403	410
10	457	454	423	430	440	437	410	430	420	430	437	443	450
11	393	400	319	326	372	368	358	368	358	372	375	379	386
12	443	440	347	351	347	351	330	361	372	372	375	389	393
13	403	400	308	308	294	297	330	326	326	330	340	358	361
14	416	416	393	396	407	403	368	410	403	413	416	427	423
1	368	368	308	308	316	308	275	312	304	319	326	333	337
Av.	420	421	370	372	384	383	373	391	391	394	401	409	414
Max.	499	480	477	483	496	496	502	512	509	525	525	537	544
Min.	368	368	308	308	294	297	279	308	308	319	319	333	337
Cylinder base, °F.													
1	229	235	211	216	218	220	216	220	225	229	235	239	243
2	253	255	239	241	245	248	251	253	255	255	260	263	267
3	235	239	220	225	227	229	229	232	237	237	239	243	248
4	267	272	248	253	260	263	274	272	269	272	274	293	293
5	201	196	216	220	227	232	235	243	241	243	248	248	253
6	281	286	281	286	293	279	281	289	289	291	295	309	314
7†													
8	243	245	235	237	241	243	248	248	251	255	258	263	263
9	297	300	286	277	281	†	267	269	267	277	279	281	283
10	265	267	253	258	263	263	267	269	267	277	279	281	283
11	183	183	161	163	173	173	171	173	176	178	181	181	186
12	267	269	239	241	251	253	245	255	258	265	279	274	277
13	248	248	208	213	201	206	196	220	225	227	235	243	248
14	260	263	248	251	258	258	245	260	258	265	267	272	272
Av.	248	251	234	237	241	239	238	245	246	249	254	259	262
Max.	297	300	286	286	293	279	281	289	289	291	295	309	314
Min.	183	183	161	163	173	173	171	173	176	178	181	181	186

TABLE III—*Concluded*

WATER INJECTION TESTS

Engine started 3.00 p.m., off, 5.37 p.m.; restarted, 6.03 p.m., off, 6.41 p.m.

Cold junction, 52° F.   Barometer, 30.25 in. of mercury.   Sp. gr. of fuel, 0.710.   Velocity of cooling air, 119 m.p.h. (at 32° F.).

Time	4.30*	4.33**	4.55	4.58	5.02	5.05	5.09	5.13	5.16	5.30	5.23	5.26	5.29
Temperature plugs, °F.													
1	544	544	474	474	490	477	440	493	480	496	502	512	518
2	599	596	537	544	550	553	537	562	565	572	575	587	593
3	611	611	556	559	562	559	534	569	572	581	593	599	608
4	620	620	559	562	584	587	587	608	602	608	608	608	617
5	572	572	477	480	506	509	499	534	531	547	544	544	544
6	677	680	641	647	665	659	674	680	680	701	709	723	729
7	602	605	569	575	593	593	599	602	599	614	620	626	629
8	659	656	638	638	656	656	665	677	674	696	696	712	717
9	599	602	569	569	584	587	584	593	590	599	602	611	611
10	641	641	605	608	620	620	611	608	608	629	629	644	647
11†													
12	626	629	531	534	537	537	531	553	556	565	569	587	587
13†													
14	614	614	593	596	608	602	599	605	602	517	626	635	635
Av.	614	614	582	566	580	578	572	590	588	602	606	616	620
Max.	677	680	641	647	665	659	674	680	680	701	709	723	729
Min.	544	544	474	474	490	477	440	493	480	496	502	512	518

* *No water.*   ** *Water turned on after readings were taken.*   † *Out of order.*

TABLE IV

WATER INJECTION TESTS

Engine started, 9.35 a.m.   Barometer, 30.3 in. of mercury.   Sp. gr. of fuel, 0.710.   Oil heater on throughout test.   Ethyl aviation gasoline 87 octane number.   CFR motor method

Time	10.08*	10.11*	10.18**	10.24	10.27	10.30	10.35	10.37	10.41	10.43	10.46	10.51	10.54	10.58	11.03
Water flow															
lb./hr.	—	—	—	120	120	144	144	191	193	221	221	247	247	273	273
lb./100 lb. fuel	—	—	—	38	38	45	45	59	59	68	68	76	75	85	83
Fuel															
pints/hr.(FM)	351	348	352	358	360	363	364	364	366	368	366	369	372	364	368
lb./b.hp./hr.(FM)	0.737	0.734	0.736	0.714	0.720	0.718	0.725	0.733	0.725	0.732	0.728	0.765	0.774	0.779	0.834
R.p.m.	1696	1690	1693	1704	1697	1697	1690	1682	1696	1699	1698	1696	1704	1685	1682
B.hp.	424	422	425	446	445	449	447	442	449	446	447	429	428	416	393
B.hp.	438	436	439	461	460	464	462	457	464	461	462	443	442	430	406
Manifold press., in. of Hg	35.0	35.0	35.0	35.0	34.9	35.0	35.0	35.0	35.0	35.0	35.0	35.0	35.0	35.0	35.0
Intake air, °F.	99	99	97	97	97	97	97	97	97	97	96	95	95	95	95
Charge temp., °F.	138	133	138	107	107	103	103	98	103	98	98	98	98	98	98
Cooling air, °F., (at 112 m.p.hr.)	36	36	36	36	36	36	36	36	36	36	36	36	36	36	36
Oil															
Press.	77	76	75	75	75	75	74	74	74	74	74	74	75	75	75
Inlet press.	53	54	55	58	59	59	59	59	58	58	58	58	57	56	56
Outlet press.	57	57	55	55	55	54	53	52	52	52	51	51	50	49	48
Temp. rise, °F.	4	3	0	-3	-4	-5	-6	-7	-6	-6	-7	-7	-7	-7	-8
Cylinder head, °F.															
1	382	382	378	326	322	307	311	285	281	285	277	258	254	251	251
2	396	399	396	364	361	350	354	333	340	340	333	311	304	300	289
3	389	389	389	361	361	350	354	322	329	326	322	285	277	281	262
4	433	433	426	389	389	375	378	350	350	350	347	319	322	318	314
5	430	430	426	357	361	350	354	307	418	411	407	285	292	292	292
6	464	464	457	413	410	410	410	392	403	413	413	396	396	396	389
7	423	423	413	385	389	382	385	375	382	378	378	364	357	371	375
8	421	424	467	457	453	447	444	433	427	440	437	426	417	410	417

TABLE IV—*Continued*
WATER INJECTION TESTS

Engine started, 9.35 a.m. Barometer, 30.3 in. of mercury. Sp. gr. of fuel, 0.710. Oil heater on throughout test. Ethyl aviation gasoline, 87 octane number. CFR motor method.

Time	10.08*	10.11*	10.18**	10.24	10.27	10.30	10.35	10.37	10.41	10.43	10.46	10.51	10.54	10.58	11.03
Cylinder head, °F.—Conc.															
9	403	406	406	382	385	378	378	364	371	371	368	350	343	336	343
10	437	440	437	368	368	361	361	333	343	329	333	318	311	307	314
11	406	410	413	364	361	354	354	340	343	343	326	326	322	322	326
12	450	450	447	357	357	340	333	300	300	277	270	176	176	204	98
13	385	389	382	307	314	292	289	215	228	215	215	180	180	176	164
14	420	423	423	371	371	368	364	336	350	350	343	318	311	300	300
1	382	—	378	322	322	311	311	277	289	281	277	254	254	247	247
Av.	417	419	419	372	372	362	362	335	348	345	341	308	304	305	295
Max.	464	464	467	457	453	447	444	433	427	440	437	426	417	410	417
Min.	382	382	378	307	314	292	289	215	228	215	215	176	176	176	98
Cylinder base, °F.															
1	245	247	242	232	228	221	221	210	204	206	202	188	178	178	173
2	263	265	260	255	251	249	251	265	251	260	255	234	223	223	196
3	245	249	247	245	240	234	234	228	226	223	223	204	196	193	183
4	281	283	279	273	268	260	260	253	247	251	249	237	228	221	210
5	263	263	260	234	234	232	234	212	212	210	208	240	186	183	181
6	306	301	298	261	275	275	277	273	279	277	268	265	255	226	218
7	249	249	245	234	234	230	230	226	223	226	226	221	218	215	212
8	296	298	293	286	283	279	279	279	270	275	273	265	255	253	249
9	277	273	263	263	263	251	251	245	240	245	258	232	221	+	202
10	273	277	277	255	255	263	268	240	249	242	237	215	210	210	149
11	196	199	204	188	186	183	183	166	168	168	166	155	152	152	146
12	268	263	260	240	237	230	232	237	206	196	191	171	166	168	163
13	258	255	253	226	228	212	212	181	183	183	181	171	168	168	181
14	263	263	263	245	245	242	240	221	228	226	223	202	196	188	181
Av.	263	263	260	247	245	240	241	231	228	228	226	214	204	198	189
Max.	306	301	298	286	283	279	279	279	279	277	273	265	255	253	249
Min.	196	199	204	188	186	183	183	166	168	168	166	155	152	152	146

TABLE IV—*Concluded*
WATER INJECTION TESTS

Engine started, 9.35 a.m. Barometer, 30.3 in. of mercury. Sp. gr. of fuel, 0.710. Oil heater on throughout test. Ethyl aviation gasoline, 87 octane number. CFR motor method.

Time	10.08*	10.11*	10.18**	10.24	10.27	10.30	10.35	10.37	10.41	10.43	10.46	10.51	10.54	10.58	11.03
Temperature plugs, °F.															
1	550	550	544	471	467	453	453	403	417	497	†	444	440	440	417
2	594	594	591	544	541	535	535	490	512	506	500	417	417	426	385
3	609	612	612	560	557	547	547	493	519	500	497	467	467	467	460
4	615	615	612	557	557	547	547	497	512	512	509	361	385	378	382
5	606	603	597	493	497	490	484	392	444	417	413				
6	660	663	660	†											
7	603	603	594	544	544	487	480	†							
8	660	663	657	612	609	603	603	563	575	575	569	541	538	528	528
9	615	609	609	569	569	566	563	512	547	538	531	493	484	480	487
10	588	591	588	525	512	519	509	464	487	474	474	450	440	433	444
11	585	588	588	503	509	503	503	467	484	474	467	440	440	437	440
12	642	539	633	535	531	512	512	426	450	396	396	270	274	270	159
13	550	554	563	440	453	426	417	343	368	322	318	254	258	247	224
14	563	563	563	519	516	506	503	484	497	480	474	426	426	406	368
Av.	603	603	601	529	528	515	512	461	484	474	468	415	415	410	390
Max.	660	663	660	612	609	603	603	563	575	575	569	541	538	528	528
Min.	550	554	544	471	453	426	417	392	368	322	318	254	258	247	159

Before the engine was stopped, it was found that with the water injection off, the power had fallen off and the consumption of fuel had risen rapidly 400 points per hr. This was later found to be due to fouled spark plugs and a loose induction pipe.

During the readings at 10.58 the vibration of the engine became excessive and was still greater when the 11.03 readings were taken.

* No water.   ** Water turned on after readings were taken.   † Out of order.

TABLE V

WATER AND ALCOHOL INJECTION TESTS

Alcohol 46½% of water/alcohol blend by weight.   Engine started, 3.15 p.m.   Barometer, 29.90 in. of mercury.   Sp. gr. of fuel, 0.710

Time	3.27*	3.30**	3.35	3.43	3.47	3.49	3.51	3.54	3.59	4.01	4.05
Pints fuel/hr.(FM)	354	354	357	364	370	370	375	380	379	374	388
Fuel only, lb./b.hp./hr.(FM)	0.818	0.814	0.802	0.808	0.813	0.813	0.826	0.833	0.842	0.842	0.989
Alcohol and fuel, lb./b.hp./hr.	0.818	0.814	0.878	0.882	0.940	0.940	1.015	1.020	1.060	1.071	1.285
Lb./hr. alcohol and water	—	—	66	66	114	114	167	167	197	197	226
Lb. water/100 lb. fuel	—	—	11	11	19	19	27	27	32	32	35
Lb. alcohol/100 lb. fuel	—	—	10	9	16	16	23	23	27	27	30
R.p.m.	1704	1707	1697	1699	1701	1697	1691	1701	1704	1696	1700
B.hp.	385	387	396	401	405	405	404	406	401	395	349
B.hp.	401	403	411	416	420	419	418	420	415	408	360
Manifold press., in. of Hg	35.0	35.0	34.9	35.0	35.0	35.0	34.9	35.0	35.1	35.0	35.0
Intake air, °F.	104	104	102	100	99	98	98	98	97	97	97
Charge temp., °F.	138	138	112	107	103	103	98	94	94	94	94
Cooling air, °F. (at 112 m.p.hr.)	38	38	38	37	37	37	37	37	37	37	37
Oil											
Press.	77	77	77	77	77	77	76	76	76	76	76
Inlet press.	40	42	48	49	52	52	52	53	53	53	53
Outlet press.	50	48	47	47	47	47	47	46	45	46	45
Temp. rise, °F.	10	6	−1	−2	−5	−5	−5	−7	−8	−7	−8
Cylinder head, °F.											
1	399	403	380	371	361	350	333	322	304	300	266
2	392	392	378	364	354	350	326	322	304	300	270
3	406	406	392	371	361	357	333	326	304	300	266
4	450	453	430	417	403	396	378	375	368	364	350
5	426	423	403	389	375	364	350	343	326	326	292
6†											
7	444	444	420	399	385	375	364	371	371	368	361

TABLE V—*Continued*

WATER AND ALCOHOL INJECTION TESTS

Alcohol 46¼% of water/alcohol blend by weight.   Barometer, 29.90 in. of mercury.   Engine started, 3.15 p.m.   Sp. gr. of fuel, 0.710

Time	3.27*	3.30**	3.35	3.43	3.47	3.49	3.51	3.54	3.59	4.01	4.05
Cylinder head, °F.—Conc.											
8	112	112	103	103	98	98	94	94	89	89	89
9	433	433	423	399	399	399	385	385	385	385	385
10	490	490	460	444	413	410	382	371	371	371	368
11	426	426	403	396	375	375	357	354	371	371	340
12	457	457	420	406	368	364	311	304	277	277	212
13	444	444	403	392	361	354	281	277	231	196	89
14	457	457	433	426	413	406	392	389	371	371	343
1	403	403	382	371	354	354	322	322	300	300	266
Av.	410	411	388	375	311	354	330	326	313	309	279
Max.	490	490	460	444	413	410	385	385	385	385	385
Min.	112	112	103	103	98	98	94	94	89	89	89
Cylinder base, °F.											
1	240	245	242	232	230	228	226	215	210	208	191
2	258	265	260	253	249	247	242	237	228	230	215
3	245	249	247	237	234	232	228	223	212	212	196
4	275	281	279	265	263	260	253	251	247	247	237
5	273	273	263	247	245	242	234	232	223	223	255
6†											
7	228	237	230	230	221	226	218	221	210	210	210
8	178	183	181	176	173	173	168	166	163	163	161
9	251	253	258	247	237	234	223	228	226	226	234
10	277	281	268	258	255	249	234	232	193	232	221
11	206	206	199	193	188	186	176	171	166	166	161
12	258	263	258	240	228	226	218	210	206	202	163
13	270	275	258	251	240	234	206	202	181	173	140
14	268	270	263	258	249	247	240	237	232	228	210
Av.	248	252	247	237	232	230	220	217	207	209	200
Max.	277	281	279	265	263	260	253	251	247	247	255
Min.	178	183	181	176	173	173	168	166	163	163	140

TABLE V—*Concluded*

WATER AND ALCOHOL INJECTION TESTS

Alcohol 46⅓% of water/alcohol blend by weight.   Engine started, 3.15 p.m.   Barometer, 29.90 in. of mercury.   Sp. gr. of fuel, 0.710

Time	3.27*	3.30**	3.35	3.43	3.47	3.49	3.51	3.54	3.59	4.01	4.05
Temperature plugs, °F.											
1†											
2	597	603	575	550	531	524	490	487	460	460	417
3	621	621	597	566	544	538	497	490	453	450	385
4	621	624	597	572	547	541	516	516	503	497	471
5	615	609	575	554	524	519	490	487	460	453	417
6†											
7	636	639	600	575	541	535	516	512	509	509	497
8†											
9	618	615	591	579	554	550	528	531	519	519	516
10	651	654	606	585	547	535	506	503	500	490	487
11	597	603	563	550	524	522	497	487·	484	503	453
12	645	645	597	579	528	522	460	450	413	410	318
13	627	627	569	547	500	497	392	392	314	247	150
14	609	609	579	569	544	541	523	523	500	467	450
Av.	621	622	586	566	535	529	492	489	465	455	415
Max.	651	654	606	585	554	550	528	531	519	519	516
Min.	597	603	563	547	500	497	392	392	314	247	150

* *No water.*   ** *Water turned on after readings were taken.*   † *Out of order.*

THE HEAT CAPACITY OF BISMUTH FROM −80° TO 120° C.[1]

BY H. L. BRONSON[2] AND L. E. MacHATTIE[3]

Abstract

The mean heat capacity of bismuth over 10° intervals has been determined from −80° to 120° C. by means of adiabatic electrical heating in a copper jacket. The maximum deviation of any individual point from a smooth curve is 0.1%, and the error in the absolute values obtained is considered to be not more than 0.1%. No discontinuities or irregularities were found; in fact, the experimental results are represented to within the limits of experimental error by the linear equation:

$$C_p = 0.1238_5 + 4.45 \times 10^{-5}t,$$

where t is the Centigrade temperature, and the units are joules per gram per degree. The equation:

$$C_p = \frac{1}{209.0} D\left(\frac{119}{T}\right) + 3.99_7 \times 10^{-7}T^{1.703}$$

was found to fit the mean experimental curve as closely as the graph could be read (0.02%). T is the absolute temperature and $D(119/T)$ the Debye function for C_v per mole. C_p is given in joules per gram per degree. A calculation of C_p from non-thermal data gives values about 3% low.

Introduction

This paper describes a continuation of the work of Bronson and Wilson (3). The same apparatus and method have been applied to the measurement of the heat capacity of bismuth.

As is well known, many of the properties of bismuth are peculiar. Besides being very diamagnetic it has a specific resistance higher than that of most if not all metals, and it expands on solidifying. Goetz and Jacobs (6) reported discontinuities or rapid changes in the coefficient of expansion of the crystal lattice spacing of bismuth. Gruneisen's law, then, might lead one to suspect similar peculiarities in the heat capacity. From this it would seem that the investigation of the heat capacity might be of considerable interest.

Preliminary Work

All the apparatus was re-calibrated and the thermal insulation was adjusted again as though the apparatus were being assembled for the first time. The aim was to keep temperature variations over the inside surface of the copper jacket within 0.01° C. However, these adjustments required much time, and there was no certainty that after the adjustments were made the thermal

conditions would be sufficiently well reproduced following removal and replacement of the copper jacket, or with varying values of relative humidity. It was therefore decided to ascertain the magnitude of the error that would be introduced by large temperature differences in the jacket.

Determinations were made with the silver specimen used by Bronson and Wilson, current being supplied to the heating coils on the sides and bottom of the jacket but not to the top coil. This gave a temperature difference between the bottom and top of the jacket of 0.5° C. at 93° C. After the jacket had been brought to a steady temperature following a temperature rise, the platinum thermometer indicated a falling temperature for 20 min. owing to the redistribution of heat flow from the heating coil on the upper side of the jacket. Here, then, was an opportunity to so adjust the position of the platinum thermometer that it would indicate the mean temperature of the thermojunctions in the jacket, a point about which there had previously been some uncertainty. The thermometer was raised until it registered a steady temperature after a rise, and friction tape was wrapped around its stem to hold it in the new position. An X-ray photograph showed that this held the middle of the platinum coil within 1 mm. of the joint between the two halves of the jacket. Two measurements then made with the silver specimen at 77° and 88° C. showed the surprisingly small deviations of 0.06 and 0.09% respectively from the experimental values of Bronson and Wilson.

Since it was thus found that a much rougher approximation of temperature uniformity in the jacket was sufficient, adjustments were made to keep temperature variations within 0.05° C. before measurements were taken.

Measurements

Several series of determinations were made as described by Bronson and Wilson, the only difference being that the series taken with the calorimeter surrounded by solid carbon dioxide were extended to 40° and 80° C. instead of to 30° and 40° C.

As a check on these measurements with the copper jacket, several determinations near room temperature were made, the water bath and jacket employed by Bronson, Chisholm, and Dockerty (2) being used. These measurements were 0.07% higher than the mean of the others; this is considered quite satisfactory agreement. Although this apparatus is similar in principle, it should be emphasized that the differential thermocouples, the suspension wires and method of suspension, the size of the jacket cavity, and the thermal relation between the thermometer and the jacket thermocouple junctions are all physically different, and hence provide some assurance that no unsuspected blunder or large systematic error has crept in.

In all, 65 heat capacity determinations were made. The results were plotted on large-scale graph paper on which 2 mm. represented 1 in the fourth figure of the value of C_p. Mean experimental values for every 20° were determined by stretching a fine black wire over short sections of the graph and moving it until it appeared to be the best line through the points. This

was done several times. The averages of the values so obtained are given in Table I, Column II.

No indications of any discontinuity in the heat capacity curve or in its slope were found in the temperature range covered.

Empirical Equations

It was found that, within the limits of experimental error, a linear equation would represent the experimental results over the whole temperature range. The equation in terms of Centigrade temperature is:

$$C_p = 0.1238_5 + 4.45 \times 10^{-5}t, \tag{1}$$

where C_p is the number of joules per gram per degree.

Since, however, the experimental graph appears to be concave downwards from −80° to 0° C. and concave upwards from 0° to 120° C. (Table I, Column IV), an attempt was made to obtain a closer fit by use of an equation of the form $C_p = \dfrac{1}{M} D\left(\dfrac{\theta}{T}\right) + AT^n$, where M is the molecular weight, $D\left(\dfrac{\theta}{T}\right)$ is the Debye function for C_v per mole, and T is the absolute temperature.

TABLE I

I Temp., °C.	II Experimental graph	III Equation (1)	IV Difference II–III	V Equation (2)	VI Difference II–V
120	0.1292_8	0.1291_9	$+0.0000_9$	0.1292_8	0.0000_0
100	$.1283_4$	$.1283_0$	$+ \quad 0_4$	$.1283_3$	$+ \quad 0_1$
80	$.1273_9$	$.1274_1$	$- \quad 0_2$	$.1274_0$	$- \quad 0_1$
60	$.1264_9$	$.1265_2$	$- \quad 0_3$	$.1264_9$	0_0
40	$.1256_1$	$.1256_3$	$- \quad 0_2$	$.1256_0$	$+ \quad 0_1$
20	$.1247_2$	$.1247_4$	$- \quad 0_2$	$.1247_3$	$- \quad 0_1$
0	$.1238_5$	$.1238_5$	0_0	$.1238_6$	$- \quad 0_1$
−20	$.1230_1$	$.1229_6$	$+ \quad 0_5$	$.1229_9$	$+ \quad 0_2$
−40	$.1221_0$	$.1220_7$	$+ \quad 0_3$	$.1221_1$	$- \quad 0_1$
−60	$.1212_0$	$.1211_8$	$+ \quad 0_2$	$.1212_0$	0_0
−80	$.1202_5$	$.1202_9$	$- \quad 0_4$	$.1202_4$	$+ \quad 0_1$

The constants θ, A, and n, in this equation were determined empirically as follows. By trial and error it was found possible to obtain a value of θ, the characteristic temperature, such that $C_p - \dfrac{1}{M} D\left(\dfrac{\theta}{T}\right)$ could be accurately represented by a term of the form AT^n. This means that a plot of $C_p - \dfrac{1}{M} D\left(\dfrac{\theta}{T}\right)$ against T on logarithmic paper would yield a straight line from which A and n could be determined. The value so found was 119 to the nearest integer. This is considerably greater than the value 107 calculated from previous low temperature, heat capacity measurements (8), but is in tolerably good agreement with the value 116 calculated from elastic constants (see note in Table II). Too much significance should not be

attached to the value 119, for this value obviously depends on the form of the term or terms chosen to represent $C_p - \dfrac{1}{M} D\left(\dfrac{\theta}{T}\right)$. The equation obtained is:

$$C_p = \frac{1}{209.0} D\left(\frac{119}{T}\right) + 3.99_7 \times 10^{-7} T^{1.703} \tag{2}$$

in joules per gram per degree. Values given by this equation and the differences between these and the experimental results are given in Table I, Columns V and VI, from which it will be seen that the equation represents the experimental results as accurately as these can be read from the graph. Moreover its slope agrees well with that of the experimental graph at the two extremities of the range. This agreement indicates that the equation can probably be extrapolated with safety for some distance. This cannot be done with the linear equation.

In connection with Equation (2) it is well to draw attention to the fact that at 120° C. a change of 1 in the fourth figure of the exponent of T changes the fifth figure of C_p by 6, and a change of 1 in the third figure of A changes the fifth figure of C_p by 3. However, a small change in one of these quantities can be practically compensated for by a change in the other. Thus the accuracy to which each must be expressed in order that a certain accuracy in the calculated value of C_p (Table I, Column V) may be obtained is greater than the accuracy of determination of their absolute values. As for the characteristic temperature, a change of 1 in it just produces a detectable curve in the logarithmic plot.

Since the relative accuracy of values of the heat capacity at different temperatures is greater than their absolute accuracy, the agreement of Equation (2) with the experimental results within narrower limits than the probable experimental error would seem to be more than coincidence and may have theoretical significance.

Sources of Error

An analysis of the batch of bismuth from which the specimen was made has been supplied by the Consolidated Mining and Smelting Company of Canada; it showed the following impurities: Pb, less than 0.002% (by spectrograph); S, 0.020%; Cu, 0.0022%; As, less than 0.00005%.

The bismuth equivalent of the specimen was calculated in the usual way (3). The equivalent of all non-bismuth components amounted to 0.63% of the total bismuth equivalent, and of this, about half was that of metals whose specific heat is known to within 1%.

In most of the determinations in which the calorimeter was surrounded by dry ice there was a downward temperature drift when the jacket-to-specimen thermocouple indicated no temperature difference. The average of the rates of drift before and after a measurement was assumed for the heating period and a correction applied. The correction for the greatest drift was 0.25%. There are reasons for believing that the drift was not due to sublimation of

frost or evaporation of moisture on the specimen, but its cause has not been definitely ascertained. Satisfactory evidence, however, that the drift has not introduced any appreciable systematic error in the determinations is found in the fact that where the series of measurements taken with the calorimeter surrounded by solid carbon dioxide overlap those taken with room temperature surroundings no difference is noticeable in the scattering of the individual points of the two series about the mean. This overlapping extended from 10° to 80° C.

The systematic error in the estimation of which there is more uncertainty than in any other lies in the heat transfer between jacket and specimen during the heating period. Transfer will take place if the lag between the mean temperature of the jacket thermocouple junctions and the jacket surface is not equal to the lag between the mean temperatures of the junctions in the specimen and its surface. This error cannot be detected by changing the rate of heating or the temperature interval of a determination. Seemingly, the only possible way to detect the change is to use a specimen in a container whose heat capacity can be determined when full and when empty, thus using it as a transfer instrument. As stated by Bronson and Wilson, it is considered unlikely that this error would be as large as that due to a constant temperature difference of 0.01° C., which a rough calculation shows would cause an error of 0.06%.

Of the factors in the expression for the heat capacity, it is estimated that the temperature interval has the largest probable error. It is unlikely that this error is as great as 0.05%.

The maximum deviation of any point from a smooth curve is 0.1%, and the average deviation, 0.03%.

Theoretical Heat Capacity

A calculation of the heat capacity of bismuth from non-thermal data is shown in Table II, from which it is seen that the calculated values are low by about 3%. Part of this difference may be due to the values of θ, α, β chosen and the number of free electrons assumed per atom. However, if five free electrons per atom are assumed, and θ, α, and β are each changed by 10% in the direction to increase the calculated C_p, the discrepancy is only halved. Actual errors in the constants as great as this and in the right direction seem improbable; consequently, one must conclude either that another term is

TABLE II

Temperature, °C.	30	75
θ	116	116
$\frac{1}{M}\left(D\frac{\theta}{T}\right)$	0.1184$_8$	0.1186$_9$
$10^5\alpha$	3.96	4.33
ρ	9.79	9.79
$10^{12}\beta$	2.98	3.05
$\dfrac{\alpha^2 T}{\rho\beta}$	0.0016$_3$	0.0021$_9$
c_s	0.0015$_3$	0.0017$_4$
C_p, calc.	0.1216	0.1226
C_p, obs.	0.1252	0.1272
Difference, %	2.9	3.6

NOTE—*Sources of data:*

θ—*Calculation of Debye (5) but using recent values of constants.*

α—*I.C.T. (7) (Fizeau).*

ρ—*Measured.*

β—*I.C.T. (7) (Bridgman).*

c_s—*Calculated from formulas given in Reference (9), on the assumption of one free electron per atom.*

needed in the expression for the heat capacity or that the assumption of harmonic oscillations in the crystal lattice is not valid for bismuth at ordinary temperatures.

This discrepancy has been noted by Carpenter and Harle (4) and attributed to anharmonic oscillations.

Results of Previous Observers

A comparison of values obtained in the present work with those in the International Critical Tables and some of the more recent work is given in Table III. The equation given in the I.C.T. as representing "best" values is:

$$C_p = 25.4 + 0.0116t \quad (25° \text{ to } 200° \text{ C.})$$

where C_p is in joules per gram-atom. In the same units Equation (1) becomes:

$$C_p = 25.88 + 0.00930t$$

TABLE III

Source	Date	Temperature, °C.	Value	Accuracy claimed	Writers' value	Difference
I.C.T. (7) "best" values		30	25.7$_6$	"Rarely better than 1%"	26.16	1.5% low
		70	26.2$_3$		26.53	1.2% low
		120	26.8$_0$		27.00	0.74% low
Anderson (1)	1930	−60	5.94	1%	6.050	1.8% low
		−20	6.02		6.141	2.0% low
		20	6.09		6.227	2.2% low
Carpenter and Harle (4)	1932	33	6.18	1.3%	6.255	1.2% low
		99.6	6.35		6.405	0.86% low
Thomas and Davies (10)	1937	20	.0308$_8$		.02979	3.7% high

Acknowledgment

References

1. ANDERSON, C. T.   J. Am. Chem. Soc. 52 : 2720-2723.   1930.
2. BRONSON, H. L., CHISHOLM, H. M. and DOCKERTY, S. M.   Can. J. Research, 8 : 282-303.   1933.
3. BRONSON, H. L. and WILSON, A. J. C.   Can. J. Research, A, 14 : 181-193.   1936.
4. CARPENTER, L. G. and HARLE, T. F.   Proc. Roy. Soc. 136 : 243-250.   1932.
5. DEBYE, P.   Ann. Physik, 39 : 789-839.   1912.
6. GOETZ, A. and JACOBS, R. B.   Phys. Rev. 51 : 159-164.   1937.
7. INTERNATIONAL CRITICAL TABLES.   McGraw-Hill Book Company, New York.   1933.
8. KEESOM, W. H. and VAN DEN ENDE, J. N.   Proc. Acad. Sci. Amsterdam, 34: 210-211.   1931.
9. STONER, E. C.   Phil. Mag. 21 : 145-160.   1936.
10. THOMAS, W. J. and DAVIES, R. M.   Phil. Mag. 24 : 713-744.   1937.

PRODUCTION AND FREQUENCY MEASUREMENT OF CURRENTS HAVING FREQUENCIES FROM 10 TO 100 CYCLES PER SECOND[1]

By A. L. Clark[2] and L. Katz[3]

Abstract

A low frequency dynatron oscillator with a range of 10 to 100 cycles per sec. and a power output of 10 watts is described. The frequency is measured by taking photographs, at intervals of one second, of two pointers on a small synchronous motor powered by the current whose frequency is to be measured. The stability of the oscillations and the accuracy of the frequency measurements are such that frequencies may be maintained and measured to 1 part in 30,000, over a period of several hours.

It is sometimes found necessary, in the laboratory, to have a supply of alternating current of low and variable frequency. The need for such a current arose in connection with the design of an apparatus for the measurement of the ratio of the specific heats of gases.
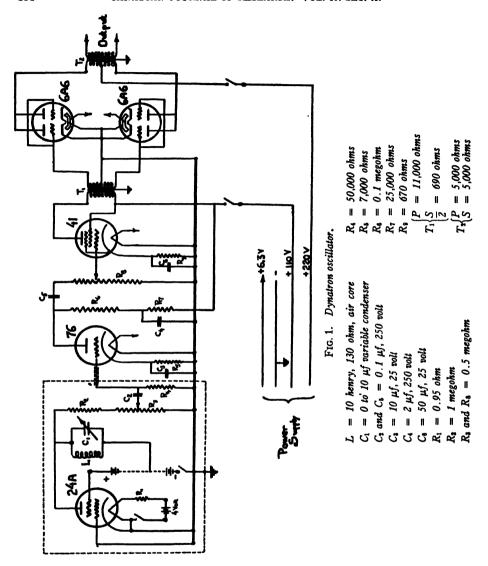
Production and measurement of high frequency currents have been satisfactorily accomplished with the design of crystal oscillators, coupled with multi-vibrators and high frequency synchronous motors, which, though excellent in performance, are costly to build and offer only discrete submultiples of the fundamental period of the crystal. This paper describes an oscillator that is comparatively inexpensive to build and that has a wide range of frequency output and exceptional stability. An accurate means of measuring the frequency is also described.

The oscillator with three stages of amplification is shown in Fig. 1. It is of the dynatron type, using the negative resistance of a 24-A tube.*

For stability the dynatron is powered entirely by batteries; however, any steady supply should prove satisfactory. The correct plate and screen-grid voltages to be used depend on the individual tube characteristics, and are found experimentally. The particular tube used was found to operate best with 115 volts on the screen and 32.4 volts on the plate. Under these conditions it has a screen emission of 11.5 ma. To minimize the effect of temperature changes, an air-core inductance is used since the permeability of an iron core changes with temperature, and this would affect the frequency. L, Fig. 1, is an air-core inductance and C_1 is a mica condenser.

* It has been recently found that the negative-transconductance between the third and second grids of an RCA-57 tube is better fitted for this purpose.

FIG. 1. *Dynatron oscillator.*

L = 10 henry, 130 ohm, air core
C_1 = 0 to 10 μf variable condenser
C_2 and C_5 = 0.1 μf, 250 volt
C_3 = 10 μf, 25 volt
C_4 = 2 μf, 250 volt
C_6 = 50 μf, 25 volt
R_1 = 0.95 ohm
R_2 = 1 megohm
R_3 and R_5 = 0.5 megohm

R_4 = 50,000 ohms
R_5 = 7,000 ohms
R_6 = 0.1 megohm
R_7 = 25,000 ohms
R_8 = 670 ohms
$T_1 \begin{cases} P = 11,000 \text{ ohms} \\ \dfrac{S}{2} = 690 \text{ ohms} \end{cases}$
$T_2 \begin{cases} P = 5,000 \text{ ohms} \\ S = 5,000 \text{ ohms} \end{cases}$

The proper sizes of inductance and capacity are effectively determined by the negative resistance of the tube and frequency output desired, according to the equations (1, p. 174)—

$$\frac{R}{L} + \frac{1}{C(-R_p)} = 0 \tag{1}$$

$$f = \frac{1}{2\pi} \sqrt{\frac{1}{LC} - \left(\frac{R}{2L} + \frac{1}{C(-R_p)}\right)^2} \cong \frac{1}{2\pi \sqrt{LC}}, \tag{2}$$

where L, C, and R are respectively the inductance, capacity, and resistance of the tank circuit, and $-R_p$ is the negative resistance of the tube, which is measured experimentally.

If C in Equations (1) and (2) is eliminated—

$$\frac{L^2}{R} \cong - \frac{(-R_p)}{4\pi^2 f^2} \, . \tag{3}$$

The greater part of the tank circuit resistance is due to the inductance; thus Equation (3) actually gives the proper ratio between L and R for the coil, in terms of the tube negative resistance and frequency desired. From this ratio it is possible to determine the most efficient type of inductance to be used, and then the correct capacity is calculated by means of either Equation (1) or (2). By use of these calculations for a frequency of 10 to 100 cycles, L was fixed at 10 henrys, R at 130 ohms and C was made variable up to 10 μf.
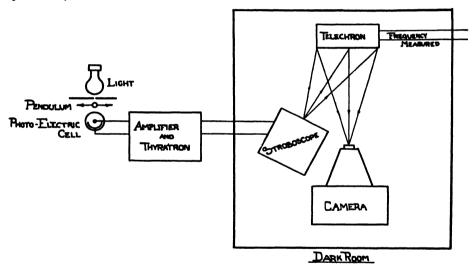
FIG. 2. *Method of measuring the frequency.*

The variable 10 μf. condenser was constructed as follows. Four sets of 10 mica condensers of capacities of 1 μf., 0.1μf., 0.01 μf., and 0.001 μf. were used. Each set was placed in a semicircle and a rotating dial allowed to connect the individual condensers, one at a time, in parallel. The four dials were connected together. With this arrangement it is possible to obtain any capacity between 0.001 and 10 μf. Finer adjustments are made by placing an ordinary radio condenser in parallel with this set-up.

To measure the frequency, high speed photographs are taken, at intervals of one second, of two pointers on a small synchronous motor powered by the oscillator. The frequency is then determined from the positions of the pointers on these photographs. The method is illustrated in Fig. 2. The

pendulum of an accurate clock interrupts a light beam falling on a photo-electric cell: this gives, at intervals of one second, impulses which when amplified are used to actuate a thyratron. The thyratron in turn discharges a condenser through the primary of a spark coil, and provides a control spark for flashing a stroboscope.* Photographs of the pointers on the synchronous motor are then taken by the light of the stroboscope flash, and the frequency is determined.
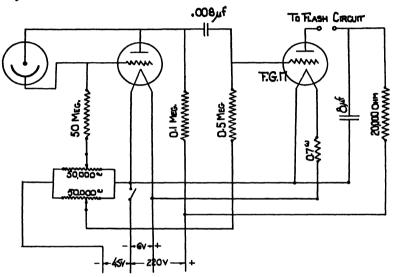
FIG. 3.   *Wiring diagram of photoelectric cell with amplifier and thyratron.   Type VB Westinghouse photoelectric cell.*

The actual wiring diagram of the photoelectric cell and thyratron and of the stroboscope are shown in Figs. 3 and 4, respectively. The mechanical details of the clock mechanism embodying the light system and photo-electric cell are shown in Fig. 5.

The two pointers on the synchronous motor were so geared that one makes one revolution in 50 cycles while the other makes one revolution per cycle. The dial, which is 5 in. in diameter, is divided into 100 equal parts; consequently, the frequency may be estimated to 1/1000 part of a cycle.

The photographs are taken on a piece of standard 35 mm. movie film wrapped around a drum. By pressing a key the drum is caused to rotate through an angle of 24 degrees (15 picture frames per circumference) with a slight lag behind the flashing of the stroboscope. The drum was rotated by means of an electromagnet and a spacer mechanism from an old typewriter. A small 60 tooth gear, attached to the "second" hand spindle of the clock, gave impulses for energizing the magnet. The angle of the lag mentioned is controlled by the position of the gear-wheel on the "second" hand spindle.

* *The argon filled lamp and design of the stroboscope were kindly supplied by Mr. H. E. Edgerton of the Massachusetts Institute of Technology.*

The stroboscope, synchronous motor, and camera (fitted with an f 8 lens) were placed in a dark room, and the camera lens was opened.   By depressing two keys (No. 1 in the stroboscope circuit, to control the flashing of the stroboscope, and No. 2 in the camera mechanism to control the rotation of
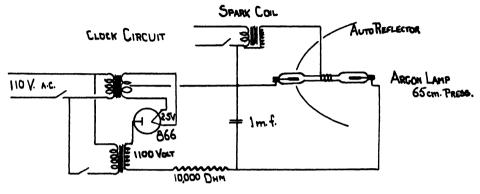
FIG. 4.   *Stroboscope circuit.*
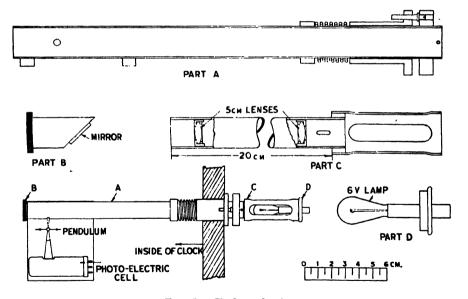
FIG. 5.   *Clock mechanism.*

the drum) the stroboscope was caused to flash, and this was followed slightly later by a rotation of the drum.   Key No. 2 is released and the next nine consecutive flashes are allowed to fall on the second frame of the film; the eleventh flash is then recorded on the third frame by pressing key No. 2 immediately after the ninth flash.   Thus the difference in the readings of the telechron pointers in the first and third frames plus some whole number

of revolutions* gives the number of cycles over a period of 10 sec. This process could be repeated for any number of flashes. Since the two halves of the pendulum swing may not be equal in length, it is important that the duration of a frequency measurement be an even number of seconds (corresponding to equal numbers of left- and right-hand halves of the pendulum swing).

The synchronous motor, of a type generally used in electric clockst, was placed directly across the oscillator output in parallel with the load. No variation in the frequency could be detected with changes in the load.

Table I summarizes the results of a test to determine how the frequency output of the oscillator varied from second to second.

The first column shows the readings of the pointers, to the estimated third decimal place, as recorded on the film. The second gives the difference between consecutive readings in the first column. It will be noticed that the frequencies, as shown, agree only in alternate pairs. This is because the photoelectric cell is not exactly in the centre of the pendulum swing. However, no error is introduced if the average frequency over one complete pendulum swing or two seconds, is taken, as shown in Column 3. It is seen that the maximum deviation from the mean value is only 1 part in 27,000.

To check the variation of the frequency over a somewhat longer period of time, say 15 min., the test summarized in Table II was made. Here the frequency was measured at five-minute intervals, the average over six consecutive seconds being taken, to give greater

TABLE I

VARIATION IN FREQUENCY FROM SECOND TO SECOND

Photograph reading	Difference	Average per pair
23.505		
	27.485	
0.990		27.489
	27.494	
27.484		
	27.482	
5.966		27.488
	27.494	
33.460		
	27.483	
10.940		27.490
	27.497	
38.440		
	27.480	
15.920		27.488
	27.497	
43.417		
	27.482	
20.899		27.489
	27.497	
48.396		
	27.480	
25.876		27.489
	27.498	
3.374		
Total average		27.489

TABLE II
VARIATION IN FREQUENCY OVER A PERIOD OF 15 MIN.

Time, min.	0	5	10	15	Mean
Average frequency over 6 sec.	27.421	27.421	27.421₅	· 27.422	27.421₄

weight to the third decimal place. The frequency varied less than 1 part in 30,000, or 1/1000 of a cycle.

As may be seen from the results in Table III, the oscillator shows equally good characteristics over a much longer period of time. On the basis of the average frequency for a 10 sec. period, the output varied 1 part in 270,000 in a run of 5½ hr.

TABLE III

VARIATION OF FREQUENCY OVER A PERIOD OF 5½ HR.

Time, hr:	0	5	6	10.5	Mean
Average frequency over 10 sec.	Oscillator started	27.3923	27.3924	27.3924	27.3924

The oscillator and frequency measuring device mutually check each other; thus if one or the other were not functioning properly, results as consistent as those shown in the tables could not be obtained. Table I indicates, to within the accuracy of frequency measurement, that the variation in the period of a pendulum oscillation from second to second is not large enough to affect the results appreciably. The *absolute* value of the frequency depends, of course, on the rate of the clock. This was checked against radio time signals and was found to be constant to within 3 sec. in 24 hr. or 1 part in 90,000.

The entire equipment has been found to be very flexible and reliable in operation. The output is large enough to drive the telechron and leave enough power for many purposes. The ease with which the frequency may be maintained at any desired value has been most satisfactory.

Acknowledgments

References

1. HUND, A. High frequency measurements. McGraw-Hill Book Company, New York. 1933.

THE REMOVAL OF WALL DEPOSITS BY HIGH FREQUENCY DISCHARGES[1]

By R. H. Hay[2]

Abstract

When a high frequency discharge is maintained between external sleeve electrodes in a tube coated with a thin metallic film, the film is removed from some regions and deposited in others, to give patterns which vary with frequency, pressure, the nature of the gas carrying the discharge, the nature of the film, and the tube diameter. Frequencies of 3.0, 60, and 300 megacycles per sec. have been used with discharges in air, nitrogen, oxygen, and hydrogen, at pressures ranging from 0.07 to 3.5 mm. of mercury and with coatings of silver and, in some cases, of sulphur. Tubes of 18 and 38 mm. outside diameter were used with a standard electrode spacing of 8 cm. and an electrode width of 1 cm.

Evidence is given that the removal is of two types: (i) local, taking place underneath the electrodes; and (ii) general, occurring adjacent to the positive column of the discharge. The cause of both types is found in the bombardment by positive ions: the local, or electrode, effect varies inversely as the pressure and the frequency; the general removal is independent of frequency, but varies directly as the pressure and the gas ion mobility, and inversely as the radius of the tube.

In interpreting the results, use is made of the hypothesis that the high frequency discharge is in effect two d-c. discharges with the electrodes as cathodes and the positive column as an effective anode. Verification has been found in the alteration of the positive column, the Faraday dark space, and the negative glow, with pressure variation and the variation of electrode spacing, and in the reaction of the negative glow to a transverse magnetic field.

Deposition regions are identified with the intersection of the negative glow and the tube wall, but no satisfactory explanation is offered for the fine structure sometimes observed in such regions.

Introduction

In 1933, C. W. Clapp, working in the laboratory of Prof. J. K. Robertson, observed that the high frequency discharge induced by sleeve electrodes removed a previously deposited metallic coating from those portions of the tube walls which lay beneath the electrodes. Subsequently, Robertson removed the coating from the entire inner surface of a tube by moving the electrodes from one position to another, using a tube the coating on which had resisted the action of a hot flame.

In a preliminary investigation of this phenomenon, Robertson and Clapp (13) subjected glass tubes, lightly silvered on the inner walls, to high frequency discharges at various pressures and at a constant frequency. They found that there was evidence of a distinct removal pattern which depended upon

the nature of the discharge, the time of exposure, and the temperature of the tube, and that patterns could be obtained by silvering a tube after it had been subjected to the discharge.

At about the time that Robertson and Clapp studied this phenomenon, Banerji, Ganguli, and Bhattacharya (1, 3) observed the formation of regularly arranged deposits in a similar type of discharge tube. After identifying the deposits as mercury vapor that had diffused over from a McLeod gauge, they were led to examine the patterns formed by various substances, some of which were electropositive and some electronegative. Furthermore, they investigated the electric fields in the discharge by means of a modified probe method, and found gradients from tube wall to axis which varied in sign and in magnitude along the axis. Regions in which the gradient is of greatest magnitude were found to correspond to areas where deposits are formed on the wall, the deposits of electropositive materials being in general complementary to those of electronegative materials.

Since Robertson and Clapp had made only a preliminary examination of the phenomenon, and since the explanation of the deposit offered by Banerji and co-workers (1, 3) was not completely satisfactory for some of the removal patterns, the present investigation was undertaken.

Experimental

Three sources of high frequency power were used: a single ended series-fed, 100-watt Hartley oscillator using a Mullard TX3-200 tube; a 40-watt push-pull oscillator using two 304B Western Electric tubes; and a special push-pull oscillator, also using the 304B tubes, built from plans kindly supplied by the Bell Telephone Laboratories, New York. The first oscillator covers, by the use of plug-in coils, the range 1.5 to 12 megacycles per sec.; the second is designed for 60 megacycles; and the third supplies about 7 to 10 watts at 300 megacycles. Frequency measurements were made with a General Radio wavemeter for all frequencies except the highest, for which a Lecher wire system was employed.

Three methods of forming metallic coatings on the inner surfaces of the glass tubes were tried: cathodic sputtering, evaporation, and silvering by means of the Brashear, or Rochelle salt, process. The first two presented difficulties which it was felt could not be overcome successfully in the time at the writer's disposal, so the Brashear process was finally used. Glass tubes, cut in lengths of 16 to 20 in., were thoroughly soaked in warm chromic acid, rinsed in tap water, then in distilled water, and silvered lightly while still wet. The layers of silver, as nearly uniform as it was possible to make them, were of "half-thickness". Too thick a coating is undesirable as it may stop the discharge; a heavy layer also makes it difficult to examine the action of the discharge on the silver. For the most part, the tubes used were of 16 mm. inside diameter although some observations were made with tubes of 34 mm. inside diameter. Some of the tubes were coated with sulphur by passing fumes from melted sulphur through them. Flowers of sulphur condensed on the tube walls and formed a fairly satisfactory layer.

Pressure was measured by means of an insensitive McLeod gauge situated close to the pump and shut off from the discharge tube except when readings were being taken.   Pressure in the discharge tubes was regulated by a needle valve placed between the reservoir and the discharge tube.   This valve was by-passed by a tap which, normally kept closed, could be opened to wash out the system with the carrier gas.   A rotary switch, inserted in the cathode-to-ground circuits of the oscillators, closed the contacts one second out of every two.   To minimize thermal effects, an electric fan was used to cool the tubes during exposure to the discharge.   When sulphur-coated tubes were used at low frequency and high pressure, the power supply was cut off for 30 to 60 sec. after every few flashes to ensure minimum heat action.   Even this precaution was not altogether successful, however, for some of the sulphur tubes show, at low frequency and high pressure, evidence of thermal removal. Tests showed that the glass must begin to soften before heat has any noticeable effect on the silver, and since no tube was allowed to become more than perceptibly warm, heat was not a factor in the formation of silver removal patterns.

The length of exposure to the action of the discharge was usually two to seven minutes, with a few exceptions of twelve and twenty-five minutes. The higher the frequency or the lower the pressure, the longer the exposure necessary to cause visible changes in the silver film.   The changes were slightly slower in air than in oxygen and nitrogen; in hydrogen they were slightly faster than in the other gases.   Gases subject to the same conditions of pressure and frequency were given equal exposures.

Results

The patterns shown in Figs. 2 to 5 are drawn as longitudinal cross sections of the silver films, black representing silver.   All estimations of the amount of removal (or deposit) were made visually.   The original thickness of the film is scaled as three-quarters of an inch and the longitudinal scale is slightly reduced from full size.   These drawings reproduce, within the limits of the visual method used, the variations in the silver layers on the tube walls.

As the removal patterns seem, in general, to correspond to the different types of discharge observed, these types have been described in detail.   There are two broad classifications, a low frequency series occurring at 15 megacycles per sec. and lower, and a high frequency series occurring at 60 and 300 megacycles per sec.

The first series is sketched in Fig. 1 and is composed of six types: *A*, *B*, *C*, *D*, *E*, and *F*.   The pressure at which each occurs is given in the figure.   The only one for which the pressure is critical is Type *B*, the transition from *B* to *A*, or *B* to *C* being sudden.   In all others the transition is gradual, and the division into types is arbitrarily based on the pressure increments.   All types occurred in air, nitrogen, and oxygen, the differences between gases being in the colors of the various parts of the discharge.   The colors indicated are those observed when air was used.   The parts marked "rose" and "pink"

in Fig. 1 generally become yellowish and more brilliant in nitrogen—especially in Types C to F; in oxygen the luminosity is much less and there are few colors other than blue and rose. Types D, E, and F cause very marked afterglows in all three gases. Exposures in silvered tubes were made, in general, with Types B, D, and F, although silver patterns in air were obtained with all six types. Type F is extinguished at a pressure of 10.7 mm. of mercury, while Type A continues at the lowest pressure obtainable with the Hyvac pump.
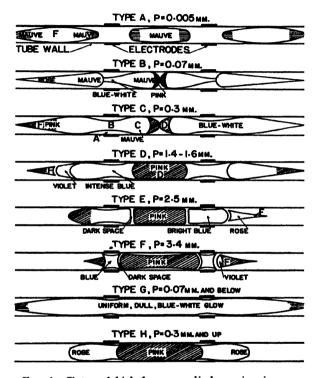
FIG. 1   *Types of high frequency discharge in air.*

As shown in Fig. 1, the high frequency series has but two types. Type G (again referring to air) occurs at pressures of 0.005 mm. of mercury and changes gradually, by a shortening of the long central pencils, to Type H which continues until a pressure of 2.0 mm. of mercury is reached, when the discharge is extinguished. As in the other series the main difference observable with different gases is one of color, with oxygen less luminous. The 60 megacycle oxygen discharge is extinguished at 0.6 mm. but continues at the lowest pressure obtainable. At 300 megacycles the discharge sometimes must be primed with a momentary discharge from a spark coil or by opening and closing the plate supply switch rapidly. The high frequency series of discharges does not heat the tube as much as the low frequency series, this
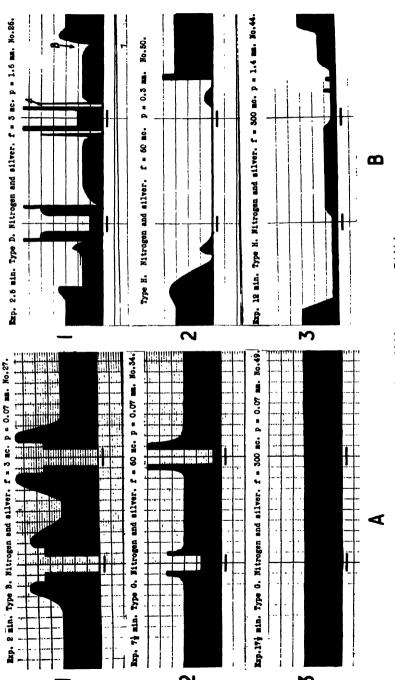
FIG. 2. *Frequency variation at (A) low pressure, (B) high pressure.*

being due, in part, to the lower power of the high frequency oscillators. Greater heat was developed, in general, at high pressure than at low pressure.

A large number of patterns was obtained, air, nitrogen, oxygen, and hydrogen being used as the carrier gases, at pressures of 0.07 to 3.5 mm. of mercury and at frequencies of 3, 60, and 300 megacycles per sec. Of these patterns, only a few representative ones are reproduced in this paper. While the evidence obtained was not always conclusive, certain main points have been fairly well established:

(1) Removal of silver is of two kinds, that occurring in localized fashion, as under the electrodes (No. 1, Fig. 2, *A*)—*the electrode effect*—and that occurring over large areas of the tube (Nos. 2 and 3, Fig. 2, *B*)—*the general removal*. Both occur simultaneously in some patterns and only one in others. The electrode effect is most noticeable at low pressures and low frequencies. The general removal occurs at higher pressures at all frequencies, and, is definitely associated with the pink or yellow glows marked F, in discharge Types *C*, *D*, *E*, and *F*, Fig. 1.

(2) Increase in frequency causes a decrease in electrode effect until it disappears altogether at 300 megacycles. A decrease in pattern complexity is also observed as frequency is increased (Fig. 2).

(3) As shown in Fig. 2, pressure alteration causes variation of the patterns. Pressure increase results in an increase in the general removal and a decrease in the electrode effect. Pattern complexity is greatest at an intermediate pressure and low frequency.

(4) A comparison of silver and sulphur patterns (Fig. 4) suggests that the two substances are complementary in their reactions to the discharge. At high pressure and low frequency, this effect is partly masked by thermal removal of the sulphur, but it is quite apparent at high frequencies and low pressure.

Influence of Carrier Gas

Oxygen and air produced the same effect on silver films as nitrogen. Hydrogen was used with both silver and sulphur coatings, and its effect on the silver (Fig. 5, *A*) is striking in that for all frequencies there is no general removal as there is with heavier gases. Further reference will be made to this point. The sulphur patterns (Fig. 5, *B*) show the effect of chemical removal, as well as electrical effects, for the odor of hydrogen sulphide was very marked at the Hyvac pump, especially during exposures made at low frequency and pressures greater than 1 mm. of mercury. It is interesting to note that removal by chemical combination occurs adjacent to, and at, those places subjected to the electrode effect.

Variation with Width of Tube

A series of exposures was made with nitrogen in wide tubes in order to test certain hypotheses which will be advanced later in the discussion of the general removal. At low frequency, the patterns obtained were similar to

Exp. 7¼ min. Type G. Nitrogen and silver. f = 60 mc. p = 0.07 mm. No.34.

Type H. Nitrogen and silver. f = 60 mc. p = 0.3 mm. No.50.

Exp. 17½ min. Type G. Nitrogen and silver. f = 300 mc. p = 0.07 mm. No.49.

Exp. 12 min. Type H. Nitrogen and silver. f = 300 mc. p = 1.4 mm. No.44.

Exp. 2 min. Type B. Nitrogen and silver. f = 3 mc. p = 0.07 mm. No.27.

Exp. 2.5 min. Type D. Nitrogen and silver. f = 3 mc. p = 1.6 mm. No.26.

Exp. 2 min. Type F. Nitrogen and silver. f = 3 mc. p = 3.4 mm. No.28.

FIG. 3. *Pressure variation at (A) low frequency, (B) and (C) high frequencies.*
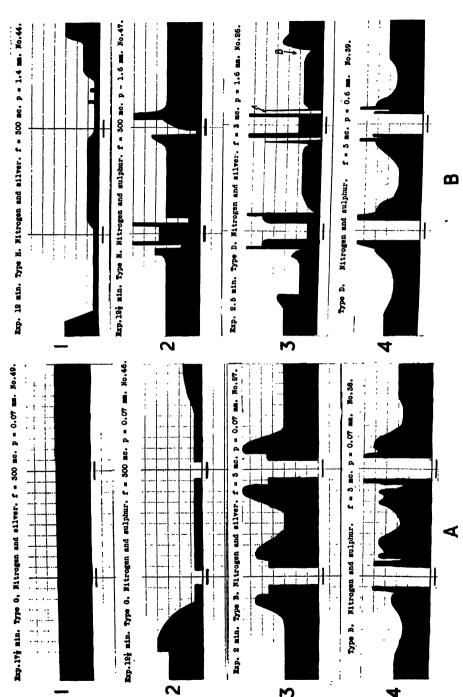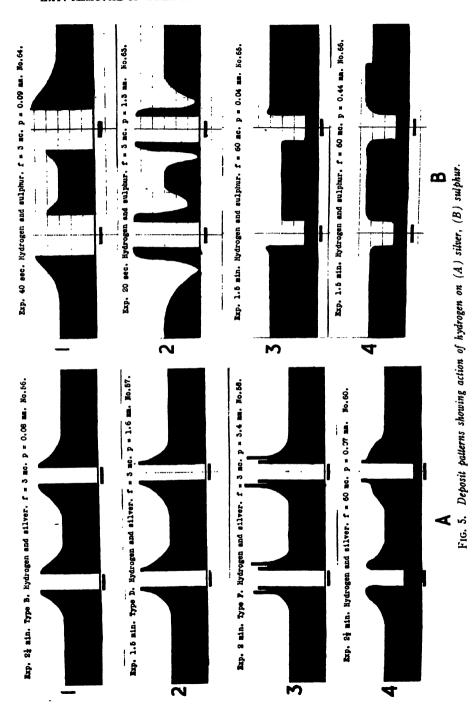
FIG. 4. *Comparison of deposit patterns for silver and sulphur at (A) low pressure, (B) high pressure.*

FIG. 5. *Deposit patterns showing action of hydrogen on (A) silver, (B) sulphur.*

No. 1, Fig. 2, *A*, and showed no general removal, no matter what type of discharge took place in the tube. At 60 megacycles per sec., however, a curious reversal of the behavior observed with narrower tubes took place, for at low pressure with a Type *G* discharge a general removal was observed over the region between the electrodes. At high pressure no general removal occurred, the pattern being composed of electrode removal and deposit areas. The Type *G* discharge was observed to fill the tube entirely, leaving only a very thin dark space next the tube wall.

Spectroscopic Observations

In an endeavor to relate the removal pattern with the mechanism of the discharge, a series of spectrograms was taken of various regions of each of the different types of nitrogen discharges. Characteristic results are given in Fig. 6 in which the portions of the discharge associated with the individual spectrograms are clearly indicated. It will be observed in Fig. 6 that the region under the electrode is one of high ionization as indicated by the preponderance of lines and first negative band heads. The deposit region immediately adjacent to the electrode shows a spectrum containing first and second positive band heads and a few first negative heads. The spectrum of the region midway between the electrodes is composed almost entirely of first and second positive band heads. These facts indicate that the region of highest ionization is beneath the electrodes and that as one moves away from there toward the yellow glow in the middle of the tube, ionization decreases and the luminosity of the glow is due to the presence of large numbers of excited molecules.

Spectra taken of discharges at ultra high frequency show the differences between the yellow and the blue glows much more strikingly. When only the blue glow is present (*i.e.*, Type *G* at low pressure) and only the electrode effect is present, the spectra were found to be line and first negative even in the inter-electrode regions. On the other hand, at higher pressures, when the yellow glow (Type *H*) is present, and the removal is entirely of the general type, the spectra show first and second positive band systems for the regions under the electrodes as well as for those between them.

The spectroscopic evidence strongly suggests that the conditions for electrode removal without general removal (Type *G* discharge) are associated with high ionization, while the general removal is linked with a discharge region of low ionization.

The Electrode Effect   **Discussion**

The experimental results associated with the electrode effect and summarized above suggest that the cause is a positive ion bombardment of the tube walls beneath the electrodes. The effect of such a bombardment on the glass walls has been noted by several workers (14, p. 459) and would explain the observations of Robertson and Clapp (13) that a silver pattern can be obtained by silvering a clear tube after it has been subjected to the discharge. The disintegration of those portions of a paper lining which lay

PLATE I
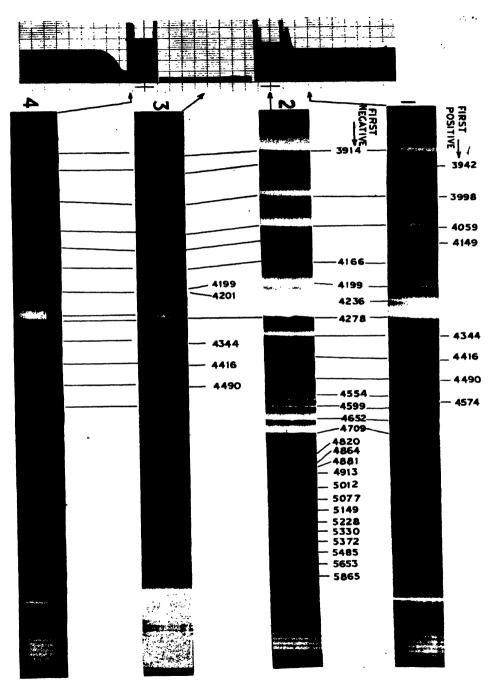
FIG. 6.   *Type F.   Nitrogen and silver.   f = 3 mc.   p = 3.4 mm.*

beneath the electrodes and close to the glass walls is further proof of the existence of such a bombardment.

According to Townsend (17, p. 302; 18), Banerji and Ganguli (2) and others, the high frequency discharge, either with external sleeve electrodes or with internal electrodes, shows alternately every half cycle the same divisions in front of the electrodes as does the d-c. discharge. The high frequency and the greater luminosity at the cathode combine to make each electrode appear to be a cathode. With reference to discharge Type *C*, Fig. 1, A is the cathode dark space and B is the negative glow merging into C, the Faraday dark space, which is succeeded by D, the positive column. The reactions of these regions to the application of transverse magnetic fields, to changes of pressure, and to alteration of the electrode separation were the same as the reactions of corresponding portions of the d-c. discharge.

Assuming such a positive ion bombardment and considering the expressions for maximum velocity and energy, and maximum travel in one-half cycle (which can be obtained by integrating the equations of motion of an ion in an alternating field) one can conclude:

(1) That electrode removal should decrease with increase of frequency,

(2) That at a given frequency (3 megacycles) the removal should decrease with increase of pressure,

(3) That at ultra high frequencies, the maximum half-cycle travel is so small that pressure variation should have no effect on the removal.

Fig. 2, *A* supports the first conclusion, while Fig. 3 shows that the second is true. It is more difficult to support the third, for at ultra-high frequencies and high pressures the electrode effect is masked by general removal.

The same expressions for energy and half-cycle travel suggest that a gas such as hydrogen should be a more active agent than nitrogen. Robertson and Clapp (13) found this to be so, but the results of the present work, while supporting their findings in general, do not indicate differences as great as they observed between the effects of the two gases.

A surprising observation was that d-c. discharges and 60 cycle alternating discharges did not cause any removal of the silver film. A tentative explanation is that at low frequencies the conductance of the thin film is such as to prevent a bombarding discharge. Another possible explanation may be found in the known variation of the dielectric properties of glass with frequency. This change may also be accompanied by changes in the surface structure. However, the unsatisfactory state of the theories of glass dielectrics and the lack of agreement between theory and experimental data make this approach one of extreme difficulty (12, p. 171 *et seq.*).

General Removal

General removal occurs opposite the positive column (D and F, Type *D*, Fig. 1) of the discharge. Of the theories of glow discharges in gases, the plasma theory of Compton, Tonks and Langmuir (4, 10, 11, 15, 16) provides the best explanation for this effect. Treating the positive column as a plasma

we see that there will exist a slow radial drift of positive ions from tube axis to wall, and that at the edge of the plasma, the positive ion sheath, or positive space charge created by the high negative wall charge, may give positive ions energies as high as 13 or 15 volts (10), which have been shown to be sufficient to cause cathodic sputtering of silver (14, p. 458). The smaller the tube radius the greater will be the energies imparted to the ions by the positive ion sheaths.

Consideration of these conditions occurring with plasmas leads to the following conclusions:

    (1) General removal should be independent of frequency since the plasma conditions are independent of this parameter.

    (2) General removal should occur along any part of the tube that is adjacent to the plasma, and should not be localized.

Fig. 2, *B*, No. 3, Fig. 3, *A*, and No. 2, Fig. 3, *C*, all give strong support to these conclusions.

    (3) Patterns obtained with nitrogen in wide tubes should show decrease in general removal; the actual results observed showed no general removal at all.

    (4) Owing to the high mobility of the hydrogen positive ion, the action of hydrogen in narrow tubes should be like that of nitrogen in wide tubes. The results shown in Fig. 5, *A*, are striking fulfilment of this expectation.

That the plasma conditions are responsible for the general removal receives further support from low pressure patterns. An electrode spacing of 8 cm. is insufficient to allow the plasma to form in the region between the electrodes at low pressure, but it is formed in the regions beyond each electrode. Silver patterns were obtained which showed general removal opposite such extra-electrode plasmas, so several silvered tubes were subjected to the Types *A* and *B* discharges with the electrodes spaced sufficiently apart to allow the formation of a plasma between the electrodes. These tubes showed plain evidence of general removal opposite all plasmas.

The spectra of nitrogen discharges in the regions of general removal are, almost without exception, first and second positive band systems; this indicates the presence of many excited molecules. The ionization potential of nitrogen is 16.8 volts, while the excitation potentials for the first and second positive band systems are 9.5 and 12 volts respectively (6). The excitation potential for the first negative system is 18.5 volts. The absence of first negative bands and lines in all plasma spectrograms is strong support for the assumption that electron energies are low in the plasmas, and is additional evidence in favor of the view of Langmuir and Tonks (10, 15, 16) that little recombination occurs in the plasma, but rather, at the tube wall in narrow tubes or at the plasma boundary in wide tubes.

Possibility of Chemical Action

The discharges with a positive column, or plasma, were accompanied by afterglows of short duration which, in the nitrogen discharge, may have indicated the presence of active nitrogen. This possibility suggests that at least part of the general removal may have been due to chemical combination between silver and active nitrogen to form silver nitride. Such action is possible (19) but it does not seem at all likely. In the first place, the formation of a layer of silver nitride, which, according to Willey, is inert to active nitrogen, would prevent further action unless one assumes that silver nitride is more easily sputtered than is silver, or that the heat liberated on the conversion of the active nitrogen to the inert variety is insufficient to vaporize the silver nitride. The first assumption is not likely to be correct, since silver is very easily sputtered in nitrogen, but the second is not so easily disposed of, and remains as a possibility difficult either to prove or to disprove. It is conceivable, however, that positive ion bombardment might detonate the silver nitride crystals, thus permitting further chemical action. Attention has already been directed to a removal beneath, and adjacent to, the electrodes, and to the strong odor of hydrogen sulphide at the pump during exposure in a tube coated with sulphur and filled with hydrogen. Chemical combination was undoubtedly responsible for a large part of this removal (See Fig. 5, *B*).

The Behavior of Sulphur

Fig. 4 shows that the action of the nitrogen discharge on silver is opposite to that on sulphur. A possible explanation for this complementary behavior may be found in the differences in the structures of the thin films formed on the glass. The silver was chemically precipitated, was black in color and resisted removal by washing. It formed a layer of small, closely connected crystals fairly firmly bound to the glass. On the other hand, the sulphur layer, formed by the condensation of visible sulphur vapor, could be washed, or even jarred to some extent, from the tube wall; it was, therefore, coarser and much less adherent to the glass.

In the experiment in which silver was removed and sulphur was not, the possible factors causing removal of the silver were positive ion bombardment and chemical action. The same positive ion bombardment of the sulphur layer obtains since the discharges are the same in both experiments. No data are available as to the ease with which sulphur may be sputtered, but its non-removal under low pressure conditions suggests that it is not very great. The discharge has some effect on the sulphur coat, however, for the coarse, yellowish-white layer was altered to a more finely divided, more adherent, yellow, almost glazed coat. A tentative explanation is that electrons reaching the wall are attached to sulphur atoms to form sulphur ions, thus becoming more difficult to remove than are the free electrons on the silver surface. The bombarding positive ions may then recombine on the sulphur surface, the resulting heat of recombination melting the sulphur and reducing the coarse structure to a finer one.

The fact that there seems to be no known compound of sulphur and nitrogen, and that the electron configurations of the two elements render such a combination very unlikely, rule out the possibility of sulphur removal by chemical action. Furthermore, the action of hydrogen on sulphur coated tubes (Fig. 5, *B*) indicates that chemical combination takes place only at those portions of the tube wall which are subjected to positive ion bombardment—*i.e.*, beneath the electrodes or opposite plasmas. Frequency and pressure, which affect the intensity of positive ion bombardment at the electrodes, affect the chemical action as well.

Deposition of Silver Adjacent to the Electrodes

Four points of evidence indicate that the deposition of silver in the regions on both sides of the electrodes is closely connected with the negative glow and the Faraday dark space:

(1) When the negative glow is general, as in Types *B* and *C*, Fig. 1, and the boundary between it and the Faraday dark space is poorly defined, the silver deposit is broad and lacks fine structure (No. 1, Fig. 3, *A*).

(2) When the negative glow is restricted and its boundaries are sharply defined (Types *D*, *E*, and *F*, Fig. 1), the silver deposit is more compressed and possesses fine structure (Nos. 2 and 3, Fig. 3, *A*).

(3) When the cathode head of the negative glow was shifted by the application of a transverse magnetic field, the boundaries of the deposit were shifted in the same manner and by the same amount.

(4) When the silver was removed from half the length of the tube and the electrodes were placed so that the edge of the silvered portion came half-way between them, silver was deposited on either side of that electrode which was over clear glass. Here, too, deposition occurred adjacent to the negative glow.

The formation of fine structure in the deposit areas remains to be explained. Banerji and Ganguli (3) report the existence of limited regions on the tube wall which are positive with respect to the tube axis and which would repel positive ions and thus prevent a deposit of silver. Careful examination might show that these regions (fine structure) correspond to the edges of Faraday dark spaces. Keyston (9) and Tonks and Langmuir (15) report the presence of double negative glows and Faraday dark spaces. These have not been observed in this work, but, nevertheless, they may be present, for in the case recorded by Langmuir they were observed only with the aid of a low power microscope. If more refined methods of observation of the discharge and measurements of the deposit reveal that multiple negative glows and dark spaces exist under the conditions which produce fine structure in the deposit areas, the appearance of a fine structure in the deposit would be explained.

Acknowledgments

The writer wishes to express his thanks to Prof. J. K. Robertson, at whose suggestion and under whose direction this work was carried out, for his kindly and helpful suggestions and for his unfailing interest; and to Prof. H. H. Stewart of the Electrical Engineering Department for his help and advice in the design and construction of the Hartley oscillator.

References

1. BANERJI, D. and BHATTACHARYA, D.   Phil. Mag. 17 : 313-316.   1934.
2. BANERJI, D. and GANGULI, R.   Phil. Mag. 11 : 410-422.   1931.
3. BANERJI, D. and GANGULI, R.   Phil. Mag. 15 : 676-681.   1933.
4. COMPTON, K. T. and LANGMUIR, I.   Rev. Modern Phys. 2 : 123-242.   1930.
5. DEWEY, JANE M.   Phys. Rev. 32 : 918-921.   1928.
6. DUNCAN, D. C.   Astrophys. J. 62 : 145-167.   1925.
7. HAYNER, LUCY J.   Z. Physik, 35 : 365-386.   1926.
8. KENTY, C.   Phys. Rev. 32 : 624-635.   1928.
9. KEYSTON, J. E.   Phil. Mag. 15 : 1162-1173.   1933.
10. LANGMUIR, I.   J. Franklin Inst. 214 : 275-298.   1932.
11. LANGMUIR, I. and COMPTON, K. T.   Rev. Modern Phys. 3 : 191-257.   1931.
12. LITTLETON, J. T. and MOREY, G. W.   The electrical properties of gases.   John Wiley and Sons, New York.   1933.
13. ROBERTSON, J. K. and CLAPP, C. W.   Nature, 132 : 479-480.   1933.
14. THOMSON, J. J.   Conduction of electricity through gases.   Vol. 2.   Cambridge University Press.   1928.
15. TONKS, L. and LANGMUIR, I.   Phys. Rev. 33 : 195-210.   1929.
16. TONKS, L. and LANGMUIR, I.   Phys. Rev. 34 : 876-922.   1929.
17. TOWNSEND, J. S.   Electricity in gases.   Oxford University Press, London.   1915.
18. TOWNSEND, J. S.   Phil. Mag. 13 : 745-759.   1932.
19. WILLEY, E. J. B.   J. Chem. Soc. 2188-2196.   1927.

THE SURFACE TENSION OF SOME DILUTE SOLUTIONS[1]

BY W. C. FISHER[2] AND C. A. MACKAY[3]

Abstract

Surface tension measurements have been made on lauric acid at temperatures above its melting point, on aqueous solutions of butyric and lauric acids, and on methyl acetate and sodium oleate. The results for the solutions are compared with those calculated by means of a recent theory.

Introduction

In recent years considerable interest has been shown in surface phenomena, much work having been done both on pure liquids and on solutions. In particular, it has been shown by several workers, whose results are summarized by Bond (3) and Puls (11), that the surface tensions of many pure liquids reach a steady or static value in a very short time, of the order of 0.005 sec., after a fresh surface is formed. It is probable that the initial surface tension exceeds its static value, but the experimental evidence at present is not quite conclusive (4). On the other hand, there is no doubt that the static value of the surface tensions of some solutions is reached only after a much longer period, even amounting to a week according to Adam and Shute (1). Milner (10) has suggested that the change of the surface tensions of solutions depends on the diffusion of the solute into or out of the surface, and that time is required for equilibrium to be reached. Bond and Puls (4) have worked out a mathematical theory based on Milner's hypothesis, from which they have derived an equation for the change of the surface tension of dilute solutions with time, assuming that there is loss of neither solvent nor solute by chemical action or evaporation. Their equation will be considered after the experimental results have been given.

To measure surface tension several methods are available, and a choice must be made of one appropriate to the particular problem. If it is intended to investigate the rate of change of the surface tension with time, the surface should not be disturbed during the period that observations are taken. This requirement is met by a method described by Ferguson and Hakes (6), in which the surface tension is found from the air pressure that is just sufficient to prevent the test liquid from rising in a capillary tube. There are the additional advantages in the method that it is not necessary to have a length ·

of capillary tube of uniform bore, which is always difficult to procure, nor is it necessary to measure the contact angle.

Method

Only a brief description of the method will be given here. The tip of a vertical capillary tube is placed at a known depth below the surface of the liquid to be tested. A small air pressure is applied to the meniscus until it is forced to the bottom of the tube, where it is held at the exact level of the tip. The air pressure is read on a suitable manometer. The experiment is repeated with the tip at various convenient depths, such as each centimetre, below the surface. Ferguson and Hakes show that if the pressure corresponding to each position of the tip is read in terms of a difference of height in a manometer, the relation between a given manometer reading h and the surface tension γ is given by the equation

$$dh = d'(h' - r/3) + 2\gamma/gr , \tag{1}$$

where d is the density of the manometer liquid, d' the density of the test liquid, h' the depth of the tip below the surface of the liquid, r the radius of the tip, and g the acceleration of gravity. If a graph is plotted between dh and $(h' - r/3)$ the intercept on the dh axis gives the surface tension when the radius of the tip is known.

Experimental

Distilled water was used in the manometer, which was read with a measuring microscope, giving readings reproducible to within 2.5×10^{-3} cm. The height of the meniscus in the capillary tube was observed through a second microscope mounted close to the first. The liquid to be examined was held in a small glass tube in a thermostat, at a temperature recorded by a copper-constantan thermocouple. The air pressure on the meniscus was regulated by varying the amount of water in a large bottle, which was connected to the capillary tube. A fine control was easily obtained by means of a much smaller vessel in series with the bottle. To reduce variations in temperature, all connecting tubes and vessels were covered with a thick layer of cotton batting. The whole apparatus was set up on rubber stoppers, in a basement room; consequently, jars were reduced to a minimum. After several trials, it was found possible to make a satisfactory glass tip by drawing down a thick walled capillary tube, dipping it in turpentine, and scratching it with a fine file before breaking it off. In this way a clean surface was obtained that was perpendicular to the axis of the tube, with no chips on the inner edge observable under a lower power microscope. The tip had an inner mean diameter of 0.0974 cm.

As a check on the suitability of the apparatus, and the accuracy with which determinations of the surface tension could be made, some preliminary measurements with distilled water were carried out. The manometer was read for five different depths of the tip below the surface of the liquid. To obtain

the best fitting straight line from the experimental data, the method of a residual plot (8, p. 60) was found to be convenient. The result for 25.3° C. was a surface tension of 72.23 dynes per cm. To compare this figure with others, it was reduced to 15° C. and 20° C., the rate of change given in the International Critical Tables being used. At 15° C. the surface tension was found to be 73.76 dynes per cm.; and at 20° C., 73.02 dynes per cm. A few recent determinations are given for comparison; at 15° C. Bond (3) gives 73.83, Ferguson and Hakes (6) 73.54, and Warren (13), as a mean of the results of 13 workers, gives 73.65 dynes per cm. Timmermans and Bodson (12) find the surface tension at 20° C. to be 72.9 dynes per cm. The agreement between these figures and ours suggests that our experimental error is no more than 0.2 dynes per cm., and it may be considerably smaller.

An additional check was available. Two years ago, J. H. Buck made a series of measurements, by the drop weight method, on a $4N$ solution of redistilled butyric acid, over a range of temperatures from 12° to 27° C. Buck's solution was stored in an air-tight glass bottle in a dark closet. His work was repeated, the same solution being used, though no tests were made to determine the concentration, which may have changed slightly in two years. The results are shown in Table I, where our values are marked F. and M.

TABLE I

COMPARISON OF MEASUREMENTS OF SURFACE TENSION (DYNES PER CM.) OF $4N$ BUTYRIC
ACID SOLUTION

Temp., °C.	12.8	17.2	21.0	25.1	27.7
Buck	28.68	28.42	28.17	27.92	27.74
F. and M.	28.49	28.17	27.81	27.79	27.49

The mean difference between the surface tensions found by means of the two methods is 0.24 dynes per cm., and the temperature coefficient is almost identical, 0.62 dynes per cm. for each degree.

When the static value of the surface tension of a solution had been found or was already known from other work, a simple procedure, which avoided disturbing the surface, was followed to determine the time rate of change of the surface tension. The tip was placed at a fixed depth, for example, 3 cm. below the surface of the solution. A fresh surface was formed by blowing several air bubbles from the tip; then, as the surface tension varied, the pressure necessary to hold the meniscus at the exact bottom of the capillary tube was read at frequent intervals, timed by means of an electrical stop watch. To obtain the rate of change of the surface tension from these observations, Equation (1) was altered slightly. Let γ_1 and γ_2 be the surface tension at t_1 and t_2 seconds, after a fresh surface is formed. Then since the tip is at a constant depth,

$$\gamma_2 = \gamma_1 - \tfrac{1}{2}dgr(h_1 - h_2) \tag{2}$$

where h_1 and h_2 are the manometer readings. If γ_1 is the static value of the surface tension, γ_2 may be found from observations of h_1 and h_2. The method

is useful only to determine rather slow changes in the surface tension, since it requires about 15 sec. to make the necessary readings. The three solutions chosen for experiment were methyl acetate, sodium oleate, and lauric acid in water.

Methyl Acetate

Though the vapor pressure of methyl acetate is so great that the concentration changes appreciably in a few minutes, a series of runs was made with a molar solution. The acetate was supplied by the Eastman Kodak Company. The surface tension increased in 10 min. from 47.0 to 50.5 dynes per cm. at a temperature of 20° C., an increase due in part to a change in concentration. Whether the age of the surface has an effect on the surface tension could not be detected with certainty from the present experiments, owing to the rapid variation in the concentration.

Sodium Oleate

To decrease the rate of change of the surface tension to a convenient value, a concentration of $M/4000$ was used. It was found that in every case the surface tension decreased with the age of the surface, but that successive runs were not reproducible within the limits expected from the results on water and butyric acid, the variations for a given surface age being as great as 3 dynes per cm. Bigelow and Washburn (2) report that they experienced the same difficulty with some of their very dilute solutions. It has been suggested by Harkins and Meyers (9) that this may be due to the entrance into the solution of metallic ions from the glass vessel. Fig. 1, *A*, shows a typical curve. For a fresh surface the rate of change of the surface tension was so great that no reading could be made until one minute after the meniscus was formed in the capillary tube. The irregularities in the points along the curve are probably due to slight jars or variations in air pressure which disturb the surface. A small intentional change in air pressure caused an increase in the surface tension from 50.2 to 52.8 dynes per cm. Had the observations been continued for an even longer period than that shown in Fig. 1, as was done on one or two occasions, the surface tension would have decreased very slowly until a final static value was reached.

Lauric Acid

Pure lauric acid, melting at 42.6° C., was supplied by the Eastman Kodak Company. Since it seems that very few measurements of the surface tension of pure lauric acid have been made, the surface tension was determined at several temperatures between 44° and 63° C. Table II gives the results.

TABLE II
SURFACE TENSION OF LAURIC ACID, M.P. 42.6° C.

Temp., °C.	44.4	47.5	53.6	63.2
Dynes per cm.	28.63	28.35	27.86	26.96

The acid is nearly insoluble in water; consequently, no attempt was made to measure the concentration of the solutions. Either a saturated solution or the same solution diluted with an equal volume of distilled water was used. The latter concentration is referred to as half-saturated. At temperatures above the melting point of the acid, the surface tension measurements of the solutions were not reproducible with a reasonable experimental error. No
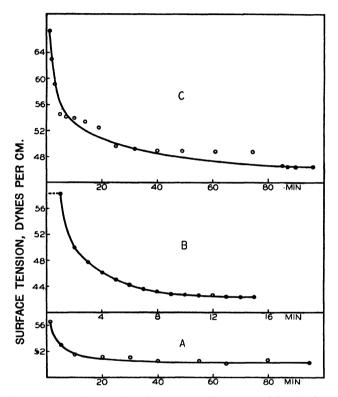
FIG. 1. *Decrease of surface tension with the age of the surface of the solution. A. Sodium oleate, M/4000 concentration at 22.1° C. B. Lauric acid solution saturated at 22.2° C. C. Lauric acid solution half-saturated at 25.9° C.*

explanation is offered at the present time. No difficulty was experienced in repeating experiments at temperatures below 42° C., and several series of readings were made to determine the static surface tension from 25° to 42° C. Table III gives the results.

TABLE III

STATIC SURFACE TENSION OF A SATURATED SOLUTION OF LAURIC ACID

Temp., °C.	25.3	30.4	39.4	41.5
Dynes per cm.	40.46	37.18	32.05	29.63

Cary and Rideal (5) measured the surface tension of a monomolecular film of lauric acid on water which was slightly acidic. They give a graph which shows that at 25° C. the film has a surface tension of approximately 48 dynes per cm., decreasing 0.73 dynes per cm. for each degree rise in temperature. The corresponding figure from Table III is 0.70 dynes per cm., but the surface tension of the solution was about 7 dynes lower.

Many experiments were made on the variation of the surface tension as the surface aged. Fig. 1, B, shows the mean result at 22.2° C. The separate runs agreed quite well, in contrast to the sodium oleate experiments. It was noticed at once that the surface tension did not change appreciably in the first minute after a new surface was formed, while for sodium oleate the decrease was so rapid during this period that the method of observation was too slow to permit the taking of accurate readings. At higher temperatures, the initial period of constant surface tension was shorter.

The experiments were repeated with the half-saturated solution of lauric acid. The static value of the surface tension was found to be 46.4 dynes per cm. at 25.9° C., while that of the saturated solution was 40.1 dynes per cm. at the same temperature. It also took considerably longer for the surface tension of the more dilute solution to reach the static value. Fig. 1, C, shows a typical curve of the change of the surface tension with the age of the surface at 25.9° C. Whenever a fresh surface was formed by blowing off a few bubbles of air from the capillary tip, the surface tension returned to its initial value and began to decrease at the same rate as before. As was already mentioned, there was a period of inactivity with the saturated solution of lauric acid. The weaker solution may have acted in the same way, but with such a short period that it was not observed. Ferguson and Sharp (7) found that several acids, as well as sodium oleate, had an initial constant surface tension and that at lower temperatures the effect lasted longer.

In the introduction it has been mentioned that Bond and Puls (4) have derived an equation for the relation between the surface tension and the age of the surface of a solution. Their equation for a constant temperature is

$$\frac{(\gamma_0 - \bar{\gamma}) - (\gamma_0 - \gamma)}{\gamma_0 - \bar{\gamma}} = e^{-\frac{2}{\sqrt{\pi}}\sqrt{\frac{t}{T}}}, \tag{3}$$

where γ_0 is the surface tension of water, γ the surface tension t seconds after a new surface is formed, $\bar{\gamma}$ the static surface tension, and T the time for the surface tension to pass halfway to its static value. The equation holds only for dilute solutions, in which the surface concentration is assumed to change by the diffusion of the solute to or from the solution. To compare the theory with experiment the equation may be written

$$\frac{\gamma_0 - \gamma}{\gamma_0 - \bar{\gamma}} = 1 - e^{-\frac{2}{\sqrt{\pi}}\sqrt{\frac{t}{T}}}. \tag{4}$$

A.graph of the equation was drawn with t expressed in terms of T as abscissa and $\dfrac{(\gamma_0 - \gamma)}{(\gamma_0 - \bar{\gamma})}$ as the ordinate. For any given solution, the experimental value of $\dfrac{(\gamma_0 - \gamma)}{(\gamma_0 - \bar{\gamma})}$ was found for time t. Then T was so chosen that the best fit was obtained between the observed points and the theoretical graph, when t was expressed in terms of T. This has been done in Fig. 2, A, for sodium oleate. The points show that when T is 2.0 min., the surface tension increases too rapidly at first and too slowly later on. No value of T can be found that would place the experimental points along the graph. Fig. 2, B, shows
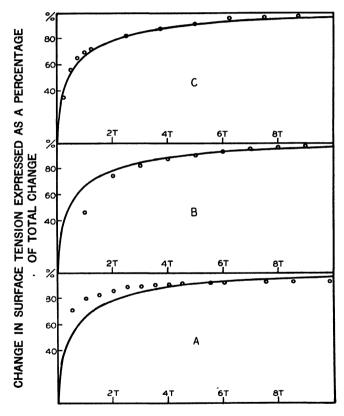
Fig. 2. *Comparison between theoretical and experimental rates of decrease of surface tension. A. Sodium oleate solution. T = 2.0 min. B. Lauric acid saturated solution. T = 1.0 min. C. Lauric acid half-saturated solution. T = 8.0 min.*

the comparison between theory and experiment for a saturated lauric acid solution, when T is 1.0 min. The initial period of constant surface tension is not accounted for in the theory; consequently, the points fit the theoretical

curve only when t is greater than $2T$. The best agreement between theory and experiment was obtained for a half-saturated lauric acid solution. This is shown in Fig. 2, C, when T is 8.0 min. Too much weight should not be given to these curves, but they do lend some support to the Milner hypothesis. It is hoped to carry on additional work to determine the effect of temperature and inorganic ions on the surface tensions of solutions such as those used in this study.

References

1. ADAM, N. K. and SHUTE, H. L.   Trans. Faraday Soc. 34 : 758-765.   1938.
2. BIGELOW, S. L. and WASHBURN, E. R.   J. Phys. Chem. 32 : 321-353.   1928.
3. BOND, W. N.   Proc. Phys. Soc. 47 : 549-558.   1935.
4. BOND, W. N. and PULS, H. O.   Phil. Mag. 24 : 864-888.   1937.
5. CARY, A. and RIDEAL, E. K.   Proc. Roy. Soc. London, 109 : 318-330.   1925.
6. FERGUSON, A. and HAKES, J. A.   Proc. Phys. Soc. 41 : 214-222.   1929.
7. FERGUSON, A. and SHARP, L. E.   Variation of surface tension with time.   *In* Reports on progress in physics, published by The Physical Society, pp. 40-41.   The University Press, Cambridge.   1934.
8. GOODWIN, H. M.   Elements of the precision of measurements and graphical methods. McGraw-Hill Book Company, New York.   1920.
9. HARKINS, W. D. and MEYERS, R. J.   Nature, 139 : 367.   1937.
10. MILNER, S. R.   Phil. Mag. 13 : 96-110.   1907.
11. PULS, H. O.   Phil. Mag. 22 : 970-982.   1936.
12. TIMMERMANS, J. and BODSON, H.   Compt. rend. 204 : 1804-1807.   1937.
13. WARREN, E. L.   Phil. Mag. 4 : 358-386.   1927.

VIBRATIONS ON POWER LINES IN A STEADY WIND[1]

V. RESONANCE OF STRINGS WITH STRENGTHENED ENDS

By R. RUEDY[2]

Abstract

The resonance frequencies, and in particular all the overtones of a string along which the linear density varies according to the law $\rho(1 + \lambda x/L)^m$, are slightly higher than the frequencies of a uniform string of the same total mass when the ratio between the mass of an element at the end and a corresponding element at the centre is varied between 1 and 25. In order to bring a string with strengthened ends into resonance it is necessary not only that the force acting on unit length of the string be of the same frequency as one of the resonance frequencies, and that its strength varies along the string in proportion to the amplitudes of the corresponding standing waves, but it must also be proportional to the mass of each element. It is therefore more difficult to produce true resonance in a string with strengthened ends than in a uniform string.

Comparison between the Frequencies of Strengthened and of Uniform Strings

On the assumption that the mass per unit length increases along a string according to the law $\rho_0(1 \pm \lambda x/L)^m$, where the lower sign applies to negative values of x on strings that are symmetrical with respect to the origin and of total length $l = 2L$, the frequencies corresponding to wave-shapes giving an odd number of loops follow from the equation

$$J_{\frac{m+1}{m+2}}\left(\frac{\pi/\lambda}{m+2}\frac{\nu}{\nu_0}\right) J_{-\frac{1}{m+2}}\left(\frac{\pi/\lambda}{m+2}\frac{\nu}{\nu_0}(1+\lambda)^{\frac{m+2}{2}}\right)$$
$$+ J_{-\frac{m+1}{m+2}}\left(\frac{\pi/\lambda}{m+2}\frac{\nu}{\nu_0}\right) J_{-\frac{1}{m+2}}\left(\frac{\pi/\lambda}{m+2}\frac{\nu}{\nu_0}(1+\lambda)^{\frac{m+2}{2}}\right) = 0.$$

The frequency ν_0, which appears in the independent variable, is the fundamental frequency $(S/16\rho_0 L^2)^{\frac{1}{2}}$ of the uniform string of total length l; in the treatment of the strengthened string this frequency is replaced by the smallest solution ν_1 of the equation just mentioned. The frequency of standing waves that have an odd number of loops is determined by the condition that a loop lies at the very centre of the string, whereas the ends remain motionless;

for the vibrations that produce an even number of loops the ends and the centre are at rest, and the possible frequencies follow from the equation

$$J_{\frac{1}{m+2}}\left(\frac{\pi/\lambda}{m+2}\frac{\nu}{\nu_0}\right)J_{-\frac{1}{m+2}}\left(\frac{\pi/\lambda}{m+2}\frac{\nu}{\nu_0}(1+\lambda)^{\frac{m+2}{2}}\right)$$
$$- J_{-\frac{1}{m+2}}\left(\frac{\pi/\lambda}{m+2}\frac{\nu}{\nu_0}\right)J_{\frac{1}{m+2}}\left(\frac{\pi/\lambda}{m+2}\frac{\nu}{\nu_0}(1+\lambda)^{\frac{m+2}{2}}\right) = 0.$$

The approximate ratios ν/ν_0 between the allowed frequencies of the strengthened string and the fundamental frequency ν_0 of the uniform string are given in Table I for two degrees of strengthening, namely for $(1+\lambda)^m = 4$ and $(1+\lambda)^m = 16$.

TABLE I

COMPARISON BETWEEN THE FREQUENCIES ν OF STRINGS WITH STRENGTHENED ENDS AND THE LOWEST FREQUENCY ν_0 OF THE CORRESPONDING UNIFORM STRING.

—	$(1+\lambda)^m = 4$			$(1+\lambda)^m = 16$		
	$m = 1$ $\lambda = 3$	$m = 2$ $\lambda = 1$	$m = 6$ $\lambda = 0.26$	$m = 1$ $\lambda = 15$	$m = 2$ $\lambda = 3$	$m = 6$ $\lambda = 0.587$
ν_1/ν_0	0.74	0.75	0.76		0.48	
ν_2/ν_0	1.21	1.30	1.39		0.76	
ν_3/ν_0	1.98	2.00	2.00	1.20	1.30	
ν_4/ν_0	2.59	2.67	2.74	1.55	1.60	1.64
ν_5/ν_0	3.18	3.3	3.4	1.92	2.00	2.05
ν_6/ν_0	3.87	4.0	4.1	2.25	2.44	2.66
$\frac{\pi}{\lambda(m+2)}$	0.35	0.785	1.51	0.07	0.26	0.66

The natural frequencies of the string for which $(1+\lambda)^m = 4$ are about 5/3 times as large as those for $(1+\lambda)^m = 16$, and about twice as large as the frequencies of the string for which the degree of strengthening is 25.

With the exception of the first few harmonics, the natural frequencies of the uniform string of unit mass ρ_0 are $1/\gamma$ times as large as the corresponding resonance frequencies of the string along which the mass of unit length increases from the value ρ_0 at the centre to the value $\rho_0 Q$ at the ends. The reduction factor

$$\gamma = \frac{m+2}{2}\frac{\lambda}{(1+\lambda)^{\frac{m+2}{2}}-1} = \frac{Q^{\frac{1}{m}}-1}{Q^{\frac{m+2}{2m}}-1}\frac{m+2}{2}$$

is constant for given values of Q and m. In other words, as far as the higher frequencies are concerned, the string behaves as though it had a uniform linear density equal to ρ_0/γ^2 grams per unit length, and the successive overtones are therefore separated by constant intervals. It is useful to examine in this connection whether the values ρ_0/γ^2 of the density are higher or lower than the average density of the strengthened string, that is, to determine how

much the same amount of material reduces the frequencies of vibration when it is concentrated near the ends instead of being uniformly distributed.

If the ratio between the mass of unit length at the end and the corresponding mass at the centre is

$$Q = (1 + \lambda)^m,$$

which corresponds to the assumed increase in mass along the string according to the law $\rho_0(1 + \lambda x/L)^m$, the average mass per unit length is

$$\rho = \frac{\rho_0}{L}\int_0^L (1+\lambda x/L)^m dx = \frac{(1+\lambda)^{m+1}-1}{\lambda(m+1)}\,\rho_0 = \frac{Q^{\frac{m+1}{m}}-1}{(m+1)(Q^{\frac{1}{m}}-1)}\,\rho_0$$

Thus a linear increase in density gives of course an average density equal to $\rho_0(1 + Q)/2$ or $2.5\rho_0$ for $Q = 4$ and $13\rho_0$ for $Q = 25$, whereas the values of ρ_0/γ^2 are 2.5 and 11.5, respectively. The higher frequencies remain, therefore, about the same whether the distribution be linear or uniform, providing only that the total mass of the string remains constant.

The same conclusion holds for all the distributions of the type $\rho_0(1 + \lambda x/L)^m$, regardless of the value for m. When, in particular, after a certain ratio Q has been chosen, successively larger values are given to m, decreasing values result for λ, since $(1 + \lambda)^m = Q$ or $\lambda = Q^{\frac{1}{m}} - 1$. At the limit

$$\rho = \frac{(1+\lambda)^{m+1}-1}{\lambda(m+1)}\,\rho_0 = \frac{Q^{\frac{1}{m}+1}-1}{(Q^{\frac{1}{m}}-1)(m+1)}\,\rho_0 = \frac{Q-1}{\ln Q}\,\rho_0 \text{ for } m = \infty.$$

The limit of the fraction is 2.16 for $Q = 4$, and 7.46 for $Q = 25$, in place of the averages 2.5 and 13 for the linear increase in density. The limit of γ, on the other hand, for the standing waves with an even number of loops, is

$$\gamma = \frac{2(\sqrt{Q}-1)}{\ln Q} \text{ for } m = \infty$$

that is

$$\gamma_\infty = 1.44 \text{ for } Q = 4$$
$$\gamma_\infty = 2.48 \text{ for } Q = 25,$$

and a uniform string giving, above the second or third overtone, the same resonance frequencies as the string with strengthened ends would, therefore, have to possess a mass equal to $2.07\rho_0$ per unit length for a ratio Q equal to 4, and a uniform mass $6.15\rho_0$ per unit length for $Q = 25$, values that do not differ greatly from the average mass of the non-uniform string. As regards the reduction in the frequency of the resonance vibration, it is most pronounced for the uniform distribution of the mass.

In order to complete the comparison between the behavior of strengthened and of uniform strings it is necessary to study also the amplitudes produced by an external force along the string with strengthened ends. Before this problem is dealt with, however, the solution obtained when m tends to infinity is

worthy of a brief treatment from a different viewpoint. At the limiting value of m the use of the Bessel functions $J_{1/\mu}$ and $J_{-1/\mu}$ ceases to give two independent solutions, so that $J_{-1/\mu}$ must be replaced, for instance, by Weber's function:

$$Y_0(\beta\xi) = \frac{2}{\pi}\left(ln\frac{\beta\xi}{2}+\gamma\right)J_0(\beta\xi) - \frac{2}{\pi}\sum_{r=1}^{\infty}(-1)^r \cdot \frac{(\beta\xi/2)^{2r}}{(r!)^2}\left(1+\frac{1}{2}+\frac{1}{3}\cdots\frac{1}{r}\right),$$

where $\gamma = 0.5772$ is Euler's constant.

At the same time the variable is

$$\frac{\pi}{\lambda(m+2)}(1+\lambda x/L)^{\frac{m+2}{2}} = \frac{\pi}{ln\,Q}Q^{\xi/2}\text{ (for }m=\infty)$$

and the frequency equation becomes

$$J_0\left(\frac{\pi}{ln\,Q}\frac{\nu}{\nu_0}\right)Y_0\left(\frac{\pi}{ln\,Q}\frac{\nu}{\nu_0}\sqrt{Q}\right) = J_0\left(\frac{\pi}{ln\,Q}\frac{\nu}{\nu_0}\sqrt{Q}\right)Y_0\left(\frac{\pi}{ln\,Q}\frac{\nu}{\nu_0}\right).$$

Hence for large values of m the resonance frequencies of the strengthened string are determined by the same equation that gives the natural frequencies of vibration of a stretched annular membrane clamped between an outer circle of radius 1 and an inner circle of radius $(1 + \lambda)^{(m+2)/2} = Q^{\frac{1}{2}}$. This equation is considered in detail in the theory of loud-speakers. The higher overtones obey the equation

$$J_0(\beta b)\,Y_0(\beta a) - J_0(\beta a)\,Y_0(\beta b) \doteq \sin\left(\beta a-\frac{\pi}{4}\right)\cos\left(\beta b-\frac{\pi}{4}\right)$$

$$- \sin\left(\beta b-\frac{\pi}{4}\right)\cos\left(\beta a-\frac{\pi}{4}\right) \doteq \sin\beta(a-b)$$

so that

$$\frac{\nu}{\nu_0} = n\frac{ln\,Q}{1-\sqrt{Q}}.$$

This result confirms the conclusion that the higher overtones are separated by equal frequency intervals.

Forced Vibrations of the String with Strengthened Ends in the Absence of Damping

The equation of motion of a string set into vibration by an alternating force $F(x)\cos 2\pi\nu t$ or $F(x)\epsilon^{-i\omega t}$ dynes per cm. and opposed by $R\partial y/\partial t$, a frictional force assumed to be proportional to the velocity but virtually independent of the frequency, is

$$m(x)\frac{\partial^2 y}{\partial t^2} = S\frac{\partial^2 y}{\partial x^2} + F(x)\epsilon^{-i\omega t} - R\frac{\partial y}{\partial t}$$

$$\frac{\partial^2 y}{\partial t^2} = \frac{S}{m(x)}\frac{\partial^2 y}{\partial x^2} + \frac{F(x)}{m(x)}\epsilon^{-i\omega t} - \frac{R}{m(x)}\frac{\partial y}{\partial t}.$$

On the assumption that a solution exists such that

$$y = Y(x)T(t)$$

and that, apart from a possible lag, the time function $T(t)$ is the same for the forced motion and the external force, the equation

$$- \omega^2 Y = \frac{S}{m(x)} \frac{d^2 Y}{dx^2} + \frac{F(x)}{m(x)} - i\omega \frac{R}{m(x)} Y$$

or

$$\frac{d^2 Y}{dx^2} + \frac{\omega^2}{S} m(x) Y = - \frac{F(x)}{S} - i\omega \frac{R}{S} Y$$

is obtained for the relation between the variables Y and x. When distances and displacements are expressed as fractions of the length L of the string on one side of the origin, putting $\eta = y/L$ and $\xi = 1 + \lambda x/L$

$$m(x) = \rho(\xi) = \rho_0(1 + \lambda x/L)^m = \rho_0 \xi^m,$$

the shape of the string is at any given moment determined by

$$\frac{d^2\eta}{d\xi^2} + \frac{\omega^2}{4\lambda^2 v_0^2} \xi^m \eta = - \frac{LF(\xi)}{S\lambda^2} - \frac{i\omega}{\lambda^2} \frac{R}{S} L^2 \eta .$$

In the absence of the terms on the right-hand side, the solution of the equation yields the undamped free motion of the string:

$$\eta = C_1 \sqrt{\xi} J_{\frac{1}{m+2}}\left(\frac{\pi/\lambda}{m+2} \frac{v}{v_0} \xi^{\frac{m+2}{2}}\right) + C_2 \sqrt{\xi} J_{-\frac{1}{m+2}}\left(\frac{\pi/\lambda}{m+2} \frac{v}{v_0} \xi^{\frac{m+2}{2}}\right).$$

If the solution

$$\eta = C_1 y_1 + C_2 y_2$$

of the reduced equation, called the complementary function for the complete equation, is known, the general solution of the complete equation may always be obtained in terms of quadratures by assuming F, C_1, and C_2 to be functions of ξ and applying Lagrange's method of the variation of the constants of integration. For a differential equation of the second order with second member $P(\xi) = -LF(\xi)/S\lambda^2$, the general solution is

$$\eta = c_1 y_1 + c_2 y_2 - y_1 \int \frac{y_2 P(\xi)}{y_1 y_2' - y_2 y_1'} + y_2 \int \frac{y_1 P(\xi)}{y_1 y_2' - y_2 y_1'}$$

or

$$\eta = c_1 y_1 + c_2 y_2 - y_1 C_1(\xi) + y_2 C_2(\xi).$$

When

$$y_1 = \sqrt{\xi} J_{\frac{1}{\mu}}\left(\frac{\pi/\lambda}{m+2} \frac{v}{v_0} \xi^{\frac{m+2}{2}}\right) = \sqrt{\xi} J_{\frac{1}{\mu}}\left(\beta \xi^{\frac{m+2}{2}}\right)$$

$$y_2 = \sqrt{\xi} J_{-\frac{1}{\mu}}\left(\frac{\pi/\lambda}{m+2} \frac{v}{v_0} \xi^{\frac{m+2}{2}}\right) = \sqrt{\xi} J_{-\frac{1}{\mu}}\left(\beta \xi^{\frac{m+2}{2}}\right)$$

then

$$y_1 y_2' - y_2 y_1' = - \frac{\sin \pi/\mu}{\pi/\mu} .$$

The integrals for C_1 and C_2 can be evaluated when $P(\xi)$ is represented by certain simple functions. From experiments with ordinary strings it is known that in order to produce full resonance the applied force has to agree not only in frequency with one of the natural frequencies of vibration of the string, but it must also vary in strength along the string according to the relation expressing the amplitudes of the stationary waves on the string, so that it is always in phase with the motion. However, with these assumptions the amplitudes become infinite, and the solution is without great practical interest. A different law will be considered for the force that acts upon the strengthened string, namely

$$\frac{F(\xi)}{\xi^m} = A^+ J_{\frac{1}{\mu}}\left(\frac{\pi/\lambda}{m+2}\frac{\nu}{\nu_0}\xi^{\frac{m+2}{2}}\right) + A' J_{-\frac{1}{\mu}}\left(\frac{\pi/\lambda}{m+2}\frac{\nu}{\nu_0}\xi^{\frac{m+2}{2}}\right),$$

where ν, the frequency of the external force, may have any value but is supposed to differ, even if only slightly, from the frequency ν_n corresponding to a standing wave. The amplitudes A^+ and A' have the dimensions MT^{-2} of a force referred to unit length.

By a change in the variable to $z = \xi^{\frac{m+2}{2}}$ the well known formulas for the integral of a product of two Bessel functions become

$$\frac{m+2}{2}(\alpha^2-\beta^2)\int \xi^{m+1} J_{\frac{1}{\mu}}\left(\alpha\xi^{\frac{m+2}{2}}\right) J_{-\frac{1}{\mu}}\left(\beta\xi^{\frac{m+2}{2}}\right) d\xi$$

$$= \frac{2}{\mu} J_{\frac{1}{\mu}}\left(\alpha\xi^{\frac{m+2}{2}}\right) J_{-\frac{1}{\mu}}\left(\beta\xi^{\frac{m+2}{2}}\right) + \beta\xi^{\frac{m+2}{2}} J_{\frac{1}{\mu}}\left(\alpha\xi^{\frac{m+2}{2}}\right) J_{-\frac{1}{\mu}-1}\left(\beta\xi^{\frac{m+2}{2}}\right)$$

$$- \alpha\xi^{\frac{m+2}{2}} J_{\frac{1}{\mu}-1}\left(\alpha\xi^{\frac{m+2}{2}}\right) J_{-\frac{1}{\mu}}\left(\beta\xi^{\frac{m+2}{2}}\right)$$

$$\frac{m+2}{2}(\alpha^2-\beta^2)\int \xi^{m+1} J_{\frac{1}{\mu}}\left(\alpha\xi^{\frac{m+2}{2}}\right) J_{\frac{1}{\mu}}\left(\beta\xi^{\frac{m+2}{2}}\right) d\xi$$

$$= \xi^{\frac{m+2}{2}}\left(\beta J_{\frac{1}{\mu}}\left(\alpha\xi^{\frac{m+2}{2}}\right) J_{\frac{1}{\mu}-1}\left(\beta\xi^{\frac{m+2}{2}}\right) - \alpha J_{\frac{1}{\mu}-1}\left(\alpha\xi^{\frac{m+2}{2}}\right) J_{\frac{1}{\mu}}\left(\beta\xi^{\frac{m+2}{2}}\right)\right)$$

$$= \xi^{\frac{m+2}{2}}\left(\alpha J_{\frac{1}{\mu}+1}\left(\alpha\xi^{\frac{m+2}{2}}\right) J_{\frac{1}{\mu}}\left(\beta\xi^{\frac{m+2}{2}}\right) - \beta J_{\frac{1}{\mu}}\left(\alpha\xi^{\frac{m+2}{2}}\right) J_{\frac{1}{\mu}+1}\left(\beta\xi^{\frac{m+2}{2}}\right)\right)$$

for any two Bessel functions, where

$$\alpha^2 = \frac{4L^2\pi^2/\lambda^2}{(m+2)^2}\nu^2\frac{\rho_0}{S}, \qquad \beta^2 = \frac{4L^2\pi^2/\lambda^2}{(m+2)^2}\nu_n^2\frac{\rho_0}{S}$$

The factor α refers to the external force, the factor β to the resonance frequencies of a string of arbitrary length.

With $\mu = m + 2$ the final solution, valid when ν differs from ν_n, or α differs from β, is

$$\eta = c_1 y_1 + c_2 y_2 + \frac{4L}{(m+2)^2(\alpha^2-\beta^2)}\left(A^+\sqrt{\xi}J_{\frac{1}{m+2}}\left(\alpha\xi^{\frac{m+2}{2}}\right) + A'\sqrt{\xi}J_{-\frac{1}{m+2}}\left(\alpha\xi^{\frac{m+2}{2}}\right)\right)$$

or

$$\frac{\eta}{\sqrt{\xi}} = c_1 J_{\frac{1}{m+2}}\left(\beta\xi^{\frac{m+2}{2}}\right) + c_2 J_{-\frac{1}{m+2}}\left(\beta\xi^{\frac{m+2}{2}}\right)$$
$$+ \frac{1}{\rho_0\pi^2 L(\nu^2-\nu_n^2)}\left(A^+ J_{\frac{1}{m+2}}\left(\alpha\xi^{\frac{m+2}{2}}\right) + A' J_{-\frac{1}{m+2}}\left(\alpha\xi^{\frac{m+2}{2}}\right)\right).$$

It consists of two parts, the free vibration normally dying down after a time, and the forced vibration that takes place at the frequency of the external force. Two constants are available for the fulfilment of two boundary conditions, for instance, $\eta = 0$ for $\xi = a = 1$, and $\eta = 0$ for $\xi = b = 1 + \lambda$, relations holding for standing waves with an even number of loops over the length l. There follows in this case

$$\sigma c_1 D = A^+\left(J_{\frac{1}{m+2}}(\alpha, a)\, J_{-\frac{1}{m+2}}(\beta, b) - J_{\frac{1}{m+2}}(\alpha, b)\, J_{-\frac{1}{m+2}}(\beta, a)\right)$$
$$+ A'\left(J_{-\frac{1}{m+2}}(\alpha, a)\, J_{-\frac{1}{m+2}}(\beta, b) - J_{-\frac{1}{m+2}}(\alpha, b)\, J_{-\frac{1}{m+2}}(\beta, a)\right)$$

and

$$\sigma c_2 D = A^+\left(J_{\frac{1}{m+2}}(\alpha, b)\, J_{\frac{1}{m+2}}(\beta, a) - J_{\frac{1}{m+2}}(\alpha, a)\, J_{\frac{1}{m+2}}(\beta, b)\right)$$
$$+ A'\left(J_{-\frac{1}{m+2}}(\alpha, b)\, J_{\frac{1}{m+2}}(\beta, a) - J_{-\frac{1}{m+2}}(\alpha, a)\, J_{\frac{1}{m+2}}(\beta, b)\right)$$

where α, a, is written for $\alpha\, a^{\frac{m+2}{2}}$, and β, b, for $\beta\, b^{\frac{m+2}{2}}$

$$\sigma = \frac{1}{\rho_0\pi^2 L(\nu^2-\nu_n^2)}$$

$$D = J_{\frac{1}{m+2}}(\beta, a)\, J_{-\frac{1}{m+2}}(\beta, b) - J_{-\frac{1}{m+2}}(\beta, a)\, J_{\frac{1}{m+2}}(\beta, b).$$

As the external frequency ν approaches ν_n, the coefficients A^+ and A', and the expressions σ and D, tend toward zero, but the denominator of c_1 and c_2 decreases at a more rapid rate than the numerator, so that large amplitudes result even with small forces A^+ and A'.

When the frequency ν of the applied force is equal to one of the resonance frequencies ν_n of the string, the integrals leading to the value of $C_1(\xi)$ and $C_2(\xi)$ appear in the indeterminate form $0 : 0$ and must be replaced by

$$\frac{m+2}{2}\int \xi^{m+1} J_\mu^2\left(\alpha\xi^{\frac{m+2}{2}}\right) d\xi = \frac{\xi^{\frac{m+2}{2}}}{2} J_\mu^2\left(\alpha\xi^{\frac{m+2}{2}}\right) - \frac{\xi^{\frac{m+2}{2}}}{2} J_{\mu-1}\left(\alpha\xi^{\frac{m+2}{2}}\right) J_{\mu+1}\left(\alpha\xi^{\frac{m+2}{2}}\right)$$

$$\frac{m+2}{2}\int \xi^{m+1} J_\mu\left(\alpha\xi^{\frac{m+2}{2}}\right) J_{-\mu}\left(\alpha\xi^{\frac{m+2}{2}}\right) d\xi = \frac{\xi^{m+2}}{4}\left(2 J_\mu J_{-\mu} + J_{\mu-1} J_{-\mu-1} + J_{\mu+1} J_{-\mu+1}\right).$$

The resulting motion is represented by

$$\frac{\eta}{\sqrt{\xi}} = c_1 J_{\frac{1}{m+2}}\left(\alpha\xi^{\frac{m+2}{2}}\right) + c_2 J_{-\frac{1}{m+2}}\left(\alpha\xi^{\frac{m+2}{2}}\right)$$
$$- \frac{1}{2(m+2)L\rho_0\nu^2}\left(A^+ J_{\frac{1}{m+2}}\left(\alpha\xi^{\frac{m+2}{2}}\right) + A' J_{-\frac{1}{m+2}}\left(\alpha\xi^{\frac{m+2}{2}}\right)\right).$$

For a string of finite length both the free and the forced motion, therefore, satisfy the boundary conditions.

The shapes of the fundamental and of the first and second overtones are illustrated for $m = 2$ (square law) and $Q = 4$ in Fig. 1 and for $Q = 16$ in Fig. 2. The forces necessary to maintain these standing waves are also plotted in arbitrary units. As a comparison, the shape of a sinusoidal wave, the third harmonic, is shown with the second overtone.
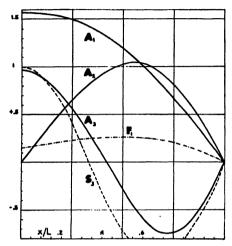
FIG. 1. *Wave-shapes y/L when $Q = 4$ for the fundamental (A_1), the first (A_2) and second overtone (A_3), the sinusoidal wave (S_3), and the force F_1 required to maintain A_1.*

FIG. 2. *Wave-shapes y/L when $Q = 16$ for the fundamental (A_1), the first (A_2) and second (A_3) overtone, the sinusoidal wave (S_3), and the forces required to maintain A_1 and A_2.*

$$A_1 = 0.807 \sqrt{\xi}\, J_{\frac{1}{4}}\left(0.79 \times 0.75\xi^{\frac{m+2}{2}}\right)$$
$$+ \sqrt{\xi}\, J_{-\frac{1}{4}}\left(0.79 \times 0.75\xi^{\frac{m+2}{2}}\right)$$

$$A_2 = 2\sqrt{\xi}\, J_{\frac{1}{4}}\left(0.79 \times 1.3\xi^{\frac{m+2}{2}}\right)$$
$$- 2.28\sqrt{\xi}\, J_{-\frac{1}{4}}\left(0.79 \times 1.3\xi^{\frac{m+2}{2}}\right)$$

$$A_3 = 2\sqrt{\xi}\, J_{\frac{1}{4}}\left(0.79 \times 2\xi^{\frac{m+2}{2}}\right)$$
$$- 0.8\sqrt{\xi}\, J_{-\frac{1}{4}}\left(0.79 \times 2\xi^{\frac{m+2}{2}}\right)$$

$$F_1 = \xi^m A_1/10.$$

$$A_1 = 0.5\sqrt{\xi}\, J_{-\frac{1}{4}}\left(0.26 \times 0.5\xi^{\frac{m+2}{2}}\right)$$

$$A_2 = \sqrt{\xi}\, J_{\frac{1}{4}}\left(0.26 \times 0.76\xi^{\frac{m+2}{2}}\right)$$
$$- 0.43\sqrt{\xi}\, J_{-\frac{1}{4}}\left(0.26 \times 0.76\xi^{\frac{m+2}{2}}\right)$$

$$A_3 = 0.24\sqrt{\xi}\, J_{\frac{1}{4}}\left(0.26 \times 1.3\xi^{\frac{m+2}{2}}\right)$$
$$+ 0.33\sqrt{\xi}\, J_{-\frac{1}{4}}\left(0.26 \times 1.3\xi^{\frac{m+2}{2}}\right)$$

$$F_1 = \xi^m A_1/10$$

$$F_2 = \xi^m A_2/5.$$

Resonance of a Dampened String with Strengthened Ends

The response of a strengthened string subject to a dampening force during its motion can be determined with the aid of the general equations by introducing the complex pulsation $w = 2\pi\nu + ik$. Since however the free vibrations

die down in the course of time, the boundary equations are fulfilled only on the two conditions that the forced vibration takes place at the frequency of the external force and also in the simple shape of standing waves, whatever the frequency.

On the assumption that a solution exists in the form

$$y(x, t) = Y(x) \cos (pt - \epsilon)$$

for the equation of motion

$$\frac{\partial^2 y}{\partial t^2} = \frac{T}{\rho} \frac{\partial^2 y}{\partial x^2} + \frac{F}{\rho} \cos 2\pi \nu t - \frac{R}{\rho} \frac{\partial y}{\partial t}$$

and writing

$$F \cos pt = F \cos 2\pi \nu t = F \cos ((pt - \epsilon) + \epsilon)$$

a relation is obtained that contains $\sin (pt + \epsilon)$ and $\cos (pt + \epsilon)$. Since this relation must hold for all values of t, the terms containing the factor $\sin (pt + \epsilon)$ and the terms containing the factor $\cos (pt + \epsilon)$ must separately add up to zero, so that

$$\frac{d^2 Y}{dx^2} + p^2 \frac{\rho}{S} Y + \frac{F(x)}{S} \cos \epsilon = 0,$$

and, regardless of any variation of the mass ρ per unit length along the string,

$$Y(x) = \frac{F(x)}{Rp} \sin \epsilon \text{ (providing that } \epsilon \neq 0)$$

so that

$$\tan \epsilon = \frac{Rp Y/\rho}{\frac{S}{\rho} \frac{d^2 Y}{dx^2} + p^2 Y} .$$

The angle by which the motion lags in phase behind the applied force is independent of the law for $F(x)$ but varies with the relation that exists between Y'' and Y', the two variables that appear in the equation of the free motion of the string. When, in particular, the span of length l vibrates under the influence of the external force in the same manner as an undamped string, then

$$\frac{S}{\rho} \frac{d^2 Y(x)}{dx^2} = - \omega^2 Y(x) \text{ and } Y = \rho \frac{\cos \epsilon F(x)}{\omega^2 - p^2}$$

$$\tan \epsilon = \frac{Rp/\rho}{\omega^2 - p^2}$$

$$\sin \epsilon = \frac{Rp/\rho}{\sqrt{(\omega^2 - p^2)^2 + R^2 p^2/\rho^2}},$$

where ω is one of the pulsations $2\pi \nu_n$ that correspond to the resonance frequencies ν_n of the undamped string of length l. The losses caused by friction are exactly balanced by the applied force. Though this force may

have any frequency, its strength must vary with x in proportion to the amplitudes of one of the standing waves of the freely vibrating string, because

$$Y(x) = \frac{F(x)}{Rp \sin \epsilon} = \frac{F(x)}{\rho \sqrt{(\omega^2 - p^2)^2 + R^2 p^2 / \rho^2}} .$$

With $\quad F(x) = (1 + \lambda x/L)^{m + \frac{1}{2}} \left(A^+ J_{\frac{1}{m+2}}\left(\alpha \xi^{\frac{m+2}{2}}\right) + A' J_{-\frac{1}{m+2}}\left(\alpha \xi^{\frac{m+2}{2}}\right) \right),$

that is, if the force varies along the string at the same rate as the product of the mass and the amplitude of the free vibrations, whatever law these vibrations may obey, and if

$$R(x) = R(1 + \lambda x/L)^m$$

at least approximately, while $\alpha = \dfrac{\pi}{\lambda(m+2)} \dfrac{\nu}{\nu_0} = \dfrac{p}{2\lambda(m+2)\nu_0}$, then

$$Y(x) = \frac{A^+ \sqrt{\xi} J_{\frac{1}{m+2}}\left(\alpha \xi^{\frac{m+2}{2}}\right) + A' \sqrt{\xi} J_{-\frac{1}{m+2}}\left(\alpha \xi^{\frac{m+2}{2}}\right)}{\rho_0 \sqrt{(\omega^2 - p^2)^2 + R^2 p^2 / \rho_0^2}}$$

so that undistorted resonance becomes possible. It will be seen that it is more difficult to fulfil the conditions for resonance in strengthened strings than in uniform strings, so that the amplitudes of vibration are reduced.

In practice, owing to the complicated changes in the amplitude that accompany higher overtones, only forces corresponding in distribution to the amplitudes of the fundamental frequency ν_1 need be considered, and, in special instances, only one of the functions $J_{\frac{1}{(m+2)}}$ or $J_{-\frac{1}{(m+2)}}$.

Special Solutions

The complete solution of the equation

$$\frac{d^2 Y}{dx^2} + \frac{4\pi^2 \nu^2 \rho_0}{S} Y = 0$$

for the shape of the vibratory string of uniform mass per unit length is

$$Y(x) = C^+ \epsilon^{\frac{2\pi\nu}{c} z} + C' \epsilon^{-\frac{2\pi\nu}{c} z} .$$

On the assumption that the ends of the string at $x = a$ and at $x = b$ are stationary, the values obtained for C^+/C' at these two points lead to the equation $\cos 2\pi\nu(b - a)/c = 0$, and give for the allowed frequencies the formula

$$\nu_n = \frac{n}{2l} \sqrt{\frac{S}{\rho_0}} .$$

This same result is obtained for either C^+ or C' equal to zero. When similar calculations are carried out for the string with strengthened ends, the solutions secured for a vanishing A^+ or A' are found to differ from the solutions that are valid when neither A^+ nor A' is negligible. The assumptions that A',

for instance, is zero, and that the points $x = 0$ and $x = L$ remain at rest, give

$$J_{\frac{1}{m+2}}\left(\frac{\pi/\lambda}{m+2}\frac{\nu}{\nu_0}\right) = 0 \qquad \text{at } x = 0$$

and

$$J_{\frac{1}{m+2}}\left(\frac{\pi/\lambda}{m+2}\frac{\nu}{\nu_0}(1+\lambda)^{\frac{m+2}{2}}\right) = 0 \qquad \text{at } x = L,$$

whereas when the string is at rest only at $x = L$, but has a loop at $x = 0$,

so that for $\qquad \eta = \sqrt{\xi}\, J_{\frac{1}{m+2}}\left(\frac{\pi/\lambda}{m+2}\frac{\nu}{\nu_0}\xi^{\frac{m+2}{2}}\right)$

$$\frac{\partial \eta}{\partial \xi} = \frac{\nu}{2\nu_0}\frac{\pi}{\lambda}\xi^{\frac{m+1}{2}}J_{-\frac{1}{m+2}}\left(\frac{\pi/\lambda}{m+2}\frac{\nu}{\nu_0}\xi^{\frac{m+2}{2}}\right) = 0 \quad \text{at } x = 0 \text{ or } \xi = 1,$$

there follows the additional solution

$$J_{-\frac{m+1}{m+2}}\left(\frac{\pi/\lambda}{m+2}\frac{\nu}{\nu_0}\right) = 0.$$

A third series of frequencies satisfying the boundary conditions is obtained for the alternative $A^+ = 0$ by merely changing the sign of the parameters of the three Bessel functions. With the exception of the two or three smallest solutions, the roots of the Bessel functions $J_\mu(z)$ are given quite closely by the values following from the asymptotic expansion of $J_\mu(z)$ and lead to the result

$$z = (2\mu + 1 \mp 2k), \text{ where } k = 1, 3, 5, \ldots$$

The resonance frequencies ν obtained from the roots of $J_{\pm 1/(m+2)}$ and $J_{\pm(m+1)/(m+2)}$, or from J_0 and J_1 when m is very large, differ slightly from the solutions that follow from the complete equation for standing waves with an odd or an even number of loops. The complete equation contains the new solutions as a simple and evident choice that fulfils the boundary conditions when the external force lacks components of the form A^+J_μ or $A'J_{-\mu}$.

Section A

INDEX TO VOLUME XVI

Authors

Section A

INDEX TO VOLUME XVI

Subjects

ERRATUM

Sec. A, p. 153, under "Details of engine" for "Rated b.hp. at 11,500 ft. . . . ." read "Rated b.hp., 385, at 11,500 ft. . . . ."

CANADIAN

JOURNAL OF

RESEARCH

VOLUME XVI

SECTION B

January to December, 1938

CANADA

A NEW METHOD FOR THE ANALYSIS OF MIXTURES OF CHLORINE, PHOSGENE, AND NITROSYL CHLORIDE[1]

By E. W. R. STEACIE[2] AND W. McF. SMITH[3]
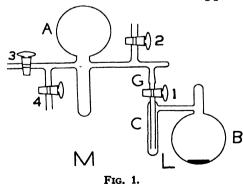
Abstract

A new method for the analysis of mixtures of chlorine, phosgene, and nitrosyl chloride has been developed. The basis of the method is the difference in the action of these gases on mercury: phosgene is inert, nitrosyl chloride attacks mercury yielding an equimolecular amount of nitric oxide, while chlorine is completely absorbed. The extension of the scheme to the analysis of mixtures containing nitric oxide and nitrogen dioxide has also been investigated.

Introduction

The analysis of mixtures of nitrosyl chloride, phosgene, and chlorine is a matter of considerable difficulty because of the corrosive nature of the gases and of the ease with which they hydrolyze. A simple scheme for the analysis of such mixtures has been developed in connection with an investigation of the thermal decomposition products of chloropicrin (2). The method depends upon the action of the above-mentioned gases on mercury. Phosgene is inert, nitrosyl chloride attacks mercury yielding an equimolecular amount of nitric oxide, while chlorine attacks mercury and is completely absorbed. The decrease in the volume or pressure of the mixture is thus an indication of the amount of chlorine present, while the amount of nitric oxide formed under the same circumstances is a measure of the nitrosyl chloride.

Apparatus

FIG. 1.

The apparatus used is illustrated in Fig. 1. Because of the action of chlorine and nitrosyl chloride on mercury, pressure measurements were made with an all-glass manometer of the spoon type. The gauge was contained in a glass jacket in which the air pressure could be regulated, and was used as a null-instrument, the pressure inside the gauge being balanced by air in the jacket, and the air pressure

then read on a mercury manometer.   Stopcocks were greased with Apiezon N grease, which was found to be quite satisfactory.   The bulb A served to provide the system with the necessary volume, and carried a protuberance to allow freezing-out of the gases.   Stopcock 2 led to the pressure gauge, 3 to the pumping system, and 4 to the inlet for the sample.   In the subsequent discussion this section of the apparatus will be referred to as section M.

The protective scum which forms on mercury when in contact with nitrosyl chloride or chlorine necessitates a thorough shaking of the absorption vessel. Consequently the unit composed of the bulb B containing mercury, the trap C, and stopcock 1 was connected to the rest of the system by the ground joint G. This entire section (denoted by L) could be removed and shaken.   The volume of the bulb B was approximately the same as that of A, while the trap C was made as small as possible so that cooling the trap had only a negligible effect (in the absence of condensation) on the pressure in the system L.

Procedure

The sample was introduced into section M of the apparatus by condensation or merely by expansion, and the pressure, P_1, produced by the gases at room temperature was read on the gauge.   The gases were then condensed in the tube below A with liquid air.   Trap C was then surrounded with liquid air, stopcock 1 opened, and the condensed gases were allowed to warm up and distil into C.   When this was complete, as registered by the pressure gauge, stopcock 1 was closed and air was admitted to section M.   Section L was then removed and shaken until no color was perceptible in the products when condensed in the trap C.   Section L was then reconnected to the system, and section M evacuated.   With stopcocks 3 and 4 closed and liquid air around trap C, stopcock 1 was opened.   The liquid air was then removed from around trap C and replaced by a frozen saturated solution of carbon dioxide in acetone*.

At this temperature phosgene has a negligible vapor pressure, but nitric oxide is entirely in the vapor phase.   The nitric oxide pressure, P_2, was then measured, the trap allowed to warm to room temperature, and the total pressure, P_3, was measured.   We then have:

Original pressure of sample in $M + L$ $= P_1 \times \dfrac{\text{volume of } M}{\text{volume of } M + L}$

Partial pressure of NOCl in sample $= P_2$

Partial pressure of $COCl_2$ in sample $= P_3 - P_2$

Partial pressure of Cl_2 in sample $= \text{(Original pressure)} - P_3$

Experimental Test of the Method

In order to test the reliability of the method the action of phosgene, nitrosyl chloride, and chlorine, singly and in mixtures, was examined.   The phosgene used was manufactured by Kahlbaum.   Nitrosyl chloride was made from

---

* *This refrigerant, whose temperature is approximately* $-103°$ *C., is easily made by freezing with liquid air a solution of acetone which has been saturated with carbon dioxide by cooling down with solid carbon dioxide.   Its use was suggested and examined by Mr. N. W. F. Phillips of this laboratory, and it has been found to be a very convenient method of obtaining a reproducible temperature considerably lower than that of solid carbon dioxide.*

sodium nitrite and phosphorus oxychloride, as described by Skinner (1), and fractionally distilled several times. Chlorine was obtained from commercial cylinders and distilled before use.

It was found that phosgene was unaffected by mercury, as indicated by the following data:

Pressure of $COCl_2$ in M prior to shaking with mercury   = 8.95 cm.
Pressure of $COCl_2$ in $M + L$ prior to shaking with mercury (calc.) = 5.2
Pressure of $COCl_2$ in $M + L$ after shaking with mercury   = 5.25

Nitrosyl chloride attacked mercury readily, the red-brown color of the gas disappearing. The vapor pressure of the resulting gas was approximately that of nitric oxide. Thus

Pressure of $NOCl$ in M = 9.6 cm.
Pressure of $NOCl$ in $M + L$ (calc.)   = 5.4

After shaking with mercury

Pressure in $M + L$ with trap C at $-183°$ C.   = 0.4
Pressure in $M + L$ with trap C at $-103°$ C.   = 5.5
Pressure in $M + L$ with trap C at $20°$ C.   = 5.5

Chlorine was almost completely absorbed on shaking with mercury, the very small residual pressure being presumably due to impurities. Thus, for example,

Pressure of Cl_2 in M prior to shaking with mercury   = 58.2 cm.
Pressure in $M + L$ after shaking with mercury   = 0.3

The data for a number of experiments with known mixtures of the constituents follow.

Phosgene and Chlorine

Sample	$COCl_2$	=	6.35 cm.	Cl_2	=	8.55 cm.
Found			6.4			8.55

Nitrosyl Chloride and Chlorine

Sample	$NOCl$	=	6.1	Cl_2	=	14.3
Found			6.05			14.3

Nitrosyl Chloride and Chlorine

Sample	$NOCl$	=	4.0	Cl_2	=	7.7
Found			3.95			7.7

Nitrosyl Chloride and Phosgene

Sample	$NOCl$	=	10.55	$COCl_2$	=	7.55
Found			10.6			7.6

Nitrosyl Chloride, Phosgene, and Chlorine

Sample	$NOCl$	=	9.8	$COCl_2$	=	5.95	Cl_2 =	5.2
Found			9.75			6.0		5.2

Nitrosyl Chloride, Phosgene, and Chlorine

Sample	$NOCl$	=	6.5	$COCl_2$	=	10.8	Cl_2 =	6.3
Found			6.45			11.0		6.15

Mixtures Containing Nitric Oxide

It may happen that nitric oxide is also present.   In the case of a mixture of nitric oxide, phosgene, and nitrosyl chloride, the nitric oxide may be thoroughly separated from the other gases by freezing the entire mixture with liquid air, and warming to $-103°$ C.   It was found experimentally that the solubility of nitric oxide in small amounts of nitrosyl chloride or phosgene was not detectable.

If chlorine is also present in the mixture, the composition will vary with the length of time that chlorine and nitric oxide are present together, since the rate of recombination to form nitrosyl chloride is appreciable at room temperature, and the mixture will finally contain only chlorine or nitric oxide, depending upon which of the two is in excess.   Separation of the free nitric oxide from chlorine, nitrosyl chloride, and phosgene may be effected at $-103°$ C. if the chlorine does not constitute a large fraction of the gases. Otherwise, recombination of the nitric oxide and chlorine should be effected before the analysis is attempted.   Owing to the termolecular nature of the gaseous reaction, the recombination at low pressures is slow.   However, since the temperature coefficient of the reaction is very small, the rate of recombination may be greatly increased by condensation of the gases, so that the whole process is complete in a few hours.   The pressure drop during this time is a measure of the amount of recombination.   The resulting mixture may then be easily analyzed since it contains only nitric oxide, phosgene, and nitrosyl chloride, or chlorine, nitrosyl chloride, and phosgene.

Mixtures Containing Nitrogen Dioxide

The presence of nitrogen dioxide is a much more serious complication.   At room temperature nitrogen dioxide is considerably associated to nitrogen tetroxide, the amount of association depending on the pressure.   An examination of the action of this gas on mercury, the extent of the association being taken into consideration, indicated that nitrogen dioxide is replaced by one-half its molecular quantity of nitric oxide, a nitrate of mercury presumably being formed.   In the absence of chlorine, the quantity of nitrogen dioxide in a mixture of nitrogen dioxide, phosgene, and nitrosyl chloride may therefore be indicated by the pressure drop on reaction with mercury.   The amount of nitrogen dioxide is, of course, not equal to twice the pressure drop on account of association, but, since the amount of association is known as a function of the pressure, the calculation may easily be made.

If nitric oxide and nitrogen dioxide are both present, the formation of nitrogen trioxide occurs at low temperatures and causes the retention of some nitric oxide when the separation at $-103°$ C. is attempted.   Moreover, it was found that the amount of nitric oxide combined with nitrogen dioxide was considerably less than the equivalent amount, even when nitric oxide was in excess, and that the value was not very reproducible.

When chlorine is present with nitrogen dioxide both are found to act independently on mercury in the manner indicated above.   In such a case the

pressure drop on shaking with mercury depends on the amount of each, but the relative amounts of each can be determined only from the nitric oxide formed if nitrosyl chloride is absent.

It is apparent, therefore, that the method is not satisfactory when nitrogen dioxide is present unless the mixture consists only of nitrosyl chloride, phosgene, and nitrogen dioxide, or of phosgene, nitrogen dioxide, and chlorine. It is, however, entirely satisfactory when nitrogen dioxide is absent.   Moreover, it should also prove of value for the determination of nitrosyl chloride and chlorine in mixtures with other gases which have a negligible vapor pressure at $-103°$ C.

References

1. SKINNER, G. S.   J. Am. Chem. Soc. 46 : 731-741.   1924.
2. STEACIE, E. W. R. and SMITH, W. McF.   J. Chem. Phys.   In press.

CANADIAN BENTONITES[1]

By Wilfred Gallay[2]

Abstract

A number of Canadian bentonites were investigated as refining and bleaching agents for a variety of industrially important petroleum and fatty oils including the following: lubricating oil distillates, cracked motor fuel distillates; peanut, cottonseed, coconut, and palm oils; lard and beef tallow; linseed oil; pilchard oil; used crank-case oils, insulating oils, and dry cleaning solvents. The raw materials and test methods were chosen to conform to industrial practice. Canadian clays were chiefly from the four western provinces, and comparisons are shown with the results obtained on several imported clays now in use. Several Canadian bentonites show good results in the bleaching of fatty oils and petroleum distillates. Bentonite from the Morden, Manitoba, district possesses unusually high adsorbent power, and in the activated condition its effect on all the raw materials tested is much superior, within the limits of the laboratory test methods employed, to that of all other bentonites examined in this investigation. Optimum methods of activation of these bentonites are discussed. Low silica to alumina ratio and high percentage of combined water are the outstanding characteristics of Morden bentonite, in comparison with adsorbent clays from other sources. Bentonites were not found suitable for use in the vapor phase percolation treatment of cracked distillates.

The present work was undertaken for the purpose of assessing, in a preliminary way at least, the value of a number of Canadian deposits of bentonitic clays for industrial purposes, chiefly the refining and bleaching of various petroleum and fatty oils. The occurrence of most of the known deposits has been described in publications of the Department of Mines, Ottawa, (1), but very few data have been available with regard to their possible applications. Consumption of these materials in Canada is supplied practically entirely by imports.

Adsorbent earths may be divided into two general classes; (1) fuller's earth, (2) bentonite clays. Fuller's earths find their chief industrial applications in the bleaching of fatty oils and in the refining of cracked petroleum distillates by vapor phase percolation. No deposit of fuller's earth has been found in Canada; it is therefore imported from Great Britain and various ections of the United States. Bentonitic clays have found important industrial applications in recent years, the largest of which is in the refining of petroleum distillates. Spence (1) has compiled a list of these applications. The term "bentonite" was first applied to the hydrous aluminium silicates of the Fort Benton formation in Wyoming, but has since been applied to other earths of somewhat similar character in various parts of the world. The known Canadian deposits of bentonitic clays, however, differ importantly in properties from Wyoming bentonite, as do also various deposits in the United States. Wyoming bentonite forms a stable suspension in water, whereas the bentonitic clays settle quite rapidly, being apparently closer to the isoelectric point. Wyoming bentonite possesses the property of swelling enormously in water and yields a stiff gel at concentrations as low as 5%. The

bentonitic clays swell only moderately. In tests of emulsifying power, finely dispersed 1 : 1 aqueous emulsions of a fairly viscous white oil of the medicinal type were produced with Wyoming bentonite; these were stable for several weeks. Corresponding tests on a variety of Canadian bentonitic clays failed to produce emulsions. The same holds true in the case of detergent power, the Wyoming bentonite being much superior in this regard both in laboratory and industrial trials. In adsorbent power, however, this order is reversed. The Wyoming bentonite is quite inferior to many bentonitic clays for refining and bleaching purposes. Despite these differences, the term bentonite has been widely applied to the general class of clays discussed in the present work, without distinction from the Wyoming type.

The adsorbent quality of bentonite is due to the extent and quality of the surface area developed by the action of weathering agents. It is probable that activation of the naturally found bentonites performs the same function. The adsorbent power of bentonites from various deposits differs enormously, and the order of merit varies further in many cases depending on the nature of the material to be adsorbed. Chemical analyses, although they show wide variation in the silica-alumina ratio and proportion of such materials as magnesia, lime, and iron, offer no clue and bear no apparent relation to the adsorbent power. Available methods of particle size determination by purely physical means are too gross to yield any information of value with regard to the extent of specific surface. Attempts have been made to set up standard tests of adsorbent power, dye solutions chiefly being used as substrates, but conclusions drawn from such tests have been found inapplicable in practical adsorbent tests on a variety of industrial materials. The evaluation of bentonites as adsorbents, therefore, remains entirely empirical, and tests must be made on the raw materials as used industrially. In the present work, contact was made with the industries concerned, and samples of raw material that are identical with those which are refined or bleached on an industrial scale were secured for test. The test methods, furthermore, corresponded as closely as possible either with the methods actually used industrially, or with methods that are capable of direct interpretation in terms of large-scale practice.

Preparation and Activation of Bentonites

Bentonites occur naturally in beds in hydrated condition and must be dried and ground before use. They may be dried either at ordinary temperature in protected stock piles, or at elevated temperatures in various types of continuous or batch driers, or by a combination of air and oven drying. From time to time, the writer has received reports which indicate that the drying of bentonite at a fairly high temperature, say at about 450° C., increases its adsorbent capacity. Calcination tests at temperatures from 300° to about 700° C., followed by adsorption tests, have, however, shown in all cases investigated that the bleaching power decreases with increased temperature of drying in this range. There are indications also that extended drying periods at temperatures above 200° C. also reduce the adsorbent quality of

the bentonite.   Drying must therefore be effected by indirect heat at temperatures below a maximum which may be readily ascertained for the bentonite being processed.   Industrial practice generally requires a product out 80 to 95% minus 200 mesh, and a variety of grinding means, *e.g.*, a mmer mill, are suitable for this purpose.

For some applications an untreated bentonite, *i.e.*, a crude bentonite merely dried and ground, serves the purpose.   For other uses, chiefly in the refining of petroleum distillates by the contact method, bentonites are treated to enhance greatly their adsorbent powers.   This treatment is commonly termed activation.

Activation of a bentonite consists essentially of treatment with an acid solution at an elevated temperature, followed by filtration, washing, drying, and grinding.   Since bentonites of better quality disintegrate rapidly in water, a coarse preliminary grinding is sufficient for the activation process. The material is then placed in an acid-resistant vessel, *e.g.*, wood, or lead-lined, with an acid solution, and the mixture is heated to boiling by direct steam which may be introduced in such a form as to serve also for agitation of the mixture.   Sulphuric acid in a number of tests has proved superior to hydrochloric acid for bentonite activation.   A part of the alumina and of the impurities are soluble in the acid, and it is probable that the specific surface is greatly increased by acid treatment; this results in increased adsorbent power.   Some bentonites are not improved by activation, and in these instances it is found that little alumina dissolves.   It is probable that the proportion of combined alumina differs in different bentonites.

Since a given amount of acid is more effective at higher concentrations, the amount of acid solution should be kept at a minimum consistent with ease of agitation and later transfer to a filter.   A slurry that can be stirred readily is desirable.   The optimum proportion of acid for activation was found to vary widely with different bentonites.   In all cases a maximum was found, above which the adsorbent power of the product decreased.   The range of this optimum for different bentonites was 25 to 100% by weight of the bentonite, with many at about 40 to 50%.   These proportions of acid were used in the laboratory in a total solution two to two and one-half times the weight of the dry bentonite.   It is evident that this amount of acid would be appreciably reduced in processing on an industrial scale, since slurries of much higher clay concentration could be handled.   The time of treatment necessary to produce a most efficient product varied from one and one-half to five hours, depending on the ease with which the bentonite is attacked by the acid.

After acid treatment, and if necessary, suitable dilution and thickening, the clay is filtered in a vacuum filter of the continuous type, and washed on the filter.   In some cases, the hardness of the water used in this washing affected the product appreciably, distilled water proving much better than tap water.   In other cases, no difference due to this factor was noted. Generally an activated clay, unless specially neutralized, contains 2 to 3%

of mineral acid calculated as hydrochloric acid. After washing, the treated clay is dried at a controlled temperature by indirect heat and is then ground to 200 mesh.

It is to be especially emphasized that the determination of the optimum procedure for the activation of a bentonite is entirely empirical, and particular attention must be paid to the actual bentonite that is to be produced on an industrial scale.

Morden Bentonite

It is immediately noted from the experimental results below, that the bentonite from the deposit near Morden, Manitoba, possesses, for a variety of petroleum and fatty oils, unusually high bleaching power. This bentonite in the crude state is very active, its activity approaching in many instances that of industrially used activated clay, and in some cases it is greater. Morden bentonite is furthermore readily susceptible to activation, yielding an activated product that possesses far greater adsorbent power than any other clay examined in this laboratory, including industrial activated earths from the United States, Germany, and France. Particular mention is therefore made of the occurrence and properties of this bentonite. While laboratory tests of refining power undoubtedly yield much information of direct value, it is to be noted that trials on full plant scale are indispensable in the final evaluation of a bleaching earth.

This deposit occurs over a very large area, but has been examined chiefly over a section of about 1000 acres, some four miles north of Thornhill, Manitoba, about equidistant between the Canadian Pacific and Canadian National Railways. Some development has taken place in two underground workings and on one surface strip. The bed is horizontal and appears to be remarkably uniform in thickness. This is particularly well observed on the two edges of a wide ravine that has been eroded through this area. The bentonite occurs in several beds interspersed with layers of shale. The total thickness of the bentonitic material is about three feet. The amount of overburden varies greatly, but a large area is so placed as to make stripping operations quite feasible. Unofficial estimates of available tonnage, made by mining authorities, give the figure at about 6000 tons of recoverable bentonite per acre. The bentonite is cream-colored to yellow and contains considerable moisture, which however it loses rapidly on exposure.

The analyses of three samples taken independently from various portions of the deposit show the following: SiO_2, 51.6, 51.2, 49.8%; Al_2O_3, 24.2, 24.0, 23.9%; MgO, 0.3, 0.3, 0.8%; CaO, 0.5, 0.6, 0.8%; Fe_2O_3, traces; loss at 120° C., 7.8%; total loss on ignition, 23.6, 23.9, 24.3%. These show a silica to alumina ratio of 2.13, 2.13, and 2.09 as compared with ratios of about 2.3 for Wyoming bentonite, Montmorillonite, and Pyrophyllite. Spence (1) obtained an average ratio of about 3.4 for 15 bentonitic clays; the lowest ratios being 2.23 and 2.27 for Death Valley and Wyoming bentonites respectively. In none of these instances however does the amount

of combined water approach that in the Morden bentonite, and this may be of great significance in relation to adsorbent power.

A typical fuller's earth widely used industrially in the bleaching of fatty oils showed the following: SiO_2, 53.7%; Al_2O_3, 15.6%; MgO, 3.5%; CaO, 4%; Fe_2O_3, 6.5%; loss at 120° C., 8.3%; total loss on ignition 15.5%. It is important to note that fuller's earth contains very much less combined water than the bentonite.

Morden bentonite is activated by relatively low proportions of sulphuric acid. When a volume of acid solution two and one-half times the weight of the bentonite is used, optimum results are obtained with 50% of sulphuric acid based on the weight of bentonite. If the volume of acid solution is materially reduced, the amount of sulphuric acid can be reduced to about 35%. The activated clay can be filtered and washed readily, and after drying is so soft that it may be disintegrated by hand rubbing. The hardness of water used in washing this treated bentonite does not appear to affect the bleaching qualities. The amounts of lime and magnesia present are so low as to obviate any necessity for pretreatment with brine to effect a base exchange and to ensure a minimum of insoluble sulphates.

CLAY LEGEND

Clay No.	Source	Clay No.	Source
1	Utah	17, 17a	Saskatchewan
2a	California	18, 18a	Saskatchewan
3, 3a	Morden, Man.	19, 19a	Saskatchewan
4, 4a	Alberta	20, 20a	Saskatchewan
5	Alberta	21, 21a	Saskatchewan
6	Alberta	22	Ontario
7	Alberta	23	Great Britain
8	Alberta	24	Ontario
9, 9a	British Columbia	25	Saskatchewan
10	Alberta	26	Saskatchewan
11	Alberta	27	Georgia
12	Alberta	28	Saskatchewan
13	Alberta	29	New Brunswick
14	British Columbia	30a	France
15, 15a	Saskatchewan	31a	Germany
16, 16a	Saskatchewan	32	British Columbia

NOTE:—*a* = *activated.*

Lubricating Oil Distillates

The elimination of certain undesirable constituents from lubricating oil distillates is generally carried out by treatment either with sulphuric acid or one of a number of selective solvents. Sulphuric acid brings about the polymerization of unsaturated constituents followed by a partial coagulation of these polymers to an acid sludge. An appreciable amount of acid remains suspended in the treated oil together with some of the chemically attacked constituents in colloidal dispersion. If water alone is then used, exhaustive

washing is necessary to remove the residual acid, and no effect is obtained with respect to the colloidally dispersed polymers. Neutralization with alkali is also ineffective in this regard, with the added disadvantage of the liability of emulsion formation. The use of an efficient adsorptive clay, however, results not only in the adsorption and removal of the colloidally dissolved undesirable constituents but also in the total removal of mineral acid.

In recent years a number of solvents have been shown to possess more or less sharply defined preferential solvent power for the undesirable components of lubricating distillates, and lubricating oils treated by this means have recently attained considerable industrial importance. Selective solvent treatment of the distillates always lessens and in some cases eliminates entirely the need for acid treatment, and thus effects also a decrease in the amount of adsorptive finishing agents. Bleaching clays, however, are commonly used in the processing of this class of oils also.

Two methods have been employed in conjunction with the use of adsorbent clays. The older is the percolation method in which, as the name implies, the distillate is percolated by various means through a column of the adsorbent. The method is obviously slow, it entails a serious loss of oil through adsorption, and can be used only in the case of an adsorbent earth that retains a comparatively coarse particle size. The contact method is of considerably greater importance. In this method, the distillate is intimately mixed with a comparatively small amount of adsorbent, and the mixture is heated for a few minutes, following which the finished oil is separated in a filter press.

The amount of clay used varies with the type of oil being processed, with the efficiency of the clay, and with the characteristics desired in the finished oil, but ranges generally from about 3 to 8%. The temperature and time of contact varies also over a considerable range. A highly active and efficient clay is desirable, since filter cake losses of oil are considerably reduced.

Procedure (Distillates 1–6)

For the present purpose, six representative lubricating oil distillates of varying S.A.E. ratings were chosen. Of these, Distillates 1 and 2 were solvent treated oils and were treated with clay directly. The other four distillates were acid treated before being finished with clay. Since a "sour" or acid treated oil is unstable and chemical changes are continuously apparent in it, these four distillates were acid treated in larger batches, and portions of the sour oil subjected to clay treatment on the same day. In this way any error due to slight variation in the effect of the acid was obviated in any of the series.

The clay contacting was carried out as follows. The distillate (400 cc.) was thoroughly mixed with the amount of clay shown in the tables and the mixture poured into a one litre, three necked flask, to which were fitted a constant speed stirrer, carbon dioxide inlet tube, and thermometer. The flask was then immersed in a thermostat to a standard depth above the level of the mixture in the flask. The contents was stirred, an atmosphere of

carbon dioxide being maintained in the flask until the temperature noted in the tables was reached. Then the flask was removed and the oil filtered.

The contact temperatures used in these tests were all much lower than those employed in current refinery practice, and it is well known that the sorptive power varies greatly with the temperature. The efficiencies at various temperatures, as determined on two of the lubricating distillates, indicates, however, the order of results which may be expected at the higher temperatures.

Color was determined by means of an optical head from a Dubosc colorimeter in conjunction with two 20 in. tubes, one fitted with a tap near the bottom. The depth of the standard was maintained the same and the depth of the unknown changed by gradually removing oil through the side tube and tap.

Efficiency. One adsorbent clay, imported from the United States and of considerable industrial importance, was chosen as standard, and the results obtained with other clays were expressed in terms relative to those obtained with this standard Clay 1. Experiments on the same oil with varying amounts of clay showed that straight lines were obtained when the color number (depth of oil in the colorimeter) was plotted against the percentage of clay used. The oil obtained by refining with Clay 1 was used in each series as the color standard. Hence the relative merit of a clay may be read graphically (Figs. 1 to 6) by simple comparison of the abscissa value of the point of intersection of the line with any chosen value for the color number.

The term "efficiency" as used in these series represents the bleaching power of the adsorbent as compared with the Standard Clay 1, which is represented as having an efficiency equal to 1.0 in each series. For example, an efficiency of 3.0 means that one pound of the clay in question is as effective as three pounds of the standard clay.

Color. The method of color measurement described above was adopted in order to provide an accurate means of comparison of the relative bleaching powers of the clays. In order to relate these to the standard industrial colorimeter, color values are reported also in a number of instances as determined in the Tag-Robinson colorimeter.

It will be noted that the correlation between the efficiency ratings made and those which might be assumed from the Tag-Robinson readings, although in nearly all cases in the same order, is in several instances not as close as might be expected. The color readings made in the special colorimeter are undoubtedly more accurate, but even after this is taken into consideration, several unexplained discrepancies remain.

Lubricating Distillate 1

This distillate is a solvent treated one and no acid treatment was carried out.

The experiments carried out with Clays 2 and 3 show that very satisfactory checks in the efficiency values are obtained at different levels of clay concentration. It is interesting to note that the efficiencies range from 0.2 to

TABLE I

EFFICIENCIES OF CLAYS ON DISTILLATE No. 1

Thermostat temp., 120° C.; maximum contact temp., 105° C.

Clay No.	Clay, %	Color No.	Efficiency	Tag-Robinson color	Clay No.	Clay, %	Color No.	Efficiency	Tag-Robinson color
1	1	3.8	1.0		4	4	7.5	0.8	
1	2	5.6	1.0		4a	4	33.8	4.4	18
1	4	9.4	1.0		5	4	3.2	0.2	
1	6	13.6	1.0	$17\frac{1}{4}+$	6	4	10.0	1.1	
1	8	16.4	1.0		7	4	10.6	1.2	
1	10	19.7	1.0		8	4	7.0	0.8	
2a	2	20.0	5.0	$17\frac{1}{4}+$	9	4	8.5	0.9	
2a	4	36.0	4.7		9a	4	23.5	3.0	
3	1	8.2	3.4		10a	4	30.8	4.0	
3	2	13.8	3.3	$17\frac{1}{4}+$	11	4	7.8	0.8	
3	4	25.0	3.2		12	4	8.7	0.9	
3a₁	2	24.4	6.2		13	4	5.8	0.5	
3a₂	2	25.4	6.4		14	4	6.7	0.6	
3a₃	2	31.5	8.1						

NOTE:—"*a*" *denotes activated;* "*a₁, a₂,*" *etc., activated under different conditions.*

8.1 in this series. By far the most efficient clay of this series is Clay 3, which in the unactivated state shows the extremely high figure of 3.3. In addition to this great activity in the crude state, the efficiency is raised to 8.1 by activation, 65% greater than that of Clay 2a, which is the best of the industrially important earths examined during this investigation, and which may be regarded as a standard activated clay.

In order to determine the effect of temperature on the bleaching efficiency of clays, further experiments were carried out at varying temperatures, all other conditions being maintained the same.

TABLE II

EFFECT OF TEMPERATURE ON BLEACHING EFFICIENCY

DISTILLATE 1

Clay No.	Clay, %	Color No. at max. contact temp.			Efficiency at max. contact temp.		
		105° C.	149° C.	188° C.	105° C.	149° C.	188° C.
1	4	9.4	27.6	24.1	1.00	3.50	3.06
3	4	25.0	42.8	32.6	3.30	5.62	4.15
3a	4	61.5	74.6	80.6	8.10	9.80	10.80
9	4	8.5	21.7	18.6	0.90	2.75	2.30
9a	4	23.5	25.8	20.8	3.00	3.25	2.61
4	4	7.5	14.8	14.5	0.80	1.76	1.73
4a	4	33.8	34.5	16.5	4.40	4.43	2.00

It is noted that there is an optimum temperature of treatment for a contact clay above which its decolorizing capacity decreases. The optimum temperature of contact for the highly efficient Clay 3a is not yet reached at 188° C.,

which is close to the flash point of this light distillate.   The figures in Table II for the efficiencies are all based on the results obtained at 105° C. with Standard Clay 1.

Fig. 1 shows the relation between color number and clay concentration at 105° C.
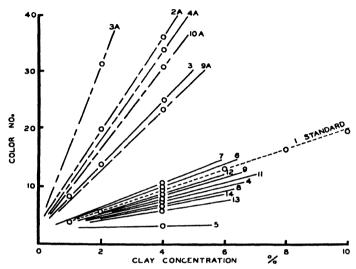
FIG. 1.   *Efficiency of clays on Lubricating Distillate 1 (solvent treated)*

TABLE III

ANALYSIS OF SOME FINISHED OILS FROM DISTILLATE 1

Clay No.	Clay, %	S.E. No.	Sp. gr. 60°/60° F.	Before oxidation		After oxidation		Coke No. diff.	Visc.-ox. ratio
				Visc. at 100° F.	Coke No.	Visc. at 100° F.	Coke No.		
1	1	57	0.888	248	0.06	385	0.61	0.55	1.56
1	2	58	0.888	245	0.08	276	0.17	0.09	1.12
1	4	54	0.888	249	0.09	287	0.20	0.11	1.17
1	6	57	0.887	247	0.07	294	0.16	0.09	1.19
1	8	58	0.887 ·	247	0.07	290	0.17	0.10	1.18
1	10	62	0.888	247	0.05	361	0.33	0.28	1.46*
2a	2	41	0.888	247	0.05	310	0.25	0.20	1.25
2a	4	46	0.888	247	0.07	300	0.17	0.10	1.21
10	4	58	0.887	247	0.05	326	0.32	0.27	1.32
8	4	56	0.887	247	0.14	303	0.23	0.09	1.23
3	4	56	0.888	247	0.17	307	0.21	0.04	1.24
3	2	55	0.888	247	0.04	320	0.28	0.24	1.29
4a	4	57	0.887	247	0.15	288	0.32	0.17	1.17
9a	4	55	0.887	247	0.17	276	0.26	0.09	1.12
3	1	58	0.888	247	0.03	293	0.21	0.18	1.19
3a₁	2	53	0.888	247	0.07	297	0.40	0.33	1.20
3a₂	1	62	. 0.888	247	0.15	301	0.30	0.15	1.22

* *This oil underwent a longer period of oxidation, hence the higher viscosity-oxidation ratio.*

A partial analysis of the refined oils obtained with different clays on Distillate 1 is shown in Table III. The oxidation resistance and coke number tests were carried out according to British Air Ministry General Specification Number D.T.D. 109 for Mineral Lubricating Oils, except that six hours' oxidation was used. The steam emulsification number was obtained by the standard A.S.T.M. method.

It is noted that only with Clay 1, of comparatively low efficiency, when used in the concentration of only 1%, is there obtained a relatively higher viscosity-oxidation ratio or lower resistance to oxidation. The coke number difference is also the highest in this instance.

Lubricating Distillate 2

This distillate is a solvent treated one and no acid treatment was carried out.

TABLE IV

EFFICIENCIES OF CLAYS ON DISTILLATE 2

Thermostat temp., 200° C.; maximum contact temp., 175° C.

Clay No.	Clay, %	Color No.	Efficiency	Clay No.	Clay, %	Color No.	Efficiency
1	2	18.0	1.0	3a₂	1	19.5	2.8
1	4	22.2	1.0	3a₂	2	25.4	2.9
1	6	26.0	1.0	4	4	18.8	0.63
1	10	33.9	1.0	4a	2	19.6	1.42
2a	2	20.5	1.65	6	4	16.9	0.38
2a	2	20.6	1.68	7	4	23.0	1.12
2a	4	28.7	1.83	9	4	22.7	1.10
3	1	16.4	1.25	9a	2	20.2	1.58
3	2	18.9	1.25	10a	4	25.9	1.50
3	4	23.7	1.22				

The most efficient clay in this series is again Clay 3, both in the crude and activated states. Very good checks were obtained on several clays at different concentration levels. Clay 3a is 65% more efficient than Clay 2a. This same relation was obtained on Distillate 1. Distillate 2 is a very heavy one corresponding to about S.A.E. 60, and hence generally lower values are found for the efficiencies, as compared with those for Distillate 1, corresponding to about S.A.E. 10.

Table V shows the results obtained in refining Distillate 2 at various temperatures, all other conditions being the same.

TABLE V

EFFECT OF TEMPERATURE ON BLEACHING EFFICIENCY DISTILLATE 2

Clay No.	Efficiency at max. contact temp.		
	175° C.	232° C.	274° C.
1	1.0	1.70	1.50
3	1.25	2.04	2.38
3a	2.85	4.40	3.80
9	1.10	0.94	0.96
9a	1.58	1.38	1.36
4	0.63	0.75	0.70
4a	1.42	1.36	1.33

In the case of Clay 3, the optimum temperature of contact has not been reached at 274° C. The efficiencies are based on the results obtained at 175° C. with Standard Clay 1.

Fig. 2 shows the relation between color number and clay concentration at 175° C.
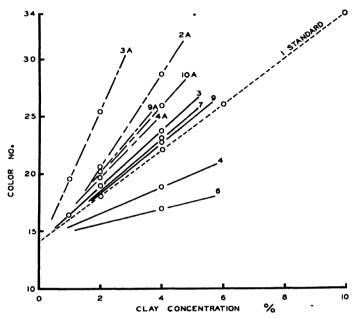
FIG. 2.　*Efficiency of clays on Lubricating Distillate 2 (solvent treated).*

Table VI shows a partial analysis of the refined oils obtained with different clays on Distillate 2. The oxidation was carried out for 12 hr. according to the specification noted above.

TABLE VI

ANALYSIS OF SOME FINISHED OILS FROM DISTILLATE 2

Clay No.	Clay, %	S.E. No.	Before oxidation		After oxidation		Coke No. diff.	Visc.-ox. ratio
			Visc. at 100° F.	Coke No.	Visc. at 100° F.	Coke No.		
1	10	225	2276	0.41	2454	0.80	0.39	1.08
1	6	230	2252	0.54	2489	1.10	0.56	1.10
3a	1	229	2259	0.46	2498	1.02	0.56	1.10
3a	2	224	2267	0.47	—	—	—	—
2a	4	223	2229	0.53	—	—	—	—
3	4	217	2271	0.70	—	—	—	—
3	2	216	2245	0.56	2477	1.05	0.49	1.10
9	4	223	2250	0.55	2805	1.21	0.66	1.23
7	4	221	2246	0.57	2624	1.25	0.68	1.17

NOTE:—*Oxidation test—British Admiralty Test D.T.D. 109, 12 hr.*

Lubricating Distillate 3

For each of Distillates 3 to 6, a number of preliminary experiments were performed in acid treating, in order to determine the optimum time of treatment and time and speed of centrifuging.

Several batches of 2500 cc. of Distillate 3 were vigorously stirred with 50 gm. of concentrated sulphuric acid, and treatment was maintained at room temperature for 30 min. The oil was then centrifuged at 2000 r.p.m. for 15 min. The supernatant oils from all batches were mixed to form one stock for clay treatment.

TABLE VII

EFFICIENCIES OF CLAYS ON DISTILLATE 3

Thermostat temp., 120° C.; Maximum contact temp., 105° C.

Clay No.	Clay, %	Color No.	Effi- ciency	Tag- Robinson color	Clay No.	Clay, %	Color No.	Effi- ciency	Tag- Robinson color
1	1	20.5	1.0		3a	2	40.6	4.12	14¼
1	2	22.4	1.0		4	4	29.9	1.11	
1	4	28.7	1.0	14¼	4a	2	35.4	3.20	
1	8	40.0	1.0		6	4	29.6	1.09	
2a	2	37.5	3.58	13¼	7	4	31.6	1.26	
3	2	32.3	2.55		9	4	31.1	1.22	
3	4	46.5	2.58	15½	9a	2	35.0	3.12	
3a	1	29.4	4.25						

Clay 3 and its activated form are outstanding in the efficiencies afforded in the refining of this light distillate. Some representative analyses are shown in Table VIII. The oxidations were carried out for six hours only.

TABLE VIII

ANALYSES OF SOME FINISHED OILS FROM DISTILLATE 3

Clay No.	Clay, %	S.E. No.	Before oxidation		After oxidation		Coke No. diff.	Visc.-ox. ratio
			Visc. at 100° F.	Coke No.	Visc. at 100° F.	Coke No.		
3a	1	38	104	0.09	112	0.17	0.08	1.08
2a	2	39	105	0.10	111	0.21	0.11	1.06
9	4	38	105	0.08	112	0.17	0.09	1.07
4	4	39	104	0.08	111	0.21	0.13	1.07
1	4	40	105	0.09	112	0.29	0.20	1.07
3	4	41	104	0.08	112	0.22	0.14	1.08

NOTE:—*Oxidation test—British Admiralty Test D.T.D. 109, 6 hr.*

These analyses show practically no differences among these oils beyond experimental error.
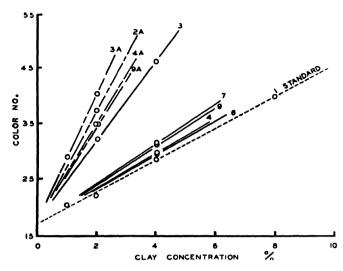
FIG. 3.   *Efficiency of clays on Lubricating Distillate 3.*

Lubricating Distillate 4

Several batches of 2500 cc. of the distillate were stirred vigorously with 100 gm. of concentrated sulphuric acid, and the treatment was maintained at room temperature for 25 min.   The sludge settled well and treatment with water was found unnecessary.   The mixtures were centrifuged at 2000 r.p.m. for 15 min. after an initial short settling period.   The centrifuged oils were then mixed to provide a uniform stock for clay treatment.

TABLE IX
EFFICIENCIES OF CLAYS ON DISTILLATE 4
Thermostat temp., 190° C.; maximum contact temp., 175° C.

Clay No.	Clay, %	Color No.	Effi- ciency	Tag- Robinson color	Clay No.	Clay, %	Color No.	Effi- ciency	Tag- Robinson color
1	2	25.1	1.0		3a	2	38.0	4.40	9¼
1	6	32.8	1.0	9¼	3a	6	69.6	4.25	
1	10	40.0	1.0		4	4	24.0	0.41	
3	2	25.9	1.35		4a	4	42.3	2.78	
3	6	37.8	1.46	9¼	9	6	36.0	1.31	9+
3a	0.5	24.6	3.80	8¾+	9a	4	43.9	3.00	

The highest efficiencies are shown by Clays 3 and 3a, for crude and activated earths respectively.   Some analyses are given in Table X, the oxidation period being 12 hr.

TABLE X
ANALYSES OF SOME FINISHED OILS FROM DISTILLATE 4

Clay No.	Clay, %	S.E. No.	Before oxidation		After oxidation		Coke No. diff.	Visc.-ox. ratio
			Visc. at 100° F.	Coke No.	Visc. at 100° F.	Coke No.		
1	6	79	414	0.19	421	0.31	0.12	1.02
3	4	79	401	0.19	422	0.38	0.19	1.05
9	6	79	408	0.19	418	0.32	0.13	1.02
4	4	79	403	0.21	416	0.31	0.10	1.03
9a	4	79	418	0.18	428	0.32	0.14	1.02
3a	2	79	400	0.18	415	0.24	0.06	1.01

NOTE:—*British Admiralty Test D.T.D. 109, 6 hr.*

Practically no differences are found among these oils refined to varying color values by these clays.
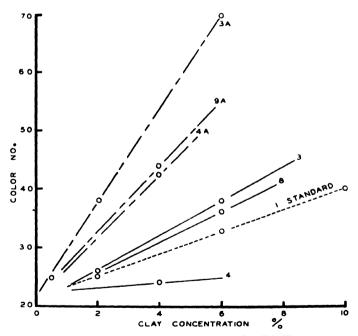
FIG. 4. *Efficiency of clays on Lubricating Distillate 4.*

Lubricating Distillate 5

This was a light distillate of viscosity corresponding to about S.A.E. 10. Batches of 2500 cc. were stirred vigorously with 50 gm. of concentrated sulphuric acid and treated for 15 min. Good coalescence of the sludge particles was obtained. The acid-treated oils were centrifuged at 2000 r.p.m. for 15 min. and the stocks mixed.

TABLE XI

Efficiencies of Clays on Distillate 5

Thermostat temp., 120° C.; maximum contact temp., 105° C.

Clay No.	Clay, %	Color No.	Effi- ciency	Tag- Robinson color	Clay No.	Clay, %	Color No.	Effi- ciency	Tag- Robinson color
1	2	25.1	1.0		3a	2	30.4	3.53	18¼
1	6	30.0	1.0	18¼	3a	6	43.4	3.46	
1	10	33.1	1.0		4	4	24.4	0.35	
3	1	24.6	1.50		4a	4	30.7	1.81	
3	2	26.5	1.65		9	4	30.2	1.71	18¼+
3	6	32.9	1.60	18½	9a	4	32.0	2.16	

The order of efficiencies of the clays on this very light lubricating distillate was similar to that obtained in other series, Clays 3 and *3a* being the best.
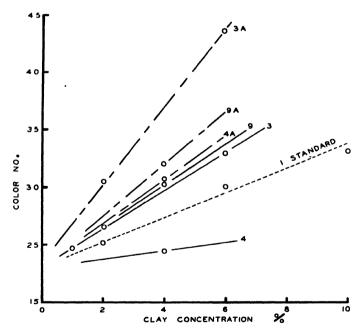
FIG. 5.   *Efficiency of clays on Lubricating Distillate 5.*

Lubricating Distillate 6

This distillate was the heaviest of this series, S.A.E. about 60 to 70, and the viscosity of the oil was found to render efficient stirring at room temperature impossible. Centrifuging was found ineffective in settling the sludge in the acid treated oil without further treatment. The procedure finally adopted was as follows: batches of 2500 cc. of the distillate were treated with 100 gm. of concentrated sulphuric acid, and the mixture was stirred

vigorously for 30 min., the temperature being maintained at 50° C. After 20 min. of treatment, 25 cc. of water was added to each batch; this resulted in a good coalescence of the colloidally dispersed acid sludge. After centrifuging at 2000 r.p.m. for 15 min., the centrifuged stocks were mixed.

TABLE XII

EFFICIENCIES OF CLAYS ON DISTILLATE 6

Clay No.	Clay, %	Color No.	Effi- ciency	Tag- Robinson color	Clay No.	Clay, %	Color No.	Effi- ciency	Tag- Robinson color
1	4	24.9	1.0		3a	6	72.0	3.75	
1	6	30.0	1.0	8¾+	4	6	19.8	0.35	
3	4	28.3	1.37		4a	4	36.0	2.07	
3	6	36.0	1.37	9	9	6	27.3	0.83	
3a	4	53.1	3.75	9¼	9a	4	32.5	1.77	

Clay 3 and its activated form are the most efficient of the crude and activated clays, respectively, in this series.
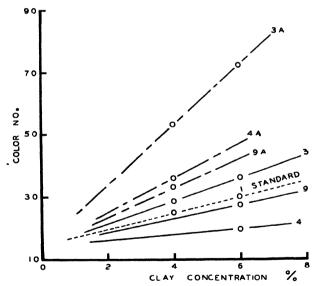
FIG. 6. *Efficiency of clays on Lubricating Distillate 6.*

Lubricating Distillate 7

This is a solvent treated distillate corresponding to about S.A.E. 30 in viscosity, and was adopted in later work as the standard unfinished oil for the preliminary testing of an unknown bleaching clay. The contact procedure used in connection with this distillate was that used by the laboratories of a Canadian oil refining company. To 300 gm. of the distillate in a standard

beaker was added 6% of the clay, and the mixture was thoroughly agitated. Then the temperature was raised to 149° C. over a period of 15 min. by direct heat, with agitation at a standard rate. The oil was then filtered and the color measured in the Tag-Robinson colorimeter.

Clays 15 to 21 were received from the Department of Ceramic Engineering, University of Saskatchewan, for test as to possibilities as bleaching clays. These materials were activated under different conditions and tested on Distillate 7, the above refining procedure being followed. The color shown last in each horizontal series is the maximum bleaching effect obtained. Results with Clays 2a and 3a are shown in comparison.

TABLE XIII
DECOLORIZING POWER OF SOME SASKATCHEWAN CLAYS

Activated clay No.	Clay, %	Tag-Robinson colors				Activated clay No.	Clay, %	Tag-Robinson colors			
15	6	16½	16¼+	16¼+	16¼+	21	6	17+	17¾	18¼+	18¼+
16	6	16½+	16¾+	16¼+	16¼+						
17	6	16½+	16¼+	16¾+	16¼+	2	2				16¾
18	6	16¾+	17	17	17¼	2	6				18
19	6		17	17¼	17¼+	3	6				18¼+
20	6	16¾	17½	17¼	17¼+						

These clays are the most important in a series investigated by Worcester (3) during the course of this work, and since that time described by him also elsewhere (4). His results show that all these clays when activated, with the exception of Clay 19, are superior in bleaching power to the standard imported Clay 2a. In his tests, the standard oil was a used crank-case oil, whereas, as is shown in a later section of this work, results obtained on used crank-case oil do not necessarily represent efficiencies on new distillates. Furthermore, the concentration of clay was 20%, very much higher than any level industrially feasible.

It will be noted from the figures of maximum color removal (highest Tag-Robinson color values), that in only one case, viz., Clay 21a, are the results superior to those obtained with the standard activated Clay 2a. Clay 21a is approximately equal in efficiency on Distillate 7 to Clay 3a, which was found to possess unusually high bleaching power on all the other lubricating distillates examined. It is to be noted (4), however, that Clay 21 has been found thus far in a bed which at the point of sampling was only 18 in. thick.

Cracked Motor Fuel Distillates

Three general methods are used in the clay treatment of cracked motor fuel distillates, viz., (a) contact method, (b) vapor phase percolation, (c) continuous countercurrent method.

(a) Contact Method

This method is similar to that already described for lubricating oil distillates and involves the agitation of the cracked distillate with clay, followed by

filtration.   The method is of little importance in Canadian refineries, and was not used in the present investigation.

(b) Vapor-phase Percolation

This method is widely used in units commonly termed Gray Towers, designed and marketed by the Gray Processes Corporation.   In these towers, cracked distillate is percolated through a column of refining clay, which exerts a polymerizing action on the unsaturated components.   The polymers formed are returned to the re-run still or the cracking plant for further processing, and the refined distillate is condensed.   The Gray Tower may consist of two shells, wherein the vapors ascend the outer shell of the tower and then percolate downwards through the clay supported in the inner shell by a perforated plate surmounted by a fine mesh screen, generally of spiral weave monel metal.   The temperature of the clay is maintained by the ascending vapors around the inner shell.   In another type, the tower consists of a single well-lagged shell containing the clay, and the vapors pass directly through the clay.   In this case, the small amount of condensate serves to dilute the rather viscous polymers and render them more readily removable from the clay.   The clay used is commonly 30 to 60 mesh in size, and the working pressure in the tower is usually from 50 to 60 lb., although pressures as high as 225 lb. have been used.

For the laboratory testing of refining clays by the vapor-phase percolation method, the apparatus shown in Fig. 7 was used.   *A* is a well-lagged steel still-pot, fitted with rounded bottom, drain valve, opening for filling with

FIG. 7.   *Laboratory apparatus for the refining of cracked distillate.*

crude distillate, and union connection to the model Gray Tower B. The contents of A are heated electrically by outside heating coils, and the heat is controlled by rheostats and ammeter. The treating tower, B, with lagged cover, C, dismantled, is shown in detailed cross section in Fig. 8. D is the condenser for the refined distillate, and at E is shown the outlet for the polymers formed. F (Fig. 7) is the Saybolt chromometer used in color measurement of the refined distillates.
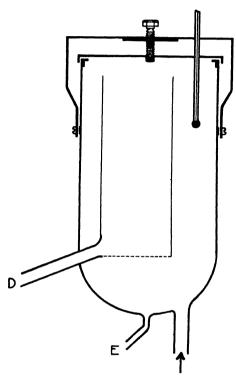
FIG. 8.   *Diagram of model Gray Tower (B in Fig. 7).*

The refining clays used industrially in Gray Tower units are of the fuller's earth type, and the screen size is carefully controlled, generally 30 to 60 mesh and largely 40 to 50 mesh. There is no disintegration of the clay during use and revivification. Several trial runs were made in the apparatus shown, a fuller's earth that is standard for this purpose being used, and excellent bleaching capacities were obtained. A large number of trials were made with a variety of bentonitic clays such as used in the previous section on lubricating distillates, but in all cases a lesser bleaching capacity was obtained. It was noted that with all bentonites, although introduced in 30 to 60 mesh size, the refining was very slow, and it is probable that the lengthy contact with these active materials caused further chemical changes in the lowest part of the tower. Examination of the clay charge after a run showed a disintegration and packing in the bentonites which caused excess pressure in the tower. It was concluded therefore that the bentonitic type of clays is not suitable for use in the vapor-phase percolation process.

(c) Continuous Countercurrent Method

This method of clay treatment of cracked distillates, introduced comparatively recently and of great importance in Canadian oil refineries, has been fully described elsewhere (2). In this process the pressure distillate, after a lye wash to remove hydrogen sulphide, is fed to a still and from there to the clay treating tower. The latter is a conventional bubble-tower, fed at the top by a heavy slurry of clay in a finished naphtha. The ascending vapors of crude distillate pass through the clay slurry and are condensed, the

spent slurry overflowing from a weir on each plate to a settling chamber. The refining process is continuous. The polymers formed during the process are adsorbed by the refining clay.

A laboratory method used for testing a refining clay to serve in the above process was developed in the laboratories of Imperial Oil Limited, Sarnia, Ont. It yields results that may be interpreted in terms of industrial scale refining.* This laboratory procedure was used in the present work. The raw distillate was first thoroughly shaken with 15 Bé. sodium hydroxide solution (20 cc. per 500 cc. distillate), separated, and thoroughly washed three times with water. It was then filtered through several thicknesses of filter paper to remove the last traces of moisture. From 500 cc. of this washed distillate in a 500 cc. distilling flask there was then distilled (A.S.T.M. apparatus) 425 cc. with an end point of 185° C. For the clay treatment, 140 cc. of the last-named distillate was thoroughly mixed with 1% of clay, placed in a Vigreux flask of special design, and distilled until 118 cc. was recovered. The finished distillate was then filtered to remove the last traces of moisture and the color was read on a Saybolt chromometer with enclosed illumination. The raw distillate used had an initial b.p. of 38° C., and an end b.p. of 193° C.

TABLE XIV
CLAY TREATMENT OF CRACKED DISTILLATES

Clay No.	Clay, %	Color	Color drop after storage	Clay No.	Clay, %	Color	Color drop after storage
1	1	+30	8	1	1	+30	10
3	1	+30	10	3	1	+30	9
3a	1	+30	0	4	1	+19	0
1	1	+29	10	1	1	+29	12
9	1	+25	6	13	1	+17	0
9a	1	+26	1	22	1	+18	0
1	1	+29	11	1	½	+27	14
4	1	+19	0	3	½	+29	14
14	1	+21	0	7	1	+26	13

Table XIV shows the results obtained in some of the refining experiments. The color measuring instrument reads to a maximum value of +30, and superior colors are noted by this same figure. The refined distillates were allowed to stand for about 10 weeks in the dark at room temperature, following which the colors were measured again. The last column of Table XIV shows the color drop, *i.e.*, the increase of color during this period. Sufficient distillate was obtained in the first distillation for three second distillations on the same day. One of these three on each day was a distillation over Clay 1, which was used as a standard.

The only clay of this series equal to the standard in decolorizing efficiency is Clay 3 and its activated form. From the refining experiments where only

*A modification of this method is now employed as a routine test method in the laboratories of Imperial Oil Limited.

½% of clay was used, it would appear that Clay 3 is somewhat more efficient than Clay 1. The results obtained after storage show, as might be expected, that the gasolines with poor original color have a low color drop, in some cases nil or even some little improvement. The cases of Clays 3a and 9a are of importance, since they show that the action of an activated clay with some residual acid yields a more stable gasoline than does a crude clay in so far as is shown by color hold. No gum tests were carried out, and no appreciable development of odor was noted during storage.

Soap and Packing House Oils and Fats

A number of bleaching clays were tested with regard to their activity in the bleaching of animal and vegetable oils used for edible and soap purposes. Some of the oils had been alkali refined before the tests were made, other oils used were samples of type oils that had not been alkali refined. The standard clay for comparison in these tests was an industrially important fuller's earth (Clay 23) commonly used in the soap and packing house industries. No activated carbons were used in conjunction with the clays.

The apparatus and method used conformed with the specifications of the American Oil Chemists Society, the oil-clay standard stirrer being driven at 250 r.p.m. A thermostat was used to control the heating in all cases. Color measurements were made in a Lovibond tintometer with enclosed illumination, a 5¼ in. silvered cell being used.

The bleaching time was 5 min. in all cases (Tables XV to XX). Determinations of free fatty acid (F.F.A.) were made according to the standard method of the American Oil Chemists Society and are expressed as oleic acid.

Prime Steam Lard

TABLE XV
BLEACHING OF PRIME STEAM LARD
Alkali refined; bleaching temp. 69° C.

Clay No.	Clay, %	Color			F.F.A., %
		Red	Yellow	Blue	
23 (Standard)	1	3.3	0.3	0.7	
23	½	5.2	0 3	1.7	0.59
3	1	1.1	0.1	0.0	
3	½	2.7	0.2	0.0	
9	1	2.7	0.1	0.0	
3a	¼	2.2	0.3	0.0	0.55
5	1	5.5	4.0	5.4	
11	1	6.4	2.0	2.3	
6	1	6.1	2.0	2.6	
4	1	9.0	2.0	2.1	
24	1	3.9	0.8	0.8	
Unbleached					0.57

Clay 3 possesses an efficiency several times that of the Standard Clay 23, and in the activated form produces an excellent bleach at the low concentration of ¼%. No excess acidity is afforded by the activated clay at this concentration.

Beef Tallow

TABLE XVI

BLEACHING OF BEEF TALLOW

Alkali refined; bleaching temp. 82° C.

Clay No.	Clay, %	Color		Clay No.	Clay, %	Color	
		Red	Yellow			Red	Yellow
23 (Standard)	1	+30	1.0	3	½	13.4	1.0
23	3	15.0	0.8	4	1	2.6	3.2
3a	1	1.6	0.1	9	1	+30	1.0
3a	½	+30	1.0	9	3	12.4	0.8
3	1	5.8	0.4	5	3	+30	2.4

During the progress of this work, yellow Lovibond glasses of values 30 to 50 were not available, hence all colors over 29.9 are recorded as +30.

Clay 3 has an extraordinarily high bleaching efficiency in comparison with the standard clay. Although the amount of clay generally used with beef tallow is low, concentrations as high as 3% were used to bring the color within a measurable range. Clay 3a, at a concentration of 1%, bleaches the oil almost water white.

Cottonseed Oil

This oil is the most important industrially of this series, and two series of bleach tests were carried out on alkali refined oils obtained from two sources.

TABLE XVII

BLEACHING OF COTTONSEED OILS

Both oils alkali refined; bleaching temp., 120° C.

Clay No.	Clay, %	Color, Oil No. 1		Color, Oil No. 2		F.F.A., %	
		Yellow	Red	Yellow	Red	Oil No. 1	Oil No. 2
23 (Std.)	6	25	2.0	23	2.4	0.07	0.08
3a	3	10	1.0	12	1.2	0.17	0.21
3a	2	16	1.3	18	1.4		
3a	1	26	2.4	24	2.5		
9	3	21	1.6	23	2.2	0.06	0.11
5	6	+30	3.0				
4	6	+30	3.0	+30	6.0		
6	6	+30	3.0	+30	4.0		
14	6	30	2.4				
22	6	+30	3.0	+30	6.0		
3	6	24	1.8	22	2.0	0.14	0.12

Clay 3a is shown to be about six times as efficient in bleaching action as the Standard Clay 23. Clay 3 possesses slightly greater bleaching power than the standard. Clay 9 was noted to be a slow filtering clay. The F.F.A. of oils bleached by Clays 3a and 3 are higher than the maximum allowable in commercial practice, but this factor can probably be greatly· reduced by pretreatment of the clay.

Peanut Oil

Two unbleached peanut oils were used in these tests. Peanut Oil 1 had been alkali refined and Peanut Oil 2 was a type oil which had not been alkali refined.

TABLE XVIII

Bleaching temp., 120° C.

Clay No.	Clay, %	Color, Oil No. 1		Color, Oil No. 2		F.F.A., %	
		Yellow	Red	Yellow	Red	Oil No. 1	Oil No. 2
23 (Std.)	6	8.2	1.1	16.0	2.0	0.04	0.76
3	6	8.2	1.1	8.4	1.3	0.14	0.86
3a	2	7.6	1.0	10.0	1.4	0.12	0.91
9	6	8.3	1.2	10.0	1.4	0.04	0.81
4	6	23.0	1.8	29.0	3.0		
12	6	12.0	1.3	16.0	2.1		
6	6	15.0	1.5				
11	6	14.0	1.4				
5	6	20.0	1.7				
14	6			15.0	2.0		

Clay 3 has about the same bleaching power as the standard on the alkali refined oil, and Clay 3a has a greater bleaching power than the standard when used at only one-third the concentration of the latter. The F.F.A. of the resultant oils are again higher than the maximum allowable. Clay 9 again shows good bleaching power but slow filtration. The F.F.A. with Clay 9 is low; the same was true with Cottonseed Oil 1.

A third series on peanut oil was carried out in an investigation of the merits of the Saskatchewan bentonitic clays referred to above. The clays were used in the unactivated state and fuller's earth (Clay 23) was used as standard; 6% clay was used in all cases.

TABLE XVIII (a)

BLEACHING OF PEANUT OIL BY SASKATCHEWAN CLAYS

Alkali refined; bleaching temp., 120° C.

Clay No.	Color		F.F.A., %
	Yellow	Red	
23 (Standard)	8.4	0.9	0.03
15	8.5	0.9	0.04
16	9.0	0.9	0.05
17	8.5	1.0	0.05
18	10.7	1.0	0.06
25	14.0	1.3	0.06
26	13.0	1.3	0.07
19	11.0	1.0	0.06
20	9.1	0.9	0.06
21	7.1	0.9	0.06
15+16+17 (Mixed)	8 7	0.9	
18+25+26 (Mixed)	12.6	1.1	

Several clays of this group show a bleaching power approximately equal to the standard, together with the important fact that the bleached oils are low in F.F.A. Since Clays 15, 16, 17, 18, 25, and 26 occur naturally in these groups, mixtures were also tested in the proportions in which they are found in the two deposits.

Coconut Oil

Clay 3 in the crude state possesses a bleaching power several times that of the stand-

ard. Clay *3a* yields a much better bleach than does Clay *2a*, an industrially important activated clay, and shows an unusually high decolorizing power on this oil.

Palm Oil

Clays 3 and *3a* are again shown to possess outstanding bleaching power on this highly colored oil.

Soybean Oil. The standard Clay 3, even at a concentration as high as 10%, produced an oil which was too highly colored for measurement. Six percent of Clay *3a* produced an oil that was slightly over 30 yellow and 3.3 red.

Speed of Filtration. This is an important characteristic of a clay from the point of view of industrial practice. The apparatus used to determine this efficiency was a single plate vertical press set in an electrically controlled thermo-

TABLE XIX

BLEACHING OF COCONUT OIL

Not alkali refined; bleaching temp., 120° C.

Clay No.	Clay, %	Color		F.F.A., %
		Yellow	Red	
23 (Standard)	6	11.0	2.0	4.60
3	6	3.7	0.6	4.80
3	6	3.4	0.7	
3a	2	5.4	0.9	5.09
2a	2	8.4	1.6	5.01
9	6	7.2	1.2	4.68
4	6	17.0	3.0	
5	6	16.3	3.0	

TABLE XX

BLEACHING OF PALM OIL

Not alkali refined; bleaching temp., 120° C.

Clay No.	Clay, %	Color		F.F.A., %
		Yellow	Red	
23 (Standard)	6	70	17	5.09
3	6	50	12	5.69
3a	6	24	44	5.69
9	6	62	15	5.64
4	6	75	18	
6	6	70	17	

stat. Pressure was applied through a reduction valve from a cylinder of nitrogen. A monel metal filter cloth was first tried but was discarded in favor of a standard cloth. Cottonseed oil (300 cc.) was thoroughly mixed with 6% of clay and a clay bed built up under 12 lb. pressure. Then the filtrate was recirculated through the clay bed at 24 lb. pressure and readings of the speed of filtration were made. Under these conditions, the speed of filtration of Clay 3 was 0.56 cc. per sec. as compared with 0.45 cc. per sec. for the standard fuller's earth (Clay 23).

Oil retention. The loss due to retention of the oil by the bleaching medium is an appreciable factor in commercial practice. The clay beds obtained in the previous section were extracted for several hours in a Sohxlet with ether and acetone. The oil retention of Clay 3 was found to be 35.8%, based on the weight of dry clay, as compared with a value of 56.6% found for the standard Clay 23.

Linseed Oil

After expression and removal from the meal residue, crude linseed oil is generally filtered and alkali refined. The refined oil is then treated with a decolorizing clay to yield the finished unbodied oil. A clay of the fuller's

earth type is commonly used in contact with the raw oil at an elevated temperature until a color of predetermined value is reached. The color is measured in the Lovibond tintometer. At the time of these measurements, no color glasses between 30 and 50 in the yellow were available, and therefore results are expressed in Table XXI as measured in a 1 cm. glass cell. Most of the yellow values are over 30, when measured with the $5\frac{1}{4}$ in. cell.

The amount of clay shown in Table XXI was heated with the oil in a thermostat to 82° C. for the time indicated. Vigorous stirring at a standard rate was used. The oil was filtered on a Büchner, and the color and other analytical determinations were made. The standard clay used (Clay 27) is an industrially important one for this purpose. The oil was a sample of alkali refined unbleached oil. The free fatty acid is expressed as oleic.

TABLE XXI

BLEACHING OF LINSEED OIL

Clay No.	Clay, %	Time of treatment, min.	Color (1 cm. cell)		F.F.A., %
			Yellow	Red	
27 (Standard)	3	30	26.5	1.5	0.57
27	3	60	25.0	2.0	
27	3	120	+30	0.9	
27	5	30	13	1.0	
27	5	60	9.1	1.0	
27	6	60	4.9	0.6	
27	10	60	2.3	0.3	
2a	6	60	2.6	0.5	
2a	10	60	2.3	0.3	
3	6	60	4.0	0.9	0.58
3	10	60	3.0	0.3	
3a	2.3	30	2.8	0.8	0.61
4	2.3	30	+30	2.1	
4a	2.3	30	20.9	0.9	0.61
5	2.3	30	+30	1.9	
6	2.3	30	+30	2.0	
7	2.3	30	+30	2.0	
8	2.3	30	+30	1.8	
9	2.3	30	23.9	2.0	
11	2.3	30	+30	2.0	
12	2.3	30	+30	3.0	
13	2.3	30	+30	2.1	
14	2.3	30	+30	1.7	
28	2.3	30	+30	1.9	
Unbleached					0.60

Among the unactivated earths, Clays 3 and 9 show somewhat greater bleaching powers than does the standard fuller's earth. With linseed oil, Clay 3a shows an extraordinary decolorizing efficiency, with consequent decrease in oil-absorption losses in the filter cake. Furthermore, with this activated clay an almost colorless oil is produced at a low level of clay concentration, and such oils are important industrially for special applications. The acidities of the finished oils are almost identical in those measured.

It was further noted that upon bodying some of these bleached oils at 600° F., the best color was obtained with the oil that had been bleached by Clay 3*a*; this shows that there is no reversion in color. The ash contents of these oils showed practically no difference from the ash content of the oil bleached by the standard clay.

Pilchard Oil

A sample of partly destearinated pilchard oil, with F.F.A. content of 0.53% expressed as oleic, was alkali refined with a slight excess of 19 Bé. sodium hydroxide. The foots were allowed to settle and the oil was clarified by centrifuging. The procedure used in bleaching was the same as that described for the soap and packing house oils. The bleaching temperature was 120° C. and the bleaching time five minutes. Owing to the unavailability of higher value yellow slides, color measurements were made in a 1 cm. glass cell in the Lovibond tintometer.

TABLE XXII

BLEACHING OF PILCHARD OIL

Clay No.	Clay, %	Color		Clay No.	Clay, %	Color	
		Yellow	Red			Yellow	Red
2*a*	2	2.2	0.0	6	6	5.3	0.3
2*a*	6	1.4	0.0	7	6	4.0	0.1
3	3	2.6	0.0	9	6	2.0	0.0
3	6	1.3	0.0	9*a*	6	1.1	0.0
3*a*	2	1.3	0.0	11	6	3.3	0.1
3*a*	6	0.4	0.0	14	6	2.3	0.0
4	6	5.3	0.5	29	6	5.0	0.1

Among the unactivated earths, Clay 3 shows the greatest bleaching power, with Clay 9 second. Clay 3*a* shows an unusually high efficiency, much greater than that of Clay 2*a*, a standard industrial activated clay. Clay 9*a* effects a good bleach, and it is important to note that the location of this clay is closest to that of the pilchard oil refining industry in Canada.

Reclamation of Used Oils

The efficiency of a number of these bentonitic clays in the treatment of used crank-case oils was investigated, and some analytical determinations were made on the recovered lubricants. The amount of clay necessary varies: (1) with the viscosity of the oil, heavier oils requiring larger amounts of clay; (2) with the cleanliness of oil, since the presence of coagulated grease and other foreign material increases the amount of clay that must be used; (3) with the color desired in the recovered oil; (4) with the adsorbent quality of the clay. The used oil is generally allowed to settle first and is drawn from the top of the container. The amount of activated clay employed ranges normally from 5 to 12%. The temperature maintained for clay treatment is generally in

the region of the flash point of the oil.   In conjunction with the clay treatment, crank-case dilution is commonly removed by steaming before the treated oil is filtered from the adsorbent.   Industrially, activated clays are employed almost exclusively for this purpose, chiefly owing to the fact that no un-activated clay that can produce the desired effects in sufficiently low concen-tration has been available.

FIG. 9. *Apparatus employed for the refining of used lubricating oils (half-gallon capacity).*

In the present work, some of the tests were carried out on a small scale, using 200 cc. of oil and heating to 200° C. in a thermostat.   No steam distillation of the diluents was carried out, and on these oils, color was the only ana-lytical determination made.   Other tests were carried out in a larger apparatus, shown in Fig. 9, of one-half gallon capacity, with attached steam generator and accessories, immersion electrical heating, and attached filter press. Analytical determinations were carried out on some of these recovered oils, and also on the corresponding unused oil.   Table XXIII shows some of the results obtained.   The used oils were obtained in the case of Oil 1 from an auto-mobile crank-case and in the case of Oils 2 and 3 from an aeroplane crank-case after some 500 miles of use.   Similar results were obtained in several other cases, on oils recovered after 1000 to 2000 miles of use.

It is noted in Table XXIII and in other data that the analytical results obtained for the re-covered oils are very good.   Low viscosity-oxidation ratios, showing good resistance to oxidation, are obtained after proper treatment with a good adsorbent clay.   Some variations are obtained in the viscosities, and in flash and fire points owing to unavoidable experimental differences in the steam distillation of diluents. It should be emphasized that the quality of a reclaimed oil, at least in so far as is shown by laboratory analysis, depends on the procedure and reagents used in the reclaiming process.   Mere washing, filtering, or centrifuging, or the use of poor adsorbents will not yield analytical characteristics that indicate an oil of good quality.

The colors of the recovered oils, as in the case of the lubricating oil dis-tillates, varied widely, depending on the clay used.   The clays found most efficient for the new distillates, *e.g.*, Clay 3a, were found also to be the most efficient in the refining of the used oils.   The poorer clays however did not

TABLE XXIII
ANALYSES OF RECLAIMED CRANK-CASE OILS

Oil	Sp. gr. 60°/60° F.	Flash pt., °F.	Fire pt., °F.	Pour pt., °F.	Viscosity index	Viscosity-oxidation ratio	Coke No. diff.	Total acidity Mg. KOH per 100 gm. oil
1 Original	0.892	445	515	− 5	119	1.52	0.72	7.0
Reclaimed	0.897	445	536	− 6	90	1.42	0.69	7.4
Reclaimed	0.897	435	526	− 8	105	1.49	0.66	6.2
2 Original	0.893	565	630	+18	108	1.50	0.95	4.2
Reclaimed	0.891	541	587	+15	103	1.49	0.77	5.5
3 Original	0.890	540	600	+14	106	1.29	0.83	6.0
Reclaimed	0.903	550	580	+18	100	1.31	0.74	3.8
Reclaimed	0.894	520	605	+16	92	1.23	0.87	4.0
Relcaimed	0.894	525	615	+18	97	1.32	0.82	4.1
Reclaimed	0.893	510	600	+12	98	1.49	0.92	5.5
Reclaimed	0.894	525	615	+12	100	1.25	0.66	3.8
Reclaimed	0.893	535	590	+10	95	1.16	1.02	3.9
Reclaimed	0.898	520	605	+14	96	1.40	1.05	1.9
Reclaimed	0.898	525	605	+10	101	1.43	1.06	3.1
Reclaimed	0.898	520	575	+16	100	1.41	0.85	6.4

Viscosity-oxidation ratio and coke number difference determined according to specification No. D. T. D. 109 of the British Air Ministry; all other tests according to A.S.T.M. methods.

show the same order of merit in the two types of oils, and it must be concluded that the refining results obtained with used crank-case oils as a medium cannot be presumed to hold also for new lubricating distillates. In several instances, Clays 3a and 2a produced recovered oils of color better than that of the corresponding original oil. Among the unactivated clays, Clay 3 was by far the most efficient, with Clay 1 second.

Some clays were tested also in the recovery of a used insulating oil taken from a transformer after some years of use. The clays were used in a concentration of 5%, and the treating temperature was 140° C.

Practically no differences were found in the viscosities, flash points, and acidities of the recovered oil. The tendency to sludge formation was determined in two ways:

1. Samples of the oils were heated in an air oven with little draft to 120° C.

2. Samples were heated to 120° C. in open beakers immersed in a thermostat. The demulsification number was determined according to the A.S.T.M. method.

In Sludge Test 1, all had formed sludge at the end of the seven day period. In Sludge Test 2, only Clay 9a produced a recovered oil that passed the test.

Dry-cleaning solvents are recovered either by distillation, the process commonly used for trichlorethylene, or by filtration through a decolorizing carbon together with a filter aid. A series of tests in which bentonitic clays were used showed the following general results. Used trichlorethylene, containing no soap and containing sufficient grease to be opaque in thin layers

TABLE XXIV
ANALYSES OF RECLAIMED INSULATING OILS

Clay No.	Demuls. No., sec.	Sludge tests			
		1	2		
		7 days	7 days	10 days	15 days
24	33		Medium	Heavy	Heavy
32	30		Trace	Medium	Heavy
9	30	Medium	Medium	Heavy	Heavy
9a	34	Trace	Nil	Trace	Medium
2a	31	Medium	Trace	Medium	Heavy
30a	30	Heavy			
31a	32	Light			

and dark brown in color, was shaken at room temperature with 1% of several unactivated and activated clays. After filtering, the solvent was perfectly clear and water white. A sample of used dry-cleaners' naphtha containing soap was also treated with clays, and the method was compared with the recovery process used at present by determining total solids after clay treatment and filtering. It was found that the use of 3.5% of Clay 3a yielded a recovered naphtha of the same solid content as that obtained by the industrially used process, with the added advantage of a much superior color.

Acknowledgment

References

1. SPENCE, H. S.   Mines Branch, Department of Mines, Canada, Bulletin No. 626.   1924.

2. WILLSON, C. O.   Oil and Gas J. 31 (45) : 61-62.   1933.

3. WORCESTER, W. G.   Bulletin No. 16, Department of Railways, Labour and Industries, Saskatchewan.   Aug. 10. 1934.

4. WORCESTER, W. G.   Trans. Can. Inst. Min. and Met. 40 : 438-451.   1937.

ACTION OF PHENYLMAGNESIUM BROMIDE ON ANTHRAQUINONES[1]

By C. F. H. Allen[2] and R. W. McGibbon[3]

Abstract

This preliminary report of the action of phenylmagnesium bromide on anthraquinone contains the description of a procedure for avoiding the recovery of large amounts of unchanged quinone, with consequent increasing of the yield. Butyl ether is preferable to toluene for "forced" Grignard reactions.

Anthraquinones react with Grignard reagents to give a variety of products, usually in low yields, with much quinone being recovered. In no case, however, has any product formed by 1,4-addition been described. The yields of diol reported were usually low, and it seemed possible that this might be accounted for in part by the production of substituted anthraquinones. It was first thought advisable to standardize the procedure used, in view of the discrepancies recorded in the literature for yields of diol (2). Since the work has been interrupted by the illness of the junior author and cannot be resumed for some time, it seems advisable to make a record of the work at this point.

Every previous worker has mentioned the presence of a large amount of anthraquinone in the reaction product. While a small part of this may be explained by a reduction by the Grignard reagent (2), the use of a large excess of the latter avoids this complication.* Kovache (6) pointed out that, owing to its insolubility in ether, the use of finely divided quinone, with vigorous stirring, was essential; in agreement with Kovache, it is our opinion that low yields are almost entirely due to this slight solubility, coupled with the precipitation, on the surface of the large particles, of the magnesium complex formed.

By changing the solvent to butyl ether, in which the quinone is much more soluble, and by a preliminary recrystallization from this solvent or chlorbenzene with rapid cooling to ensure formation of small crystals, the yield of diol was easily raised to 80%; only traces of anthraquinone were found in the product. With β-methylanthraquinone, which is much more soluble, no unchanged starting material was recovered. The yield was 86% in butyl ether and 66% in ethyl ether.

The procedure involved the formation of phenylmagnesium bromide in diethyl ether in the usual way, addition first of the solid quinone, then the butyl ether and distillation of the ethyl ether. These are conditions for a

* Care must be taken, of course, that the stirring is not so vigorous that the suspended quinone is removed from the sphere of action by being thrown upon the upper walls of the flask.

"forced" Grignard reaction. Since it was possible that the type of product might have been related to these differences (1, 3, 4, 5), the residual gum was investigated, but no solids could be isolated, nor was there any evidence of a product that might have resulted from a 1,4-addition of the phenylmagnesium bromide. It may be pointed out that butyl ether is more suitable for forced reactions than toluene, in which the organo-metallic complexes are usually very sparingly soluble.

Experimental

All the reactions were carried out in the usual apparatus and in an inert atmosphere. To three equivalents of phenylmagnesium bromide (from 27.4 gm. of bromobenzene, 3.8 gm. of magnesium and 60 cc. of ethyl ether) was added 5 gm. of anthraquinone and 80 cc. of butyl ether, and the whole heated in an oil bath at 100° to 105° C., the ethyl ether being allowed to distil off. Most of the quinone appeared to have reacted after one and one-half hours; if there were any large particles they were visible on the bottom of the flask when stirring was discontinued, and were unaffected by a further two and one-half hours of refluxing. The clear solution was decanted and decomposed with 100 cc. of 3.6% hydrochloric acid, and steam distilled until all the solvent and diphenyl had been removed (1500 cc. of distillate), and the granular residue (10.8 gm.) was filtered and air dried. The large particles mentioned above did not dissolve in fresh butyl ether, until pulverized to expose fresh surface; they proved to be unchanged quinone. The quantity varied in different runs, but was never more than 0.1 gm., and sometimes there was none.

The crude product was boiled with methanol, filtered from insoluble inorganic material, and the solvent distilled; 6.9 gm. (80%) of diol was obtained by collecting successive crops of crystals. The use of acetone for recrystallization followed by benzene took less time; acetone alone forms a solvated diol containing two parts of acetone to one of diol. There was always some oily material left, which with concentrated sulphuric acid did not show the halochromism characteristic either of the diol or of the oxanthrone.

References

1. ALLEN, C. F. H. and GILMAN, L. J. Am. Chem. Soc. 58 : 937-940. 1936.
2. BARNETT, E. DE B., COOK, J. W., and WILTSHIRE, J. J. J. Chem. Soc. 1724-1732*. 1927.
3. DUFRAISSE, C., and LEBRAS, J. Bull soc. chim. [5] 4 : 1037-1045. 1937.
4. DUFRAISSE, C., and HORCLORS, R. Bull. soc. chim. [5] 3 : 1894-1905. 1936.
5. DUFRAISSE, C., and VELLUZ, L. Bull. soc. chim. [5] 3 : 1905-1913. 1936.
6. KOVACHE, A. Ann. de chem., 10 : 184-238. 1918.

   * *This also gives earlier references.*

CONTRIBUTION TO THE STUDY OF THE PRECIPITATION OF CHROMATES[1]

By P. E. PELLETIER[2], L. CLOUTIER[3], AND PAUL E. GAGNON[3]

Abstract

A study was made of the precipitation of the chromates of copper, cadmium, cobalt, zinc, and iron at room temperature. The concentration of the reacting metallic salt solutions was kept constant, and that of the potassium chromate solutions was varied regularly. Solutions were mixed in less than one-tenth of a second, and the rate of mixing was accurately determined. The ratio of oxide to chromium trioxide was found by analysis for chromium trioxide and the metal on the same portion of the precipitate. If the ratio remained constant with varying concentrations of reactants, a definite compound was indicated. The composition of the precipitates obtained with copper salts approached that of the normal chromate. Cadmium and cobaltous salts always gave normal chromates. Zinc and ferric salts yielded only basic mixtures.

Introduction

The products obtained in a great number of reactions often vary according to the mode of mixing the reagents. This is especially true with solutions which, upon mixture, are likely to give rise to basic compounds. Thus Thümmel (18) noticed that in pouring a solution of alkaline carbonate into a solution of mercuric chloride, mercuric oxychloride is formed, while if the solution of mercuric chloride is added to that of the alkaline carbonate, mercuric oxide is precipitated. Such solutions, according to the method in which the precipitation is carried out, usually give a series of mixtures the composition of which varies between that of the hydroxide and that of the less basic compound. These mixtures have sometimes been considered as definite compounds. This explains the great number of basic compounds mentioned in the literature.

Therefore, when it is possible to obtain a number of precipitates and it is desired to obtain one of constant composition, it is important that the reactants be mixed not only in given proportions but also as intimately as possible, in minimum time, before the precipitate is formed (8).

For this purpose Jolibois (9) designed an apparatus with which he systematically studied various precipitations (10).

One of the authors applied the same technique to the precipitation of lead chromates. He found that not only a normal chromate, but also two definite

basic compounds (2), were formed. In view of these results the authors decided to undertake the study of the precipitation of the chromates of copper, cadmium, cobalt, zinc, and iron.

The composition of the precipitates obtained with copper salts approached that of the normal chromate when the concentration of the potassium chromate solutions was increased regularly. The salts of cadmium and cobalt (cobaltous) gave only normal chromates. No definite compound was obtained with zinc or ferric salts.

The authors have also studied the action of mixtures of potassium hydroxide and potassium chromate on the above-mentioned salts. In every experiment they obtained only precipitates the basicity of which increased very rapidly to that of the hydroxide as the value of the ratio of potassium oxide to chromium trioxide in the solutions increased. Under similar conditions, the lead salts furnished two definite basic chromates (2).

Apparatus

The authors deem it desirable to repeat here the description of the apparatus and procedure (3) employed (Fig. 1).
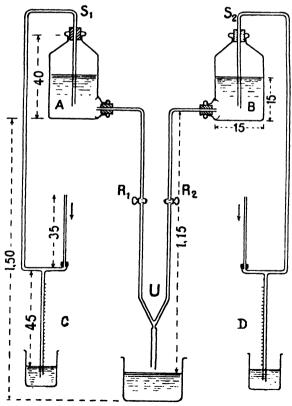
FIG. 1. *Mixing apparatus.*

"The apparatus consists of two Mariotte flasks in which are placed two solutions A and B of known concentrations. By means of two stopcocks, R_1 and R_2, the flow of the solutions in the two tubes, which are joined in U, can be regulated. At the point U, the solutions mix very rapidly in less than 1/10th of a second. A precipitate is then formed in a homogeneous liquid. Air is drawn into the Mariotte flasks according to the rate of flow of the liquids. The rate of flow is measured by means of two Venturi tubes, *i.e.*, two capillary tubes and two coloured solutions.

"The apparatus is calibrated in such a way that when the coloured liquids are at the same level in the two tubes C and D, the rates of flow are the same."

"Such an apparatus enables us to study systematically a precipitation. We keep the concentration of the solution A constant, we precipitate with different solutions B of increasing concentration and each time we study the composition of the precipitate."

A curve can be constructed by plotting the different values of the molar ratio of oxide to chromium trioxide in the precipitates against the molar ratio of chromium trioxide to oxide in the solutions.

If the composition of the precipitates remains constant with varying concentrations of reagent B, in different experiments, only one phase is present, *i.e.*, one definite compound (12). A mixture is indicated if, under the same conditions, the composition of the precipitate varies.

Results

Copper Chromates

Vauquelin (19) stated that when potassium chromate is added to a solution of a neutral copper salt, a chestnut brown precipitate is formed, which, according to Gerhardt (6) and Freese (4), consists of $K_2O . 3CuO . 3CrO_3 . 2H_2O$, or according to Gröger (7), of $KCu_2(OH)(CrO_4)_2 . H_2O$. Skormin (17) obtained the compound $4CuO . CrO_3 . 3H_2O$ by the action of an alkaline solution of potassium chromate in excess on a solution of copper sulphate. According to Rosenfeld (15, 16), the compound $3CuO . CrO_3 . 2H_2O$ is formed when potassium chromate is added to a solution of copper sulphate.

None of the compounds mentioned were obtained by the present authors, who treated solutions of copper nitrate, $M/20$, with solutions of potassium chromate that ranged in concentration from $M/40$ to $5/8 M$.

The composition of the precipitate obtained approximates that of the compound $K_2O . 3CuO . 3CrO_3 . 2H_2O$ analyzed by Gerhardt (6) and Freese (4). However, the former precipitate has a greater proportion of copper than the latter. Furthermore, by means of a test with perchloric acid on a portion of the solution containing the dissolved precipitates, the authors have proved the total absence of potassium in each of the precipitates obtained.

The precipitates were filtered off, washed with cold water until free from potassium chromate, and dried at 80° C.; 0.5 to 1.0 gm. of the precipitate was then heated with 10 cc. of 10% potassium hydroxide solution, and the whole diluted to 200 cc. Copper hydroxide was filtered off, and well washed with hot water—until it did not contain any chromium. It was then dissolved in 12% sulphuric acid and the copper was determined electrolytically.

The filtrate from the copper hydroxide contained potassium chromate which was determined by iodometric titration.

The results obtained are given in Table I and Fig. 2.

TABLE I

COPPER NITRATE ($M/20$) AND POTASSIUM CHROMATE ($M/40$ to $5/8$ M)

Conc. of solutions, moles per litre		Molar ratio CrO_3/CuO in solutions	Analysis of precipitates, gm.		Molar ratio CuO/CrO_3 in precipitates	Average
$Cu(NO_3)_2$	K_2CrO_4		CuO	CrO_3		
0.05	0.025	0.5	0.4380	0.2082	2.644	
			0.3091	0.1459	2.664	
			0.5405	0.2577	2.636	2.64
0.05	0.05	1.0	0.5784	0.2845	2.555	
			0.4400	0.2174	2.540	
			0.5154	0.2465	2.568	
			0.4549	0.2248	2.548	2.55
0.05	0.075	1.5	0.3755	0.2645	1.780	
			0.2999	0.2123	1.776	1.78
0.05	0.10	2.0	0.4857	0.4736	1.289	
			0.3169	0.3169	1.282	1.28
0.05	0.15	3.0	0.2009	0.2108	1.181	
			0.2736	0.2932	1.173	
			0.2740	0.2889	1.165	1.17
0.05	0.20	4.0	0.2596	0.2799	1.165	
			0.2594	0.2819	1.157	1.16
0.05	0.25	5.0	0.2985	0.3382	1.110	
			0.2694	0.3059	1.110	1.11
0.05	0.30	6.0	0.2506	0.2862	1.101	
			0.2581	0.2969	1.092	1.10
0.05	0.40	8.0	0.2364	0.2739	1.092	
			0.2021	0.2336	1.088	1.09
0.05	0.50	10.0	0.2924	0.3416	1.076	
			0.2556	0.2999	1.071	1.07
0.05	0.625	12.5	0.2737	0.3286	1.062	1.06

Cadmium Chromates

Several basic chromates of cadmium were prepared from boiling solutions of a cadmium salt and potassium chromate: $3CdO .2CdCrO_4 . 8H_2O$ (13); $CdO . CdCrO_4 . H_2O$ (5); $4CdO . 3CdCrO_4$ with 4.5 to 6.0 H_2O (17).

The nature of the product obtained depends on the time of contact of the precipitate with boiling water. Consequently, the composition of the basic salts of cadmium chromate remains to be determined.

A solution of cadmium nitrate, $M/20$, was used. The concentration of the potassium chromate solutions varied from $M/20$ to $M/2$. By precipitating at room temperature, only the normal chromate was obtained, whatever the concentration.
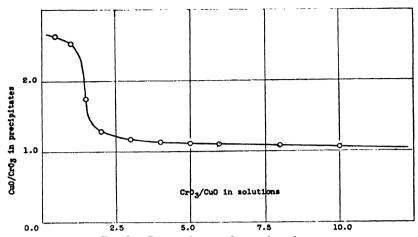
FIG. 2.   *Copper nitrate and potassium chromate.*

The precipitates, dried at 80° C., were dissolved in dilute acetic acid, and chromium was determined by the usual method as lead chromate. The filtrate was then treated with sulphuric acid and the excess of lead was removed as lead sulphate. The cadmium was then precipitated with potassium carbonate and determined as cadmium oxide.

Table II and Fig. 3 show the results obtained.

TABLE II

CADMIUM NITRATE ($M/20$) AND POTASSIUM CHROMATE ($M/20$ to $M/2$)

Conc. of solutions, moles per litre		Molar ratio CrO_3/CdO in solutions	Analysis of precipitates, gm.		Molar ratio CdO/CrO_3 in precipitates	Average
$Cd(NO_3)_2$	K_2CrO_4		CdO	CrO_3		
0.05	0.05	1.0	0.3836	0.2977	1.004	
			0.3591	0.2784	1.005	1.00
0.05	0.10	2.0	0.4017	0.3111	1.006	
			0.3085	0.2389	1.006	1.01
0.05	0.25	5.0	0.5210	0.4084	0.998	
			0.4893	0.3773	1.001	1.00
0.05	0.50	10.0	0.3283	0.2583	0.990	
			0.4254	0.3291	1.007	1.00

Cobaltous Chromates

Briggs (1) prepared the normal cobaltous chromate by mixing solutions of cobaltous acetate and potassium chromate.

The authors likewise obtained a normal chromate by treating a solution of cobaltous nitrate, $M/20$, with different solutions of potassium chromate, $M/20$ to $M/2$. Under the conditions of the experiments, the basic compounds mentioned in the literature were not obtained.
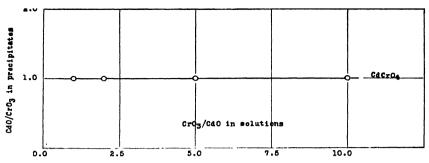
FIG. 3.   *Cadmium nitrate and potassium chromate.*

The precipitates, dried at 80° C., were treated with 20% potassium hydroxide, water was added, and cobalt hydroxide was filtered off. After complete removal of potassium chromate by washing with hot water, chromium was determined in the filtrate by iodometric titration. The cobalt hydroxide was dissolved in a mixture of hydrogen peroxide and dilute sulphuric acid, and the cobalt was determined electrolytically.

The results are shown in Table III and Fig. 4.

TABLE III

COBALT NITRATE ($M/20$) AND POTASSIUM CHROMATE ($M/20$ TO $M/2$)

Conc. of solutions, moles per litre		Molar ratio CrO_3/CoO in solutions	Analysis of precipitates, gm.		Molar ratio CoO/CrO_3 in precipitates	Average
$Co(NO_3)_2$	K_2CrO_4		CoO	CrO_3		
0.05	0.05	1.0	0.1457	0.1979	0.983	
			0.2317	0.3081	1.000	0.99
0.05	0.15	3.0	0.1565	0.2085	1.002	
			0.1561	0.2081	1.001	1.00
0.05	0.25	5.0	0.1376	0.1852	0.991	
			0.3455	0.4645	0.990	0.99
0.05	0.50	10.0	0.1837	0.2408	1.015	
			0.1474	0.1937	1.015	1.01
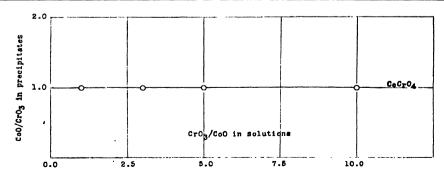
FIG. 4.   *Cobalt nitrate and potassium chromate.*

Zinc Chromates

The normal zinc chromate is difficult to prepare, owing to the fact that in the presence of a large amount of water it is readily hydrolyzed to basic salts. This is the reason why a great many basic salts have been reported. A number of these salts of indefinite composition form the so-called zinc yellow.

A solution of zinc nitrate, $M/20$, was treated with solutions of potassium chromate ranging in concentration from $M/20$ to $3/4$ M.

The precipitates, dried at 80° C., were dissolved in dilute acetic acid. Chromium was determined as lead chromate. The excess of lead was removed as lead sulphate, and the zinc was then determined as zinc ammonium phosphate.

The results obtained are given in Table IV and Fig. 5.

FIG. 5. *Zinc nitrate and potassium chromate.*
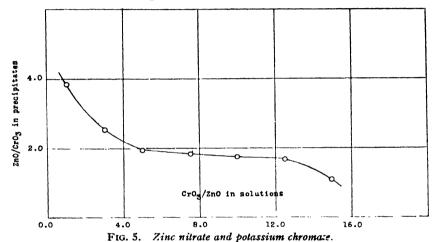
TABLE IV
ZINC NITRATE ($M/20$) AND POTASSIUM CHROMATE ($M/20$ to $3/4$ M)

Conc. of solutions, moles per litre		Molar ratio CrO_3/ZnO in solutions	Analysis of precipitates, gm.		Molar ratio ZnO/CrO_3 in precipitates	Average
$Zn(NO_3)_2$	K_2CrO_4		ZnO	CrO_3		
0.05	0.05	1.0	0.3325	0.1057	3.864	
			0.5268	0.1675	3.864	3.86
0.05	0.15	3.0	0.2769	0.1353	2.514	
			0.3741	0.1820	2.526	2.52
0.05	0.25	5.0	0.4255	0.2773	1.886	
			0.2730	0.2218	1.882	1.88
0.05	0.375	7.5	0.3214	0.2197	1.798	
			0.3510	0.2396	1.781	1.78
0.05	0.50	10.0	0.4836	0.3381	1.769	
			0.2452	0.1723	1.759	
			0.2380	0.1652	1.770	1.77
0.05	0.625	12.5	0.2453	0.1764	1.710	
			0.2872	0.2078	1.699	1.70
0.05	0.75	15.0	0.3788	0.3782	1.179	
			0.3073	0.3185	1.186	
			0.1826	0.1908	1.177	
			0.1889	0.1965	1.182	1.18

Iron Chromates

A solution of ferric chloride, $M/10$, was treated with solutions of potassium chromate of concentrations from $M/10$ to $M/2$.

The precipitates, dried at 80° C., were dissolved in dilute hydrochloric acid (10%). Iron was determined as ferric oxide, and chromium as sesquioxide or volumetrically by iodometric titration.

No definite compound was obtained, as is shown in Table V and Fig. 6.
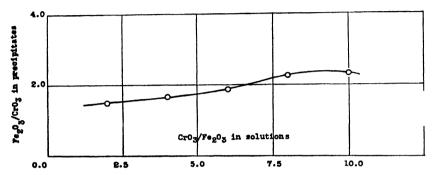
FIG. 6.   *Ferric chloride and potassium chromate.*

TABLE V

FERRIC CHLORIDE ($M/10$) AND POTASSIUM CHROMATE ($M/10$ to $M/2$)

Conc. of solutions, moles per litre		Molar ratio CrO_3/Fe_2O_3 in solutions	Analysis of precipitates, gm.		Molar ratio Fe_2O_3/CrO_3 in precipitates	Average
$FeCl_3$	K_2CrO_4		Fe_2O_3	CrO_3		
0.10	0.10	2.0	0.2383	0.0992	1.503	
			0.2168	0.0910	1.492	
			0.2118	0.0871	1.523	1.51
0.10	0.20	4.0	0.2305	0.0824	1.665	
			0.2288	0.0847	1.643	
			0.2701	0.1020	1.660	1.65
0.10	0.30	6.0	0.3323	0.1105	1.883	
			0.1937	0.0648	1.871	1.88
0.10	0.40	8.0	0.3360	0.0930	2.262	
			0.1901	0.0525	2.268	2.26
0.10	0.50	10.0	0.3441	0.0922	2.327	
		.	0.2281	0.0613	2.330	
			0.1887	0.0508	2.327	2.33

References

1. BRIGGS, S. H. C.   Z. anorg. chem. 63 : 325-329.   1909.
2. CLOUTIER, L.   Ann. chim. (10) 19 : 2-77.   1933.
3. CLOUTIER, L., PELLETIER, P. E., and GAGNON, P. E.   Trans. Roy. Soc. Can. III, 30 : 149-164.   1936.

4. FREESE, C.   Ann. Physik, 140 : 242-253.   1870.

5. FREESE, C.   Ber. 2 : 476-479.   1868.

6. GERHARDT, C.   J. Pharm. Chim. (3) 22 : 57.   1847.

7. GRÖGER, M.   Sitzber. Akad. Wiss. Wien, 113 : 155-171.   1903.

8. JOLIBOIS, P.   Bull. soc. chim. ind. (5) I : 597-613.   1934.

9. JOLIBOIS, P.   Compt. rend. 169 : 1095-1098.   1919.

10. JOLIBOIS, P., BOSSUET, R., and CHEVRY.   Compt. rend. 172 : 373-375.   1921.

11. JOLIBOIS, P. and BOSSUET, R.   Compt. rend. 174 : 1625-1628.   1922.

12. JOLIBOIS, P. and CLOUTIER, L.   Compt. rend. 195 : 795-797.   1932.

13. MALAGUTI, F. J. and SARZEAU, M.   Ann. chim. phys. (3) 9 : 431-463.   1844.

14. MILLER, W. H. and KENRICK, F. B.   J. Phys. Chem. 7 : 259-268.   1903.

15. ROSENFELD, M.   Ber. 12 : 954-959.   1879.

16. ROSENFELD, M.   Ber. 13 : 1469-1475.   1880.

17. SKORMIN, B.   Dissert.   Berlin.   1896.

18. THÜMMEL, K.   Arch. Pharm. 223 : 953-973.   1885.

19. VAUQUELIN, M.   Ann. chim. phys. (1) 70 : 70-94.   1809.

WILDIERS' BIOS AND THE LACTIC ACID BACTERIA[1]

THE RELATION OF BIOS TO THE WATER-SOLUBLE B-VITAMINS

By Blythe Alfred Eagles[2], Olga Okulitch[3], and Arthur Stephen Kadzielawa[4]

Abstract

The influence of three distinct activators prepared from tomatoes, yeast, or liver, on the metabolism of two species of lactic acid bacteria has been studied. One of these activators is Bios II A, and the other two have been shown to be components constituting Bios II B. On the basis of their physical and chemical properties, it is suggested that the growth stimulants required by the lactic acid bacteria are identical with certain of the heat-stable accessory food factors of the Vitamin-B complex essential for the growth of animals.

In two papers (3, 16) from this laboratory it was shown that the Bios of Wildiers exerts a marked influence on the acid-producing abilities of the lactic acid bacteria. In addition, evidence in support of the multiple nature of Wildiers' Bios as demonstrated by Miller, Eastcott, and Maconachie (13) for the growth of yeasts, was presented for the betacocci and those streptococci which normally find milk a poor nutrient substrate. Enrichment of milk with three distinct activators (Bios I, Bios II A, and Bios II B) prepared from alfalfa, yeast, or tomatoes, evidently provided not only ideal growth conditions for these micro-organisms, but a substrate as well for their most intensive metabolism.

The vitamin requirements of the lactic acid bacteria have been investigated by Orla-Jensen and co-workers (14). They have demonstrated that all true lactic acid bacteria require two activators, lactoflavin and "milk bios". "Milk bios" is a thermostable, alkali-fast substance present in milk and adsorbed by activated charcoal. It is considered to be identical with pantothenic acid described by Williams and Saunders (20); and it is also suggested by Orla-Jensen and co-workers that it is identical with Vitamin B_6 (1, 8). Further, they have shown that the lactic acid rod forms require in addition to lactoflavin and "milk bios" an activator present in whey and not adsorbed by activated charcoal. Vitamin B_1 was found to play no role in the physiological activities of the lactic acid micro-organisms.

In a study of the accessory nutritive factors required by the lactic acid bacteria, Snell, Strong, and Peterson (17) have recently reported the presence, in an alcohol extract of liver, of an acidic ether-extractable substance essential for the normal growth of 14 species of lactic acid bacteria. This substance

is rather labile to heat, acid, and especially to alkali, is adsorbed by charcoal but not by Lloyd's reagent, and is not precipitated by phosphotungstic acid.

As work has progressed on the activator requirements of the betacocci, communications describing the nature of the essential dietary factors of the heat-stable portion of the Vitamin-B complex required for the growth of the rat and of the chick have appeared from other laboratories. A detailed summary of the properties of the constituents of the Vitamin-B complex is to be found in the paper by Edgar and Macrae (6).

Edgar and Macrae (4, 5, 6) describe the separation from autoclaved yeast extract of two heat-stable factors necessary for the optimum growth of rats maintained on a Vitamin B-free diet and receiving lactoflavin and Vitamin B_1. One factor is present in the filtrate after exhaustive extraction with fuller's earth, while the second is contained in the eluate from the fuller's earth adsorbate after the removal of lactoflavin. The fuller's earth filtrate factor is adsorbed by Norite charcoal at pH 1.2 and is not precipitated by phosphotungstic acid.

Elvehjem and Koehn (7) first described a fuller's earth filtrate factor present in an aqueous liver extract and necessary for the growth of the chick. This factor was later investigated by Lepkovsky and Jukes (9). Unlike the yeast filtrate factor of Edgar and Macrae, the liver filtrate factor is not adsorbed by Norite charcoal.

The yeast fuller's earth adsorbate factor may be similar to, or identical with, the factor obtained by Lepkovsky and co-workers (10) from the fuller's earth adsorbate from rice bran extracts. In certain respects Edgar and Macrae's adsorbate factor resembles the Vitamin B_6 investigated by Birch and György (1). Edgar and Macrae, and Lepkovsky and co-workers do not describe the properties of their respective adsorbate factors, in so far as their adsorption by charcoal or precipitation by phosphotungstic acid are concerned. Vitamin B_6 is adsorbed by fuller's earth at pH 2.5, but not by charcoal at pH 6.0, and is precipitated by phosphotungstic acid.

A review of the literature on the question of the relation of Bios to the Vitamin-B complex shows that the evidence is overwhelmingly against the suggested identity of Bios and Vitamin B_1. In their early work on the fractionation of Bios, Miller and co-workers (2,11) showed that neither Bios I nor Bios II (adsorbed by charcoal) cured avian polyneuritis or promoted the growth of rats. However, in the light of the more recent work on the multiple nature of the Bios factors required for the growth of yeasts (12, 18, 19), and of the demonstration of several heat-stable dietary factors essential for the nutrition of the rat, it appeared not improbable to assume that a relation might exist between the Bios factors and certain of the B-vitamins. A study of the chemical and physical properties of the factors constituting the Bios of Wildiers and the Vitamin-B complex strongly suggested to us that the Bios activators, which we have shown are required by the lactic acid bacteria for their most intensive metabolism, are identical with certain of the heat-stable components of the Vitamin-B complex.

In an attempt to establish the validity of the writers' hypotheses, fractionation of tomato juice, by means of a combination of the procedures used for the differentiation of the Bios constituents and for the characterization of the heat-stable components of the Vitamin-B complex, was undertaken. The behavior of the respective entities towards adsorption by charcoal and by fuller's earth, and towards precipitation by phosphotungstic acid, was used as a basis for separation.

Experimental

The filtrate resulting from the treatment of the contents of two tins of tomato juice with tannic acid and lead acetate, with subsequent removal of hydrogen sulphide, was used as the starting material for the preparation of the various fractions (12). This filtrate was divided into two equal portions, Filtrates 1 and 2.

Filtrate 1 was treated after the manner of Miller (12) for the separation of Bios II *A* and Bios II *B*. These Bios preparations were concentrated to 100 cc. and 50 cc. quantities respectively. A fuller's earth filtrate factor and a fuller's earth adsorbate factor were prepared from Filtrate 2 after the manner of Edgar and Macrae. These vitamin factors were also concentrated to 100 cc. and 50 cc. quantities respectively. An aliquot equivalent to one-fifth of the volume of each of the Bios and vitamin concentrates was retained for the purpose of determining its influence on the acid-producing abilities of the lactic acid micro-organisms.

Fuller's earth filtrate and adsorbate fractions were prepared by the procedure of Edgar and Macrae from the remainder of each of the Bios concentrates after they had been made up to a volume of 600 cc. Each of the resulting fractions was concentrated to the volume of the solution from which it was prepared.

The four fractions thus obtained were:—

Fuller's earth filtrate of Bios II *A*—   Fraction 1
Fuller's earth adsorbate of Bios II *A*—   Fraction 2
Fuller's earth filtrate of Bios II *B*—   Fraction 3
Fuller's earth adsorbate of Bios II *B*—   Fraction 4

Charcoal adsorbate and filtrate fractions were prepared by the procedure of Miller from the remainder of the fuller's earth filtrate and fuller's earth adsorbate factors. Each solution was made up to a volume of 600 cc. prior to treatment with charcoal, and each of the resulting fractions was concentrated to the volume of the solution from which it was prepared.

The four fractions thus obtained were:—

Charcoal filtrate of fuller's earth filtrate—   Fraction 5
Charcoal adsorbate of fuller's earth filtrate—   Fraction 6
Charcoal filtrate of fuller's earth adsorbate—   Fraction 7
Charcoal adsorbate of fuller's earth adsorbate— Fraction 8

An aliquot equivalent to one-quarter of the volume of each of the eight fractions was retained for the purpose of determining its influence on the acid-producing ability of the lactic acid micro-organisms.

A phosphotungstic acid precipitation was carried out on the remainder of each of the eight fractions. Each fraction was diluted to a volume of 200 cc., adjusted to contain 5% of sulphuric acid by volume, and precipitation was effected with 20% phosphotungstic acid in 5% sulphuric acid. The phosphotungstic acid precipitates and filtrates were freed from phosphotungstic acid in the usual manner, and each of the resulting solutions was concentrated to the volume of the solution from which it was prepared. Fraction 3 failed to yield a phosphotungstic acid precipitate.

The influence of each of the preparations, when added to milk as an enriching entity, on the acid-producing abilities of cultures EMB_1173 and

TABLE I

TITRATABLE ACIDITY IN GRAMS LACTIC ACID PER LITRE

Medium employed as substrate	Culture number	
	EMB_1173	EMB_2173
Milk	3.6	1.6
Milk + 0.15% yeast extract	6.5	3.4
Milk + Bios II A	7.4	7.4
Milk + Fraction 1	7.2	6.3
Milk + PTA* precipitate of Fraction 1	3.6	1.8
Milk + PTA filtrate of Fraction 1	4.5	4.7
Milk + Fraction 2	3.6	1.8
Milk + PTA precipitate of Fraction 2	3.6	1.6
Milk + PTA filtrate of Fraction 2	3.6	1.6
Milk + Bios II B	5.4	3.6
Milk + Fraction 3	4.7	3.6
Milk + PTA precipitate of Fraction 3	—	—
Milk + PTA filtrate of Fraction 3	3.4	1.6
Milk + Fraction 4	6.3	3.2
Milk + PTA precipitate of Fraction 4	5.6	2.7
Milk + PTA filtrate of Fraction 4	3.6	1.6
Milk + Fuller's earth filtrate factor	6.8	3.6
Milk + Eraction 5	5.6	4.1
Milk + PTA precipitate of Fraction 5	3.6	1.6
Milk + PTA filtrate of Fraction 5	5.9	4.7
Milk + Fraction 6	5.9	2.7
Milk + PTA precipitate of Fraction 6	4.3	1.6
Milk + PTA filtrate of Fraction 6	6.1	1.8
Milk + Fuller's earth adsorbate factor	5.2	2.9
Milk + Fraction 7	3.2	1.1
Milk + PTA precipitate of Fraction 7	3.6	1.6
Milk + PTA filtrate of Fraction 7	4.3	1.6
Milk + Fraction 8	5.4	3.4
Milk + PTA precipitate of Fraction 8	5.9	2.9
Milk + PTA filtrate of Fraction 8	3.6	2.0

* PTA *stands for phosphotungstic acid.*

EMB$_2$173 (15, 16) was determined. The enrichment was added at the rate of 1% in all cases. Milk and milk enriched with 0.15% autolyzed yeast extract served as controls. Culture EMB$_1$173 is an atypical strain of *Streptococcus cremoris* (Orla-Jensen) responding markedly to the enrichment of milk with yeast extract. Culture EMB$_2$173 is to be classified as a strain of *Betacoccus cremoris* (Knudsen and Sørensen). Procedures followed throughout the fermentation study have been described previously (15). The results of the determinations of the total titratable acidity produced by each of the cultures are given in Table I.

When the data for the acid production of cultures EMB$_1$173 and EMB$_2$173 are considered, it is obvious that enrichment of milk with either Bios II *A* or Bios II *B* has a marked stimulating effect on the vital activity of the micro-organisms, and that the influence of Bios II *A*, particularly in the case of culture EMB$_2$173, is more marked than that of Bios II *B*, previous results being thus confirmed (3) (Table I).

The addition of the fuller's earth filtrate factor or of the fuller's earth adsorbate factor has a marked stimulating effect on the vital activity of both micro-organisms. The total titratable acidity produced by culture EMB$_1$173 in milk enriched with the fuller's earth filtrate factor is equal to that produced when Bios II *A* is employed as the enriching entity. It would appear that culture EMB$_2$173 is stimulated to a greater extent by Bios II *A* than by the fuller's earth filtrate factor. It is difficult at this time to provide an adequate explanation of this phenomenon; it is possible, however, that the sensitivity of the organism to varying concentrations of the active principles accounts for the apparent discrepancy observed in the stimulating abilities of accessory factors, which resemble each other in many respects. The activation produced by enrichment of milk with the fuller's earth adsorbate factor is practically identical with that obtained by the addition of Bios II *B* in the case of both micro-organisms.

A study of the influence of the eight fractions prepared from Bios II *A*, Bios II *B*, the fuller's earth filtrate factor, and the fuller's earth adsorbate factor on the activity of the micro-organisms shows clearly that a relation exists between the Bios constituents and the heat-stable components of the Vitamin-B complex.

On the basis of the adsorption reactions employed for the preparation of these fractions, a close resemblance in the acid-stimulating abilities of Fractions 1 and 5, 2 and 7, 3 and 6, 4 and 8, respectively, is to be expected. The results detailed in Table I bear out this expectation. It is evident that we are dealing with only four distinct fractions. The fractions that are adsorbed by fuller's earth but not by charcoal, Fractions 2 and 7, are inactive. Marked stimulating ability is to be found, however, in all other fractions. It is apparent that we are concerned with three distinct activating entities: a factor adsorbed by charcoal and by fuller's earth, Fractions 4 and 8; a factor adsorbed by charcoal but not by fuller's earth, Fractions 3 and 6; and a factor that is not adsorbed by either charcoal or fuller's earth, Fractions 1 and 5.

Confirmation of these results was obtained when the solutions resulting from the treatment of the respective active fractions with phosphotungstic acid were employed as enriching entities. Of the active factors, only the one adsorbed by both fuller's earth and charcoal is precipitated by phosphotungstic acid. Regardless of the order in which the adsorbents are employed for the separation of the respective fractions, corresponding pairs of factors react similarly in so far as their precipitability by phosphotungstic acid is concerned. Although neither of the factors that are adsorbed by charcoal but not by fuller's earth is precipitated by phosphotungstic acid, a difference in the behavior of the respective solutions containing this factor towards phosphotungstic acid was observed. Fraction 3, which was prepared by adsorption on charcoal prior to treatment with fuller's earth, yielded no precipitate, and the factor became inactivated by the addition of phosphotungstic acid. Fraction 7, on the other hand, yielded a phosphotungstic acid precipitate, the filtrate retaining the stimulating activity of the fraction.

Fractionation of Bios II A yielded two fractions, only one of which was active, Fraction 1. Fraction 5, obtained from the fuller's earth filtrate factor, exhibited similar chemical, physical, and biological characteristics. On the basis of its chemical and physical properties, the Bios II A of Miller would appear to be identical with the liver filtrate factor described by Elvehjem and Koehn, and Lepkovsky and Jukes.

Treatment of Bios II B with fuller's earth yields two active components, Fractions 3 and 4, a filtrate factor not precipitable by phosphotungstic acid, and an adsorbate factor precipitable by this reagent. Fraction 6, obtained from the fuller's earth filtrate factor, was similar to Fraction 3. Fraction 8, the fraction adsorbed by charcoal from the fuller's earth adsorbate factor, resembled Fraction 4.

The activating constituent of Bios II B not adsorbed by fuller's earth is similar to the fuller's earth filtrate factor described by Edgar and Macrae.

From a study of the properties of the other active component of Bios II B, adsorbed by fuller's earth and precipitated by phosphotungstic acid, it would appear that this activator is distinct from any of the dietary factors of the Vitamin-B complex described by various workers. It resembles in certain respects the Vitamin B_6 of Birch and György and the factor obtained from rice bran extracts by Lepkovsky and co-workers. Unlike Vitamin B_6, this component of Bios II B is adsorbed by Norite charcoal even at pH 6.

To establish more clearly the relation between the Bios factors and the constituents of the Vitamin-B complex, fractionation of liver and yeast extracts, the principal materials used as sources of the B-vitamins, was undertaken.

When an aqueous extract of either of these materials, autoclaved for five hours at 120° C., was fractionated, the stimulating abilities of the resulting activators were found to be similar to those of corresponding entities prepared from canned tomato juice. Thus, canned tomato juice, autoclaved yeast

extract, or autoclaved liver extract may serve as sources of the three distinct activators.

In an attempt to obtain further evidence supporting the hypothesis that two of the three activators required by the lactic acid bacteria are similar to the factors described by Edgar and Macrae, fractionation of an autoclaved extract of brewers' yeast was carried out, the method described by these workers being followed in strict detail. In their procedure, adsorption with fuller's earth is carried out directly on an acid extract of the material, without an intervening tannic acid and lead acetate precipitation. Fractions corresponding to their fuller's earth adsorbate and filtrate factors were prepared.

The filtrate remaining after successive treatment with fuller's earth and charcoal should contain the Bios II A entity. This filtrate did exhibit slight stimulating ability, which however did not approach that exhibited by Fractions 1 and 5, obtained when the procedure of Miller, using a tannic acid and a lead acetate precipitation, was employed. It would appear that in the procedure of Edgar and Macrae this factor may be partially removed by treatment with fuller's earth. Although we have not carried out tests on the activity of the washings of the fuller's earth prior to elution, it is possible that the II A factor may be found therein. Of the two factors described by Edgar and Macrae, one is adsorbed by charcoal and the other by both charcoal and fuller's earth. It is to be noted that Edgar and Macrae do not describe a factor possessing the properties of Fractions 1 and 5. As shown above, each of these fractions is identical with Bios II A and the liver filtrate factor of Elvehjem and Koehn, and is not to be found in appreciable quantities in the filtrate after treatment of an activated yeast extract with fuller's earth and charcoal after the manner of Edgar and Macrae.

If the Bios II B fraction, which contains the two factors described by Edgar and Macrae, was prepared from an unautoclaved extract of brewers' yeast, it was found to exert only a slight influence on the acid-producing abilities of the micro-organisms. Subsequent autoclaving of this fraction, however, resulted in an increased activity approximating the activity possessed by the Bios II B prepared from an extract of yeast autoclaved prior to fractionation.

The three activators were also separated from an autoclaved extract of fresh hog's liver, by use of the procedures employed in the fractionation of brewers' yeast. No Bios II A activity was obtained when direct adsorption with fuller's earth and charcoal was employed. Unless the liver extract was autoclaved prior to fractionation, the Bios II B fraction possessed only slight stimulating activity.

On consideration of the results as a whole, it is evident that three distinct growth stimulants other than Bios I (inositol) are present in tomato juice, autoclaved yeast extract, and in autoclaved liver extract, and that these activators are essential for the most intensive metabolism of certain lactic acid bacteria. One of these activators is Bios II A, and the other two have been shown to be components constituting Bios II B.

Although it has been impossible to carry out confirmatory biological testing of the factors on laboratory animals, the nature of the physical and chemical characteristics of the activators, combined with the results obtained when lactic acid micro-organisms have been used as an index of the activating power of the entities, strongly suggests that these factors required by the lactic acid bacteria are identical with certain of the heat-stable accessory food factors of the Vitamin-B complex.

References

1. BIRCH, T. W. and GYÖRGY, P.   Biochem. J. 30 : 304-315.   1936.
2. DEAS, J.   J. Biol. Chem. 61 : 5-8.   1924.
3. EAGLES, B. A., WOOD, A. J., and BOWEN, J. F.   Can. J. Research, B, 14 : 151-154.   1936.
4. EDGAR, C. E., MACRAE, T. F., and VIVANCO, F.   Biochem. J. 31 : 879-885.   1937.
5. EDGAR, C. E. and MACRAE, T. F.   Biochem. J. 31 : 886-892.   1937.
6. EDGAR, C. E. and MACRAE, T. F.   Biochem. J. 31 : 893-902.   1937.
7. ELVEHJEM, C. A. and KOEHN, C. J.   J. Biol. Chem. 108 : 709-728.   1935.
8. GYÖRGY, P.   Biochem. J. 29 : 741-759.   1935.
9. LEPKOVSKY, S. and JUKES, T. H.   J. Biol. Chem. 114 : 109-116.   1936.
10. LEPKOVSKY, S., JUKES, T. H., and KRAUSE, M. E.   J. Biol. Chem. 115 : 557-566.   1936.
11. LUCAS, G. H. W.   J. Phys. Chem. 28 : 1180-1200.   1924.
12. MILLER, W. L.   Trans. Roy. Soc. Canada, 30, III : 99-103.   1936.
13. MILLER, W. L., EASTCOTT, E. V., and MACONACHIE, J. E.   J. Am. Chem. Soc. 55 : 1502-1517.   1933.
14. ORLA-JENSEN, S., OTTE, N. C., and SNOG-KJAER, A.   The vitamin and nitrogen requirements of the lactic acid bacteria.   D. Kgl. Danske Vidensk. Selsk. Skrifter, Naturv. og Math. Afd., 9, Raekke, VI. 6.   Copehagen.   1936.
15. SADLER, W., EAGLES, B. A., and PENDRAY, G.   Can. J. Research, 7 : 370-377.   1932.
16. SADLER, W., EAGLES, B. A., BOWEN, J. F., and WOOD, A. J.   Can. J. Research, B, 14 : 139-150.   1936.
17. SNELL, E. E., STRONG, F. M., and PETERSON, W. H.   Biochem. J. 31 : 1789-1799.   1937.
18. WILLIAMS, R. J., WILSON, J. L., and AHE, F. H. V. DER.   J. Am. Chem. Soc. 49 : 227-235.   1927.
19. WILLIAMS, R. J. and BRADWAY, E. M.   J. Am. Chem. Soc. 53 : 783-789.   1931.
20. WILLIAMS, R. J. and SAUNDERS, D. H.   Biochem. J. 28 : 1887-1893.   1934.

STUDIES ON LIGNIN AND RELATED COMPOUNDS

XXXIII. ISOLATION OF ACETOVANILLONE FROM WASTE SULPHITE PULP LIQUOR[1]

By Irene K. Buckland[2], George H. Tomlinson II[3]
And Harold Hibbert[4]

Abstract

Waste sulphite pulp liquor (obtained in the manufacture of a commercial sulphite pulp from soft woods, principally spruce and balsam) on treatment with aqueous alkali gave vanillin, acetovanillone, phenolic substances, and a tarry resinous product. The yield of acetovanillone is about 5.5% of that of the vanillin formed, or about 0.3% calculated on the basis of the lignin present.

Introduction

In a previous note (3) announcement was made of the discovery that small quantities of acetovanillone can be obtained from waste sulphite pulp liquor (from soft wood). In the present communication a description is given of the isolation of this compound, and its identification with the pure synthetic product.

A commercial waste sulphite pulp liquor on similar treatment yielded, in addition to vanillin, a viscous oil, which, after treatment, was found to contain *(a)* phenolic substances, *(b)* a crystalline solid, and *(c)* a residual tar, in yields of 3.2, 5.5, and 49.5%, respectively, of the weight of the vanillin found.

The crystalline solid, after suitable purification, was shown to be acetovanillone, identical in all its physical and chemical properties with the pure synthetic product.

The phenolic substances and the tarry residue are being investigated.

The fact that acetovanillone gives no precipitate with *m*-nitrobenzoyl hydrazine proves that its presence does not interfere with the estimation of vanillin by means of this reagent (6).

Experimental

Waste sulphite liquor* (114 litres), obtained in the commercial manufacture of a sulphite pulp from soft woods (principally spruce and balsam), was heated with sodium hydroxide under pressure, and the vanillin (297.5 gm.) extracted from the reaction mixture with benzene, the procedure previously outlined for the small-scale preparation (6) being followed. Removal of the

solvent left 178.3 gm. of a dark viscous oil, which was distilled under reduced pressure. Three fractions were isolated. Fraction 1 (9.7 gm.) was a mixture of phenolic substances, b.p. 56° to 86° C. at 5.2 mm. initial pressure—diminishing to 1 mm. as the distillation proceeded; Fraction 2, b.p. 140° to 160° C. at 2 mm., bath temperature 230° C., crystalline solid (16.4 gm.); Fraction 3, residual tar (147.2 gm.).

Identification of the Crystalline Product (Fraction 2)

This was redistilled and gave two fractions: *(a)* a mixture of an oil with a crystalline solid (1.0 gm.), b.p. 60° to 80° C. at 2 mm.; *(b)* a white crystalline solid as principal fraction, b.p. 157° to 180° C. at 1.7 mm. On recrystallization of the latter product from benzene it was obtained in the form of broad colorless leaflets, m.p. 114.5° C.; OCH_3, 18.7, 18.6%. Calcd. for acetovanillone: $(C_9H_{10}O_3)$: OCH_3, 18.68%.

The semicarbazone was prepared from semicarbazide hydrochloride and sodium acetate in alcohol solution (50%); m.p. 165.5° to 166° C.

Identity of the Crystalline Product with Synthetic Acetovanillone

Attempts to prepare acetovanillone from guaiacol acetate by treatment with anhydrous aluminium chloride (4) were unsuccessful, the acetate being recovered unchanged. A similar result was found by Barch (2), who, however, by using the modified procedure of Baltzly and Bass (1), showed that the Fries rearrangement could be carried out in nitrobenzene as solvent.

Method

A solution of aluminium chloride (34 gm.) in 125 gm. of nitrobenzene was added, with stirring, to 25 gm. of guaiacol acetate; the mixture was then cooled to 0° C. and stirred for 20 hr. at room temperature. The orange-red reaction mixture was poured on cracked ice, and then extracted with three volumes of ether. The extract was neutralized by shaking with aqueous bicarbonate. The ether was evaporated off and the residue distilled under diminished pressure. The nitrobenzene and guaiacol acetate distilled over at 77° to 81° C. at 2.2 to 1.0 mm., and then 12 gm. of an oily solid at 132° to 140° C. at 1.0 mm. The latter fraction was purified by recrystallization from benzene and obtained in the form of fine white needles; yield, 6.0 gm. m.p. 115° C.; (m.p. reported (5) 115° C.).

A mixture of this and the acetovanillone obtained from waste sulphite pulp liquor showed no lowering in melting point (114° to 115° C.).

The semicarbazone of the synthetic acetovanillone was prepared in the manner described above; m.p., 164.5° to 165.5° C.; mixed melting point with previous preparation, 164.5° to 165.5° C.

Reaction with Ferric Chloride

Both preparations of acetovanillone (synthetic, and that from waste sulphite pulp liquor) gave the same typical reaction with ferric chloride; namely, a blue coloration which disappeared on heating, owing to precipitation of dehydro-diacetovanillone.

Attempted Preparation of m-Nitrobenzoyl Hydrazone of Acetovanillone

Acetovanillone was found to give no precipitate with *m*-nitrobenzoyl hydrazine (such as is obtained with vanillin) by the method described previously (6).

References

1. BALTZLY, R. and BASS, A., J. Am. Chem. Soc. 55 : 4292-4294. 1933.

2. BARCH, W. E. J. Am. Chem. Soc. 57 : 2330. 1935.

3. BUCKLAND, I. K., TOMLINSON, G. H. and HIBBERT, H. J. Am. Chem. Soc. 59 : 597.
      1937.

4. MOTTERN, H. J. Am. Chem. Soc. 56 : 2107-2108. 1934.

5. TIEMANN, F. Ber. 24: 2855–2862. 1891.

6. TOMLINSON, G. H. and HIBBERT, H. J. Am. Chem. Soc. 58 : 345-353. 1936.

AN ALKALOID FROM *DELPHINIUM BROWNII* RYDB.[1]

By Richard H. F. Manske[2]

Abstract

Delphinium brownii contains a total of 0.5% of alkaloids, hydrolysis of which yields a crystalline base, probably $C_{22}H_{37}O_7N$ or $C_{23}H_{39}O_7N$, together with anthranilic and methylsuccinic acids. Mannitol is present in considerable amounts.

The chemistry of the *Delphinium* alkaloids, even more so than that of the *Aconitum* alkaloids, is still in the earliest stages of development. Though both classes have been known for many years, little knowledge of the constitution of even a single individual is available. The classical methods employed for the structural study of many other alkaloids fail entirely, or yield results which at present are not susceptible of satisfactory interpretation. The nature of the functional groups in aconitine appears now to have been established (1) although the carbon skeleton remains to be determined.

Most of the positive results in the chemistry of these alkaloids, which, because of their closely related botanical origin may be considered chemically similar, are confined to hydrolytic cleavage, identification of the acid fragments, and characterization of the basic moiety. Benzoic and acetic acids are commonly obtained. Several of the aconite alkaloids have yielded anthranilic acid which itself is combined with succinic acid in the form of an anil (3).

The alkaloid now obtained from *Delphinium brownii* Rydb. belongs to the anthranilic type, in that hydrolysis yields anthranilic acid. Instead of succinic acid, however, the corresponding anil is derived from methylsuccinic acid, and this appears to be the first isolation of the latter from natural sources. It may be pertinent to point out that methylsuccinic acid contains the isoprene carbon skeleton which is also present in tiglic and angelic acids, $\beta\beta$-dimethylacrylic acid (senecioic acid), and reductic acid, all of which occur naturally. The hypothesis that the *Delphinium* and *Aconitum* alkaloids are isoprene derivatives is an attractive one. However, selenium dehydrogenation, which has been so conspicuously successful with terpenes and steroids, is of less utility with nitrogenous bases.

The main alkaloid of *Delphinium brownii* Rydb., for which no name is as yet proposed, has not been obtained crystalline. Combination with a number of acids which include hydrochloric, sulphuric, acetic, oxalic, nitric, perchloric, and phosphoric has likewise failed to yield a crystalline product. Hydrolysis with methanolic potassium hydroxide yields, in addition to the organic acids already mentioned, a well crystallized base, which was also isolated without intentional hydrolysis from the crude alkaloid. No ultimate proof of the homogeneity of the hydrolytic base is available. Nevertheless, its repeated preparation and apparently identical properties when

different lots of plant material were examined can scarcely be coincidental. Analytical figures are intermediate between those for $C_{22}H_{37}O_7N$ and $C_{22}H_{39}O_7N$, and the presence of three or four methoxyl groups is indicated. Molecular weight determinations indicate a smaller molecule, and $C_{20}H_{33}O_6N$ containing three methoxyls is not entirely excluded. An attempt to obtain a benzoyl derivative yielded an amorphous product, and a decision as to the correct formula must await further work.

Finally, it may be mentioned that *D. brownii*, like many other *Delphinium* species (2), contains a relatively large amount of mannitol.

Experimental

Isolation of the Total Alkaloids

The plant was collected in southern Alberta, where it grows wild. The dried and ground aerial portion was extracted with methanol and the solvent removed from the extract. Water was added and sufficient hydrochloric acid to insure acidity to Congo red. The mixture was heated on a steam bath to coagulate the fats and resin, and then cooled. In general it was then possible to decant the clear aqueous solution from the insoluble portion. (It is convenient to work with such dilutions that a litre of final extract is prepared from 1 to 2 kilos of plant material.) The aqueous solution was filtered with a little charcoal and extracted several times with ether (LC). It was then basified with excess ammonium hydroxide and extracted with ether until no more extract was obtained. In some experiments a small amount of the total base crystallized from the concentrated ether extract. This proved to be identical with the hydrolytic base described later. It was difficult to purify, and the author is greatly indebted to Dr. E. H. Charlesworth for carrying out this purification and identification.

The crude total alkaloid was dissolved in dilute oxalic acid and the filtered solution repeatedly extracted with ether. When this solution was basified with potassium hydroxide and the base again extracted with large volumes of ether, a pale colored alkaloid containing virtually no neutral material was obtained. The yield by this procedure was 0.50%.

In an earlier attempt to obtain a single individual in a crystalline condition, an ethereal solution containing 40 gm. of total alkaloid was fractionally extracted with six successive equal portions of dilute hydrochloric acid, and the base regenerated from each extract. The last two were combined, and thus five fractions of alkaloid were obtained. No crystalline material was obtainable from any of these fractions. Hydrolysis with alkali yielded in each case approximately the same amount of crystalline hydrolytic base.

Isolation of Mannitol

The ammoniacal solution from which the crude alkaloid had been extracted was filtered and evaporated *in vacuo* to a thick syrup. This was extracted with successive portions of hot methanol, and the extracts were evaporated

to a thin syrup. After several days the crystalline product which had separated was filtered off. It was then recrystallized from dilute methanol, 95% ethanol, and water in the order named. It then melted at 166° C.* either alone or in admixture with an authentic specimen. The author takes this opportunity to note that the same carbohydrate alcohol has been found in relatively large amounts in *Lactarius deceptivus* Pk. The estimated total amount of mannitol in the *Delphinium* is about 1.5%.

Hydrolysis of the Alkaloid

A solution of the purified alkaloid in methanol was treated with twice its weight of potassium hydroxide in 50% aqueous solution. It was heated on a steam bath for 12 hr., diluted with water, and the methanol evaporated. During the last-mentioned process the crude hydrolytic base gradually crystallized. After cooling, the mixture was filtered and washed with water and ether alternately. There remained a colorless crystalline residue which was further purified by recrystallizing from ether in a Soxhlet extractor. Final purification was effected by dissolving a portion in dilute methanol and adding hot water and a nucleus to the filtered solution. As thus obtained, this base melts at 120° to 121° C., some sintering taking place several degrees lower. For analysis the substance was dried in a high vacuum over phosphorus pentoxide for 24 hr. Found: C, 62.12, 62.14; H, 8.62, 8.86; N, 3.30; 3.22; OMe, 26.10, 29.26, 23.51, 25.23%. M.W. 307, 315 (Rast). Calcd. for $C_{22}H_{37}O_7N$: C, 61.82; H, 8.67; N, 3.28; 3 OMe, 22.81%. The optical activity of $[\alpha]_D^{22} = +52.2°$ ($c = 0.8$ in methanol) points to a similarity to, if not identity with, lycoctonine (3).

The ether washings from the crude base deposited a small amount of crystalline material on long standing, and a further small amount was obtained by repeating the hydrolysis. There remained a not inappreciable amount of virtually colorless resinous base, the examination of which is still in progress.

Isolation of Anthranilic and Methylsuccinic Acids

The aqueous alkaline filtrate from the preparation of the above-mentioned crystalline base was rendered just acid with hydrochloric acid and filtered from a small amount of amorphous precipitate. It was repeatedly extracted with ether, and the combined extracts were evaporated to a small volume. The crystalline product thus obtained was filtered off and recrystallized three times from hot water. It melted at 145° C. and this melting point was not depressed when the substance was admixed with a specimen of anthranilic acid. Esterification with methanol yielded the characteristic odor of synthetic grape flavor. Calcd. for $C_7H_7O_2N$; C, 61.31; H, 5.11; N, 10.22%. Found: C, 61.27; H, 5.13; N, 10.40%.

The filtrate from the crude anthranilic acid was evaporated to dryness and the residue recrystallized twice from dry ether. It was obtained in colorless fine prisms which melted at 112° C. and showed no optical activity

* *All melting points are corrected.*

in water ($c = 0.8$).   When it was admixed with a specimen of synthetic methylsuccinic acid melting at 114° C., there was no observable depression in melting point.   It gave the characteristic fluorescine test with great brilliance when heated with resorcinol and sulphuric acid.   Calcd. for $C_5H_8O_4$; C, 45.46; H, 6.06%.   Found: C, 45.67; H, 6.18%.

No indication of the presence of acetic, benzoic, or other acids was obtained in any of the hydrolysis experiments.

References

1. FREUDENBERG, W.   Ber. 69 : 1962-1965.   1936.
2. JARETZKY, R. and SCHAUB, C.   Arch. Pharm. 271 : 171-174.   1933.
3. SCHULZE, H. and BIERLING, E.   Arch. Pharm. 251 : 8-49.   1913.

A NEW METHOD FOR THE DETERMINATION OF VARIOUS FIBRES IN MIXTURES, WITH SPECIAL REFERENCE TO THE DETERMINATION OF LANITAL IN WOOL-LANITAL MIXTURES[1]

By P. Larose[2]

Abstract

The method of Da Schio (1) for the determination of lanital in lanital-wool mixtures has been tried and found to be unreliable. A new and satisfactory method has been developed. This method makes use of the difference in the specific gravities of wool and lanital to separate the fibres by means of a liquid of intermediate specific gravity. The Herzog-Skinkle method has been found to give results that are a little high. The method devised by the author is also applicable to wool-cotton and wool-staple rayon mixtures. Results of tests carried out on various mixtures and by various methods are given.

No special difficulties have been experienced in the determination of various types of fibres in mixtures. The fibres that were usually found together differed sufficiently in some chemical property to make a separation by chemical means possible, with a reasonable degree of success. However, with the introduction of lanital-wool* mixtures, a new problem presented itself; that of separating two fibres differing little in chemical properties. The difficulty is very similar to that encountered when the separation of cotton and viscose rayon was studied. It was found that differences in solubility in solutions of calcium thiocyanate gave a fairly good separation of the fibres. Da Schio proposed for the separation of lanital from wool a method based on the same principle, *i.e.*, the difference in rate of solubility of the two fibres in sodium hydroxide solutions.

The writer briefly reviewed Da Schio's method in a previous article (2) and pointed out its weakness. Further reference will be made to his method subsequently.

The problem was approached in a different manner by the writer, who tried to effect a separation by virtue of the difference in specific gravities of various fibres.

Following preliminary experiments which indicated that such a method would be feasible, determinations were made on two wool-lanital fabrics and on a wool-lanital top, which were the only samples available to the author. Unfortunately, all contained about equal quantities of lanital and wool, so that the method has not been given a fair trial with a wide variety of fabrics.

The principle of the method is such that its application is not limited to lanital-wool mixtures. With wool-cotton and wool-viscose rayon mixtures the method gave results that agreed well with those obtained with standard chemical methods, as the figures given later will show.

Da Schio's Method

In order to try out the method proposed by Da Schio, two mixtures were prepared from known quantities of pure wool and pure lanital. The first contained 66.8% of lanital by weight; the other, 38.1%.

The directions given by Da Schio were closely followed except as regards the temperature, which, inadvertently, was allowed to rise from 31° to 35° C. during the tests, and the results obtained were 59.3 and 34.7%, respectively, for the two mixtures, when the correction of 12.3% for the loss of lanital was made as required by Da Schio's method. However, the lanital blank, carried out simultaneously, gave a loss of 21.7%. If this figure is used in correcting for the loss of lanital, the calculated results are 66.4 and 38.9%, respectively, which show very good agreement with the actual amounts. It must be emphasized, nevertheless, that such agreement is possible only when a blank determination is made at the time that the samples are analyzed, and probably only when the same type of lanital as that present in the mixtures is used. These conditions obtained in the above-mentioned test. The difference between the 21.7% loss noted in the experiment and that of 12.3% given by Da Schio is due in part to the fact that the average temperature (33° C.) in this experiment was 2° higher than that recommended by Da Schio.

A wool-lanital top supposed to contain 50% of lanital was analyzed by this method, and at the same time a blank determination was made with some pure lanital tops obtained from the same source. The blank showed a loss in lanital of 9.2%, which gave a corrected figure of 49.3% of lanital in the mixed top.

A determination carried out subsequently on the pure lanital top treated in the same way showed a loss of 13.7%. The difference between this figure and the previous result of 9.2% may be due to some small change in the conditions of the experiments. These figures suffice to show the sensitivity of the method to small changes in the experimental conditions, and, no doubt, to differences between various lots of lanital.

The extreme precaution that has to be taken to obtain good results by this method makes it rather inconvenient for routine testing.

Separation Based on Differences in Specific Gravity
(Flotation Method)

Preliminary experiments indicated that although the difference in the specific gravities of lanital and wool is small, it is sufficient to enable a separation to be made by a flotation method. Lanital sinks in a liquid of specific gravity 1.300, but floats in one of specific gravity 1.310; wool floats in a liquid of specific gravity 1.320 but sinks in one of specific gravity 1.310. Consequently, if wool and lanital are present in a liquid of specific gravity 1.310, the lanital should float and the wool should sink, provided that the fibres are free to separate.

The success of the author's method depends largely upon the cutting of the yarn—the cut pieces should be as short as possible so as to permit easy

separation in the liquid. With the lanital-wool yarn investigated, the writer obtained good results with lengths of 1 mm. or less. The best length depends on the twist and the parallelism of the fibres of the yarn; the more twisted and the less parallel the fibres, the shorter they should be cut. Since the yarn tested had very little twist, the 1 mm. length probably represents the maximum length consistent with good results in the analysis of any yarn. The time of cutting is decreased considerably by holding several strands of the yarn together between the thumb and forefinger of the left hand and cutting them with sharp scissors, the bunch of yarns being pushed along as the cutting progresses.

When a sufficiently large sample of the cut ends has been obtained, it is transferred to the liquid adjusted to the correct specific gravity. The size of the sample may vary with the size of the vessel in which the separation is to be made. The writer found it best to use a large test tube, about 1 in. in diameter, and a sample weighing from 0.2 to 0.3 gm. The liquid used is a mixture of toluene and carbon tetrachloride. Other liquids could be employed, of course, but these two are very convenient as they are generally found in most laboratories.

The cut material is transferred to the test tube, and the liquid is added until the vessel is about three-quarters full. The tube is closed with a stopper, and the contents well shaken in order to separate the small bits of fibres. It is then left standing in an upright position and time allowed for the lanital to rise to the top and the wool fibres to sink. Two hours was generally found to be sufficient, although sometimes a longer period was required for proper separation to take place.

The tube is then opened and about half the liquid, carrying the floating lanital, is decanted into a filter paper in a funnel. Care must be taken during this operation not to agitate the tube so as to disturb the wool which has settled at the bottom. The remaining portion of the liquid with the wool is then poured on another filter paper. The separated fibres are then dried and weighed. The writer prefers weighing both portions of the separated fibres rather than weighing the original sample and then only one portion of separated fibres; the lanital, for example. If for any reason the separation fails, the operation of the original weighing is saved.

Since the regain of lanital is only slightly higher than that of wool, it is not necessary for practical purposes to weigh the fibres in the dry condition; it is sufficient to let them condition in the laboratory before weighing.

The success of the separation can be verified by examining some of the separated fibres under the microscope; any admixture of wool fibres with the lanital, or *vice versa*, is easily discerned. In general, the amount of one fibre mixed with the other was found to be small, but when it was fairly large each of the separated portions was treated in the same manner as the original sample, and in this way a complete separation was effected. The possibility of checking the complete separation of the fibres in this way is a decided advantage.

The small quantity of material necessary for the test is also an advantage when the sample available is small, although it may not be as representative of the whole fabric as a larger sample would be. The method is so simple, however, and involves so little work that if a representative result is desired, several determinations can be made simultaneously with yarns taken from various parts of the cloth.

In the wool-lanital fabric tested by the writer, the variation along the yarn was fairly large, and several determinations had to be carried out to obtain a fair average value. It seems that the spinning of wool-lanital yarn offers some difficulties, and that the technique is not yet such that a yarn of constant composition throughout its length can be spun.

In order to check the method, the correct percentage of lanital in the fabric had to be known. To obtain this value, the writer had recourse to the tedious procedure of separating by hand the individual fibres in small samples and examining them under the microscope. The separated fibres were weighed on a micro-balance. It was found later that this separation could be made easier by dyeing the yarn with a dye such as Direct Sky Blue F.F. This dyes the lanital fibres directly from a cold water solution, but the wool is hardly affected. This is applicable, of course, only to light-colored fibres. By examining against a dark background the fibres picked from the yarn, it was fairly easy with the naked eye to distinguish the lanital from the wool fibres. The length of yarn used for the separation by means of the microscope was 3 in. while that employed in the separation of the dyed fibres by naked eye was 6 in. The dyeing of the yarn, however, introduced a complication in the determination owing to the increase in weight of the lanital resulting from the addition of the dye. A correction had to be made for this increase. This was determined by means of a blank test with a yarn weighed before and after dyeing.

Results

The first wool-lanital fabric on which most of the tests were performed was a checked material made from four colored yarns; yellow, white, grey, and brown in both warp and weft. Reference has already been made to the variation in lanital content. The following figures represent the percentage of lanital as determined by visual separation:

        Yellow: warp, 51.8
                 weft, 47.8, 46.8, 47.9, 46.9
        Grey: warp, 51.6
                 weft, 48.6, 43.2, 48.3
        White: warp, 49.9
                 weft, 50.8, 48.0, 52.0
        Brown: warp, 48.5
                 weft: 49.7, 42.7

Mean of all results, 48.4% lanital.

Owing to this high variation from sample to sample, it is difficult to judge, by comparison with these results, the accuracy of any one determination by the flotation method. However, as pointed out before, a microscopic examination of the separated fibres would show to what degree the separation had been successful, and hence would indicate roughly the degree of accuracy.

The following are the results obtained with the flotation method, the percentage of lanital being given:

Yellow: warp, 51.5, 53.5
weft, 51.6, 48.0, 42.9
Grey: warp, 46.8
weft, 46.8, 50.6, 44.1
White: warp, 50.2, 55.0, 44.9
weft, 48.2, 50.8, 43.5, 47.2, 50.8
Brown: warp, 53.8, 49.0
weft, 48.3
Mixed yarns: 47.2, 48.3
Mean of all results, 48.8% lanital.

The wool-lanital top that was used in testing Da Schio's method was also analyzed by the flotation method. Two determinations gave 49.3 and 48.2% of lanital, while a separation by visual means gave 48.9% of lanital.

A second lanital-wool fabric was analyzed. This was a small piece taken from an advertisement in a textile periodical. It was said to contain 50% of lanital and 50% of wool. The flotation method gave 50.8% of lanital. This determination was made with only 0.11 gm. of material.

A small sample, 0.13 gm., of this fabric, tested according to Da Schio's method, showed 45.7% of lanital when a loss of 12.3% was used as a blank correction, but 51.1% when 21.7% was the correction employed.

Determination of Lanital by the Herzog-Skinkle Method

Skinkle (3) used a modification of a method first proposed by Herzog for the determination of mohair in wool-mohair mixtures. In Herzog's method, in which the composition of the blend is determined by examining the fibres under a microscope and counting the number of each kind, use is made of the formula

$$\text{Percentage of Fibre } A = \frac{N_a G_a}{N_a G_a + N_b G_b} \times 100$$

where N_a is the number of fibres of constituent A,
  N_b is the number of fibres of constituent B,
  G_a is the weight of Fibres A per unit length,
  G_b is the weight of Fibres B per unit length.

The fibres are so cut that the average lengths of Fibres A and B are approximately the same.

Skinkle assumes that animal hairs are circular and that all have the same density. The weight per unit length would, therefore, be proportional to d^2, d being the diameter of the fibre. The formula then reduces to

$$\text{Percentage of Fibre } A = \frac{N_a d_a^2}{N_a d_a^2 + N_b d_b^2} \times 100 \,.$$

It is sufficient to count the number of fibres and to measure their mean diameter.

Since the apparent density of lanital differs from that of wool by only 1% or less, the error introduced in the percentage composition by assuming equal density would be, for a 1 : 1 mixture, about 0.25%, which, for all practical purposes, can be neglected.

The measurement of the diameter, on the other hand, has to be done very accurately to obtain good results.

In the fabric analyzed the mean diameter of the lanital fibres was found to be 22.2 μ, and that of the wool fibres, 20.6μ, these figures being the mean of those for 1100 fibres of each. An error of 0.2μ (which is not unreasonable) in the determination of the diameter would result in an error of 1% in the actual fibre content of the wool-lanital fabric tested.

Skinkle's method was applied to fibres cut in the same manner as those tested by the flotation method. It was assumed that, from the method of cutting, the average length of the wool fibres would be the same as that of the lanital fibres. Fourteen determinations were carried out on the various colored yarns and the same order of variation shown in the other methods was found. The mean of all determinations was 54.3% of lanital. If the difference in diameter was neglected and the percentage composition calculated from the number of fibres only, the value found for lanital was 51.0%. Similar results were obtained when $\frac{1}{4}$ in. sections of the yarn were cut, the fibres teased out, and counted under the microscope.

The method of cutting short lengths with two razor blades clamped together, as advocated by Skinkle, was also tried. The percentage of lanital found by counting fibres was 50.2%.

This method apparently gives, for the lanital in wool-lanital blends, results that are somewhat too high. This is perhaps due to the fact that the lanital fibres are not solid, but contain a number of cylindrical pores or canals which may be observed when the fibres are cross sectioned. The calculation of the percentage by means of Skinkle's formula is based on the supposition that the fibres are solid cylinders. If the lanital fibres are pierced by a series of longitudinal canals, the value used for the density in the transformation of Herzog's formula would have to be appreciably less than the true density of lanital.

Application of the Flotation Method to Other Blends

The application of the flotation method to the analysis of fibre mixtures other than wool-lanital is exemplified by the following results, which were obtained with two wool-staple rayon mixtures and two wool-cotton mixtures.

For the separation of the fibres in these mixtures, the toluene-carbon tetra-chloride solution was adjusted to a specific gravity (1.40) intermediate between that of wool and that of cotton or rayon.

The first wool-staple rayon yarn examined was from an automobile upholstery fabric. Analysis of the fabric by chemical means (sulphuric acid method) gave a wool content of 45.8% in the warp and 42.9% in the weft, while the corresponding figures by the flotation method were 49.6 and 47.5%. The high results of the flotation method are largely due to the presence of small bits of the original highly twisted yarn mixed with the wool.

Better results were obtained with the other wool-viscose yarn which was from a dress material and not twisted to the same extent. The percentages of wool in this material as found by various methods are:

By chemical means (H_2SO_4 method):   38.2, 37.3; mean 37.8%
By chemical means ($Ca(CNS)_2$ method):   38.4, 37.9; mean 38.2%
Separation of fibres under microscope: 36.8, 36.2; mean 36.5%
By flotation: 35.6, 35.6, 36.0; mean 35.7%

A second sample of a similar fabric gave

By H_2SO_4 method: 36.1%
By $Ca(CNS)_2$ method: 35.5%
By flotation method: 36.0, 35.2, 36.0%.

The wool-cotton mixtures analyzed were both flannels. The first sample, tested by the sulphuric acid method, gave 46.5 and 45.6% of wool; mean, 46.1%. The flotation method gave 47.0, 47.3, and 46.9%; mean, 47.1%.

The second sample analyzed in the same way gave 61.2% of wool by the sulphuric acid method, and 60.6 and 62.4%, or a mean of 61.5%, by the flotation method.

The figures quoted are sufficient to show that the flotation method gives results that, on the whole, compare very favorably with those obtained by means of the ordinary chemical methods. It has the advantage of requiring less manipulation, and, moreover, it is possible to check the accuracy of the results by examination of the fibres under the microscope.

References

1. DA SCHIO, E.   Boll. assoc. ital. chim. tessile color, 12 : 180.   1936.
2. LAROSE, P.   Can. Textile J. 54, 15 : 32-33.   1937.
3. SKINKLE, J. H.   Am. Dyestuff Reporter, 26 : 119-120.   1937.

THE ISOLATION OF GUAIACOL FROM WASTE SULPHITE LIQUOR

Buckland, Tomlinson, and Hibbert (1, 2) have reported the isolation of acetovanillone from a waste sulphite liquor from soft woods; this has now been shown to be a degradation product of pure lignin sulphonic acid (3). In addition, a volatile phenolic, unidentified oil was obtained by them which has now been identified, by means of its boiling point and the p-nitrobenzoyl and p-toluene sulphonic esters, as guaiacol. The ratio of acetovanillone to guaiacol was approximately 4 : 1.

Investigation of a similar oil from lignin sulphonic acid from hard woods is in progress.

1. BUCKLAND, I. K., TOMLINSON, G. H., and HIBBERT, H. J. Am. Chem. Soc. 59 : 597. 1937.
2. BUCKLAND, I. K., TOMLINSON, G. H., and HIBBERT, H. Can. J. Research, B, 16 : 54-56. 1938.
3. LEGER, F. J. and HIBBERT, H. J. Am. Chem. Soc. 60 : March, 1938.

FRANK LEGER
HAROLD HIBBERT

PULP AND PAPER RESEARCH INSTITUTE,
McGILL UNIVERSITY,
MONTREAL, CANADA.
MANUSCRIPT RECEIVED FEBRUARY 14, 1938.

THE CONVERSION OF FURFURYL ALCOHOL TO LEVULINIC ACID

Pummerer and co-workers (1, 2) have reported the conversion of furfuryl alcohol to methyl levulinate by the action of methanolic hydrochloric acid. Tchitchibabine (4, pp. 563-568) later confirmed the former authors' results.

The mechanism proposed for this conversion, involving the migration of a hydroxyl or methoxyl group from a 1 to a 5 carbon atom, this occurring either before or after ring opening, is clearly unsatisfactory. For this reason, a study of the reaction has been carried out in these laboratories.

The theory now proposed is similar to that offered by Scott and Johnson (3) for the conversion of furfuryl chloride to methyl pyromucic acid.

While addition of the elements of water is assumed in explaining the mechanism, those of methanol or mineral acid may actually be the ones which enter into the reaction. The first step involves 1 : 4 addition of the elements of water to the conjugated systems in furfuryl alcohol, followed by elimination in the carbinol and 2 position as shown (II).

$$\underset{\text{(III)}}{\overset{\displaystyle H_2C\text{——}CH_2}{O=C\diagdown_{O}\diagup C=CH_3}} \qquad \text{or} \qquad \underset{\text{(IV)}}{\overset{\displaystyle H_2C\text{——}CH}{O=C\diagdown_{O}\diagup C\text{—}CH_3}}$$

From II, through a 1,3 hydrogen migration and ketonization of the resulting enol, or migration of the conjugated system into the furane ring, α or β angelica lactone (III and IV respectively) is formed.

By ring opening through addition of water, or by addition of the elements of water to the double bond, the open chain or the ring form of levulinic acid is formed from (III) or (IV).

$$\overset{\displaystyle H_2C\text{——}CH_2}{\underset{\underset{OH}{\displaystyle O=C}}{}\qquad \underset{\underset{O}{\displaystyle C}}{}\text{—}CH_3} \qquad \text{or} \qquad \overset{\displaystyle H_2C\text{——}CH_2}{O=C\diagdown_{O\cdot}\diagup \overset{OH}{\underset{CH_3}{C}}}$$

This same mechanism is also capable of explaining the formation of levulinic acid from hydroxy methyl furfural, and of γ-keto pimelic acid from furyl acrylic acid. It also serves to explain many other anomalies associated with ring opening in the furane series.

Although the experimental proof of this mechanism is still somewhat incomplete, evidence has been secured for most of the intermediate steps. It is offered here since it appears that this conversion of furane. derivatives may have a definite bearing on the formation of lignin in the plant.

1. PUMMERER, R., BIRKHOFFER, L., and GUYOT, O. Ber. 68, B: 480-493. 1935.
2. PUMMERER, R. and GUMP, W. Ber. 56, B: 999-1008. 1923.
3. SCOTT, E. W. and JOHNSON, J. R. J. Am. Chem. Soc. 54 : 2549-2556. 1932.
4. TCHITCHIBABINE, A. E. Chimie et Industrie, Special No. March, 1932.

FRANK LEGER,
HAROLD HIBBERT.

PULP AND PAPER RESEARCH INSTITUTE,
McGILL UNIVERSITY,
MONTREAL, CANADA.

THE STRUCTURE OF LIGNIN

In recent investigations on the structure of lignin there has been a marked tendency to consider it either as derived from an oxyconiferyl aldehyde (Freudenberg) or as originating from an unstable carbohydrate, the latter undergoing a metamorphosis to lignin only during the process of extraction from the plant (Hilpert).

Neither view is supported by adequate experimental evidence and it is difficult to reconcile with such theories the recent discovery in ·these laboratories of guaiacol, vanillin, acetovanillone, syringic aldehyde, acetosyringone,

etc., as decomposition products of lignin sulphonic acids. On the other hand, these and numerous other reactions find a satisfactory explanation if the basic lignin building-constituent is viewed as arising from the condensation of guaiacol with fructose or one of its derivatives according to the following scheme:

In the case of the furane intermediates derived directly from fructose, it is not necessary that the furane ring should actually open in the initial stages of the synthesis. As is indicated in the preceding note, intermediates VII and VIII might very well originate by addition of water to the hypothetical ring (VI), derived from furfuryl alcohol, followed by ring opening through addition of water.

Each of these can then condense with one or two moles of guaiacol as shown above. Similarly the open-chain form of fructuronic acid can give rise to (III).

According to this "guaiacol theory of lignin formation", lignin represents essentially a condensation product of guaiacol with a 4-keto-oxy-pentanal

$$(-\overset{|}{\underset{|}{C}}-\overset{|}{\underset{|}{C}}O-\overset{|}{\underset{|}{C}}-\overset{|}{\underset{|}{C}}-\overset{H}{\underset{|}{C}}=O).$$

The many-sided character of the lignin complex, as will be shown in a forthcoming article, finds a satisfactory explanation when viewed from the above standpoint. In hard woods, the guaiacyl- is partly replaced by the syringyl-radical.

HAROLD HIBBERT.

PULP AND PAPER RESEARCH INSTITUTE,
McGILL UNIVERSITY,
MONTREAL, CANADA.

THE STRUCTURE OF DEXTRAN
NOTE ON "THE STRUCTURE OF DEXTRAN SYNTHESIZED BY THE ACTION OF *LEUCONOSTOC MESENTERIOIDES* ON SUCROSE" BY FOWLER, BUCKLAND, BRAUNS, AND HIBBERT[1]

BY F. E. BRAUNS[2]

Since a preliminary experiment on the alcoholysis of methylated dextran revealed that three different methylated methyl glucosides are obtained, two principal requirements must be fulfilled in order to determine the structure of dextran: first, the dextran must be methylated completely, as on hydrolysis of an incompletely methylated dextran more lower-methylated glucoses are obtained; second, the different methylated glucosides have to be separated quantitatively in order to determine the exact ratio of dimethyl, trimethyl, and tetramethyl methyl glucosides. Such a quantitative separation cannot be carried out by fractional distillation, as has been confirmed by other carbohydrate chemists.

Such a quantitative separation has *not* been accomplished in the work described, and therefore it is not possible to decide definitely the structure of dextran. In Experiment I, in which 7.5 gm. of the original hydrolysis products was separated, the loss during the separation was .18.4%, and, when this loss is allocated *pro rata* to these methyl glucoside fractions, the corrected yields are 1.70, 4.34, and 1.47** gm. for dimethyl, trimethyl, and tetramethyl methyl glucosides, respectively, as given in Table I of the paper. These corrected values, however, are not used in the calculation of the yields of methyl glucosides in the various ratios. If the corrected values as given in percentage in Column 3 of Table A are used, the actual yields of the three glucosides, compared with those calculated for a ratio of 1 : 3 : 1, would be 120.5, 96.4, and 92.5%, respectively, instead of 99.3, 78.3, and 75.5. This experiment, therefore, actually indicates that dextran is not a 1 : 3 : 1 polymer. If, however, the loss is allocated to the trimethyl and tetramethyl methyl glucosides only, on the assumption that the loss first occurred during the separation of these two, as indicated in Experiment II, the corrected values as given in Column 4 are obtained; these agree with the

---

TABLE A

YIELDS OF METHYL GLUCOSIDES

Methyl glucoside isolated	Yield from 7.5 gm. of hydrolyzed methylated dextran				Yield from 4.55 gm. hydrolyzed methylated dextran			Theoretical yield of dimethyl, trimethyl, and tetramethyl methyl glucosides in %, on the basis of the ratios shown			
	Gm.	%	Per cent corrected for the loss according to		Gm.	%	Per cent corrected for the loss	1:1:1	1:2:1	1:3:1	1:4:1
			Hibbert†	Brauns††							
Dimethyl methyl glucoside Mol. wt. 222.15	1.40	18.7	22.67	18.7	0.69**	15.2	15.2	31.4	23.5	18.8	15.7
Trimethyl methyl glucoside Mol. wt. 236.16	3.52*	46.9	57.87	60.6	2.35	51.7	67.3	33.3	50.0	60.0	66.6
Tetramethyl methyl glucoside Mol. wt. 250.18	1.20	16.0	19.6	20.7	0.61	13.4	17.5	35.3	26.5	21.2	17.7
Total yield	6.12	81.6	100.14	100.0	3.65	80.3	100.0				
Loss during separation		18.4				19.7					

* *Does not contain the 0.05 gr. of Frac. Vc. since this residue was not crystalline and was not analyzed.*

** *Value taken from Miss Fowler's thesis.*

† *Allocated to all three glucosides.*

†† *Allocated to trimethyl and tetramethyl glucosides.*

values for a 1 : 3 : 1 polymer. For a ratio of 1 : 2 : 1, the yields actually found, calculated as percentage of the theoretical values, are 79.5, 94.0, and 60.3% (as given in Column 6 of Table I of the paper); whereas the corresponding corrected yields are 96.6, 115.7, and 73.8%.

In the second experiment, in which 4.55 gm. of hydrolyzed methylated dextran is used for a quantitative separation, the refractive index of 1.455 for the mixture of tetramethyl and trimethyl methyl glucosides is applied for the determination of the ratio of the amounts of each present, which is thus found to be 25% tetramethyl to 75% trimethyl methyl glucoside. A glance at the refractive indices given in the literature for the various methylated methyl glucosides prepared by different investigators, shows that the refractive indices, even of the same methyl methyl glucoside, vary over a comparatively wide range, so that they cannot be used as a basis for quantitative analytical calculations. On the other hand, if average refractive indices are used, it can be seen that the refractive indices for mixtures are too close together to permit their being used as a basis for the calculation of the amounts of two different methyl methyl glucosides in a mixture of the two. If for a mixture with $n_D = 1.455$, the calculated ratio is 25% tetramethyl to 75% trimethyl methyl glucoside, the ratio for a mixture with $n_D = 1.454$ would be 33.3 to 66.6%, and for one with $n_D = 1.456$, it would be 16.6 to 84.4%. Nor do the yields of the isolated dimethyl, trimethyl, and tetramethyl methyl glucosides in the second experiment justify the statement that dextran is a 1 : 3 : 1 polymer. In the fifth and sixth columns of Table A, the yields of dimethyl, trimethyl, and tetramethyl methyl glucosides actually found are given. After removal of the dimethyl methyl glucoside (0.69 gm.), a yield of 3.85 gm. of a mixture of trimethyl and tetramethyl methyl glucosides is obtained; this shows that the loss of 19.7% of the total yield at the end of the separation occurred during the fractionation of the tetramethyl from the trimethyl methyl glucoside. When this loss is allocated in a ratio of 51.7 to 13.4% to the trimethyl and tetramethyl methyl glucoside fractions, respectively, their yields become 67.3 and 17.5%. The total yields of dimethyl, trimethyl, and tetramethyl methyl glucosides in the second experiment are, therefore, 15.2, 67.3, and 17.5% (Column 7, Table A); these figures agree with those for a 1 : 4 : 1 polymer (Column 11, Table A).

This detailed statement clearly indicates that it cannot be decided definitely whether dextran is a 1 : 2 : 1, 1 : 3 : 1, or 1 : 4 : 1 polymer on the basis of the information contained in the paper under discussion. This question can be solved only by a quantitative separation of the methylated methyl glucosides obtained on alcoholysis of fully methylated dextran.

ANOLOBINE, AN ALKALOID FROM
ASIMINA TRILOBA DUNAL[1]

By Richard H. F. Manske[2]

Abstract

An alkaloid, for which the name anolobine is now suggested, has been isolated from the bark of *Asimina triloba* Dunal, the North American papaw. It is best represented by $C_{17}H_{17}O_3N$ and contains one phenolic hydroxyl group. Gaebel's reaction indicates a methylenedioxy group. The nitrogen is secondary. Exhaustive methylation and oxidation of the final vinyl compound has yielded 4-methoxyphthalic acid, and this observation together with a knowledge of analogous alkaloids from related plants has made it possible to designate a highly plausible structure for anolobine. A glycoside was found in the leaves although it does not appear to be present in the bark.

The alkaloids of the Natural Family, Anonaceae, have received only scant attention. *A priori*, a close chemical correspondence between alkaloids of this family and those of Menispermaceae and Lauraceae is to be suspected. Botanical classification includes the three families in the Natural Order Ranunculales.

The family, of which *Asimina triloba* Dunal is the only Canadian representative, is widely distributed throughout the tropics. The genus, *Anona*, regarded by some botanists as synonymous with *Asimina*, is represented in the tropical Americas by a number of species, some of which have yielded alkaloids, though so far of undetermined structure (3, 4, 6). It was therefore of interest to investigate the plant named in the title. It grows as a shrub or a small tree, and the pulp of the fruit, known as the North American papaw, is edible when fully mature.

The examination of the leaves failed to reveal more than doubtful traces of alkaloids. The bark contained about 0.05% of total alkaloid whether it was collected in summer or in winter. Though minute amounts of other bases appear to be present, the only alkaloid thus far obtained crystalline constitutes nearly 90% of the total. This alkaloid, for which the name anolobine is now proposed, is best represented by $C_{17}H_{17}O_3N$. Its monophenolic nature is proved by the preparation from it of a non-phenolic monomethyl ether, $C_{18}H_{19}O_3N$. The remaining two oxygens are almost certainly present in a methylenedioxy group. It readily gives a precipitate of the red phloroglucide in Gaebel's test, although the formal proof of the presence of such a group is still lacking. The nitrogen atom is secondary. The phenolic base, as well as its methyl ether, yields a water insoluble nitrosamine, which is soluble in ether and gives Liebermann's nitroso reaction with great brilliance.

Methylation of the methyl ether yields a mixture containing a moderate quantity of the quaternary iodide, and this on decomposition with strong

alkali yields an optically inactive methine, $C_{20}H_{23}O_3N$. Further degradation of the latter via its methiodide yields a hydrocarbon which is at least partly polymerized. On the assumption that anolobine is an aporphine alkaloid, this hydrocarbon on oxidation should yield a methoxy-methylene-dioxy-phenanthrene carboxylic acid. The main product obtained however proved to be identical with 4-methoxyphthalic acid. There was obtained ónly a minute amount of an acid which might have been a derivative of phenanthrene.

This observation serves to locate the phenolic hydroxyl as in Formulas (I) or (II), the process of oxidation having destroyed the benzene nucleus carrying the methylenedioxy group. The first of these is excluded because the methine

(I)   (II)

of anolobine methyl ether is certainly not identical with that of laureline, which on the basis of degradative experiments (1) and a synthesis (5) is the ON-dimethyl derivative of (I). The allocation of the methylenedioxy group to the position assigned to it is based on analogy with its similar position in virtually all known aporphine alkaloids. Formula (II) is therefore ascribable to anolobine with a considerable degree of certainty, although a rigorous proof by synthesis is desirable. The author takes this opportunity to invite anyone interested to undertake such a problem.

Anolobine   **Experimental**

The dried bark of *Asimina triloba* Dunal, collected in southwestern Ontario, was extracted with methanol and the solvent removed from the extract. The addition of water and enough hydrochloric acid to yield a solution acid to Congo red caused the separation of a rather low melting fat, which was separated only with difficulty. The clear aqueous solution which was ultimately obtained was first extracted several times with ether, then basified with excess ammonia, and extracted with ether again. In some experiments the second extraction was carried out with chloroform, but in either case the large amount of inorganic precipitate made the separation a tedious one.

Removal of the solvent from the extract yielded a residue that crystallized readily in contact with methanol when crystals for inoculation were available. Owing to its sparing solubility in methanol, the crude anolobine as thus

obtained could be readily purified by washing with this solvent in which the colored impurities were to a large extent soluble. Repeated recrystallization from chloroform-methanol, or purification via the sparingly soluble hydrochloride, yielded brilliant colorless prisms, which when placed in a bath at 245° C.* melted to a dark tar at 262° C., some darkening taking place about 10° lower. Anolobine dissolves in sulphuric acid to form an intense green solution, which on gentle warming becomes olive in color; on further heating, the color changes to brown. Nitric acid yields a pink solution which becomes orange colored on warming. Calcd. for $C_{17}H_{17}O_3N$: C, 72.08; H, 6.01; N, 4.95%. Found: C, 72.77; H, 5.54; N, 5.11%.

Anolobine is laevorotatory, giving a value, $[\alpha]_D^{27°} = -22.5°$ in the solvent made by mixing equal volumes of chloroform and absolute methanol ($c = 0.4$).

Anolobine O-Methyl Ether

A suspension of 2 gm. of anolobine in 50 cc. of chloroform containing some methanol was treated with an ethereal solution of diazomethane. The alkaloid slowly dissolved as the liberation of nitrogen proceeded. After 24 hr. the alkaloid had dissolved and the reaction appeared to be completed. Removal of the organic solvents and addition of dilute hydrochloric acid yielded a sparingly soluble hydrochloride. The filtered solution of the latter in hot water was basified with excess alkali, and the liberated base extracted with ether. The washed extract was evaporated to a small volume. The methyl ether of anolobine crystallized readily. It was recrystallized first from dry ether, in which it is only sparingly soluble, and then from methanol-ether. It was obtained in colorless fine needles, which melt at 97° C. and in contact with air gradually develop a slight greenish color. It dissolves in cold sulphuric acid to form a colorless solution which rapidly becomes pink. Gentle heating deepens this color, which on progressive heating becomes olive and then dark olive blue. Dilution with water yields a Prussian blue solution.

The methyl ether, like the parent alkaloid, yields an ether soluble precipitate when its solution in dilute acid is treated with sodium nitrite. The precipitate yields an intense blue color in Liebermann's test for nitroso compounds. Calcd. for $C_{18}H_{19}O_3N$: C, 72.73; H, 6.40; N, 4.71; 1 OMe, 10.44%; M.W. 297. Found: C, 71.31; H, 5.97; N, 4.86; OMe, 10.29%; M.W. 302. $[\alpha]_D^{27°} = -27.9°$ ($c = 0.4$ in absolute methanol).

Anolobine O-Methyl Ether Methine

The fact that anolobine is a secondary base is satisfactorily demonstrated by the mixed nature of the product obtained when the methyl ether is treated with methyl iodide. A solution of the alkaloid in methanol on treatment with methyl iodide yielded an almost instantaneous precipitate of the crystalline, though not homogenous, addition product. The organic solvents used were boiled off, and the residue was dissolved in a large volume of boiling water. The filtered solution was rapidly cooled and basified with an excess of potassium hydroxide. The mixture of secondary and tertiary bases thus liberated was extracted with ether and treated again with methyl iodide. The quaternary

* *Melting points are corrected.*

methiodide crystallized for the greater part from the cooled solution, and was decomposed by heating for 24 hr. on a steam bath in strongly alkaline solution. The liberated methine base was extracted from the cooled solution, and a further small quantity obtained by heating the aqueous solution again.

The methine as thus obtained crystallized readily when its ether solution was evaporated. It was recrystallized from dry ether and obtained in long colorless needles that melt at 99° C. In admixture with anolobine O-methyl ether, this substance was completely liquid at 84° C. In absolute methanol it was optically inactive ($c = 0.4$). Calcd. for $C_{20}H_{23}O_3N$: C, 73.85; H, 7.08; N, 4.31; 1OMe, 9.54%. Found: C, 74.24; H, 6.51; N, 4.57; OMe, 9.48%.

4-Methoxyphthalic Acid

The above-described methine on treatment with methyl iodide in methanol yielded a very sparingly soluble methiodide. This was decomposed by heating on the steam bath with an excess of aqueous potassium hydroxide. After an interval of 24 hr. the solution was cooled and the liberated hydrocarbon extracted with ether. This process was repeated until no more hydrocarbon was obtained, and until the methiodide had virtually disappeared. The hydrocarbon was definitely crystalline although a portion of it appeared to be polymeric. It was oxidized with potassium permanganate in acetone solution containing a little water until the permanganate color was permanent for five to six hours. Water was then added and the acetone boiled off, and the precipitate of manganese dioxide dissolved in a stream of sulphur dioxide. The acidified solution (hydrochloric acid) was thoroughly extracted with ether. Removal of the solvent yielded a residue which largely crystallized although it was evidently a mixture. The greater portion of it was very soluble in water, and this fraction was extracted from a very small amount of a sparingly soluble acid. The latter was dissolved in dilute sodium bicarbonate solution and the filtrate acidified. In the course of several days the sparingly soluble acid separated in slender prisms that melted at 204° C. After recrystallization from methanol, it melted at 207° C. The amount of this acid was insufficient for an analysis, in spite of the fact that a total of 3.7 gm. of anolobine was used in these experiments. It seems highly probable, however, that it is 3 : 4 methylenedioxy-7-methoxy-phenanthrene-1-carboxylic acid.

The readily soluble portion of the oxidation product was distilled up to 115° C. at 1 mm. and the distillate redistilled at 110° at 1 mm. It then melted at 95° C. After one recrystallization from benzene-petroleum ether it melted at 96° C., and in admixture with an authentic specimen of 4-methoxyphthalic anhydride melting at 98° C. (2) it melted at 97° to 98° C.

The methyl-imide was distilled *in vacuo* and after one recrystallization from methanol melted at 158° C. either alone or in admixture with a synthetic specimen. The ethyl-imide was prepared and distilled in the same manner. It was recrystallized from petroleum ether, and either alone or admixed with an authentic specimen it melted at 79° C. Calcd. for $C_{11}H_{11}O_3N$: N, 6.83%. Found in synthetic specimen: N, 6.69%.

Isolation of a Glycoside (?)

The dried leaves (1910 gm.) collected in August were examined for alkaloids. The clear aqueous solution obtained from the methanolic extract was allowed to remain for several days, during which time a sparingly soluble substance crystallized. This was filtered off, washed, and dried. It was dissolved in a small volume of methanol in which it is readily soluble, and the hot filtered solution cautiously treated with hot water. Pale yellow fine needles in stellate aggregates were thus obtained. After filtering, washing, and drying, this substance, which is probably a glycoside, melted at 186° C., sintering slightly at 184° to 185° C. It does not contain methoxyl, and the analyses are in agreement with the dihydrate of $C_{21}H_{24}O_{11}$, although $C_{21}H_{22}O_{11}$ is not entirely excluded and is more probable on structural grounds. Calcd. for $C_{21}H_{24}O_{11} \cdot 2H_2O$: C, 51.64; H, 5.74%. Found: C, 51.04; H, 5.51%.

Only the merest trace of alkaloid was found in the leaves, and its presence here may be attributable to admixture of a small amount of bark from the younger twigs which was peeled off as the leaves were stripped from the tree. The glycoside was not found in the bark.

References

1. BARGER, G. and GIRARDET, A. Helv. Chim. Acta., 14 : 481-504. 1931.
2. BENTLEY, W. H. and WEIZMANN, C. J. Chem. Soc. 91 : 98-104. 1907.
3. REYES, F. R. and SANTOS, A. C. Philippine J. Sci. 44 : 409-410. 1931.
4. SANTOS, A. C. Philippine J. Sci. 43 : 561. 1930.
5. SCHLITTLER, E. Helv. Chim. Acta. 15 : 394-402. 1932.
6. TRIMURTI, N. J. Indian Inst. Sciences, 7 : 232. 1924.

THE ALKALOIDS OF FUMARIACEOUS PLANTS

XVI. SOME MISCELLANEOUS OBSERVATIONS[1]

By Richard H. F. Manske[2]

Abstract

Eleven new alkaloids are described. They have been obtained from mother liquors from plants whose investigation has already been reported. The present record deals with *Dicentra cucullaria* (three)[*], *D. eximia* (four), *Corydalis aurea* (seven), and *C. sempervirens* (two). For convenient reference all new alkaloids in this series of communications have been given a number following the letter F, and a table is included in which the salient features are summarized.

Alkaloid F 23 (formerly -η) has now been obtained from *C. sempervirens*. It is shown to be the optical antipode of *d*-adlumine, and a mixture of the two has yielded the *dl*-form.

The thoroughness with which the alkaloids of a particular plant may be isolated and characterized depends, in addition to the amount of material available, on the number of alkaloids present and on their crystallizability either as free bases or as simple derivatives. With mixtures of unknown constituents, crystallization of an individual is frequently a matter of chance, dependent, among other factors, on time and on the absolute amount. It may be permissible, therefore, to reiterate that the investigations which the author has recorded in this field from time to time cannot be regarded as exhaustive. In general, at the time of publication, small amounts of un-crystallized mother liquors remained, and the further examination of these seemed unprofitable until more material became available, or until spontaneous crystallization took place. The nucleus required to induce crystallization of a particular fraction of some of the mother liquors was obtained from a new and higher yielding source.

In the following summary the names of the alkaloids thus far isolated are shown after the name of the plant from which they were obtained. Those in parentheses have been previously reported and are included to complete the record.

Dicentra cucullaria,—(protopine, cryptopine, α-allocryptopine, bicuculline, corlumine), cularine, cularidine, ochotensine.

Corydalis sempervirens,—(protopine, cryptopine, bicuculline, capnoidine), F 20, F 23.

Dicentra eximia,—(protopine, dicentrine, glaucine, corydine, glaucentrine), cularine, F 21, F 29, F 30.

Corydalis aurea,—(protopine, bicuculline, capaurine, capauridine, corydaline, *el*-tetrahydropalmatine, corypalline), *dl*-tetrahydropalmatine, α-allocrytopine, aurotensine, cordrastine, F 24, F 27, F 28.

---

[*] *Number of hitherto unreported alkaloids.*

At the outset of these investigations it was not realized that so many new alkaloids would be found in the Fumariaceae family. When a definite name could not be coined on one basis or another, resort was had to the letters of the Greek alphabet to designate new or supposedly new alkaloids. The limitations of such a system have now become apparent. More than 30 alkaloids for which no name has yet been evolved and which appear to be new have already been isolated. It is therefore proposed to allocate to each of these alkaloids a number following the letter F (from Fumariaceae). Furthermore, in order to systematize the record, all aklaloids found by the author whether they have already been given a name or a Greek letter are reclassified. Table I, including 11 hitherto unreported alkaloids, is a review as well as a summary.

TABLE I

No.	Name or designation	M.p., °C.*	Formula	Functional groups	References
F 1	Bicuculline (α)	177	$C_{20}H_{17}O_6N$	2 O_2CH_2	2, 3, 4, 6, 8, 12, 13, 15
F 2	d-Adlumine	180	$C_{21}H_{23}O_6N$	O_2CH_2; 2OMe	4, 5
F 3	Adlumidine	235	$C_{19}H_{15}O_6N$	2 O_2CH_2(?)	4
F 4	Capnoidine	238	$C_{19}H_{15}O_6N$	2 O_2CH_2(?)	6, 12
F 5	Glaucentrine (δ)	148	$C_{20}H_{23}O_4N$	3OMe; OH	7, 9, 10
F 6	Capaurine	164	$C_{21}H_{27}O_5N$	4OMe; OH	8
F 7	Capauridine	208	$C_{21}H_{27}O_5N$	4OMe; OH	8
F 8	Corypalline	164	$C_{11}H_{15}O_2N$	OMe; OH	14
F 9	Cularine	115	$C_{20}H_{23}O_4N$	3OMe	**
F 10	Cularidine	157	$C_{19}H_{21}O_4N$	2OMe; OH	**
F 11	Corlumine	159	$C_{21}H_{23}O_6N$	O_2CH_2; 2OMe	11, 12, 13
F 12	Corlumidine	236	$C_{20}H_{19}O_6N$	O_2CH_2; OMe; OH	11, 12, 14
F 13	θ	183	$C_{18}H_{17}O_4N$	O_2CH_2; OMe; OH	12, 13
F 14	κ	198	$C_{20}H_{19}O_5N$	O_2CH_2(?)	13
F 15	λ	212	$C_{19}H_{19}O_5N$	O_2CH_2(?); 2OMe	13
F 16	μ	236	$C_{18}H_{17}O_4N$	O_2CH_2(?); 2OMe	13
F 17	Ochotensine (ι)	248	$C_{21}H_{23}O_4N$	O_2CH_2(?); OMe; OH	13
F 18	Aurotensine	128	$C_{19}H_{21}O_4N$	2OMe; 2OH	**
F 19	Cordrastine	196	$C_{22}H_{25}O_6N$	4OMe	**
F 20		221	$C_{18}H_{23}O_5N$		**
F 21		80	$C_{20}H_{25}O_5N$	4OMe	**
F 22		238	$C_{37}H_{46}O_{10}N_2$	3OMe	1
F 23	l-Adlumine η	180	$C_{21}H_{23}O_6N$	O_2CH_2; 2OMe	12
F 24		138	$C_{19}H_{23}O_4N$	3OMe; OH	**
F 25	υ	230	$C_{19}H_{17}O_6N$	O_2CH_2(?); NMe	15
F 26	Cryptocavine	223	$C_{22}H_{23}O_6N$	O_2CH_2; 2OMe	15
F 27		148	$C_{21}H_{25}O_5N$	4OMe	**
F 28		135	$C_{17}H_{19}O_3N$	2OMe; OH	**
F 29		262	$C_{18}H_{21}O_4N$	2OMe; 2OH	**
F 30		102	$C_{19}H_{21}O_4N$	3OMe	**
F 31		216	$C_{18}H_{19}O_5N$	O_2CH_2(?)	15

* Melting points are corrected.
** Alkaloids that are discussed in this paper.

Special interest attaches to alkaloid F 23, formerly alkaloid-η (12). Although it has been available in only very small amounts, it is now shown to be the optical antipode of d-adlumine (15) from *Adlumia fungosa*. With d-adlumine it yields dl-adlumine which crystallizes in stout prisms quite distinct from either of its parents. The constitution of l-adlumine has also been formally

demonstrated by hydrolytic oxidation. The acidic and basic fragments thus obtained were characterized in each case by a Cannizzaro rearrangement which yielded 3 : 4-methylene-dioxy-phthalide and 1-keto-2-methyl-6 : 7-dimethoxy-tetrahydro-isoquinoline respectively.

Experimental

In the following résumé the known alkaloids which have not previously been described as occurring in the plants mentioned are only briefly recorded. The new alkaloids and their isolation are described in greater detail. The nomenclature of the various fractions is that previously recorded (4).

α-Allocryptopine and Corlumine from D. cucullaria

The mother liquors which had accumulated as the result of isolating the known alkaloids from 93 kg. of plant material (tubers and aerial portion) were combined and reworked (4). The protopine fraction (BS) finally crystallized for the greater part, and when this alkaloid was recrystallized from chloroform-methanol it melted at 160° C.* This melting point was not depressed when the alkaloid was admixed with an authentic specimen of α-allocryptopine.

The mother liquor from which the bicuculline had been crystallized was clarified in methanol with charcoal and seeded with a crystal of corlumine. Crystallization was immediate, and recrystallization yielded colorless fine needles, melting alone or admixed with an authentic specimen at 159° C. The total yield was 0.04%.

The final mother liquor on long standing deposited a small amount of corlumine and with it a small amount (0.1 gm.) of a very sparingly soluble alkaloid. Hot methanol removed the former, and the latter was recrystallized from hot chloroform, in which it is only sparingly soluble. This proved to be identical with F 17 (alkaloid-ι), first isolated from *C. sibirica* (13). Its relative abundance in *C. ochotensis*, a plant now under investigation, suggests the name *ochotensine*.

Glaucentrine

This is the name now given to an alkaloid first isolated from *D. eximia* and later from *D. formosa* and *D. oregana*. It was obtained crystalline only as the hydrochloride and referred to as alkaloid-δ (7, 9, 10). The free base has now been obtained crystalline. For this purpose the purified hydrochloride was dissolved in water, treated with aqueous sodium bicarbonate, and the liberated base extracted with purified ether. The washed and dried solution (sodium sulphate) was evaporated to a small volume. The alkaloid separated for the greater part as a viscous resin. Dry methanol was added until the solution just became homogeneous, and the solution was placed in the ice chest. The base crystallized after some time. It was filtered off, washed first with ether containing a little methanol, and then with dry ether in which it is only sparingly soluble. Colorless fine prisms melting at 148° C.

* *All melting points are corrected.*

were thus obtained. Analyses† indicate the formula $C_{20}H_{23}O_4N$. Calcd.: C, 70.38; H, 6.75; N, 4.00%. Found: C, 70.02; H, 6.84; N, 4.05%.

The previous formula (9), $C_{21}H_{25}O_5N$, is erroneous, although the presence of three methoxyl groups is clearly indicated. The hydrochloride was found to contain 23.84% methoxyl; $C_{20}H_{23}O_4N$. HCl requires 24.64%. Final evidence for the correctness of the new formula was obtained when it was observed that the fully methylated alkaloid (diazomethane) is identical with *d*-glaucine. Glaucentrine therefore is O-desmethylglaucine. Work is in progress with the object of determining which of the four possible formulas is correct.

Alkaloid F 29

The fractions (BSE and EES) from *D. eximia*, which yielded glaucentrine, contained another alkaloid that crystallized with great facility in one particular experiment, and its subsequent isolation from the mother liquor was readily accomplished. The phenolic bases regenerated from the mother liquors obtained in the isolation of glaucentrine hydrochloride crystallized readily in contact with methanol. The base is virtually insoluble even in hot methanol, and was recrystallized from much boiling chloroform, and more conveniently from hot dioxane and methanol. It was then obtained in brilliant colorless prisms which began to darken at 250° to 255° C. and melted to an orange colored liquid at 262° C. The yield was 0.007%. Analysis indicate two methoxyl groups in $C_{19}H_{21}O_4N$. Calcd.: C, 69.74; H, 6.40; N, 4.28; 2OMe, 18.89%. Found: C, 69.67; H, 6.49; N, 4.65; OMe, 18.83%.

The presence of two hydroxyl groups in this alkaloid is confirmed by the preparation of its dimethyl ether. For this purpose an ethereal solution of diazomethane was added to a solution of the base in dioxane. After 24 hr. the non-phenolic base was purified as the hydrochloride, which is only sparingly soluble in cold water. This salt melts to an orange colored liquid at 236° to 237° C. The free base prepared from the hydrochloride was recrystallized from hot methanol (moderately soluble) and washed with ether in which it is sparingly soluble. Large stout prisms melting at 177° C. were thus obtained. Dissolved in sulphuric acid, the crystals yielded a colorless solution which on heating exhibited the following color changes—dirty olive, blue with a pink cast, and finally deep blue. Calcd. for $C_{21}H_{25}O_4N$; C, 70.99; H, 7.04; 4OMe, 34.93%. Found: C, 71.08; H, 7.18; OMe, 34.72%.

The diethyl ether was prepared in the same manner. The hydrochloride is readily soluble in dioxane and was purified by recrystallization from water. The free base was recrystallized from ether–petroleum-ether; the colorless prisms thus obtained melt at 131° C. Calcd. for $C_{23}H_{29}O_4N$; 2OMe and 2OEt as 4OMe, 32.38%. Found: OMe and OEt as OMe, 31.93%.

Corydalis aurea

To date, a total of 49 kg. of this plant has been worked over, and, aside from a large supply of mother liquors which have yielded no crystals, 14 alkaloids

† *Analyses are the means of satisfactory duplicates.*

have already been isolated. The recent discovery of corypalline (14) in the seeds is an indication that the genus *Corydalis* differs chemically from *Papaver* in that the seeds of the latter are devoid of alkaloids. The large number of alkaloids makes any exact description of their isolation difficult.

The crude tetrahydropalmatine obtained from fraction (BC) was recrystallized as the hydrochloride; a small amount of a very sparingly soluble salt was obtained. The latter salt was recrystallized several times from much boiling water, and it then consisted of pale yellow fine needles. The free base was generated from this by adding ammonia to a rapidly cooled aqueous solution of the salt. The caseous precipitate readily became granular as the base crystallized. It was recrystallized from methanol and obtained in colorless elongated plates which melt at 148° C. This is not identical with *dl*-tetrahydropalmatine described below. Its non-identity with several new alkaloids, all of approximately the same melting point and empirical composition, which have been isolated from other sources, does not help to elucidate its nature. It is F 27 and is best represented by $C_{21}H_{25}O_4N$, containing four methoxyl groups. Calcd.: C, 70.98; H, 7.04; N, 3.94; 4OMe, 34.93%. Found: C, 71.05; H, 7.00; N, 3.99; OMe, 34.84%.

Since the author's first paper on *C. aurea* (8), Eppson (16) has investigated the same plant. His C_1, m.p. 138° to 140° C., is almost certainly *l*-tetrahydropalmatine, in that the optical rotation and the methoxyl content are approximately correct. C_2 is probably identical with the author's F 27, although its identity with the alkaloid of *C. ambigua* of the same melting point is less certain.

The author has isolated from other sources at least one more alkaloid of approximately the same composition and melting point. Eppson's D_2 is almost certainly a slightly impure specimen of the low melting form of protopine.

The mother liquor from which the *l*-tetrahydropalmatine had been crystallized was converted to hydrochloride. On cooling, a mixture of two hydrochlorides separated—fine needles, readily soluble on warming, and stout, highly refracting polyhedra only slowly soluble. The two were separated by gently warming a suspension of them in water. The filtrate redeposited the fine needles. Each fraction was recrystallized. The stout polyhedra yielded *d*-corydaline, and the fine needles on appropriate treatment yielded a base which was recrystallized from methanol; it then melted at 152° C. In admixture with a specimen of *dl*-tetrahydropalmatine, prepared from *l*-tetrahydropalmatine by oxidation with iodine and reduction of the palmatine iodide thus formed with zinc and hydrochloric acid, there was no depression in melting point. Calcd. for: $C_{21}H_{25}O_4N$; C, 70.98; H, 7.04; N, 3.94; 4OMe, 34.93%. Found: C, 71.16; H, 7.07; N, 4.31; OMe, 34.99%.

Aurotensine is the name now given to an alkaloid which has been isolated not only from *C. aurea*, but also from *C. ochotensis* and *Fumaria officinalis*. Furthermore, it is of interest to note that its dimethyl ether is the main alkaloid found in another species; namely, *C. caseana*, the investigation of which will be recorded shortly. It occurs in fractions (BSE and EES), from

which it is conveniently isolated as the sparingly soluble hydrochloride. The free base was regenerated from the hydrochloride by cautiously treating a rapidly cooled aqueous solution with dilute ammonia. It was recrystallized by adding a little water to a concentrated methanolic solution. Colorless, flat rhombic plates were thus obtained. It melts at 128° C., losing water of crystallization at the same time. Calcd. for $C_{19}H_{21}O_4N$: C, 69.74; H, 6.40; N, 4.28; 2OMe, 18.89%. Found: C, 68.51, H, 6.62; N, 4.29; OMe, 19.61%. This formula is confirmed by the analysis of the dimethyl ether, which will be described in another communication.

Cordrastine

The existence of hydrastine, adlumine, and corlumine, and of bicuculline in nature renders the existence of the tetramethoxy analogue highly probable. On one occasion the protopine fraction from *C. aurea* was contaminated with a small amount of a second base which was separated from the former as its readily soluble hydrobromide. The regenerated base was recrystallized from chloroform-methanol, and then consisted of colorless fine needles which melted with previous darkening at 196° C. Though the formal proof of its structure is lacking, this alkaloid, for which the name *cordrastine* is now proposed, is almost certainly represented by Formula A. A trace of this base, when heated with manganese dioxide in dilute sulphuric acid, yielded a strongly fluorescent solution, a behavior reminiscent of that of other phthalide-isoquinoline alkaloids. The analytical figures are in excellent agreement with those required by theory, although sufficient material for only one set of analyses was available. Calcd. for $C_{22}H_{25}O_6N$: C, 66.17; H, 6.27; N, 3.51; 4OMe, 30.08%. Found, C, 66.41; H, 6.32; N, 3.43; OMe, 29.37%.

(A)

Alkaloid F 24

The ether extract (EEC) from a large lot of *C. aurea* in contact with methanol deposited a mixture of bases, the more soluble of which was repeatedly recrystallized from hot methanol. It was ultimately obtained in colorless fine prisms that melted at 138° C. Found: C, 69.65; H, 7.05; N, 4.41; OMe, 27.33%. Calcd. for $C_{19}H_{23}O_4N$; C, 69.72; H, 7.03; N, 4.28; 3OMe, 28.44%.

Alkaloid F 28

The fraction (ES) was freed of non-phenolic alkaloids, and the phenolic bases were regenerated by adding ammonium chloride to the alkaline solution. The filtered, washed, and dried precipitate readily recrystallized in contact with methanol. It was washed with cold methanol in which it is moderately soluble (m.p. 135° C.), and recrystallized from a large volume of ether. Colorless fine needles melting at 135° C. were thus obtained. In admixture with F 24 it was completely liquid at 130° C. Found: C, 72.17; H, 7.03; N, 5.09; OMe, 20.64%. Calcd. for $C_{17}H_{19}O_3N$: C, 71.58; H, 6.67; N, 4.91; 2 OMe, 21.76%.

Cularine

There are certain alkaloids which are repeatedly encountered, and among these protopine is the only one which has been isolated from all plants in the Fumariaceae family which have been subjected to more than a cursory examination. Cryptopine and allocryptopine have each been found in six out of twenty species investigated by the author. Bicuculline has been found in nine species, and the new alkaloid, now referred to as *cularine*, has been isolated from five species; namely, *D. cucullaria*, *D. eximia*, *D. formosa*, *D. oregana*, and *C. claviculata*. It is expected that a communication dealing with the last named plant will be placed on record in the near future. Cularine crystallizes in large stout prisms only when it is quite pure, or if crystals for seeding are available, and until a method of purification was discovered it constituted the major portion of the uncrystallizable bases in the fraction (BC) from the plants mentioned. It was discovered, however, that it yielded a sparingly soluble acid oxalate and this could be recrystallized only from large volumes of hot water or methanol, and the alkaloid regenerated from the oxalate with excess alkali crystallizes readily from ether in which it is only moderately soluble. It melts sharply at 115° C. and shows $[\alpha]_D^{25} = + 285°$ ($c = 0.8$ in methanol). The simple formula $C_{20}H_{23}O_4N$, containing three methoxyl groups, is in good agreement with the analytical values, but some work on its degradation points to twice this formula. Calcd. for $C_{20}H_{23}O_4N$: C, 70.38; H, 6.75; N, 4.11; 3OMe, 27.27%. Found: C, 70.27; H, 6.90; N, 4.28; OMe, 27.32%.

Its presence in *D. eximia* and *D. formosa* is limited to several parts per million of the dry weight, and its isolation and definite identification was possible only with the relatively large amounts of these plants available. The properties of the oxalate greatly simplified the work. The other plants contain somewhat larger amounts.

The sparingly soluble oxalate obtained from *D. eximia* was a mixture from which the cularine salt was separated by extraction with hot water. The less soluble salt could not be redissolved in a reasonable amount of boiling water. It was dissolved in dilute hydrochloric acid, and the alkaloid regenerated by adding an excess of potassium hydroxide and extracting with ether. The washed and dried extract on evaporation to a small volume deposited a

new alkaloid in colorless fine needles. When recrystallized from ether, in which it is only slightly soluble, this alkaloid melted sharply at 102° C. It is alkaloid F 30 and is best represented by $C_{19}H_{21}O_4N$. Calcd. for $C_{19}H_{21}O_4N$: C, 69.74; H, 6.40; N, 4.28; 3OMe, 28.34%. Found: C, 69.75; H, 6.48; N, 4.59; OMe, 28.92%.

It is non-phenolic, and the presence of three methoxyls, as well as the analytical figures, indicates a close relation to cularine, of which it appears to be the N-desmethyl derivative. The amount of this alkaloid is limited to about 1 gm. in 35 kilos of dried plant. Nevertheless, Hoffmann degradation has yielded a small amount of base, characterized as the picrate, which appears to be identical with that of the methine of cularine.

Alkaloid F 21

The alkaloids in the mother liquor from the isolation of cularine and F 30 from *D. eximia* as oxalates were regenerated with alkali and extracted, with ether. No crystals could be obtained directly from this product. It was treated with acetic anhydride, warmed gently, and allowed to remain in the ice chest for a week. Water was added and when the anhydride had disappeared the mixture was extracted with ether. The aqueous solution yielded a small amount of glaucine. The ether extract was freed of solvent and the residue heated for 36 hr. with methanolic potassium hydroxide. The basic portion was converted to hydrochloride in hot water. On cooling, a sparingly soluble hydrochloride, melting at 256° C. without effervescence but some darkening, separated in slender prisms. The free base was regenerated from this and crystallized first from ether and then from methanol-ether. Colorless rectangular plates melting at 80° C. were thus obtained. Alkaloid F 21 dissolves in cold sulphuric acid to form an orange colored solution, which on heating exhibits the following color changes:— yellow, green, blue, purple, and finally brown at a high temperature. The yield was 0.1 gm. from 35 kilos. Found: C, 66.74; H, 7.08; N, 3.97; OMe, 32.47%. Calcd. for $C_{20}H_{25}O_5N$: C, 66.85; H, 6.96; N, 3.90; 4OMe, 34.54%.

Cularidine

The fractions (BSE and EES) from *D. cucullaria* are relatively small. Each was neutralized with hydrochloric acid in methanol, and the concentrated solution treated with dry ether until the turbidity was permanent, and then with sufficient acetone to redissolve the precipitate. In the course of months a small amount of crystalline hydrochloride had separated from each fraction. This proved to be sparingly soluble in methanol or cold water, and was recrystallized from the former. The free base was liberated by means of ammonia and taken up in ether. The new alkaloid, *cularidine*, crystallized readily when the ether solution was evaporated to a small volume. It was recrystallized from methanol-ether and obtained in colorless fine needles melting sharply at 157° C. The analytical figures are in fair agreement with $C_{19}H_{21}O_4N$, containing two methoxyls, but the crucial observation that it yields cularine on methylation with diazomethane is more important.

It therefore is O-desmethylcularine. Calcd. for $C_{19}H_{21}O_4N$: C, 69.74; H, 6.40; N, 4.28; 2OMe, 18.88%. Found: C, 68.94; H, 6.57; N, 4.44; OMe, 18.59%.

Corydalis sempervirens

l-Adlumine (Alkaloid F 23)

This alkaloid, which previously has been referred to as alkaloid-η, and which was obtained from *C. scouleri* (12), has also been isolated from this plant. The fraction (BS), from which the greater portion of protopine and cryptopine had been removed, was heated with methanolic potash, water was added, and the methanol boiled off. The aqueous alkaline solution was decanted from the insoluble bases through a filter, and the filtrate treated with an excess of ammonium chloride. The precipitated base was filtered off, and redissolved in hot dilute hydrochloric acid. The base was reprecipitated with ammonia, filtered off, dried, and recrystallized from chloroform-methanol. Colorless six-sided plates of F 23 were thus obtained. It melted sharply at 180° C., and this melting point was not depressed when the alkaloid was admixed with a specimen from *C. scouleri*. The optical activity is opposite in sign but equal in degrees to that of adlumine from *A. fungosa*, namely $[\alpha]_D^{22} = -42.5°$ ($c = 0.8$ in chloroform).

The *dl*-form of adlumine was prepared by dissolving 0.064 gm. of each of the *d*- and *l*-forms in chloroform and evaporating to a thin syrup. Methanol was then added and the remainder of the chloroform evaporated. On cooling, stout short prisms melting sharply at 190° C. were obtained. It is interesting to note that a mixture of approximately equal amounts of the *d*- and the *dl*-forms was completely liquid at 175° C.; this confirms the earlier observation that a mixture of the *d*- and *l*-forms had a melting point lower than that of either individual.

The hydrolytic oxidation with dilute nitric acid was carried out as with *d*-adlumine (5). · Owing to the paucity of material only 0.2 gm. was available for the experiment. The acid fragment was converted by alkali treatment into the sparingly soluble 3 : 4-methylene-dioxy-phthalide which, when recrystallized twice from water, melted sharply at 232° C. either alone or in admixture with an authentic specimen. The basic fragment was also heated with alkali. The 1-keto-2-methyl-6 : 7-dimethoxy-tetrahydro-isoquinoline was isolated as previously described and recrystallized from ether. It melted at 125° C., and in admixture with an authentic specimen from adlumine (m.p. 126° C.) it melted at 125° to 126° C.

Alkaloid F 20

After the known alkaloids of *C. sempervirens* (3) were separated, all the mother liquors were combined, dissolved in dilute hydrochloric acid, filtered, and the bases precipitated by the addition of ammonia. The aqueous filtrate was extracted with ether and the extracts were evaporated to a small volume. The crystals which separated were recrystallized twice from methanol in which this base, F 20, is slightly soluble, Colorless prisms

melting at 221° C. were thus obtained. Calcd. for $C_{18}H_{23}O_5N$: C, 64.86; H, 6.91; N, 4.20%. Found: C, 64.42; H, 7.08; N. 4.37%. Methoxyl is absent.

It may be added that alkaloid-γ, previously reported from this source (6), has been identified as a slightly impure specimen of protopine.

Dicentra canadensis

Alkaloid F 22

In a previous communication dealing with this plant (1) the author recorded the isolation of a substance having the formula $C_{37}H_{38}O_{10}N_2$. It was regarded as neutral owing to its insolubility in hydrochloric acid. It has now been found that it yields a crystalline hydrochloride when its solution in chloroform-methanol is treated with a methanolic solution of hydrogen chloride. The pale yellow product obtained under these conditions is readily soluble in chloroform, only sparingly soluble in hot methanol, and virtually insoluble in hot water. It melts at 286° C. to an orange colored resin, sintering at a temperature several degrees lower.

The analyses are in good agreement with $C_{37}H_{39}O_9N_2Cl$. As in the free base, three methoxyl groups appear to be present. The loss of an oxygen atom is probably attributable to the formation of the chloride, rather than of the hydrochloride, from the base which is now regarded as quaternary. The base would then require the formula $C_{37}H_{40}O_{10}N_2$, which is also in satisfactory agreement with the analyses previously given. Calcd. for $C_{37}H_{39}O_9N_2Cl$: C, 64.30; H, 5.65; N, 4.05; Cl, 5.14; 3OMe, 13.47%. Found: C, 64.43; H, 5.77; N, 3.95; Cl, 5.69; OMe, 13.77%.

References

1. MANSKE, R. H. F.   Can. J. Research, 7: 258-264.   1932.
2. MANSKE, R. H. F.   Can. J. Research, 7: 265-269.   1932.
3. MANSKE, R. H. F.   Can. J. Research, 8: 142-146.   1933.
4. MANSKE, R. H. F.   Can. J. Research, 8: 210-216.   1933.
5. MANSKE, R. H. F.   Can. J. Research, 8: 404-406.   1933.
6. MANSKE, R. H. F.   Can. J. Research, 8: 407-411.   1933.
7. MANSKE, R. H. F.   Can. J. Research, 8: 592-599.   1933.
8. MANSKE, R. H. F.   Can. J. Research, 9: 436-442.   1933.
9. MANSKE, R. H. F.   Can. J. Research, 10: 521-526.   1934.
10. MANSKE, R. H. F.   Can. J. Research, 10: 765-770.   1934.
11. MANSKE, R. H. F.   Can. J. Research, B, 14: 325-327.   1936.
12. MANSKE, R. H. F.   Can. J. Research, B, 14: 347-353.   1936.
13. MANSKE, R. H. F.   Can. J. Research, B, 14: 354-359.   1936.
14. MANSKE, R. H. F.   Can. J. Research, B, 15: 159-167.   1937.
15. MANSKE, R. H. F.   Can. J. Research, B, 15: 274-277.   1937.
16. EPPSON, H.   J. Am. Pharm. Assoc. 24: 113-115.   1935.

A STUDY OF THE IRON IN A PODSOL SOIL BY MEANS OF AN IMPROVED DIPYRIDYL METHOD[1]

By W. J. Dyer[2] and W. D. McFarlane[3]

Abstract

An accurate determination of the ferrous and ferric iron content of a colored soil extract is possible by the direct application of the dipyridyl method when an Evelyn photoelectric colorimeter and a suitable light filter are employed.

It is shown that a sodium carbonate treatment of a podsol soil increases the water extractable iron and organic matter. The soluble iron is contained in the humic acid fraction. Since the iron in these extracts reacts quantitatively with $\alpha\alpha'$-dipyridyl, it is believed to be entirely combined in a manner similar to that of the soluble unionized complexes of iron with hydroxy organic acids.

Part I. An Improved Method for the Determination of Ferrous and Ferric Iron in Soil Extracts

The reagent $\alpha\alpha'$-dipyridyl reacts only with ferrous iron which is not bound to nitrogen, and has been used by Hill (3) and McFarlane (6) for the determination of iron. Recently Ignatieff (5) proposed a method for the determination of ferrous iron in soil solutions which employs this reagent. Aluminium chloride is used to decolorize the solution before the dipyridyl colorimetry is carried out, but the pink color of the ferrous dipyridyl complex is modified by this treatment.

The authors have developed a procedure, employing an Evelyn photoelectric colorimeter (2) and a 520 M light filter, by which accurate estimations of the ferrous dipyridyl color can be made even in humic acid solutions, without removing extraneous color. When this method is applied to a solution of the humic acid fraction or to soil extracts, the results indicate that in the presence of a reducing agent all the iron reacts with dipyridyl.

Experimental

An aliquot of the approximately neutral solution containing 10 to 20 γ of iron is placed in a 25 ml. volumetric flask. About 10 ml. of 10 N ammonium acetate solution (pH approximately 6.1) and 1 ml. of a 0.005 M solution of $\alpha\alpha'$-dipyridyl containing 1.0 ml. of 1 N hydrochloric acid per 100 ml. is added. If ferrous iron is to be determined, the solution is diluted to 25 ml. with the acetate buffer, and mixed. To determine the total iron (Fe^{++} + Fe^{+++}) a trace of sodium hydrosulphite (iron-free) is added to reduce the iron, before the solution is diluted to 25 ml. After the solutions are allowed to stand, the color intensity is measured in an Evelyn photoelectric colorimeter, Filter 520 M being used. Usually the color attains its maximum intensity in a few minutes, but when large amounts of organic matter are present it

may be necessary to let the solution stand for five hours before the color intensity is measured. To compensate for the color of the extract, the colorimeter is adjusted to read 100% transmission of light with a blank solution prepared in a manner identical with that of the preparation of the colored solution but to which no dipyridyl has been added. The ferrous dipyridyl concentration is then determined by reference to calibration data that have been previously prepared, as described below.

The approximate absorption curve of the ferrous dipyridyl was determined with the Evelyn colorimeter from measurements made on the light transmission of the pink color at the different wave-lengths of light transmitted by different filters. The curve was similar to that obtained by McFarlane (6) by spectrometry, and shows the maximum absorption at about 520 millimicrons. Accordingly, the 520 M filter was used for the determination.
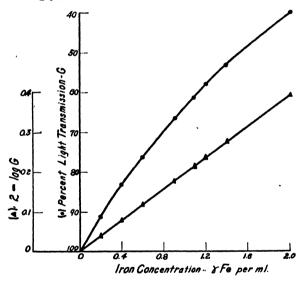
FIG. 1. *The relation between the concentration of iron and the color intensity of ferrous dipyridyl solutions.*

Hill (3) states that the ferrous dipyridyl complex is stable at pH values between 3.5 and 8.5. Since our method of measuring the color intensity is more sensitive than the methods formerly used, this point was investigated more fully. The results showed that the complex is undissociated in the pH range 3.2 to 8.2. Within this range of pH a very slight fading of the color with increasing acidity was noted, but the difference is not significant. The concentration of dipyridyl in 1 ml. of the reagent is twice the theoretical amount required to react with 2×10^{-5} gm. of iron. This excess is in accordance with Hill's recommendations.

The calibration data were obtained by application of the above procedure to standard solutions of ferrous ammonium sulphate. A calibration curve may be plotted, as in Fig. 1, which shows the relation between photometer

readings and iron concentration, or, if Beer's law is applicable, a constant may be calculated from the relation

$$C = \frac{2 - \log G}{K_1}$$

in which C is the concentration, G is the corrected galvanometer reading, and K_1 is a constant. If K_1 is calculated from the readings with different concentrations of iron, it is evident that Beer's law will be applicable over the range in which the values for K_1 are constant. From the straight line relation between iron concentration and $2 - \log G$, as shown in Fig. 1, it is evident that K_1 is constant over the range plotted. By calculation, K_1 is found to be 0.197 ± 0.002, with a maximum variation of 0.005.

Part II.   The Organic Combination of the Iron Extracted by Alkali from Podsol Soil

When a typical Quebec Appalachian upland podsol soil is treated, in the autumn, with 1,000 lb. of sodium carbonate per acre, a marked increase in the yield of oats is obtained.* The oat straw has a bright golden yellow color and contains about 25 mg. of iron per 100 gm. of dry matter, whereas the straw from the untreated control plots has a rust color and an iron content of about 12 mg. per 100 gm. of dry matter.

Experiments are described below which show that a significant amount of iron can be extracted with alkalis from this podsol soil. When a sodium carbonate or pyridine extract of this soil is fractionated, practically all the dissolved iron is found in the humic acid fraction. Burke and co-workers (1) and Olsen (7) have shown that humic acid holds iron in solution at a pH greater than 6.0, and that iron so combined has a stimulating effect on the growth of plants and soil micro-organisms. Presumably the iron is combined with α-hydroxy acids to form soluble unionized complexes (Smythe and Schmidt (8) and Hopkins (4)). However, humic acid as obtained from soil always contains nitrogen, and it is of interest to know whether any of the iron in the humic acid fraction is linked to nitrogen. The authors' analysis by the dipyridyl method indicates that no significant amount of the iron in the humic acid fraction of this soil is bound in the form of an iron-nitrogen complex. Since all the iron reacts directly with dipyridyl, the dipyridyl method becomes particularly valuable for the rapid determination of ferric and ferrous iron in soil extracts. The results in general indicate that the beneficial effect of sodium carbonate on the oat crop is due, in part at least, to its rendering more iron available to the plants.

Experimental

To examine the effect of sodium carbonate on the soil, a number of glass percolators were set up each containing a kilogram of soil which had been treated with a known amount of a sodium carbonate solution. Percolation

* *Unpublished data—Macdonald College Soil Fertility Committee, 1937.*

was carried out immediately by pouring enough water on the surface of the soil to give one litre of percolate. Analysis of the percolates (Table I) showed

TABLE I

ANALYSIS OF WATER PERCOLATES OF SODIUM CARBONATE TREATED SOIL

Test No.	Amount of sodium carbonate, lb. per acre	pH	Organic matter, gm. per 100 gm. soil	Iron, mg. per 100 gm. soil
1	Nil	5.23	0.173	0.47
2	2,000	5.90	0.185	0.85
3	4,000	6.36	0.250	2.30

that the organic matter and iron content, and the pH of the percolates, increase with the amount of sodium carbonate added. Sodium carbonate, therefore, increases the solubility of organic matter and of iron.

To investigate further the effect of alkalis on the soil iron, extraction of the soil with sodium carbonate and with pyridine was next carried out. A sample of 100 gm. of the podsol soil was refluxed for four hours with 500 ml. of pyridine. The filtrate was evaporated nearly to dryness *in vacuo*. The residue was shaken with ether and water, and the voluminous precipitate which separated in the ether layer was filtered off and dried. The ether and water solutions were evaporated to dryness separately. Analysis of the three fractions (Table II) showed that 92.1% of the iron in the extract was contained in the humic acid precipitate.

TABLE II

Fraction	Organic matter, gm.	Total iron, mg. extracted from 100 gm. of soil
Ether residue	0.190	1.30
Water residue	0.371	0.33
Precipitate	1.283	19.00

In a second experiment, 100 gm. of soil, ground to pass a 100-mesh sieve, was extracted overnight by continuous shaking with 500 ml. of cold pyridine. The material was filtered; the residue was refluxed with 500 ml. of pyridine at 115°. C. for four hours, and filtered. Each filtrate was evaporated nearly to dryness *in vacuo*, the residue extracted with ether, filtered, and dried. The analysis of these humic acid fractions is shown in Table III, (1) and (2).

In further experiments, 20-gm. samples of the soil were extracted by continuous shaking with 500 ml. of a 1% sodium carbonate solution for 24 hr. One sample had been previously leached with 200 ml. of 1% hydrochloric acid solution. This treatment liberates the humic acid held as the insoluble calcium humate. The extracts were filtered and the humic acid was precipitated with an excess of 10% hydrochloric acid. The precipitates were dried and analyzed, with the results shown in Table III, (3) and (4).

TABLE III

ANALYSIS OF HUMIC ACID FRACTIONS

Extracting agent	Humic acid residues			Total iron in humic acid fraction of 100 gm. of soil, mg.	Iron in humic acid fraction as per cent of total soil iron*
	Weight, gm. per 100 gm. soil	Nitrogen, %	Iron, %		
Pyridine at 25° C. (1)	0.350	—	3.7	1.4	0.12
Pyridine at 115° C. (2)	0.804	1.98	19.4	19.4	1.64
Sodium carbonate—direct (3)	4.535	2.48	4.8	21.5	1.82
Sodium carbonate—after leaching with HCl (4)	6.550	2.62	14.4	94.0	7.97

* *The total iron content of this soil is 1.18%.*

Evidently, direct extraction with sodium carbonate or pyridine dissolves only a small amount, about 1.7%, of the total iron in the soil. Nevertheless, an increase of this magnitude in the available iron would be quite significant so far as plant nutrition is concerned. A comparison of the results in Tables I and III shows that direct percolation of the soil does dissolve a considerable amount (about 10%) of the total alkali soluble iron. Pretreatment with hydrochloric acid increases the proportion of the total iron which is subsequently extracted by sodium carbonate to about 8.0%. The total iron content of the humic acid fractions was determined by ashing a weighed quantity in a vitreosil dish at 500° C., dissolving the ash in 5 ml. of 6 N hydrochloric acid, and applying the dipyridyl method.

To determine whether all the iron in the humic acid fraction reacts directly with dipyridyl, the following experiment was carried out. A weighed portion, about 60 mg. of the solid, was dissolved in warm 5% ammonium hydroxide solution and filtered. The total iron in an aliquot of this solution was determined after ashing. Iron that reacted directly with dipyridyl was determined by adding the reagents plus sodium hydrosulphite to a neutralized aliquot of the solution as described above. The blank compensated for the color of the test solution, and complete recovery of added iron in such solutions could be obtained.

Examination of one humic acid preparation gave:—

——	Micrograms of iron per ml. solution
Total iron (average of 12 estimations)	7.86 ± 0.30
Iron reacting directly with dipyridyl (average of 8 estimations)	7.87 ± 0.06

It may be concluded, therefore, that in this humic acid fraction, which contained 2.48% of nitrogen, no significant amount of the iron is combined with nitrogen.

References

1. BURK, D., LINEWEAVER, H., and HORNER, C. K. Soil Science, 33: 413–453; 455–487. 1932.
2. EVELYN, K. A. J. Biol. Chem. 115: 63–75. 1936.
3. HILL, R. Proc. Roy. Soc. London, B, 107: 205–214. 1931.
4. HOPKINS, E. F. Bot. Gaz. 89: 209–240. 1930.
5. IGNATIEFF, V. J. Soc. Chem. Ind. 56: 407 T–410 T. 1937.
6. McFARLANE, W. D. J. Ind. Eng. Chem. Anal. Ed. 8: 124–126. 1936.
7. OLSEN, C. Compt. Rend. Lab. Carlsberg, 18: 1–16. 1930.
8. SMYTHE, C. V. and SCHMIDT, C. L. A. J. Biol. Chem., 88: 241–269. 1930.

AN IMPROVED METHOD FOR THE DETERMINATION OF PHOSPHATE BY PHOTOELECTRIC COLORIMETRY[1]

By W. J. Dyer[2] and C. L. Wrenshall[3]

Abstract

A sensitive and accurate method for the determination of phosphate, involving the application of the Evelyn photoelectric colorimeter to the ceruleomolybdate reaction, is described. This technique makes it possible to differentiate phosphate phosphorus from other forms of phosphorus.

Conditions affecting the rate and extent of color development have been studied. The results show that the maximum color intensity is developed in about five minutes after addition of the reducing agent. The determination may be made in the presence of extraneous color, and soil organic matter does not interfere with the reaction. Under the conditions specified, using light filters, Beer's law applies to the reaction in soil extracts as well as in pure solutions in the range 0.02 to 0.40 parts per million of phosphorus.

Introduction

The concentration of phosphate phosphorus in natural waters and soil extracts is often extremely low; consequently, methods of the highest sensitivity are required for its determination. Comparison of the stated sensitivities attained by the several procedures which have been proposed for the development of the so-called ceruleomolybdate blue color shows that the Truog and Meyer (11) method is capable of the highest sensitivity; it produces an appreciable blue color in the presence of 0.02 parts per million (p.p.m.) of phosphate phosphorus. This procedure is at present in widespread use for the visual colorimetry of phosphate in a variety of soil extracts. It has the advantage that the manipulations are simple and rapid. There is a justifiable general tendency to regard the results of this and other similar methods as rough estimations, valuable only for purposes of comparison. The characteristics of the reaction, which is subject to certain interferences, and which produces an unstable color that increases to a maximum intensity and then gradually fades, have apparently not been accurately defined. Furthermore, precise visual readings are not possible when the solution to be tested is already tinted, as soil extracts so frequently are.

The use of the single-cell type of photoelectric colorimeter* equipped with light filters, described by Evelyn (7), has enabled the writers to make a more exact study of the reaction than has been reported hitherto, and thus to define the conditions under which the concentration of phosphate phosphorus may be determined with a higher degree of accuracy. Determinations may be

carried out on highly colored soil extracts with virtually no impairment of accuracy. This permits the full realization of the aim of Parker and Fudge (10) who proposed the determination of inorganic phosphate phosphorus in the soil extract by direct colorimetry, total phosphorus after ignition, and, by difference, phosphorus present in forms other than orthophosphate, that is presumably combined in organic molecules.

Three recent papers (6, 8, 12) describe techniques for the determination of phosphate by photoelectric colorimetry. The higher sensitivity of the reaction employed in the present work, and the use of light filters selected with reference to the light absorption of the ceruleomolybdate blue color, lead to distinct advantages.

The reaction on which the method depends is a reduction of molybdate by stannous chloride in the presence of phosphate. In the reaction the blue compound, phospho-conjugated ceruleomolybdate, is formed. According to Deniges (4, 5) this compound has the formula $[(MoO_3)_4 . MoO_2]_2 . H_3PO_4 . 4H_2O$. Reduction is effected in the presence of sulphuric acid of such concentration that the reduction of molybdate to the true molybdenum blue, $MoO_2 . 4MoO_3$, is inhibited. Arsenate or antimonate, if present, act as chromogens in the same way as does phosphate.

Experimental

In the proposed method the blue color is developed in a suitably diluted aliquot of the solution to be analyzed, contained in a colorimeter tube, and the maximum intensity of the color is determined by the deflection shown on the galvanometer. The concentration of phosphate in the final solution may be obtained by reference to a calibration curve, or, since the reaction conforms to Beer's law, it may be calculated from the following relation:

$$C = \frac{2 - \log G}{K_1} ,$$

where C is the concentration, G the corrected galvanometer reading (tables of $2 - \log G$ are provided with the instrument), and K_1 is a constant. The calibration curve, or the constant K_1, is previously established by using solutions of known phosphate concentration.

REAGENTS

The reagents used were those specified by Truog and Meyer (11), namely:

(1) Acid molybdate reagent; 2.5% ammonium molybdate in 10 N sulphuric acid.

(2) Stannous chloride; 25 gm. of $SnCl_2 . 2H_2O$ dissolved in 100 ml. of concentrated hydrochloric acid, made up to one litre, and preserved from oxidation by means of a layer of mineral oil.

(3) Standard phosphate; contains 5 p.p.m. of phosphorus as phosphate.

The acid molybdate reagent is stable for at least six months if protected from direct sunlight. The stannous chloride deteriorates slowly and should

be discarded after about one month.   The reagents should give a satisfactory blank test.   A phosphate solution of known strength should be tested daily to check reagents and other conditions affecting the calibration constant.

The proportions of sulphuric acid and molybdate have been thoroughly investigated by Truog and Meyer (11) and lately by Holman and Pollard (9); it has been found that the ratio recommended by the former was satisfactory.

PROCEDURE

An aliquot of sample solution is introduced into a 50 ml. volumetric flask, diluted with distilled water to approximately 45 ml., 2 ml. of acid molybdate reagent is added and the contents immediately mixed.   Water is added to bring the volume to exactly 50 ml., and the contents is again thoroughly mixed.   The dilution of the original sample should be such as to give a final concentration of phosphate phosphorus between 0.02 and 0.4 p.p.m.   A 10 ml. aliquot is pipetted into a colorimeter tube placed in the colorimeter, and the rheostat so adjusted that the galvanometer shows a reading of 100, the 660 filter being used.   One drop of stannous chloride reagent is then mixed with the contents of the tube, and the galvanometer reading is observed five minutes after the addition of the stannous chloride. The concentration of phosphate phosphorus in the final solution is obtained by reference to calibration data, and that of the original solution by taking into account the dilution of the sample.

The method of setting the blank corrects for any color in the solution that absorbs light passing the 660 filter; consequently, interference from extraneous colors in the sample solution is eliminated.   The slight increase in volume due to the addition of stannous chloride need not be considered, as it is the same in standards and unknowns, and hence is included in the calibration.

If only small quantities of sample solution are available, the whole procedure may be carried out in the colorimeter tube, as follows: pipette 10 ml. of sample solution into a colorimeter tube, add 0.4 ml. of acid molybdate, and mix. Adjust to the blank setting, add stannous chloride, and determine the color intensity as directed above.   For this technique, a special calibration should be made, care being taken that the standard phosphate solutions are tested in identical manner.

If a photoelectric colorimeter is not available, valuable work may be done with a balancing type visual colorimeter of large capacity, such as the Kenni-cott-Campbell-Hurley colorimeter*, or by nesslerization.   The visual tech-nique is applicable between the limits of phosphate concentration stated above, and the colors are not sufficiently intense to be matched in an ordinary colorimeter of small capacity.   The colors should be developed simultaneously in the standard and in the unknown solutions, the directions of Truog and Meyer (11) being followed, and the comparison should be made five minutes after the addition of the stannous chloride.   Visual comparisons are never entirely satisfactory, however, when the sample solutions are appreciably tinted.

Obtainable from the Arthur H. Thomas Co.. Philadelphia. U.S.A.

INVESTIGATION OF THE REACTION

Selection of the Color Filter

The approximate absorption curve of a blue solution prepared by the above-mentioned procedure was obtained by the use of a series of filters, each transmitting narrow portions of the visible spectrum. The percentage of the total light transmitted by the blue solution in each range of wavelengths was determined. The absorption curve is shown in Fig. 1. The peak of absorption occurs in the red near 660 millimicrons. Accordingly, the 660 filter, standard with the instrument, was used for this determination.
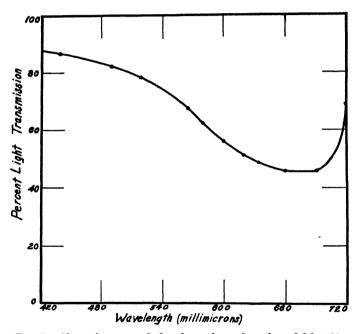
FIG. 1. *Absorption curve of phospho-conjugated ceruleomolybdate blue.*

Effect of Stannous Chloride

Chapman (2) has made a preliminary study of this effect, using glass color standards, and he noted that the intensity of the blue color was influenced by the amount of stannous chloride added. This point has been further investigated. A series of 10 ml. aliquots containing the required amount of acid molybdate reagent was prepared from each of three standard phosphate solutions, from a soil extract, and from pure water. Graded amounts of the stannous chloride reagent were added to each series, and the color development was measured. The results are shown in Fig. 2. The amount of stannous chloride used by Truog and Meyer (11) corresponds to the 0.03 ml. addition, and 0.05 ml. was the amount used in this investigation. It is evident that the amount of stannous chloride added has a definite effect

on the intensity of the color developed. Apparently the effect is due to reduction of the ammonium molybdate itself, since the color of the blank increases with increasing amounts of reducing agent just as does that of the solutions containing phosphate. The behavior of the soil extract is the same as that of pure solutions. Evidently the amount of stannous chloride added should be kept reasonably constant, although small variations from the recommended level will not introduce appreciable errors.
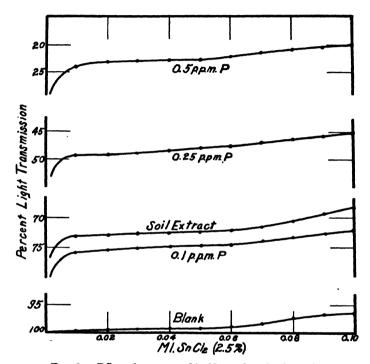
FIG. 2. *Effect of stannous chloride on the color intensity.*

Rate of Reaction

The rates of color development and fading for this reaction have not previously been accurately charted. Fig. 3 shows results obtained by measuring the intensity of the blue color in terms of percentage light transmission at several intervals after the addition of stannous chloride. A soil extract and standard solutions containing three different concentrations of phosphate were examined.

These results show that the maximum color is developed five minutes after the addition of stannous chloride. In solutions of lower phosphate content this maximum intensity is maintained for five minutes or more, but fading begins sooner at the higher concentrations. It seems likely that the earlier fading in the higher range is responsible for the fact that Beer's law is not
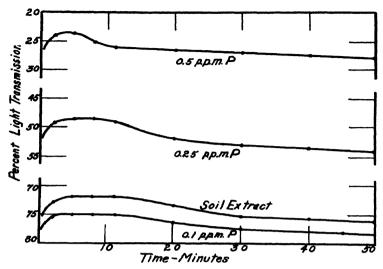
FIG. 3.   *Rate of development and fading of color intensity.*
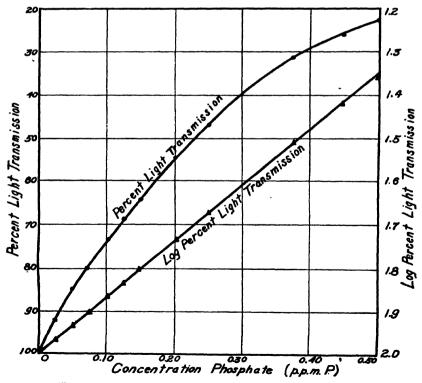
FIG. 4.   *Calibration curve and application of Beer's law.*

applicable to solutions containing more than about 0.4 p.p.m. of phosphorus. It would also account for inaccuracies in techniques in which the time of reading is not rigidly standardized, and where comparisons are made in the range of concentrations greater than 0.5 p.p.m. of phosphorus.

The effect of permitting a considerable period to elapse between the addition of acid molybdate reagent and the addition of stannous chloride was investigated, pure phosphate solutions, phosphate solutions containing 5 p.p.m. of ferric iron, and water extracts of soils being used. A delay of as much as two hours in the addition of stannous chloride was without effect, but longer intervals caused an appreciable diminution of the intensity of the color. With soil extracts containing organic matter, it was found advisable to proceed directly, as a cloudiness sometimes developed on long standing after the addition of acid molybdate.

Calibration Curve and Beer's Law ✓

Solutions of phosphate of known concentration were tested by the procedure described above; the resulting calibration curve is shown in Fig. 4, in which percentage light transmission is plotted against phosphate concentration.

The straight line relation between the logarithm of percentage light transmission and phosphorus concentration shows that in pure solutions ranging in concentration up to 0.4 p.p.m. of phosphorus, or somewhat higher, the reaction conforms with Beer's law. The constant, K_1, has a value of 1.315 ±0.014.

Under reasonably uniform external conditions the calibration values remain constant over long periods. Wide fluctuations in temperature should be avoided; it has been observed that lowering the temperature of the solutions from 26° to 21° C. reduces the intensity of the blue color, with a corresponding decrease in the value of K_1. Calibrations should be made for each instrument under prevailing operating conditions, and K_1 should be checked frequently.

The validity of the application of Beer's law to the determination of phosphate in soil extracts was tested. Known amounts of phosphate were added to soil extracts, determinations were made, and the amounts determined were compared with the known additions. Typical results are shown in Table I.

TABLE I

APPLICATION OF BEER'S LAW TO SOIL EXTRACT DETERMINATIONS

Added phosphate, p.p.m. P	Readings	Phosphate, p.p.m. P		Recovery, %
		Found	Increase	
Soil extract	93.75, 94.0, 94.0	0.020	—	—
0.025	87.0, 87.0, 87.0	0.045	0.025	100.0
0.050	81.0, 81.0, 80.75	0.070	0.050	100.0
0.100	69.75, 70.0, 70.0	0.119	0.099	99.0
0.100	69.75, 70.0, 69.5	0.120	0.100	100.0
0.150	60.5, 60.0, 60.0	0.168	0.148	98.7
0.200	52.0, 51.75, 51.75	0.218	0.198	99.0
0.300	38.5, 37.75, 37.75	0.323	0.303	101.0
0.400	28.0, 28.0, 27.75	0.422	0.402	100.5

The recovery of added phosphate is seen to agree closely with the known additions. As a further test, soil extracts were diluted to different extents, and the concentration of phosphate in the original extracts was calculated from the concentrations in the final solutions. Results are given in Table II.

TABLE II

EFFECT OF ORGANIC MATTER (IN COLORED SOIL EXTRACTS)

Extract	Aliquot (ml.) diluted to 50 ml.	Phosphate found, p.p.m. P	Conc. of phosphate in extract, p.p.m. P
(a)	10	0.098	0.490
	10	0.099	0.495
	20	0.202	0.505
(d)	20	0.023	0.057
	40	0.043	0.054
(e)	20	0.030	0.075
	40	0.062	0.077

From Tables I and II it is evident that the calculation based on Beer's law applies to soil extracts as well as to pure solutions. Table II shows that the extent of dilution of the original extract does not materially influence the result. This is of special interest in view of the statement of Holman and Pollard (9) that dissolved soil organic matter interfered with the reaction in such a way that higher results were obtained in the more dilute extract. This type of interference has not been encountered here. We have noted one case in which the light transmission was interfered with by the formation of a colloidal precipitate which appeared on addition of the acid molybdate reagent.

INTERFERING SUBSTANCES AND CONDITIONS

The effect of the common inorganic acids and their salts has been adequately defined by Chapman (2) and by Holman and Pollard (9).

Organic Acids

Citric acid, which is commonly used in making soil extracts, inhibits the normal reaction, even when present in low concentration. Davies and Davies (3) found that citric, oxalic, tartaric, malic, lactic, and glycollic acids interfered with the Bell-Doisy and Fiske-Subbarow methods, and showed that citric and malic acids form molybdate complexes.

Table III records the effects of some organic acids on the color development in a phosphate solution containing 0.2 p.p.m. of phosphorus.

The data show that α-hydroxy acids, and oxalic acid, have a marked inhibiting action on the color development, while the other acids had little or no effect.

The successful application of the method to water extracts of soil indicates that interfering organic substances are seldom if ever present in concentrations high enough to affect the reaction.

Ferric Iron

Truog and Meyer (11) believed that ferric iron seriously interferes with the reaction by retarding the rate of color development and causing a greenish

TABLE III
EFFECT OF ORGANIC ACIDS

Acid	Acid conc. in final soln., %	Phosphorus, p.p.m., found at various time intervals after addition of stannous chloride		
		5 min.	10 min.	20 min.
Citric	0.9	0	—	—
	0.1	0.03	0.04	0.05
	0.02	0	—	—
Tartaric	0.2	0.052	—	0.065
Acetic, CH_3COOH	0.2	0.200	0.200	0.180
Glycollic, $CH_2OH.COOH$	0.2	0.175	0.162	0.150
Oxalic, $COOH.COOH$	0.2	0	0	0
Trichloracetic, CCl_3COOH	0.2	0.200	0.196	0.180
	2.5	0.168	0.172	0.162
Propionic, CH_3CH_2COOH	0.2	0.200	—	—
Lactic, $CH_3.CHOH.COOH$	0.02	0.200	—	—
	0.4	0.100	0.125	0.125
Hydracrylic, $CH_2OH.CH_2.COOH$	0.2	0.200	0.193	0.180
Malonic, $COOH.CH_2.COOH$	0.2	0.200	0.200	0.186
Hydroxymalonic, $COOH.CHOH.COOH$	0.2	0	—	—

TABLE IV
EFFECT OF FERRIC IRON

Ferric iron added, p.p.m. Fe	Phosphorus found, p.p.m. P	Deviation	
		p.p.m.	%
0	0.195		
1	0.194	−0.001	−0.5
2	0.191	−0.004	−2.0
3	0.191	−0.004	−2.0
4	0.187	−0.008	−4.1
5	0.189	−0.006	−3.1
6	0.188	−0.007	−3.6
7	0.191	−0.004	−2.0
8	0.190	−0.005	−2.6
9	0.187	−0.008	−4.1
15	0.195*	0	0
20	0.198†	+0.003	+1.5
30	0.201†	+0.006	+3.1
40	0.196†	+0.001	+0.5

Faded rapidly.

† *Faded very rapidly with maximum color development at about four minutes.*

tinge to develop, but stated that the effect was probably not serious if the concentration was less than 4 to 6 p.p.m. of iron. Under our conditions we have not found the effect to increase with increasing iron concentration to the same extent as did these workers, and a rapid rate of fading has been observed rather than a retardation of the color development. Table IV shows results obtained by applying the standard technique to solutions containing 0 to 40 p.p.m. of ferric iron, added as ferric chloride.

Evidently the color development was slightly inhibited in solutions containing 0 to 15 p.p.m. of iron; in solutions containing more than 15 p.p.m. of iron, the maximum color intensity was reached sooner, about four minutes after the addition of stannous chloride, and thereafter the color faded very rapidly. This makes high concentrations of ferric iron highly undesirable. Lower concentrations do not appear to introduce a serious error, but for accurate results the concentration of ferric iron should not exceed about 1 p.p.m.

In general, the writers have found that the iron content of soil extracts has not been high enough to cause interference at the final dilution.

Ferrous Iron

The general practice is to eliminate ferric iron by reducing it to ferrous iron, which has been considered not to interfere. Chapman (2) stated that ferrous iron may reduce the color development if the addition of stannous chloride is delayed after the addition of the acid molybdate. This point has been further investigated.

Ferrous iron was added to phosphate solutions in the form of a solution of ferrous ammonium sulphate. The stannous chloride was introduced at the desired time interval after the addition of acid molybdate. The results are shown in Table V.

TABLE V

EFFECT OF FERROUS IRON WITH DELAYED ADDITION OF STANNOUS CHLORIDE

Solution	Time interval between addition of molybdate and stannous chloride, min.	Phosphorus found, p.p.m. P	Deviation	
			p.p.m.	%
Blank + 1 p.p.m. Fe	1	0.0		
	2	0.0		
	5	0.0		
Phosphate soln.		0.191		
Phosphate soln. + 1 p.p.m. Fe	¼	0.191	0.0	0
	½	0.186	0.005	2.6
	¾	0.187	0.004	2.1
	1	0.185	0.006	3.4
	2	0.180	0.011	5.8
	5	0.162	0.029	15.2
Phosphate soln.		0.191		
Phosphate soln. + 2 p.p.m. Fe	½	0.185	0.006	3.4
	1	0.182	0.009	4.7
	2	0.173	0.018	9.4
	5	0.152	0.039	20.5
Phosphate soln.	1	0.183		
	2	0.183		
	5	0.183		
Phosphate soln. + 5 p.p.m. Fe	½	0.182	0.001	0.5
	1	0.163	0.020	11.0
	2	0.147	0.036	19.7
	5	0.132	0.051	27.9

It is evident that ferrous iron definitely inhibits the color development if any considerable time elapses between the addition of molybdate and the addition of stannous chloride. The effect is progressive with increasing time intervals. Even 1 p.p.m. of ferrous iron is sufficient to have an appreciable effect. With intervals of 15 sec. no effect could be detected. Evidently it is essential that the stannous chloride be added immediately (within 15 sec.) after the acid molybdate, if ferrous iron is present in the sample solution. In a previous paragraph it was noted that under normal circumstances intervals up to two hours do not affect the results.

PRECISION AND ACCURACY

The data of Tables I and VII, in which results of duplicate determinations are listed, show the high degree of precision attained by means of this technique. As there is no personal factor involved in making the readings, the same calibration may be used by different investigators without additional errors arising.

The accuracy of the method may be judged from data in Table I, in which the recovery of known amounts of added phosphate is reported.

The photometric technique has also been applied to the determination of total phosphorus in soil following fusion with magnesium nitrate, and in Table VI the results are compared with those of the standard A.O.A.C. titration of ammonium phosphomolybdate (1, p. 10).

TABLE VI

COMPARISON OF TOTAL SOIL PHOSPHORUS BY TITRATION AND COLORIMETRIC METHODS

Soil number	Total phosphorus, % of soil			
	Titration	Av.	Colorimetric	Av.
Macdonald College	0.1024 0.1019	0.1021	0.100 0.100	0.100
1	0.0798 0.0780	0.0789	0.072 0.073	0.0725
2	0.0946 0.0990	0.0968	0.094 0.099	0.0965
3	0.0782 0.0786	0.0784	0.078 0.077	0.0775

The results of the photometric method are in close agreement with those of the standard method, in spite of the high dilution factor involved. This indicates the high degree of accuracy that has been attained.

The method described has been used in this laboratory for the past six months in determining the phosphorus contents of a variety of soil extracts, and has proved highly satisfactory. A feature of this work has been the differentiation of inorganic and organic phosphorus on the basis that the

former reacts directly to give the blue color, while the latter reacts only after the organic matter has been destroyed by ignition. A series of results are given in Table VII.

TABLE VII

ORGANIC AND INORGANIC PHOSPHORUS IN SOIL EXTRACTS

Soil number	Phosphorus in extract, p.p.m. P						Organic phosphorus	
	Inorganic phosphorus			Total phosphorus				
	a^*	b	Av.	a	b	Av.	p.p.m. P	%
Water extracts (1 : 5)								
1†	0.038	0.045	0.041	0.490	0.510	0.500	0.459	91.9
	0.042	0.040						
2	0.945	0.965	0.958	2.40	2.48	2.44	1.482	60.7
	0.935	0.985						
3	0.040	0.040	0.041	0.404	0.400	0.402	0.361	89.8
	0.041	0.043						
4	0.075	0.062	0.070	0.238	0.268	0.253	0.183	72.4
	0.080	0.062						
9	0.216	0.205	0.211	0.770	0.730	0.750	0.539	71.9
	0.220	0.205						
Acid extracts (1 : 200)								
1	0.034	0.035	0.034	0.085	0.080	0.082	0.048	58.5
2	0.106	0.110	0.108	0.140	0.146	0.143	0.035	24.5
3	0.072	0.073	0.072	0.097	0.106	0.101	0.029	28.6
4	0.141	0.141	0.140	0.135	0.145	0.140	0.000	0
9	0.280	0.254	0.267	0.277	0.262	0.269	0.002	0.8

* *a and b represent duplicate extractions.*
† *Soil 1 is a Brown Forest; Soil 2, a Muck; Soil 3, a Calcareous Loam; and Soils 4 and 9 are Podsols.*

In all the water extracts, and in most of the acid extracts, a considerable proportion of the phosphorus present appears to be combined in organic molecules. Thus there is an essential difference between procedures which determine the phosphorus of an extract after ignition and those which depend on direct colorimetry in the original solution, although this fact does not seem to have been generally recognized.

References

ASSOCIATION OF OFFICIAL AGRICULTURAL CHEMISTS. Methods of Analysis, 3rd. ed. 1930.
CHAPMAN, H. D. Soil Sci. 33 : 125-135. 1932.
DAVIES, D. and DAVIES, W. Biochem. J. 26 : 2046-2056. 1932.
DENIGES, G. Compt. Rend. 171 : 802-804. 1920.
DENIGES, G. Compt. Rend. 184 : 687-689. 1927.
EDDY, C. W. and DE EDS, F. J. Ind. Eng. Chem., Anal. Ed. 9 : 12-14. 1937.
EVELYN, K. A. J. Biol. Chem. 115 : 63-75. 1936.
GOODLOE, P. J. Ind. Eng. Chem., Anal. Ed. 9 : 527-529. 1937.
HOLMAN, W. M. and POLLARD, A. S. J. Soc. Chem. Ind. 56 : 339T-343T. 1937.
PARKER, F. W. and FUDGE, J. F. Soil Sci. 24 : 109-117. 1927.
TRUOG, E., and MEYER, A. H. J. Ind. Eng. Chem., Anal. Ed. 1 : 136-139. 1929.
ZINZADZE, C. J. Ind. Eng. Chem., Anal. Ed. 7 : 227-230. 1935.

INDUCED ASYMMETRY AND OPTICAL RESOLUTION OF 2-PHENYLPYRIDINE DERIVATIVES[1]

BY J. G. BRECKENRIDGE[2] AND O. C. SMITH[3]

Abstract

It was shown in 1927 that quinine, when combined with a diphenic acid derivative, gave a salt with an optical rotation in the opposite direction to that of the free alkaloid ("Kuhn's effect"). The present authors have prepared the salts of four of the cinchona alkaloids with 2-phenylpyridine-2':3-dicarboxylic acid, and find similar results. In addition, a partial optical resolution of a derivative of this acid has been effected, the dextro-form of the methiodide of the dimethyl ester having been isolated.

The first example of the type of so-called asymmetric induction described here was observed by Kuhn and Albrecht (4), when, on preparing the quinine salt of 4:4'-dinitrodiphenic acid, they obtained a dextrorotatory product having $[\alpha]_D^{22°} + 110°$ in chloroform. The theory was advanced that the alkaloid induced an asymmetric configuration in the remainder of the molecule, the asymmetry disappearing on removal of the alkaloid, since an inactive acid only could be liberated from the salt. Since then other examples of what is known as "Kuhn's effect" have been observed—Bell and Robinson (1) with 4-nitrodiphenic acid, and Lesslie and Turner (5) with diphenic acid itself—the free acid in each case not having the necessary substituent groups in the 6-positions to show the well known asymmetry of various other derivatives. This subject has been reviewed by Ritchie (7).

A compound of a type similar to diphenic acid is 2-phenylpyridine-2':3-dicarboxylic acid (I).

(I)

(II)

It was thought that it might be of interest to form the salts of (I) with several of the cinchona alkaloids, and possibly provide another example of Kuhn's

effect. Accordingly, the salts of (I) with quinine, quinidine, cinchonine, and cinchonidine were prepared, examined in the polarimeter, and their specific rotations calculated. The results obtained with the free alkaloids and their salts are given in Table I.

TABLE I

SPECIFIC ROTATIONS OF THE FREE ALKALOIDS AND THEIR SALTS

		Quinine	Quinidine	Cinchonine	Cinchonidine
Alkaloids					
	c	2.14	2.10	0.37	2.12
	$[\alpha]_{5461}^{22}$	$-143°$	$+258°$	$+277°$	$-94°$
Salts					
	c	3.03	2.90	3.04	2.96
	$[\alpha]_{5461}^{22}$	$+244°$	$-206°$	$-250°$	$+303°$
	$[\alpha]_{5780}^{22}$	$+209°$	$-175°$	$-211°$	$+259°$
	$[\alpha]_{4358}^{22}$	$+476°$	$-412°$	$-516°$	$+617°$
	$[M]_{5461}^{22}$	$+2175°$	$-1835°$	$-2078°$	$+2519°$

The rotations were measured in chloroform in a 20 cm. tube, and, with the exception of cinchonine, the concentrations used were such that the amount of alkaloid present, both free and in the salt, would be approximately the same.

Lesslie and Turner (5) observed mutarotation both in the initial mixture of diphenic acid and alkaloid, and in solutions of the crystallized salts. In the present work, solutions of the salts showed a constant rotation, the first reading being taken three minutes after the salt was wetted, a mixture of two volumes of ethanol to one volume of chloroform being used, but the muta-rotation in the freshly prepared solution was just observable. Equivalent quantities of the acid·and each alkaloid were dissolved in ethanol, mixed, made up to a known volume, and the first readings taken one and one-half minutes after mixing. Observations were made at intervals for 48 hr. The rotation increased noticeably during the first two minutes of observation, but thereafter remained constant. Apparently with (I) the activation process is very much more rapid than it is with diphenic acid, although the two compounds are very similar.

Attempts have been made to resolve derivatives of (I), use being made of the conveniently situated nitrogen atom. Chalmers, Lions, and Robson (2) worked with the strychnine and brucine salts of the methosulphate, but could obtain no evidence of resolution, and the present authors attempted the preparation of salts of the cinchona alkaloids with both the metho- and etho-sulphates, but were unsuccessful. A crystalline salt could not be isolated, the usual result being the recovery of the metho- or etho-sulphate of the alkaloid. However, a partial resolution of the methiodide of the dimethyl ester (II) was effected by the use of silver α-bromocamphor-π-sulphonate,

the dextro-form of (II) being isolated. The silver salt of (I) was treated with methyl iodide to obtain the ester, which was heated with more methyl iodide in a sealed tube, and the resulting methiodide was treated with silver bromocamphor sulphonate. The crystalline bromocamphor sulphonate obtained showed a rotation in chloroform ($c = 2.0$) of 4.28° for λ 5461Å, from which the specific rotation $[\alpha]_{5461}^{22} = +107°$, and $[M]_{5461}^{22} = +637°$. The methiodide, recovered by shaking a chloroform solution of the bromo-camphor sulphonate with aqueous potassium iodide and precipitating with ether, gave a rotation in chloroform ($c = 0.30$) of 0.94° for λ 5461Å, from which $[\alpha]_{5461}^{22} = +156.7°$, and $[M]_{5461}^{22} = +648°$. All rotations were measured in a 20 cm. tube. The value recorded for the methiodide was unaltered after two recrystallizations, and an experiment carried out in ethanol solution showed no change in rotation after heating to 70° C. for three hours.

This is evidently another process of activation rather than resolution, similar to several already recorded (6), whereby one form only crystallizes (in this case the *d*-bromocamphor sulphonate *d*-complex). In previous instances it was found possible to obtain the other form by changing the solvent or method of crystallization—in the present work the amount of material available was insufficient to permit the writers to proceed further, and it was felt that the isolation of the *d*-form was sufficient proof of the point in question.

Experimental

α-Naphthoquinoline was prepared according to the method of Chalmers, Lions, and Robson (2), boric acid and ferrous sulphate being added, as in the modification of Skraup's quinoline synthesis given by Cohn (3). The naphthoquinoline was oxidized to the acid; yield, about 45%. (The authors wish to acknowledge the assistance of J. N. Robinson of this Department in carrying out the above-mentioned synthesis and some preliminary experiments.)

The general procedure in preparing the salts was as follows. The acid (1.5 gm.) in hot 25% ethanol was added to the calculated amount of the anhydrous alkaloid in hot 95% ethanol (4.00 gm. for quinine and quinidine, 3.63 gm. for cinchonine and cinchonidine). The mixture was filtered, evaporated to crystallization, and the product recrystallized from a suitable solvent.

Quinine salt. Recrystallized three times from 80% ethanol; orthorhombic crystals; yield, 80%. Calcd. for $C_{13}H_9O_4N . 2(C_{20}H_{24}O_2N_2)$: C, 71.3; H, 6.45%. Found: C, 71.1; H, 6.49%.

Quinidine salt. Recrystallized twice from a mixture of ethyl acetate (75%) and ethanol (25%); well formed monoclinic crystals; yield, 80%. Calcd. values as above. Found: C, 71.2; H, 6.36%.

Cinchonine salt. Recrystallized twice from 95% ethanol; small needles; yield, 60%. Calcd. for $C_{13}H_9O_4N . 2(C_{19}H_{22}ON_2)$: C, 73.6; H, 6.43%. Found: C, 73.4; H, 6.51%.

Cinchonidine salt. Recrystallized three times from 25% ethanol; ortho-rhombic crystals; yield, 87%. Calcd. values as for cinchonine salt. Found: C, 73.9; H, 6.50%.

A detailed crystallographic examination of these salts has been carried out by Dr. M. A. Peacock, Department of Mineralogy, the results to be published elsewhere shortly.

Polarimetric observations. The alkaloid or salt was dissolved in 17 cc. of chloroform, and the rotation measured at 22° C. in a 20 cm. tube.

TABLE II
POLARIMETRIC OBSERVATIONS

Compound	Mol. wt.	Wt. used	α_{5461}	α_{5780}	α_{4358}	$[\alpha]_{5461}$
Quinine	324	0.3629	− 6.1	—	—	−143°
Quinidine	324	0.3570	+10.8	—	—	+258°
Cinchonine	294	0.0626	+ 2.0	—	—	+277°
Cinchonidine	294	0.3602	− 4.0	—	—	− 94°
Quinine salt	891	0.5060	+14.5	+12.5	+28.3	+244°
		0.5151	+14.8	+12.7	+28.9	+244°
Quinidine salt	891	0.5002	−12.1	−10.3	—	−206°
		0.4921	−11.9	−10.2	−23.9	−206°
Cinchonine salt	831	0.5015	−14.8	−12.5	−30.8	−250°
		0.5167	−15.2	−12.8	−31.4	−250°
Cinchonidine salt	831	0.4950	+17.6	+15.0	—	+302°
		0.5031	+17.9	+15.3	+36.5	+303°

Mutarotation experiments. The quinine salt (1.00 gm.) was dissolved in 100 cc. of a mixture of two volumes of ethanol and one volume of chloroform, and the rotation observed in a 40 cm. tube, the first reading being taken three minutes after the salt was wetted. Observed rotations were: $\alpha_{5461} = +3.51°$, $\alpha_{5780} = +3.00°$; this gave $[\alpha]_{5461} = +87.5°$, $[\alpha]_{5780} = +75°$. These values were unchanged after more than 48 hr.

Acid (1.50 gm.) and quinidine (4.00 gm.), both in 95% ethanol, were mixed, the volume was made up to 200 cc., and observed in a 40 cm. tube, the first reading being taken two minutes after mixing; $\alpha_{5780} = −2.66°$. The rotation increased rapidly, and after about one minute of observation had risen to $\alpha_{5780} = −2.91°$, equivalent to $[\alpha]_{5780} = −26.4°$; this value remained unchanged after more than 48 hr. The mutarotation was too rapid to allow accurate and reproducible readings, but its existence could not be doubted.

Experiments similar to the above were carried out with the other salts and similar results obtained. It will be seen that the specific rotations with alcohol present are very much lower than those taken in chloroform—this was also observed with diphenic acid.

Preparation of the Methiodide of the Dimethyl Ester (II)

A portion (10 gm.) of the acid (I) was dissolved in 2000 cc. of distilled water, and the silver salt precipitated by addition of 15 gm. of silver nitrate

and 15 gm. of ammonium acetate in distilled water. The silver salt was dried, refluxed, and shaken for several hours with excess of methyl iodide in ether. The mixture was filtered, the ether removed, and the residual reddish oil heated in a sealed tube with excess of methyl iodide at 100° C. for four hours. The resulting gum crystallized from acetone-ether as yellow crystals; m.p. 149° C.* Recrystallization gave faintly yellow clusters, m.p. 151° C., which remained unchanged after another crystallization. Calcd. for $C_{16}H_{16}O_4NI$: C, 46.5; H, 3.90; I, 30.7%. Found:† C, 46.2, 46.9; H, 3.93, 3.82; I, 30.5%.

A portion (1.80 gm.) of (II) in 60 cc. of 50% methanol was added to 1.92 gm. of silver bromocamphor sulphonate in 30 cc. of distilled water. The mixture was filtered, evaporated *in vacuo*, and the resulting colorless glass crystallized from acetone-ether as small white needles. Recrystallization gave 0.90 gm. of product, m.p. 210° C. Calcd. for $C_{26}H_{30}O_8NSBr$: C, 52.3; H, 5.07; Br, 13.4%. Found:† C, 52.5, 52.5; H, 4.90, 4.79; Br, 13.4%.

A portion (0.500 gm.) of the above-mentioned product in 25 cc. of chloroform in a 20 cm. tube gave $\alpha^{22}_{5461} = +4.28°$, $\alpha_{5780} = +3.75°$, from which $[\alpha]_{5461} = +107°$ and $[M]_{5461} = +637°$; 0.100 gm. in 5 cc. of ethanol gave $\alpha_{5461} = +3.33°$, $\alpha_{5780} = +2.80°$, from which $[\alpha]_{5461} = +83°$, and $[M]_{5461} = +495°$. These and all subsequent rotations were measured in a 20 cm. tube at 22° C.

The solution of the bromocamphor sulphonate in chloroform was shaken with aqueous potassium iodide, the resulting yellow chloroform layer was separated, dried over anhydrous calcium sulphate (Drierite), and the methiodide crystallized by addition of ether; 0.22 gm. was obtained as minute, faintly yellow crystals, m.p. 151° C.

The methiodide (0.0150 gm.) in 5 cc. of .chloroform showed rotations of $\alpha_{5461} = +0.94°$, $\alpha_{5780} = +0.73°$, from which $[\alpha]_{5461} = +156.7°$ and $[M]_{5461} = +648°$. Recrystallization of the methiodide gave a product having exactly the same rotation. A portion (0.0150 gm.) in 5 cc. of 95% ethanol showed rotations of $\alpha_{5461} = +0.18°$, $\alpha_{5780} = +0.12°$, and these values were unchanged after the solution was heated at about 70° C. for several hours. From the residues resulting from the above-mentioned experiments, the methiodide recovered gave exactly the same results, and it is apparent that the compound is optically pure.

References

1. Bell, F. and Robinson, P. H.   J. Chem. Soc. 2234-2239. 1927.
2. Chalmers, A. J., Lions, F., and Robson, A. O.   J. Proc. Roy. Soc. N.S.Wales, 320-326. 1931.
3. Cohn, E. W.   J. Am. Chem. Soc. 52 : 3685-3688. 1930.
4. Kuhn, R. and Albrecht, O.   Ann. 455 : 272-299. 1927.
5. Lesslie, M. S. and Turner, E. E.   J. Chem. Soc. 347-350. 1934.
6. Mills, W. H. and Breckenridge, J. G.   J. Chem. Soc. 2209-2216. 1932.
7. Ritchie, P. D.   Asymmetric synthesis and asymmetric induction.   Oxford University Press. 1933.

* *Melting points are corrected.*
† *Carbon-hydrogen microanalyses by Dr. H. Stantial, Department of Chemistry.*

CONTRIBUTION À L'ÉTUDE D'*ACER SACCHARUM*

II. LA PRÉSENCE D'AMYLASES DANS LA SÈVE D'ÉRABLE ET LES PRODUITS D'HYDROLYSE[1]

PAR ELPHÈGE BOIS[2] ET ARISTIDE NADEAU[3]

Résumé

Les glucides de la sève d'*Acer saccharum* proviennent de l'hydrolyse enzymatique de l'amidon dans les racines. Le seul sucre réducteur présent dans la sève d'érable est le cellobiose, ce qui explique la valeur du pouvoir rotatoire des sirops d'érable avant et après l'interversion. Les amylases de la sève d'érable hydrolysent l'amidon en sucrose et cellobiose, non en maltose, d'où les noms de sucrogène-amylase et cellobiogène-amylase.

Introduction

Bien que les opinions émises sur l'activité des amylases depuis Dubrunfaut, Payen, et Persoz (1830) jusqu'à nos jours, divergent, toutes s'accordent pour affirmer que l'amidon est dédoublé en maltose; seuls Giri et Sreenivasan (4) à notre connaissance, font remarquer que dans le cas de l'amylase de pH optimum 7.0, le point final de la coloration avec l'iode est obtenu sans formation mesurable de maltose. Cette observation démontre, selon ces auteurs, que pendant les premiers stades de la digestion de l'amidon, cette enzyme ne produit pas de groupe réducteur durant les premiers temps de sa présence dans les plantes.

Les travaux faits jusqu'ici sur la sève d'érable avaient surtout pour objet la fabrication du sirop (1, 13), la reconnaissance de sa falsification (6, 7, 11), l'étude de son arome (3, 10, 12) et ses micro-organismes (2).

Jones et Bradlee (8, pp. 137, 138), cependant, ont étudié la teneur de l'érable en hydrates de carbone suivant les saisons et admettent que leur transformation est due à l'activité de certains ferments. Ils ont trouvé, ce que nous avons aussi vérifié, qu'à l'automne, la richesse en sucrose de l'érable, soit dans le tronc au niveau de l'entaille, soit dans les racines, est très faible, tandis que la teneur en amidon est très forte surtout dans les racines. A mesure que la saison avance nous avons constaté un gain en sucrose allant jusqu'à 80% et un autre gain 7 à 8 fois plus grand en sucre réducteur; par contre il y a perte en amidon d'environ 30%.

Partie expérimentale

Cette diminution de l'amidon a été constatée aussi dans l'examen de coupes minces. Ces coupes ont été faites sur des racines fraîchement arrachées, puis mises entre lame et lamelle et traitées uniquement avec une solution d'iode. Pendant l'hiver on constate la présence de nombreux petits grains

d'amidon dans les vaisseaux. Au temps de la coulée, la plupart des vaisseaux sont vides. Les grains d'amidon ont disparu. Cette transformation est vraisemblablement le résultat de l'activité de certains ferments.

Si on ajoute une solution d'amidon à de la sève d'érable, on constate après quelques heures la disparition de l'amidon ou du moins l'absence de réaction avec l'iode (12). Tout semble se passer comme dans le cas d'une suspension d'amidon en présence de salive, d'extrait de malt ou de taka-diastase. Nous avons étudié systématiquement cette action de la sève sur l'amidon en fonction de la température et du pH.

La cueillette de la sève se faisait au printemps dans des fioles contenant une quantité suffisante de toluène pour empêcher tout développement microbien; elle était conservée dans la glacière.

Influence de la température

On détermine la vitesse d'hydrolyse d'une solution d'amidon en présence de sève d'érable à différentes températures. L'expérience est faite au moyen d'une solution d'amidon à 1% et d'une quantité égale de sève tamponnée à pH 6.6 à 6.8 moyen de solutions $M/15$ de phosphates monopotassique et disodique. Le pH désiré est obtenu par un mélange de l'une et de l'autre

TABLEAU I

HYDROLYSE DE L'AMIDON À pH CONSTANT (6.6 À 6.8)

T, °C.	Après 17 h.	Après 24 h.	Après 40 h.	Après 48 h.
2	Violet	Rouge violet	Rouge brun	Rouge brun
8	Rouge violet	Rouge brun	Brun rouge	Brun rouge
15	Rouge brun	Brun rouge	Brun	Brun clair
20	Rouge brun	Brun	–	–
40	Brun	–	–	–
50	Brun	–	–	–
60	Brun rouge	Brun	Brun clair	–

solution en proportion déterminée. Au bout d'intervalles de temps fixes, on prélève 2 cc. de la solution à laquelle on ajoute cinq gouttes d'une solution d'iode $N/50$. La coloration obtenue indique la plus ou moins grande hydrolyse de l'amidon.

A 2° C., tableau I, on constate une coloration rouge brun même après 48 h. Pour le même temps à 8° C. la coloration est brune, tandis qu'à 15° C. elle est d'un brun clair. A 20° C. aucune coloration avec l'iode après 40 h. A 40° et 50° C. moins de 24 h. suffisent pour une réaction négative. A 60° C. légère coloration brune après 40 h. Si la solution est portée à 80° C. pendant quelque temps, il n'y a plus d'hydrolyse; la coloration bleue persiste; les ferments sont détruits à cette température. Les températures entre 40° à 50° C. semblent donc être les plus favorables.

Influence du pH

Les mêmes solutions d'amidon et de ferments maintenues à 40° C. sont tamponnées cette fois-ci à differents pH à partir de 4.0 à 7.5 au moyen de

mélanges en différentes proportions de solutions $M/15$ de phosphates mono-
potassique et disodique. Les résultats obtenus sont indiqués dans le ta-
bleau II. Comme on le voit à pH 4.2 une coloration rouge brun persiste
après 48 h.; de pH 5.5 à pH 6.75, moins de 20 h. suffisent pour une réaction
négative, tandis qu'il faut un peu plus de 48 h. à pH 7.5.

Des résultats sensiblement les mêmes sont obtenus à 50° C. (tableau III).
La zone de pH la plus favorable s'écend comme dans le premier cas de pH
5.2 à pH 6.7. Cette température semble être moins favorable pour les pH
extrêmes. Ces faits suffisent pour prouver sans aucun doute la présence des
ferments du amylase dans la sève d'érable.

TABLEAU II

HYDROLYSE DE L'AMIDON À TEMPÉRATURE CONSTANTE (40° C).

pH moyen	Après 17 h.	Après 24 h.	Après 40 h.	Après 48 h.
4.20	Rouge brun	Rouge brun	Rouge brun	Rouge brun
4.79	Brun	Brun	–	–
5.38	Brun	–	–	–
5.77	Brun	–	–	–
6.16	Brun	–	–	–
6.75	Brun	–	–	–
7.46	Brun rouge	Brun	Brun	Brun clair

TABLEAU III

HYDROLYSE DE L'AMIDON À TEMPÉRATURE CONSTANTE (50° C.)

pH moyen	Après 17 h.	Après 24 h.	Après 40 h.	Après 48 h.
4.03	Violet	Rouge brun	Rouge brun	Rouge brun
4.84	Brun rouge	Brun	Brun	Brun clair
5.20	Brun	–	–	–
5.81	Brun	–	–	–
6.17	Brun	–	–	–
6.67	Brun	–	–	–
7.42	Rouge brun	Brun rouge	Brun rouge	Brun

Les produits d'hydrolyse

Poussant plus avant nos recherches, nous avons voulu caractériser le ou
les produits formés par le dédoublement de l'amidon. Puisque les glucides
de réserve se trouvent emmagasinés dans les racines et que durant l'hiver
nous voyions disparaître l'amidon de ces racines, nous avons cru y trouver
ses produits de transformation. D'autre part on constate aussi dans le
dosage des sucres du sirop d'érable qu'il y a une faible quantité de sucre réduc-
teur qui ne peut pas provenir de l'interversion du sucrose. Nous avons
d'ailleurs trouvé que tout échantillon de sève d'érable, malgré les précautions
prises lors de la récolte pour empêcher l'interversion du sucrose, possédait
un pouvoir réducteur supérieur au pouvoir réducteur d'une solution de
sucrose de même concentration. Certains admettent la présence de lévulose
(1); nous avons donc recherché la nature de ce produit réducteur.

Cellobiose

(a) *Dans les racines.* Nos études ont porté d'abord sur les racines. Débarrassées complètement de leur écorce, elles étaient réduites en pulpe. On traite 100 g. de cette pulpe par deux litres d'alcool éthylique à 80% pendant 30 min. à l'ébullition en présence de carbonate de calcium pour neutraliser les acides. Après filtration et distillation de la solution alcoolique, le résidu est repris par l'eau, et décoloré au noir animal. On ajoute 100 cc. de la solution obtenue, contenant 3% de solide environ, à 5 g. de chlorhydrate de phénylhydrazine purifié et 10 g. d'acétate de sodium. On chauffe le tout au bain-marie pendant une heure. Il y a formation d'une osazone à chaud. Après l'avoir filtrée et purifiée, on détermine sa forme cristalline et sa solubilité comme glucosazone (P.F., 205° C.). Par refroidissement le filtrat laisse déposer une osazone jaune brun, cristallisée en aiguilles groupées en forme d'oursin. Cette osazone purifiée par recristallisation dans l'alcool a un point de fusion de 198° C.

(b) *Dans la sève.* La même methode employée avec de la sève fraîche donne des résultats semblables. Avec 250 cc. de sève fraîche, chauffée au bain-marie pendant une heure en présence de 7 g. de chlorhydrate de phényl-hydrazine et 14 g. d'acétate de sodium, il y a formation tantôt des deux mêmes osazones, tantôt uniquement de l'osazone cristallisée en aiguilles groupées en forme d'oursin. Le glucose, présent dans certains cas, peut provenir de l'hydrolyse du sucrose ou du cellobiose.

(c) *Amidon en présence de sève.* Les mêmes résultats sont obtenus avec de la sève en présence d'amidon. La sève est dialysée dans des sacs de cellophane jusqu'à disparition des sucres. Deux cents centimètres cubes de sève ainsi traitée et une quantité égale d'une solution d'amidon à 1% sont tamponnées à pH 6.5 au moyen de tampon aux phosphates comme plus haut. Le tout est placé à 37° C. jusqu'à disparition de la coloration avec l'iode. La solution est alors filtrée, puis additionnée de 10 g. de chlorhydrate de phénylhydrazine et de 20 g. d'acétate de sodium. Les osazones obtenues dans les conditions mentionnées plus haut, sont identiques à celles trouvées précédemment. Nous faisons remarquer que dans les trois cas nous n'avons jamais obtenu la maltosazone.

Le dosage de l'azote par la méthode Kjeldahl sur cette osazone cristallisée en aiguilles groupées en forme d'oursin donne 10.6% d'azote (valeur théorique, 10.77%), ce qui prouve la présence d'un sucre réducteur en C_{12}. De plus l'osazone obtenue à partir d'une solution de cellobiose authentique, a donné la même forme crystalline, la même solubilité et le même point de fusion (198° C.). Le mélange des deux osazones donne le même point de fusion. Le sucre réducteur formé est bien du cellobiose.

2. *Sucrose*

La présence de sucrose dans la sève nous a conduits à chercher s'il n'y avait pas formation de ce sucre dans l'hydrolyse de l'amidon par les ferments de la sève d'érable. Une solution d'amidon à 1% et de la sève dialysée sont

tamponnées à pH 6.6 au moyen de tampons aux phosphates et laissées à 17° à 18° C. environ, jusqu'à l'absence de réaction avec l'iode.   Le dosage des sucres est fait par la méthode Munson et Walker, avant et après traitement par l'invertase, au début et à la fin de l'hydrolyse.   Une augmentation en sucre correspondant à 30% de la quantité théorique de formation de sucrose est alors constatée.   Comme l'action de l'invertase employée était nulle sur une solution de cellobiose et aussi sur la solution d'amidon, cette augmentation ne peut être attribuée qu'à la transformation de l'amidon en sucrose.

Discussions et conclusions

1. Nos travaux permettent de corriger et de développer, en partie du moins, la théorie de la génèse du sucre d'érable.   Chez *Acer saccharum*, les glucides résultant de la fonction chlorophyllienne au niveau des feuilles pendant l'été, sont transportées au fur et à mesure de leur production dans les racines, où ils se transforment en amidon.   Tous les vaisseaux libériens et les rayons médullaires en sont gonflés.   Durant l'hiver, suivant les variations de la température, cet amidon s'hydrolyse en faible quantité, puis au printemps le phénomène s'accentue brusquement et l'amidon disparaît pour donner naissance à deux glucides en C_{12}: le sucrose et le cellobiose, que nous trouvons dans la sève au moment de la coulée.

2. Le seul sucre réducteur présent dans la sève au moment de sa sortie de l'érable est le cellobiose.

Déjà en 1911, Bryan (1, p. 64) luttait contre l'affirmation de la présence de sucre interverti dans la sève d'érable, qu'on expliquait alors par une hydrolyse du sucrose par les cellules de l'arbre qui devaient y trouver un combustible plus apte à être utilisé.

Bryan mettait aussi en doute une deuxième hypothèse basée sur les différences entre les dosages chimiques et polarimétriques des glucides de la sève. En effet, on constatait que la valeur du pouvoir rotatoire, avant comme après l'interversion, était toujours inférieure à ce qu'elle aurait dû être si l'on n'avait eu affaire qu'au sucrose.   L'on admettait alors la présence de lévulose dont le pouvoir rotatoire $[\alpha]_D = -92°$.

Après bien des mesures et des dosages, Bryan concluait que si le lévulose est présent, il doit tout de même être accompagné d'une autre substance optiquement active.

Avec le cellobiose, nous avons une explication de ces lectures trop faibles au polarimètre.   Nous sommes en présence de sucrose, $[\alpha]_D = +66°$, et de cellobiose, $[\alpha]_D = +35°$.   Donc avant l'interversion la lecture est plus faible que pour une solution de sucrose de même concentration.   Après l'hydrolyse, nous avons: sucre interverti $[\alpha]_D = -19.84°$, et le glucose, $[\alpha]_D = +52°$ provenant du cellobiose, la lecture est encore inférieure à celle d'une solution de sucre interverti seul.   La preuve que nous n'avons que du cellobiose comme sucre réducteur, découle de l'obtention de son unique phénylosazone caractérisée par son point de fusion mixte, sa teneur en azote, sa cristallisation et sa solubilité.

3. Il y a dans la sève d'*Acer saccharum* deux ferments du type amylase. Les premiers qui aient signalé l'hydrolyse de l'amidon par la sève d'érable n'ont donné aucune preuve que le phénomène était enzymatique.

Nous apportons ces preuves: un chauffage de la sève à 80° C. fait disparaître ses propriétés amylolytiques, la dialyse de la sève amène une diminution de ces propriétés par séparation du ou des co-ferments. L'action de la sève sur l'amidon, contrôlée par la réaction avec l'iode, varie suivant la température et la concentration en ions hydrogène. Elle est plus marquée à 40° à 50° C. et dans la zone de pH compris entre 5.3 à 6.7.

4. Ces ferments hydrolysent, *in vitro*, une solution d'amidon en cellobiose et sucrose sans production de maltose. C'est croyons-nous, la première fois que ce fait est observé et étudié.

Cette conclusion est des plus importantes. Il était admis, d'une part (Haworth (5)) que la caractéristique de l'amidon, c'était son hydrolyse en maltose, tandis que celle de la cellulose c'était son hydrolyse en cellobiose. L'étude de ces deux polysaccharides et de leurs dérivées immédiats était pour ainsi dire, basée sur cette admission. D'après les résultats obtenus ici, il faudrait modifier les hypothèses émises jusqu'à aujourd'hui sur la constitution de l'amidon et admettre que les cycles pyraniques et furaniques coexistent dans la chaîne d'amidon.

D'autre part, il était aussi reconnu que dans les feuilles des plantes, il y a, durant le jour, par ordre d'importance, du sucrose, des hexoses, et de l'amidon. Durant la nuit la quantité de l'amidon croît aux dépens des autres glucides. On admettait donc la formation des hydrates de carbone d'après cette suite de phénomènes.

$$CO_2 + H_2O \longrightarrow HCOH$$
$$Amidon \longleftarrow C_6H_{12}O_6 \underset{Nuit}{\overset{Jour}{\rightleftharpoons}} Sucrose$$

Mais cet amidon disparaissait de quelle façon? "In none of the starch-bearing (Miller (9, p. 436)) leaves were they able to detect maltose, . . ." (9, p. 440) ". . . since so far as anyone knows, cane sugar does not arise directly from starch."

Nous avons démontré la transformation de l'amidon en sucrose, *in vitro*; nous l'avons constaté chez les racines de l'érable et nous croyons que dans les feuilles il en est de même.

5. Les enzymes contenues dans la sève d'*Acer saccharum* qui hydrolysent l'amidon en sucrose et cellobiose; nous les avons nommées: sucrogène-amylase et cellobiogène-amylase. Elles se distinguent nettement des amylases connues à date par les produits formés.

Le prénom "sucrogène" indique bien ici le phénomène hydrolytique observé, et nous l'employons par opposition à saccharogène-amylase déjà connu, qui désigne le ferment hydrolysant l'amidon en un sucre en C_{12} (maltose) tandis que le dextrinogène-amylase indique une hydrolyse partielle de l'amidon.

La sucrogène-amylase se rapproche du type β-amylase parce qu'au voisinage de la température optimum, la coloration avec l'iode persiste longtemps. La cellobiogène-amylase semble appartenir au type α-amylase.

Bibliographie

1. BRYAN, A. H.   U.S. Dept. Agr. Bur. Chem. Bull. 134.   1911.
2. EDSEN, H. A., JONES, C. H., ET CARPENTER, C. W.   Vermont Agr. Expt. Sta. Bull. 167. 1912.
3. FINDLAY, G. H. ET SNELL, J. F.   Can. J. Research, B, 13 : 269-275.   1935.
4. GIRI, K. V. ET SREENIVASAN, A.   Nature, 138 : 406-407.   1936.
5. HAWORTH, W. N. ET HIRST, E. L.   Trans. Faraday Soc. 29 : 14-17.   1933.
6. JONES, C. H.   Vermont Agr. Expt. Sta. Rept. 17 : 446-459.   1904.
7. JONES, C. H.   Vermont Agr. Expt. Sta. Rept. 18 : 315-339.   1905.
8. JONES, C. H. ET BRADLEE, J. L.   Vermont Agr. Expt. Sta. Bull. 358.   1933.
9. MILLER, E. C.   Plant physiology.   McGraw-Hill Book Company, New York.   1931.
10. NELSON, E. K.   J. Am. Chem. Soc. 50 : 2006-2012.   1928.
11. RISI, J. ET BOIS, E.   Recherches analytiques sur la matière aromatique des produits de l'érable à sucre.   Contribution de l'École Supérieure de Chimie, Université Laval, No. 1.   1933.
12. RISI, J. ET LABRIE, A.   Can. J. Research, B, 13 : 175-184.   1935.
13. VAILLANCOURT, C.   Erablières.   Ministère de l'Agriculture Bull. 72.   1927.

CONTRIBUTION À L'ÉTUDE D'*ACER SACCHARUM*

III. ACTIVITÉ DES AMYLASES DE LA SÈVE D'ÉRABLE[1]

PAR ELPHÈGE BOIS[2] ET ARISTIDE NADEAU[3]

Résumé

Les conditions optima de l'activité de la sucrogène-amylase sont: un pH de 6.6 et une température de 8° C.; tandis que la cellobiogène-amylase a son maximum d'action à 50° C. et à pH 4.8.

L'activité de ces amylases augmente à mesure que la saison de coulée avance. Au printemps, le pH de la sève est précisément le pH optimum de formation du sucrose (pH 6.6). De plus la température de cette saison (0° à 15° C.) est favorable à la formation du sucrose qui cesse avec la venue des jours chauds.

Introduction

Après avoir reconnu l'existence d'amylases dans la sève d'érable et avoir caractérisé les glucides résultants de leur action sur l'amidon, nous sommes en mesure de poursuivre l'étude de ces ferments et de déterminer dans quelles conditions leur travail est effectué. Nous pourrons ainsi vérifier ce que nous avons déjà avancé (2) au sujet du maximum d'activité, qui, d'après les travaux de Sherman, Thomas et Caldwell (14), doit-être voisin du minimum de pouvoir tampon analogue au point isoélectrique.

La mesure de l'activité se fera en déterminant à intervalles fixes, les quantités de sucre réducteur (cellobiose) et de sucrose produites au cours de l'hydrolyse d'une solution d'amidon par la sève d'érable en faisant varier la température et le pH.

Ce sont les deux facteurs les mieux étudiés à date. Ils font l'objet d'un grand nombre de travaux dont les conclusions sont plus ou moins contradictoires. Il est juste de dire avec Kopaczewski (4) que l'activité des amylases est influencée par la pureté et l'âge des enzymes, par la composition et l'état physique du substrat, par les conditions expérimentales et par la concentration des cations ou anions présents à côté de l'ion H^+; autant de facteurs qui peuvent faire varier les résultats.

Partie expérimentale

A. TECHNIQUE DES MANIPULATIONS

Préparation de la solution d'amidon

L'amidon soluble pesé est délayé dans un peu d'eau chaude. L'ébullition est continuée pendant deux minutes, puis le tout est refroidi aussi rapidement que possible. Le volume d'eau est ensuite ajusté de manière que la solution soit de concentration égale à 1%.

[2] *Professeur de Biochimie à l'Université Laval.*
[3] *Etudiant gradué, de l'Université Laval, Boursier du National Research Council of Canada.*

Les ferments

La sève cueillie au temps de la coulée (mars, avril) contient, en plus des ferments, une quantité de sucrose qui varie de 1 à 4% et quelques centièmes de un pour cent de cellobiose.

Les essais d'élimination de ces glucides (précipitation, dialyse, ultrafiltration) nous ont toujours laissé une solution de ferments de faible activité.

C'est donc avec de la sève telle qu'obtenue de l'arbre que nous avons fait nos expériences. Pour la conserver, elle était mise en bouteille avec une quantité suffisante de toluène pour la saturer et maintenue dans un endroit frais, environ 12° C. Ce mode de conservation est efficace pour une période de quelques mois. Les manipulations qui ont servi à l'obtention des courbes 1-2-3 ont été faites à la fin de l'été avec cette sève.

Pour les périodes de conservation plus longues (8 à 12 mois), la sève fraîche était concentrée dans le vide, à une température inférieure à 25° C., jusqu'à une teneur de 60% en solide. Ce sirop était ensuite saturé de toluène et conservé à la glacière. Pour l'emploi, il suffisait de le diluer jusqu'à la concentration de la sève originale, c'est-à-dire 4 à 5% de solide, déterminée au moyen du réfractomètre.

Le pouvoir amylolytique pouvait se maintenir de cette façon, tandis que chez la sève non concentrée, il diminuait, déjà de 50% après huit mois. Nous avons pu contrôler que cette perte était proportionnelle à la transformation du sucrose contenu dans la sève en sucre interverti; les sels présents favorisaient cette interversion.

Le sucre interverti jouerait vis-à-vis de la sucrogène-amylase et la cellobiogène-amylase le rôle d'inhibiteur, tout comme il a été établi pour le β-maltose vis-à-vis les β-amylases (16, p. 138).

De plus, dans la sève concentrée dans le vide, dialysée jusqu'à la disparition du sucrose et du sucre réducteur, tamponnée à pH 6.8, et saturée de toluène, nous avons constaté l'apparition du sucre réducteur, après un séjour de 10 mois à la glacière. Ce qui indique la présence dans la sève d'érable de glucides supérieures, non dialysables, intermédiaires de l'amidon, qu'on est convenu d'appeler encore des achroodextrines.

La sève uniquement concentrée dans le vide s'est par contre toujours montrée stable.

Les tampons

Les solutions tampons servant à fixer le pH des liquides à hydrolyser, étaient préparées au moyen de quantités variables de solution $M/15$ de phosphate disodique, phosphate monopotassique et d'acide phosphorique. Le pH était determiné à l'électrode à la quinhydrone au début et à la fin de l'hydrolyse sur chaque liqueur à l'étude. Les pH se sont maintenus à peu près constants (± 0.05) tout le temps de l'hydrolyse.

La température

Pour les températures de 60° C. à 4 0° C., nous avions recours à un bain d'eau muni d'un agitateur et d'un thermostat qui permettaient de régler et

de maintenir la température à $\pm 0.5°$; un système de refrigération par circulation d'eau froide était ajusté pour la température de 16° C., tandis que nous avons aménagé des compartiments dans la glacière pour les séries d'expériences faites à 8° C. et à 2° C.

Les témoins

La présence de cellobiose, de sucrose et de dextrine dans la sève servant d'agent d'hydrolyse, nous posait tout un problème, à savoir: quelles seraient nos expériences témoins? Nous ne prétendons pas l'avoir tranché d'une façon précise, mais nous croyons avoir établi une marge de sécurité suffisante pour les conclusions que nous voulons tirer de ce travail.

Une étude des modifications des glucides de la sève suivant les variations de la température et du pH, nous a permis de fixer un maximum entre les pH 6.5 et 6.8. Comme l'augmentation en sucre ne dépassait pas 10 mg. dans 25 cc. de solution, il n'y a pas eu de corrections de faites pour cette augmentation dans les graphiques qui suivent. Par mesure de précaution, pour chaque température étudiée, un essai témoin a été fait où le volume d'amidon était remplacé par une quantité égale d'eau. C'est le témoin compagnon.

Nous avions en plus les témoins au temps zéro, ce qui nous permettait d'apprécier l'influence des mélanges de sève, d'amidon et de tampon sur nos déterminations quantitatives des sucres formés.

Les dosages

La méthode de Bang (7, p. 1189) au sulfocyanure cuivrique, employée par plusieurs, Ohlsson et ses collaborateurs en particulier (9, 10, 11, 12), nous a servi au début et les résultats s'accordent suffisamment avec ceux que nous publions. La teinte du virage nous semblait d'appréciation délicate avec le changement d'éclairage; par ailleurs, la sève d'érable contenant une quantité appréciable de sucrose, 3 à 4%, cette microméthode était débordée lorsqu'il s'agissait de doser le sucre total.

Nous avons ensuite préféré augmenter le volume des liqueurs en expérience et nous avons adopté pour le dosage du sucre réducteur (cellobiose) et du sucrose, la méthode Munson et Walker (A.O.A.C.). La défécation est faite par addition d'une suspension d'alumine, l'interversion du sucrose par une solution d'invertase d'activité standard tamponnée à pH 4.5 au moyen d'acide acétique $N/5$.

Les quantités de glucides (cellobiose en présence de sucrose et sucrose ou mieux sucre interverti en présence de cellobiose) correspondant au poids du cuivre trouvé, étaient déterminées au moyen de deux courbes: (*a*) l'une obtenue avec une solution de sucrose et de cellobiose de concentration bien déterminée (1%; c'était en moyenne la teneur de nos liqueurs à doser). Le dosage du sucre réducteur était fait sur les quantités croissantes de cette solution; (*b*) l'autre, avec les mêmes quantités, mais après traitement par l'invertase. Tous nos dosages, soit pour établir nos courbes, soit pour déterminer les quantités de sucre formé au cours de l'hydrolyse, soit pour les témoins, étaient donc faits dans des conditions identiques.

Calcul des dosages

Dans un premier dosage: l'amidon + sève + tampon, au temps zéro, on obtient une quantité de sucre réducteur:

$$R_1 = \text{sucre interverti} + \text{sucre réducteur contenu dans}$$
$$\text{l'amidon} + \text{cellobiose de la sève.}$$

Après l'action de l'invertase on obtient:

$$R_2 = R_1 + \text{sucrose de la sève.}$$
$$R_2 - R_1 = S_1, \text{ sucrose de la sève.}$$

Après 17, 24, 40, et 48 h. d'hydrolyse on dose une quantité de sucre

$$R_3 = R_1 + \text{cellobiose venant de l'amidon}$$
$$\text{d'où } R_3 - R_1 = R_5, \text{ cellobiose formé.}$$

Après l'action de l'invertase on obtient:

$$R_4 = R_2 + R_5 + \text{sucrose venant de l'amidon}$$
$$\text{d'où } R_4 - R_2 - R_5 = S_2, \text{ sucrose formé.}$$
$$\text{ou } S_2 = R_4 - R_2 - R_3 + R_1.$$

Les graphiques qui suivent indiquent la quantité en milligrammes de sucre réducteur (cellobiose (R_5)) ou de sucrose (S_2) formé dans 25 cc. de solution, à une température déterminée et en fonction du pH.   Chaque courbe indique la quantité de sucre produit aux différentes étapes de l'hydrolyse: 17, 24, 40, 48, ou 65 h.

L'hydrolyse

Les mélanges hydrolytiques étaient constitués comme suit:

1 volume de la solution d'amidon 1%, saturée de toluène.

1 volume de sève d'érable, saturée de toluène.

0.25 volume de la solution tampon.

Ils étaient faits dans des bouteilles bouchées à l'émeri.   La concentration en amidon était donc de 0.44%.

B. Résultats

1. Les essais préliminaires nous ont permis d'observer qu'aux températures supérieures à 65° C. la sève d'érable n'amenait qu'une très faible hydrolyse de l'amidon et lorsqu'elle était maintenue 10 min. à 70° C., elle perdait toute activité; on admet alors la destruction des enzymes.

Les résultats que nous présentons des experiences faites à 60°, 50°, et 40° C. forment un groupe homogène, c'est-à-dire que la solution d'amidon et de la sève employée étaient les mêmes pour toute la série des manipulations.

Nous remarquons en premier lieu que la formation de sucrose est nulle à ces températures, du moins elle n'est pas appréciable dans des conditions où nous avons dû opérer.   De plus, le sucrose présent dans la sève subit une interversion d'autant plus forte que la température est plus élevée.   Les témoins nous l'indiquent clairement.   Nous savons d'après Bertrand et Holderer (1) que 72 mg. de cuivre correspondent à 51.8 mg. de cellobiose, aussi à 37 mg. de sucre interverti ou 35.15 mg. de sucrose.

Or à 60° C., la plus forte quantité de sucre réducteur (exprimé en cellobiose) du témoin est 12.7 mg., ce qui représenterait 8.63 mg. de sucrose contenu dans le mélange au début de l'hydrolyse.   A 50° C. on obtient 6.6 mg. ce qui correspond à 4.5 mg. de sucrose, et à 40° C., 3.2 mg. correspondant à 2.2 mg. de sucrose.

Ce sucre représente au plus 0.1 de l'augmentation du pouvoir réducteur de la solution à l'étude.   Nous pouvons donc admettre que nos courbes, tout en n'étant pas exactes doivent indiquer l'allure générale du phénomène.

A 60° C. (Fig. 1), la formation du sucre réducteur, cellobiose passe par un maximum à pH 4.8 (33 mg. dans 25 cc. après 48 h. équivalent à 30% de l'amidon mis à hydrolyser).   L'activité diminue avec l'augmentation de la valeur du pH.
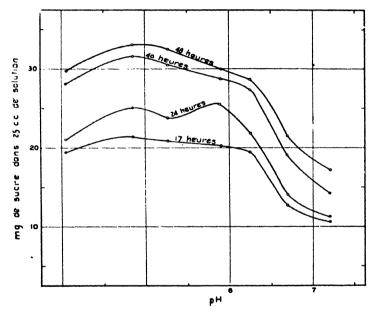
FIG. 1.   *Sucre réducteur à 60° C.*

A 50° C. (Fig. 2) nous avons deux maxima, le premier à pH 4.8 avec une production de cellobiose égale à 35.4% de l'amidon, et un second à pH 6.6 où la quantité de sucre réducteur représente 45.4% de l'amidon.

Ce second maximum ne se retrouve pas chez les autres courbes.   Nous avons répété l'hydrolyse dans les mêmes conditions avec un autre échantillon de sève et une nouvelle solution d'amidon.   Nous avons constaté la même anomalie, c'est-à-dire un second maximum à pH 6.6, mais inférieur cette fois au premier maximum à pH 4.8 pour les courbes après 40 et 48 h. d'hydrolyse, et égal au premier pour celles après 17 et 24 h. d'hydrolyse.   Nous reconnaissons être dans la zone critique où plusieurs facteurs entrent en jeu, nous le verrons plus loin.
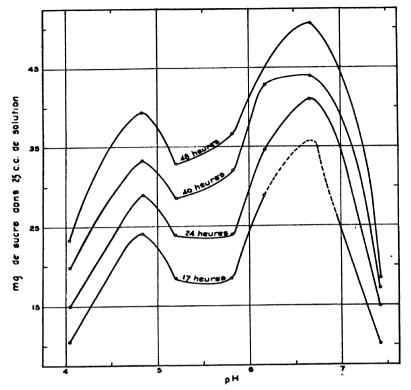
FIG. 2.   *Sucre réducteur à 50° C.*
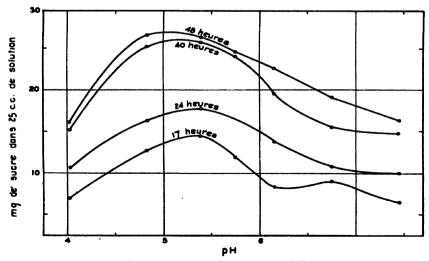
FIG. 3.   *Sucre réducteur à 40° C.*

A 40° C. (Fig. 3) la quantité de sucre réducteur formé ne dépasse pas 26.6 mg. dans 25 cc. de l'hydrolysat, ce qui équivaut à la transformation de 24.1% d'amidon. A cette température nous remarquons que le pH optimum oscille entre 4.8 et 5.3.

2. Nous ne mentionnerons pas les expériences faites entre 40° et 16° C., elles sont d'intérêt tout à faire secondaire, puisque nous passons par une étape intermédiaire des activités des deux amylases. Nous retrouvons d'une manière plus accentuée dans les courbes qui suivent, les mêmes phenomènes: diminution de l'activité de la cellobiogène-amylase et apparition de l'activité de la sucrogène-amylase.

Les hydrolyses faites à 16°, 8°, et 2° C. forment un second groupe homogène. A 16° C. (Fig. 4) la formation de sucre réducteur ne représente plus que 17.7% de l'amidon (19.5 mg.) à pH 4.8 le plus favorable; tandis qu'aux pH extrêmes, la quantité de cellobiose est très faible, inférieure à 10 mg.
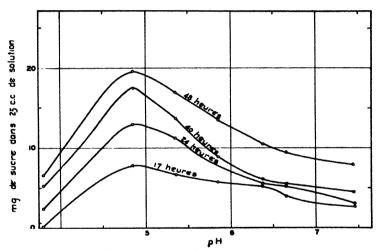
FIG. 4.   *Sucre réducteur à 16° C.*

La production du sucrose (Fig. 5) ne fait plus de doute, le maximum s'établit à pH 6.6 avec 32.4 mg. ce qui indique une hydrolyse de l'amidon égale à 29%.   Un total de (29 + 17.7 = 46.7%).

A 8° C. (Fig. 6) la cellobiogène-amylase devient moins active, le pH optimum prend une valeur plus élevée, 5.4 au lieu de 4.8, et la quantité de sucre réducteur formé ne représente que 13% de l'amidon.

Pour le sucrose (Fig. 7), cette température s'est révélée la plus favorable, la quantité de sucre augmente légèrement aux pH les plus bas, puis s'accentue considérablement pour marquer un maximum à pH 6.6. La proportion d'amidon ici transformée en sucrose est de 40%; l'hydrolyse totale (40 + 13 = 53%).

Notons encore que dans les conditions les plus favorables, même après 65 h. d'hydrolyse, il reste une quantité d'amidon non transformé que nous

évaluons à 30%.   C'est la partie moins soluble, non colorable par l'iode que l'on est convenu d'appeler "amylopectine".

De plus les témoins compagnons de 24 h. et de 65 h., soit pour le sucre réducteur ou le sucrose, sont les mêmes, indice que du côté de la sève la réaction est complète.
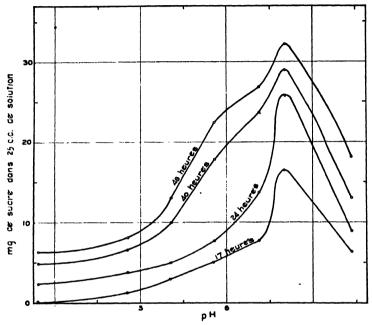
FIG. 5.   *Sucrose à 16° C.*
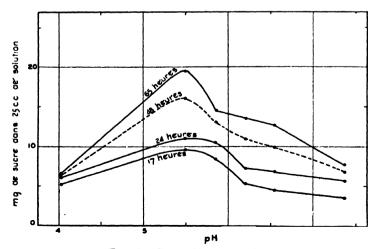
FIG. 6.   *Sucre réducteur à 8° C.*
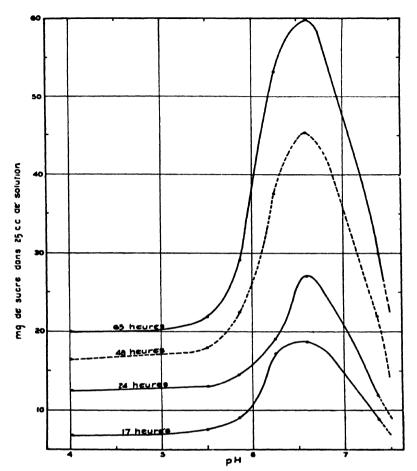
FIG. 7. *Sucrose à 8° C.*
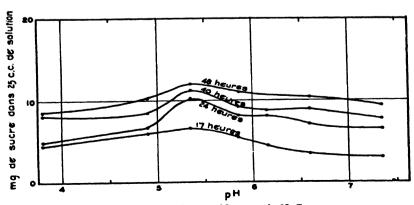
FIG. 8. *Sucre réducteur à 2° C.*

A 2° C. (Fig. 8) le cellobiose formé n'équivaut plus qu'à 10% de l'amidon à pH 5.35.   L'activité de la cellobiogène-amylase est de nouveau déplacée vers un pH plus élevé.
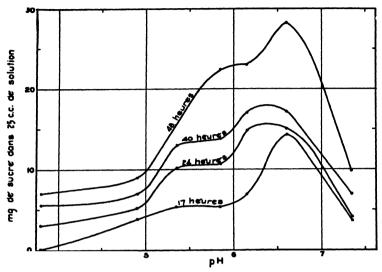
FIG. 9.   *Sucrose à 2° C.*
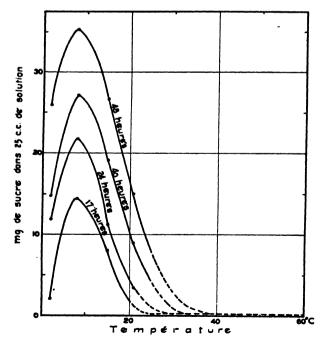
FIG. 10.   *Sucrose à pH 6.62.*

La formation de sucrose (Fig. 9) est encore importante; à pH 6.6, 28.3 mg. après 48 h. ou 23.6% de l'amidon transformé en sucrose.   Il restait sans doute de l'amidon intact puisque la réaction avec l'iode était encore positive au moment du dernier dosage.

Chez l'érable

Certaines constatations faites au printemps sur la sève fraîche, apportent quelques faits nouveaux qui viennent confirmer les résultats déjà obtenus. Chaque jour, le pH a été déterminé au moyen de l'électrode à la quinhydrone. La sève, provenant toujours d'une même entaille, a un pH qui se maintient aux environs de 6.6.   La présence de pluie ou de neige a pour effet d'augmenter le pH.   Il atteint parfois 7.4, surtout à la fin de la saison quand l'entaille vieillit et que la température devient plus chaude.   Mais la sève revient à son pH normal (pH 6.6) si une nouvelle entaille est faite.

Nous avons donc entrepris un troisième groupe de déterminations qui pourront nous donner quelques renseignements sur les phénomènes dont l'*Acer saccharum* est le siège au printemps.

Un même mélange d'amidon et de sève, tamponné à pH 6.62, a été mis à hydrolyser à différentes températures.   Les résultats font l'objet des courbes Figs. 10 et 11.   Les maxima à 8° C. pour la formation de sucrose et à 50° C.
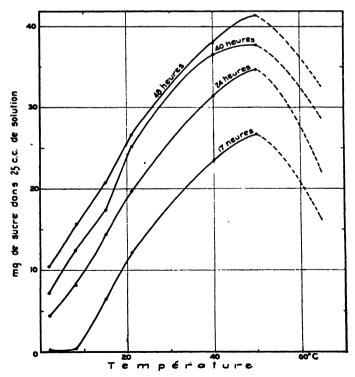
FIG. 11.   *Sucre réducteur à pH 6.62.*

pour celle du sucre réducteur, le cellobiose, confirment bien ce que nous venons de présenter, et nous font voir que l'élaboration de sucrose l'emporte du beaucoup sur celle du cellobiose aux mois de mars et d'avril.

C'est en effet lorsque la température oscille autour de 8° C. (45° F.) que l'écoulement de la sève est le plus abondant et il s'arrête avec la venue des jours chauds.

Nous avons aussi mesuré la vitesse d'hydrolyse d'une solution d'amidon en présence de sève pendant tout le temps de la coulée. Chaque jour, une série de tubes contenant 2 cc. de sève fraîchement cueillie, 1 cc. d'amidon soluble et 1 cc. de tampon aux phosphates (pH 6.6) le tout saturé de toluène, sont placés à 37° C.

Au début du printemps, il faut un séjour de 40 h. environ à cette température pour que la réaction avec l'iode soit négative; au milieu de la saison 24 h. suffisent et à la fin, 20 h. La quantité de ferments dans la sève croît donc à mesure que la saison de coulée progresse.

Discussions et conclusions

1. D'après nos recherches, les conditions optima de l'activité de la sucrogène-amylase sont: pH 6.6 et une température de 8° C.

Pour la cellobiogène-amylase nous ne pouvons pas être aussi catégorique pour le moment, les courbes obtenues aux températures supérieures à 40° C., nous indiquent bien que le pH optimum est 4.8 et qu'il se déplace vers pH 5.3 à mesure que la température baisse, mais à 50° C. nous sommes en présence d'un second maximum à pH 6.6 qui semble être le résultat d'un ou de plusieurs phénomènes secondaires. Soit interversion du sucrose à mesure de sa formation (1 mg. de sucre interverti = 2.66 mg. Cu), soit l'hydrolyse du cellobiose en deux glucoses (1 mg. de glucose = 2.04 mg. Cu; tandis que 1 mg. de cellobiose = 1.38 mg. Cu). Peut-être encore s'agit-il d'une modification d'un des constituants de l'amidon, l'amylopectine par exemple.

2. Le pH optimum de formation du sucrose, le pH 6.6, est dans la zône d'un des minima de pouvoir tampon situé à pH 6.5 à 6.7. L'autre minimum à pH 4.6 à 4.9 correspond assez bien à pH optimum compris entre 4.8 et 5.4 de formation de sucre réducteur (2).

Ces faits confirment les résultats de Sherman, Thomas, et Caldwell (14) à savoir; l'activité maximum des ferments se trouve au voisinage du point iso-électrique.

3. Les solutions ou suspensions d'amidon telles que préparées couramment ne sont pas entièrement hydrolysées par les deux amylases contenues dans la sève d'érable.

Les autres amylases agissent d'une façon analogue. Le pourcentage de la partie réfraetaire varie avec le mode de préparation et de l'amidon et de

sa solution, tout comme les proportions d'amylase et d'amylopectine de plusieurs auteurs: entre autres, Maquenne et Roux (8), Gatin-Gruzewska (3), Ling et Nanji (5, 6), ou amylogène et amylon de Reich et Damansky (13).

Remerciement

Nous tenons à remercier M. l'abbé Alexandre Vachon, directeur de l'École Supérieure de Chimie, Université Laval, pour l'encouragement qu'il nous a accordé au cours de l'éxécution de ce travail.

Bibliographie

1. BERTRAND, G. et HOLDERER, M.   Compt. rend. 168 : 1016-1017.   1919.
2. BOIS, E. et NADEAU, A.   Can. J. Research, B, 14 : 373-380.   1936.
3. GATIN-GRUZEWSKA, M.   Compt. rend. 146 : 540-542.   1908.
4. KOPACZEWSKI, W.   Bull. assoc. chim. 53 : 344-356.   1936.
5. LING, A. R. et NANJI, D. R.   J. Chem. Soc. 123 : 2666-2688.   1923.
6. LING, A. R. et NANJI, D. R.   J. Chem. Soc. 127 : 629-656.   1925.
7. MATHEWS, A. P.   Physiological chemistry.   William Wood and Company, New York.   1931.
8. MAQUENNE, L. et ROUX, E.   Ann. chim. phys. 9 : 179-220.   1906.
9. NORTH, O. G. et OHLSSON, E.   Z. physiol. Chem. 214 : 89-100.   1932.
10. OHLSSON, E.   Compt. rend. trav. lab. Carlsberg. 16, No. 7 : 1-68.   1926.
11. OHLSSON, E.   Z. physiol. Chem. 189 : 17-63.   1930.
12. OHLSSON, E. et UDDENBERG, C. E.   Z. physiol. Chem. 221 : 165-173.   1933.
13. REICH, W. S. et DAMANSKY, A. F.   Bull. soc. chim. biol. 19 : 357-391.   1937.
14. SHERMAN, H. C., THOMAS, A. W., et CALDWELL, M. L.   J. Am. Chem. Soc. 46 : 1711-1717.   1924.
15. SUTRA, A.   La constitution de l'amidon, Actualités scientifiques.   Herman et Cie, Paris.   1934.
16. TAUBER, H.   Enzyme chemistry.   John Wiley and Sons, New York.   1937.

A STUDY OF THE VISCOSITY METHOD FOR THE DETERMINATION OF DAMAGE IN SILK[1]

By Audrey S. Tweedie[2]

Abstract

A method described by Trotman and Bell for the detection of damage in silk by measuring the viscosity of its solution in aqueous zinc chloride has been studied.

The effect of the temperature and the time of digestion on the viscosity has been investigated, and it is shown that a higher temperature with a shorter period of digestion gives equally satisfactory results, and is more convenient for a routine test.

The mechanism of the change in viscosity with time of digestion has been studied, and it is shown to be a dispersion process followed by hydrolysis of the silk.

Damage to weighted silk may be determined by this method if the silk is deweighted before dispersion in the zinc chloride solution.

The method has been used to determine the damage resulting from the treatment of silk with boiling dilute acid, boiling dilute alkali, light, and superheated steam. The viscosity of the damaged silk has been correlated with its tensile strength to give the viscosity method a quantitative basis. The amino nitrogen content of the silk was also determined and has been correlated with the tensile strength and viscosity. The results show that there is a difference between the hydrolysis of silk occurring in boiling dilute acid and that occurring during the corresponding alkali treatment. In the former, hydrolysis of the silk with formation of free amino groups occurs previous to dispersion, whereas in alkali it appears that the disintegration of the fibre into fibrils takes place very readily and that the fibrils are then rapidly dispersed in the alkaline solution before appreciable hydrolysis can occur. That the photochemical decomposition of silk is an oxidation process is confirmed. The action of steam appears to differ from that of acid, alkali, or light.

Introduction

Trotman and Bell (7) described a method for detecting damage in silk by measuring the viscosity of a zinc chloride solution of the silk. They applied the method to silk damaged by various chemical agents, *e.g.*, acid, alkali, and others, and later (8) reported results of an extension of the work, which included the determination of the effect of different degumming processes, dyeing, and the action of light.

Several interesting points in the papers mentioned (7, 8) appeared to merit further investigation. For example, the value of the method in the examination of faulty consumer goods would be greatly enhanced if it could be applied to weighted silks, which comprise most finished silk materials and garments. Furthermore, correlation of the change in viscosity of silk with change in other factors, such as its tensile strength under different conditions, *e.g.*, exposure to light, acid treatment, and other factors, would increase the usefulness of the viscosity test as a quantitative measure of damage. It was in order to investigate such points that the work described in this paper was undertaken.

Materials and Methods

Silk Used

The following varieties of woven silk goods were used:

Silk *A*. A crêpe, containing no weighting or finishing materials. This piece had been stored in the dark since its purchase about two years prior to these experiments.

Silk *B*. A crêpe, containing weighting and finishing materials.

Silk *C*. A crêpe, containing finishing materials only.

Silk *D*. Parachute silk, plain weave, weight 2 oz. per sq. yd., containing no weighting or finishing materials.

Silk *E*. A crêpe, dyed blue, weighted, from an old silk cushion cover. This was so much rotted that it was falling apart.

Removal of Finishing and Weighting Materials from Silk

For the removal of finishing materials, the silk was extracted with petroleum ether, and then washed thoroughly by immersing in distilled water at a temperature of 60° C., removing, and squeezing. This was done a number of times and the process repeated in several changes of water.

For removal of weighting, the silk, after the finishing materials had been removed, was worked thoroughly in 2% hydrofluoric acid at 60° to 70° C. for 20 min. It was then rinsed in distilled water, worked well for 20 min. in a 2% sodium carbonate solution at 60° to 65° C. and finally thoroughly rinsed in distilled water.

Viscosity Measurement

The viscosity measurements were made with a 2.5% (weight per volume) solution of the silk in an aqueous zinc chloride solution of density 1.67 at 20° C. The weight of silk used was the conditioned weight at 65% relative humidity and 70° F. The weighed amount of silk, cut into small pieces, was placed in a small flask, and the required volume of zinc chloride solution added. The flask was then stoppered and placed in an oven at the given temperature for the required length of time with occasional swirling of the flask to ensure mixing of the contents*. It was then cooled in water to 20° C., the solution transferred to a viscosimeter (British Cotton Industries Research Association X-type viscosimeter), and the viscosity at 20° C. measured.

Tensile Strength Measurements

These were made with a Suter machine on material conditioned at 65% relative humidity and 70° F. The measurements were made in the warp direction only, and each value given in the table is the mean of 10 determinations carried out on strips 1 in. in width.

Amino Nitrogen Determination

The amino nitrogen content of the silk was measured by the Van Slyke method (9). A Van Slyke macro-apparatus was used with a 3 ml. gas burette substituted for the standard 40 ml. burette, as the volumes of nitrogen measured were small. For the reaction between nitrous acid and silk, 15 cc. of nitrous acid solution, 10 cc. of water (air free), and 5 cc. of silk solution

---

* *This operation is referred to in this paper as "digestion".*

were used instead of the 20 cc. of nitrous acid solution and the 10 cc. of protein solution specified in the original Van Slyke method.   In place of the suspension of powdered silk used by other workers in the determination of amino nitrogen, the zinc chloride solution of silk (from viscosity determinations) was used.   The amino nitrogen content of the silk is calculated as percentage of the dry weight of silk present in the solution.

Harris (1), in a study of the photochemical decomposition of silk, had determined the amino nitrogen content of silk after dissolving it in a 50% lithium bromide solution, but his later work was done on suspensions of finely powdered silk in distilled water.   However, in their latest paper (5), Harris and co-workers mention the difficulty of preparing suspensions sufficiently uniform to assure the addition of an accurately known amount of protein for each determination.   By using a zinc chloride solution of silk instead of an aqueous suspension, the weight of silk in a given volume is accurately known, but the actual volume delivered to the reaction chamber varies slightly with the viscosity of the solution, since the solution does not drain freely from the walls of the burette.   However, the resulting error is small.

The zinc chloride solution causes the evolution of about three times as much nitric oxide as that caused by water, and this necessitated the use of an extra bulb below the gas pipette for storage of this gas before absorption.   Difficulty with frothing and with the formation of a jelly-like mass of deaminized protein was experienced with the solutions of less-degraded silk.

Tests were made to determine the completeness of the reaction between the silk and the nitrous acid after various times of reaction, Table I.   These showed that the reaction is virtually complete after five minutes; to provide a margin of safety a standard 6-min. shaking period was chosen.

The volume of nitrogen obtained in blank determinations was about half that obtained with undegraded or slightly degraded silk, *e.g.*, 0.41 and 0.79 cc. of nitrogen respectively.   Thus, slight variations in the size of the blank resulted in relatively high variations in the calculated amino nitrogen content of the silk.   Consequently, blank determinations were made for every sample of silk tested.

TABLE I

THE RATE OF REACTION BETWEEN NITROUS ACID AND SILK

Silk used	Time of reaction, min.	Amino nitrogen, % ± 0.02
Silk *D*—3½ hr. digestion at 45° C.	5	0.18
	10	0.20
	15	0.20
Silk *D*—18 hr. digestion at 45° C.	3	0.29
	5	0.31
	10	0.32
	14	0.29
Silk *D*—old solution–digested two to four months previously	3	1.20
	5	1.29
	10	1.35
	14	1.34

Kanagy and Harris (4) found variations in the quantity of nitrogen evolved with variation in the age of the sodium nitrite solution. In the present experiments it was found that much greater variations resulted from the alkaline permanganate solution used in the absorption pipette. This solution was made up from air-free water. To remove air inadvertently introduced, the solution was shaken in an evacuated flask before use. Even with these precautions the result of the first, and often of the second, blank, after the absorbing solution was changed, was high, and had to be discarded.

Results and Discussion

Effect of the Temperature and Time of Digestion on the Viscosity

Trotman and Bell (7) found that the viscosity of a solution of silk in zinc chloride depends on the temperature at which the silk is dissolved. In their early experiments they heated the silk with the solvent in a tube placed in boiling water, and then cooled the tube rapidly to 20° C., but they found it difficult to obtain a constant initial viscosity even when the heating period was timed with a stop-watch. They finally adopted the method of digesting the silk in the zinc chloride solution in a small stoppered bottle at 37° C. for exactly six hours, cooling to 20° C., and measuring the viscosity. The author of this paper found six hours a rather inconvenient length of time, as it was then necessary to make the viscosity measurements towards the end of the day; this prevented any further experimentation of a lengthy nature on those solutions that day. Trotman and Bell make no mention of trials at moderate temperatures other than 37° C., so it was decided to investigate the relation between the viscosity and the time and temperature of digestion, in the hope that a shorter period at a higher temperature might be equally satisfactory. Experiments were carried out at three temperatures, 37°, 45°, and 60° C., and with time intervals varying from 1 to 75 hr. The results are shown in Table II and Fig. 1.
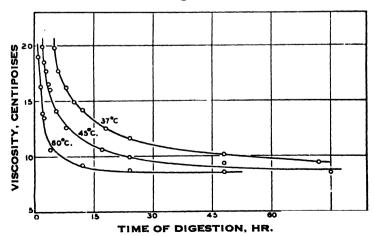
FIG. 1.   *Variation of viscosity with time of digestion at three different temperatures.*

Some time after completion of this work, a translation was obtained of a paper by Tanizaki (6) on the regeneration of fibroin. In this paper, data are given for the relation between the time of digestion (10 to 120 min.) at 124° C. and the viscosity (in seconds) of the resulting zinc-chloride–fibroin solution. The curve obtained on plotting viscosity against time of digestion is similar to the curves obtained by the present author, although the concentration of fibroin used was somewhat lower.

TABLE II

EFFECT OF TEMPERATURE ON THE VARIATION OF VISCOSITY OF SILK *A*
WITH TIME OF DIGESTION

Time of digestion, hr.	Temperature of digestion, °C.		
	37	45	60
	Viscosity, centipoises		
1	—	—	19.0
1.5	—	—	16.3
2	—	19.9	13.9
2.5	—	18.5	13.5
3	—	17.7	—
3.5	—	16.5	—
4	—	16.0	10.6
5	19.8	—	—
5.5	—	14.1	—
6	17.7	—	—
8	16.2	12.6	—
10	14.9	—	—
12	14.2	—	9.2
17	—	10.6	—
18	12.5	—	—
24	11.6	9.9	8.7
48	10.1	9.3	8.5
72	9.4	—	—
75	—	8.5	—

It will be seen that three hours' digestion at 45° C. gives the same viscosity as is obtained with six hours at 37° C. Moreover, the rate of decrease of viscosity with increasing time of digestion at 45° C. is only slightly greater than that at 37° C. at this part of the curve. At 60° C. the viscosity changes much more rapidly, and consequently very exact control of the digestion time would be necessary at this temperature. It was, therefore, decided to adopt the three-hour period of digestion at 45° C. for all further work.

From the figures given in Table II, it might be concluded that a two-hour period at 45° C. would be quite satisfactory. However, Silk *A* was somewhat degraded as a result of its two-year storage, and it dispersed fairly rapidly in the zinc chloride solution. With an undegraded silk such as Silk *D*, used in later experiments, a three-hour digestion period is necessary for the dispersion, and this period was therefore adopted as standard.

If from the curves shown in Fig. 1, the ratio of the time of digestion at 37° C. to that required at 45° C. to give the same viscosity is determined,

it is found that the ratio is virtually constant throughout the whole viscosity range, its average value being 2.2. The same holds true for the ratio of the time of digestion at 45° C. to that at 60° C., the average value in this case being 2.5. However, the experimental error at 60° C. is greater than that at the lower temperatures, and consequently the agreement between the various determinations of the ratio is not so good. The constancy of the two series of ratios is shown in Fig. 2, in which the three curves from Fig. 1 are replotted with the digestion periods at 37° C. and 60° C., calculated to their corresponding values at 45° C. For clearness, the logarithm of the time of digestion has been plotted against the viscosity. The three series of points fall closely on the same curve; this shows that the only effect of raising the digestion temperature is to increase the rate of reaction.
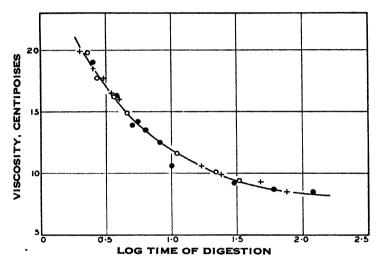
FIG. 2.   +, *Digestion at 45° C.*   O, *Digestion at 37° C.; time of digestion ÷ 2.2 to give equivalent period at 45° C.*   ●, *Digestion at 60° C.; time of digestion × 2.5 to give equivalent period at 45° C.*

An attempt was made to use a procedure for dissolving the silk similar to that adopted for the cuprammonium viscosity test on cotton. This involved placing the zinc chloride solution and the silk directly in the viscosimeter, together with two $\frac{3}{16}$ in. ball bearings to aid agitation, and then fastening the tube to a wheel that was made to rotate for 24 hr. at room temperature. The viscosity of a sample of Silk A, after this procedure, was 18.0 centipoises, which is very close to the figure of 17.7 as determined with the standard procedure. The quantity of silk used with the zinc chloride solution is several times that of the cotton used with the cuprammonium solution, and consequently occupies a large volume in the viscosimeter; thus it was difficult to mix the silk and the zinc chloride solution efficiently. Altogether this procedure is much less satisfactory than that involving digestion at a raised temperature.

Viscosity of Undamaged Degummed Silk

Trotman and Bell (7) concluded, from their results with Italian, Chinese, and Japanese silks, that the viscosity of a 2.5% solution of undamaged, degummed silk should not be less than 19.0 centipoises, and that a viscosity greater than 21.0 centipoises would indicate incomplete degumming. That the latter statement is not necessarily true is shown by the fact that the sample of Silk *D* examined by the present author had a viscosity of 23.7 centipoises. This silk as purchased was degummed, but a piece of the material was given a further treatment for one hour in a 25% (based on the weight of the silk) soap bath at 95° C. to obviate the possibility of the initial degumming being incomplete. The viscosity of the silk thus treated was 22.9 centipoises. The high viscosity of this silk may be explained by the high quality of the raw silk used and the careful processing involved in the manufacture of this type of material.

Application of the Method to Silk Containing Finishing and Weighting Materials

The only piece of silk on hand which contained finishing materials, but no weighting, was extracted with petrolic ether to remove any oily or waxy substances, and then dissolved in the zinc chloride. The resulting solution was very cloudy owing to the presence of suspended particles of those finishing materials not soluble in petrolic ether. These should, therefore, also be removed before the silk is tested by the viscosity method.

Weighted silk does not dissolve in zinc chloride solution and must, therefore, be deweighted before testing. It was found that the hydrofluoric acid deweighting treatment caused only a small drop in viscosity when applied to samples of unweighted silk. With weighted silk, the treatment would be expected to cause less damage, since the silk fibres are protected by the metallic salts during part of the time of treatment. The only sample of undamaged weighted silk (Silk *B*) that was on hand was deweighted by the hydrofluoric acid method, and its viscosity was then determined. The value of 22.0 centipoises that was obtained would certainly place this silk in the undamaged class.

The method was also applied to the piece of rotted Silk *E*. After deweighting, the fabric was cut up finely and thoroughly mixed to ensure uniform sampling. As can be seen from Table III, the viscosity of the zinc chloride solution of this silk under the standard conditions was very low.

TABLE III

VISCOSITY OF DEWEIGHTED SILKS AND THE EFFECT OF THE DEWEIGHTING TREATMENT ON THE VISCOSITY OF UNWEIGHTED SILK

Silk	Treatment	Viscosity, centipoises
C	Extracted and washed	19.8
C	Subjected to deweighting treatment	19.5
D	Untreated	23.7
D	Subjected to deweighting treatment	21.7
B	Deweighted	22.0
E	Deweighted	10.4
F	Deweighted	11.4
G	Deweighted	10.5

Two other samples of old, very rotten, weighted silk (Silks *F* and *G*) had viscosities very close to that of the blue silk already discussed.

Effect of Treatment with Sodium Chloride and Hydrochloric Acid

An attempt was made to damage silk with sodium chloride and hydrochloric acid solutions according to the procedure followed by Trotman and Bell (7) of soaking the silk in 10% sodium chloride for six hours or in 0.1 N hydrochloric acid for 12 hr., then squeezing and drying. The drying temperature was not specified, so this was taken to be room temperature. After drying, the silk was conditioned, thoroughly rinsed to remove free sodium chloride, dried, and reconditioned. Its viscosity was then determined. The results are given in Table IV.

TABLE IV

THE VISCOSITY OF SILK AFTER SODIUM CHLORIDE, HYDROCHLORIC ACID, AND HEAT TREATMENTS

Silk	Treatment	Viscosity, centipoises
A*	Untreated	19.9
	Soaked 10 hr. in 10% NaCl, dried at 25° C.	19.3
	Soaked 12 hr. in 0.1 N HCl, dried at 25° C.	17.8
	Soaked 24 hr. in 0.1 N HCl, dried at 25° C.	16.5
	Soaked 3 hr. in 0.1 N HCl, dried at 105° C. for 3 hr.	12.5
	Soaked 0.5 hr. in 0.1 N HCl, dried at 105° C. for 1.5 hr.	13.3
	Soaked 0.5 hr. in 0.1 N HCl, dried at 105° C. for 24 hr.	12.6
	Kept at 105° C. for 72 hr.	17.5
	Boiled 18 min. in 0.1 N HCl, rinsed, dried at 25° C.	13.3
D	Original	23.7
	Wetted-out with distilled water, dried at 105° C. for 0.5 hr., repeated 3 times	22.1
	Boiled in distilled water for 20 min.	21.6

* *This work was done before the standard three-hour period of digestion was adopted. For this type of silk the two-hour period gave good results.*

The sodium chloride treatment caused little change in the viscosity of the silk, whereas Trotman and Bell noted a drop in viscosity from 21.8 to 18.3 centipoises under the same conditions.

The hydrochloric acid treatment caused a drop in viscosity from 19.9 to 17.8 centipoises, which is very small compared to the drop from 21.8 to 12.3 centipoises observed by Trotman and Bell. Increasing the period of soaking in the acid from 12 to 24 hr. and omitting the rinse, resulted in a further drop of 1.3 centipoises.

The viscosity of silk treated with hydrochloric acid and dried at 105° C. was in close approximation to that found by Trotman and Bell. Apparently then, heating is necessary in the treatment of silk with dilute hydrochloric acid to cause appreciable damage and the resultant large drop in viscosity. Heating untreated silk for 72 hr. at 105° C. caused a drop in viscosity of 2.4 centipoises, and it may, therefore, be concluded that for short periods at this temperature the change would be comparatively small. Three repetitions of the wetting in distilled water and drying for 30 min. at 105° C. each time also resulted in little change, as did boiling the silk in distilled water for

20 min.   Varying the time of soaking in acid and the time of drying at 105° C. showed that most of the damage to the silk resulted during the short period of time necessary to actually dry the silk and evaporate the hydrochloric acid; *i.e.*, the hot hydrochloric acid caused the damage.   This was verified by boiling the silk in 0.1 N hydrochloric acid for 18 min.   The viscosity of the silk after this treatment was identical with that of the silk soaked in 0.1 N acid and dried at 105° C. for 1.5 hr.

Study of the Mechanism Resulting in Change of Viscosity with Increasing Time of Digestion

The relation between viscosity and time of digestion was studied for Silks A, D, and E.   The results are given in Table V and are plotted in Fig. 3.

TABLE V

VARIATION OF VISCOSITY WITH TIME OF DIGESTION
FOR SEVERAL SAMPLES OF SILK

Time of digestion, hr.	Viscosity at 20° C., centipoises		
	Silk D	Silk A	Silk E
1	—	—	10.8
2	—	19.9	10.7
2.5	—	18.5	—
3	23.7	17.7	10.4
3.5	20.8	16.5	—
4	—	16.0	10.3
5.5	—	14.1	—
6	15.3	—	—
7	—	—	10.1
8	—	12.6	—
10	—	—	9.6
12	12.4	—	—
15	—	—	9.2
17	—	10.6	—
18	—	—	—
24	10.1	9.9	9.0
48	9.2	9.3	8.4
72	9.2	—	8.4
75	—	8.5	—
97.5	8.6	—	—
240	8.3	—	—

It will be seen that with increasing age of, or damage to, the silk, there is a flattening of the curves toward the time axis; that is, the viscosity for any given period of digestion decreases with increasing degree of damage to the silk. The physical appearance of the zinc chloride solution of these silks shows a parallel change.   After one and a half hours of digestion at 45° C., Silk E had completely dissolved and formed a clear solution, whereas the other silks still showed some fabric structure, and even after three hours of digestion their solutions had a frosty appearance due to the presence of minute particles of silk fibre which were visible under the microscope.   Furthermore, Silk D, which had the highest viscosity under the standard conditions, required the longest digestion period to give a clear solution.

It appears from these observations that the change in viscosity over the first portion, at least, of the curve obtained by plotting viscosity against time of digestion represents a change in the degree of dispersion of the silk in the zinc chloride solution.   A natural assumption would be that the silk fibre is gradually broken down into its ultimate units through rupture (by the mechanical forces involved in swelling) of the bonds holding these units together· in the fibre structure.   Theoretically, the viscosity at this

stage would be the true viscosity of a solution of silk "molecules" in zinc chloride solution. At this period, and probably earlier, there is the possibility of the silk molecule being attacked chemically by the products of hydrolysis of a salt such as zinc chloride. Acid hydrolysis resulting in the formation
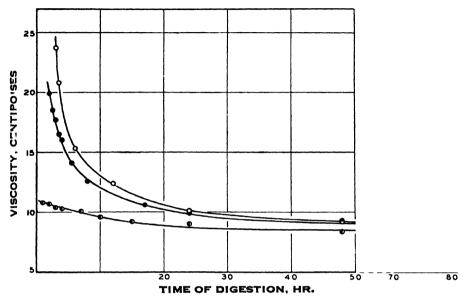
FIG. 3. *Relation between viscosity and time of digestion at 45° C. for Silks A, D, and E, of different age. Top curve, Silk D; middle curve, Silk A; bottom curve, Silk E.*

of free amino groups could be expected. It was decided to check this possibility by determining the amino nitrogen content of the zinc chloride solution of Silk D after different times of digestion, and to compare these figures with those from samples of Silk D which had been hydrolyzed to varying degrees by boiling with dilute hydrochloric acid and then subjected to the standard viscosity treatment. The relation between viscosity and amino nitrogen content of these two series of silk solutions is shown in Tables VI and VII and in Fig. 4.

It will be seen that both series of figures lie on the same curve. Unfortunately

TABLE VI

THE VISCOSITY AND AMINO NITROGEN CONTENT OF SILK D AFTER VARIOUS PERIODS OF DIGESTION

Heating period		Viscosity, centipoises	Amino nitrogen, %
Hr.	Temp., °C.		
3	45	23.7	0.22
3.5	45	20.8	0.20
6	45	15.3	0.20
12	45	12.4	0.28
18	45	10.6	0.31
24	45	10.1	0.48
48	45	9.2	0.62
97.5	45	8.6	0.95
240	45	8.3	1.82
72	37	9.6	0.53
168	37	8.8	0.75

the highest amino nitrogen content observed for the silk boiled in hydro-chloric acid was only 0.48%. When the silk was given more drastic treat-ment with the acid it fell to pieces. There is no increase in amino nitrogen until the viscosity of the silk solution drops below 15 centipoises. Beyond this point, decrease in viscosity is accompanied by increase in amino nitrogen content until the viscosity reaches a limiting value, while the amino nitrogen content continues to increase. Two solutions of silk digested at 37° C. gave results that fall on the same curve. It will be noted that there is no
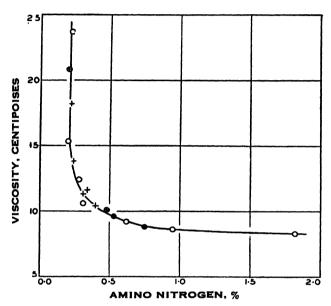
FIG. 4. *Relation between viscosity and amino nitrogen content of Silk D.* O, *after various periods of digestion at 45° C.* *After various periods of digestion at 37° C.* +, *Acid treated silk.*

TABLE VII

THE TENSILE STRENGTH, VISCOSITY, AND AMINO NITROGEN CONTENT OF SILK *D* AFTER TREAT-MENT WITH DILUTE HYDROCHLORIC ACID

Acid treatment		Viscosity, centipoises	Amino nitrogen, %	Tensile strength, lb. per in.
Time of boil, min.	HCl conc., normality			
0	0.0	23.7	0.22	47.0
5	0.05	20.9	0.20	45.5
5	0.1	18.2	0.22	44.5
20	0.1	13.8	0.24	41.5
5	0.5	11.6	0.34	39.5
6	0.6	11.3	0.31	34.5
7	0.7	10.4	0.40	23.5
6	0.8	10.5	—	19.5
5	0.9	10.2	0.48	9.0
5	1.0	9.9	0.49	7.5

change in amino nitrogen content when the digestion period is less than six hours; this indicates that there is no appreciable degradation of the silk in the three hour digestion period adopted as standard.

The experimental results recorded here appear to justify the hypothesis advanced in the earlier part of this section. Trotman and Bell (7) noted the fall in viscosity on prolonged digestion at 37° C. and on keeping the solution at room temperature, but stated that it did not appear to be due to hydrolysis. They dialyzed a zinc chloride solution of silk (age not given) and found neither peptones nor amino acids in the dialysate. However, the dilution involved in dialysis might easily mask the presence of such small amounts of amino nitrogen as are present.

Relation Between Viscosity and Tensile Strength of Silk Damaged in Various Ways

This relation was investigated for samples of Silk *D* which had been damaged (*a*) by boiling with hydrochloric acid of various concentrations, (*b*) by exposure in a fugitometer at an average temperature of 36° C., (*c*) by exposure in a fugitometer at an average temperature of 96° C., (*d*) by boiling with sodium hydroxide of various concentrations, and (*e*) by steaming at a pressure of 15 lb. for various periods. The results are given in Tables VII, VIII, IX, X, and in Fig. 5.
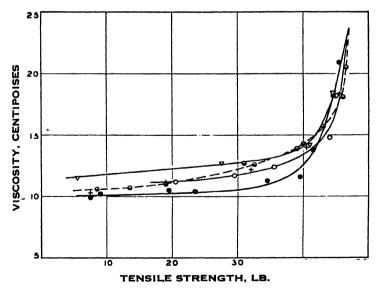
FIG. 5. *Viscosity–tensile-strength relation for Silk D damaged by:— steaming under pressure, O; dilute sodium hydroxide, ▽; dilute hydrochloric acid, ●; exposure in fugitometer at 36° C. (⊖) and 96° C. (+).*

· Although the results obtained with each of the treatments give slightly different curves, all four curves are of the same general type, and the viscosity method can, therefore, be used to detect damage of a chemical or photochemi-

TABLE VIII

THE TENSILE STRENGTH, VISCOSITY, AND AMINO NITROGEN CONTENT OF SILK EXPOSED IN A
FUGITOMETER AT TWO DIFFERENT TEMPERATURES FOR VARIOUS PERIODS

Silk	Time of exposure, hr.	Viscosity, centipoises	Tensile strength, lb. per in.	Amino nitrogen, %
D, exposed at 36° C.	0	23.7	47.0	0.20
	3	20.5	46.5	—
	6	18.1	46.0	—
	12	15.7	43.0	—
	18	14.3	40.0	—
	24	13.9	39.0	—
	36	12.6	32.5	—
	48	12.7	31.0	—
	72	11.0	19.0	—
	97	10.7	13.5	0.18
	120	10.6	8.5	0.19
D, exposed at 96° C.	2	18.4	45.5	—
	8	14.0	40.5	—
	17	12.2	32.0	—
	24	11.2	19.0	—
	48	10.3	7.5	—

TABLE IX

THE TENSILE STRENGTH, VISCOSITY, AND AMINO NITROGEN CONTENT OF SILK D TREATED WITH
DILUTE ALKALI

Alkali treatment		Viscosity, centipoises	Tensile strength, lb. per in.	Amino nitrogen, %
Time of boil, min.	NaOH conc., normality			
5	0.05	18.4	44.5	—
5	0.1	14.2	41.0	—
5	0.15	12.7	27.5	—
5	0.25	11.5	5.5	0.21

TABLE X

THE TENSILE STRENGTH, VISCOSITY, AND AMINO
NITROGEN CONTENT OF SILK D STEAMED AT
15 LB. PRESSURE

Time of steaming, hr.	Viscosity, centipoises	Tensile strength, lb. per in.	Amino nitrogen, %
3	18.2	45.0	—
8	14.8	44.0	—
18	12.4	35.5	—
26	11.7	29.5	0.21
40	11.2	20.5	0.22

cal nature to silk. The initial large drop in viscosity is accompanied by only a small change in tensile strength; these results parallel those obtained with cotton with the cuprammonium viscosity method. This makes the viscosity method especially valuable, in that damage is readily detected even when the tensile strength shows little change, a condition that would likely obtain when the processing methods are faulty. The method may also be used to differentiate between chemical damage and that caused by mechanical means.

Differences in the Action of Certain Agents that Cause Damage to Silk

(i) Dilute Acid

As has already been mentioned, boiling hydrochloric acid causes hydrolysis of silk, with a resulting increase in its amino nitrogen content. This is accompanied by a decrease in tensile strength and a slight yellowing of the silk. The relation between the amino nitrogen content of the acid-damaged silk and its viscosity has been shown in Fig. 4. In Fig. 6 the tensile strength of the silk is plotted against its amino nitrogen content. It will be seen that down to the point where the silk has lost half of its original strength, the amino nitrogen content may be considered as varying linearly with the tensile strength. With further hydrolysis the change in amino nitrogen content is less rapid than that in tensile strength.
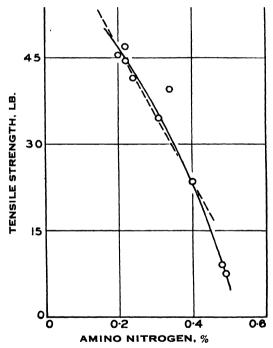
FIG. 6. *Relation between tensile strength and amino nitrogen content of silk damaged by dilute hydrochloric acid.*

(ii) Light

Harris (1) showed that the amino nitrogen content was not changed during the deterioration of silk by the action of light in the presence of oxygen. This fact has been confirmed by the writer with samples of silk exposed in the fugitometer for 97 and 120 hr., respectively. The results are given in Table VIII.

By reference to Fig. 5, it can be seen that the relation between viscosity and tensile strength of silk exposed in the fugitometer at 36° C. is the same as that of silk exposed at 96° C. In other words, the action taking place under the two sets of conditions is similar. In Fig. 7 the tensile strength of the silk is plotted against the time of exposure in the fugitometer for both temperatures; a much more rapid decrease in tensile strength at the higher temperature is shown. The form of the curves is very similar to that of the curves obtained by Harris and Jessup (2) with untreated silk exposed at 70° C.
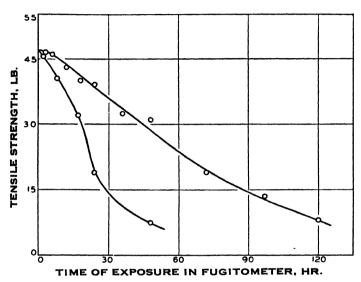
FIG. 7. *Relation between tensile strength and time of exposure of Silk D in a fugitometer. Upper curve, 36° C.; lower curve, 96° C.*

In Fig. 8 the logarithm of the time of exposure is plotted against the logarithm of the viscosity of the silk for both temperatures. A straight line relation is obtained, and, moreover, the two lines are parallel, except for a short distance at their upper ends. At 36° C. $\log V/\log T$ increases during the initial period of exposure until it reaches a certain value that remains constant during further exposure, whereas at 96° C. $\log V/\log T$ initially decreases until it attains its constant value. At both temperatures, approximately the same time (1.5 to 2 hr.) is required for attainment of this constant value.

The relative humidity of the air in the fugitometer was not controlled in these experiments, and consequently the moisture content of the silk would be quite different at the two temperatures used. The action of the two factors, temperature and humidity, cannot therefore be differentiated in this experiment.

Exposure to light in the fugitometer causes the white silk to become yellowish. While the viscosity measurements on these silks were being made, it was noted that there was a definite gradation in the color of the zinc chloride

solutions with time of exposure. The color varied from water-white through yellow to light yellow-brown, the color deepening with increasing time of exposure to light. This color may be due directly to the modified silk or to small amounts of some secondary product which may be split off under the action of light.
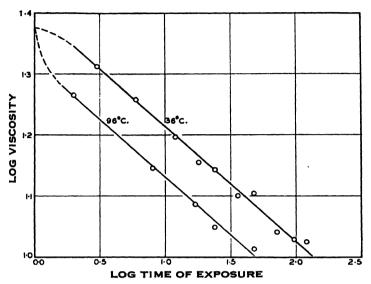
FIG. 8. *Relation between logarithm of viscosity and logarithm of the time of exposure of Silk D in a fugitometer at two different temperatures.*

(iii) Dilute Alkali

The action of a boiling dilute solution of sodium hydroxide on silk is quite different from that of boiling dilute hydrochloric acid. When silk is boiled in dilute sodium hydroxide there is a loss in weight, which increases with increasing concentration of the alkali. The loss is very marked when the silk is boiled for five minutes in 0.25 N sodium hydroxide, whereas the weight of silk is little changed when it is boiled for the same length of time in hydrochloric acid solution of even four times this normality. The decrease in tensile strength of silk fabric boiled in dilute alkali is due partly therefore to the loss of silk, whereas with the acid treatment, the loss in tensile strength appears to be almost wholly due to modification of the molecular structure of the silk fibre. This is indicated by its increasing amino nitrogen content. The amino nitrogen content of the sample of silk that had been boiled in the 0.25 N sodium hydroxide solution was unchanged, although its viscosity and tensile strength were low.

It has been stated by Jordan Lloyd and Marriott (3) that the swelling of silk fibroin in dilute alkaline solutions is accompanied by a splitting of the fibre into fibrils and by a softening of the protein. From the present experiments, it appears that in the boiling alkali this disintegration into fibrils

takes place very rapidly in the more exposed fibres, and that these fibrils are then speedily dispersed in the alkaline solution before the alkali can cause their hydrolysis to any appreciable extent.   In other words, alkaline hydrolysis of the silk "molecules", with resulting formation of free amino groups, takes place only after the silk has been dispersed, whereas in the acid hydrolysis, the formation of free amino groups occurs previous to dispersion.   Jordan Lloyd and Marriott (3) have previously suggested that the splitting of the fibre into fibrils in acid solution probably takes place at a plane of cleavage different from that in alkaline solution.

(iv) Steaming

Silk may be hydrolyzed also by steaming under pressure for prolonged periods.   It appeared interesting to ascertain whether the mechanism of the early stages of damage to silk resulting from such steaming shows any resemblance to that involved in the early stages of acid or alkali damage. Samples of Silk *D* which had been steamed under 15 lb. pressure (250° F.) for 26 and 40 hr., respectively, were tested for their amino nitrogen content. The results are given in Table IX.   The change in amino nitrogen content is so small as to be of doubtful significance.   The only conclusion that can be drawn from this very limited experimentation is that the breakdown of fibre structure by steaming under pressure is, in the early stages at least, different from that caused by boiling with dilute acid.   Judged from the appearance of the silk, the damage is also different from that caused by alkali, notably in the freedom of the silk from the stiffness, translucency, and thinning that resulted from alkali treatment, and in the pronounced brown coloration that develops on steaming.   In the last named respect, it more closely resembles silk that has been exposed for several days in the fugitometer.

Altogether, the results given in this section fit in very well with the view advanced by Jordan Lloyd and Marriott (3), that different reagents may be expected to attack different "faults" in the crystal structure of a protein fibre, such as silk, and to influence the properties in different ways.

References

1. HARRIS, M.   Bur. Standards J. Research, 13 : 151-155.   1934.
2. HARRIS, M. and JESSUP, D. A.   Bur. Standards J. Research, 7 : 1179-1184.   1931.
3. JORDAN LLOYD, D. and MARRIOTT, R. H.   Trans. Faraday Soc., 29 : 1228-1240.   1933.
4. KANAGY, J. R. and HARRIS, M.   Bur. Standards J. Research, 14 : 563-573.   1935.
5. RUTHERFORD, H. A., HARRIS, M. and SMITH, A. L.   Am. Dyestuff Reporter, 26 : P650-P655.   1937.
6. TANIZAKI, T.   J. Agr. Chem. Soc. Japan, 12 : 343-347.   1936.
7. TROTMAN, S. R. and BELL, H. S.   J. Soc. Chem. Ind. 54 : 141T-142T.   1935.
8. TROTMAN, S. R.   J. Soc. Chem. Ind. 35 : 325T-327T.   1936.
9. VAN SLYKE, D. D.   J. Biol. Chem. 12 : 277-284.   1912.

THE STRUCTURE OF DEXTRAN SYNTHESIZED BY *LEUCONOSTOC DEXTRANICUS*

Investigation of dextran (*L.d.*) obtained by the action of *Leuconostoc dextranicus* on sucrose, and carefully purified by electrodialysis, followed by methylation and hydrolysis, has led to the surprising result that the hydrolysis products are free from tetramethyl methyl glucoside, within the limits of experimental accuracy. The principal product of hydrolysis is 2,3,4-trimethyl methyl glucoside, but in addition about 10% of a dimethyl methyl glucoside is also formed.

The identity of the dimethyl methyl glucoside has not yet been completely established, but inasmuch as the synthesis of the three dimethyl methyl glucosides in question is approaching completion, this problem should be clarified in the near future.

The significance of these results lies in the fact that no evidence of the presence of any "end groups" has been found; this proves that we are not dealing with a short chain polymer either with or without side chains. On the contrary the accumulated evidence points to the substance being a linear polymer in which the terminal units of one chain are in chemical union with members of adjacent chains to form a network-like structure. In such a case the sugar representing the terminal groups would be present in such small quantity in the hydrolytic products as to render its detection almost impossible.

E. C. FAIRHEAD
M. J. HUNTER
HAROLD HIBBERT.

DIVISION OF INDUSTRIAL AND CELLULOSE CHEMISTRY,
McGILL UNIVERSITY,
MONTREAL, CANADA.
MARCH 17, 1938.

THE ISOLATION OF GUAIACOL AND PYROGALLOL 1,3-DIMETHYL ETHER FROM HARDWOOD WASTE SULPHITE LIQUOR

Treatment of a hardwood waste sulphite liquor (obtained by pulping a mixture of beech, birch, and maple woods), with sodium hydroxide (9%) at 150° C., yields, in addition to acetosyringone (1), guaiacol and pyrogallol 1,3-dimethyl ether.

Guaiacol was identified as its *p*-nitrobenzoyl ester (melting point, 104° to 105° C.; mixed melting point, 104° to 105° C.). Pyrogallol 1,3-dimethyl ether was identified by comparison of the *p*-nitrobenzoyl ester (melting point, 155° to 156° C.; mixed melting point, 155° to 156° C.) and côrulignon oxidation products with those obtained from an authentic sample of the material.

Investigation of a corresponding volatile phenol fraction from birch lignin sulphonic acid is in progress.

1. LEGER, F. J. and HIBBERT, H. J. Am. Chem. Soc. 60 : 565-567. 1938.

FRANK LEGER
HAROLD HIBBERT.

PULP AND PAPER RESEARCH INSTITUTE,
McGILL UNIVERSITY,
MONTREAL, CANADA.
MARCH 29, 1938.

THE ALKALOIDS OF FUMARIACEOUS PLANTS

XVII. *CORYDALIS CASEANA* A. GRAY[1]

BY RICHARD H. F. MANSKE[2] AND M. R. MILLER[3]

Abstract

A chemical examination of *Corydalis caseana* has yielded a total of ten alkaloids. Of these, protopine, α-allocryptopine, bicuculline, corypalmine, and scoulerine are known alkaloids. The remaining five appear to be new and include: *caseanine*, $C_{21}H_{25}O_4N$; *casealutine* and *alkaloid F34*, isomeric and represented by $C_{20}H_{23}O_4N$; *alkaloid F33*, $C_{19}H_{21}O_4N$; and *alkaloid F35*, $C_{20}H_{23}O_4N$. The new alkaloids are phenolic except caseanine which is the monomethyl ether of casealutine and the dimethyl ether of aurotensine.

Corydalis caseana A. Gray, a species native to high moist canyons of the Plumas National Forest, California, has been subjected to a preliminary examination by one of the present authors (4). Owing to the pressure of other duties its further investigation was temporarily suspended. More material was however collected, and some of the fractions were examined in the National Research Laboratories, Ottawa, Canada. The present joint communication is thus the result of the collaborative undertaking.

Of the ten alkaloids thus far isolated, only five, namely, protopine, α-allo-cryptopine, bicuculline, corypalmine, and scoulerine have been previously encountered, and with the exception of corypalmine are all present in *C. scouleri* (2). The remaining five alkaloids, though by no means conclusively characterized, appear to be new. Of these, *caseanine* (F36) is the most abundant. Its probable empirical formula, $C_{21}H_{25}O_4N$, containing four methoxyl groups, is identical with that of tetrahydropalmatine, of glaucine, and of methylpavine (5). Its possible identity with an optically active form of the last is under consideration. Incidentally, it is the dimethyl ether of aurotensine (3). The remaining four alkaloids, F32, F33, F34, and F35, which were present in small amounts only, are all phenolic. For their further examination more material will be required, although one of them, F32, has been encountered in another species, *C. lutea*, now under investigation. On methylation it yields caseanine, and since it contains only one hydroxyl group it is one of the four possible O-desmethyl derivatives of caseanine. The term *casealutine*, derived from the specific names of its two botanical sources, is proposed for this alkaloid.

Experimental

The procedure developed by one of us (1) was used to effect a separation into the various fractions. In the following summary the numbering of the alkaloids is sequential to that recently recorded (3). There was available a total of 5.5 kg. of dried plant material.

Base hydrochlorides extracted from aqueous solution by means of chloroform—

BC—Non-phenolic bases,—Caseanine (F36), Bicuculline.
BCE and EEC—Phenolic bases precipitated by carbon dioxide,—*l*-corypalmine, F32, F33, F34, F35.

Base hydrochlorides not extracted from aqueous solution by means of chloroform—

BS—Non-phenolic bases,—Protopine, α-Allocryptopine.
BSE and EES—Phenolic bases precipitated by carbon dioxide,—Scoulerine, F33.

Bicuculline

The fraction (BC), which had been thoroughly washed with water and dried, was dissolved in hot methanol. The base, which rapidly separated in crystalline form, was filtered off. It melted at 195° C.* Admixture with a specimen of bicuculline melting at 196° C. caused no depression in the melting point. It was further characterized by conversion to the low melting form (m.p. 177° C.) which proved to be identical with an authentic specimen. The yield was 0.20%.

Caseanine (F36)

The methanolic filtrate from the bicuculline was boiled with charcoal, filtered, and evaporated to a small volume. An excess of oxalic acid in sufficient water was added to effect complete solution. No salt separated in the course of several days. The solution was then thoroughly exhausted with ether†, filtered with charcoal, and basified in small portions with ammonia. The liberated base was extracted with ether in which it was sparingly, though completely, soluble. The washed ether solution on partial evaporation deposited colorless stout needles which melted at 114° C. with the evolution of vapors, evidently water. This hydrate, when recrystallized from ether, melted at 115 to 116° C. and slowly lost its water of crystallization at room temperature. It then melted at 137 to 139° C. Total yield, 0.40%.

Caseanine is easily obtained in anhydrous, almost colorless prisms when its solution in benzene, which has been heated to expel water, is cautiously treated with petroleum ether. As thus obtained it melts sharply at 142° C. It dissolves in sulphuric acid to give a colorless solution. On heating, the solution becomes pink and finally brown; this color changes to purple when the solution is cooled. Found: C, 71.03; H, 7.04; N, 3.99; OMe, 33.75%. Calcd. for $C_{21}H_{25}O_4N$: C, 70.99; H, 7.04; N, 3.94; 4OMe, 34.93%.

All melting points are corrected.

† *It has been the experience of one of the authors (R. H. F. M.) that the extraction of oxalic acid solutions with ether is a more effective procedure for purifying crude alkaloids than extraction of mineral acid solutions.*

The *picrate* was recrystallized from hot water containing a little methanol. The pale yellow needles thus obtained melted not quite sharply at 112 to 113° C., and this melting point was not depressed when the substance was admixed with a specimen of aurotensine dimethyl ether picrate.

The hydrochloride is only sparingly soluble in cold water, crystallizing from a hot solution in colorless fine needles.

Alkaloid F33

The fraction (BCE) was dissolved in chloroform-methanol, filtered, and the solution evaporated to a small volume. Colorless fine needles rapidly separated, and these induced crystallization when introduced into a methanolic solution of (EEC). The combined product from the two fractions was redissolved in hot chloroform, in which it is only sparingly soluble. The solution was rapidly evaporated to a small volume and treated with methanol. The base then crystallized at once. After filtering off, washing, and drying, it melted at 257° C. with slight previous darkening. It has a strong tendency to become electrified, and its transfer to a bottle is difficult even in a beam of ultra-violet light. Its empirical formula, its phenolic nature, and the presence of two methoxyl groups indicate that it may be a second di-O-desmethyl-caseanine. Found: C, 69.44; H, 6.69; OMe, 17.40%. Calcd. for $C_{19}H_{21}O_4N$; C, 69.74; H, 6.40; 2OMe, 18.89%.

Casealutine (F32)

The filtrate from the crystallization of alkaloid F 33 on slight evaporation deposited a second base. This was recrystallized from chloroform-methanol and was then obtained in colorless stout prisms which melt to a dark tar at 230° C. The colorless solution in sulphuric acid becomes pink, olive, and finally purple on progressive heating, the last becoming more intense on cooling again. Found: C, 70.14; H, 6.86; N, 4.58; OMe, 26.64%. Calcd. for $C_{20}H_{23}O_4N$; C, 70.38; H, 6.75; N, 4.10; 3OMe, 27.27%.

A small portion of casealutine was suspended in methanol and treated with an ethereal solution of diazomethane. In the course of about ten days the alkaloid was completely dissolved. The solvents were evaporated and the residue was dissolved in dilute hydrochloric acid; this yielded a sparingly soluble hydrochloride. The regenerated non-phenolic base was recrystallized from ether, and thus yielded the sparingly soluble hydrate of caseanine, which either alone or admixed with an authentic specimen melted at 115 to 116° C. The anhydrous base was prepared by recrystallization from benzene-petroleum ether. It melted at 142° C.; admixture with anhydrous caseanine did not depress the melting point.

l-Corypalmine

The mother liquors from the casealutine and especially those from fraction (EEC) after some time deposited a mixture of bases. These were extracted with several successive portions of hot methanol (the residue consisted of impure casealutine) and the extracts evaporated somewhat. The colorless

base which crystallized on cooling was recrystallized from chloroform-methanol, and it then melted at 226° C. when placed in a bath at 210° C. In admixture with a specimen of *l*-corypalmine, which melted at the same temperature and which on methylation yielded *l*-tetrahydropalmatine, there was no depression in the melting point. In admixture with casealutine it was completely liquid at 214° C. The color reactions with sulphuric acid are similar, although when carried out side by side the differences are evident. In the cold acid, *l*-corypalmine yields a colorless solution which on heating undergoes the following color changes,—pale pink, then almost colorless to olive, and finally intense purple, which, on dilution with water, becomes bright orange with a reddish cast.

Alkaloid F34

The more soluble portions of fractions (BCE and EEC) deposited on long standing a further mixture of crystalline bases. A series of fractional crystallizations yielded a more soluble base which was finally recrystallized from chloroform-methanol. The colorless needles appeared completely homogeneous and melted at 218° C., sintering and darkening at a temperature several degrees lower. In admixture with either *l*-corypalmine or with casealutine it was completely liquid below 210° C. Its colorless solution in sulphuric acid became yellow and then pink on gentle warming and brown on heating; on cooling, the solution became purple. The analyses indicate that it is isomeric with casealutine. Found: C, 70.04; H, 6.92; N, 4.28; OMe, 26.65%. Calcd. for: $C_{20}H_{23}O_4N$; C, 70.38; H, 6.75; N, 4.10; 3OMe, 27.27%.

Alkaloid F35

The final mother liquor from (BCE and EEC), which yielded no more crystalline alkaloids, was neutralized with hydrobromic acid and evaporated to a thin syrup. The sparingly soluble hydrobromide which separated in the course of several days was recrystallized from hot methanol-acetone. It was dissolved in hot water, in which it is sparingly soluble, and the rapidly cooled solution basified with ammonia. The crystalline precipitate thus obtained was recrystallized from hot methanol by the cautious addition of hot water. Large, well defined colorless plates melting sharply at 145° C. were thus obtained. No solvent of crystallization appears to be present in the crystals. The alkaloid dissolves in cold sulphuric acid to give a colorless solution which develops a pale pink color on prolonged heating only. Found: C, 70.43; H, 6.84; N, 3.98; OMe, 26.68%. Calcd. for $C_{20}H_{23}O_4N$; C, 70.38; H, 6.75; N, 4.10; 3OMe, 27.27%.

Methylation with diazomethane yielded a methyl ether which when recrystallized from methanol-ether melted at 186° C. It gave the same color reaction with sulphuric acid as its phenolic precursor.

Protopine and α-Allocryptopine

The isolation of protopine in a state of purity is in general a facile procedure. In the present instance no difficulty was encountered in separating it from

the allocryptopine, which appears to be the only other alkaloid in the fraction (BS). The yield of protopine was 0.10%.

A small amount of α-allocryptopine was also obtained from fractions (BC and EC). In all cases the protopine was eliminated as hydrobromide, and the purified α-allocryptopine melted at 160° C. Comparison with an authentic specimen failed to reveal any differences. The yield was 0.16% and this is the only plant, in so far as the authors are aware, in which the amount of allocryptopine is greater than that of protopine.

l-Scoulerine

The fractions (BSE and EES) in contact with methanol yielded a small amount of alkaloid F33. The filtrate from the latter was neutralized with hydrochloric acid and evaporated to a small volume. A sparingly soluble hydrochloride readily crystallized. The free alkaloid was regenerated from this and recrystallized from methanol-ether. It melted at 193 to 194° C. and in admixture with an authentic specimen of *l*-scoulerine from *C. scouleri* it melted at 194° to 195° C. The entire specimen, which weighed approximately 50 mg., was methylated with diazomethane in methanol ether. The non-phenolic base thus obtained when recrystallized from ether melted sharply at 142° C. either alone or in admixture with a specimen of *l*-tetrahydropalmatine.

Fumaric Acid

The isolation of pure fumaric acid from the fraction (LC), as in previous cases, was relatively simple, although the amount present is probably not more than 0.1%.

References

1. MANSKE, R. H. F.   Can. J. Research, 8 : 210-216.   1933.
2. MANSKE, R. H. F.   Can. J. Research, B, 14 : 347-353.   1936.
3. MANSKE, R. H. F.   Can. J. Research. B, 16 : 81-90.   1938.
4. MILLER, M. R.   J. Agr. Research, 42 : 239-243.   1931.
5. PYMAN, F. L. and REYNOLDS, W. C.   J. Chem. Soc. 97 : 1320-1328.   1910.

LINOLEIC ACID AND ITS ISOMERS[1]

By J. W. McCutcheon[2]

Abstract

Linoleic acid has been prepared from sunflower seed oil by a modification of Rollett's method. The melting point of the solid tetrabromostearic acid is placed at 115.2° C. The boiling point, specific gravity, iodine value, and refractive index of the ethyl ester and the melting point of the free acid were determined. Linoleamide was prepared, and its melting point is placed at approximately 58° C. Through rebromination of the prepared linoleic acid, the isomeric liquid tetrabromostearic acid was isolated, and is described. Its reduced acid is shown to be identical with that derived from the solid isomer. From these data and additional data from the literature, it was concluded that bromination and debromination cause no *cis-trans* isomerization, and that the two pairs of optically active enantiomorphous bromo derivatives exist, not because of their derivation from different acids, but rather because of the four asymmetric carbon atoms which they contain. Therefore, only one naturally occurring linoleic acid is at present known which is identical with that produced through reduction of the tetrabromide that melts at 115.2° C. or the corresponding liquid derivative. No attempt is made to assign any particular *cis-trans* configuration to this acid, or to exclude the theoretical existence of three others.

An investigation of the hydrogenation process as applied to vegetable and animal oils was carried out recently by the author. A review of the literature revealed the problem to be very complex, largely owing to the difficulty of obtaining elementary pure raw materials. Linoleic acid is the most common and simplest acid available for the study of selective hydrogenation, but it has been used very little, possibly owing to the difficulty of preparation and the uncertainty regarding the product obtained. The work of those who did use it was open to the criticism that the product was not pure (23) or did not represent the natural acid (20). Hence, it was suggested that, as a preliminary to the further study of hydrogenation, an investigation be conducted on the preparation of this acid, with the object of obtaining it in a pure state and studying its isomerism.

Linoleic acid occurs to the extent of about 25 to 50% in the semidrying oils such as cottonseed, peanut, soybean, and others. It has been shown by Hilditch and Vidyarthi (7), Riebsomer and Nesty (16), Smit (20) and others, chiefly through oxidation reactions, to be the $\Delta^{9,12}$ octadecadienoic acid, of which, according to Inoue and Suzuki (9), four possible *cis-trans* isomerides should exist.

Up to the present, the method of Rollett (17) has been the only one available for the preparation of this acid in any degree of purity, although very recently several interesting papers have appeared that suggest the use of freezing mixtures (3, 4). Rollett's method depends on the bromination of the liberated fatty acids of the oil, the separation of the solid tetrabromostearic acid, and its subsequent reduction by means of zinc. That these operations cause no

bond shift has been shown by Smit (20), Suzuki and Inoue (21), Hilditch and Vidyarthi (7), Hilditch and Green (6), and others, although it has been apparent from the first that stereoisomerism does occur, since less than 50% of the theoretical quantity of the solid tetrabromide is precipitated. Only two isomers, a solid, m.p. 113° to 115° C., and a liquid, exist, the proportions formed being generally given as 40 to 50% solid and the remainder liquid (6, 14, 17, 22).

It was suspected for some time that a third (22) and even a fourth (18) isomer did exist. These were shown by Palmer and Wright (15) and later by Smit (20) to be merely the ethyl or methyl ester of the tetrabromide, formed during crystallization.

The so-called solid, or α-tetrabromide, is a snow white, crystalline compound readily soluble in sulphuric ether, alcohol, glacial acetic acid, and other solvents, but sparingly soluble in petroleum ether. Its melting point has been generally recorded as 113° to 115° C. (11, p. 202; 17, 22), but one result places it at 116° to 117° C. (20).

The liquid, or β-tetrabromide, differs from the solid in its ready solubility in petroleum ether. Both these tetrabromo compounds when reduced to the acid and rebrominated yield further mixtures of the same two isomers.

The solid isomer yields on reduction α-linoleic acid, which is generally considered to be identical with the naturally occurring product; both give on mild oxidation the same two sativic acids, m.p. 155° and 173° C. (6). As far as can be learned, no data regarding the acid or esters from the liquid tetrabromide have been published, with the exception of those of Hilditch and Green (6), who report finding very small amounts of the same sativic acids as obtained from the solid derivative.

Rollett believed that there occurred only one linoleic acid which gave two bromo derivatives, each representing a racemic compound. Hilditch and Green (6) also believed that only one natural linoleic acid is present in seed fats, as does Smit (20), who added, however, the opinion that the bromination probably causes a Walden inversion, so that the derived product may not be the same as the natural one. Nicolet (13) believes that isomerization occurs in bromination, and thus accounts for the two tetrabromides as being produced from two or even more linoleic acids. In conclusion, it may be mentioned that van Loon (12) and van der Veen (24) point out the fallacy of designating the derived acids from the α- and β-tetrabromides with the same appellation because of the isomerism known to occur.

The investigation described herein had for its object *(a)* the establishment of additional constants of the esters of the solid tetrabromo derivative, and *(b)* the preparation of the liquid derivative in a state pure enough for its comparison with the solid derivative.

Experimental Data

The Raw Material

Sunflower seed oil was chosen not only because of its exceedingly high content of linoleic acid, but also because of the complete absence of linolenic

or more highly unsaturated acids. The analyses given in Table I, except for a rather high unsaponifiable content, closely correspond to the normal values for such an oil.

TABLE I

ANALYSIS OF THE SUNFLOWER SEED OIL USED

Free fatty acid (as oleic, refined oil), %	0.07	Analysis of the fatty acids, %	
Color	4.5 red/35.0 yellow		
Iodine value (Wijs)	128.2	Saturated acids (Twitchell)	10.0
Saponification value	193.4	Oleic acid (by calculation)	31.0
Total fatty acids, %	95.6	Linoleic acid (by calculation)	57.2
Hexabromide test (absence of linolenic acid)	Negative	Unsaponifiable	1.8
Unsaponifiable, %	1.78		
Iodine value of unsaponifiable	149.7		

Preparation of the Fatty Acids   •

In the preparation of the fatty acids the method recommended by the American Oil Chemists' Society (1) was closely followed, the usual care being taken to avoid oxidation. Yields of 90 to 92% were readily obtained, and the product was preserved in an atmosphere of carbon dioxide.

The Bromination

The bromination, debromination, and esterification were carried out in a manner similar to the method of Rollett (17), the main differences being; (i) the bromination was carried out at 20° to 25° C. rather than at zero; (ii) a special purification process for the solid tetrabromide was introduced; (iii) debromination and esterification were carried out as two separate steps; (iv) the esterification was completed in the absence of zinc.

A solution of 30 ml. of liquid bromine in 400 ml. of petroleum ether was sprayed into a mixture of 100 gm. of the fatty acids and 1600 ml. of the ether over a period of about 15 to 20 min., the temperature being held between 20 and 25° C. The petroleum ether (b.p. 40° to 60° C.) conformed to the standards required in extraction work by the methods of the American Oil Chemists' Society (1). Table II indicates the yields obtained in the bromination of various batches.

TABLE II

YIELDS OF SOLID TETRABROMIDE OBTAINED FROM VARIOUS BATCHES

Batch	Weight of oil taken, gm.	Weight of tetrabromide, gm.	Corr. m.p., °C.	Yield, % of theoretical
1	100	48.9	112.6	36.2
2	100	48.8	113.0	36.2
3	100	57.0	114.0	49.1*
4	1060 (5 batches)	465.5	114.1	36.5†
5	20 (pure linoleic acid)	20.4	114.2	47.6*

High yield due to the use of tetrabromide-saturated petroleum ether and the residue-containing beakers from previous batches.

† *This batch was prepared in April, 1936.*

Through subsequent work on the solubility of the tetrabromide in petroleum ether, the true yield is believed to be 50% of theory. This is obtained by allowing a solubility of 2 gm. of the bromide in 1000 ml. of petroleum ether, and adding a manipulative loss of 12%. This conclusion appears justified by the findings with Batches 3 and 5.

Purification of the Tetrabromides

A pilot lot of 10 gm. was refluxed for one hour at 47° C. with petroleum ether, filtered, dried, and screened. A second lot was treated similarly twice. Both products had identical melting points (114.7° C.*), which checked well with the value (114.6° C.) obtained in the previous year.

However, in some experiments conducted at this time to determine the solubility of the tetrabromide in boiling petroleum ether, it was noted that the filtrate from some of the hot solutions showed definite, needle shaped crystals. By reworking these, about 1 or 2 gm. of beautifully crystalline needles, which formed in clusters, was obtained. Under the high power microscope they were found to be transparent and somewhat square at the ends. It was concluded that this product would be exceptionally suited to the checking of the true melting point of the tetrabromide. The results on this sample were 115.2, 115.2, 115.1, 115.2 (very fine capillary), 115.2 (closed tube method). Average, 115.2° C.

From this work it was concluded that the solid tetrabromide could not be sufficiently purified by simply washing it with petroleum ether. After several trials with small pilot batches, the following methods were adopted and applied successfully not only to the material that melted at 114.7° C. but also to the residues from Batch 1 (m.p. 112.6° C.) to raise the melting point to 115.1° C. The yield for each crystallization was about 80%. However, there is no doubt that greater yields could be obtained with larger batches.

Method 1

To 15 gm. of the tetrabromide in a 2000 ml. beaker was added 600 ml. of petroleum ether. The height to which the solvent rose was marked so that a correction could be made for losses during boiling. The mixture was brought to a vigorous boil on a water bath, and then just sufficient absolute ethyl alcohol to completely dissolve the whole precipitate was added slowly. Repeated experiments gave values very close to 5% by volume (30 ml.) under these conditions. The hot solution was filtered with suction through a 4 in. Büchner to remove any foreign material, and it was then chilled to 0° C. The chilled solution was filtered and washed with 300 to 400 ml. of fresh petroleum ether.

The color of the filtrate indicates whether one crystallization is sufficient. Owing to the fine, easily broken down texture of the material, it is not necessary to screen the product. Altogether, 80.8 gm. of the compound was so prepared.

Although this method was satisfactory with a well washed crude material of melting point 114.5° C. or higher, the low temperature crystallization was

* *All melting points determined by the author are corrected.*

not very satisfactory for materials less pure, since there was a tendency for the liquid tetrabromide to co-precipitate. Method 2, suggested by the work of Smit (20), was developed in order to obviate this difficulty.

Method 2

Tetrabromide (100 gm.) was dissolved in 200 to 300 ml. of sulphuric ether and filtered. The ether was then evaporated to incipient crystallization (about 100 ml.) and diluted with petroleum ether to about 1500 ml. The solution was then cooled to 15° to 20° C., filtered, and washed. Yields approximated 70 to 80%.

The purified crystals are snow white, and have a slight silver sheen. When viewed under the high power microscope they appear as long narrow rectangular plates with square ends. With lower magnification they appear needle shaped. They melt without decomposition to a pure white solid, but traces of impurity will cause a decided browning. The bromine content was 53.20%; theoretical, 53.28%.

Solubility of the Tetrabromide in Petroleum Ether

Although this was not intensively studied, experiments indicated that the solubility varied from about 0.4 gm. per 100 ml. at 45° C. to about 0.1 gm. at 0° C. Solutions showed a great tendency to become supersaturated even in the presence of excess tetrabromide.

Debromination and Esterification

The debromination was carried out with 40-gm. lots of the tetrabromide in 300 ml. Erlenmeyers, about 35 gm. of 20 mesh zinc metal being used. After the first vigorous exothermic reaction was over, the whole was refluxed 30 min. before any alcoholic hydrochloric acid was added. Esterification was carried out in the usual manner with 4 N alcoholic hydrochloric acid for two hours. The zinc was then removed, and the solution refluxed for an additional hour. The color of the product during these operations will vary from pale straw to water white, depending on the purity of the tetrabromide used. The ester was separated with a brine solution, washed, filtered, and distilled under high vacuum. The product was a water white liquid. Yields obtained with a number of batches are given in Table III.

TABLE III

YIELDS OF ETHYL LINOLEATE FROM TETRABROMOSTEARIC ACID

Weight of tetrabromide used, gm.	40	100	93.6	171.9
Weight of ethyl ester recovered, gm.	16.7	42.2	42.1	74.0
Yield, % of theoretical	81.3	82.4	87.9	84.4

The product distils at constant temperature without the formation of any residue, and the acidity should be less than 0.25% calculated as linoleic acid.

The acid is obtained from the ester, as required, by the method of cold saponification outlined by Rollett (17). Except for the 50% loss of tetrabromostearic acid by the formation of the liquid isomer, the yields vary from

about 80 to 90%, depending on the number of manipulations involved. From the accumulated data of experiments with numerous batches, the yields given in Table IV may be expected.

TABLE IV

SUMMARY OF TYPICAL YIELDS—SUNFLOWER SEED OIL TO LINOLEIC ACID

Substance used	Amount, gm.	Substance obtained	Amount, gm.
Sunflower seed oil	100	Fatty acids	87
Fatty acids	87	Tetrabromide	42.5
Tetrabromide	42.5	Purified tetrabromide	35
Purified tetrabromide	35	Distilled ethyl ester	14.6
Distilled ethyl ester	14.6	Linoleic acid	12.5

It was observed that, as compared with the free acid, the pure ester was an extremely stable compound. The iodine value, refractive index, and color samples kept in ordinary two ounce white-glass bottles for more than a year at room temperatures remained virtually unchanged. For this reason it was considered advisable to determine, as far as possible, the constants of the ester rather than of the free acid. The following are a few of the constants that have been determined:—ethyl ester—the boiling point, specific gravity, refractive index, and iodine value: free acid—the melting point. The linoleamide was prepared from the free acid.

The Boiling Point of the Ethyl Ester

The distilling apparatus consisted of two Pyrex 50 ml., round bottomed flasks so joined together by a short piece of 8 mm. Pyrex tubing that one might be used as the distilling flask and the other as the receiver, alternately (Fig. 1). Thus it was possible to repeat conveniently the determinations with the minimum loss in transfer, and also to check whether any decomposition was taking place.

The vacuum gauge was of the Bennert mercury manometer type with movable milk glass scale, 13 cm. each way from zero, i.e., a 0 to 260 mm. range. The readings were taken with
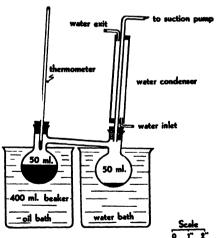
FIG. 1. *Distilling apparatus.*

the aid of a three-inch reading glass, and the observer checked his method of reading the meniscus by taking the zero reading on the manometer alone.

The vacuum control apparatus as constructed was identical with that described by Schierholtz (19). After a preliminary adjustment no difficulty

was experienced in maintaining the vacuum at various values between 1 and 20 mm. of mercury with no observable fluctuations in the meniscus.

The temperature was taken with an ordinary −10° to 360° C. mercury thermometer, which was graduated in 1° C. divisions. The over-all length was 16 in., with 27° to the inch. It was checked against a thermometer supplied with a U.S. Bureau of Standards' certificate and table of corrections. At temperatures 197°, 202°, and 206° C. no differences could be noted between the thermometers when the corrections were made. The effect of a vacuum on the bulb was studied by setting up the unit in a water bath held at a very definite temperature close to that of the room, and reading the thermometer before and after the pressure was reduced to 1 mm., due care being taken to allow the heat developed to be dissipated. The correction caused by expansion of the bulb under such reduced pressure was found to be 0.2° C., and was therefore neglected in subsequent work.

Operation

The distilling flask was heated in an oil bath. No bumping occurred except at a pressure of 17 mm. Bumping was probably minimized by the design of the apparatus which permitted no drops to form on the outlet tube. A very slight rise in temperature was noted toward the end of the distillations; this was attributed to the gradual increase of vapor head in the flask. For this reason the flasks were reversed when about two-thirds of the product had distilled over.

An assistant aided in recording the data; this made the simultaneous recording of pressure and temperature possible. The distillation was maintained for several minutes until the temperature and pressure became constant. Finally, after a series of increasing pressures, the original low pressure was restored in order that a possible change in boiling point due to decomposition could be checked. No change was noted. The data obtained are given in Table V.

TABLE V

BOILING POINT DATA FOR ETHYL LINOLEATE, TAKEN AT VARIOUS REDUCED PRESSURES

Pressure, mm.	2.5	4.5	6	12	17	2.5
Temperature uncorrected, °C.	171.0	184.0	190.5	208.5	220.0	170.5
Temperature corrected, °C.	175	187.5	193.5	212	224	173

Final values are given to the nearest one-half degree. None of the previous values obtained by the author under less exacting conditions differ by more than a very small fraction from the values given in Table V. These results are presented graphically in Fig. 2.

Specific Gravity of the Ethyl Ester

The specific gravity of the ethyl ester was determined in the usual way with a 10 ml. Gay-Lussac type specific gravity bottle that had been standardized with freshly boiled distilled water. Thermometer and weights were checked against standard equipment, and the necessary corrections made. The data and results are given in Table VI.

TABLE VI
SPECIFIC GRAVITY OF ETHYL LINOLEATE

—	Temp., °C.	Grams	Specific gravity
Air wt. of pycnometer (P)		8.0004, 8.0004	
P + water	15.5	17.9769, 17.9768	Apparent, 0.8844 (15.5°/4° C.)
P + water	25.0	17.9594, 17.9596	True, 0.8846 (15.5°/4° C.)
P + ester	15.5	16.8323, 16.8323	Apparent, 0.8775 (25.0°/4° C.)
P + ester	25.0	16.7652, 16.7652	True, 0.8776 (25.0°/4° C.)

Humidity, 50%; brass weights, density 8.4.
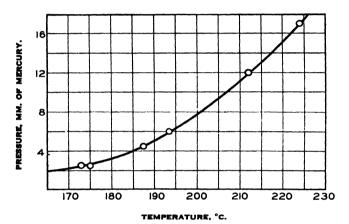
FIG. 2.   *Boiling point curve of ethyl linoleate.*
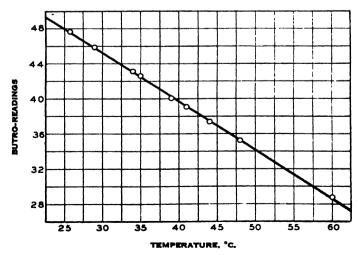
FIG. 3.   *Butro-refractometer readings for ethyl linoleate at various temperatures.*

Refractive Index of the Ethyl Ester

The refractive index was determined by means of a butro-refractometer, with light filtered through a dichromate solution so as to approximate sodium light. The results are presented in Table VII, and graphically in Fig. 3.

TABLE VII

REFRACTIVE INDEX OF THE ETHYL ESTER OF LINOLEIC ACID

Temp., °C.	25.8	29.0	34.0	35.0	39.0	41.0	44.0	48.0	60.0
Butro-reading	47.70	45.85	43.10	42.60	40.25	39.10	37.40	35.20	28.75
Refractive index	1.4578	1.4565	1.4546	1.4542	1.4526	1.4518	1.4505	1.4489	1.4443

NOTE:—*Temperatures were read to 0.1° C., but in controlling the rise in temperature it was convenient to hold them at the even values.*

The values 1.4488, 1.4491, and 1.4486 were obtained for the refractive index at 48.0° C. of three lots of esters that were prepared the previous year.

Iodine Value

The iodine value of the ethyl ester, as determined by means of the Wijs method (1), was *(a)* 162.29, *(b)* 162.49; average, 162.39. These results agree well with those of Rollett (17) and van der Veen (25).

The Melting Point of Linoleic Acid

Ordinary melting point tubes were filled with linoleic acid and immersed in a beaker of alcohol chilled with solid carbon dioxide to about −65° C. The acid froze immediately to a white solid. By transferring the tubes to an alcohol bath at −30° C. and allowing the bath to warm gradually, a fairly sharp melting point was noted between −8° and −9° C., with duplicate samples prepared from different batches of the ethyl ester. One of these samples, however, after standing for several days in an atmosphere of carbon dioxide, was observed to have a melting point of −13° to −14° C. A fresh sample again gave the melting point of −8° to −9° C., which did not change when the sample, in the form of a thin film, was exposed to the atmosphere for 30 min. Lewkowitsch (11, p. 184) has suggested that oleic acid is dimorphous, having melting points of about 4° and 14° C. Possibly linoleic resembles oleic in this respect, and indeed both values, approximately, have been reported by different workers (8, 20).

In an endeavor to settle the above question an attempt was made to study the transition points by means of the dilatometric method (5, p. 274). The attempt was unsuccessful, but it is hoped that this work will be pursued at a later date.

Linoleamide and Its Preparation

Linoleamide was prepared according to the method of Aschan (2). After a number of preliminary experiments with pure oleic acid from which crude oleamide of melting point 72° to 73° C. was obtained, a small pilot batch of linoleamide was prepared (m.p. 57° C.). Both the oleamide and the linoleamide were soft, soapy, non-crystalline substances, very difficult to filter. The details of the preparation follow.

Ten grams of the linoleic acid was weighed into a four ounce glass-stoppered bottle and 2 ml. of phosphorus trichloride added. The mixture was shaken at intervals for several hours and allowed to stand overnight. The supernatent acid chloride was then transferred to a small glass-stoppered dropping funnel and slowly run into about 400 ml. of well agitated concentrated ammonia solution held at 0° C. in an ice bath. The ammonia solution was diluted to about four times its volume with distilled water and extracted with chloroform. The solvent was distilled off and the oily residue (about 5 ml.) was taken up with about 75 ml. of absolute ethyl alcohol, and filtered.

The filtrate was chilled until about 75% or more of the solid had precipitated. A small portion was laid aside for melting point determination, and the remainder was again dissolved and reprecipitated, m.p. 57° to 58° C.

After several days the soapy material in all samples had separated into two phases: a substance having a fibrous structure, and an amber liquid. The possibility of the presence of two isomers became apparent. After five weeks, however, a careful microscopic examination of the liquid and solid phases failed to reveal any crystalline structure. In fact, the fibrous material was found to be in a state of gradual decomposition. The conclusion reached was that only one substance was originally present, but that on standing it gradually oxidized and polymerized. The sample had been kept in a small glass-stoppered bottle, and it was not considered likely that sufficient oxygen was present to cause the complete change observed.

The Preparation of the Liquid Tetrabromide

Since the liquid tetrabromide can be obtained only by difference, considerable care must be taken to use nothing but pure linoleic acid as starting material. Twenty grams of the linoleic acid was prepared from the 43 gm. of triple-distilled ethyl ester as described previously. It was brominated in the usual manner except for the following differences:—

(a) The petroleum ether was the recovered material from previous brominations, so as to insure against the possible formation of non-volatile bromo addition products. In addition a small blank was run for such residues. None was found.

(b) The temperature of bromination was held from −10° C. at the beginning to −2° C. at the end.

(c) The amount of bromine was increased from 6 to 10 ml.

The solid tetrabromide was filtered in the usual way and washed with three lots of 300 ml. of petroleum ether cooled to −20° C. It was quite granular and easily worked over. The melting point of the crude tetrabromide was 112.7° C.; that of the recrystallized tetrabromide was 114.8° C. The yield was 20.0 gm.

The filtrate was then chilled to −20° C., whereupon a brown gummy viscous material began to separate out; it did not completely redissolve until the temperature had risen to −10° C. At 0° C. a small, hard, horny mass still remained undissolved; when this was filtered off, dissolved in boiling

petroleum ether, and chilled again to $-20°$ C. a fine white material that was identified as the solid tetrabromide was obtained.   Yield, 0.3 gm.

The main filtrate was then chilled to approximately $-65°$ C. in an alcoholic bath containing solid carbon dioxide.   The liquid tetrabromide formed a thick viscous layer on the sides and bottom of the beaker.   The solid tetrabromide still remaining in solution formed a fine white suspension, which was readily removed by filtration.   Yield, 0.1 gm.

Total yield of solid tetrabromide:— $20.0 + 0.3 + 0.1 = 20.4$ gm., equivalent to 47.6% of the theoretical.

The liquid tetrabromide remaining in the bottom of the beaker was dissolved in fresh petroleum ether and transferred to a 250 ml. Soxhlet flask.   By alternately warming and chilling to about $-65°$ C. it was possible to wash the liquid compound by decantation.   After the first wash the filtrates were almost colorless.   The final product was a pale straw colored viscous syrup. The first filtrate when concentrated also gave a similar product in almost equal quantity; this indicates that even at $-65°$ C. the liquid tetrabromide is considerably soluble in petroleum ether.

The total weight of liquid tetrabromide was 12.1 gm., although no attempt was made to obtain a quantitative yield.   From this, 3.4 gm. of the ethyl ester was prepared in the usual manner, and its boiling point determined. This was repeated on a larger scale, 25.2 gm. of ethyl ester being prepared from the tetrabromide that melts at $115.0°$ C.   After the solid isomer had been filtered off at $-1°$ C., the liquid was obtained by evaporation of the petroleum ether under a current of carbon dioxide gas.   The yield was 25.1 gm., or 49.2% of the theoretical.   This product was esterified in the usual way, no difficulty being experienced, and distilled three times; a water white liquid was obtained.   The constants determined for these compounds are compared in Table VIII with previous values obtained for the solid tetrabromo derivative.

TABLE VIII

COMPARISON OF SOME PHYSICAL CONSTANTS OF ETHYL LINOLEATE PREPARED FROM BOTH THE SOLID AND THE LIQUID TETRABROMOSTEARIC ACID

Lot	Boiling point values					Refractive index (25.1 gm. lot)			
						Liquid tetrabromo derivative		Solid tetrabromo derivative	
	Pressure, mm.	Ester from liquid tetra-bromide, °C.	Ester from solid tetra-bromide*, °C.	Temp., °C.		Butro-reading	Refractive index	Butro-reading	Refractive index
3.4 gm.	5	190	190	48.0		35.05	1.4488	35.20	1.4489
3.4 gm.	12	215	212	38.0		40.60	1.4528	40.72	1.4529
25.1 gm.	11	208.5	209						

True specific gravity (15.5°/4° C.) of ethyl ester is:— 0.8845, liquid derivative; 0.8846, solid derivative.

* See Fig. 2.

The constants given in Table VIII agree within the limits of experimental error and point to the identity of the products. It is to be noted that the refractive index of the liquid tetrabromo derivative is lower than that of the solid, as would be expected, since it contains the accumulated impurities.

In addition, the liquid tetrabromide was prepared from the 35.4 gm. lot of ester obtained during April of 1936. A modification consisting in the removal of the excess bromine by shaking out with thiosulphate solution followed by thorough washing was introduced. Both liquid bromides were pale straw colored liquids that set to a semi-solid mass on standing overnight. They had a peculiar varnish-like odor. Some acrolein, which was finally traced to the petroleum ether, was present in each liquid. Although this would have no effect on the ester derivative, it was considered advisable to repeat the preparation of liquid tetrabromide to decide whether the crystallization observed after standing was caused by such impurities.

Petroleum ether of boiling point 30° to 55° C. was brominated and distilled. A 100 ml. sample of this material was then rebrominated and redistilled. No residue remained at 60° C. and there was only a very faint odor suggesting acrolein. A portion (15.0 gm.) of the 40.2 gm. lot of linoleic ethyl ester prepared during April, 1936, was saponified and brominated in the usual way. The solid tetrabromide was filtered off, and the filtrate chilled to −5° C. and refiltered. The excess bromine was boiled off and the ether solution concentrated to about 30 ml. It was then chilled to about −65° C. in an alcohol bath containing solid carbon dioxide, whereupon the liquid tetrabromide separated out as a thick milky gum adhering to the walls of the beaker. The ether was poured off, and fresh ether added. In this manner the bromide was washed three times by decantation. It was then transferred to a 25 ml. ampoule, and the final traces of solvent were removed by warming under a pressure of $\frac{1}{2}$ to 1 mm. The product darkened somewhat during the latter process, but it was considered advisable to ensure the removal of acrolein should any be present. The ampoule was then sealed off under a pressure of 1 mm. or less.

The warmed material was a dark pale straw colored substance resembling melted rosin. When the ampoule was immersed in a bath at −65° C. for a few minutes, the bromo compound became solid, and fractured along the walls of the tube. These fractures disappeared almost immediately on removal of the tube from the cold bath. The tube was rotated and the material thus spread in a film over the surface of the tube, which was then chilled, but crystallization did not occur. After the material had stood at room temperature for 24 hr., however, crystals appeared. The conclusion was then drawn that this phenomenon was not due to impurities as originally suspected. The bromine content was found to be 53.12%, theoretical 53.28%. When the acid from the liquid derivative was again brominated, the yield of solid tetrabromide was that usually observed.

Discussion of Results

The Melting Point of the Solid Tetrabromostearic Acid

The melting point of the solid tetrabromide has been placed by the author's work at 115.2° C., a value close to that generally accepted. With many samples of crude material the author has obtained values ranging from 113° to 114.7° C., which, with some samples, could not be raised after repeated pulverizing and washing. Without recrystallization the maximum melting point obtained for any sample was 114.7° C. On the other hand, with only one recrystallization the minimum value obtained was 114.7° C., and the maximum, 115.1° C., although all values were obtained with fairly large batches. This possibly explains the variations previously recorded in the literature. The value 116° to 117° C. given by Smit (20) appears to be too high. He used, as raw materials, oils known to contain linolenic acid. Since this acid also forms liquid stereoisomers with bromine, the difficulty of completely removing them by precipitation can be appreciated. That traces of these acids probably contaminated Smit's tetrabromo compound is indicated by the abnormally high iodine value recorded for both the acid and the ester: 181.9 (theoretical 181.1) and 174.4 (theoretical 172.5) respectively. That substitution of bromine in the acid was not the cause of the present author's lower result was carefully ascertained by running a separate test wherein this possibility was reduced to a minimum, by keeping the time of contact between bromine and acid down to five minutes and the temperature from $-10°$ C. at the beginning to $-2°$ C. at the end. The resulting crude material was identical in melting point with that of other batches.

The Iodine Value

The iodine value obtained is somewhat lower than the theoretical, but the author feels that this is no indication of impurity since the values agree very closely with those of Rollett (17) and van der Veen (25). This finds support in the work of Waterman and co-workers (26), and, more recently, in that by de Kok, Waterman and Westen (10), who indicate that the iodine value is always lower than the theoretical unsaturation as measured by the hydrogen absorption.

Isomerism

As regards the isomerism in the bromo compounds, the author presents a few deductions on the mechanism of the change which have been brought to a focus partly through the work described in the present paper, and partly through the accumulated data in the literature.

Granted that isomerization does occur, we may conclude that it does so either in the bromination, in the debromination, or in both.

If isomerization occurs during the debromination process only, we would have to conclude that two naturally occurring linoleic acids exist in various oils as 1 : 1 mixtures. The prepared linoleic acids from the tetrabromides would also then be 1 : 1 mixtures. In view of the uniformity in the boiling

points of various samples of the ethyl ester, the constant yield under varying conditions of bromination, and the fact that only one linoleamide is produced, it is difficult to believe that such a condition does exist.

If isomerization occurs both in the bromination and the debromination processes, then, in order that both acids derived from the solid and liquid bromo compounds be identical, it would follow again that both the natural and derived linoleic acids would be 1 : 1 mixtures of two isomers, and the same objections mentioned above would apply. It would also be necessary in the latter case to assume a very complicated system of conversion.

If isomerization occurred during the bromination process only, we would be forced to conclude that the debromination of each would produce different isomeric linoleic acids, a fact not substantiated by the present work, unless the isomerides occurred only in the bromo compounds and disappeared on their reduction. Now it is very difficult to conceive of a *cis-trans* isomerization that would fulfil this condition, and indeed there is considerable evidence to show that we are not here dealing with such a type. For example, Nicolet (13) has shown that when oleic and elaidic acids (known *cis-trans* modifications) are brominated and debrominated they regenerate their respective parent acids only. Bromination and debromination of these acids thus do not cause *cis-trans* isomerization. In addition, it has been shown by Hilditch and Green (6) that when oleic acid is oxidized with alkaline permanganate solution it yields an hydroxy acid of melting point 132° C., whereas if it is oxidized with hydrogen peroxide in acetic acid, it yields an acid of melting point 95° C. Elaidic acid, the *cis-trans* isomeride, however, yields with permanganate an acid that melts at 95° C., and with peroxide an acid that melts at 132° C. It may be concluded, then, that one of these reagents has caused a *cis-trans* isomerization. Now it is generally agreed (6, 11, p. 203; 22) that natural linoleic acid and the acid derived from the solid tetrabromostearic acid yield on mild oxidation with alkaline permanganate two sativic acids of melting points 173° and 155° C. If now these two acids are *cis-trans* modifications resolv-

TABLE IX
SOME HYDROXY ACIDS AND THEIR MELTING POINTS

Starting material	Melting points (°C.) of the hydroxy acids produced by	
	Alkaline KMnO₄	H₂O₂ in acetic acid
Oleic	132	95
Elaidic	95	132
Linoleic	155⎫ 173⎭	146⎫ 126⎭

able into each other, then it would be expected that the peroxide oxidations should yield two acids of similar melting points. This is not so, however, as is shown by Hilditch and Green (6). The product obtained is a mixture of two new sativic acids of melting points 146° and 126° C. (Table IX).

For the above reasons then we will abandon the idea that the transformation observed is of the *cis-trans* type. If now we examine the structure of linoleic
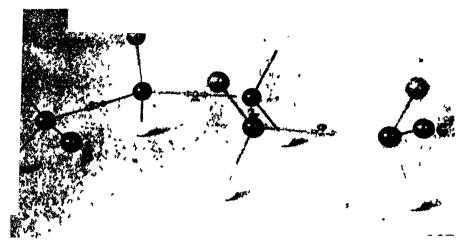
acid by means of a model, it will be seen that there is the possibility that the bromine may enter the compound in four different ways, forming two pairs of optically active compounds, which in no way interfere with the *cis-trans* arrangement chosen or the conception of free rotation in the bromo compounds.   If we conceive of the possibility of the bromine breaking the double bond either up or down, independently, we may obtain a rough picture of the thought in mind.   Smit (20) made a vague reference to such a conception when he drew attention to the fact that after one double bond is oxidized, isomerization may occur in the manner in which the second one is filled.   He did not however consider this from the viewpoint of transformation in the bromo or hydroxy compounds only, but rather in the light of a Walden inversion, which of course would imply isomerization of the reduced compounds as well.

The following formulas and figures partly illustrate this conception:

In the figures of the models, Figs. 4 and 5, the CH_3—$(CH_2)_4$— group is represented by a blue ball, marked B, and the

$$—(CH_2)_7 —C\diagup\!\!\!\diagdown\begin{matrix}O\\OH\end{matrix}$$

group by a green ball marked G.   In both models the double bond has been split and the bromine atoms (yellow) added on.   Fig. 4 illustrates (i) and (ii), where all the bromines lie on one side of the molecule; Fig. 5 illustrates (iii) and (iv).

It should be noted that in the preparation of the models a *cis-trans* form must be chosen and maintained.   The convention has been adopted that when the two bromines are removed and the bonds joined, two white balls or hydrogen atoms on the same side represent a `cis-form.   In the above case the models are of the *cis-cis* type.

Fig 4
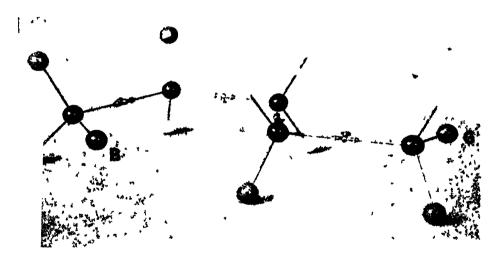
Fig 5

Possibly the liquid tetrabromide possesses the bromines in line as in the first pair of acids ((i) and (ii)), thus allowing a packing of the molecules in a polymerization and slow crystallization effect This would account for the wide differences in the physical properties of the solid and liquid compounds. Since debromination would regenerate the parent acid, it explains why both bromo compounds yield identical linoleic acids, and also offers an explanation for formation of equivalent amounts of the isomers in each case. It would then follow that only one natural linoleic acid exists which is identical with

that formed by the debromination of either tetrabromostearic acid. The terms α and β when applied to the solid and liquid tetrabromo compounds would still be valid, but meaningless when applied to the derived acids.

This conception would also allow of the formation of only one bromide of oleic acid and two of linoleic, a conception substantiated by experimental data. It would predict four from linolenic acid. Although four such isomers have not yet been isolated, it is significant that yields of only 23 to 24% of solid hexabromide have been obtained by the bromination of this acid (11, p. 211). Since derived products would have the same opportunity for isomerization, only one hydroxy derivative from oleic acid and two from linoleic would be expected. This is confirmed by the data. It would predict the existence of four hexahydroxystearic acids from linolenic, but this has not yet been confirmed.

In conclusion, the author wishes to acknowledge his indebtedness to the large amount of work done by others in this field, and hopes this paper may stimulate further interest in the subject. The problem as to whether linoleic acid is dimorphous, whether the solid tetrabromide is resolvable into a mixture of two optically active isomers, or whether four isomeric hydroxy acids may be derived from linolenic acid, should prove most interesting subjects for study.

Acknowledgments

References

1. AMERICAN OIL CHEMISTS' SOCIETY. Official and Tentative Methods. 1937.

2. ASCHAN, O. Ber. 31 : 2344-2350. 1898.

3. BROWN, J. B. Oil Colour Trades J. 90 : 1350. 1936.

4. BROWN, J. B. and STONER, G. G. J. Am. Chem. Soc. 59 : 3-6. 1937.

5. FINDLAY, A. Practical physical chemistry. 4th ed. Longmans, Green and Company. London. 1923.

6. HILDITCH, T. P. and GREEN, T. G. Biochem. J. 29 : 1552-1563. 1935.

7. HILDITCH, T. P. and VIDYARTHI, N. L. Proc. Roy. Soc. (London), 122, A : 563-570. 1929.

8. HOLDE, D. and GENTNER, R. Ber. 58, B : 1067-1071. 1925.

9. INOUE, Y. and SUZUKI, B. Proc. Imp. Acad. (Tokyo), 7 : 15-18. 1931.

10. KOK, W. J. C. DE, WATERMAN, H. I., and WESTEN, H. A. VAN. J. Soc. Chem. Ind. 55 : 225-228T. 1936.

11. LEWKOWITSCH, J. Chemical technology and analysis of oils, fats, and waxes. Vol. 1. 6th. ed. Macmillan and Company Ltd., London. 1921.

12. LOON, J. VAN. Chem. Umschau Fette, Öle, Wachse Harze, 38 : 279-281. 1931.

13. NICOLET, B. H. J. Am. Chem. Soc. 43 : 2122-2125. 1921.

14. NICOLET, B. H. and COX, H. L. J. Am. Chem. Soc. 44 : 144-152. 1922.

15. PALMER, L. S. and WRIGHT, P. A. Ind. Eng. Chem. 6 : 822-823. 1914.

16. RIEBSOMER, J. L. and NESTY, G. A. J. Am. Chem. Soc. 56 : 1784-1785. 1934.

17. ROLLETT, A. Z. physiol. Chem. 62 : 410-421. 1909.

18. SANTIAGO, S. and WEST, A. P. Philippine J. Sci. 32 : 41-52. 1927.

19. SCHIERHOLTZ, O. J. Ind. Eng. Chem. (Anal. Ed.) 7 : 284. 1935.

20. SMIT, W. C. Rec. trav. chim. 49 : 539-551. 1930.

21. SUZUKI, B. and INOUE, Y. Proc. Imp. Acad. (Tokyo), 6 : 266-268. 1930.

22. TAKAHASHI, K. J. Tokyo Chem. Soc. 40 : 233-289. 1919.

23. VEEN, H. VAN DER. Verfkroniek, 4 : 19-21. 1931.

24. VEEN, H. VAN DER. Chem. Umschau Fette, Öle, Wachse Harze, 38 : 117-120. 1931.

25. VEEN, H. VAN DER. Chem. Umschau Fette, Öle, Wachse Harze, 39 : 104-109. 1932.

26. WATERMAN, H. I., BERTRAM, S. H., and WESTEN, H. A. VAN. J. Soc. Chem. Ind. 48 : 50-51T. 1929.

THE KINETICS OF THE DECOMPOSITION REACTIONS OF THE LOWER PARAFFINS

I. n-BUTANE[1]

By E. W. R. STEACIE[2] AND I. E. PUDDINGTON[3]

Abstract

The kinetics of the thermal decomposition of n-butane has been investigated at pressures from 5 to 60 cm. and temperatures from 513 to 572° C. The initial first order rate constants at high pressures are given by

$$\log_{10} k = 12.71 - \frac{58700}{2.3RT} \text{ sec.}^{-1}.$$

The results are in good agreement with the work of Frey and Hepp, but differ greatly from that of Paul and Marek. The reaction rate falls off strongly with diminishing pressure; this is rather surprising for a molecule as complex as butane. The first order constants in a given run fall rapidly as the reaction progresses. The last two facts suggest that chain processes may be involved.

A large number of analyses of the products of reaction have been made at various pressures, temperatures, and stages of the reaction, the method being that of low-temperature fractional distillation. The products are virtually independent of temperature and pressure over the range investigated. The initial products, obtained by extrapolation to zero decomposition, are:—H_2, 2.9; CH_4, 33.9; C_3H_6, 33.9; C_2H_4, 15.2; C_2H_6, 14.1%. The mechanism of the reaction is discussed, and the results are compared with those of the other paraffin decompositions.

Introduction

In recent papers from this laboratory (38, 39, 42) dealing with the decomposition of the alkyl nitrites, it has been concluded that for a series of homologous compounds decomposing by identical mechanisms the activation energy should decrease only very slowly as the series is ascended. (Or, perhaps, remain constant if the compounds are sufficiently complex, as found by Coffin and his co-workers (3, 4, 25).)

From the point of view of the influence of chemical configuration on the reaction rate, the thermal decomposition reactions of the paraffin hydrocarbons offer unique and interesting possibilities. These reactions are also of interest by comparison with the mercury photosensitized decompositions (21, 24, 41, 43), and with the reactions of hydrogen atoms with the hydrocarbons (1, 15, 16, 34, 35, 40, 44).

The available information on the reactions of the lower paraffins has recently been reviewed by one of us (36). If the velocity constants of the decomposition reactions are expressed in the customary way by

$$k = Ae^{-E/RT},$$

we have the values of A and E given in Table I for the paraffins from methane to hexane.

It is obvious from the table that there is no agreement whatsoever among the results of different workers, and it therefore seemed worth while re-in-

vestigating some of the reactions accurately, with special emphasis on the determination of the temperature coefficient.   In considering the results given in Table I, we would naturally expect that even if the results of different workers are widely different, those obtained in the same laboratory should be at least roughly comparable.   From this point of view the wide difference between the results for normal and isobutane obtained by Paul and Marek is noteworthy, and it is a matter of considerable interest to determine whether or not this difference is fictitious.   It was therefore decided to re-investigate the butane decompositions first, and the present paper deals with that of n-butane.   .

TABLE I

SUMMARY OF THE RESULTS OF DIFFERENT OBSERVERS FOR THE KINETICS OF THE PARAFFIN DECOMPOSITIONS

Paraffin	Observer	$\log_{10} A$	E, Kcal.
CH_4	Kassel (20)	12.00	79.4
C_2H_6	Marek and McCluer (22)	15.12	73.2
	recalculated (26)	16.06	77.7
	Sachsse (32)	14.1	69.8
C_3H_8	Marek and McCluer (22)	13.44	62.1
	Paul and Marek (26)	16.60	74.9
n-C_4H_{10}	Frey and Hepp (14)	13.53	61.4
	Paul and Marek (26)	17.05	73.9
iso-C_4H_{10}	Paul and Marek (26)	14.89	66.0
n-C_5H_{12}	Frey and Hepp (14)	13.4	61.2
iso-C_5H_{12}	Frey and Hepp (14)	12.93	58.6
n-C_6H_{14}	Frey and Hepp (14)	12.43	55.5
	Dintzes et al. (8, 9)	14.58	64.5

The first investigations of this reaction were those of Pease (27) and of Pease and Durgan (28).   It was shown that the reaction was homogeneous, the products being almost entirely as represented by the three equations

$$(1)\quad C_4H_{10} = C_4H_8 + H_2$$
$$(2)\quad C_4H_{10} = C_3H_6 + CH_4$$
$$(3)\quad C_4H_{10} = C_2H_4 + C_2H_6 .$$

The rate of the reaction was only roughly measured.

Hurd and Spence (18) investigated the products of the reaction only, and concluded that Reactions (2) and (3) were the main processes.   Cambron (2) suggested that the reaction

$$C_4H_{10} = 2C_2H_4 + H_2$$

also occurs at high temperatures.

Reference has already been made to the kinetic results of Frey and Hepp. The main trouble with their work from a kinetic standpoint lies in the fact

that they worked at two temperatures only, and hence their value of the temperature coefficient is not as reliable as it might otherwise be.   Also, they did not study the effect of varying pressure on the rate to any great extent, and their results are not detailed enough to enable any decision to be made regarding the falling-off in rate at low pressures.   Frey and Hepp made very thorough analyses of the products of the reaction by low-temperature fractional distillation.   A typical analysis at 575° C. and 74.5 cm. pressure after 10% decomposition was: H_2, 5.0; CH_4, 32.1; C_2H_4, 16.3; C_2H_6, 13.2; C_3H_6, 31.1; C_3H_8, 2.2%.

Marek and Neuhaus (23) made analyses at various stages of the reaction, and concluded that the initial products were:—

	CH_4	C_3H_6	C_2H_6	C_2H_4	H_2	C_4H_8	C_3H_8
At 600° C.	24.3	24.3	17.3	17.3	8.0	8.0	0.0
At 650° C.	24.0	24.0	18.4	19.4	6.2	6.2	0.5(?)

Their values for hydrogen and butylene are thus considerably higher than those of Frey and Hepp and of Hurd and Spence.

The kinetic results of Paul and Marek have been summarized in Table I. Their work was done by a flow method, as was that of Frey and Hepp.   One source of uncertainty in their work was the temperature of the reaction vessel. They used a preheater to prevent excessive cooling of the reaction vessel by the flowing gases.   This was at too high a temperature, however, and in some cases 20% of the reaction occurred in the preheater.   They correct for this, but on account of the fact that their experiments are thus made with partially decomposed butane it is impossible to get initial rates from their work.   Their work, also, yields no information concerning the falling-off in rate at low pressures.

Some experiments on the rate of the reaction were also made by Witham (45), who also used a flow method.   His rates vary so much with contact time, that little information can be obtained from them.

Experimental

In the present investigation the static method was used, so as to enable accurate temperature control, and to permit the investigation of the effect of pressure on the rate of reaction.   A comparatively large reaction vessel was used, so that sufficient products were available to permit accurate analysis, and a large number of analyses were made.   In this way it was possible to combine the advantages of the static and flow methods.

The apparatus is shown diagrammatically in Fig. 1.   The reaction vessel was a transparent quartz flask of about 750 cc. capacity, and was connected through a graded seal to a capillary mercury manometer, and through a stopcock to a storage bulb, pumps, McLeod gauge, etc.   The manometer was wound with

nichrome wire and heated electrically to a temperature of 105° C. to prevent condensation of the decomposition products. The reaction vessel was heated in an electric furnace, the temperature of which could be controlled manually to within ± 1°. The maximum temperature gradient along the furnace was less than 1.5°. The temperature was measured by means of a chromel-alumel thermocouple in conjunction with a potentiometer. The thermo-couple was standardized at 0° C. and at the boiling point of sulphur.

An expansion bulb of two litres capacity connected in series with a trap was used to collect samples for analysis. The sample was obtained, after the reaction had proceeded to the desired extent, by opening a stopcock con-necting the reaction vessel with the expansion chamber for 10 sec. By cooling the trap with liquid air the pressure in the expansion chamber was kept low and most of the gas in the reaction vessel could be removed in a single expan-sion. There was no danger of fractionating the sample by this method, since the expansion occurred rapidly through narrow tubing. Where neces-sary, several runs were made under identical conditions and the products combined to give a sample large enough for accurate analysis (about 600 cc.).
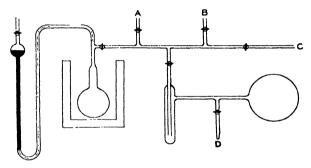
Fig. 1. *Apparatus. A, storage bulb; B, purification apparatus; C, pump; D, Toepler pump.*

The sample was transferred by means of a Toepler pump to a portable mercury gas-holder, and was then analyzed by low-temperature fractional distillation in an apparatus of the Podbielniak type. On samples of 600 cc. of gas an accuracy of about 0.2 to 0.3% could be obtained.

Prior to making a run the apparatus was evacuated to a pressure of 10^{-4} mm. Differences in ultimate pressure and in time of evacuation had no noticeable effect on the reaction rate.

C.p. butane, obtained in cylinders from the Ohio Chemical and Mfg. Co., was used. It was stated by the manufacturers to be at least 99% n-butane. The cylinder gas was fractionally distilled twice, the middle portion being retained each time. It was stored as a gas in a 10-litre flask connected to the apparatus.

The reaction was followed by observing the rate of change of pressure. Rates were measured at temperatures from 513° to 572° C., and at initial pressures from 5 to 60 cm. The products were examined over the same

temperature range at various initial pressures, and at various stages of the reaction, so as to permit an accurate interpretation of the results obtained by observing the pressure change.   The "initial products" were found by extrapolating to zero conversion in the usual way.   The time for a 12.5, 25, or 50% pressure increase was used as a measure of the rate of reaction.
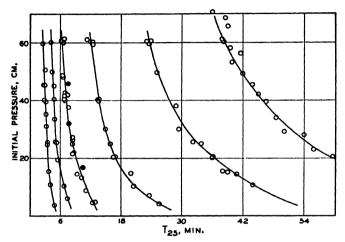
FIG. 2.   *Effect of pressure and temperature on the rate of reaction.   The curves from left to right represent respectively 572°, 562°, 552°, 538°, 522°, 513° C.   Black circles represent results of experiments made in a packed reaction vessel.*

The Rate of the Reaction   **Results**

The rates of the first few experiments made in the apparatus were somewhat erratic, but after about 10 runs the rate became completely reproducible. The results of the early runs were discarded.   On removing the reaction vessel at the end of the investigation it was found to be covered with a thin

TABLE II
DATA FOR A TYPICAL EXPERIMENT AT 552° C.
Initial pressure = 24.80 cm.

Time, min.	ΔP, cm.	k, sec.$^{-1}$	Time, min.	ΔP, cm.	k, sec.$^{-1}$
0	–	–	40	15.34	4.03×10^{-4}
1	1.10	7.48×10^{-4}	50	17.40	4.05
2	2.01	7.04	60	18.87	3.96
4	3.45	6.23	70	19.70	3.77
6	4.50	5.54	80	20.70	3.75
8	5.45	5.18	90	21.70	3.84
10	6.47	5.04	100	22.38	3.84
14	8.10	4.72	130	23.82	4.12
18	9.53	4.51	170	24.85	–
22	10.76	4.30	290	26.01	–
26	11.90	4.19	410	26.40	–
30	13.00	4.14	530	26.48	–

coherent layer of carbon. During the investigation a small quantity of tar-like polymer distilled from the reaction vessel into the connecting tubing. The quantity of such material formed, however, was insufficient to enable its identification. In any case, the amount of tar formed per run was too small to make any measurable difference in the gas analyses or in the pressure readings.

Several runs were carried to completion, the time required being about 14 hr. at 552° C. The pressure increase at completion was between 107 and 109%. As analysis showed that an increase in pressure of 25% corresponded exactly to 25% decomposition, it appears that secondary reactions account for the slight increase in pressure over the theoretical 100%.

TABLE III

THE VARIATION OF REACTION RATE WITH PRESSURE AND TEMPERATURE

Initial pressure, cm.	T_{25}, min.	Initial pressure, cm.	T_{25}, min.	Initial pressure, cm.	T_{25}, min.
Temperature, 513° C.					
10.80	75.0	38.90	46.2	58.50	39.5
15.10	64.5	39.80	46.5	60.10	38.1
20.15	59.5	42.16	45.0	61 20	38.0
22.30	56.0	45.40	43.2	65.45	39.0
27.90	54.0	49.30	42.0	68.80	38.7
29.30	50.4	53.35	39.8	70.60	36.0
34.20	48.5	56.50	41.7		
Temperature, 522° C.					
5.75	54.0	20.15	36.0	38.40	28.2
10.70	44.0	20.40	36.0	49.40	25.2
14.75	41.0	24.95	34.2	59.50	23.6
15.20	39.0	25.38	32.2	60.40	23.2
15.45	38.0	30.20	29.5	60.60	23 9
Temperature, 538° C.					
4.25	25.5	20.60	16.5	40.70	13.5
7.08	23.7	25.00	16.0	59.50	12.5
10.31	20.5	29.95	15.0	60.20	12.0
14.80	19.0	40.00	13.6	60.20	12.5
20.25⁻	16.8	40.10	13.6	61.20	11.2
Temperature, 562° C.					
6.00	7.5	25.60	5.3	45.20	4.7
10.20	6.7	30.30	5.1	49.50	4.5
19.45	5.5	33.70	4.7	60.10	4.2
25 45	5.6	40.60	4.6		
Temperature, 572° C.					
4.65	4.7	31.10	3.4	45.40	3.0
10.90	4.2	35.00	3.1	45.40	2.7
15.40	3.8	39.50	3.1	50.20	3.0
25.38	3.6	39.80	2.9	59.50	2.5
25.20	3.5				

<div align="center">

TABLE III—*Concluded*

THE VARIATION OF REACTION RATE WITH PRESSURE AND TEMPERATURE

</div>

Initial pressure, cm.	T_{25}, min.	T_{50}, min.	Initial pressure, cm.	T_{25}, min.	T_{50}, min.
Temperature, 552° C.					
4.15	12.4	40.0	40.20	7.1	21.0
4.90	13.0	39.0	40.60	6.8	20.2
8.90	11.0	33.2	41.10	7.0	21.0
13.60	10.0	29.3	41.60	7.2	21.6
21.75	8.8	25.5	42.50	7.0	21.1
22.20	8.6	26.0	47.90	6.6	19.7
25.10	8.3	24.6	48.60	6.4	19.3
26.60	8.4	26.0	59.80	6.5	19.2
27.00	8.5	25.5	60.00	6.4	17.7
32.40	7.7	23.2	61.30	6.7	18.3
37.30	7.7	22.2			
Temperature, 552° C.—Packed reaction vessel					
14.88	10.0	28.5	45.65	7.7	20.0
30.25	7.8	33.3			

Data for a typical run at 552° C. are given in Table II. The unimolecular constants in the table are calculated on the assumption that 100% pressure increase corresponds to completion. For the early stages of the reaction it would make little difference if the constants were calculated on the assumption of 108% pressure increase at completion. Justification for the use of the pressure change as a measure of the extent to which the reaction has progressed will be given in a later section.

Table III shows the effect of temperature and of initial pressure on the rate of reaction. In the table T_{25} denotes the time for a 25% increase in pressure, and T_{50} that for a 50% increase in pressure. It will be shown later that these correspond to 24.9 and 46.3% decomposition respectively.

It will be seen from the data of Table III that the rate, as inferred from T_{25} or T_{50}, falls off with diminishing pressure. In order to get high-pressure rates, $T_{12.5}$, T_{25}, or T_{50} was plotted against the reciprocal of the pressure and extrapolated to infinite pressure, as shown in Fig. 3. The values of the infinite pressure rate constants given in Table IV were thus obtained.

In Table IV in addition to the values of the high-pressure rate constants the limiting ratios of T_{25} to $T_{12.5}$, and of T_{50} to T_{25} have been tabulated. It will be shown later that $T_{12.5}$, T_{25}, and T_{50} correspond to 12.5, 24.9, and 46.3% reaction respectively. Whence it follows that the theoretical values of the two ratios are both 2.16 for a first order reaction. These are much lower than the experimental values.

The fact that the theoretical values of these ratios do not hold is in accord with the results of Table II, which show that the first order constants in an individual run fall off strongly as the reaction progresses. Similar behavior

has been noted by Dintzes and co-workers (5, 6, 7) in the decompositions of ethane and propane, and this is undoubtedly due to the existence of secondary changes of some kind.

TABLE IV

LIMITING HIGH PRESSURE RATE CONSTANTS

Temper- ature, °C.	$T_{12.5}$, sec.	T_{25}, sec.	T_{50}, sec.	$\dfrac{T_{25}}{T_{12.5}}$	$\dfrac{T_{50}}{T_{25}}$	$k_\infty \times 10^4$, sec.$^{-1}$, calculated from T_{25}
513	573	1788	–	3.12	–	1.61
522	339	1092	–	3.22	–	2.64
538	198	600	–	3.30	–	4.69
552	101	342	840	3.39	2.46	8.41
562	69.6	216	504	3.11	2.33	13.3
572	–	120	297	–	2.47	24.0
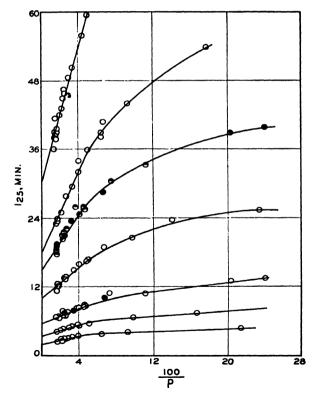
FIG. 3. *Extrapolation of rates to infinite pressure. From top to bottom the curves represent successively: T_{25} at 513° C., open circles; T_{25} at 522° C., open circles; T_{50} at 552° C., half-black circles; T_{25} at 538° C., open circles; T_{25} at 552° C., open circles; T_{25} at 562° C., open circles; T_{25} at 572° C., open circles. Full black circles represent results of experiments made in a packed reaction vessel.*

This divergence of the constants from the theoretical behavior raises the question of the validity of using $T_{12.5}$ or T_{25} as a measure of the rate of reaction, since the calculated velocity constant will depend on the extent to which the reaction has progressed. From the point of view of the determination of the activation energy of the reaction, the important point is whether or not the reaction rate curves have identical forms at different temperatures. If they do, then the relative values of the velocity constants at different temperatures inferred from the time to any given fractional amount of reaction will be in the same ratio, and the calculated value of the activation energy will not be affected by the drift of the first order rate constants. The simplest way of checking the form of the reaction rate curves is to compare values of the ratios $T_{25}/T_{12.5}$ and T_{50}/T_{25} at various temperatures and pressures. If these ratios remain constant there is no doubt that the curves are affine.
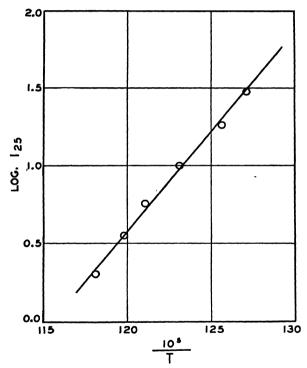
FIG. 4.   *The effect of temperature on the rate of reaction.*

Table V gives data of this sort for typical runs. It is obvious from Tables IV and V that there is no significant change in the values of the ratios with changing temperature at any given pressure, including the extrapolated values at infinite pressure. We may therefore use the values given in Table IV to calculate the activation energy of the reaction, and this has been done graphically in Fig. 4. From the slope of the line a value of 58,700 cal. per mole is obtained for the energy of activation. From this value we obtain for

TABLE V

VALUES OF T_{50}/T_{25} AND $T_{25}/T_{12.5}$ AT VARIOUS TEMPERATURES AND PRESSURES

Temperature, °C.	$T_{12.5}$, sec.	T_{25}, sec.	T_{50}, sec.	$\dfrac{T_{25}}{T_{12.5}}$	$\dfrac{T_{50}}{T_{25}}$
Initial pressure, 50 cm.					
513	894	2544	–	2.84	–
522	534	1512	–	2.83	–
538	269	762	–	2.83	–
552	145	420	1182	2.90	2.82
562	94.8	270	738	2.85	2.73
572	–	169	486	–	2.87
Initial pressure, 33.3 cm.					
513	1056	2922	–	2.78	–
522	630	1716	–	2.72	–
538	305	840	–	2.75	–
552	167	456	1356	2.73	2.97
562	107	295	858	2.76	2.91
572	–	192	582	–	3.02
Initial pressure, 25 cm.					
513	–	–	–	–	–
522	729	1920	–	2.63	–
538	339	924	–	2.72	–
552	189	493	1524	2.61	3.08
562	117	324	972	2.76	3.01
572	–	216	675	–	3.13

the high pressure rate of reaction as a function of temperature the equation

$$\log_{10} k = 12.54 - \frac{58700}{2.3RT} \text{ sec.}^{-1} .$$

High pressure rates obtained from values of T_{50} or $T_{12.5}$ give identical values of the activation energy, thereby justifying the use of times to fractional amounts of reaction as a measure of the rate.

As pointed out above, the velocity constants fall off in an individual run as the reaction progresses. The true rate of reaction is, of course, the initial rate and not that obtained at a later stage. Extrapolation of the results to obtain initial rates is not easy, but the indications from a large number of runs are that the initial velocity constants are almost exactly 50% higher than those calculated at 25% completion. Hence for the *initial* high pressure rate we have

$$\log_{10} k = 12.71 - \frac{58700}{2.3RT} \text{ sec.}^{-1}$$

The full circles in Fig. 3 represent runs made in a reaction bulb packed with broken silica tubing, the surface-volume ratio of which was approximately 15 times greater than that of the empty vessel. These experiments prove that the reaction is not appreciably heterogeneous.

The Products of the Reaction

Analyses of the products of the reaction were made by low-temperature fractional distillation on samples removed at $T_{12.5}$, T_{25}, and T_{50} at initial pressures from 20 to 60 cm., over the whole temperature range. Analyses from runs at lower initial pressures were not feasible on account of the small amount of products available. The results of the analyses are given in Tables VI and VII.

TABLE VI

THE PRODUCTS OF THE REACTION AT VARIOUS TEMPERATURES AND AN INITIAL PRESSURE OF 60 CM.

Temperature, °C.	513	522	538	552	562	572	Mean
			Products, mole per cent				
Sample withdrawn at T_{50}							
H_2	2.0	2.8	1.5	1.8	0.5	1.7	1.7
CH_4	39.1	38.2	38.7	40.0	40.5	38.9	39.2
C_2H_4	15.1	15.9	15.8	16.0	15.8	16.2	15.8
C_2H_6	14.1	14.2	14.2	12.6	13.5	12.6	13.5
C_3H_6	29.8	28.8	29.5	29.6	29.7	30.2	29.6
% C_4H_{10} decomposed	45.0	45.2	45.4	50.2	45.7	46.0	46.3
Sample withdrawn at T_{25}							
H_2	0.0	2.0	1.2	0.5	2.0	—	1.1
CH_4	36.0	36.2	36.0	39.0	35.5	—	36.5
C_2H_4	16.1	15.8	15.9	15.8	16.3	—	16.0
C_2H_6	13.9	12.0	13.3	12.6	13.7	—	13.1
C_3H_6	33.9	34.0	33.5	32.2	32.9	—	33.3
% C_4H_{10} decomposed	23.1	24.6	24.7	26.2	25.8	—	24.9
Sample withdrawn at $T_{12.5}$							
H_2	2.1	1.5	0.8	2.5	—	—	1.7
CH_4	33.5	36.0	37.4	34.7	—	—	35.4
C_2H_4	15.0	14.9	15.4	15.7	—	—	15.2
C_2H_6	14.7	14.6	13.8	13.5	—	—	14.2
C_3H_6	34.7	33.0	32.5	33.6	—	—	33.5
% C_4H_{10} decomposed	11.4	12.7	13.5	12.7	—	—	12.6

It follows from Table VI that T_{50}, T_{25}, and $T_{12.5}$, as measured by the pressure change, really correspond to 46.5, 24.9, and 12.6% decomposition respectively.

In the analyses reported above, hydrogen and methane were distilled off together, and this fraction was analyzed for the separate constituents by combustion. Butene has frequently been reported as a product of the decomposition. With small samples it is difficult to detect since its boiling point is close to that of butane, which is of course present in large quantity. In a number of cases attempts were made to determine butene by analyzing the butane-butene fraction from a distillation for unsaturates, by use of

fuming sulphuric acid as the absorbent in a Burrell gas analysis apparatus. The method is complicated to some extent by the fact that some butane is absorbed by the reagent, and blank runs had to be made to correct for this. The results indicated that if any butene were present its amount was not more than 1%, and even this small amount may have been partly due to propylene which had not been perfectly cut from butane. It may therefore be concluded that no significant amount of butene is present, and it has not been reported in the tables.

It follows from Table VII that there is no noticeable variation of products with changes in initial pressure over the range from 20 to 60 cm. Owing to the difficulty in obtaining a sample sufficiently large for analysis, no attempt was made to determine the products of runs made at lower initial pressures.

Table VI shows that over the range used there is little variation in the products of reaction with temperature. In view of this, mean values of products at T_{50}, T_{25}, and $T_{12.5}$ have been used in extrapolating to zero conversion to get the initial products. Fig. 5 shows the result of this extrapolation. If we assume the difference between the percentages of methane and propylene to be due to hydrogen, the following percentages are obtained for the initial products: H_2, 2.9; CH_4,

TABLE VII

THE PRODUCTS OF THE REACTION AT VARIOUS INITIAL PRESSURES

Initial pressure, cm.	60	40	20
Products, mole per cent			
552° C. Sample withdrawn at T_{50}			
H_2	1.8	1.5	2.4
CH_4	40.0	38.6	39.1
C_2H_4	16.0	17.8	17.0
C_2H_6	12.6	12.8	12.8
C_3H_6	29.6	29.2	28.8
% C_4H_{10} decomposed	50.2	46.4	47.0
552° C. Sample withdrawn at T_{25}			
H_2	0.5	2.4	0.9
CH_4	39.0	36.0	36.5
C_2H_4	15.8	18.4	16.4
C_2H_6	12.6	11.7	13.8
C_3H_6	32.2	31.6	32.2
% C_4H_{10} decomposed	26.2	26.3	24.1
552° C. Sample withdrawn at $T_{12.5}$			
H_2	2.5	1.4	—
CH_4	34.7	36.6	—
C_2H_4	15.7	15.0	—
C_2H_6	13.5	13.7	—
C_3H_6	33.6	33.4	—
% C_4H_{10} decomposed	12.7	13.6	—
538° C. Sample withdrawn at T_{25}			
H_2	1.2	0.3	—
CH_4	36.0	36.5	—
C_2H_4	15.9	16.1	—
C_2H_6	13.3	13.3	—
C_3H_6	33.5	33.2	—
% C_4H_{10} decomposed	24.7	24.5	—

33.9; C_3H_6, 33.9; C_2H_4, 15.2; C_2H_6, 14.1. The fact that the quantity of ethylene is greater than that of ethane may be due to the occurrence to a small extent of the reaction postulated by Cambron

$$C_4H_{10} = 2C_2H_4 + H_2 ,$$

or perhaps more likely to a small amount of secondary dehydrogenation of ethane,

$$C_2H_6 = C_2H_4 + H_2 .$$

The hydrogen-carbon ratio calculated from the mean values of the products in Table VI has the values 2.59, 2.52, and 2.52 at T_{50}, T_{25}, and $T_{12.5}$ respectively. This is in satisfactory agreement with the theoretical value of 2.50, and indicates that no appreciable quantity of tar or higher polymers can have been formed during the early stages of the reaction. The hydrogen-carbon ratio for the initial products, as obtained by extrapolation, is 2.52.
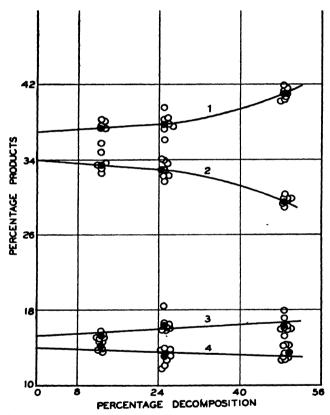
FIG. 5. *Extrapolation to determine initial products of the reaction. Curve 1 represents* $CH_4 + H_2$; *Curve 2,* C_2H_6; *Curve 3,* C_2H_4; *Curve 4,* C_3H_6. *Open circles represent actual analyses; black circles represent mean values.*

Discussion

The Products of the Reaction

The products obtained by previous workers have been discussed in the Introduction. The products reported above show excellent general agreement with the work of Hurd and Spence (18) and of Frey and Hepp (14). The agreement with the work of Marek and Neuhaus (23) is not good. Thus for the ratio $(CH_4 + C_3H_6)/(C_2H_4 + C_2H_6)$ our work indicates a value of about

2.3 for the initial products at temperatures up to 572° C., in agreement with Frey and Hepp's value at 575° C. and 10% decomposition of 2.15. Marek and Neuhaus from the initial products at 600° C., however, obtain a value of 1.4, and the discrepancy cannot be attributed to the difference in temperature, since all observers agree that temperature has little effect on the products in this range.

Our results are in qualitative agreement with Rice's suggested free radical mechanism (31), inasmuch as the only important products are CH_4, C_3H_6, C_2H_4, and C_2H_6. However, the Rice mechanism indicates a value for the above ratio of 1.33, which is very different from that found. Actually, however, this ratio, on the Rice mechanism, is entirely dependent on purely arbitrary assumptions regarding the relative reactivity of primary and secondary hydrogen atoms, and it would not be difficult to devise a free radical mechanism which would agree with the products found.

The Rate of the Reaction

If we compare the values of E, A, and of the velocity constant at, say, 575° C. with those of other workers, we obtain, using the initial rates from our work,

	E, Kcal.	$\log_{10} A$	k_{575}, sec.$^{-1}$
Frey and Hepp	61.4	13.53	4.8×10^{-3}
Paul and Marek	73.9	17.05	9.8×10^{-3}
Steacie and Puddington	58.7	12.71	3.7×10^{-3}

In view of the limited number of experiments made by Frey and Hepp, the agreement of their work with ours is entirely satisfactory. There is, however, a very large discrepancy between these results and those of Paul and Marek, amounting to 15 Kcal. in E and over 10,000 in A.

One cause of uncertainty in previous work has been the use of k's determined at atmospheric pressure in determining E, instead of the use of high pressure k's. The falling-off in rate with pressure varies with temperature, and hence activation energies determined from observed velocities at lower pressures will be too high. Thus from our results we get

True E	58.7 Kcal.
E from P = 76 cm.	66.2
E from P = 50 cm.	66.4
E from P = 33 cm. =	66.7
E from P = 25 cm. =	67.0.

In other words the activation energy determined from experiments at atmospheric pressure is about 7.5 Kcal. too high. The results of Paul and Marek and of Frey and Hepp were obtained at atmospheric pressure, and should therefore be too high by approximately the same amount. If we arbitrarily correct them, we obtain

Frey and Hepp	54.5 Kcal.
Paul and Marek	67.0
Present work	58.7.

This gives somewhat better agreement, although the results of Paul and Marek are still definitely far too high by comparison.

In Table I we have given a summary of kinetic data for the paraffin decompositions. In view of the present work it appears probable that the results of Marek and his co-workers may be too high in all cases, and that those of Frey and Hepp are to be preferred when available. On this basis it may be tentatively suggested that the best values of the activation energies of the paraffin decompositions are not far from: CH_4, 79; C_2H_6, 70; C_3H_8, 62; n-C_4H_{10}, 59; n-C_5H_{12}, 56; n-C_6H_{14}, 55 Kcal. In other words, it is probable that there is a steady decrease in the activation energy as we ascend the series, leading to a limiting value for the higher members of about 55 Kcal.

As pointed out above, the products of the reaction do not vary significantly within the temperature range investigated. The activation energies of the separate decompositions

$$C_4H_{10} \; = \; CH_4 + C_3H_6 \tag{1}$$

and

$$C_4H_{10} \; = \; C_2H_4 + C_2H_6 \tag{2}$$

therefore appear to be identical and equal to the observed value for the over-all reaction of 58.7 Kcal. We may also apportion the velocity constants between the separate reactions and write for the initial high pressure rates:

$$\log_{10} k_1 \; = \; 12.55 - \frac{58700}{2.3RT} \; \text{sec.}^{-1}$$

$$\log_{10} k_2 \; = \; 12.19 - \frac{58700}{2.3RT} \; \text{sec.}^{-1}.$$

Free Radicals in the Butane Decomposition

It has been shown by Rice, Johnston, and Evering (30) that free radicals can be detected in the high temperature decomposition of n-butane, and Rice and Johnston (29) have found the activation energy of the free radical split to be 65.4 Kcal. Rice has suggested (31) that the ordinary thermal decomposition at lower temperatures occurs by a free radical chain mechanism. As we have shown above, the Rice scheme leads to the correct products of the reaction, although the relative amounts of the various products are not in good agreement with his predictions.

The kinetic consequences of such free radical chain mechanisms have been found to be in general disagreement with experiment for ethane and propane (see (36) for a full discussion). In the case of butane, however, there is a great deal of evidence to show that radicals are involved in the thermal decomposition, at least to some extent. Thus by various methods Heckert and Mack (17), Frey (13), Echols and Pease (10, 11), Sickman and Rice (33), and Steacie and Folkins (37) have shown that chain decomposition of n-butane can be initiated by radicals, or that chains occur in the ordinary thermal decomposition to some extent. The present investigation has shown that the activation energy of the decomposition is 58.7 Kcal., which is very little

below Rice and Johnston's estimate of 65.4 Kcal. for the split into radicals. In other words, if we assume a chain mechanism, the over-all activation energy is only slightly lower than the activation energy for the primary step, and it appears therefore that in this case it is possible that the primary step is a split into radicals, followed by the setting up of quite short chains. Similar considerations would apply to all the higher hydrocarbons, since it seems probable that the thermal and free radical activation energies are converging to the same value for the higher paraffins. However, it remains for further work to decide the question.

The Effect of Pressure on the Rate of Reaction

It will be seen from the data of Table III and Figs. 2 and 3 that the rate of reaction falls off with diminishing pressure at quite high pressures. The Kassel equation for the effect of pressure on the rate is (19)

$$k/k_\infty = \left(1 - e^{-\frac{h\nu}{kT}}\right)^s \sum_{j=m}^{\infty} \frac{\left(\begin{array}{c} j - m + s - 1 \\ j - m \end{array}\right) e^{-(j-m)h\nu/kT}}{1 + \dfrac{A(j - m + s - 1)! \, j!}{aN(j - m)! \, (s - 1)!}}$$

where N is the number of molecules per cubic centimetre, a is a collision factor which involves the molecular diameter σ, s is the number of oscillators in the molecule ($(3n - 6)$, where n is the number of atoms) less the number of C—H bonds, since the C—H valence vibrations are not likely to be thermally excited at the temperature in question, j is the number of vibrational quanta possessed by the molecule, m is the number of quanta which must be localized in the pertinent bond in order that reaction may occur, and ν is the frequency of the oscillators, all of which are for simplicity assumed to be identical. If we apply the equation, putting

$$s = 26$$
$$\sigma = 4 \times 10^{-8} \text{ cm.}$$
$$N_0 m h\nu = 58.7 \text{ Kcal. } (N_0 = \text{Avogadro's number}),$$

we find that for all values of ν from 200 to 3000 cm.$^{-1}$ no falling off in rate is predicted until pressures below 1 mm. are reached. If we assume that half the molecule is "frozen" from the point of view of the reaction, and put

$$s = 6$$
$$\sigma = 4 \times 10^{-8} \text{ cm.}$$
$$m = 18$$
$$\nu = 1141 \text{ cm.}^{-1},$$

we get perfect agreement with experiment, as shown by Fig. 6, in which the line represents the theoretical curve and the circles the experimental points at 552° C. Such a freezing-out of part of the molecule is, perhaps, plausible in the case of a molecule such as diethyl ether where there is an atom in the centre which differs from those at the ends, and which might make energy transfer difficult owing to the difference in the frequency of the valence

vibrations.   It seems, however, very unlikely that such an explanation could be valid in the case of a molecule like butane which contains nothing but C—H and C—C bonds.   It is therefore much more likely that this surprisingly great falling-off in rate for a molecule as complex as butane is to be ascribed to chain processes.   It should also be pointed out that the variation in the drift of the unimolecular constants with pressure, as shown by Table V, although small, may be a complicating factor.   It is hoped that further work will throw some light on this point.
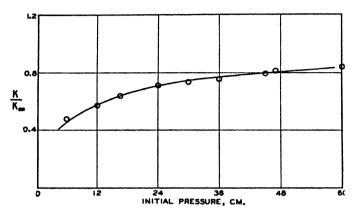
FIG. 6.   *The falling-off in rate with diminishing pressure.   Circles represent typical experimental results at 552° C.   The curve is theoretical, using, $s = 6$, $\sigma = 4 \times 10^{-8}$ cm., $m = 18$, $v = 1141$ cm.$^{-1}$.*

An investigation of the decomposition of isobutane and of normal pentane is in progress.   It is planned to extend the work in the future to propane and other hydrocarbons, and it is hoped that eventually sufficient accurate data will be available to enable a more extended discussion of the influence of chemical configuration on the reaction rate.

References

1. BONHOEFFER, K. F. and HARTECK, P.   Z. physik. Chem. 139 : 64-74.   1928.
2. CAMBRON, A.   Can. J. Research, 7 : 646-661.   1932.
3. COFFIN, C. C., DACEY, J. R. and PARLEE, N. A. D.   Can. J. Research, B, 15 : 247-253.   1937.
4. DACEY, J. R. and COFFIN, C. C.   Can. J. Research, B, 15 : 260-263.   1937.
5. DINTZES, A. I. and FROST, A. V.   J. Gen. Chem. U.S.S.R. 3 : 747-758.   1933.
6. DINTZES, A. I. and FROST, A. V.   Compt. rend. acad. sci. U.R.S.S. 4 : 153-157.   1933.
7. DINTZES, A. I. and FROST, A. V.   Compt rend. acad. sci. U.R.S.S. 5 : 513.   1934.
8. DINTZES, A. I. and FROST, A. V.   J. Gen. Chem. U.S.S.R. 4 : 610-615.   1934.
9. DINTZES, A. I. and ZHERKO, A. V.   J. Gen. Chem. U.S.S.R. 6 : 68-74.   1936.
10. ECHOLS, L. S. and PEASE, R. N.   J. Am. Chem. Soc. 58 : 1317.   1936.
11. ECHOLS, L. S. and PEASE, R. N.   J. Am. Chem. Soc. 59 : 766-767.   1937.
12. EGLOFF, G.   Reactions of the pure hydrocarbons.   Reinhold Publishing Co.   New York.   1937.
13. FREY, F. E.   Ind. Eng. Chem. 26 : 198-203.   1934.
14. FREY, F. E. and HEPP, H. J.   Ind. Eng. Chem. 25 : 441-449.   1933.

15. GEIB, K. H. and HARTECK, P.   Z. physik. Chem. A, 170 : 1-19.   1934.
16. GEIB, K. H. and STEACIE, E. W. R.   Z. physik. Chem. B, 29 : 215-224.   1935.
17. HECKERT, W. W. and MACK, E.   J. Am. Chem. Soc. 51 : 2706-2717.   1929.
18. HURD, C. D. and SPENCE, L. U.   J. Am. Chem. Soc. 51 : 3353-3362.   1929.
19. KASSEL, L. S.   Kinetics of homogeneous gas reactions.   Chemical Catalog Co., New York.   1932.
20. KASSEL, L. S.   J. Am. Chem. Soc. 54 : 3949-3961.   1932.
21. KEMULA, W., MRAZEK, S. and TOLLOCZKO, S.   Collection Czechoslov. Chem. Communications, 5 : 263-278.   1933.
22. MAREK, L. F. and McCLUER, W. B.   Ind. Eng. Chem. 23 : 878-881.   1931.
23. MAREK, L. F. and NEUHAUS, M.   Ind. Eng. Chem. 24 : 400-402.   1932.
24. MORIKAWA, K., BENEDICT, W. S. and TAYLOR, H. S.   J. Chem. Physics, 5 : 212-225.   1937.
25. PARLEE, N. A. D., DACEY, J. R. and COFFIN, C. C.   Can. J. Research, B, 15 : 254-259.   1937.
26. PAUL, R. E. and MAREK, L. F.   Ind. Eng. Chem. 26 : 454-457.   1934.
27. PEASE, R. N.   J. Am. Chem. Soc. 50 : 1779-1785.   1928.
28. PEASE, R. N. and DURGAN, E. S.   J. Am. Chem. Soc. 52 : 1262-1267.   1930.
29. RICE, F. O. and JOHNSTON, W. R.   J. Am. Chem. Soc. 56 : 214-219.   1934.
30. RICE, F. O., JOHNSTON, W. R. and EVERING, B. L.   J. Am. Chem. Soc. 54 : 3529-3543.   1932.
31. RICE, F. O. and RICE, K. K.   The aliphatic free radicals.   Johns Hopkins Press, Baltimore.   1935.
32. SACHSSE, H.   Z. physik. Chem. B, 31 : 87-104.   1935.
33. SICKMAN, D. V. and RICE, O. K.   J. Chem. Physics, 4 : 608-613.   1936.
34. STEACIE, E. W. R.   Can. J. Research, B, 15 : 264-273.   1937.
35. STEACIE, E. W. R.   J. Chem Physics, 6 : 37-40.   1938.
36. STEACIE, E. W. R.   Chem. Revs.   April, 1938.
37. STEACIE, E. W. R. and FOLKINS, H. O.   Unpublished work.
38. STEACIE, E. W. R. and KATZ, S.   J. Chem. Physics, 5 : 125-130.   1937.
39. STEACIE, E. W. R., KATZ, S., ROSENBERG, S. L. and SMITH, W. McF.   Can. J. Research, B, 14 : 268-274.   1936.
40. STEACIE, E. W. R. and PHILLIPS, N. W. F.   J. Chem. Physics, 4 : 461-468.   1936.
41. STEACIE, E. W. R. and PHILLIPS, N. W. F.   J. Chem. Physics, 6 : 179-187.   1938.
42. STEACIE, E. W. R. and SMITH, W. McF.   J. Chem. Physics, 4 : 504-507.   1936.
43. TAYLOR, H. S. and HILL, D. G.   J. Am. Chem. Soc. 51 : 2922-2936.   1929.
44. TRENNER, N. R., MORIKAWA, K. and TAYLOR, H. S.   J. Chem. Physics, 5 : 203-211.   1937.
45. WITHAM, W. C.   Ph.D. Thesis, Columbia University, 1934.   Quoted from Egloff (12).

THE HEATS OF ADSORPTION OF ALKALIS BY STANDARD CELLULOSE[1]

By J. L. MORRISON[2], W. BOYD CAMPBELL[3], AND O. MAASS[4]

Abstract

The heats of adsorption of aqueous sodium, potassium, and lithium hydroxides, and some salt solutions by cotton cellulose have been measured. The adsorption of alkali by cellulose seems to be ionic rather than molecular; more particularly, it appears to be closely related to the availability of the H^+ ion from the very weakly acidic cellulose, and of the OH^- ion from the electrolyte.

The nature of the adsorption of alkalis by cellulose has been the subject of considerable speculation. Fresh interest in this subject has been revived by a paper by Bancroft and Calkin (2), in which the authors report the results of measurements of a so-called true adsorption of sodium hydroxide on cellulose.

Generally two distinct methods have been used to measure the amount of adsorption, a change-in-titre method (9, 11, 15, 16, 17), and a centrifuge method (2, 6, 12). The results obtained by investigators using different methods, or even the same method, vary widely. As a consequence, different investigators are at variance regarding the theoretical deductions as to the adsorption mechanism concerned. Heuser and Bartunek (9) imply a molecular compound formation between the alkali and the cellulose molecules in proportions such as $(C_6H_{10}O_5)_2LiOH$, $(C_6H_{10}O_5)_2NaOH$. On the other hand, Bancroft and Calkin are of the opinion that a simple "adsorption" takes place. Neale (14), from considerations of measurements of heats of adsorption, postulates the formation of a hydrolyzable sodium cellulosate.

It was thought that further and more accurate measurements of the heats of adsorption of alkalis by cellulose might yield additional information in regard to the adsorption mechanisms involved. So far the only measurements of this type recorded in the literature are those of Barratt and Lewis (3), Neale (14), and Chilikin (5), who used sodium hydroxide. The present investigation includes the study of the adsorption by standard cellulose of sodium hydroxide, as well as of lithium and potassium hydroxides, and some salt solutions.

Experimental Technique

A description of the apparatus (a rotating adiabatic calorimeter) and the procedure has been given in a previous paper (13). All samples were taken from one lot of cellulose. The alkali solutions were made up to the desired strength and analyzed before being transferred by means of a weight pipette to the calorimeter, care being taken to prevent access of carbon dioxide. The sodium and lithium hydroxides were free from carbonate. The potassium hydroxide contained 2% of potassium carbonate. Measurements were also made with potassium carbonate, sodium chloride, and sodium-chloride–sodium-hydroxide solutions. All chemicals employed were of c.p. quality.

Results

The heats of adsorption of solutions of lithium, sodium, and potassium hydroxides, by standard cellulose, were determined. The data are presented in Table I and are plotted in Figs. 1 and 3. The best obtainable specific heat data (4, 8) were used to calculate the results, and the corrections for heat of vaporization were made from vapor pressure data (10, pp. 370 and 373).

The heats of adsorption of a sodium chloride and two potassium carbonate solutions by the standard cellulose were measured. A similar determination was made with a sodium-chloride–sodium-hydroxide solution prepared from the above-mentioned sodium chloride solution to which was added sodium hydroxide to the extent of 2.81% of the total solution. The values obtained for these miscellaneous determinations are given in Table II.

TABLE I

HEATS OF ADSORPTION OF ALKALIS BY STANDARD CELLULOSE AT 25° C.

Alkali	Concentration, weight %	Individual determinations, calories per gram dry cellulose				Mean, cal. per gm.
LiOH	2.66		12.38		12.50	12.44
	5.48		14.30		14.22	14.26
NaOH	0.95	11.49	11.17	11.18	11.47	11.30
	1.89	11.84	11.86	11.74	11.79	11.81
	4.28		12.55	12.55	12.66	12.58
	5.40			13.24	13.29	13.27
	6.55		13.60	13.54	13.69	13.61
	8.20		14.78	14.84	14.53	14.71
	11.39			17.85	17.73	17.79
	14.23			25.14	25.31	25.22
	16.00			28.23	28.30	28.26
	18.14			30.50	30.63	30.56
KOH	3.69			12.59	12.68	12.64
	6.25			13.65	13.55	13.60
	7.94		14.53	14.33	14.60	14.49
	11.36		16.00	16.17	15.98	16.05
	13.52			17.74	17.81	17.78

The heat evolved by the salt-alkali mixture was 11.50 cal. This is interesting since the heat evolved by an alkali solution of the same concentration but containing no sodium chloride was 12.18 cal.

TABLE II

HEATS OF ADSORPTION OF VARIOUS SOLUTIONS BY STANDARD CELLULOSE

Reagent	Individual determinations, calories per gram cellulose		Mean, cal. per gm.
(a) Water	10.20	10.18	10.19
(b) NaCl soln. (16.6% wt.)	10.02	10.12	10.07
(c) NaCl–NaOH (16.6% + 2.81%)	11.53	11.47	11.50
(d) NaOH (2.81%-curve)			12.18
(e) K₂CO₃ soln. (3.1% wt.)			10.32
(f) K₂CO₃ soln. (14.7% wt.)			10.20

The concentrated sodium chloride solution gives a value somewhat less than that of water, the strong carbonate a value much the same as that of water, and the weaker carbonate solution a value higher than that of water. These facts, as well as the rest of the results given in Tables I and II, merit discussion.

Discussion

It was pointed out in the introduction that determinations of the heats of adsorption of sodium hydroxide by cotton cellulose were made by Neale. In Table III a comparison is made of the values he obtained in the same concentration range with those obtained here. The agreement of the results with solutions of 10.70 and 15.20% concentration is excellent.

TABLE III

A COMPARISON OF NEALE'S VALUES AND THE AUTHORS' FOR HEATS OF ADSORPTION OF SODIUM HYDROXIDE BY COTTON CELLULOSE

Sodium hydroxide, percentage by weight	8.08	10.70	13.90	15.20
Neale's values, calculated to present basis, cal.	12.92	16.85	25.72	27.84
Present values (curve), cal.	14.50	16.90	24.80	27.82

In Neale's determinations the cellulose was first permitted to adsorb the vapor (water) of the alkali solution before the reaction heat was measured. By the use of vapor pressure data (10, pp. 370 and 373), Argue and Maass's heat of adsorption data (1), and Walker's sorption isotherms (18), it was possible to recalculate Neale's measurements to the same basis as that of the present values.

Neale considered that all the heat of reaction was evolved in five minutes. In the present investigation it was observed that, although most of the heat was given out in the first three or four minutes, at least 25 or more minutes was required for all the heat to be evolved.

With soda-boiled cotton and a solution of 2.99 moles of sodium hydroxide per 1000 gm. of water, Neale's results (14, p. 389) varied from 1.18 to 1.30 kg-cal. per mole of cellulose, or from 7.28 to 8.02 cal. per gm. of cellulose. The largest variation in the present work, which occurred at the beginning

of the investigation on alkalis, was with 0.95% sodium hydroxide solution. For the four determinations at this concentration, the results varied from 11.17 to 11.49 cal. per gm. of cellulose. In all other determinations the variation was usually much less than 0.3 cal. It may be concluded that the present work affords the most accurate calorimetric data on alkali adsorption by cellulose to date.
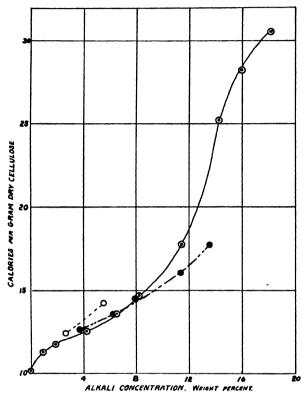
FIG. 1. *Heat of adsorption of alkalis by cotton cellulose.* O, *Lithium hydroxide;* ⊙, *sodium hydroxide;* ●, *potassium hydroxide.*

The amount of alkali sorbed by cellulose has been determined by a large number of investigators. The results of Heuser and Bartunek (9) may quite profitably be considered, since they determined the relative adsorptions of several alkalis, including the three considered here. A relation between the amount sorbed and the heat evolved was sought by comparing Heuser and Bartunek's data with the thermal data. In Figs. 1 and 2 are plotted the heats evolved and the amounts adsorbed, respectively, for different percentages by weight of the three alkalis, lithium, sodium, and potassium hydroxides. The similarity in regard to the relative positions of the two sets of curves is striking. It would appear that the heat evolved is some measure of the amount of substance adsorbed.

Measurements of the amount of substance adsorbed have always been attended with experimental difficulties, and reference to the literature will show that the results of different investigators vary widely. The accuracy of the heat measurements as made by means of the adiabatic calorimeter is such that one may consider measurements of this type a more accurate measure of the amount of material adsorbed.
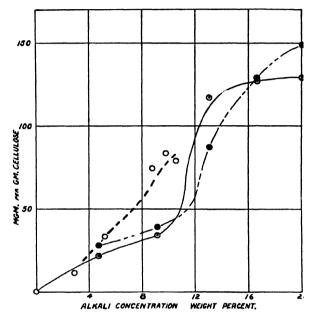
FIG. 2. *Adsorption of alkalis by cotton cellulose (Heuser and Bartunek).* O, *Lithium hydroxide;* ⊙, *sodium hydroxide;* ●, *potassium hydroxide.*

The question arises whether the adsorption is molecular or ionic, or of some other type. Many investigators have postulated cellulose adsorption compounds of the type (cellulose)sodium hydroxide, etc., implying a molecular adsorption. It would appear from the order of the heats of adsorption, when plotted on a molar basis as in Fig. 3, and also from the comparison of weight values with those of Heuser and Bartunek, that it may be molecular. That is, compounds of higher molecular weights give higher heats of adsorption. But the differences, though greater than experimental error, are too small to be accounted for on this basis. On the molar basis (Fig. 3) the curves of heats of adsorption of sodium hydroxide and lithium hydroxide are nearly overlapping, yet the molecular weights of these compounds are 24 and 40. Some other explanation is therefore required.

Neale supplies a clue to the possible explanation. From his investigations (14) he concludes that cellulose in the presence of a strong base acts as a weak acid, yielding small amounts of H^+ ion. These H^+ ions presumably

come from the hydroxyl groups known to be present in cellulose.   His hypothesis is that these H^+ ions neutralize the OH^- ions of the base to form water, and the alkali cation attaches itself to the oxygen of the cellulose much in the same manner as in salt formation.   The cellulosate is very sensitive to hydrolysis, so that the presence of water virtually keeps it dissociated.   The present results will now be discussed in the light of this hypothesis.
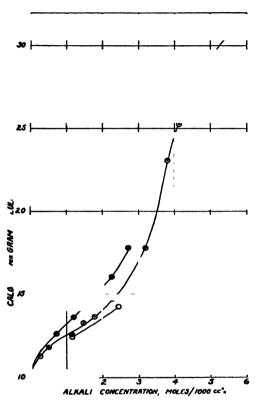
FIG. 3.   *Heat of adsorption of alkalis by cotton cellulose.*   O, *Lithium hydroxide;*   O, *sodium hydroxide;*   ●, *potassium hydroxide.*

It has already been pointed out that two phenomena may be noted in regard to the evolution of heat when the results are plotted on a molar basis.   The magnitudes of the heats evolved are similar for the three alkalis, and, at the same time, there js a well defined order of these magnitudes, namely, for lithium hydroxide, sodium hydroxide, and largest, potassium hydroxide. The strengths of these alkalis are quite similar, yielding a similar OH^- ion concentration.   But the cations are hydrated in the order, Li^+, Na^+, and least, K^+.   A plausible explanation would be that the hydration of the cation influenced the availability of the OH^- ion. The most hydrated Li^+ ion would partly prevent its OH^- from forming water with the hydrogen from the weakly acidic cellulose. Further, the ease with which the cation could attach itself to the cellulose, subsequent to the neutralization process, would be influenced in the same direction by hydration.   These considerations would explain the variations in the quantity of heat evolved.

Further evidence based on the shape of the curves of heat of adsorption supports Neale's speculations.   At first there is a rapid increase in the amount of heat evolved, then a slowing at about 5% (by weight) concentration. Two processes may cause this.   Ordinary swelling, by increasing the surface, may make available an increased number of H^+ ions from the cellulose; but as maximum swelling is approached these H^+ ions become used up and a slowing of the neutralization process may occur.   Also, the OH^- ion concentration due to the alkali does not increase as fast as does the molecular concentration. Both phenomena may be taking place simultaneously.   After the slowing of

the process there is a very rapid increase in the amount of heat evolved, and then a decrease (sodium hydroxide, Fig. 3). It is known that a drastic change occurs, beginning when the sodium hydroxide concentration is 10% (weight). A whole new surface is opened up and a superabundance of H^+ ions may now be made available; this would account for the large increase in heat evolution. But again, the new surface is used up, and a slowing of the process occurs when the concentration is greater than 15%.

It may be noted here that the rapid rise in the heat evolved at concentrations higher than 10% is even more pronounced than is apparent in Fig. 3. In another paper it will be shown that the heat of mercerization, the heat involved in the drastic change of the structure of cellulose at mercerizing strengths of alkalis, is endothermic. Consequently, the true adsorption heat is even larger than it appears, and an even steeper curve results.

Still further evidence for this (and Neale's) mechanism is supplied by the data regarding heats evolved when various salt solutions and a salt-alkali solution react with cellulose. With ordinary strong sodium chloride solution ((*b*), Table II) in which there is certainly a superabundance of Na^+ ions, the heat evolved is slightly less than that when water alone is used. Apparently, sodium chloride is not adsorbed appreciably by cellulose; it probably only competes with cellulose for water. Its influence, in depressing the amount of heat evolved, as compared with that evolved in water alone, may be called a "bulk" effect, reducing the water concentration.

The heat evolved in a solution containing sodium hydroxide (2.81%) and the same amount of sodium chloride as that in the solution mentioned above (16.6%) ((*c*), Table II) is considerably less than that given out in a solution of the same alkali concentration but containing no sodium chloride. Moreover, the difference is much more than can be accounted for by the "bulk" effect that sodium chloride exhibits. The only explanation seems to be that the OH^- ion concentration is affected. The presence of an excess of Na^+ ions increases the amount of molecular sodium hydroxide, but decreases the availability of OH^- ions. Two conditions appear to be evident; (i) the adsorption phenomenon is probably not molecular, and (ii) the availability of OH^- ions seems to be of prime importance in the adsorption process.

The results obtained with potassium carbonate solutions provide only further support for these ideas. The heat evolved in a solution of low concentration is measurably greater than that in water alone. It is well known that a solution of this salt has an excess OH^- concentration, and, though small, it is apparently sufficient to form water from the H^+ ions of the very weakly acidic cellulose. On the other hand, the heat given out in a concentrated carbonate solution is the same as that in water. Apparently, the "bulk" effect of the salt in the water solution balances the effect of the OH^- ion concentration.

It has been considered that the evolution of heat is due to the ionization of very weakly acidic cellulose, and to the subsequent processes of water formation and alkali cation adsorption. But it cannot be said how much is contributed by any of these processes.

Very recently Bancroft and Calkin (2) published what they considered was the most accurate measure of the amount of adsorption of sodium hydroxide by cellulose.   It is of interest to compare their results with those of
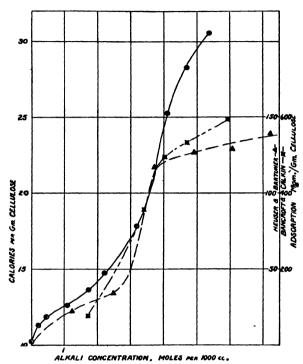
FIG. 4.   *Comparison of heat of adsorption with amount of adsorption of sodium hydroxide by cellulose.*

Heuser and Bartunek, and with the present thermal data, as in Fig. 4.   The first portion of Heuser and Bartunek's curve seems to follow very closely the variations of the curve of heat evolved.

References

 1. ARGUE, G. H. and MAASS, O.   Can. J. Research, 12 : 564-574.   1935.
 2. BANCROFT, W. D. and CALKIN, J. B.   J. Phys. Chem. 39 : 1-9.   1935.
 3. BARRATT, T. and LEWIS, J. W.   J. Textile Inst. 13 : 113-120.   1922.
 4. BERTETTI, J. W. and McCABE, W. L.   Ind. Eng. Chem. 28 : 375-378.   1936.
 5. CHILIKIN, M. M.   Zhur. Priklad. Khim. 3 : 221-230.   1930; Chem. Abstr. 24 : 3899.   1930.
 6. COWARD, H. F. and SPENCER, L.   J. Textile Inst. 14 : T28-T32.   1923.
 7. GUCKER, F. T. and SCHMINKE, K. H.   J. Am. Chem. Soc. 54 : 1358-1378.   1932.
 8. GUCKER, F. T. and SCHMINKE, K. H.   J. Am. Chem. Soc. 55 : 1013-1019.   1933.
 9. HEUSER, E. and BARTUNEK, R.   Cellulosechem. 6 : 19-26.   1925.
10. INTERNATIONAL CRITICAL TABLES. McGraw-Hill Book Company, New York. Vol. 3. 1928.
11. JOYNER, R. A.   J. Chem. Soc. Trans. 121 : 2395-2409.   1922.
12. LEIGHTON, A.   J. Phys. Chem. 20 : 32-50.   1916.
13. MORRISON, J. L., CAMPBELL, W. BOYD, and MAASS, O.   Can. J. Research, B, 15 : 447-456.
        1937.
14. NEALE, S. M.   J. Textile Inst. 20 : 373-400.   1929.
15. VIEWEG, W.   Ber. 40 : 3876-3883.   1907.
16. VIEWEG, W.   Ber. 41 : 3269-3275.   1908.
17. VIEWEG, W.   Ber. 57 : 1917-1921.   1924.
18. WALKER, F.   Ph.D. Thesis, McGill University.   1937.

THE REACTION OF OXYGEN ATOMS WITH METHANE[1]

By E. W. R. Steacie[2] and N. A. D. Parlee[3]

Abstract

The reaction of oxygen atoms, produced by the discharge tube method, with methane has been investigated at temperatures from 30° to 330° C. The products of the reaction are carbon monoxide, carbon dioxide, and water. Ethane is absent. The activation energy is approximately 8 Kcal. It is concluded that either

(a) The reaction postulated by Norrish

$$O + CH_4 = CH_2 + H_2O$$

does not occur to any great extent, or

(b) The reaction

$$CH_2 + CH_4 = C_2H_6$$

has an activation energy greater than 11 to 12 Kcal.

Introduction

There is considerable uncertainty regarding the theoretical basis of the oxidation reactions of the hydrocarbons. According to the hydroxylation theory, which was proposed by Bone (3), and has been mainly upheld by him and his co-workers, the fundamental reactions in the oxidation of methane are

$$CH_4 + \tfrac{1}{2}O_2 = CH_3OH \tag{1}$$

$$CH_3OH + \tfrac{1}{2}O_2 = H_2CO + H_2O \tag{2}$$

The peroxidation theory (4) assumes, on the other hand, that the first stage in oxidation reactions is the formation of an unstable peroxide which initiates chain processes by means of which reactivity is handed on from the active products (peroxides) to the reactant molecules.

Neither of these theories is wholly satisfactory, and Norrish (10) has suggested a theory which is somewhat of a compromise between the other two. He suggests that the initial steps in the oxidation of methane are:

$$O + CH_4 = CH_2 + H_2O \tag{3}$$

$$CH_2 + O_2 = CH_2O + O \tag{4}$$

thus setting up chain processes in which the carriers are methylene radicals and oxygen atoms.

If Norrish's assumptions are correct, then it should be possible, by the Wood-Bonhoeffer method, to cause Reaction (3) to occur to a large extent by introducing atomic oxygen in high concentration into methane. If under these circumstances Reaction (3) occurs largely, then in addition to Reaction (4) there is also the possibility of

$$CH_2 + CH_4 = C_2H_6 . \tag{5}$$

No direct information is available as to the rate of Reaction (5), but its occurrence has been suggested by Kassel (7) as a step in the decomposition

of methane. Kassel suggests a mechanism for the methane decomposition which fits the experimental data excellently. The arguments on which this mechanism is based lead to the conclusion that Reaction (5) has the high activation energy of 44 Kcal. Of course, a successful mechanism is not necessarily unique, and the evidence that E_5 is 44 Kcal. is thus rather speculative.

Belchetz and Rideal (1, 2) investigated the primary split of methane into radicals at high temperatures and concluded that the primary reaction was

$$CH_4 = CH_2 + H_2 . \qquad (6)$$

On the other hand, Rice and Dooley (11, 12), using the Rice technique, were unable to detect the methylene radical, and found only methyl radicals in the methane decomposition. They consider the primary split to be

$$CH_4 = CH_3 + H . \qquad \cdot \qquad (7)$$

They also discuss the possibility of the methyl radicals having been formed by secondary processes. If this is so, then the absence of methylene radicals in their experiments must be ascribed to either Reaction (5) or

$$CH_4 + CH_2 = 2CH_3 \qquad (8)$$

being fast enough to keep the concentration of methylene radicals down to a low value. They show that for this to occur either Reaction (8), or more likely Reaction (5), would have to have an activation energy less than 12 Kcal., which they consider to be too low.

The consensus of opinion is thus that Reaction (5) has a high activation energy. However, the evidence is very uncertain, and it appeared to be possible that Reaction (5) was a rapid reaction, and that the discrepancy between the work of Rice and Dooley and that of Belchetz and Rideal might be ascribed to its occurrence.

It follows that if the primary step in the methane oxidation is that postulated by Norrish, as appears likely, then there is the possibility of ethane formation by Reaction (5). If this were found to be the case it would lend support to the Norrish mechanism, and at the same time approximately define the activation energy of Reaction (5). If no ethane were found, the result would be somewhat inconclusive, since its absence could be due to the non-occurrence of either Reactions (3) or (5). It appeared, however, to be worth investigating the possibility of the occurrence of ethane in the reaction of oxygen atoms with methane.

The reaction of oxygen atoms with methane has been investigated by Harteck and Kopsch (6). They used the usual Wood-Bonhoeffer type of apparatus, and froze the condensable products out of the flowing stream by means of a liquid air trap. With this method the only condensable products were carbon dioxide and water, since carbon monoxide and ethane would have passed through the trap and been lost. They found more water than

carbon dioxide, approximately in the ratio of 2 : 1 by weight, instead of 1 : 1.22 as required if the reaction went completely by

$$4O + CH_4 = CO_2 + 2H_2O .$$

They therefore concluded that carbon monoxide was formed as well. From the water formed they calculated the following percentage oxidation of methane in various experiments. The oxygen atom concentration in these experiments was approximately 30%.

Temperature, °C.	30	100	189
Percentage of methane reacted	1.0, 0.9, 1.1	2.1, 2.0	5.9, 6.5

The carbon dioxide formed in these experiments must have come from some intermediate product, such as formic acid, since the oxidation of carbon monoxide by oxygen atoms is quite slow. The results indicated an activation energy for the reaction of approximately 7 Kcal. (5).

Experimental

The apparatus was essentially the same as that used by one of us in previous investigations of hydrogen atom reactions (13, 14).

The discharge was operated with an applied voltage of about 3500 across the tube and a 5000 ohm resistance. The current was maintained at 320 milliamperes by means of a rheostat in the primary of the transformer. The reaction chamber had a diameter of 7 cm. and a length of 70 cm., and was surrounded by an electric furnace which could be slipped up and down the tube to permit observation when the efficiency of wall poisoning, etc., was being tested. Two tubes entered the reaction vessel from below, one of which contained a thermocouple; the other served as an inlet for methane.

In these experiments no attempt was made to measure the oxygen atom concentration, since the main purpose of the investigation was the determination of the products of the reaction. However, from the intensity of the afterglow, as compared with previous observations of the same kind with known oxygen atom concentrations, it was approximately 20% at room temperature. The uncertainty in this value is certainly less than a factor of 2.

The walls of the apparatus were poisoned by rinsing with a 5% solution of phosphoric acid in the usual way.

Tank oxygen was used. It contained no appreciable impurity other than a small amount of nitrogen and the rare gases. The oxygen was admitted to the discharge through a calibrated capillary flowmeter.

Methane was secured in cylinders from the Ohio Chemical and Manufacturing Co. It was purified by distillation and stored in a large reservoir. In making an experiment it was expanded into two successively smaller reservoirs of known volume. The smaller of these volumes was connected

to the apparatus through a capillary flowmeter. By adjusting the pressure in the smaller reservoir it was possible to secure any desired rate of flow, and by observing the change in pressure in the secondary storage volume the amount of gas used could be accurately calculated.

After leaving the reaction vessel the gas passed through a trap at $-80°$ C. in order that easily condensable products would be removed, and then through the high-speed diffusion pump. After leaving the pump the gas passed through a large trap at $-183°$ C. which contained silica gel. This served to remove methane and other low-boiling gases. The residual gas then went to an oil pump.

At the end of an experiment the silica gel trap was allowed to warm up, and the gas was desorbed and expanded into a large storage volume. The last of the adsorbed gas was removed with a Toepler pump and pumped into the same volume, and the total volume of recovered gas was then measured. Blank runs showed that all the methane and about 85% of the oxygen were trapped by the gel. It was safe, therefore, to assume that all gases with boiling points higher than that of methane would be completely recovered. On account of its comparatively small amount, carbon monoxide was also completely recovered. (It should be noted that in spite of its slightly lower boiling point, carbon monoxide is more strongly adsorbed by silica gel than is oxygen (9).)

Analyses of the gaseous products were made in a Burrell gas analysis apparatus for oxygen, carbon dioxide, unsaturated hydrocarbons, carbon monoxide, and saturated hydrocarbons. The hydrocarbon fraction of the reaction products was analyzed in a low-temperature fractional distillation apparatus of the Podbielniak type. As large quantities of oxygen interfered with the distillation, it was necessary to remove oxygen before the distillation. It was also necessary to remove carbon dioxide since it sublimes at atmospheric pressure. These gases were therefore removed prior to the distillation by shaking the sample with a sodium-hydrosulphite–potassium-hydroxide solution.

Experimental Results

The Products of the Reaction

The products of the reaction at various temperatures are given in Table I. It will be seen from the table that the amount of carbon dioxide formed is in good agreement with the findings of Harteck and Kopsch. Harteck and Kopsch could not determine carbon monoxide with their experimental arrangement, and they therefore inferred its amount from the water formed. Our results indicate a considerably greater formation of carbon monoxide than that inferred by them. This is possibly due to the adsorption of water on the walls, which may have cut down the observed water formation in their work. In our case, water could not be determined since the walls of the apparatus were poisoned with a solution of phosphoric acid. Part of the discrepancy is also due to the fact that we used a larger reaction vessel, and hence the contact time in our work was greater than in theirs. They did not calculate collision

yields from their experiments, so that the latter point cannot be directly verified. Geib (5), however, has estimated an activation energy of 7 Kcal. from their work which would indicate a collision yield very similar to that obtained by us. The two investigations may therefore be considered to be in satisfactory agreement.

TABLE I

THE PRODUCTS OF THE REACTION

(See Table II for pressures, flow rates, etc.)

| Run No. | Temperature, °C. | Methane used, cc. | Ratio O_2/CH_4 | Percentage CH_4 converted to | | | Total percentage reaction |
				CO	CO_2	C_2H_6 or heavier	
1	37	415	4.0	10.5	—	None	10.5
2	200	550	4.0	27.1	5.7	None	32.8
3	201	608	4.0	28.1	7.3	None	35.4
4	303	697	4.0	33.4	21.9	None*	55.3
5	330	490	4.0	30.2	19.2	None*	49.4
6	315	700	4.0	31.3	19.7	None*	51.0

* *Combustion analyses of the hydrocarbon fraction from Runs 4, 5, and 6 confirmed the absence of ethane.*

It is significant that no appreciable quantity of formic acid, formaldehyde, or any other intermediate oxidation product is formed. This leads to the conclusion that the primary reaction of oxygen atoms with methane is slow compared with the later steps which continue until the methane has been completely oxidized to carbon monoxide, carbon dioxide, and water. This slow primary step may well be that suggested by Norrish

$$O + CH_4 = CH_2 + H_2O .$$

Since the reaction

$$O + CO = CO_2$$

is comparatively slow (6), the carbon dioxide formed cannot have resulted from the oxidation of carbon monoxide, at least at room temperature. It seems probable therefore that the next steps in the oxidation may be

$$CH_2 + O = CH_2O$$
$$CH_2 + O_2 = CH_2O_2 ,$$

and that these are followed by the oxidation of formaldehyde and formic acid. It has been shown by Geib (5) that the reaction of oxygen atoms with formaldehyde yields mainly carbon monoxide, while formic acid yields mainly carbon dioxide. Both reactions are rapid at room temperature, the activation energies being below 7 Kcal.

The absence of ethane or other saturated hydrocarbons leaves the evidence for the Norrish mechanism inconclusive, since we have the alternative possibilities:

(a) The reaction

$$O + CH_4 = CH_2 + H_2O$$

TABLE II

REACTION OF METHANE WITH OXYGEN ATOMS

Atom concentration, assumed 20%; volume of reaction vessel, 1370 cc.

Run No.	Temperature, °C.	Pressure, mm.	Methane flow, cc./sec., at N.T.P.	Oxygen flow, cc./sec., at N.T.P.	Total flow cc./sec., at experimental conditions (corrected for presence of atoms)	Reaction time, sec.	Partial pressure of oxygen atoms, cm.	No. of collisions per sec. by one CH_4 molecule with oxygen atoms	No. of collisions by one CH_4 molecule with oxygen atoms in reaction time	Percentage reaction	Collision yield	Activation energy, Kcal., on assumption of a steric factor of 0.1
1	37	0.32	0.0628	0.250	919	1.49	0.0052	3.58×10^3	5.33×10^3	10.5	1.98×10^{-7}	8.1
2	200	0.34	0.0628	0.254	1334	1.03	0.0055	3.06×10^3	3.14×10^3	32.8	1.04×10^{-4}	10.8
3	201	0.33	0.0632	0.248	1350	1.01	0.0054	3.00×10^3	3.03×10^3	35.4	1.17×10^{-4}	10.7
4	303	0.33	0.0630	0.254	1678	0.82	0.0055	2.77×10^3	2.26×10^3	55.3	2.44×10^{-4}	12.1
5	330	0.35	0.0632	0.250	1639	0.84	0.0057	2.83×10^3	2.36×10^3	49.4	2.09×10^{-4}	12.9
6	315	0.32	0.0630	0.248	1732	0.79	0.0053	2.64×10^3	2.09×10^3	51.0	2.44×10^{-4}	12.4

does not occur, or

(b) The reaction

$$CH_2 + CH_4 = C_2H_6$$

is not a rapid reaction, its activation energy being greater than 11 to 12 Kcal., and hence the absence of methylene radicals in Rice and Dooley's work cannot be ascribed to its occurrence. However, it must be admitted that the situation is too complex to admit of very definite conclusions.

The Kinetics of the Reaction

Although this investigation was made primarily for the purpose of determining the products of the reaction of oxygen atoms with methane, the results are sufficiently detailed to enable an estimate of the activation energy of the process to be made as well. The data on which this estimate is based are given in Table II, an atom concentration of 20% being assumed,

$$i.e., \quad \frac{P_O}{P_O + P_{O_2}} = 0.20 .$$

It will be seen that the collision yield at room temperature leads to an activation energy of 8.1 Kcal., which is in satisfactory agreement with Geib's approximate estimate of 7 Kcal. from the results of Harteck and Kopsch.

The activation energies calculated from the collision yields at higher temperatures are considerably higher than this value. This is undoubtedly due to the fact that the atom concentration at higher temperatures is much less than that at room temperature, since the efficiency of the wall poisoning diminishes rapidly as the temperature is raised. If we assume that the atom concentration at 300° has fallen to about 2%, the activation energies calculated from experiments at higher temperatures are brought into line.

References

1. BELCHETZ, L.   Trans. Faraday Soc. 30 : 170-179.   1934.
2. BELCHETZ, L. and RIDEAL, E. K.   J. Am. Chem. Soc. 57 : 1168-1174.   1935.
3. BONE, W. A. and TOWNEND, D. T. A.   Flame and combustion in gases.   Longmans, Green and Co. London.   1927.
4. EGERTON, A.   Nature, 121 : 10.   1928.
5. GEIB, K. H.   Ergeb. exakt. Naturw. 15 : 44-105.   1936.
6. HARTECK, P. and KOPSCH, U.   Z. physik. Chem. B, 12 : 327-347.   1931.
7. KASSEL, L. S.   J. Am. Chem. Soc. 54 : 3949-3961,   1932.
8. KASSEL, L. S.   J. Am. Chem. Soc. 57 : 833-834.   1935.
9. McBAIN, J. W.   The sorption of gases and vapours by solids.   George Routledge and Sons, Ltd., London.   1932.
10. NORRISH, R. G. W.   Proc. Roy. Soc. Lond. A, 150 : 36-57.   1935.
11. RICE, F. O.   J. Am. Chem. Soc. 56 : 488-490.   1934.
12. RICE, F. O. and DOOLEY, M. D.   J. Am. Chem. Soc. 55 : 4245-4247.   1933.
13. STEACIE, E. W. R.   Can. J. Research, B, 15 : 264-273.   1937.
14. STEACIE, E. W. R.   J. Chem. Phys. 6 : 37-40.   1938.

THE POLYMERIZATION OF ISOBUTENE[1]

By E. W. R. Steacie[2] and G. Shane[3]

Abstract

An investigation of the polymerization of isobutene has been made at low temperatures and pressures, using very small percentage conversions. The reaction rate curves are pronouncedly autocatalytic in nature, and the process appears to be too complex to yield very much information concerning the kinetics of the reaction.

Introduction

Most of our knowledge of the polymerization reactions of the higher olefins comes from the work of Krauze, Nemtzov, and Soskina (2–6), who have investigated the polymerization of ethylene, propene, the butenes, and pentene at high pressures in the temperature range 300° to 400° C. The reactions are all second order, the products being mainly, but not exclusively, those corresponding to a straight association to give an olefin with twice the number of carbon atoms. The kinetic constants, together with collision efficiencies calculated by Bawn (1), are given in Table I.

TABLE I

Reaction	E, Kcal.	$\log_{10} A$	Collision efficiency
$2C_2H_4 = C_4H_8$	37.7	10.8	4×10^{-3}
$2C_3H_6 = C_6H_{12}$	37.4	10.2	1×10^{-3}
$2C_4H_8 = C_8H_{16}$	38.0	10.0	5×10^{-4}
$2iso\text{-}C_4H_8 = C_8H_{16}$	43.0	12.3	1×10^{-1}
$2C_5H_{10} = C_{10}H_{20}$	38.0	9.8	4×10^{-4}

It will be seen that, with the exception of the values for isobutene, A, E, and the collision efficiency are almost the same for all members of the series. The difference in the case of isobutene is of considerable interest, if real. However, the fact that both A and E alter in such a way as to compensate each other makes the result open to considerable suspicion. Also, a collision efficiency as great as 1/10 is very unlikely for an association reaction. It therefore seemed of interest to reinvestigate the polymerization of isobutene.

Experimental

Previous work on the olefin polymerizations has been done at high pressures, to swamp out the accompanying first order decomposition reactions. It was decided in the present work to use low pressures and very small conversions, and to follow the reaction by determining the diisobutene formed. In this way it was hoped to avoid complications due to the decomposition, and at the same time be able to work at low pressures where greater accuracy is attainable.

The method of following the progress of the reaction was as follows. Gaseous isobutene was admitted to a Pyrex bulb in an electric furnace at a measured pressure. After the lapse of a predetermined time, the contents of the reaction vessel was pumped out through a liquid air trap. The trap was then warmed to −80° C. and the unreacted isobutene was pumped away until the pressure had fallen to 0.001 mm. The contents of the trap was then evaporated, recondensed, and the trap again pumped down. The diisobutene was then re-evaporated into a known volume, and its pressure measured on an oil manometer.

Isobutene was prepared by refluxing a mixture of tertiary butyl alcohol and anhydrous oxalic acid. The resulting gas was condensed and fractionally distilled several times. A further distillation through a Podbielniak column indicated no appreciable amount of impurity.

The diisobutene from a large number of runs was collected, and this aggregate, amounting to about 1 cc., was distilled through a small column of the Podbielniak type. It gave a boiling range of 100° to 107° C. at 760 mm. pressure, in good agreement with the results of Whitmore and Wrenn (7) who found a boiling range of 100° to 105° C. for a mixture of the isomeric diisobutenes. The vapor pressure of the product was 37 mm. at 25° C. Its refractive index was $n_D^{20} = 1.422$, as compared with 1.408 to 1.415 found by Whitmore and Wrenn for the various isomers of diisobutene.

Results

The results obtained were complex. Those from a set of runs at 60 cm. initial pressure are given in Fig. 1. The pronounced "autocatalytic" nature of the reaction-time curves is noteworthy. As a consequence of this the interpretation of the results is difficult and very ·great accuracy cannot be expected. The only feasible way to treat the experimental data is to overlook all but the initial rates, i.e., those before the "breaks" in the curves occur. It is found that in this region the reaction is fairly accurately second order, in so far as the effect of varying initial concentration on the initial rate is concerned. The reaction is influenced by the surface to some extent, runs in a packed vessel indicating from 6 to 20% heterogeneity. It was also found that,
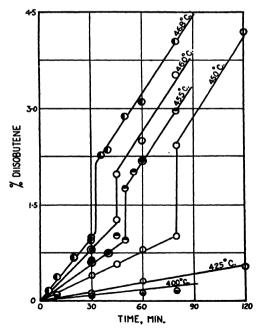
FIG. 1. *The rate of polymerization of isobutene. Initial pressure, 60 cm. The rates are expressed as percentage of diisobutene formed in terms of the initial amount of isobutene.*

as in the ethylene polymerization, small amounts of oxygen had a pronounced catalytic effect. Thus in one experiment at 400° C., 2 mm. of oxygen added to 60 cm. of isobutene increased the rate by a factor of 4.

In view of these complications, no very accurate kinetic data could be obtained. However, the temperature coefficient of the initial rate, plotted in the form of a curve of log rate against $1/T$, gave a fairly good straight line and indicated an activation energy of 43.4 Kcal., with an uncertainty of perhaps 3 to 4 Kcal. This value is in excellent agreement with the results of Krauze *et al.* From this we get for the initial rate constant

$$\log_{10} k = 9.65 - \frac{43400}{2.3RT} \text{ litre mol.}^{-1} \text{ sec.}^{-1}$$

It is apparent, therefore, that while our value for the activation energy is in good agreement with the results of Krauze, Nemtzov, and Soskina, there is a very large difference in the A factor obtained from the two investigations. Our value is in line with those found for the other olefins, and as a result the collision efficiency calculated from our work is also in line with those of the other olefins, *viz.*, approximately 4×10^{-4}.

This discrepancy between the two investigations is primarily due to the fact that our absolute rates are much lower than those of Krauze *et al.* (by a factor of about 200). The fact that the reaction is partly heterogeneous cannot account for the discrepancy, since this means that our rates are somewhat *higher* than they should be. The real causes of the discrepancy would seem to be that *(a)* the reaction is not accurately second order, and hence our results cannot be properly compared with those obtained at very high pressures, and *(b)* the complex nature of the rate curves makes accurate interpretation impossible. In view of these facts it does not seem advisable to give much weight to the previously reported high collision efficiency of the reaction.

References

1. BAWN, C. E. H. Trans. Faraday Soc. 32 : 178-187. 1936.
2. KRAUZE, M. V., NEMTZOV, M. S. and SOSKINA, E. A. Compt. rend. acad. sci. U.R.S.S. 2 : 301-306. 1934.
3. KRAUZE, M. V., NEMTZOV, M. S. and SOSKINA, E. A. Compt. rend. acad. sci. U.R.S.S. 3 : 262-267. 1934.
4. KRAUZE, M. V., NEMTZOV, M. S. and SOSKINA, E. A. J. Gen. Chem. U.S.S.R. 5 : 343-355. 1935.
5. KRAUZE, M. V., NEMTZOV, M. S. and SOSKINA, E. A. J. Gen. Chem. U.S.S.R. 5 : 356-360. 1935.
6. KRAUZE, M. V., NEMTZOV, M. S. and SOSKINA, E. A. J. Gen. Chem. U.S.S.R. 5 : 382-387. 1935.
7. WHITMORE, F. C. and WRENN, S. N. J. Am. Chem. Soc. 53 : 3136-3142. 1931.

CONTRIBUTION TO THE STRUCTURE OF DISTYRENES[1]

By Léo Marion[2]

Abstract

Dehydration of $\alpha\gamma$-diphenylbutyl alcohol with potassium bisulphate yields 1,3-diphenyl-3-butene which can be oxidized to β-phenylpropiophenone. This 3-butene isomerizes on standing to a crystalline 1,3-diphenyl-1-butene which forms a dibromo-derivative and gives benzaldehyde and hydratropic aldehyde when ozonized. If $\alpha\gamma$-diphenylbutyl alcohol is dehydrated with 20% sulphuric acid, it also yields 1, 3-diphenyl-3 butene, but this isomerizes to 1,3-diphenyl-2-butene from which acetophenone is obtained on oxidation.

Staudinger's proof of the identity of the pyrolytic distyrene with 1,3-diphenyl-3-butene is not valid since $\alpha\gamma$-diphenylpropane, present with the distyrene, produces β-phenylpropiophenone when oxidized.

When highly polymerized styrene is subjected to pyrolysis *in vacuo*, a partly depolymerized product is obtained. Recently Staudinger and Steinhofer (5) found that this product consists of a complex mixture of styrene, di-, tri-, and tetra-styrene together with saturated hydrocarbons. From the distyrene fraction, by catalytic polymerization of the ethylenic component, they succeeded in isolating $\alpha\gamma$-diphenylpropane. On oxidizing the distyrene fraction they isolated β-phenylpropiophenone, and, on the basis of this result, attributed to the ethylenic component the structure of 1,3-diphenyl-3-butene. These experiments have since been repeated and confirmed by Midgley, Henne, and Leicester (4). The properties exhibited by 1,3-diphenyl-3-butene, as will appear from the sequel, and the impossibility of isolating any crystalline dibromide from pyrolytic distyrene led the present author to doubt the validity of Staudinger and Steinhofer's interpretation of their results. A reconsideration of the oxidation of pyrolytic distyrene suggested a different interpretation. It is well known that paraffins substituted by one or more phenyl groups can be oxidized to ketones (2). Pure $\alpha\gamma$-diphenylpropane was, therefore, oxidized under conditions identical with those used by Staudinger and Steinhofer, and found to give an excellent yield of β-phenylpropiophenone. Hence, the conclusion of Staudinger and Steinhofer that pyrolytic distyrene is 1,3-diphenyl-3-butene is based on a fallacious interpretation of their results.

It was thought that the identity of the ethylenic component of pyrolytic distyrene with 1,3-diphenyl-3-butene might be proved or disproved more readily by synthetic methods, and the latter compound has now been synthesized. The ethyl ester of $\alpha\gamma$-diphenylbutyric acid (3) was reduced to the corresponding alcohol which was dehydrated either with potassium bisulphate or with sulphuric acid. Both methods of dehydration gave 1,3-diphenyl-3 butene (I) which is an unstable, colorless oil. When oxidized with potassium permanganate in acetone solution it yields the expected β-phenylpropiophenone (II).

However, 1,3-diphenyl-3-butene rapidly isomerizes on standing. When it has been obtained by potassium bisulphate dehydration, it is transformed mainly into a crystalline isomer, m.p. 47° C.,* which can be ozonized to benzaldehyde and hydratropic aldehyde, and is, therefore, 1,3-diphenyl-1-butene (III). When the dehydration has been effected with sulphuric acid, 1,3-diphenyl-3-butene isomerizes chiefly to 1,3-diphenyl-2-butene (IV). The latter, on oxidation with potassium permanganate gives acetophenone.

$$CH_2(C_6H_5)CH_2-C(C_6H_5)=CH_2 \qquad \text{(I)}$$

$$CH_2(C_6H_5)CH_2-CO(C_6H_5) \qquad \text{(II)}$$

$$CH(C_6H_5)=CH-CH(C_6H_5)CH_3 \qquad \text{(III)}$$

$$CH_2(C_6H_5)CH=C(C_6H_5)CH_3 \qquad \text{(IV)}$$

1,3-Diphenyl-1-butene forms a well characterized crystalline dibromo-derivative, m.p. 86.5° C., from which the bromine can be removed and the crystalline hydrocarbon recovered. The latter is unstable and is slowly oxidized. Even when the hydrocarbon is kept in a stoppered bottle, the odor of benzaldehyde can soon be detected. From a consideration of its oxidation products, it is apparent that the crystalline hydrocarbon must have the structure III. Likewise, the formation of β-phenylpropiophenone from the freshly prepared dehydration product of αγ-diphenylbutyl alcohol makes it impossible to assign to this hydrocarbon any structure other than that of 1,3-diphenyl-3-butene (I). This is further supported by the failure of this hydrocarbon to crystallize on inoculation with the crystalline 1,3-diphenyl-1-butene, eventually obtained from it on standing, although it crystallizes immediately if inoculated after having stood for some time.

From cinnamic acid, Stoermer and Kootz (6) have prepared a liquid disty-rene which produced benzoic acid and hydratropic aldehyde when oxidized, and is, therefore, a 1,3-diphenyl-1-butene. From this distyrene they isolated three crystalline dibromo-derivatives (m.p. 129°, 122°, and 79° C.). On repeating their work, the author isolated two dibromo-derivatives, both melting at 129° C. and melting at 102° C. when admixed, but has failed to obtain the third as a crystalline substance. Inoculation of the mother liquors from these two crystalline dibromo-derivatives with the dibromide of the crystalline isomer (m.p. 86.5° C.) failed to bring about crystallization. There seems to be no doubt that the dibromide melting at 86.5° C. is different from that melting at 79° C. Since 1,3-diphenyl-1-butene is capable of *cis-trans* isomerism and each of the isomers can form two dibromo-derivatives, it is probable that the crystalline hydrocarbon (m.p. 47° C.) is the *trans*-isomer, whereas the liquid distyrene of Stoermer and Kootz is the *cis*-compound. The dibromide, m.p. 86.5° C., described above, is thus the last missing di-bromide of the four theoretically possible.

The dibromo-derivatives of the diphenylbutenes I and IV are oils which could not be crystallized.

All melting points are corrected.

If pyrolytic distyrene is really 1,3-diphenyl-3-butene, then it should be possible, after bromination, to isolate from the product the crystalline dibromo-derivative, m.p. 86.5° C. of the isomeric 1,3-diphenyl-1-butene which is formed so readily from it. A polystyrene fraction of average molecular weight 8000 was pyrolized *in vacuo* according to the usual procedure and the distyrene fraction isolated. This, however, could not be induced to crystallize by inoculation with the crystalline 1,3-diphenyl-1-butene nor, after bromination, by inoculation with the dibromo-derivative of m.p. 86.5° C.

Experimental

Preparation of αγ-Diphenylbutyric Acid

This was best prepared by the method of Kohler and Kimball (3) from α-phenyl-β-benzoylpropionic acid by a Clemmensen reduction. The acid can also be prepared from diethyl *sodio*-phenylmalonate and phenylethylbromide in absolute alcohol. The phenyl-phenylethylmalonic ester produced is saponified, and the acid when distilled *in vacuo* yields αγ-diphenylbutyric acid which, recrystallized from petroleum ether, forms beautiful prismatic crystals, m.p. 75° C. Calcd. for $C_{16}H_{16}O_2$: C, 80.0; H, 6.66%. Found: C, 79.98; H, 6.70%.

Preparation of αγ-Diphenylbutyl Alcohol

αγ-Diphenylbutyric acid is esterified and the ester reduced by Bouveault's method with sodium and alcohol to αγ-diphenylbutyl alcohol (90% yield). The alcohol is a colorless, viscous oil, b.p. 174° to 180° at 1 mm.

Dehydration of αγ-Diphenylbutyl Alcohol with Potassium Bisulphate

The alcohol was heated for one hour with potassium bisulphate and distilled under diminished pressure, b.p. 140° C. at 2 to 3 mm. This hydrocarbon is a colorless, fairly mobile oil. A sample (1 gm.) of the hydrocarbon was dissolved in acetone and treated at room temperature with potassium permanganate added in small portions, each equivalent to half an atom of oxygen. A total of 3.5 atoms was required. The product yielded benzoic acid and a neutral oil which crystallized on standing. Recrystallized from petroleum ether, it melted at 75° C. Admixed with an authentic sample of β-phenylpropiophenone of m.p. 74° C., the mixture melted at 74° C. The ketone was converted into the oxime which, recrystallized from petroleum ether, melted at 87° to 88° C. Admixture with β-phenylpropiophenone-oxime failed to depress the melting point.

Bromination of 1,3-Diphenyl-3-butene

The hydrocarbon obtained as described above (7.7 gm.) was dissolved in chloroform, and after cooling was treated with a chloroformic solution of bromine. After the solution had stood one hour at room temperature, the excess bromine and the chloroform were evaporated under reduced pressure, and the residual oil was dissolved in boiling methanol. On cooling, the solution deposited a crop of crystals which, after one recrystallization from methanol, melted at 86.5° C. (yield, 2.6 gm.) Calcd. for $C_{16}H_{16}Br_2$: Br, 43.44%. Found, 43.66, 43.46%.

Isolation of 1,3-Diphenyl-1-butene

The crystalline dibromo-derivative, when digested with zinc dust in alcohol, yields an oil, b.p. 130° to 140° C. at 1 mm., which crystallized on cooling. Recrystallized from methanol, m.p. 47° to 47.5° C. Calcd. for $C_{16}H_{16}$: C, 92.3; H, 7.68%. Found: C, 91.30, 91.50; H, 7.65, 7.59%. The crystalline hydrocarbon, when rebrominated, yields the crystalline dibromide, m.p. 86.5° C.

Some of the original 1,3-diphenyl-3-butene which had not been brominated, but had been kept for some time, was inoculated with a crystal (m.p. 47° C.), whereupon it immediately deposited crystals, which, filtered from the accompanying oil and recrystallized, were identical with the hydrocarbon obtained from the dibromo-derivative.

The crystalline hydrocarbon (0.3 gm.) was ozonized in chloroform solution, and the ozonides were decomposed by boiling for 45 min. with water, zinc dust, and a trace of hydroquinone. The product, which had a strong odor of benzaldehyde, yielded two semicarbazones, m.p. 222° to 223° and m.p. 147° to 148° C. The first when admixed with benzaldehyde-semicarbazone (m.p. 229° C.) melted at 226° C.; the other, admixed with hydratropic aldehyde-semicarbazone (m.p. 154° C.) melted at 151° C. The hydrocarbon was also oxidized with permanganate, whereupon it yielded benzoic acid, and with chromic acid which produced benzaldehyde isolated as its semicarbazone.

Dehydration of αγ-Diphenylbutyl Alcohol with Sulphuric Acid

When αγ-diphenylbutyl alcohol is refluxed for three hours with 20% sulphuric acid, it produces 1,3-diphenyl-3-butene. After this has been allowed to stand, however, it does not deposit any crystals even when inoculated with a crystal of 1,3-diphenyl-1-butene. When this product is oxidized in acetone solution with potassium permanganate it yields β-phenylpropiophenone, m.p. 75° C. (oxime, m.p. 88° C.), and acetophenone, isolated as its semicarbazone (m.p. and mixed m.p. 207° C.), together with some benzoic acid mixed with another acid, probably phenylacetic acid. The production of acetophenone can be explained only by the presence in the mixture of 1,3-diphenyl-2-butene. Stoermer and Kootz (6) have shown that sulphuric acid brings about the isomerization of cis-1,3-diphenyl-1-butene to 1,3-diphenyl-2-butene. It is, therefore, likely in this case that some of the 1,3-diphenyl-3-butene isomerized to 1,3-diphenyl-1-butene, and that this was transformed by the sulphuric acid into 1,3-diphenyl-2-butene. During bromination, the last-named hydrocarbon lost hydrogen bromide, and the final product is an oil which could not be crystallized.

Pyrolysis of Heat-polymerized Styrene

Styrene was polymerized by heating in a sealed tube at 170° C. for 72 hr. The polymer was dissolved in benzene and fractionally precipitated with methanol. The fraction of average molecular weight 8000 (11 gm.) was pyrolyzed *in vacuo* according to the usual procedure (5), and the distyrene fraction, b.p. 144° to 150° at 3 mm., isolated by distillation (1.8 gm.).

This failed to crystallize even after inoculation with a sample of synthetic 1,3-diphenyl-1-butene.   Half of this distyrene was dissolved in chloroform and brominated at room temperature as described above.   The oily product was dissolved in methanol but failed to crystallize even in contact with a small crystal of the dibromide melting at 86.5° C.   The oily bromide was then distilled.   About one-third distilled at 170° C. at 1 mm. as a light-yellow oil, and a reddish-brown oil was left in the flask.   This residual oil, dissolved in methanol, also failed to crystallize.

Pyrolytic distyrene, after standing several weeks, failed to develop the odor of benzaldehyde as 1,3-diphenyl-3-butene invariably does.

Preparation of αγ-Diphenylpropane

β-Phenylpropiophenone (10 gm.) was reduced by the method of Clemmensen and the oily product fractionated.   A colorless oil, b.p. 120° to 122° at 1.5 mm., was collected.   This fraction was dissolved in alcohol and treated with hydroxylamine hydrochloride and sodium acetate; the product dissolved in ether was extracted with several portions of aqueous sodium hydroxide.   The oil recovered from the ether was redistilled, b.p. 124° C. at 2 mm.   Wt., 4.6 gm.   One gram of this αγ-diphenylpropane was nitrated according to the method of Bergmann and Fujise (1), and the tetranitro derivative recrystallized from chloroform-alcohol, m.p. 169° C.

Oxidation of αγ-Diphenylpropane

αγ-Diphenylpropane (1 gm.) was dissolved in glacial acetic acid and boiled for one-half hour with 0.4 gm. of chromic oxide, also dissolved in glacial acetic acid.   This yielded 0.7 gm. of an oil which soon crystallized.   Recrystallized from petroleum ether, it melted at 75° C.   Admixed with an authentic specimen of β-phenylpropiophenone it did not depress the melting point.   Half of the ketone was converted into the oxime, m.p. 87° C. before or after admixture with an authentic specimen.

Acknowledgment

References

1. BERGMANN, E. and FUJISE, S.   Ann. 483 : 65-80.   1930.
2. FRIEDEL, C. and BALSOHN, M.   Bull. soc. chim. 32 : 615-617.   1879.
3. KOHLER, E. P. and KIMBALL, R. H.   J. Am. Chem. Soc. 55 : 4632-4639.   1933.
4. MIDGLEY, T., HENNE, A. L., and LEICESTER, H. M.   J. Am. Chem. Soc. 58 : 1961-1963. 1936.
5. STAUDINGER, H. and STEINHOFER, A.   Ann. 517 : 35-53.   1935.
6. STOERMER, R. and KOOTZ, H.   Ber. 61 : 2330-2336.   1928.

A SOURCE OF MERCURY RESONANCE RADIATION OF HIGH INTENSITY FOR PHOTOCHEMICAL PURPOSES[1]

BY E. W. R. STEACIE[2] AND N. W. F. PHILLIPS[3]

Abstract

A lamp-reaction vessel system for photochemical purposes is described. This is very inexpensive and has an unusually high intensity of mercury resonance radiation (about 1.5×10^{-5} einsteins per sec.).

Introduction

A great deal of photochemical work is done by mercury photosensitization, and for this purpose a strong source of the resonance line at 2537 Å is essential. The ordinary mercury arc possesses many disadvantages. It runs hot, emits numerous lines other than the resonance lines, and the resonance lines themselves are partially reversed, even when the lamp is water cooled. On this account most recent photochemical work has been done with low pressure discharge lamps, a rare gas carrier being used. These require a starting potential of about 5000 v., but operate on 400 to 500 v. Such lamps are commercially available with very high intensities. In order to use the emitted light efficiently it is customary to employ an annular quartz reaction vessel with the lamp in the centre. Such a combination of lamp and reaction vessel is quite effective, but is very expensive. Furthermore, it lacks flexibility, since, on account of the expense, special lamps and reaction vessels cannot be designed for each investigation.

Description

To obviate the above disadvantages a lamp-reaction vessel system has been designed, which is very cheaply and easily made since only the actual emitting portion of the lamp is of quartz, the remainder being constructed of Pyrex glass. A sketch is given in Fig. 1.
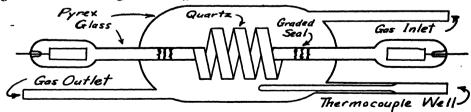
FIG. 1. *The lamp-reaction vessel system.*

The emitting portion of the lamp is a quartz spiral constructed of tubing with an outside diameter of 10 mm. This is connected by graded seals to Pyrex tubing of the same diameter. The electrode chambers, also of Pyrex, are 15 mm. in diameter and 7 cm. long. The electrodes are standard neon sign "coated" electrodes, 8 mm. in diameter and 3 cm. long. They are welded through copper to tungsten wires which are sealed through the glass. The Pyrex reaction vessel is triple sealed on as shown, and is 9 cm. in diameter and 23 cm. long. The distance from the reaction vessel to the electrode chambers is 14 cm.

The lamp is filled with neon at a pressure of 12 mm., and contains a small droplet of mercury. The filling and "bombarding" of the electrodes was done by the usual neon sign technique* (1).

The coated electrodes were found to be very cool in operation, the electrode chambers being at a temperature not greater than 35° C. This is a considerable improvement on commercial lamps of this type with plain electrodes, which run at about 150° C. The smaller heating means improved efficiency. If it is desired to investigate reactions at high temperatures, either the central part of the lamp only may be heated, the electrodes being left outside the furnace, or, on account of the small heating of the electrodes, the entire lamp including the electrodes may be placed in the furnace.

The intensity of the resonance radiation emitted by the lamp was determined by measuring the rate of hydrolysis of monochloracetic acid (2). Two concentrations of the acid were employed, 0.5 M and 0.25 M. These gave identical results; absorption was therefore complete. The solution after irradiation was analyzed by the addition of an excess of silver nitrate and back titration, after filtration of the precipitated silver chloride, with potassium thiocyanate, ferric nitrate being used as an indicator. The characteristics of the lamp are given in Table I.

TABLE I

CHARACTERISTICS OF THE LAMP

Potential, v.	Current, ma.	Input, watts	Resonance radiation emitted, einsteins/sec.	Efficiency of production of λ 2537, %
450	120	54	1.62×10^{-5}	24
495	100	50	1.49	28
495	100	50	1.48	28
495	100	50	1.50	28
503	80	40	1.36	32
572	50	29	1.22	39
655	19	—	—	—
668	11	—	—	—
706	7.7	—	—	—
708	4.2	—	—	—
713	2.5	1.8	1.54×10^{-6}	80
820	1.9	—	—	—
920	1.7	—	—	—
1000	1.5	—	—	—
	<1.5	Lamp goes out		

* *We are greatly indebted to the Claude Neon Eastern Ltd., for performing these operations.*

The efficiency in Column 5 is calculated with allowance for the fact that one-half of the tubing is Pyrex glass and is opaque to λ 2537.   As far as we are aware these are the highest efficiencies ever recorded for the production of λ 2537.   The data at 100 ma. are illustrative of the constancy of the output.   The lamp is remarkably stable at low currents, and can be operated efficiently without flickering down to 2.5 ma.   Its intensity can thus be varied tenfold in operation.

References

1. MILLER, S. C. and FINK, D. G.   Neon signs.   McGraw-Hill Book Company, New York.
         1935.
2. RUDBERG, E.   Z. Physik, 24 : 247-263.   1924.

THE KINETICS OF THE DECOMPOSITION OF CHLOROPICRIN AT LOW PRESSURES[1]

BY E. W. R. STEACIE[2] AND W. McF. SMITH[3]

Abstract

The decomposition of gaseous chloropicrin has been investigated down to pressures of 0.3 cm. At lower pressures the rate falls off. The results fit the Kassel theory for a model with 15 oscillators, a molecular diameter of 8×10^{-8} cm., and a frequency of 779 cm.$^{-1}$

Introduction

A series of simple compounds differing only in the nature of their substituents, and decomposing at conveniently low temperatures, is of value in studying the effect of chemical constitution on the reaction rate. The series of which chloropicrin is a member constitutes such a group of compounds. In a previous paper (2) it was shown that the decomposition of chloropicrin is homogeneous and unimolecular, and consequently of value for comparative study. In view of this fact it was considered advisable to investigate the behavior of chloropicrin over a wider range of pressure, and this paper describes measurements carried out between 3.0 and 0.3 cm. initial pressure.

It was shown in the previous paper that the products of the decomposition are essentially nitrosyl chloride, phosgene, nitric oxide, and chlorine as represented stoichiometrically by the equations

$$CCl_3NO_2 \longrightarrow COCl_2 + NOCl$$
$$\Updownarrow$$
$$NO + 1/2Cl_2.$$

There was evidence that the nitric oxide and chlorine are produced at a rate somewhat greater than that to be expected from the simple secondary decomposition of nitrosyl chloride.

Experimental

As in the previous work, the progress of the reaction was followed by observing the rate of pressure change in a system of constant volume. For experiments in which the initial chloropicrin pressure was greater than 1 cm. the apparatus was identical in design with that described in the preceding paper, except that mercury was replaced by butyl phthalate as a manometer liquid. As before, the pressure was measured with a glass manometer used as a null instrument, the reactant was introduced with the help of a magnetic hammer, and isolation of the system was accomplished by sealing off the connecting tubing. The dead space constituted about 5% of the reaction system.

In experiments in which the chloropicrin pressure was less than its vapor pressure at room temperature, viz., about 1.5 cm., the reactant was admitted

to the system and the system was isolated by a single stopcock greased with Apiezon N grease. The glass manometer employed in the investigation at pressures greater than 1.5 cm. was sensitive to better than 0.01 cm. of mercury, and that used for lower pressures was sensitive to 0.002 cm.

In this investigation the pressure increase at completion agreed with that to be expected from a mixture of phosgene, nitrosyl chloride, chlorine, and nitric oxide, with equilibrium established among the last three named. Thus at 161.7° C. and an initial pressure of 1.24 cm., the pressure increase at completion was 118% as compared with a calculated value of 119%.

For individual experiments the unimolecular constants calculated on the basis of the percentage pressure increase being equal to the amount of reaction show good agreement, rising somewhat with the progress of the reaction, particularly during the later stages as would be expected from the total pressure increase. On the other hand, the final equilibrium value is attained as quickly at low pressures as at high, and since the homogeneous decomposition of nitrosyl chloride is bimolecular, it would appear that nitric oxide and chlorine are produced in nearly the final equilibrium ratio during the initial decomposition, or that some surface catalyzed decomposition of nitrosyl chloride occurs. Rate constants calculated on the basis of nitric oxide and chlorine production in the final equilibrium amount show slightly better constancy than those calculated on the basis of percentage reaction corresponding to percentage pressure increase. However, the difference is small, and it has therefore been assumed that the time for a 25% pressure increase is a measure of the time for the same amount of decomposition to occur at different pressures. It is possible that on this basis a small error is introduced into the results, but in view of the semi-empirical nature of the theory of unimolecular reactions at low pressures such an error cannot be very serious.

TABLE I

COMPLETE DATA FOR TYPICAL EXPERIMENTS

Temperature, 161.7° C.

Initial pressure, 1.24 cm.			Initial pressure, 0.38 cm.		
Time, min.	Per cent reaction	$k \times 10^6$, sec.$^{-1}$	Time, min.	Per cent reaction	$k \times 10^6$, sec.$^{-1}$
5	6.8	235	6	6.7	192
10	13.6	243	12	13.5	194
15	20.9	261	18	19.2	197
20	27.4	267	24	24.7	196
25	35.3	240	30	30.2	197
30	39.6	280	36	36.5	210
35	45.5	289	42	41.0	202
40	50.0	281	49	46.1	210
51	59.5	295	55	51.5	201
60	65.5	296	60	55.8	226
80	79.0	325	71	60.0	213
100	88.0	354			

Results

Complete data for two runs are given in Table I.   The rate constants given in this table are calculated on the assumption of equality between the percentage pressure increase and the amount of reaction.   The summarized rate data for all runs are given in Table II.   The high pressure values of t_{25} and t_{50} are given in Table III.   These were obtained by plotting the corresponding values in Table II against the reciprocal of the initial pressure, and extrapolating to infinite pressure.

TABLE II
Summarized rate data

Initial pressure, cm.	t_{25}, sec.	t_{50}, sec.	Initial pressure, cm.	t_{25}, sec.	t_{50}, sec.
Temperature, 170.2° C.					
3.02	410	940	0.64	535	1270
2.08	433	972	0.59	570	1300*
1.50	446	1045	0.44	660	1390
1.07	468	1060	0.33	660	1500*
0.75	525	1180*			
Temperature, 161.7° C.					
3.40	720	1710	1.00	1080	2520*
2.74	810	1930	0.97	1127	2600
2.20	880	1860	0.81	1155	2680*
1.98	920	2120	0.73	1162	2700*
1.93	960	2210	0.61	1176	2675
1.50	957	2380	0.59	1320	3000*
1.33	1094	2400	0.52	1425	3100
1.24	1065	2400	0.52	1283	3000*
1.18	1004	2400	0.38	1455	3220*
1.12	960	2500	0.37	1500	3300*
1.06	1053	2580	0.24	1800	3960*
1.04	1100	2500			
Temperature, 153.5° C.					
2.73	1885	4180	0.67	2900	— *
1.65	2176	4980	0.60	3460	— *
1.25	2210	5200	0.54	3000	—
1.00	2560	— *	0.37	3330	— *

NOTE.—*In runs marked *, a stopcock was used in the reaction system.*

TABLE III
Extrapolated values of rate data

Temp., °C.	170.2	161.7	153.5	145.2
t_{25}, sec.	280	580	1420	3400
t_{50}, sec.	680	1470	3480	

Discussion

The falling-off in rate at low pressures in unimolecular decompositions may be described by the Kassel theory. Kassel assumes that reaction occurs when a molecule which possesses j quanta divided among s oscillators has m localized in one particular oscillator. The oscillators are considered to be identical and of frequency ν. The rate constant, k, at low pressures may then be expressed relative to the limiting high pressure rate, k_∞, by the relation

$$\frac{k}{k_\infty} = \left(1 - e^{-\frac{h\nu}{kT}}\right)^s \sum_{j-m}^{\infty} \frac{\left(\begin{array}{c} j - m + s - 1 \\ j - m \end{array}\right) e^{-\frac{(j-m)h\nu}{kT}}}{1 + \frac{A}{aN} \frac{j!\,(j - m + s - 1)!}{(j - m)!\,(j + s - 1)!}}$$

A is a measure of the rate of energy redistribution in the molecule, and is obtained empirically from the high pressure rate; a is the collision factor $4\sigma^2\left(\frac{\pi kT}{m}\right)^{\frac{1}{2}}$, where σ is the collision diameter.

In applying the relation, m must be so chosen that the value of the frequency (which is related to it by the expression $mh\nu = E/N_o$, where E is the energy of activation and N_o is Avogadro's number) is within the range of frequencies which are indicated by other data such as the Raman spectrum. The value of s is given by the relation $3(n - 2)$, where n is the number of atoms in the molecule.

Fig. 1 gives the theoretical curve for $s = 15$, $\sigma = 8 \times 10^{-8}$cm., and $m = 17$. The circles are experimental values.
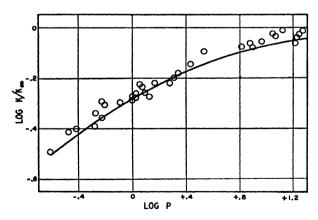
FIG. 1. *Falling-off in rate at low pressures. The circles are experimental points. The solid line is the theoretical curve for $s = 15$, $\sigma = 8 \times 10^{-8}$ cm., $\bar{\nu} = 779$ cm.$^{-1}$.*

The value of $\bar{\nu}$ corresponding to the value chosen for m is 779 cm.$^{-1}$, a value consistent with the vibrational frequencies obtained from the Raman spectrum, *viz.* 420 to 1578 cm.$^{-1}$ (1).

The value of σ is not unreasonable but is slightly greater than the collision diameter to be expected for a molecule such as chloropicrin. However, the value for effective energy exchange with high energy molecules may well be somewhat different from the ordinary collision diameter. However, the extrapolation to obtain the high pressure rate is not very accurate, and it is possible that the true value of k_∞ may be greater by a small percentage than that used. If such is the case, the curve could be fitted to the data by employing a value of σ considerably smaller.

The value of s is of particular interest. Most molecules which undergo unimolecular decomposition contain C—H bonds, which possess such a high frequency that they are not thermally excited at decomposition temperatures. As a result the value of s is less than that given by the relation $s = 3(n - 2)$. Chloropicrin, however, contains no hydrogen atoms, and consequently should have all its oscillators thermally excited at the temperatures employed here. The fact that the theoretical value of s is satisfactory thus furnishes additional confirmation of the essential truth of unimolecular theory.

References

1. MILONE, M.   Gazz. chim. ital. 63 : 453-456.   1933.
2. STEACIE, E. W. R. and SMITH, W. McF.   J. Chem. Phys. 6 : 145-149.   1938.

ANALYTICAL NOTES. I.[1]

By C. W. Davis[2]

Abstract

An organic selenide is decomposed with an oxidizing mixture containing an excess of halogen. Selenium is determined gravimetrically as the metal.

The same oxidizing mixture is used for the decomposition of an organic mercury compound commonly used as a seed disinfectant.

A method is described by means of which elements difficult to separate may be determined by using two analytical methods followed by simple algebraic calculation for the unknowns.

Solid calcium acetate is used to retain the phosphorus on ignition of soybean oils.

Selenium in Organic Compounds

Selenium, like sulphur, forms dioxides and trioxides and unites with various metals to form compounds corresponding to the sulphides. Selenic acid closely resembles sulphuric acid. An important difference is the ease with which hydrochloric acid reduces the free acid and its salts to selenious acid. Sulphur dioxide will reduce selenium in the quadrivalent state to the metal. Early literature (1) contains many references to the difficulty of accurate determination of selenium and to the interference of nitric acid with the reduction.

A distillation apparatus with ground glass joints was used to study the decomposition of ethyl diselenide with an oxidizing mixture containing an excess of halogen. Nitro-chlorate mixture converted the selenium to a stable form such as selenic acid or selenates. The distillates after the addition of water and sulphuric acid and boiling off an equal volume of liquid contained no appreciable selenium. The traces of nitric acid remaining in the mixture containing sulphuric and selenic acids do not interfere with the quantitative reduction to selenium metal, provided that the selenic acid solution is added slowly to a large excess of hydrochloric acid saturated with sulphur dioxide as described by Lundell (4).

Examples

Ethyl diselenide. Calcd.: Se, 73.2%. Found: Se, 73.2%.

B.D.H. Sodium selenite. Calcd.: Se, 45.8%. Found: Se, 46.1%.

Mercury in Organic Compounds

Since mercury is completely volatilized when its compounds are ignited or fused with sodium carbonate, and since it is partly volatilized when solutions containing its salts are evaporated or boiled, the decomposition of organic mercury compounds without loss of mercury has presented some difficulties.

Fitzgibbon (2) writes a brief survey of the well known procedures for determining mercury and recommends reduction with formaldehyde in the presence of gelatin, and titration iodometrically. This titration method was proved to be more accurate than two other methods, *viz.*, direct titration and reaction of mercuric sulphide with excess iodine. Fitzgibbon decomposes such compounds as ethyl mercuric chloride with bromine and sulphuric acid under reflux. This method of decomposition is slow because a large amount of reduced mercury rises above the acid during the procedure.

In the present work nitro-chlorate mixture was used in a narrow-necked 260 cc. Erlenmeyer flask. Decomposition was rapid, sometimes almost explosive, but on the whole the method was preferable to the slower one. Excess chlorine and nitric acid were eliminated by the addition of water and sulphuric acid and subsequent boiling until the volume was small. Several distillates were tested but no volatile mercuric chloride could be detected.

Example

Ethyl mercuric chloride. Calcd.: Hg, 75.67%. Found: Hg, 75.7, 75.5%.

Bromine and Chlorine in Organic Compounds

The quantitative separation of bromides from chlorides is difficult. According to Lundell (4), small amounts of chlorine can be separated from large amounts of bromine by oxidation with potassium bi-iodate. Separation can also be effected by oxidation with potassium permanganate and distillation, but the exact time at which all the bromine is distilled off is difficult to detect.

None of these methods proved satisfactory in an analysis of a sample of ethyl mercuric halide (prepared by means of the Grignard reagent). A simple yet accurate procedure for an unknown mixture is as follows.

Decomposition is effected by Robertson's (6) method. The halides in nitric acid solution are treated with excess silver nitrate in known amount and the excess is determined by Volhard's method. The weight of mixed silver bromide and chloride is ascertained. The amount of silver in the precipitate can be calculated from the normality and amount of silver nitrate solution that has reacted. Algebraic equations are solved in order to determine the percentages of bromine and chlorine. The method is simple and the results quite satisfactory. The general principle applied is analogous to that used in finding the approximate percentages of potassium and sodium in a mixture by calculation from the weight of their fused salts and chlorine content as determined by either Mohr's or Volhard's method. The determinations here are of interest in the analysis of commercial liquid soaps.

Example

(1) One gram of unknown yielded 0.6490 gm. of a mixture of silver bromide and silver chloride; this mixture contained 0.4014 gm. of silver. The weight of the bromine and chlorine in the mixed halides is therefore 0.2476 gm. (24.76%). If x = percentage bromine, and y = percentage chlorine, $x + y = 24.76$.

Then, $4.05x + 4.05y = 100.28$, and $2.35x + 4.05y = 64.90$, from which $x = 20.81\%$, $y = 3.95\%$.

(2) One gram of a mixed salt prepared from a soap contained 51.7% chlorine.

If x = percentage potassium chloride, and y = percentage sodium chloride, $x + y = 100$.

Then, $47.5x + 60.8y = 5170$, and $47.5x + 47.5y = 4750$, from which $x = 31.6\%$, $y = 68.4\%$.

Phosphorus in Soybean Products

The phosphorus in soybean oils is in the form of phosphatides (3) which are very readily coagulated. The decomposition of soybean oils by oxidizing acids is a laborious procedure and the large amount of reagents used interferes with the separation of phosphate.

Calcium acetate solution (5) has been used to retain the phosphorus on ignition of organic compounds such as casein. The ignition method in the present work was rapid, and it was found that the phosphorus was retained by the addition of 2 gm. of powdered calcium acetate to even 20 or 30 gm. of oil. This procedure allows the estimation of phosphorus by macro technique in oils containing very small amounts. The oil, covered with the calcium acetate in a porcelain crucible, is heated, ignited, and allowed to burn over a Bunsen flame. Ignition of residual carbon is effected in an electric muffle. The calcium phosphate and lime are dissolved in hydrochloric acid and water. Ferric chloride, in amount proportional to that of phosphate, is added to the solution. Ferric hydroxide and phosphate are precipitated with ammonia, and subsequent filtering eliminates most of the lime. The precipitate is dissolved in acid and phosphorus is determined by a standard molybdate procedure. Results can be checked by other methods of decomposition.

That this method gives good results with soybean oils is probably due to the nature of the phosphatide content. It is reasonable to believe that the addition of calcium acetate and the strong heating causes coagulation and intimate mixture of the phosphatides with calcium acetate as they settle to the bottom of the crucible.

References

1. BRADT, W. E. and LYONS, R. E.   Proc. Indiana Acad Sci. 36 : 195-201.   1926.
2. FITZGIBBON, M.   Analyst, 62 : 654-656.   1937.
3. HALLIDAY, G. E.   Oil & Soap, 14 : 103-104.   1937.
4. HILLEBRAND, W. F. and LUNDELL, G. E. F.   Applied inorganic analysis.   John Wiley and Sons, Inc., New York.   1929.
5. SHAW, R. H.   Ind. Eng. Chem. 12 : 1168-1170.   1920.
6. THORPE, J. F. and WHITELEY, M. A.   A student's manual of organic and chemical analysis, qualitative and quantitative.   Longmans, Green and Company, Ltd., London. 1926.

THE HEAT CAPACITY AT CONSTANT VOLUME OF THE SYSTEM ETHYLENE NEAR THE CRITICAL TEMPERATURE AND PRESSURE[1]

By D. B. PALL[2], J. W. BROUGHTON[3], AND O. MAASS[4]

Abstract

The heat capacity of ethylene at constant volume has been investigated through the critical range, between 6.5° and 27° C., at an average density slightly greater than the critical. The heat capacity in the immediate neighborhood of the critical temperature is found to be a function of the previous thermal treatment of the system. The results indicate the persistence of a large amount of molecular interaction in ethylene above the critical temperature, and are in agreement with the concept that the liquid state of aggregation can persist above the temperature at which the visible meniscus disappears.

Introduction

A large amount of evidence which seems to indicate that phenomena in the critical region are more complex than is indicated by the simple theory of Andrews (1) and Van der Waals has been accumulated. In particular, a series of reports from this laboratory have pointed to the persistence of the liquid state above the critical temperature, (7, 8, 9, 10). Most recently the work of Maass and Geddes (5), and of McIntosh and Maass (6), has confirmed the existence of a region in which the density of ethylene not only fails to follow the classical density-temperature parabola, but is also a function of the thermal history of the system.

These phenomena appeared to be explicable only in terms of molecular interaction. Any such molecular interaction must show up as a large effect in the heat capacity of the system, since every intermolecular bond represents an extra mode for heat absorption.

The apparatus designed to make these thermal measurements had to meet a number of exacting conditions. The pressures encountered in the critical region are high. Measurements must be made over very small temperature ranges. During the course of a run, the material should be as nearly as possible at temperature equilibrium; hence, the rate of heating must be slow.

Experimental

An adiabatic electrical calorimeter (Fig. 1) was used. *A* is a ¼ in. welded steel container, vacuum tight. *F* is a steel cylindrical bomb containing the material whose heat capacity is to be determined. The bomb is immersed in a mercury bath in the light steel container *C*. In the mercury, *D*, is a perforated steel cylinder *E*, on which is wound a copper heating element. The

supports are of bakelite cut to a knife edge at the top. Attached to the walls are 12 radiation thermels, one of which is shown at *B*. These are copper-constantan thermocouples connected in series. The leads from the bomb heater to the outer electrical circuit pass through the tube shown. Another tube serves for outside connection to the thermocouples, and a third is used for evacuation.
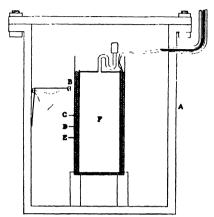
FIG. 1. *Diagram of the calorimeter.*

The outside electrical arrangements include a potentiometer which can be connected across either the bomb heating coil or a standard resistance in series with it. The thermocouples are connected directly in series with a low period, highly sensitive galvanometer, which shows a 1 cm. deflection for a 0.001° C. difference in temperature between the inner and outer parts of the calorimeter.

The calorimeter is immersed in a water bath fitted for very efficient stirring. A sensitive mercury-toluene thermoregulator made it possible to control the temperature within ±0.003° C. over long periods. The bath temperature could be controlled by hand to within less than 0.001° C.; thus heat losses in the calorimeter were quite negligible. Temperatures were measured by means of a Beckmann thermometer, which, when fitted with a special magnifying device, could with practice be read to within 0.0003° C. The absolute calibration, against a platinum resistance thermometer, was good to within 0.001°.

The bomb itself is illustrated in Fig. 2. It is constructed of welded steel, with 0.09 in. walls. The steel goose neck *D* was attached to the copper tube *C*, in which had been placed a piece of wire solder, at *E*. After the requisite amount of ethylene had been distilled in, the tube was heated at *A* to melt the solder, and pinched off at *B* after the seal had been made. The amount of ethylene distilled in was calculated to be 10.66 gm.; after a year during which the pressure in the bomb averaged 50 to 60 atm., it was weighed and opened, and the weight of ethylene was found to be 10.653 gm. It is seen, therefore, that the seal was air tight.

The time during which current was passed through the heating coil was measured by means of a chronometer. This had been calibrated and was not appreciably in error. The potentiometer and standard cell had also been calibrated to 1 part in 10,000. The
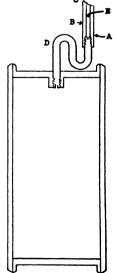
FIG. 2. *Diagram of container, showing method of sealing.*

ethylene was tank material supplied by the Ohio Chemical Company for anesthetic purposes; it was purified by low temperature distillation three times before using.

In the course of a run, the initial temperature of the bomb is determined by reading the outside temperature with no deflection in the thermel galvanometer. The heating coil is then turned on, the exact time being noted. Adiabatic conditions are maintained by raising the bath temperature simultaneously with that of the bomb, the reading of the thermel galvanometer being kept at zero. E.m.f. readings across both the heater and the standard resistance are noted at regular intervals, and the time when heating is stopped is recorded. Then, adiabatic conditions still being maintained, time is allowed for temperature equilibrium to be established in the bomb assembly, and the final temperature determined in the same way as the first. The rate of heating is about 1.5° per hr. The heat capacity is then calculated from the average value of the two e.m.f's, the heating time, and the temperature interval.

All other experimental errors were negligible compared with the error in determining temperature intervals. Although the Beckmann thermometer could be read to within 0.0003° C., it appears that owing to hysteresis effects its ultimate accuracy in measuring differences is about 1 part in 1000. This then is the accuracy of the determination of the heat capacity of the assembly—container, plus mercury, plus ethylene. When the measurements are made over very small ranges (less than 0.5° C.) this limit is of course increased.

A note should be added regarding "time lags". Outside of the range 8° to 9.5° C., temperature equilibrium after heating had been stopped was generally established in 10 min. Sometimes, however, the time required for equilibrium was much longer than this. It was considered to be of some interest to take the value of the changing temperature at intervals, until an asymptotic final value had been reached. These are included and systematized in the results under the heading "Time Lags".

Results

Heat Capacity Measurements

Values for the heat capacity of the system are given for the range 6.5° to 27° C. With the exception of the first three results in Section B of Table I, the measurements in the range 6.5° to 9.5° C. were made with two phases coexisting. The heat capacity of the system changes very rapidly in this region; consequently, it was necessary to make runs over very small temperature intervals. Furthermore, in the neighborhood of 8.5° to 9.5° C. long periods were required after heating for the establishment of equilibrium. Both these factors reduce the accuracy of the results obtained in this region compared with those in other temperature ranges.

TABLE I

HEAT CAPACITY AT CONSTANT VOLUME OF THE SYSTEM ETHYLENE BELOW THE CRITICAL TEMPERATURE. AVERAGE DENSITY = 0.2255

A				B	
Initial temperature approached from below 8° C.				Initial temperature approached from above 15° C.	
Range,°C.	Av. heat capacity, cal./°C./gm.	Range, °C.	Av. heat capacity, cal./°C./gm.	Range, °C.	Av. heat capacity, cal./°C./gm.
9.39 – 9.59	0.622	8.75 – 8.96	1.418	9.38 – 9.54	0.633
9.36 – 9.50	0.694	8.66 – 8.86	1.349	9.37 – 9.57	0.647
9.26 – 9.46	0.918	8.66 – 8.86	1.359	9.36 – 9.50	0.663
9.17 – 9.37	1.184	8.41 – 8.61	1.320	9.29 – 9.52	0.651
9.06 – 9.25	1.405	8.21 – 8.41	1.269	9.26 – 9.48	0.705
8.96 – 9.16	1.305	8.03 – 8.21	1.255	9.16 – 9.36	1.082
8.86 – 9.06	1.430	7.47 – 7.96	1.251		
8.806 – 9.075	1.402	6.49 – 7.47	1.169		
8.80 – 8.99	1.320				

Density determinations have demonstrated that near the critical temperature this property is dependent on the thermal history of the systems (4, 6). By analogy the heat capacity might also be a function of previous heat treatment; this has been tested and found to be true. In Table II, the columns headed "Homogeneous" contain the results of those measurements made by bringing the temperature of the system down from at least 5° above the critical temperature. Similarly the heading "Heterogeneous" means that the bomb temperature was brought up from at least 1.5° below the critical temperature before the run was made. Although time lags do not directly affect these results, it may be noted that for the heterogeneous type of run starting at 9.36° C. it was necessary to maintain the temperature constant for at least 14 to 16 hr. before a run was started, in order to ensure that temperature equilibrium had been established.

The maximum difference in heat capacity, depending on thermal history, is seen to be 4.5% in the range 9.36° to 9.50° and 2.6% in the range 9.36° to 10.36°.

Table III shows heat capacities of the system at temperatures higher than 13.7° C., where the material is always homogeneous. The results of Tables I and II are plotted in Fig. 3, and those of Table III, showing a minimum in the curve, in Fig. 4.
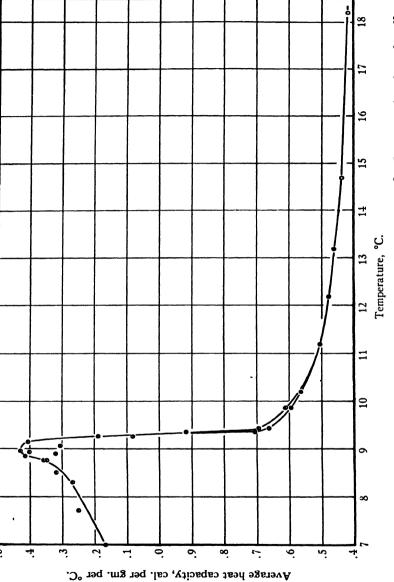
FIG. 3. *Heat capacity of ethylene, 7 to 18° C. Average density, 0.2255.* ●, *Temperature brought up from 8° or below before run started.* ◑, *Temperature brought down from above 15° before run started.*
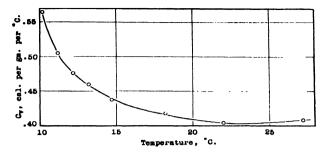
FIG. 4.   *Specific heat of ethylene at constant volume, 10 to 27° C.   Average density, 0.2255.*

TABLE II

HEAT CAPACITY OF ETHYLENE AT CONSTANT VOLUME
AVERAGE DENSITY = 0.2255

Temp. range, °C.	Heat capacity, bomb assembly, cal./°C.		Mean for bomb assembly		Absolute heat capacity, cal./°C./gm.		Difference, cal./°C./ gm.
	Homo-geneous	Hetero-geneous	Homo-geneous	Hetero-geneous	Homo-geneous	Hetero-geneous	Hetero-geneous minus homo-geneous
9.36 – 9.50	40.72 40.99 40.69 40.90 41.05	41.36 41.07 41.35 41.07	40.87	41.20	0.663	0.694	0.031
9.36 – 10.36	40.18$_5$ 40.18$_8$ 40.11$_9$	40.29$_0$ 40.37$_7$ 40.26$_3$ 40.37$_5$	40.15$_1$	40.32$_6$	0.594	0.609$_5$	0.015$_5$
9.7 – 10.7	39.88$_8$ 39.79$_3$ 39.86$_5$	39.85$_4$ 39.97$_7$ 39.87$_6$ 39.83$_4$	39.85$_3$	39.87$_9$	0.563	0.565$_5$	0.002$_5$
10.7 – 11.7	39.29$_4$ 39.22$_3$ 39.29$_7$	39.31$_9$ 39.24$_7$ 39.30$_8$	39.27$_1$	39.29$_1$	0.504	0.505$_5$	0.0015
11.7 – 12.7	39.04$_5$ 39.08$_2$ 38.98$_4$	38.95$_3$ 39.08$_5$ 38.98$_5$	39.03$_7$	39.00$_9$	0.478	0.475$_5$	−0.002$_5$
12.7 – 13.7	38.88$_8$ 38.91$_6$ 38.89$_3$	38.84$_5$ 38.91$_4$ 38.87$_3$	38.89$_9$	38.87$_3$	0.461$_5$	0.459	−0.002$_5$
9.7 – 13.7	39.26$_2$* 39.25$_9$	39.26$_5$* 39.21$_4$					

* *Mean of 1° runs.*

TABLE III

SPECIFIC HEAT OF ETHYLENE AT CONSTANT VOLUME AT TEMPERATURES GREATER THAN 13.7° C.

Range, °C.	12.7 – 16.7	15.7 – 20.7	21.0 – 23.0	26.2 – 28.2
Heat capacity of bomb assembly, cal./°C.	38.70	38.61	38.51, 38.57	38.72, 38.60
Mean C_v, cal./°C./gm.	0.438	0.417₆	0.404₅	0.408

Time Lags

Geddes and Maass have shown that in the establishment of equilibrium in the critical-temperature–critical-pressure region there is a "time lag" depending on the previous thermal history of the system. In the calorimetric measurements described here a very large number of observations were recorded in establishing the time lag curves. However, a great simplification in presentation of data is possible, for the curves obtained on plotting temperature against time have the form of first order reaction plots. If the difference between the temperature at time t and the final asymptotic temperature is denoted by ΔT,

$$\frac{d(\Delta T)}{dt} = -k\Delta T$$

or in the integrated form,

$$\frac{\Delta T_0}{\Delta T} = kt ,$$

where ΔT_0 is the value of ΔT at zero time.

TABLE IV

TIME LAG

Material heated from 8.96 to 9.16 °C. in 560 sec. Zero time counted from instant at which heating is stopped. $\Delta T_0 = 31 \times 10^{-3}$ °C. $k = 3.4 \times 10^{-4}$ sec.$^{-1}$

Time, sec.	Temp., Beckmann	$\Delta T \times 10^3$ °C.	Time, sec.	Temp., Beckmann	$\Delta T \times 10^3$ °C.
610	1.3015	16.1	2560	1.2884	4.0
670	1.3002	14.8	2920	1.2879	3.5
720	1.2988	14.4	3190	1.2866	2.2
780	1.2988	14.4	3400	1.2862	1.8
940	1.2970	12.6	3760	1.2866	2.2
1000	1.2962	11.8	3940	1.2856	1.2
1060	1.2953	10.9	4480	1.2850	0.6
1210	1.2939	9.5	4680	1.2848	0.4
1370	1.2925	8.1	5340	1.2845	0.1
1600	1.2915	7.1	5860	1.2840	−0.4
1870	1.2898	5.4	6600	1.2845	0.1
1960	1.2897	5.3	7540	1.2843	−0.1
2320	1.2884	4.0	8440	1.2847	0.3

Thus, for each of the time lag curves a straight line is obtained when log ΔT is plotted against the time.   A sample of the data recorded in establishing one of these time lags is given in Table IV, and the results are plotted with those of two other runs in Fig. 5.   The slope of these lines is read as the value of k, the rate constant.   The intercept on the zero time axis also has a meaning, since it represents the value of ΔT at zero time, and therefore corresponds to the total temperature drop.   These are the ΔT_0 values; when multiplied by the total heat capacity of the bomb assembly they give the total amount of heat absorbed by the ethylene during the lag.   For purposes of calculation, zero time is taken as half way through the heating interval.   The k and ΔT_0 values are listed in Table V and plotted against the temperatures in Figs. 6 and 7.
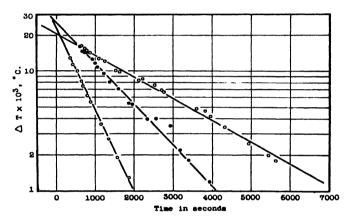
FIG. 5.   *Sample time lags.   Black circles correspond to Table IV.*
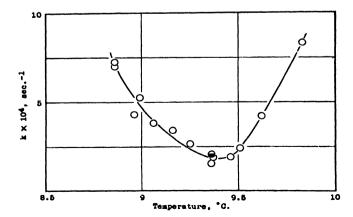
FIG. 6.   *Rate constants for time lags.   O, Temperature brought up from below 8° C.* ●, *Temperature brought down from above 14° C.*

FIG. 7. ΔT_0 for time lags. O, Temperature brought up from below 8° C. ◖, Temperature, brought down from above 14° C.

TABLE V
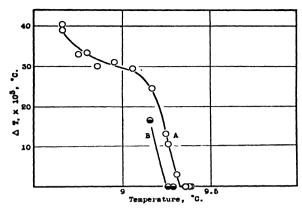
Range		Temp. interval, °C.	Time of heating, sec.	$\Delta T_0 \times 10^3$, °C.	$\Delta T_0 \times 10^3$, correct for a 0.2° interval	$k \times 10^4$ sec.$^{-1}$ $t_{1/2} = \dfrac{\log 2}{k}$
Initial temp. °C.	Final temp. °C.					
8.660	8.858	0.1981	560	38.5	39.0	7.27
8.664	8.855	0.1904	510	38.5	40.5	7.20
8.800	8.989	0.1892	505	31.5	33.5	5.36
8.746	8 856	0.2071	570	34.0	33.0	4.30
8.858	9.058	0.2005	555	30.0	30.0	3.81
8.957	9.163	0.2052	560	·32.0	31.0	3.40
9.059	9.253	0.1942	525	28.5	29.5	2.68
*9.163	9.363	0.1977	520	16.5	16.5	2.06
9.170	9.367	0.1981	510	24.2	24.5	1.88
9.253	9.356	0.1030	260	13.0	13.0	1.51
9.260	9.461	0.2011	535	10.7	10.5	1.99
9.312	9.512	0.2000	400	3	3	2.4
9.16	9.834	0.67	180	70	—	8.3
9.16	9.622	0.46	165	35	—	4.2
*9.26	9.48	0.22	500	0	—	—
*9.29	9.52	0.23	500	0	—	—
*9.37	9.57	0.2	500	0	—	—
9.36	9.50	0.16	400	0	—	—
9.38	9.7	0.32	600	0	—	—
9.39	9.59	0.2	500	0	—	—

* Initial temperature approached from above 15° C. All others approached from below 8° C.

Discussion of Results

Pressure-volume-temperature Relations

It is essential to a thorough understanding of the results that a clear picture of the P-V-T relations be carried in mind. The average density chosen was 0.2255 gm. per cc. McIntosh and Maass (6) have investigated the system at this density with respect .to dependence of density on thermal

history.   The pressure also is accurately known to be a linear function of the temperature, and to be independent of the thermal history.

When the temperature of the system is raised at constant volume from 8° C. through the critical temperature (9.5° C.), its density does not become uniform throughout, but changes in a continuous manner, the two phases persisting up to about 12.5° C., although the meniscus vanishes at 9.5° C. Thus, when the temperature is raised from 8° through the critical temperature to 12.5° the density values follow Curve A, Fig. 8.   There the density given is that of the lower phase.   If now the temperature is lowered, the density values follow Curve B.   Furthermore, liquid reappears now at 9.34° C., or 0.16° below the point at which the meniscus disappeared.   On applying heat at any temperature represented by a point on B above 9.34°, the same course is followed.   Evidently the system comprises two phases along A (for this reason it is referred to as heterogeneous); whereas along B, at temperatures greater than 9.34° C., the system is homogeneous.
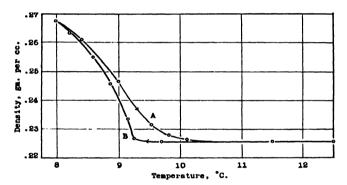
FIG. 8.   McIntosh and Maass isochore.   Average density, 0.2255.

Thermal History Effects

Consider two points on curves A and B, Fig. 8, at the same temperature, say 9.35° C.   In Fig. 3, the point on the upper curve shows a heat capacity higher than that shown by the point on the lower curve.   Suppose one assumes that these are equilibrium states, that is, that each of the systems would have the same properties after infinite time had elapsed, and furthermore that no attempt is made to distinguish any heterogeneity in the system, but it is considered as a whole—then their relative entropies can be discussed.   One can bring the temperature of the system in the first state up to say 12.5° with absorption of Heat Q_1, then bring it back to the second state at 9.35° C., during which Heat Q_2 is removed.   But Q_1 is greater than Q_2; hence, the system has undergone an increase in entropy.

Thus, on the assumption that the equilibrium state has been reached, it follows that it is possible to have in this region two systems with different entropies.   It follows too that the system of greater entropy should be the

more stable.   This is in accord with experiments which show that although the heterogeneous system can be changed to the homogeneous system without bringing the temperature of the system below the critical, the reverse change is not possible (4, 6).

An attempt can be made to form a kinetic picture of the system.   In discussing the heterogeneous system, the phase of greater density will be referred to as the condensed phase, whereas the other will be termed the vapor phase. Evidently, the structure of the condensed phase must be more complex than that of the vapor phase; *i.e.*, there is more molecular interaction.   This must correspond to an increase in the number of modes of taking up heat.   Hence it would be expected that the heterogeneous system should have a greater heat capacity than the homogeneous system (see Table III).

For similar reasons it is not surprising that thermal history should appear as a factor in the time lag results (compare curves *A* and *B*, Fig. 7).

The Maximum in the Heat Capacity Curve

The occurrence of the maximum in heat capacity at 9° C. is readily explained.   At temperatures below the critical, two phases are present.   As the temperature is raised, liquid evaporates, and the heat of vaporization is measured together with the heat capacities of liquid and vapor, as well as any changes resulting from the compression of the vapor, or expansion of the liquid.   Counteracting the effect of increased vaporization is the decreasing value of the heat of vaporization; furthermore, as the densities of liquid and vapor approach each other, a point will be reached at which the liquid will increase in mass as well as in volume, and evaporation no longer occurs.   As the temperature is raised from say 7° C. the increasing evaporation predominates, but as the critical temperature is approached, the latter factors will predominate, and the heat capacity decreases.

The Minimum in the Heat Capacity Curve

At temperatures greater than 12.5° C. the system is always homogeneous. The specific heat continues to decrease up to about 22° C.   Now, except in the critical region, C_v for ethylene shows an increase with temperature (3, 5). It can, moreover, be shown from the experimental value of $\left(\dfrac{d^2p}{dT^2}\right)_{v\ constant}$ that this should hold at the pressures considered.   This increase has been successfully explained in terms of increased absorption of heat by bond vibration at higher temperatures.   Hence the decrease in heat capacity experimentally found cannot be explained by a molecular mechanism.   Furthermore, no macroscopic changes take place.   It follows therefore that heat must be absorbed as vibrational energy by bonds representing molecular interaction.   There is therefore a large amount of intermolecular interaction in ethylene above the critical temperature, at these pressures, which does not entirely disappear until a temperature 13° C. above the critical has

been reached. At temperatures above this, a normal rise in specific heat with temperature is shown. These results are in qualitative agreement at least with those obtained by Callendar (2) for the specific heat of water. Exact comparison is not possible, since Callendar measured total heats at constant pressure.

Time Lags

It is more difficult to draw definite conclusions from the time lag data. The rate constant, k, is probably related to the value of $\frac{dp}{dv}$ and $\frac{d^2p}{dv^2}$ for the system. These approach zero at the critical temperature, at which it is seen that the rate constant shows a minimum (Fig. 6).

The ΔT_0 values correspond to the amount of "de-association" after heating through a $0.2°$ interval. These values are extraordinarily large. For instance, the absorption of heat for $\Delta T_0 = 0.030°$, $T_{initial} = 8.9°$ C., is $49.2 \times 0.030 = 1.48$ cal.; whereas during increase in temperature from $8.9°$ to $9.1°$ C., the ethylene itself absorbed $1.43 \times 10.66 \times 0.200 = 3.04$ cal.

Conclusions

It is possible to correlate very closely this work and density measurements. In neither is the classical result obtained when the system ethylene is brought through the critical temperature. Instead, the liquid state seems to persist after the meniscus has disappeared. This is shown in the one case by direct measurement of the density of the phases; in the other it is demonstrated by the difference in heat capacity of this two phase system and that of a homogeneous system, over the same range of temperature. In both, the difference in properties between the two systems becomes zero at about $10.5°$ C.

A large amount of molecular interaction exists in ethylene in the critical region. It must be concluded also that this is not confined to the condensed phase, but that the same is true of the vapor, but to a lesser degree. This follows from the decrease in heat capacity with temperature of the homogeneous system.

References

1. ANDREWS, T. J. Chem Soc. 23 : 74-95. 1870.
2. CALLENDAR, H. L. Proc. Roy. Soc. A, 120 : 460-472. 1928.
3. EUCKEN, A. and PARTS, A. Z. Physik. Chem. B, 20 : 184-194. 1933.
4. HEUSE, W. Ann. Physik. 59 : 86-94. 1919.
5. MAASS, O. and GEDDES, A. L. Phil. Trans. Roy. Soc. A, 236 : 303-332. 1937.
6. McINTOSH, R. L. and MAASS, O. To be published.
7. MARSDEN, J. and MAASS, O. Can. J. Research, B, 13 : 296-307. 1935.
8. TAPP, J. S., STEACIE, E. W. R., and MAASS, O. Can. J. Research, 9 : 217-239. 1933.
9. WINKLER, C. A. and MAASS, O. Can. J. Research, 9 : 65-79. 1933.
10. WINKLER, C. A. and MAASS, O. Can. J. Research, 9 : 613-629. 1933.

THE EFFECT OF MAGNESIUM-BASE SULPHITE-LIQUOR COMPOSITION ON THE RATE OF DELIGNIFICATION OF SPRUCE WOOD AND YIELD OF PULP[1]

By J. M. Calhoun[2], J. J. R. Cannon[3], F. H. Yorston[4], and O. Maass[5]

Abstract

The rate of delignification of resin extracted spruce wood-meal in magnesium base sulphite liquor has been determined at 130° C. over the concentration range 0.5 to 4% combined, and 2 to 10% free, sulphur dioxide. The rate of reaction is roughly proportional to the concentration of free sulphur dioxide when the combined is constant, but decreases with increase in the concentration of combined when the free is constant. The relation of the rate of delignification to the liquor composition cannot be expressed by any simple equation of the type:

$$\text{Rate of delignification} = K(\text{total SO}_2 - n \times \text{combined SO}_2),$$

where K and n are constants. The rate of cooking is somewhat greater in magnesium base sulphite liquor than in calcium base liquor of the same mole percentage composition.

The yield of pulp at any given lignin content is independent of the free sulphur dioxide over the whole concentration range, but increases with increase in the concentration of the combined to a maximum at about 3%, and decreases at slightly higher concentrations. When the concentration of combined sulphur dioxide is greater than 1% the yield of pulp obtained from magnesium base cooks is slightly higher than that from corresponding calcium base cooks.

Introduction

In an earlier paper (2) an investigation of the effect of calcium-base sulphite-liquor composition on the rate of delignification of spruce wood and yield of pulp was reported. It was found that the combined sulphur dioxide could be varied over only a comparatively small range of concentration without danger of precipitation of calcium sulphite during cooking. Therefore, the rate of delignification of spruce wood in magnesium base sulphite liquor was investigated, since the greater solubility of magnesium salts made possible a greater variation in the concentration of combined sulphur dioxide. It was hoped that this would permit a more precise correlation of the composition variables with the rate of delignification, and in addition prove an interesting comparison with the calcium system in regard to both the rate of cooking and the yield of pulp.

Sulphite liquors containing magnesia alone, or mixtures of lime and magnesia, have been used industrially to some extent. Hiller (3) states that higher yields and better quality of pulp have been obtained with magnesium base liquors, but no quantitative measurements of the rate of delignification have been made.

Experimental

The experimental procedure followed was identical in every detail with that previously described for calcium base cooks (2), and the results in the two cases are, therefore, strictly comparable. Well seasoned, white spruce wood-meal (density, 0.43; mesh 40 to 100) was prepared from a single log and extracted with alcohol-benzene (1 : 2). All cooks were carried out in 100 cc. sealed Pyrex bomb tubes at 130° C. The liquor ratio (50 : 1) was sufficiently large to minimize any concentration changes during cooking. Six samples of wood-meal were cooked for different lengths of time in each liquor used. The mean liquor concentration for a given run was taken as the average of that for all the bombs, analysis being made after cooking. The pulp was filtered, washed, oven dried, weighed, and analyzed for lignin by the Ross-Potter method (5). All yields were calculated on the resin extracted, bone-dry wood basis.

The liquor concentration as determined at room temperature was corrected, in the manner previously described, for sulphur dioxide lost to the vapor phase at 130° C. The same correction as before was applied for the time required to heat the bombs to 130° C. This was calculated to be 0.22 hr., which was subtracted from the observed time that the bombs were in the bath.

Results and Discussion

The data for a typical run are given in Table I to illustrate the calculations. The lignin as percentage of the original wood was plotted on a logarithmic scale against the observed time of cooking for each run, *e.g.*, Series *B*, Fig. 1. The yield of pulp was also plotted against the observed time of cooking for each run, *e.g.*, Series *B*, Fig. 2. The uncorrected times to 80, 90 and 95% delignification were read from the lignin curve for each run, and the yields of pulp at the corresponding times were read from the yield curve. Because of the deviations of the reaction from the first order relation no attempt was made to calculate velocity constants. As in the case of the calcium base cooks, the reciprocal of the corrected time to 90% delignification was taken as the best measure of the rate.

TABLE I

DATA FROM A TYPICAL COOK (RUN No. 83)*

Time in bath (uncorr.), hr.	Combined sulphur dioxide, %	Total sulphur dioxide (uncorr.), %	Total sulphur dioxide (corr.), %	Yield of pulp, %	Yield of non-lignin, %	Lignin, % of pulp	Lignin, % of original wood
0.75	0.97	7.99	7.93	77.3	61.5	20.4	15.8
1.50	0.94	7.86	7.72	65.7	57.3	12.8	8.4
2.25	0.93	7.76	7.70	57.1	53.6	6.04	3.45
2.75	0.91	7.82	7.79	54.1	52.6	2.76	1.49
3.25	0.91	7.84	7.76	52.3	51.0	1.94	1.01
4.00	0.88	7.79	7.67	50.5	50.0	1.01	0.51
Av.	0.92	7.84	7.76				

See Table II for details.
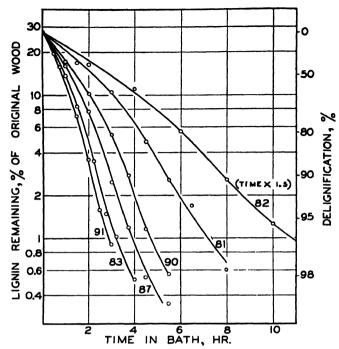
FIG. 1. *The effect of free sulphur dioxide concentration on the rate of delignification of spruce wood at 130° C.   Series B.   Magnesium base sulphite liquor; average combined sulphur dioxide 0.92%.*
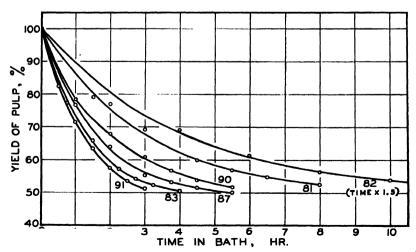
FIG. 2. *The effect of free sulphur dioxide concentration on the yield of pulp at 130° C. Series B.   Magnesium base sulphite liquor; average combined sulphur dioxide 0.9%.*

TABLE II

SUMMARY OF THE EFFECT OF COMPOSITION OF MAGNESIUM BASE SULPHITE LIQUOR ON THE DELIGNIFICATION OF SPRUCE WOOD AT 130° C.

Run No.	Average final concentration of sulphur dioxide (corrected)			80% delignification		90% delignification		95% delignification		Time to 90% delignification (corrected), hr. = $t_{90\%}$	Rate of delignification = $1/t_{90\%}$
	Combined, %	Total, %	Free (total−comb.), %	Time (uncorr.), hr.	Yield of pulp, %	Time (uncorr.), hr.	Yield of pulp, %	Time (uncorr.), hr.	Yield of pulp, %		
Series A											
105	0.40	2.15	1.75	6.40	54.3	8.28	50.3	10.25	48.0	8.06	0.124
104	0.39	3.40	3.01	3.82	54.0	4.83	50.3	5.98	47.8	4.61	0.217
102	0.45	4.70	4.25	2.70	56.8	3.53	52.7	4.32	50.2	3.31	0.302
103	0.44	6.51	6.07	2.05	57.0	2.63	52.4	3.26	50.2	2.41	0.415
107	0.45	8.63	8.18	1.57	55.3	2.00	51.0	2.45	48.4	1.78	0.562
Av.	0.43				55.5		51.3		48.9		
Series B											
82	0.88	2.44	1.56	9.13	61.0	11.78	56.6	14.60	54.0	11.56	0.086
81	0.98	3.95	2.97	4.25	60.8	5.38	57.0	6.65	54.2	5.16	0.194
90	0.92	5.01	4.09	2.96	60.8	3.75	56.7	4.34	54.3	3.53	0.283
87	0.91	6.16	5.25	2.37	60.2	3.02	55.6	3.60	53.5	2.80	0.357
83	0.92	7.76	6.84	1.89	60.6	2.40	56.3	2.88	53.5	2.18	0.458
91	0.92	9.05	8.13	1.70	60.8	2.12	56.3	2.62	52.9	1.90	0.527
Av.	0.92				60.7		56.4		53.7		
Series C											
96	1.93	4.62	2.69	6.45	63.8	8.60	59.0	10.75	56.2	8.38	0.119
92	1.92	5.64	3.72	3.85	64.7	4.83	60.6	5.86	57.8	4.61	0.217
98	1.97	7.03	5.06	2.74	62.7	3.47	58.2	4.15	55.8	3.25	0.308
84	1.90	8.59	6.69	2.00	65.5	2.56	60.6	3.15	56.5	2.34	0.427
94	1.94	10.36	8.42	1.67	64.3	2.08	59.3	2.41	56.7	1.86	0.538
Av.	1.93				64.2		59.5		56.6		

TABLE II—*Concluded*

SUMMARY OF THE EFFECT OF COMPOSITION OF MAGNESIUM BASE SULPHITE LIQUOR ON THE DELIGNIFICATION OF SPRUCE WOOD AT 130° C.—*Concluded*

Run No.	Average final concentration of sulphur dioxide (corrected)			80% delignification		90% delignification		95% delignification		Time to 90% delignification (corrected), hr. $= t_{90\%}$	Rate of delignification $= 1/t_{90\%}$
	Combined, %	Total, %	Free (total − comb.), %	Time (uncorr.), hr.	Yield of pulp, %	Time (uncorr.), hr.	Yield of pulp, %	Time (uncorr.), hr.	Yield of pulp, %		
Series D											
100	2.89	6.38	3.49	6.70	66.3	9.20	61.5	11.42	58.2	8.98	0.111
95	2.89	7.52	4.63	3.94	65.7	5.24	60.2	6.75	56.7	5.02	0.199
97	2.93	9.10	6.17	2.58	65.9	3.33	60.8	4.01	58.0	3.11	0.322
99	2.86	10.49	7.63	2.07	64.7	2.62	60.4	3.13	57.3	2.40	0.417
101	2.93	12.56	9.63	1.64	65.4	2.08	60.7	2.61	56.8	1.86	0.538
Av.	2.90				65.6		60.7		57.4		
Series E											
110	3.82	8.35	4.53	6.66	65.2	8.49	60.7	10.41	57.2	8.27	0.121
109	3.91	10.00	6.09	3.52	64.0	4.58	59.1	5.70	55.8	4.36	0.230
106	3.92	11.62	7.70	2.49	64.5	3.25	59.5	3.90	56.3	3.03	0.330
113	3.84	12.47	8.63	2.06	65.0	2.76	59.7	3.50	55.0	2.54	0.394
112	3.86	14.21	10.35	1.82	63.1	2.34	58.1	3.02	54.2	2.12	0.472
Av.	3.87				64.4		59.4		55.7		

A complete summary of the results of all runs is given in Table II. The range of concentration was from 0.5 to 4% combined, and 2 to 10% free sulphur dioxide.

The Relation of the Free Sulphur Dioxide to the Rate of Delignification

The average concentration of free sulphur dioxide (total − combined) for each run is listed in Table II, and is plotted against the rate of delignification $(1/t_{90\%})$ in Fig. 3. The dotted curve (C') is for Series C of the calcium base cooks taken from a previous paper (2) for comparison.
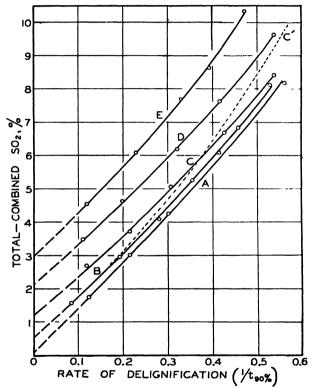
FIG. 3. *The relation of free sulphur dioxide concentration to rate of delignification of spruce wood at 130° C. Mg series A, B, C, D, E:--average combined sulphur dioxide, 0.43, 0.92, 1.93, 2.90, 3.78%, respectively. Ca series, C':--average combined sulphur dioxide, 0.90%.*

An inspection of Fig. 3 brings a number of interesting facts to light. It is observed that for magnesium base sulphite liquor the five series of combined sulphur dioxides give widely separated curves, none of which extrapolate to zero rate at zero concentration of free sulphur dioxide. Therefore, the rate of delignification of spruce wood in magnesium base sulphite liquor is decidedly not governed by the concentration of free sulphur dioxide alone, but decreases

with increasing concentration of the combined. This is contrary to the results obtained with calcium base cooks, which showed the rate of reaction to be virtually independent of the concentration of combined sulphur dioxide when the free is constant. This may possibly be due to inherent differences in the two liquors, but is more likely attributable to the fact that only a comparatively small variation in the concentration of combined sulphur dioxide is possible in the calcium base cooks because of solubility restrictions.

The rate of delignification in magnesium base sulphite liquor was also plotted for each series against the "total $- 1.5 \times$ combined sulphur dioxide," and against the "total $- 2 \times$ combined", as in the case of the calcium base cooks. The experimental data did not show any agreement with either relation. This can be made clearer in the following manner. The concentration of free sulphur dioxide for each series of combined, at the point corresponding to zero rate of delignification, was obtained by extrapolating the curves in Fig. 3. These values are listed in Table III, together with the total sulphur dioxide (free $+$ combined), and the ratio of the total to the combined, all at zero rate of delignification.

Now, if the rate of delignification were related to the liquor composition in any simple manner such as,

$$1/t_{90\%} = K \text{ [total SO}_2 - n \times \text{combined SO}_2] ,$$

where K and n are constants, then the ratio of the total to the combined sulphur dioxide at zero rate of delignification would also be constant and equal to n. If the rate of delignification were determined by the concentration of free or "excess" sulphur dioxide, n would equal 1.0, or 2.0, respectively. The last column of Table III shows that this is not so; n increases rapidly at first and then more slowly with increasing concentration of combined sulphur dioxide. Consequently, no relation of this type will fit the experimental results, and it would seem that the concentration of the active cooking agent in magnesium base sulphite liquor is not proportional to the analytical composition. Before any quantitative relation can be established,

TABLE III

THE COMPOSITION OF MAGNESIUM BASE SULPHITE LIQUOR AT POINTS CORRESPONDING TO ZERO RATE OF DELIGNIFICATION

Average combined SO₂, %	Free SO₂, %	Total SO₂, %	$\dfrac{\text{Total SO}_2}{\text{Combined SO}_2} = n$
0.43	0.10	0.53	1.23
0.92	0.45	1.37	1.49
1.93	1.20	3.13	1.62
2.90	2.10	5.00	1.73
3.87	2.95	6.82	1.76

it will be necessary to obtain equilibria data on the magnesium system, which will enable the calculation of actual ion concentrations at cooking temperatures, as in the case of the calcium system.

The ratios of the total to the combined sulphur dioxide at zero rate of delignification listed in Table III suggest that no cooking would occur in

solutions of magnesium monosulphite containing no excess sulphur dioxide. This is probably not true, since Yorston (6) found that one-third of the lignin could be removed by cooking wood in neutral sodium sulphite solutions at 130° C. However, the rate of delignification, as determined by the time to reach 90% removal of lignin, may still be zero in magnesium sulphite solutions. Even if the curves in Fig. 3 did bend downward at low concentrations of free sulphur dioxide, it is only their relative positions with which we are concerned, and the statement made regarding the inadequacy of the above equation would still hold.

Consider, now, the absolute velocities of delignification in magnesium base sulphite liquor (Fig. 3, *B*), compared with that in calcium base liquor (Fig. 3, *C'*) of the same concentration of combined sulphur dioxide (0.9%). The reaction is noticeably more rapid in magnesium base liquor than in calcium base liquor of the same mole percentage composition. This agrees with the report of Berndt (1) who suggests that the magnesium salts of lignin sulphonic acids may be more soluble than the corresponding calcium salts.

Evidence has been presented (2) to show that the rate of delignification in calcium base sulphite liquor is determined by the product of the concentrations of the hydrogen and bisulphite ions. A comparison of the reaction rates in the two systems must, therefore, be made on the basis of the true ionic concentrations at the cooking temperature. Some preliminary results of King (4) show that the partial pressure of sulphur dioxide over magnesium base liquor differs considerably from that over calcium base liquor of the same mole percentage composition. Consequently, it is probable that the hydrogen and bisulphite ion concentrations in the two systems differ, and the higher reaction velocity in magnesium base liquor may not be due to any specific effect of the metal cation itself, but, rather to different equilibria conditions prevailing in the two liquors. As soon as the vapor pressure and conductivity data regarding the magnesium system are completed, it should be possible to settle these points.

From a practical point of view, the difference in the rate of pulping in magnesium and calcium base sulphite liquors is not great enough to be of any commercial importance. The great advantage of magnesium base liquor is that the danger of precipitation of sulphites, with consequent cooking difficulties and "liming-up" of digesters, is avoided.

The Relation of the Combined Sulphur Dioxide to the Rate of Delignification

To obtain a clearer picture of the effect of the combined sulphur dioxide on the rate of delignification of spruce wood-meal in magnesium base sulphite liquor, points were taken from the curves in Fig. 3 at constant concentrations of free sulphur dioxide, and replotted against the combined. The result is shown in Fig. 4, in which the dotted lines represent areas of extrapolation.

It is observed that a symmetric family of curves is obtained, corresponding to different concentrations of free sulphur dioxide. At low concentrations of combined and high free sulphur dioxide, the reaction rate does not vary

rapidly with the combined. However, at about 2% combined the curves all bend sharply in a direction which indicates a marked decrease in the rate of cooking with increase in the combined sulphur dioxide.

At the left side of Fig. 4 a line has been drawn through the points at which the concentrations of free and combined sulphur dioxide are equal, that is, where the composition of the liquors correspond to magnesium bisulphite containing no excess sulphurous acid. The position and slope of this line show that the rate of pulping in pure magnesium bisulphite solutions, although small, is appreciable and increases slowly with increasing concentration of magnesium bisulphite.
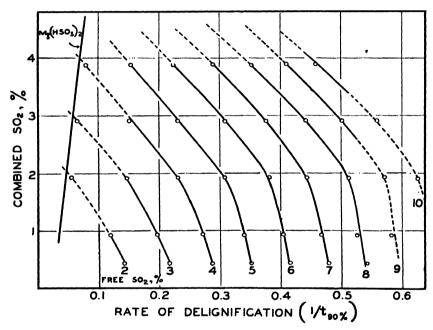
Fig. 4. *Rate of delignification of spruce wood in magnesium base sulphite liquor at 130° C. as a function of the combined sulphur dioxide concentration.*

The Effect of Liquor Composition on the Yield of Pulp

Table II shows that with magnesium base cooks the yield of pulp at a given lignin content is virtually independent of the concentration of free sulphur dioxide when the combined is constant, as was also found with calcium base cooks. In Fig. 5, the average yield of pulp for each series of combined, at 80, 90 and 95% delignification, is plotted against the average combined sulphur dioxide. The dotted curves show the same data for the calcium base cooks taken from a previous paper (2) for comparison.

It is observed that the yield of pulp from magnesium base cooks increases rapidly at first and then more slowly, reaching a maximum value at a concentration of about 3% combined sulphur dioxide, beyond which it drops slightly. Somewhat lower yields are obtained from magnesium than from calcium base cooks at low concentrations of combined sulphur dioxide, but higher yields are obtained at concentrations greater than 1% combined.

The effect of the liquor composition on the yield of pulp can be explained on the assumption that the rate of degradation of cellulose at a given temperature depends chiefly on the hydrogen ion concentration of the liquor. An increase in acidity or an increase in the length of the cook will result in a loss of yield. An increase in the concentration of combined sulphur dioxide at constant free, decreases the hydrogen ion concentration and hence increases the yield of pulp. At the same time, an increase in the concentration of combined sulphur dioxide at constant free also decreases the rate of delignification in magnesium base liquor; this lengthens the time required for cooking and so reduces the yield of pulp. These two opposing actions explain the maximum in the yield curves in Fig. 5. When the concentration of combined sulphur dioxide is constant, the rate of delignification is roughly proportional to the concentration of free sulphur dioxide. An increase in the free sulphur dioxide increases the hydrogen ion concentration of the liquor, but decreases the time required for lignin removal. This explains the approximate constancy of yield at different concentrations of free sulphur dioxide for a given concentration of combined.

FIG. 5. *The effect of the combined sulphur dioxide concentration on the yield of pulp at 130° C. —— Magnesium base; -------- calcium base. Delignification I, 80; II, 90; III, 95%.*

The difference in the yields of pulp obtained from magnesium and calcium base liquor is not great enough to be of commercial interest. With either base, the yields of pulp in these experiments with liquors containing about 1% combined sulphur dioxide are considerably higher than those obtained in sulphite mills.

Conclusion

It is impossible at the present time to discuss the theoretical significance of the data presented here on the rate of delignification of spruce wood-meal in magnesium base sulphite liquor. A knowledge of the actual concentrations of the hydrogen and bisulphite ions for the liquor compositions and temperature used is required. At the time of writing, vapor pressure and conductivity measurements are being made on the system magnesium-oxide–sulphur-dioxide–water in this laboratory by King (4). When this information is available, an interpretation of the observed effect of the liquor composition on the reaction rate should be possible. It is hoped that the data obtained will assist in elucidating the mechanism of the delignification reaction. Particular interest is attached to the high concentrations of combined sulphur dioxide, which are not possible with a calcium base liquor.

From a practical point of view it should be noted that for cooking there would appear to be an optimum liquor composition of about 1.5% combined sulphur dioxide. At lower concentrations than this the yield of pulp shows a marked decrease, and at higher, the rate of delignification is abnormally low. The use of this concentration of combined sulphur dioxide with a calcium base liquor is not feasible.

References

1. BERNDT, K. Papier-Fabr. 24 : 561, 584. 1926.
2. CALHOUN, J. M., YORSTON, F. H., and MAASS, O. Can. J. Research, B, 15 : 457-474. 1937.
3. HILLER, O. Papier-Fabr. 31 : 195. 1928.
4. KING, T. E. Unpublished results, McGill University. 1938.
5. ROSS, J. H. and POTTER, J. C. Pulp and Paper Mag. Can. 29 : 569-571. 1930.
6. YORSTON, F. H. Forest Products Laboratories of Canada, Montreal. Project 70M.
       Progress Report No. 3. 1935.

CONDUCTIVITY DATA OF AQUEOUS MIXTURES OF HYDROGEN PEROXIDE AND NITRIC ACID[1]

BY W. H. HATCHER[2] AND D. W. MACLAUCHLAN[3]

Abstract

Solutions of hydrogen peroxide and nitric acid are unstable when the concentration of the latter is greater than 50%. The conductivities of nitric acid solutions of concentrations lower than this value in water and water-peroxide mixtures have been determined, and the results indicate the formation of one or more unstable peroxides or peracids apparently incapable of ionizing.

Introduction

The present paper is an extension of the investigations of Maass and co-workers (1, 7, 8) and others (3, 5) on solutions of electrolytes in pure and in aqueous hydrogen peroxide. These have shown that inorganic salts in hydrogen peroxide as pure as 100% give conductivity curves closely resembling those obtained when pure water is used as the solvent; organic acids, on the other hand, show decreasing conductivity with increase of peroxide concentration, coincident with the formation of the so-called peracids. Also, the measured dielectric constants of hydrogen-peroxide–water mixtures, which show a maximum of 121 for 36.3% peroxide, provide no evidence that a high dielectric constant contributes directly to the ionizing power.

The following pages present the first study of the conductivity of a strong acid in hydrogen-peroxide–water mixtures.

Experimental

Preparation of Reagents

The hydrogen peroxide used throughout was prepared from 30% commercial material containing no inhibitor; this was distilled, concentrated, and, where necessary, crystallized; it contained no impurity other than water.

Nitric acid was prepared by the method of Manley and Veley (9), whose values for the conductivity of nitric acid are accepted as standard. In spite of the thoroughness of their method of preparation, it is felt that the values obtained by the dilution of highly concentrated nitric acid cannot be as trustworthy as those provided by the pure unconcentrated acid. Since the conductivities of the acid-water and acid-water-peroxide mixtures were

measured by a uniform technique in order to find any differences that might exist between the two, such slight errors as might arise from the preparation of the acid tended to cancel out.

Mixing of the Reagents

Preliminary experiments in mixing hydrogen peroxide and nitric acid showed unexpected evidence of almost explosive violence at high concentrations, whereas quite dilute solutions gave no trace of decomposition even after days of standing. It was thus early evident that the range of concentrations to be measured is restricted.

In order, therefore, to determine the limiting concentrations of reagents suitable for sustained physical measurement, various mixtures of 30 cc. or less were made in clean Pyrex test tubes and small Erlenmeyer flasks, and their behavior was carefully studied. Three types of mixtures were soon found. The first type consisted of those in which the reagents on being poured together immediately bubbled violently and then gushed forth to a height of two or three feet, crackling violently when falling on metallic gauze and occasionally igniting the bench-tops. When this occurred, the odor of ozone was very strong, brown fumes were distinctly visible, and considerable heat was developed; these reactions are listed as "instantaneous", and such mixtures termed "reactive". The second type consisted of somewhat less concentrated solutions that took from a few seconds to several hours to react, and even in those that took several hours a climax was reached which could be predicted beforehand; an originally slow ebullition increased gradually with the temperature until the latter reached 40°, 70° or even 100° C., whereupon the evolution of brown fumes became rapid; after this climax the reaction subsided rapidly. The early part of these slow reactions is due to decomposition of hydrogen peroxide by the heat of mixing of the reagents, and the reaction is delayed by cooling or using an open beaker instead of a narrow test tube. When it was possible to trap the products of these reactions, the residue represented most of the nitric acid employed but showed complete absence of any hydrogen peroxide. The third type was stable for a period of 24 hr., and is here termed "unreactive".

Fig. 1 shows a convenient representation of the limits of reactivity of these mixtures obtained by adding various volumes of nitric acid of different concentrations to 1 cc. of 62.9% hydrogen peroxide in water at 21 to 23°C. A large collection of data showed that the controlling factor in promoting reaction is

FIG. 1. *Reacting volumes of nitric acid and hydrogen peroxide; showing volumes of aqueous nitric acid of various concentrations added to one volume of 62.9% hydrogen peroxide at 21 to 23° C. A, lower limit of instantaneous reaction; B, lower limit of any noticeable reaction.*

the concentration of nitric acid rather than that of the peroxide, and that it is not possible to have a concentration of acid greater than 50% in the acid–hydrogen-peroxide–water mixture without the possibility of reaction.

Those mixtures which were "unreactive", e.g., below Curve B in Fig. 1, were made to react by heating, but even then only a mild decomposition with loss of oxygen occurred.

When the same type of container was used in the above-mentioned experiments, the results were easily reproducible; but the addition of pieces of capillary tubing largely increased the rate of decomposition, while mixing the reagents in beeswax-lined glass containers decreased it appreciably.

In order to avoid any possibility of decomposition during the measurements to be described, concentrations represented by points below Curve B, Fig. 1, were chosen, the temperature was kept from start to finish at 0° C. by means of an ice-water bath, and Pyrex containers were used throughout.

Determination of Conductivity

The method used for determining the conductivity was the static one, and the apparatus similar to that previously described (1, 3); all connecting wires were shielded in copper tubing, and the electrodes were thin sheets of gold, 4 by ¼ in., since tin and platinum were found unsuitable in the presence of both nitric acid and hydrogen peroxide. Manley and Veley (9) and Jones and Murray (5) used the a-c. method of Kohlrausch for nitric-acid–water mixtures, and although the authors obtained small differences using the static method, the accuracy of the latter method is attested by the excellent agreement with the standard values for oxalic acid.

Three cells of different diameter were used, and, standardized with potassium chloride, showed cell-constant values of 13.56, 108.03, and 579.6. A check on the procedure, molar oxalic acid being used, gave a specific conductivity at 18° C. of 589.5 × 10⁻⁴ as compared with the accepted value of 590 × 10⁻⁴. In the preparation of each mixture, the solutions of nitric acid and hydrogen peroxide, whose concentrations were accurately known, were added to the exact quantity of water required (if any); these were accurately weighed in and the specific gravity of each mixture immediately determined. For convenience of treatment the experi-
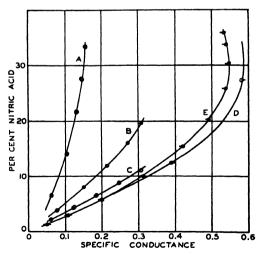
FIG. 2. *Specific conductance of nitric acid in water and hydrogen peroxide. A, water = 22 to 25% by weight; B, water = 55 to 57%; C, water = 75 to 77%; Per cent H₂O₂ = 100 − (H₂O + HNO₃); D, nitric acid in water only (authors); E, same (Manley and Veley).*

mental values obtained are shown in weight percentage unless otherwise stated.

In Fig. 2 are the curves showing the specific conductance of mixtures of nitric acid, hydrogen peroxide, and water. The discrepancy between D and E can be partly accounted for by the difficulty in obtaining pure nitric acid of high concentrations. Also the difficulty of measuring the conductivity of concentrated acids is evidenced by Newbery's value for sulphuric acid (12) which is 3% lower than that of Kohlrausch and Grotrian (6) and was substantiated by the work of Marie and Noyes (10). Incidentally Manley and Veley believed nitric acid to be a mixture of nitric acid, water, and nitrogen pentoxide.

In contrast to organic acids (3), nitric acid and hydrogen peroxide give an immediate reading which does not change with time, as shown by a mixture of 19.93% of nitric acid, 24.67% of hydrogen peroxide, and 55.40% of water whose specific conductance remained at 0.300 over a period of 24 hr.

At low concentrations of nitric acid and high concentrations of hydrogen peroxide, the effect of the latter on the conductance though small was taken into account by determining its specific conductance separately and subtracting it proportionately from the total value obtained from the mixture. These final values are those shown in Fig. 2.

Fig. 3 shows a different plotting of some of the results obtained, and Fig. 4 shows the molar conductivity of such solutions.
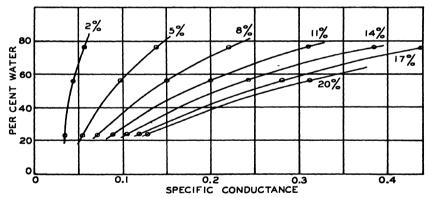
FIG. 3. *Specific conductance of nitric acid in water–hydrogen-peroxide mixtures. Weight percentages of nitric acid and water as shown; percentage of peroxide = 100 − (H_2O + HNO_3).*

The Viscosity of Nitric-acid–hydrogen-peroxide–water Mixtures

Equal volumes of 31% nitric acid and 34% hydrogen peroxide were mixed and the time of flow taken in an Ostwald viscosimeter 0° C.; the specific viscosity was found to be 1.093, whereas that of 31% nitric acid is 1.19 and that of 34% peroxide, 1.00.

The Conductivity of Sulphuric Acid in Aqueous Hydrogen Peroxide

Several determinations were made at 18° C. for comparison with the standard values, sulphuric acid, 41.7% and 87.7%, in water only, being

used: the respective specific conductances were 0.667 and 0.1076 as compared with 0.662 and 0.108 obtained by Kohlrausch and Grotrian (6). The specific conductance of 45% sulphuric acid in water at 18° C. is 0.620; the same concentration of acid with 3.34, 15.6, and 22.0% of hydrogen peroxide gave respective specific conductances of 0.536, 0.341, and 0.196.

Chemical Tests of Nitric-acid–hydrogen-peroxide Mixtures

Whereas neither hydrogen peroxide nor nitric acid shows any immediate reaction with benzene, a "reactive" mixture of the two, free from nitrous acid, produces a definite and persistent greenish-yellow coloration (11, p. 382). An "unreactive" mixture gave no such coloration but did produce iodine instantaneously on addition to a very dilute neutral solution of potassium iodide; with a more concentrated mixture—34% of peroxide and 31% of acid—a very large instantaneous precipitate of iodine was produced, though with no apparent liberation of oxygen even after several hours.

These tests, especially the latter, are considered satisfactory evidence of peracid formation.

Discussion of Results

The instability of hydrogen-peroxide–nitric-acid–water mixtures is apparently due to the formation of a highly unstable complex, which, forming immediately on the mixing of the reagents and in proportion to their concentrations, decomposes exothermally; the accumulation of this heat hastens the decomposition so that in the vicinity of certain critical concentrations the evolution of oxygen and nitrogen oxides may occur with violence. This is, of course, in line with the instability of nitric acid itself of concentrations above 70%.

This unstable complex may be a peracid or a peroxide of nitrogen, for the previously noted observation of Manley and Veley that the formula HNO_3 is an ideal expression to represent the presence of HNO_3, H_2O, and N_2O_5 all at once might be taken to suggest the existence of HNO_4, HNO_5, etc., and also N_2O_6, N_2O_7, etc. Shilov and co-workers (15) represent a reaction between nitrous acid and hydrogen peroxide as

$$2\ HNO_2 + H_2O_2 \rightarrow N_2O_4 + 2\ H_2O.$$

Friend (2, p. 333) states that at low temperatures pure hydrogen peroxide and nitrogen pentoxide together show the characteristics of a peracid; thus

$$H_2O_2 + N_2O_5 \rightarrow HNO_3 + HNO_4.$$

Raschig (14) on treating nitrous acid with 3% hydrogen peroxide solution concluded that pernitric acid is produced, which slowly decomposes into nitric acid and hydrogen peroxide:

$$HNO_4 + H_2O \rightarrow HNO_3 + H_2O_2.$$

Pollak (13) established the formation of pernitric acid from nitric acid and hydrogen peroxide in the presence of potassium bromide. Also Helbig (4) claimed the formation of an unstable N_2O_6 when a series of electrical discharges

was sent through liquid air; this substance he reported as decomposing, sometimes explosively, with the evolution of brown fumes.

In the absence of any exact quantitative data regarding the composition of these peracids either from the literature or in the work so far of the present authors, even the term "pernitric acid" is held unjustifiable.

However, the results here presented, pure nitric acid—free from nitrous acid —and pure hydrogen peroxide being used, show that the behavior of this mixture is in accord with that of mixtures in which sulphuric and many organic acids were employed in producing an electrical conductivity lower than that obtained when the acid–water mixture alone is used.
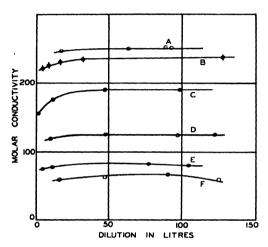
FIG. 4. *Molar conductivity of nitric acid in water and hydrogen peroxide. A, in water only (authors); B, same (Jones and Murray); C, in water and hydrogen peroxide (19.2%); D, in water and hydrogen peroxide (40.0%); E, in water and hydrogen peroxide (61.4%); F, in water and hydrogen peroxide (79.6%).*

Fig. 2 shows that at any concentration of nitric acid in a mixture of water and hydrogen peroxide the last named produces a decrease in the specific conductance approximately proportional to its concentration. This fact is better shown in Fig. 3 where extrapolation to zero water concentration indicates that solutions of pure nitric acid in pure hydrogen peroxide should give a specific conductance of approximately 0.04.

In Fig. 4 are shown the values for molar conductivity of nitric acid in water (the authors' and Jones') and in water–peroxide mixtures; thus the higher the peroxide content of the medium the less able is the solution to conduct the current. This is also exemplified by the figures in Table I. Here a small change in nitric acid and dilution but a large increase in peroxide content produce a striking decrease in molar conductivity.

The apparent unimportance of viscosity and dielectric properties points to the possible union of nitric acid and hydrogen peroxide to form a non-conducting substance as the only explanation of the results here related. Indeed it is possible, all other factors being ignored, to show that at any fixed water-content of these mixtures the observed specific conductance differs from that of nitric acid in water only by an amount

TABLE I

Nitric acid, %	Hydrogen peroxide, %	Dilution in litres	Molar conductivity
19.65	25.47	0.264	81.5
20.82	54.88	0.218	28.5

that is determined by the removal from the ionic state of molecules of nitric acid and hydrogen peroxide. Such an empirical relation, however unjustified, does suggest that the current carried is a measure of the "free" hydrogen ions in "free" water.

At any rate the values obtained definitely point to retention of the electrolyte by hydrogen peroxide apart from the possible influence of viscosity, dielectric properties, solvation of the ions by hydrogen peroxide, or changes in water aggregations.

The following equation suggests an analogy to organic peracids:—

$$x \; H_2O \; + \; HNO_3 \; \rightleftharpoons \; HNO_3(O)_x \; + \; x \; H_2O.$$
$$H^+ \stackrel{\textstyle\parallel}{+} NO_3^-$$

Sulphuric acid shows the same tendency as nitric acid to decreased conductance; this is in accord with the work of Maass and Matheson (8). Jones and Murray (5) found that oxalic and sulphuric acids cause a freezing-point depression in dilute hydrogen peroxide solutions greater than that when pure water is used as the solvent, and the opposite of this for salt solutions; from this they argued that in mixtures of acids and hydrogen peroxide the dissociation is greater, and in mixtures of salts and hydrogen peroxide there is compound formation. The peroxide content was so small, however, that these explanations do not seem convincing.

The investigation of nitric-acid–peroxide mixtures is proceeding with a view to establishing the nature of the possible peracid or peroxide involved.

References

1. CUTHBERTSON, A. C. and MAASS, O. J. Am. Chem. Soc. 52 : 489-499. 1930.
2. FRIEND, J. N. Text-book of inorganic chemistry. J. B. Lippincott, Philadelphia. Vol. VII. 1931.
3. HATCHER, W. H. and POWELL, E. C. Can. J. Research, 7 : 270-282. 1932.
4. HELBIG, D. Atti accad. Lincei, (5) 11 : ii. 57. 1902.
5. JONES, H. C. and MURRAY, G. Am. Chem. J. 30 : 205-209. 1903.
6. KOHLRAUSCH, F. and GROTRIAN, O. Pogg. Ann. 154 : 1, 215-239. 1875.
7. LINTON, E. P. and MAASS, O. J. Am. Chem. Soc. 53 : 957-964. 1931.
8. MAASS, O. and MATHESON, G. L. J. Am. Chem. Soc. 51 : 674-687. 1929.
9. MANLEY, J. J. and VELEY, V. H. Phil. Trans. (A) 191 : 365-398. 1898.
10. MARIE, C. and NOYES, W. A. J. Am. Chem. Soc. 43 : 1095-1098. 1921.
11. MELLOR, J. W. A comprehensive treatise on inorganic and theoretical chemistry. Longmans, Green & Co., New York. Vol. VIII. 1928.
12. NEWBERY, E. J. Chem. Soc. 113 : 701-707. 1918.
13. POLLAK, F. Z. anorg. allgem. Chem. 143 : 143-162. 1925.
14. RASCHIG, F. Z. angew. Chem. 17 : 1419. 1904; 20 : 694. 1907.
15. SHILOV, E. A., RUIBAKOV, A. A. and PAL., M.A. Bull. inst. polytech. Ivanovo-Vosniesensk, 15 : 85-105. (Chem. Abstr. 25 : 5826. 1931.)

THE KINETICS OF THE DECOMPOSITION REACTIONS OF THE LOWER PARAFFINS

II. ISOBUTANE[1]

BY E. W. R. STEACIE[2] AND I. E. PUDDINGTON[3]

Abstract

The kinetics of the thermal decomposition of isobutane has been investigated over an initial pressure range of from 5 to 60 cm., and at temperatures from 522 to 582° C. The initial first order rate constants at high pressures are given by

$$\log k = 13.92 - \frac{63500}{2.3\,RT} \text{ sec.}^{-1}$$

The results are in general agreement with those obtained by previous investigators. The reaction rate falls off with diminishing pressure, and the first order rate constants in a given run diminish strongly as the reaction proceeds. This behavior is similar to that of n-butane.

Analyses of the products of the reaction were made at various stages, temperatures, and initial pressures by low-temperature distillation in a still of the Podbielniak type. The initial products were found by extrapolation to be H_2, 35; CH_4, 14; C_2H_4, 0.9; C_2H_6, 0.9; C_3H_6, 14; and C_4H_8, 35%. The results are compared with those of other workers.

Introduction

In a recent paper from this laboratory (16) it was pointed out that the thermal decomposition reactions of the simple paraffin hydrocarbons offer interesting possibilities for a study of the effect of chemical configuration on the reaction rate. A review of the literature by one of us (14) has shown that the existing kinetic data are far too unreliable to enable any comparison between the various members of the paraffin series. This is particularly true of the isomers of butane. In view of this an investigation has been made of the decomposition of the two butanes. The present paper deals with that of isobutane.

Pease (10), and later Pease and Durgan (11), using a flow method, first showed that the reaction was first order and homogeneous. The velocity constant at 600° C. was found to be 7.6×10^{-3} sec.$^{-1}$, and the activation energy was very roughly estimated to be 65,000 cal.

Paul and Marek (9), using a similar method, obtained a value of 66,000 cal. for the activation energy. Their velocity constants varied from 2.8 to 32.6 $\times 10^{-3}$ sec.$^{-1}$ at temperatures from 550° to 610° C. Their work was done at low conversions, about 5% of the isobutane being decomposed.

Frey and Hepp (5) worked at one temperature only, 575° C., and found a velocity constant of 4.8×10^{-3} sec.$^{-1}$.

Marek and Neuhaus (8), Hurd and Spence (6), and others (4) examined the products of the reaction only. Their results will be discussed later.

Experimental

In this investigation a static system was used almost entirely, a flow apparatus being employed for a few runs to study the products at low conversions. As the static system and experimental technique have been described elsewhere (16), they will not be discussed here.

The flow system is shown diagrammatically in Fig. 1. Purified isobutane was stored as a liquid in a bulb connected to the apparatus by a ground joint. In series with the gas supply was a 10 litre volume which served to stabilize the pressure. Stopcocks, which had been scratched with a file, at *A* and *B*, served to control the flow of gas. The rate of flow of the gas could be estimated by turning the three-way stopcock so that the gas flowed directly into the manometer.
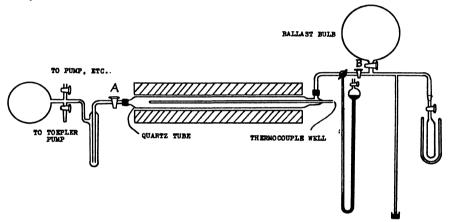
FIG. 1.   *Flow apparatus.*

The reaction vessel for the flow system was a two-foot length of transparent quartz tubing having a volume of 80 cc. Into one end was sealed a thermocouple well which extended nearly the entire length of the vessel. Since the remainder of the apparatus was of soft glass, the reaction vessel was attached with de Khotinsky cement.

The furnace consisted of a piece of $1\frac{1}{4}$ in. iron pipe wound with nichrome ribbon (0.44 ohm per ft.), and wrapped with asbestos paper. At the temperature of operation the reaction vessel had a temperature gradient of 5° from the centre to either end. The temperature of any location could be controlled to ± 1°.

A trap immersed in liquid air, in series with an expansion bulb of two litres volume, kept the back pressure sufficiently low that the rate of flow was not appreciably altered during a run. On completion of an experiment the products were expanded into the two litre bulb, pumped into a portable gas-holder by means of a Toepler pump, and transferred to the low-temperature distillation apparatus. The small capacity of the analytical still (about

one litre of gas) limited the usefulness of the flow system in studying the products at low conversions.

Isobutane of 99% purity, obtained in cylinders from the Ohio Chemical and Mfg. Co., was purified in a low temperature still of the Podbielniak type prior to use. The purified gas contained no detectable impurity.

Results

After the first few runs the rates became completely reproducible. Somewhat more polymerization to higher compounds occurred than with *n*-butane, although the total amount of higher products formed per run was negligible. After about 10 runs in the packed reaction vessel, the quartz packing became covered with a thin layer of carbon.

Runs carried to completion showed a pressure increase of about 108%. The amount in excess of 100% was doubtless due to secondary reactions, since analytical results showed that 25% pressure increase corresponded to 25% decomposition.
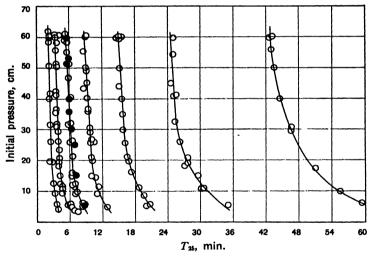
FIG. 2. *Effect of pressure on rate. Curves from left to right are for temperatures 582, 572, 562, 552, 543, 533, 522, respectively. Full circles represent determinations with reaction bulb packed with crushed quartz.*

Data for a typical run are given in Table I. Unimolecular constants are calculated on the assumption that 100% pressure increase corresponds to completion. Table II shows the effect of temperature and initial pressure on the rate of reaction. In the table, $T_{12.5}$ and T_{25} correspond to pressure increases of 12.5 and 25% respectively.

The data of Table II are shown graphically in Fig. 2. It will be seen that the rate, as inferred from the times to fractional values, falls off with diminishing initial pressure. High pressure rates were obtained by plotting the

TABLE I

DATA FOR A TYPICAL EXPERIMENT AT 562° C.

Initial pressure, 41.90 cm.

Time, min.	P, cm.	k, sec.$^{-1}$	Time, min.	P, cm.	k, sec.$^{-1}$
0.5	2.00	16.15×10^{-4}	39	29.75	5.30×10^{-4}
1	3.35	13.81	46	31.85	5.18
3	6.95	11.50	56	34.18	5.05
5	9.52	8.62	71	36.75	4.92
8	12.65	7.50	84	38.32	4.88
12	16.08	6.73	113	40.90	5.04
15	18.28	6.40	138	42.30	—
22	22.56	5.87	243	45.00	—
31	26.85	5.51	278	45.60	—

fractional times against the reciprocal of the initial pressure and extrapolating to infinite pressure as shown in Fig. 3. Table III gives the values of the rate constants obtained in this way.

The theoretical value of the ratio $T_{25}/T_{12.5}$, 2.16, is considerably lower than the experimental values. This was also observed by us in the decomposition of n-butane, and has also been noted by Dinzes (1-3) in the decomposition of ethane and propane. Since the first order constants fall off rapidly in an individual run, as shown by Table I, this is, of course, to be expected.

As pointed out before (16), reaction rate curves must have identical forms at different temperatures if the calculated value of the activation energy is to be unaffected by the drift in the rate constants as the reaction progresses. The simplest way of testing this is to compare the values of the ratio $T_{25}/T_{12.5}$ at various initial pressures and temperatures. Table IV gives data of this sort. As the value of this ratio is virtually independent of the initial pressure and temperature, the values in
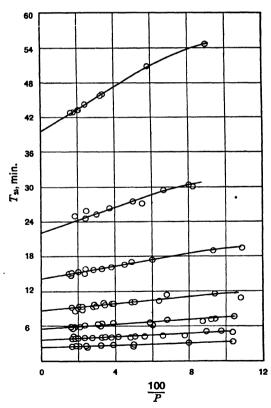
FIG. 3. *Extrapolation of rates to infinite pressure. Curves from top to bottom are for temperatures 522, 533, 543, 552, 562, 572, 582, respectively.*

TABLE II
VARIATION OF REACTION RATE WITH TEMPERATURE AND PRESSURE

Initial pressure, cm.	$T_{12.5}$, min.	T_{25}, min.	Initial pressure, cm.	$T_{,12.5}$, min.	T_{25}, min.

Temperature, 522° C.

6.10	18.0	59.0	40.40	14.2	44.8
10.78	17.5	55.4	49.62	13.3	43.3
17.40	16.0	51.0	56.40	14.0	42.8
29.50	15.0	46.5	60.20	13.2	43.0
30.40	14.8	46.5	60.25	13.3	43.2

Temperature, 533° C.

6.32	11.3	35.0	26.67	8.1	25.9
10.45	10.7	30.3	32.86	7.8	24.8
12.01	9.3	30.0	40.80	8.0	24.8
15.10	9.3	29.7	40.80	8.5	25.4
18.13	8.8	27.0	45.40	7.3	24.1
19.45	9.5	27.4	54.40	7.8	24.8
20.20	8.9	27.8	60.10	7.9	24.9

Temperature, 543° C.

5.02	6.7	19.9	35.6	5.0	15.5
5.18	8.2	20.9	40.9	5.5	15.8
8.40	6.5	19.5	42.6	4.6	15.0
10.76	6.3	19.2	49.7	5.1	15.3
16.65	5.8	17.1	49.9	4.9	15.1
20.30	5.5	16.8	59.1	5.1	15.2
21.3	5.3	16.6	60.1	4.9	14.7
27.0	5.7	16.3	60.3	4.9	15.0
30.2	5.4	15.3	60.9	4.8	15.0

Temperature, 552° C.

4.50	4.5	13.0	29.8	3.4	9.9
9.30	3.2	10.8	30.1	3.3	9.8
10.58	4.2	11.8	35.2	3.2	9.7
10.60	4.2	12.8	35.8	3.3	9.4
14.75	3.8	11.8	40.3	3.0	9.1
15.65	3.6	10.1	43.9	2.9	8.9
20.30	3.3	10.2	45.2	3.1	9.3
20.4	3.5	10.0	49.7	3.2	9.4
25.3	3.6	10.1	50.5	3.1	9.0
25.5	3.4	10.0	55.3	2.9	8.5
25.5	3.3	10.1	60.0	2.9	9.1
			60.2	3.1	9.1

TABLE II—*Concluded*

VARIATION OF REACTION RATE WITH TEMPERATURE AND PRESSURE

Initial pressure, cm.	$T_{12.5}$, min.	T_{25}, min.	Initial pressure, cm.	$T_{, 12.5}$, min.	T_{25}, min.
Temperature, 562° C.					
4.85	2.6	8.3	25.9	2.1	6.3
5.22	2.7	8.3	30.8	2.1	6.3
5.36	2.9	8.5	31.5	2.1	6.0
6.65	2.8	8.0	40.3	2.1	6.2
8.65	2.1	6.3	47.6	2.1	5.9
9.80	2.5	7.5	51.2	2.0	6.0
10.61	2.5	7.3	55.0	1.9	5.6
10.81	2.2	7.2	59.6	2.0	5.9
11.42	2.6	6.8	59.7	1.9	5.6
14.95	2.2	6.9	60.0	1.9	5.8
16.50	2.2	6.2	60.0	1.9	5.8
20.40	2.2	6.8	60.0	1.9	5.7
25.2	2.1	6.4			
Temperature, 562° C. Packed reaction vessel.					
5.01	3.1	8.8	36.9	2.0	6.1
15.2	2.6	7.6	40.0	2.1	6.3
26.0	2.4	6.6	51.2	2.0	6.0
30.0	2.0	6.1	53.6	2.1	6.1
			59.8	1.9	5.9
Temperature, 572° C.					
3.0	2.8	7.0	30.3	1.4	4.0
4.3	2.2	6.1	30.8	1.3	4.0
5.3	2.1	6.1	35.8	1.3	3.7
5.5	2.3	6.3	36.2	1.3	3.9
5.5	2.0	5.4	41.0	1.3	3.8
9.6	1.7	4.9	42.4	1.4	3.8
11.2	1.7	5.0	50.7	1.3	3.9
12.8	1.5	4.3	51.3	—	3.8
15.1	1.5	4.4	55.3	1.3	3.9
18.0	1.3	3.9	58.3	1.3	3.9
19.8	1.4	4.2	60.0	1.3	3.8
20.7	1.4	4.1	60.4	1.3	4.0
23.3	1.4	4.1	60.7	1.3	3.9
26.3	1.3	4.0			
Temperature, 582° C.					
4.1	1.1	3.6	40.2	1.0	2.4
5.1	1.4	4.0	40.8	0.9	2.7
9.6	1.1	3.2	58.2	0.7	2.2
12.4	1.1	3.2	60.0	—	2.5
19.8	0.9	2.5	60.0	0.8	2.5
19.9	1.0	2.9	61.0	0.8	2.5
25.7	1.0	2.8	61.0	0.7	2.2
31.4	1.0	2.8	62.0	0.8	2.2

TABLE III

EXTRAPOLATION OF RATE DATA TO INFINITE PRESSURE

Temperature, °C.	$T_{12.5}$, sec.	T_{25}, sec.	$T_{25}/T_{12.5}$	$k \times 10^4$, sec.$^{-1}$ (calculated from T_{25})
522	747	2382	3.15	1.21
533	408	1278	3.13	2.25
543	270	843	3.12	3.41
552	168	495	2.95	5.81
562	113	333	2.95	8.64
572	70	215	3.09	13.4
582	46	141	3.05	20.4
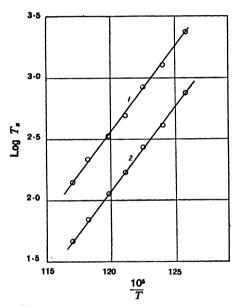
FIG. 4. *The temperature coefficient of the reaction. Curve 1, log* $T_{25} - \dfrac{10^5}{T}$ *. Curve 2, log* $T_{12.5} - \dfrac{10^5}{T}$ *.*

Table III can be used to determine the energy of activation. This has been done graphically in Fig. 4, where Curve 1 is constructed from the values of T_{25} and Curve 2 from those of $T_{12.5}$. Identical values of 63,500 calories per mole are obtained for the energy of activation in each case. Whence we obtain for the velocity constants, calculated from the values of T_{25}, the equation

$$\log_{10} k = 13.62 - \frac{63500}{2.3\,RT} \text{ sec.}^{-1}$$

Since the value of the velocity constant diminishes as the reaction proceeds, as shown by Table I, it is obvious that the above equation does not give the *initial* rate of reaction. From the data of a large number of runs, it appears that the initial rate constant is almost exactly 100% higher than that at T_{25}. Correcting for this we have for the initial high pressure rate

$$\log_{10} k = 13.92 - \frac{63500}{2.3\,RT} \text{ sec.}^{-1}$$

That the reaction is not appreciably heterogeneous is shown by the position of the full circles in Fig. 3. These points represent runs in which the reaction vessel was packed with broken silica tubing, thereby increasing the surface/volume ratio by a factor of about 15 over that of the empty vessel in which the rest of the experiments were made.

The Products of the Reaction

The products of the reaction were analyzed by low temperature fractional distillation. Samples for this purpose were taken at $T_{12.5}$, T_{25}, and T_{50} at an initial pressure of 60 cm. over the entire temperature range. One analysis was also made from an experiment with an initial pressure of 20 cm. These results are given in Table V. Results of two runs made in the flow system at decompositions of 5.3 and 7.5% are given in Table VI. The mean values of all these results indicate that T_{50}, T_{25}, and $T_{12.5}$ as inferred from the pressure change really correspond to 51.0, 25.0, and 12.0% reaction respectively.

In the analyses, hydrogen and methane were distilled off together, and this fraction analyzed by combustion. It is perhaps worth pointing out that isobutene is difficult to determine accurately since its boiling point is below and close to that of isobutane, which is pres-

TABLE IV

VALUES OF $T_{25}/T_{12.5}$ AT VARIOUS TEMPERATURES AND PRESSURES

Temperature, ° C.	$T_{25}/T_{12.5}$			
	Infinite pressure	50 cm.	25 cm.	20 cm.
582	3.05	2.99	3.11	2.90
572	3.09	3.00	2.99	3.03
562	2.95	3.02	3.08	3.14
552	2.95	2.99	3.05	3.12
543	3.12	3.09	2.98	3.05
533	3.13	3.17	3.08	3.14
522	3.15	3.16	3.20	3.20

TABLE V

THE PRODUCTS OF THE REACTION IN THE STATIC SYSTEM

Temperature, ° C.	522	543	552	562	572	582	Mean
Products, mole %	*Initial pressure = 60 cm.*		*Sampled at T_{50}*				
H_2	—	19.5	20.8	20.3	21.6	21.0	20.6
CH_4	—	38.6	37.5	36.2	36.6	36.2	37.0
C_2H_4	—	4.0	2.8	3.3	2.2	3.7	3.2
C_2H_6	—	5.2	3.9	5.0	4.4	4.1	4.3
C_3H_6	—	17.0	18.3	18.6	17.7	18.0	17.9
C_4H_8	—	15.6	16.8	16.4	17.5	17.0	16.7
% C_4H_{10} decomposed	—	51.2	50.0	52.2	50.7	50.8	51.0
Products, mole %	*Initial pressure = 60 cm.*		*Sampled at T_{25}*				
H_2	26.7	25.0	25.8	27.7	25.0	24.8	25.8
CH_4	28.5	28.2	29.1	27.2	28.5	27.8	28.2
C_2H_4	2.5	1.8	3.8	2.1	1.4	2.5	2.3
C_2H_6	3.5	3.5	2.2	2.4	2.7	2.4	2.8
C_3H_6	18.2	18.6	16.2	17.9	20.0	18.5	18.2
C_4H_8	20.5	23.0	23.3	22.9	22.7	24.0	22.7
% C_4H_{10} decomposed	25.7	24.6	25.0	22.7	27.9	24.2	25.0
Products, mole %	*Initial pressure = 60 cm.*		*Sampled at $T_{12.5}$*				
H_2	30.0	31.6	29.8	31.4	30.3	—	30.6
CH_4	20.1	21.1	20.5	21.0	20.1	—	20.6
C_2H_4	2.0	1.6	1.0	—	2.0	—	1.3
C_2H_6	2.0	1.5	2.3	—	2.1	—	1.6
C_3H_6	17.7	14.5	17.7	17.8	16.8	—	16.9
C_4H_8	28.2	29.5	28.9	29.8	28.4	—	29.0
% C_4H_{10} decomposed	11.7	12.2	12.5	12.0	13.5	—	12.0
	Initial pressure = 20 cm. Temp. = 562° C. Sampled at T_{50}						
Products, mole %	H_2 22.0, CH_4 36.0, C_2H_4 3.6, C_2H_6 3.5, C_3H_6 17.0, C_4H_8 18.0, % C_4H_{10} decomposed 48.0.						

ent in large amount, and, unless care is taken, normal butane, which is often present as an impurity in isobutane, may easily be included with it.

TABLE VI

THE PRODUCTS OF THE REACTION IN THE FLOW SYSTEM

Initial pressure = 60 cm.
Temperature = 572° C.

Products	Mole %	
H_2	33.7	30.5
CH_4	15.1	16.0
C_2H_4	—	1.5
C_2H_6	—	1.5
C_3H_6	16.3	21.0
C_4H_8	34.8	30.0
% C_4H_{10} decomposed	7.5	5.3

Small amounts of propane, of the order of 1% or less, were detected, but since an accurate separation of this small quantity from propylene is very difficult, it was included in the propylene fraction. It does not appear to be an initial product, and is probably formed by the hydrogenation of propylene.

From Table V it appears that the products are virtually independent of initial pressure and of temperature over the range examined.
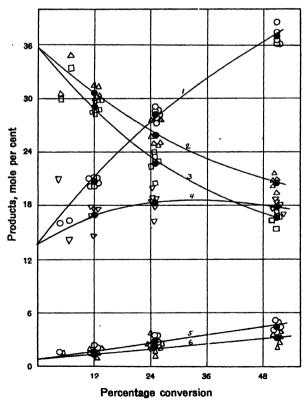
FIG. 5. *Extrapolation to initial products. Curve 1, methane; Curve 2, hydrogen; Curve 3, butylene; Curve 4, propylene; Curve 5, ethane; Curve 6, ethylene. Filled circle in each case is the mean of the group.*

Initial products were obtained graphically, as shown in Fig. 5. The extrapolated values thus obtained are:—H_2, 35.0; CH_4, 14.0; C_2H_4, 0.9; C_2H_6, 0.9; C_3H_6, 14.0; C_4H_8, 35.0 mole per cent.

Discussion

The Rate of the Reaction

Comparing the values of E and A with those of other workers, we have—

	E, Kcal.	$\log_{10} A$	K_{575}, sec.$^{-1}$
Pease and Durgan	65.0	14.23*	1.6 $\times$ 10^{-3}*
Paul and Marek	66.0	14.89	7.1 $\times$ 10^{-3}
Frey and Hepp	.—	—	4.8 $\times$ 10^{-3}
This investigation	63.5	13.92	3.0 $\times$ 10^{-3}

*Calculated from the value given for 600° C.

A similar comparison for n-butane follows—

	E, Kcal.	$\log_{10} A$	K_{575}, sec.$^{-1}$
Frey and Hepp	61.4	13.53	4.8 $\times$ 10^{-3}
Paul and Marek	73.9	17.05	9.8 $\times$ 10^{-3}
Steacie and Puddington	58.7	12.71	3.7 $\times$ 10^{-3}

In both cases the agreement of our data with those of Frey and Hepp is satisfactory. Agreement with the results of Paul and Marek is considerably better with isobutane than with n-butane. From our work it appears that while the activation energy for isobutane is somewhat higher than that for n-butane, the large difference between the two reported by Paul and Marek is fictitious.

In our paper on the decomposition of n-butane it was pointed out that the calculated value of the activation energy was somewhat higher at low pressures than at high, owing to the slight variation with temperature of the falling off in rate with pressure. From our data the difference between the true activation energy and that calculated from rates at atmospheric pressure was determined, and applied as a correction to the results obtained by other workers at atmospheric pressure. Owing to an arithmetical error, this calculated correction was too high. The proper correction is 1.7 Kcal. instead of 7.5 as given. Correcting the data for n-butane in this way, we obtain

Frey and Hepp	59.7 Kcal.
Paul and Marek	72.2
Steacie and Puddington	58.7

In other words there is now almost exact agreement with the results of Frey and Hepp.

If the same type of calculation is made for isobutane, we have

True activation energy	63.5 Kcal.
Calculated from results at	
76 cm.	63.5
33 cm.	63.6
20 cm.	64.0 .

In this particular case, therefore, there is no correction to be applied to results obtained at atmospheric pressure.

The Products of the Reaction

A comparison of the products obtained by various workers is given in Table VII. Fair agreement exists throughout, provided that the products are compared at the same degree of decomposition. The work of Frey and Hepp was done within the temperature range of this investigation, while that of Marek and Neuhaus, and Hurd and Spence was done at a slightly higher temperature (600°C.).

Qualitative agreement with the predictions of the Rice free radical theory (13) is obtained, since the chief products are H_2, C_4H_8, C_2H_6, and CH_4 as predicted. However, on the Rice theory the ratio

$$\frac{C_4H_8 + H_2}{CH_4 + C_2H_6}$$

should be equal to 1.1. Actually, the experimental value of this ratio is 2.5. Whether or not the compound decomposes by a free radical mechanism seems to be an open question at the moment. It may, however, be remarked that the value of the activation energy obtained in this work is not very much above the activation energy of the split into free radicals (12, 13), and hence it is not necessary to postulate long chains if a free radical mechanism is to hold. The falling-off in rate with diminished pressure,

TABLE VII

COMPARISON OF THE PRODUCTS OBTAINED BY VARIOUS WORKERS

Observers	Percent C_4H_{10} decomposed	H_2	CH_4	C_2H_4	C_2H_6	C_3H_6	C_3H_8	C_4H_8
Marek and Neuhaus	0.0	31.5	17.5	—	1.2	17.0	—	31.5
Steacie and Puddington	0.0	35.0	14.0	0.9	0.9	14.0	—	35.0
Frey and Hepp	17.4	24.4	21.9	1.1	1.2	16.2	5.0	30.0
Steacie and Puddington	17.4	27.6	25.4	1.8	2.2	17.8	—	25.4
Frey and Hepp	6.7	29.5	20.6	0.0	1.1	15.7	1.9	31.1
Steacie and Puddington	6.7	30.8	18.6	1.2	1.4	15.9	—	32.2
Hurd and Spence	22.0	21.3	35.5	3.5	—	17.3	—	22.5
Steacie and Puddington	22.0	26.8	26.4	2.0	2.5	18.0	—	23.9

discussed in the next section, furnishes some evidence in favor of a free radical mechanism. Furthermore, as shown by Table I, the velocity constants fall off very strongly in an individual run. In the later stages of the reaction this is partly due to the back hydrogenation reactions coming into play. In the early stages of the reaction, however, the falling-off is even more pronounced, and calculation from the equilibrium constant of the dehydrogenation reaction (4) shows that at this stage the back reaction is negligible. The effect may therefore be due to some sort of chain process.

The Effect of Pressure on the Rate of Reaction

As was the case with the normal isomer, the rate of decomposition of isobutane falls off strongly with decreased initial pressure. This effect is rather surprising for such complex molecules. If we apply the Kassel theory (7), and put the number of oscillators equal to $(3n - 6)$, where n is the number of atoms in the molecule, we obtain $s = 36$. Subtracting the number of C-H bonds, as usual, since the C-H valence vibrations are unlikely to be thermally excited at these temperatures, we get $s = 26$. With this value of s, and any reasonable assumed frequency, the theory predicts no falling-off in rate until very low pressures are reached. To get agreement with experiment it is necessary to assign to the parameters the following values:

$$s = 10$$
$$\sigma = 4 \times 10^{-8} \text{ cm.}$$
$$m = 22$$
$$\nu = 1000 \text{ cm.}^{-1}$$

Fig. 6 shows the agreement with experiment under these circumstances, the solid line representing the theoretical curve, and the circles the experimental points at 562° C.
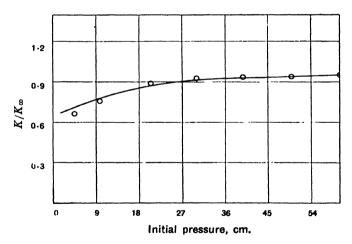
FIG. 6. *Application of Kassel equation. Solid line represents falling-off as calculated from Kassel theory. Circles represent experimental values.*

Since the isobutane molecule contains only C-C and C-H bonds, it appears unlikely that energy transmission from one part of the molecule to another should be difficult and result in the "freezing out" of some of the vibrational degrees of freedom. The effect is therefore, perhaps, to be ascribed to some complexity in the reaction such as the participation of free radicals. It is hoped that work now in progress (15) may throw further light on this point.

References

1. DINZES, A. I. and FROST, A. V.   J. Gen. Chem. (U.S.S.R.) 3 : 747-758.   1933,

2. DINZES, A. I. and FROST, A. V.   Compt. rend. acad. sci. U.R.S.S. 4 : 153-157.   1933.

3. DINZES, A. I. and FROST, A. V.   Compt. rend. acad. sci. U.R.S.S. 5 : 513-515.   1934.

4. EGLOFF, G.   The reactions of pure hydrocarbons.   Reinhold Publishing Co., New York.   1937.

5. FREY, F. E. and HEPP, H. J.   Ind. Eng. Chem. 25 : 441-449.   1933.

6. HURD, C. D. and SPENCE, L. U.   J. Am. Chem. Soc. 51 : 3353-3362.   1929.

7. KASSEL, L. S.   Kinetics of homogeneous gas reactions.   Chemical Catalog Co., New York.   1932.

8. MAREK, L. F. and NEUHAUS, M.   Ind. Eng. Chem. 25 : 516-519.   1933.

9. PAUL, R. E. and MAREK, L. F.   Ind. Eng. Chem. 26 : 454-457.   1934.

10. PEASE, R. N.   J. Am. Chem. Soc. 50 : 1779-1785.   1928.

11. PEASE, R. N. and DURGAN, E. S.   J. Am. Chem. Soc. 52 : 1262-1267.   1930.

12. RICE, F. O., JOHNSTON, W. R., and EVERING, B. C.   J. Am. Chem. Soc. 54 : 3529-3543.   1932.

13. RICE, F. O. and RICE, K. K.   The aliphatic free radicals.   Johns Hopkins Press, Baltimore.   1934.

14. STEACIE, E. W. R.   Chem. Rev.   22 : 311-402.   1938.

15. STEACIE, E. W. R. and FOLKINS, H. O.   Unpublished results.

16. STEACIE, E. W. R. and PUDDINGTON, I. E.   Can. J. Research, B, 16 : 176-193.   1938.

MEASUREMENT OF THE DIELECTRIC CONSTANT OF CELLULOSE[1]

By H. A. De Luca,[2] W. Boyd Campbell[3] and O. Maass[4]

Abstract

A method has been devised for the measurement of the dielectric constant of a material that cannot be made to completely fill a condenser. The following is the procedure adopted: Two completely miscible liquids are so chosen that the dielectric constant of the material under examination lies between the two values for the liquids. The dielectric constants of solutions of A and B ranging from 100% A to 100% B are measured. A curve is drawn showing the relation between dielectric constant and percentage composition. The condenser used is then partly filled with the fibrous material. The solutions of A and B are introduced into the condenser and the net dielectric constants are determined. A second curve is drawn showing this relation. The point of intersection of the two curves gives the composition of that liquid that has the same dielectric constant as the fibrous material.

This method has been applied to the measurement of the dielectric constant of cellulose, benzene and ethylene dichloride being used. A value of 6.1 has been obtained for this constant.

Introduction

In an effort to obtain a clearer insight in regard to the cellulose-water system, Argue and Maass (2) resorted to a measurement of the dielectric constant of the water adsorbed on cellulose. A more precise interpretation of their results was prevented at that time, however, by the lack of a value for the dielectric constant of standard cellulose. The present investigation was undertaken for the purpose of establishing such a value.

The most widely used method for the measurement of the dielectric constant is based upon the relation that defines the dielectric constant of a material as numerically equal to the ratio of the capacity of a condenser when filled with the material to the capacity of the same condenser when empty. Some difficulty is encountered in attempting to apply this method to substances (such as fibrous materials) which cannot be made to completely fill the condenser space. Argue and Maass (2) have shown on theoretical grounds that the capacity of a condenser partly filled with a given weight of a fibrous material depends on the orientation of the fibres with respect to the condenser plates. If the fibres could be made to assume a regular arrangement such as parallel or at right angles to the plates, then by using the formulas developed by the above workers it would be possible to calculate the dielectric constant of the material from a measurement of the capacity of the partly filled condenser. If, however, the fibres possess a random distribution within the condenser space, as in the case of cellulose, the above-mentioned method cannot be used.

A method has been devised for the measurement of the dielectric constant of fibrous materials having as its basis the following considerations. Consider a condenser filled with a given liquid. Let us now replace some of the liquid in the condenser space by an equal volume of fibrous material. If the dielectric constant of the latter is the same as that of the liquid, the capacity of the condenser will undergo no change and will be independent of the particular manner of distribution of the fibrous material in the condenser space. This can be proved mathematically by substitution in the formulas of Argue and Maass (2) which are given below.

$$\epsilon' = \frac{C'}{C} = \frac{1}{\dfrac{V_l}{V\epsilon_l} + \dfrac{V_f}{V\epsilon_f}} \tag{1}$$

$$\epsilon'' = \frac{C''}{C} = \frac{V_l\epsilon_l}{V} + \frac{V_f\epsilon_f}{V} \tag{2}$$

Equation (1) represents the net dielectric constant, ϵ', when the condenser, which has a capacity C when filled with a fluid of unit dielectric constant, is filled with a liquid of dielectric constant ϵ_l and fibrous material of dielectric constant ϵ_f with the *fibres parallel to the plates*. V_l is the volume of liquid and V_f that of the fibrous material; therefore $V_l + V_f = V$.

Equation (2) represents the net dielectric constant ϵ'' when the fibres are *perpendicular to the plates*.

C' and C'' are the condenser capacities in the two cases.

If $\epsilon_l = \epsilon_f = \epsilon$, Equations (1) and (2) both take the form $\epsilon' = \epsilon = \epsilon''$. In other words, the dielectric constant of the compound dielectric is independent of the particular distribution of the fibres relative to the condenser plates. Inasmuch as Equations (1) and (2) represent the extreme cases of fibre distribution, that is, parallel to the plates and at right angles, the same relation holds for any intermediate manner of distribution.

The above discussion indicates that the dielectric constant of a fibrous material can be measured provided that the condenser space unoccupied by the fibres is filled with a liquid having the same dielectric constant. Such a liquid is obtained in the following manner. Two completely miscible liquids, A and B, are so chosen that the dielectric constant of the material under examination lies somewhere between the two values for the liquids. The dielectric constants of solutions ranging from 100% A to 100% B are measured. A curve showing the relation between dielectric constant and percentage composition is drawn. The condenser used in the above-described measurements is then partly filled with the fibrous material. The solutions of A and B are introduced into the condenser and the resultant dielectric constants determined. A curve similar to the first one is drawn. The point of intersection of the two curves gives the composition and the dielectric constant of the liquid that has the same dielectric constant as the fibrous material. In this manner the dielectric constant of the fibrous material can be determined.

Experimental

Apparatus for Capacity Measurement

The heterodyne method of capacity measurement was employed. The apparatus was originally described by Smyth (8), but it has been considerably modified by other workers in this laboratory as well as by the present authors. It consists essentially of two high-frequency oscillators of the vacuum tube type and a detector-amplifier unit (Fig. 1).
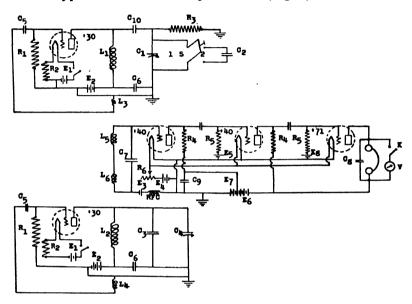
FIG. 1.   *Wiring diagram for measurement of capacity.*

R_1 = 50,000 ohms.	E_1 = 3 volts.	C_1 = 500 $\mu\mu f$.
R_2 = 15 ohms.	E_2 = 90 volts.	C_2 = Cell.
R_3 = 12,500 ohms.	E_3 = 1.5 volts.	C_3 = 500 $\mu\mu f$.
R_4 = 0.25 megohms.	E_4 = 6 volts.	C_4 = 1.200 $\mu\mu f$.
R_5 = 5 megohms.	E_5 = 3 volts.	C_5 = 0.001 μf.
R_6 = 6 ohms.	E_6 = 135 volts.	C_6 = 0.01 μf.
	E_7 = 45 volts.	C_7 = 0.00025 μf.
	E_8 = 27 volts.	C_8 = 0.002 μf.
		C_9 = 2 μf.
		C_{10} = 0.1 μf.

The two oscillator circuits are shown respectively at the top and bottom of Fig. 1. The inductances L_1 and L_2 consisted of 70 turns of No. 14 insulated copper wire wound on a form $3\frac{3}{4}$ in. in diameter. L_3 and L_4, consisting of 35 turns, were wound over L_1 and L_2 respectively. The capacitance C_1 was a precision condenser of 500 $\mu\mu f$. (General Radio, Type 247 E). C_2 was the experimental condenser containing the substance whose dielectric constant was to be measured. C_3 was approximately equal to C_1 in capacity. C_4 (about 1200 $\mu\mu f$.) was necessary to offset the capacity of the long leads used in conjunction with C_1 and C_2. A one plate vernier condenser attached to C_4 afforded a fine adjustment.

Several precautions were taken to ensure frequency stability of the oscillators. A heavy bus bar was used in wiring to avoid the capacity changes that result from the vibration of lighter wire. In order to obtain a more constant "A" voltage source, four batteries were connected in series–parallel since such an arrangement minimizes the current drain from each cell. A fixed resistor, rather than a rheostat, was used to drop this voltage to two volts. Heavy duty "B" batteries served to supply the plate voltages of the vacuum tubes. For purposes of shielding, each oscillator was housed in a sheet metal box, which was grounded. The variable condensers were included in the oscillator circuits in such a manner that the shafts, which extended beyond the metal shielding, were also grounded. The long leads, used in connecting the standard condenser and the experimental condenser to the oscillator, were shielded by placing the individual wires in copper tubing and grounding the latter.

In order to increase the accuracy with which the standard condenser could be read, it was placed in the centre of a circular wooden platform 5 ft. in diameter. A small mirror attached to the rotor shaft reflected a line image on to a millimetre scale fastened to the circumference of the platform. With this arrangement, readings could be estimated to within 0.1 mm. In order to avoid body capacity, a pulley arrangement was used so that the rotor could be turned from the edge of the platform. A vernier dial used in conjunction with the pulley system made possible a fine adjustment.

The oscillators were loosely coupled to the detector-amplifier unit (shown centrally in Fig. 1) by means of L_5 and L_6 each of which consisted of four turns of No. 22 wire on a bakelite form $2\frac{1}{2}$ in. in diameter. (By increasing the number of turns on these coils, the intensity of the beat note can be increased. The above-mentioned number of turns, however, was sufficient.) L_5 and L_6 were placed in the metal boxes containing the oscillators, adjacent to L_1 and L_2 respectively.

The detector-amplifier unit was the same as that described by Smyth (8), with the following major exception. The output stage was operated in addition as a vacuum-tube voltmeter so that a visual indication of the null point could be obtained. (This depends on so choosing the bias of the tube that it operates on the non-linear part of its grid-voltage–plate-current curve.) The above unit also was shielded by means of a sheet metal box.

Before an attempt is made to locate the null point in this set-up, the reading on the voltmeter V (the three volt range of a Weston voltmeter Model No. 290) is first adjusted to a suitable value by means of R_6. The region of zero beat is determined by using the loud-speaker. The voltmeter, however, furnishes a more convenient and more sensitive means of obtaining the exact null point. As zero beat is approached, the reading given by V gradually increases. Just before the null point is reached, the voltmeter needle begins to oscillate. The more nearly the zero beat conditions are approached, the wider is the amplitude of the oscillating needle. As the exact null point is reached, however, the needle suddenly ceases its motion. The null point

extended over a slight "dead space", which was equal to approximately 0.1 cm. on the scale. With this method the dead space was much smaller than it was when the loud-speaker alone or even a pair of earphones was used. To minimize the effect of the dead space, the same side was always taken as the null point; that is, zero beat was always approached from the same direction.

The capacity was determined as follows. Switch S is left in Position 1 and the standard condenser, C_1, is set to read zero on the scale. C_4 is then rotated until zero beat conditions obtain. Switch S is next placed in Position 2 and the standard condenser is rotated until zero beat conditions are again established. The difference between the two readings gives a measure of the capacity of C_2.

When the apparatus was first assembled, instead of a single null point, a series of zero beats was obtained; this indicated that the oscillators were beating against the carriers of broadcasting stations. It was found that the long leads to the standard condenser, even though shielded, were acting as antennas. When these were removed from the circuit, only one null point was obtained. The interfering signals were subsequently filtered out by means of R_3 and C_{10}. The value of the blocking condenser is not critical, but it should be large enough to offer but slight impedance to a current of the frequency of the oscillator. The value of R_3 was found to be quite critical, as values less than 10,000 ohms killed oscillation, while values greater than 15,000 ohms did not remove the interfering signals. No such filter circuit was necessary for the fixed oscillator as it did not include any long leads.

Calibration of the Standard Condenser

In later calculations the assumption is made that a straight line relation exists between the capacity of the standard condenser at a given setting and the corresponding scale reading. Linton and Maass (6) have shown that this is not strictly true. Accordingly, it is necessary to correct for the aberration from linearity in the above-mentioned relation. The following method was devised for calibrating the standard condenser. A small condenser was used to replace C_2 in the variable oscillator, and the displacement of the null point produced by it over successive parts of the scale was determined. The lowest value was arbitrarily chosen as the unit value, and the differences between this and the remaining readings were calculated. A curve showing the relation between reading of the standard condenser and correction was then drawn. The accuracy of this method of calibrating the condenser was investigated by measuring the capacity of a given condenser over various parts of the scale. All the corrected values were found to agree much more closely among themselves than did the uncorrected ones.

The Calculation of the Dielectric Constant

The dielectric constant, as previously mentioned, is given by the ratio C'/C, where C' is the capacity of the condenser filled with the material and C is the capacity of the condenser empty. The capacity measurements taken under experimental conditions, however, include the capacity of the leads

which connect the unknown capacity to the measuring equipment. It is therefore necessary to allow for these.

We may write:
  (i) for the condenser when empty: $L + C = kd_1$
  (ii) for the condenser when filled: $L + C' = kd_2$
  (iii) for the leads: $L = kd_3$

Where L is the lead capacity,
      C is the capacity of the condenser when empty,
      C' is the capacity of the condenser when filled,
      d_1 is the scale reading for the empty condenser plus the leads,
      d_2 is the scale reading for the filled condenser plus the leads,
      d_3 is the scale reading for the leads,
      k is the proportionality factor connecting scale reading and capacity.

The dielectric constant ϵ will be given in terms of scale readings by the relation:

$$\epsilon = \frac{kd_2 - kd_3}{kd_1 - kd_3}$$

$$\epsilon = \frac{d_2 - d_3}{d_1 - d_3} \qquad (4)$$

Since the proportionality factor k does not appear in the final expression, we are not concerned with its value. Capacity measurements have been accordingly expressed in this work in terms of the scale readings of the standard condenser.

Experimental

Preparation of the Liquids

As there was considerable doubt concerning the value of the dielectric constant of cellulose, it was necessary to choose two liquids whose dielectric constants were somewhat far apart. It was also necessary to choose liquids that would not be adsorbed by the cellulose. The hydrocarbons, which are ideally suitable because they are not appreciably adsorbed, all possess low dielectric constants. It was one of these, benzene (dielectric constant, 2.27) that was chosen for the liquid of lower dielectric constant. There are, however, very few liquids that are not likely to be adsorbed that possess a high dielectric constant. Such compounds as those containing oxygen, hydroxyl groups, nitrogen, and unsaturated carbon, which are those that exhibit high dielectric constants, are also those that are most likely to be strongly adsorbed. It was decided to use ethylene dichloride (dielectric constant, 10.1 to 10.8) as it appeared probable that it would fulfil sufficiently well the above-mentioned requirements.

C.p. benzene (tested for the absence of traces of water) and a relatively pure grade of ethylene dichloride were used. The purity of the ethylene dichloride was of no consequence in so far as its dielectric constant was con-

cerned, as no assumptions were made in this respect. On the other hand, it was necessary to determine whether any of the slight impurities present might be adsorbed. It was demonstrated experimentally, however, that ethylene dichloride, benzene, or any of the impurities that might be present were not adsorbed on the cellulose to an extent that would influence the measurement of its dielectric constant.

TABLE I
COMPOSITION OF SOLUTIONS

Solution	Wt. per cent		Solution	Wt. per cent	
	Benzene	Ethylene dichloride		Benzene	Ethylene dichloride
1	100.00	0.00	5	27.99	72.01
2	76.48	23.52	6	16.45	83.55
3	60.87	39.13	7	0.00	100.00
4	40.64	59.36	4a	31.01	68.99

Cellulose

The cellulose was prepared by the method for standard cellulose described by Argue and Maass (1).

The Dielectric Cell

The experimental condenser and its glass envelope formed the dielectric cell. The condenser consisted of two concentric brass cylinders, 0.07 cm. in thickness, 18 and 17 cm. in length, and 2.6 and 1.6 cm. in diameter, respectively. The outer cylinder was made longer than the inner one for purposes of shielding. The two cylinders were kept apart by two Pyrex rings, 0.5 cm. in thickness and 1.0 cm. in height. A vertical section 0.7 cm. wide was cut out of each ring to allow penetration of liquid into the inter-cylinder space. (The glass rings were made first and the brass cylinders chosen afterwards·to fit them very tightly.) There were four small projections on the bottom of the outer cylinder, bent inwards, upon which one of the glass rings rested. About half a centimetre from the bottom of the inner cylinder there were four projections, bent outwards, which rested on the glass ring. The other ring was similarly placed at the top of the condenser. This arrangement prevented any movement of the two cylinders relative to each other. The assembled condenser was placed in the Pyrex envelope (*C* in Fig. 2) which was 3.2 cm. inside diameter and 35 cm. in length. The additional length of the envelope (over that of the condenser) was required in order that it could be sealed without heating the cellulose. Electrical connection was made to the cylinders by means of two fine copper wires, a section of each being replaced by a small piece of thin platinum foil, in order that a glass-to-metal seal could subsequently be made by the method of Campbell (4). These arms were placed as far apart as was conveniently possible (about 6 cm.) so·that the lead capacity might be a minimum. It was necessary to

include the experimental condenser in the circuit in such a manner that the outer cylinder was grounded, in order to avoid a capacity effect between the condenser and the bath liquid. Under these conditions, the capacity of the empty condenser plus the leads was found to be the same (53.65 cm. on the capacity scale) whether or not the dielectric cell was surrounded by the bath fluid.
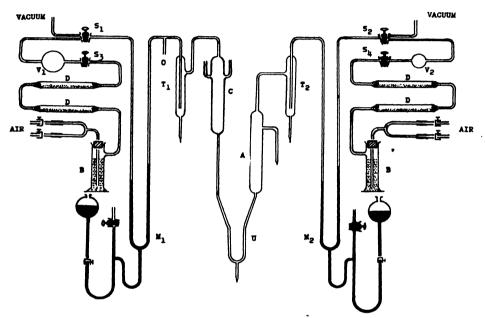
FIG. 2. *Experimental set-up for measurement of dielectric constant of cellulose.*

The Bath

The dielectric cell was immersed in a Pyrex water bath. The liquid was stirred by means of compressed air forced through an O-shaped glass tube containing small openings, and placed at the bottom of the bath around the cell. The temperature of the bath could be lowered or raised by sending a stream of cold water or a mixture of steam and air through the stirrer. Small changes in temperature were made at times by simply adding small amounts of hot or cold water. The temperature of the bath could be easily kept within $0.2°$ C. of the desired temperature ($25.0°$ C.).

Experimental Procedure

The combined capacity of the leads and the condenser filled with liquid was measured with each of the seven solutions. For this part of the work the tube coming from the bottom of the cell was not connected to the U-tube as shown in Fig. 2, but the lower end was left open so that the liquids could be drawn up into the cell. Inasmuch as it was necessary that the capacity of the leads be kept the same for this and subsequent measurements, the

platinum foil was included in the internal leads but the glass-to-metal seals were not made at this stage of the work. The fine copper leads were brought out of the arms of the cell through a cork and the seal was completed with DeKhotinsky cement. This was sufficiently air-tight since the cell was not subjected to a high vacuum at this stage.

By applying a vacuum through S_1, about 150 cc. of the liquid contained in a tall cylinder was drawn into the cell. Capacity measurements showed that it was necessary to raise and lower the liquid several times before the walls of the cylinders became thoroughly wetted. All measurements were made with the liquid at a given height, about 1 cm. above the top of the condenser. Small differences in the level of the liquid relative to this point could not be detected by capacity measurements since the capacity of the internal leads was quite small. Capacity measurements made at $25.0° \pm 0.2°$ C. usually agreed within 0.10 cm. for successive measurements on the same solution. The average values for the capacity of the condenser filled in turn with the various solutions are given in Table II. The liquid was drained from the cell at the conclusion of each measurement and the cell swept with a current of air dried by means of the sulphuric acid tower B and the two phosphorus pentoxide tubes D, D. At the same time the bath temperature was raised to 90° C.

TABLE II

CAPACITY OF CONDENSER FILLED WITH SOLUTION ONLY, AND WITH SOLUTION PLUS CELLULOSE

Solution	Capacity with solution only, cm.–units	Capacity with solution and cellulose, cm.–units	Solution	Capacity with solution only, cm.–units	Capacity with solution and cellulose, cm.–units
1	76.75	—	5	152.10	151.85
2	94.05	—	6	175.55	172.20
3	108.20	122.20	7	221.50	—
4	131.90	133.70	4a	147.00	147.05

The cell was next taken from the bath and the cellulose was packed into the condenser. It was only necessary to remove the upper glass ring from the condenser and pack cellulose into the inter-cylinder space. Considerable care was exercised in sealing the cell inasmuch as an excessive heating of the cellulose had to be avoided. The completed cell was replaced in the bath in its original position and joined to the rest of the apparatus in the manner indicated in Fig. 2.

It was first necessary to remove any water that the cellulose had adsorbed. The bath was left at room temperature and the system was evacuated through S_1, a Hy-Vac pump and a Langmuir diffusion pump being used. Evacuation was continued for three hours, and then the bath temperature was raised to 100° C. At the end of six hours evacuating at the higher temperature, the capacity of the experimental condenser had reached a constant value; this

indicated that the cellulose was thoroughly dried. With the system under vacuum and the bath temperature at 25° C., the capacity of the leads and the condenser containing the cellulose was found equal to 60.15 cm. Air, dried by passage through the two drying units, was then slowly let into the system until the pressure was atmospheric. The fact that no change took place in the capacity of the system following this operation showed that the air had been thoroughly dried.

The method of introducing the liquid into the cell filled with cellulose presented several difficulties. It was highly important that the system be under vacuum when this was carried out in order that the possibility of air bubbles being trapped among the cellulose fibres be reduced to a minimum. It was obviously impossible to use stopcocks. The difficulty was overcome by the use of frozen seals of the same composition as that of the liquid with which the cell was to be filled.

During the introduction of the liquid into the U-tube, precautions were taken that the moist air of the atmosphere did not come in contact with the cellulose. Compressed air was first introduced into the system by way of the drying unit shown on the left (Fig. 2). At the same time the sulphuric acid tower shown on the right was disconnected from the phosphorus pentoxide tubes in order to allow a point of exit for the air. The tip on the arm of A was then broken and a loosely stoppered test tube containing about 20 cc. of the liquid was placed under it. The supply of compressed air was shut off and the sulphuric acid tower again connected to the system. A Dewar flask containing solid carbon dioxide and acetone was placed around the trap T_2 to prevent the vapors of benzene and ethylene dichloride from passing through the Hy-Vac pump in subsequent operations. The freezing mixture was kept around the trap from this stage to the end of the run. Volume V_2 (about 50 cc.) was then evacuated. With S_2 closed, S_4 was partly opened. This caused the liquid to rise into the arm of A and finally to flow into the U-tube. When the arms of the U-tube were filled to a height of about 10 cm., S_4 was closed. The height of the liquid in the left-hand arm was finally adjusted to 5 cm. by introducing a slight amount of compressed air into this side of the system. A Dewar flask containing solid carbon dioxide and acetone was then placed under the tip of the U-tube, one centimetre of it being immersed in the freezing mixture. After the liquid had frozen, the freezing mixture was raised an additional centimetre. This process was repeated until all the liquid in the left-hand arm was frozen, after which atmospheric pressure was established on both sides of the frozen seal. All the liquid in the right-hand side of the U-tube was not frozen, in order that there would always be a supply ready to flow into the space resulting from the contraction that the liquid first underwent on freezing and then on reaching thermal equilibrium with the freezing mixture. It was not desirable to leave any liquid in the left-hand arm inasmuch as this side of the system was to be highly evacuated in subsequent operations.

After the frozen seal had been made, the vessel A (volume 300 cc.) was filled with the solution. A covered flask containing the solution was placed

under the arm and, by application of suitable vacuum at S_4, about 250 cc. of the liquid was drawn into the vessel A. The flask was then removed and a current of dried air was passed through the arm to remove as much as possible of the liquid remaining in it. Some difficulty was at first encountered in attempting to seal this arm owing to the fact that the charring of the liquids prevented the making of a good seal and also because the solutions were slightly inflammable. The difficulty was overcome by stoppering the arm and then gently heating before attempting to seal it.

The system to the left of the frozen seal was next evacuated for 5 to 10 hr.; the pressure was then usually about 10^{-3} mm. of mercury. The pressure above the liquid in A was reduced to the vapor pressure of the liquid, a small amount of which was allowed to boil off in order to drive out as much air as possible. It was essential that the difference between the air pressures in the evacuated spaces over both sides of the frozen seal be as small as possible in order that the liquid might not be pushed beyond the dielectric cell on the subsequent thawing of the seal.

Care had to be exercised in thawing the seals since benzene and ethylene dichloride expand on liquefying. The seal was melted by lowering the freezing mixture a half a centimetre at a time until the arch of the U-tube was reached. At this point the melting of the solid was hastened by briskly rubbing the inner part of the arch with the fingers. Following the removal of the seal, the liquid rose into the dielectric cell but to a height never more than 5 cm. above the bottom of the condenser. The liquid was then raised to a height slightly below a given point (the same as that used in the previous set of measurements) by allowing air to expand from V_2 into the space above the liquid in A. The finer adjustment in the level was made by raising the mercury in the mercury cut-off M_2. About half an hour was allowed for the liquid to reach thermal equilibrium with the bath before any capacity measurements were made. After the capacity of the system had been determined, the liquid was removed from the dielectric cell by applying a vacuum at S_2. Thus by alternate use of pressure and vacuum by means of which the cell was filled and emptied, a series of capacity measurements of the same solution could be made.

Several preliminary runs brought forth the following facts. The capacity of the condenser was found to successively increase during the first five or six times that the liquid was drawn out of the cell and sent in again. This indicated that at pressures as low as 10^{-3} mm., the cellulose fibres trapped some air bubbles which were removed a few at a time. That all the air was not removed even when the capacity of the condenser had attained a constant value was shown by the fact that the "constant value" was not the same for an entirely independent set of measurements on the same solution. This showed that some of the air bubbles were difficult to dislodge and also that the number of this type that formed was not the same for different runs. It was accordingly necessary to modify the experimental procedure. Subsequent to the thawing of the frozen seal, the liquid was sent into the cell and

drawn·out about ten times. After the liquid had been adjusted to the desired height, the frozen seal was again formed in the U-tube. Air was then let into the space above the liquid in the cell until the pressure was atmospheric. It was reasoned that any bubbles that had formed in the liquid at an air pressure of 10^{-3} mm. would most certainly be reduced to a negligible size when the external pressure was increased to atmospheric. The results indicated that this was true. It was found that owing to the contraction of the air spaces subsequent to the establishment of atmospheric pressure above the liquid, the level dropped slightly. To offset this, the liquid was raised about the same distance above the proper level before the frozen seal was made. This was probably not necessary, since, as has been shown previously, the internal lead capacity was so small that a slight difference in the level of the liquid was of no consequence.

It was considered improbable that the dielectric constant of cellulose was as low as that of Solutions 1 and 2. Accordingly the series of capacity measurements was begun with Solution 3 and continued with solutions of higher dielectric constant until the point of intersection of the two curves previously mentioned was satisfactorily established. The average values of the capacity of the leads and the condenser filled with cellulose and each of Solutions 3 to 6 are given in Table II. Two runs were carried out with each solution, the separate capacity values agreeing well within 0.10 cm.

At the conclusion of a set of capacity determinations the liquid was drained from the cell by breaking the tip on the tube below the U-tube. Air was then passed through the cell by way of the left-hand drying unit. Considerable difficulty was experienced in attempting to seal the tube below the U-tube after the liquid had been drained from the cell. The cellulose held back a considerable amount of the liquid, and it dripped continuously into the U-tube. As mentioned previously, the charring of the liquid on strong heating prevented the making of a satisfactory seal. The difficulty was overcome by the use of a solid carbon dioxide trap. A piece of asbestos was wrapped around the glass tubing in the form of a cone just below the cell. This was filled with finely powdered solid carbon dioxide. Prior to making the seal, the open tube was closed with an asbestos-protected cork and the U-tube and connecting tubing was heated. Under these conditions a satisfactory seal could be made.

The liquid held back by the cellulose was removed by evacuating the system through trap T_2 (surrounded with solid carbon dioxide and acetone). By a measurement of the capacity of the condenser, it was found that all the liquid was removed from the cellulose in three hours or less of pumping. At the end of this time, evacuation was stopped, and dried air was let into the system. The solid that collected in T_2 was carefully thawed and removed by breaking the tip at the bottom of the trap. T_2 was then sealed, a current of dried air passing through the apparatus from left to right during this operation.

It has been indicated elsewhere that experimental evidence was obtained to show that benzene, ethylene dichloride, or any of the impurities that

might be present were not adsorbed by the cellulose to an extent that would influence the measurement of the dielectric constant of cellulose. Before one of the capacity measurements in which the solution was sent into the condenser filled with cellulose only was taken, the part of the frozen seal immediately below the dielectric cell was allowed to melt. This caused the evacuated space to be filled with the vapors of the liquids. The system was allowed to stand thus for 30 min. The capacity of the condenser was then measured but no increase (over the normal capacity of the cell filled with cellulose) was found. This points to the absence in the solutions of any constituents that might be adsorbed in sufficient quantities to influence the measurements in this investigation.

It would have been impossible to carry out successfully the above experimental procedure without the inclusion of the mercury cut-offs in the system, as the vapors of the liquids had a tendency to attack the stopcock grease. The mercury in the cut-offs was accordingly kept raised at all times unless otherwise necessary. The presence of the mercury in the system is of no consequence as far as the measurements are concerned, as it has been shown by Russell, Maass, and Campbell (7) that mercury is not appreciably adsorbed by cellulose.

In Fig. 3 is shown the relation between capacity of the condenser and composition of the liquid for the sets of measurements in which (i) the condenser was filled only with the liquid (Curve 1), (ii) the condenser was filled with cellulose and liquid (Curve 2). The point of intersection of these curves was actually determined on a much larger graph than is given here, one on which the capacity measurements were plotted to the nearest 0.1 cm. and the composition values to the nearest 0.05%. The two curves were found to merge into one for a distance given by the capacity as 146.2 to 147.6 cm. and by the composition as 68.50 to 69.50%. The mean of these values, 146.9 and 69.00, respectively, was taken as the true point of intersection. A liquid of this composition was introduced into the cell, and a capacity value of 147.05 cm. was obtained; this agrees favorably with that given above.

The agreement between the value taken from the graph and the experimentally obtained value is no proof that this point is the point of intersection of the two curves. It indicates only the agreement that can be obtained between points taken off Curve 2 and the experimental values. To prove conclusively, however, that the value obtained for the point of intersection of the two curves was not far from the correct one, it was necessary to introduce the above solution into the empty condenser. (This solution will henceforth be termed Solution 4a.) The dielectric cell was therefore dismantled and the cellulose removed. It was replaced in the bath and the capacity of the condenser filled with Solution 4a was determined. It was found equal to 147.00 cm. (compared to 147.05 cm.). This shows definitely that the point previously chosen as the point of intersection lies on both Curves 1 and 2. (In other words, it indicates that no capacity change has been introduced in dismantling the condenser and again assembling it.) It was accord-

ingly necessary only to determine the dielectric constant of this solution in order to arrive at a value for the dielectric constant of cellulose.
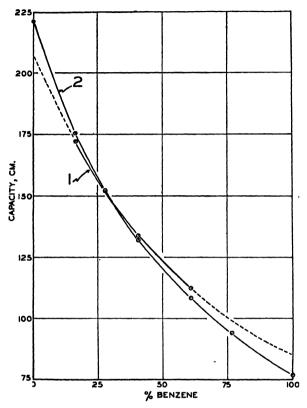
FIG. 3.   *Relation between capacity and composition.   Curve 1, solution.   Curve 2, solution plus cellulose.*

Calculation of the Dielectric Constant of Cellulose

It has been mentioned that in calculating the dielectric constant from the capacity values experimentally determined, it is necessary to allow for the capacity of the leads. A value for the effective lead capacity was obtained by substituting in Equation (4) the value of the dielectric constant of benzene and the corresponding values of d_1 and d_2. This gives:—

$$2 : 27 = \frac{76.65 - d_3,}{53.65 - d_3}$$

whence $d_3 = 35.45$.

The accuracy of this calibration was tested by measuring the dielectric constant of chloroform, for which satisfactory agreement with the values in the literature was obtained.

Now, by use of the value of d_3 and the above equation, all previous capacity measurements can be expressed in terms of the dielectric constant. These are given in Table III. These values have been plotted in Curves 1 and 2 of Fig. 4. The point of intersection gives directly the dielectric constant of cellulose. As was done previously these values were plotted on a larger scale than is shown here (to 0.01 dielectric units and 0.05%). The two curves
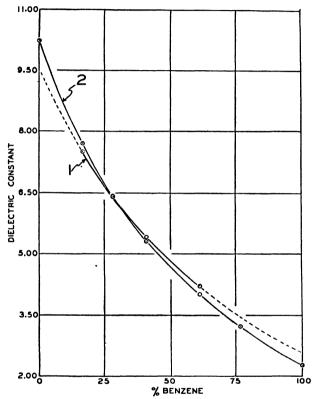
FIG. 4. *Relation between composition and dielectric constant. Curve 1, solution. Curve 2, solution plus cellulose.*

TABLE III

DIELECTRIC CONSTANT OF SOLUTION ONLY AND OF SOLUTION PLUS CELLULOSE

Solution	Dielectric constant of solution only	Dielectric constant of solution and cellulose	Solution	Dielectric constant of solution only	Dielectric constant of solution and cellulose
1	2.27	—	5	6.41	6.39
2	3.22	—	6	7.70	7.51
3	4.00	4.22	7	10.22	—
4	4.30	5.40	4a	6.13	6.13

merged into one for a distance given by the dielectric constant as 6.07 to 6.17. The mean of these values, 6.12, was taken as the dielectric constant of cellulose.

It was shown previously that the condenser possessed the same capacity when filled with cellulose and Solution 4a as when it was filled with the solution only. By substituting this capacity measurement (147.05 cm.) in Equation (1), a value of 6.13 is obtained for the dielectric constant of cellulose.

Discussion of Results

In the foregoing treatment of the subject, the values for the dielectric constant have been expressed to the nearest 0.01 unit. This has been done more to show the accuracy of which the method is capable rather than an attempt to measure the dielectric constant of cellulose to this value. It is quite probable that the dielectric constants of two samples of standard cellulose might differ by a number of times the above amount. Expressed to the nearest 0.1 unit, the value of this constant as found in this work is given as 6.1.

As mentioned previously, the literature does not contain a value for the dielectric constant of standard cellulose. It is stated in the International Critical Tables (5) that the value of ϵ for cellulose lies between 3.9 and 7.5, but the source of these data is not definitely indicated. Campbell (3) obtained a value of 6.7 for a regenerated cellulose. Stoops (9) found the dielectric constant of cellophane (which is also a regenerated cellulose) to vary from 6.7 to 7.7, the value depending on the frequency of the measuring current. The dielectric constant of standard cellulose would be expected to be different from that of a regenerated cellulose inasmuch as the treatment employed in the production of the latter alters the crystal structure. On the other hand, it is felt that in the light of the values obtained by Campbell, Stoops, and the writers, the value for the dielectric constant of cellulose should be given within smaller limits.

References

1. ARGUE, G. H. and MAASS, O. Can. J. Research, 12 : 564-574. 1935.
2. ARGUE, G. H. and MAASS, O. Can. J. Research, B, 13 : 156-166. 1935.
3. CAMPBELL, A. Proc. Roy. Soc. London, A, 78 : 196-211. 1907.
4. CAMPBELL, W. BOYD. J. Am. Chem. Soc. 51 : 2419-2420. 1929.
5. INTERNATIONAL CRITICAL TABLES, Vol. 2, p. 310. McGraw-Hill Book Co., New York. 1927.
6. LINTON, E. P. and MAASS, O. J. Am. Chem. Soc. 53 : 957-964. 1931.
7. RUSSELL, J. K., MAASS, O., and CAMPBELL, W. BOYD. Can. J. Research, B, 15 : 13-37. 1937.
8. SMYTH, C. P. Dielectric constant and molecular structure. Chemical Catalogue Co., Inc. New York. 1931.
9. STOOPS, W. N. J. Am. Chem. Soc. 56 : 1480-1483. 1934.

PERSISTENCE OF THE LIQUID STATE OF AGGREGATION ABOVE THE CRITICAL TEMPERATURE[1]

By R. L. McIntosh[2] and O. Maass[3]

Abstract

The data obtained by Maass and Geddes (7) on the properties of ethylene in the critical-temperature–critical-pressure region have been substantiated although it was shown that a small correction had to be applied to their absolute values of density. It was shown that at the critical density of ethylene the difference between the densities of the medium below and above the point at which the meniscus disappeared was a maximum. The conclusion of Mayer and Harrison (made in their recent papers on statistical mechanics of condensing systems (6, 10)) that, at a temperature just above that at which the meniscus disappeared, the pressure of the system remains constant over a considerable variation of mass per volume, has been corroborated. The effect of the presence of small measured quantities of air has been examined. The phenomena observed are explained on the basis that there is a difference between the gaseous and liquid states of aggregation with a structure assigned to the latter.

Introduction

In recent years, investigations (4, 7, 8, 9, 12, 13, 14, 17, 18, 19) of the properties of liquid-gas systems in the critical temperature region have been carried out in this laboratory. It was shown that the liquid state of aggregation can persist above the temperature* at which the visible meniscus disappears.

The present paper is a continuation of the study begun by Maass and Geddes (7) on the density of ethylene. Their experimental arrangement was such that any two of the factors, pressure, temperature, and density, could be varied, while the other was held constant. Time lags in the establishment of equilibrium densities could best be explained on the assumption of a dynamic structure in the liquid state. Measurements made at constant volume showed a persistence of a heterogeneous system until the temperature was⁻ approximately four degrees above the critical, while vapor pressure measurements showed the heterogeneous and homogeneous systems to have the same pressure within the limits of experimental accuracy. Isothermal compression and expansion were found to destroy the heterogeneity, and temperature fluctuations produced the same effect. The last two observations limit the kinds of mechanical stirring that may be employed in the

investigation of critical temperature phenomena. Mechanical stirring that does not cause local heating and cooling, or expansion and compression, does not influence the phenomena observed, either in kind or in rate of attainment of equilibrium.

The present paper shows the main features of the investigation of Maass and Geddes to be reproducible. Further evidence of the persistence of the liquid state above the classical critical temperature has been obtained with pure ethylene and with ethylene-air mixtures.

Experimental Procedure

Density, Pressure, Temperature Measurements, etc.

The experimental arrangement employed for the measurement and control of pressure, temperature, and density was developed by Maass and Geddes (7) and described by them in a recent paper that must be consulted for the appreciation of the experimental method.

Purity of Ethylene Samples

The procedure followed by Maass and Geddes for the purification of the ethylene was to distil a large volume of ethylene of 99.9% purity three times, initial and final fractions being discarded. Two samples prepared by the above-mentioned authors in this way gave identical results.

For the investigation described below, a sample was prepared in this manner and compared with others that had been distilled through a Podbielniak column. All the samples behaved in an identical manner. Particular precautions were taken to ensure the absence of air due to slight leaks in stopcocks. Before being filled, the apparatus was tested for long periods by means of a McLeod gauge.

Air-ethylene Systems

The air-ethylene samples were introduced into the apparatus as follows. Ethylene was prepared and inserted in the manner described previously (7). The stopcock in the lead to the bomb containing the ethylene was then closed, and the filling system evacuated and flushed with dry air several times. The cock in the lead from a small storage flask containing the air (the volume of which was accurately known) was opened, and the pressure read on the manometer. The cock in the bomb lead was then slowly opened, and air admitted until the desired pressure change was indicated on the manometer. The cock was then closed, and the bomb sealed off in the usual manner.

Critical Temperature of Air-ethylene Systems

It was thought possible that the temperature of disappearance of the visible meniscus might serve as a criterion of the purity of an ethylene sample. The data obtained are given in Table I.

It is seen that the critical temperature cannot be used as a test for the presence of small amounts of an inert gas. The best and quickest test for purity was found in the independence of the density of the liquid phase of the ethylene with changing ratios of liquid to vapor at 9.00° C.

TABLE I

Sample No.	1	2	3	4	5	6
Purity	100% C₂H₄	Unknown air content	100% C₂H₄	0.93% air	0.55% air	100% C₂H₄
T꜀, °C.	9.50	9.50	9.50	9.49	9.50	9.50

Experimental Results

The unusual nature and interest of the results of Maass and Geddes made the question of reproducibility an essential part of any subsequent work. The determination of typical isobars and isochores of the system ethylene was therefore repeated, particular attention being focused on the duration of time lags and the shapes of the curves.

In the course of the first experiments carried out with this object in view some air was inadvertently introduced into a sample of ethylene. The peculiarities of this system were such that it was deemed important to undertake an investigation of air-ethylene mixtures as soon as the limits of reproducibility had been determined.

Three typical isobars of samples of ethylene of satisfactory purity are given in Fig. 1. The isobars are identical in shape with those obtained by
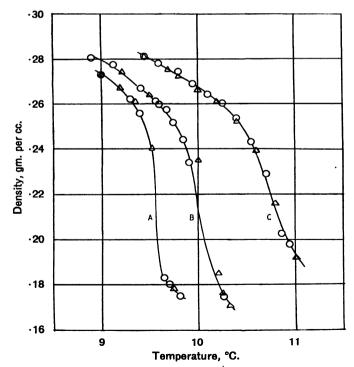
FIG. 1.   *Isobars of pure ethylene.   A, 50.10; B, 50.54; C, 51.44 atm.   Triangles denote Geddes' and Maass' values less 0.010₀ gm. per cc.*

Geddes and Maass but show a difference of 0.0100 gm./cc. in the absolute value of the density all along the curves. This is very clearly illustrated by the good agreement between the triangular points (which are the values obtained by Geddes and Maass minus a constant factor of 0.0100 gm./cc.) and the curves, which are observed values. The cause of the discrepancy can be suggested and the present values are for several reasons believed correct. It is at once apparent that the carbon dioxide pressure cannot be the cause of the divergence, for the liquid density at 9.00° C., under the vapor pressure of the ethylene alone, and obtained by keeping the centre U-tube frozen, differs by the same factor of 0.0100 gm./cc. from the values of Geddes and Maass. The most likely source of error is therefore the calibration of the glass float by Geddes and Maass. The volume constant in the present work was reproducible to 3 parts in 800, the mean of a series being of course more accurate. Moreover, duplication with an entirely new apparatus, including a new spiral and new float, gave density values agreeing with each other to 8 parts in 1000 on absolute values. Although two samples of gas were used in the work of Geddes and Maass, none of their work was repeated by them with a different experimental unit; in this investigation work was repeated with a different unit. Table II shows the reproducibility of the liquid phase density at 9.00° C., where values of the density for different liquid-vapor ratios are given, as well as a check obtained with a new experimental unit. Consequently, it may be reasonable to assume that the absolute values of the data presented here are more nearly correct, and that although no change is indicated in the relative density measurements reported by Geddes and Maass, and in the conclusions drawn therefrom, nevertheless, their values should be corrected. This has been done in the pressure-temperature curves at constant volume given below.

TABLE II

DENSITIES OF ETHYLENE LIQUID AT 9.00° C. FOR VARIOUS FILLINGS

Sample No.	Average density	Density of liquid
1	0.2161	0.2455
	.2334	.2460
	.2301	.2460
3	.2153	.2450
	.2210	.2450
	.2253	.2455
6	.2127	.2443

Densities of samples 1 and 2 were measured by means of one experimental set-up, the density of sample 3 by an entirely new set-up including new spiral and float. Samples 3 and 6 were put through the Podbielniak column. Absolute accuracy of density measurements are better than 1%. Relative accuracy of density measurements, 0.2%.

PRESSURE-TEMPERATURE CURVES OF ETHYLENE

Various pressure-temperature curves of pure ethylene have been evaluated from the corrected isobars of Geddes and Maass for several densities. These are all excellent straight lines as Fig. 7 shows, and therefore follow the behavior predicted by Ramsay and Young for such isochores. The slopes have been used to test Mills' formula (11) that $\left(\dfrac{\delta p}{\delta T}\right) V_c = \dfrac{2R}{V_c}$, where R has its usual

significance, and V_c is the critical molar volume. The calculated value of $2R/V_c$ for ethylene is 1.26 atm. per degree, while the corrected density values of Geddes and Maass' data give 1.21 atm. per degree as compared to 1.16 atm. per degree if Geddes' and Maass' uncorrected absolute values are used.

Reproducibility of Time Lags

The degree of agreement of the time lags is all that may reasonably be expected from the experimental method. Very small differences in absolute temperatures cause large changes in density, especially at those positions of the isobars where time lags are most sensitive. Moreover, the correction that must be applied for the changing mercury level involves a personal error. This is due to the fact that the temperature of the carbon dioxide has to be adjusted continuously in such a way that the proper temperature change is achieved at the desired time interval. Since the effect of pressure upon time lags and density is marked, slight differences in pressure cause divergences in the time required for equilibrium. The correct order of magnitude is therefore all that should be expected along the isobars, while much better agreement should be obtained in constant volume determinations where the U-tube is kept frozen. The results are given in Table III. In accordance with the practice initiated by Geddes and Maass, the results

TABLE III

TIME LAGS ALONG ISOBARS

Maximum time lags observed on heating $+0.20°$ *C., pressures being kept constant*

Pressure, atm.	Geddes and Maass	McIntosh and Maass		
	Pure ethylene $t_{1/2}$, min.	Pure ethylene $t_{1/2}$, min.	0.93% air $t_{1/2}$, min.	0.55% air $t_{1/2}$, min.
50.54	12	12	—	—
51.44	7.5	5	6.5	4

Time lags observed on cooling so as to produce specified density changes (in pure ethylene) pressures being kept constant at 50.54 atm.

Geddes and Maass		McIntosh and Maass	
Density change	$t_{1/2}$, min.	Density change	$t_{1/2}$, min.
0.262 to 0.245	2	0.265 to 0.254	2.8
0.240 to 0.205	8	0.245 to 0.210	7

for the isobars are expressed in terms of the time required for the density change to reach the halfway mark, called the time to half value. The agreement is good.

In Table IV the times required for the establishment of equilibrium are given for isochore runs.

TABLE IV

TIME LAGS OF ISOCHORES*

—	Pure ethylene		0.93% air	0.55% air
	Sample No. 3	Sample No. 6		
Temp. change, °C.	9.20　to 9.50	9.30　to 9.50	9.30　to 9.55	9.30　to 9.55
Density change	0.2354 to 0.2256	0.2325 to 0.2241	0.2544 to 0.2517	0.2469 to 0.2386
Time to equilibrium, min.	23	23	3	3
Temp. change, °C.	9.70　to 9.90	9.80　to 10.50	10.30　to　11.50	9.80　to 16.30
Density change	0.2094 to 0.2073	0.2175 to　0.2136	0.2175 to　0.2136	0.2346 to　0.2277
Time to equilibrium, min.	20	19	3	3

* *Geddes and Maass—approximately 20 min. in all cases.*

NOTE.—*Cooling time lags of air-ethylene isochores are of same duration as the heating, i.e., 3 min.*

For purposes of a comparison to be discussed later, the time lags for ethylene-air mixtures are included in Tables III and IV.

The time lag phenomenon first observed by Geddes and Maass, although not comprehensively reinvestigated, is shown to be reproducible within the limits of experimental error.

One Component System

The liquid and vapor densities at 9.50° C. were determined as functions of the mass per volume ratio in the following manner. The mercury level was adjusted so that the liquid or vapor phases, as the case might be, totally surrounded the float. The equilibrium density at 9.50° C. was then determined, as was the position of disappearance of the meniscus, on a scale at

TABLE V

LIQUID-VAPOR DENSITIES AT 9.50° C.

Average density	Liquid density	Vapor density	Weight liquid, gm.	Weight vapor, gm.	Total volume, cc.	Volume liquid, cc.	Volume vapor, cc.
0.1822*	0.188	0.1793	1.35	2.805	22.86	7.21	15.65
.1842*	.191	.1806	1.55	2.610	22.58	8.13	14.45
.2020	.2103	.192	3.654	2.77	31.78	17.38	14.40
.2032*	.2113	.191	2.498	1.66	20.52	11.82	8.70
.2070	.2154	.196	3.726	2.09	31.01	17.26	13.75
.2095	.2203	.194	3.965	2.46	30.64	17.99	12.65
.2153	.2255	.196	4.380	2.04	29.82	19.42	10.40
.2184	.2268	.201	4.490	1.93	29.40	19.80	9.60
.2210	.2283	.204	4.634	1.79	29.05	20.30	8.75
.2253	.2310	.210	4.670	1.73	28.50	20.25	8.25

* *These values were obtained with an entirely new apparatus, and the ethylene was purified by means of a Podbielniak still.*

the side of the bomb. The total volume at this mercury level could be cal-
culated from the average density of the medium and the weight of ethylene.
A plot of scale readings against volume gave the relative volumes of liquid
and vapor from the position of disappearance of the meniscus. The amount
and density of the phase not directly measured could then be calculated by
difference. This procedure assumes the homogeneity of each phase, and is
therefore not absolute, but such an assumption is the simplest and most
obvious. The results are given in Table V, and shown graphically in Fig. 2.
It will be noted, as indicated in the table, that the data are obtained from
different samples of pure ethylene.
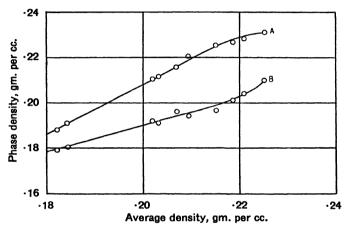
FIG. 2. *Phase densities at 9.50° C. Upper curve, liquid. Lower curve, vapor*

It is interesting to note that the vapor phase at one average density may
have a greater density than the liquid at a lower average density. According
to the classical theory there should exist no difference, and, from the definition
of equilibrium, the nature of the two phases should be independent of the
relative amounts of each phase. One is therefore led to the conclusion that
either the densities determined are not equilibrium values, a point that
cannot be directly settled since time is of infinite duration, or else some other
factor besides the relative amounts of the phases is being altered as the mass
per volume ratio is changed. This factor may well be the regional orientation,
in the nomenclature of Maass and Geddes (7) or the cybotactic groups of
Benz and Stewart (1).

For this reason the maximum divergence is to be expected at the critical
density. At the critical density the movement of the meniscus should be a
minimum, and therefore dilution of one phase by the other should also be a
minimum. If the absolute values of Geddes and Maass were employed,
the maximum would occur at a density of 0.2250 gm. per cc. and not at the
critical. This simple explanation would therefore be invalidated; this is a
good indication that the values now recorded are more nearly correct.

Constancy of Pressure with Changing Volume above the Critical Temperature

Recently Mayer and Harrison (6, 10) made some interesting calculations based on statistical mechanics as to what might be expected in the critical-temperature–critical-pressure region of a one component system. They have found experimental corroboration in the results obtained in this laboratory and went on to predict that the pressure of a system just above the critical temperature would remain constant with changing mass per volume. Specifically they predict a region above the critical temperature, as classically defined, in which the pressure-volume curves for various temperatures are characterized by $\left(\frac{\partial p}{\partial V}\right)_T = 0$. This region has an upper limit given by that temperature for which $\left(\frac{\partial p}{\partial V}\right)_T = 0$ for one point only. The isothermals of Geddes and Maass show no such region. However, the experimental points are not close enough together to settle this question definitely. The evidence given in Table VI shows the validity of Mayer and Harrison's prediction. Owing to the possible importance of this experiment the technique of manipulation may well be presented fully.

TABLE VI

DATA SHOWING CONSTANCY OF PRESSURE WITH CHANGING VOLUME AT 9.80° C.

Mercury level	Average density	Specific volume, cc.	Equilibrium density	Pressure
125	0.2178	4.591	0.2214	50.35
113	.2094	4.775	.2148	50.36
130	.2214	4.514	.2247	50.36
108	.2070	4.830	.2112	50.35

The mercury was adjusted so that the float would be completely immersed in liquid ethylene. The temperature of both the carbon dioxide and ethylene was then carefully raised, great care being taken to maintain the mercury at a constant level. The ethylene temperature was raised to 9.80° C., and the equilibrium density determined. This density measurement showed that the system had remained heterogeneous, for it was an equilibrium value, and differed from the average density at that volume. The carbon dioxide temperature was read, and the pressure corrected for the difference in the mercury levels in the two bombs.

Since the heterogeneity of the system has been shown to be destroyed by either isothermal expansion or compression, the following procedure was employed. After a pressure reading had been made, the mercury level was changed by heating or cooling the carbon dioxide slightly. The centre U-tube was then frozen by raising the dry-ice–acetone mixture about it, and the ethylene cooled to 7.51° C. As may be seen from Fig. 3, the ethylene has, below 8° C., regained its original characteristics. The temperature of the

ethylene was again raised to 9.80° C., and a density and pressure reading obtained with the new volume.

Complete Hysteresis Curve at Constant Volume

The complete hysteresis curve of ethylene, temperatures below the critical temperature being included, has been determined for the first time, and is shown in Fig. 3. The triangular points represent cooling from 10.5° C., a temperature at which the liquid phase has been nearly destroyed. No increase in density occurs on cooling until a visible meniscus forms. This has a bearing on the interpretation of the peculiar data obtained from air-ethylene mixtures, as will be shown later.
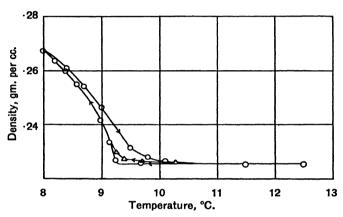
FIG. 3. *Isochore of average density 0.2253. Triangular points denote cooling from 10.5° C.*

AIR-ETHYLENE MIXTURES

A fortunate accident in the use of an ethylene sample contaminated with air had led to unexpected results with respect to the classical temperature-density curve. This sample did not yield the normal hysteresis curve of pure ethylene. The cooling curve followed the heating curve very closely. In order to determine a possible cause of such behavior, measured quantities of air and ethylene were introduced into the apparatus. Two samples, one 0.93% air by weight, the other 0.55% air, were studied.

Isobars of Air-ethylene Mixtures

Two isobars of each sample are given in Fig. 4. The time lags for both heating and cooling have already been recorded in Table III. The times to half-value agree, within the sensitivity of the method, with the values obtained for pure ethylene. Moreover, the shapes of the isobars are similar to those of the curves obtained with pure ethylene. These facts indicate that the inflections observed in isobar runs with pure ethylene are not noticeably affected by the presence of air in these concentrations. This is not so in isochore runs.

Another point of interest in these curves is the increase in density with decreasing air content. The reason for this is that the isobar systems, although at pressures well above the critical in both cases, are now not homogeneous systems (they would be if ethylene alone were present) but consist of two phases. The air is apparently largely insoluble in the liquid ethylene. This causes an increase in pressure on the system, and a corresponding increase in total volume, with a consequent decrease in the density.
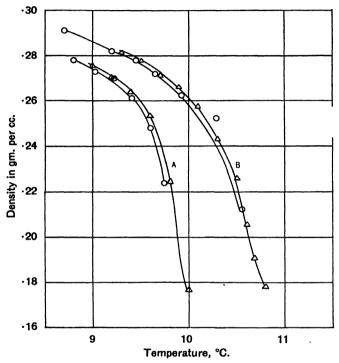
FIG. 4.   *Isobars of air-ethylene mixtures.   Circles, 0.93% air.   Triangles, 0.55% Air.*
A, 50.54; B, 51.44 atm.

Isochores of Air-ethylene Mixtures

These curves, of which typical examples are shown in Fig. 5, exhibit a behavior vastly different from that of the curves obtained with pure ethylene.

The greatest difference is the increase of density with decrease in temperature when the cooling is started above the critical, a phenomenon that has been noted for the first time.

In order to understand the complete significance of what is to follow, a brief review of previous work and theories is given.

The classical temperature-density curve has long been assumed to be parabolic in shape, with a smooth vertex. Experimental evidence had been obtained with increasing temperature nearly to the critical, but never quite

to it. The form of the curve was therefore extrapolated by means of the Cailletet-Mathias rule regarding the critical density. Traube (16), Galitzine (5), and Teichner (15) were the first to question this procedure, and recorded the observation of a density discontinuity above and below the position of disappearance of the meniscus, and that the meniscus reappeared at a temperature other than the critical. Young (20) and others failed to reproduce these results, and attempted to explain them by the theory that impurities hindered the establishment of equilibrium by slowing up of diffusion. Maass and his collaborators have traced the density-temperature curve through the entire critical region with very carefully purified materials, and confirmed the first results of Galitzine *et al*.
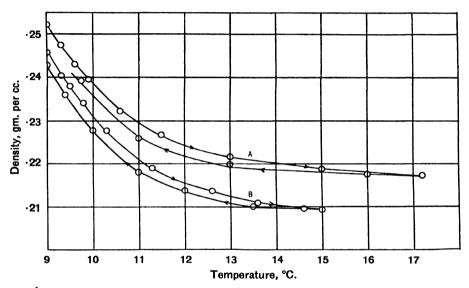
FIG. 5. *Isochores of air-ethylene mixtures. A, 0.93% air; B, 0.55% air.*

It is now believed by the present authors that if this behavior is caused by impurities, and this is regarded as improbable, a mechanism other than that proposed by Young must be assumed. Moreover, it seems doubtful that substances may be obtained pure enough for this phenomenon to disappear entirely, in the light of the work of Clark (2, 3) and that described in the present paper.

Turning again to the time lags of these runs, we see that the order of magnitude in the establishment of equilibrium density is now quite different and much smaller. This in itself indicates an entirely different type of phenomenon to be occurring. There appear two alternatives in explaining what is happening. First, either the liquid phase is destroyed and reformed, and that much more quickly in the presence of air; or second, the air causes the liquid state to persist, since it apparently is not dissolved to any great extent, by

increasing the pressure on that phase. In this case the changes of density may easily be explained by an expansion or contraction of the liquid.

A rough calculation for the 0.93% mixture gives, on the assumption that the meniscus is in the middle of the tube, and that the air is immiscible with liquid ethylene, an excess pressure of approximately three atmospheres. Certain "molecular stirring" experiments performed in the following manner support this theory.

A cooling coil was wound around the upper portion of the bomb. The coil could be maintained at 5° C. by the passage of tap water through it. The temperature of the bomb was raised to 10° C., the sliding thermostat partly lowered, and the upper portion of the bomb cooled. Violent distillation occurred, and the liquid phase was destroyed, since all parts of the sample were subjected to alternate heating and cooling. After several stirrings of this kind, and subsequent heating to 13.5°, the sample had a density of 0.2160 gm. per cc., as Table VII shows. The system is now probably homogeneous, and on cooling acts much like pure ethylene, as Fig. 6 shows, except that the temperature of condensation is now lowered.

TABLE VII
MOLECULAR STIRRING

Intermittent stirring nearly completely destroys liquid

Density	Time of stirring, min.	Temp., °C.	No. of stirrings
0.2379	0	10.00	0
.2215	25	10.00	1
.2193	21	10.00	2
.2172	15	10.00	3
.2172	12	10.00	4

System was cooled to 9.60° C. The density increased slightly to 0.2177 gm. per cc. If heated to 13.5° C., after such stirring the density falls to 0.2160 gm. per cc. On cooling from 13.5° C., the density changes as follows:—

Density	Temp., °C.	Density	Temp., °C.
0.2160	12.50	0.2211	9.40
.2166	11.00	.2227	9.10
.2182	10.00	.2355	8.90
.2197	9.60		

Condensation occurs at approximately 9.0° C.

As shown in Fig. 3, when the liquid phase is partly destroyed, no increase in density occurs on cooling. From this and the above experiments we are led to the conclusion that the liquid phase had persisted many degrees above the critical, owing to the pressure caused by the presence of the inert gas. This allows of the possibility that the phenomenon of hysteresis might entirely disappear if the purity of the substance were great enough. The care taken in purification and filling the apparatus with the pure ethylene samples makes this seem, however, a very remote one.

These investigations are being continued. Particularly the influence of added impurities, both inert and soluble ones, may help to elucidate the nature of the phenomenon. At present the most general explanation that seems plausible is that the liquid state of aggregation differs from the gaseous state
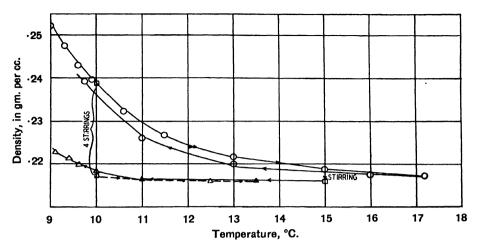
FIG. 6.   *Molecular stirring.   Circles denote reference isochore; triangles denote behavior on heating to 13.5° C. after stirring, then cooling; squares denote behavior on stirring; block triangles denote behavior subsequent to stirring.*
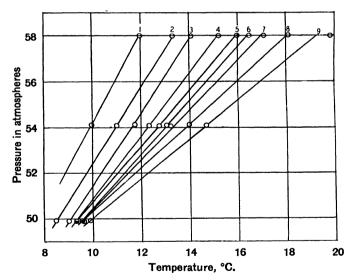
FIG. 7.   *Pressure-temperature relations for various isochores evaluated from Geddes and Maass's isobars.   Numbers denote following isochores—1, 0.290; 2, 0.275; 3, 0.262; 4, 0.240; 5, 0.220; 6, 0.205; 7, 0.190; 8, 0.170; 9, 0.148 gm. per cc.   Shaded circles denote double points.*

owing to a structure in the former.   At the critical temperature and pressure the density of the liquid has been reduced to a point at which structure tends to disappear.   Increase in pressure above the critical temperature tends to re-establish structure.

References

1. BENZ, C. A. and STEWART, G. W.   Phys. Rev. 46 : 703-706.   1934.
2. CLARK, A. L.   Trans. Roy. Soc. Can. III, 9 : 43-67.   1915.
3. CLARK, A. L.   Trans. Roy. Soc. Can. III, 18 : 329-338.   1924.
4. EDWARDS, J. and MAASS, O.   Can. J. Research, 12 : 357-371.   1935.
5. GALITZINE, B.   Wied. Ann. 50 : 521-545.   1893.
6. HARRISON, S. F. and MAYER, J. E.   J. Chem. Phys. 6 : 101-104.   1938.
7. MAASS, O. and GEDDES, A. L.   Phil. Trans. Roy. Soc. A, 236 : 303-332.   1937.
8. MARSDEN, J. and MAASS, O.   Can. J. Research, B, 13 : 296-307.   1935.
9. MARSDEN, J. and MAASS, O.   Can. J. Research, B, 14 : 90-95.   1936.
10. MAYER, J. E. and HARRISON, S. F.   J. Chem. Phys. 6 : 87-100.   1938.
11. MILLS, J. E.   J. Phys. Chem. 9 : 402-417.   1905.
12. MORRIS, H. E. and MAASS, O.   Can. J. Research, 9 : 240-251.   1933.
13. SUTHERLAND, H. S. and MAASS, O.   Can. J. Research, 5 : 48-63.   1931.
14. TAPP, J. S., STEACIE, E. W. R. and MAASS, O.   Can. J. Research, 9 : 217-239.   1933.
15. TEICHNER, G.   Ann. Physik, 13 : 595-610.   1904.
16. TRAUBE, J.   Z. anorg. allgem. Chem. 38 : 399-409.   1904.
17. WINKLER, C. A. and MAASS, O.   Can. J. Research, 6 : 458-470.   1932.
18. WINKLER, C. A. and MAASS, O.   Can. J. Research, 9 : 65-79.   1933.
19. WINKLER, C. A. and MAASS, O.   Can. J. Research, 9 : 613-629.   1933.
20. YOUNG, F. B.   Phil. Mag. 20 : 793-828.   1910.

THE MERCURY PHOTOSENSITIZED DECOMPOSITION OF ETHANE

II. THE PRODUCTION OF HYDROGEN AND THE MECHANISM OF THE REACTION[1]

BY E. W. R. STEACIE[2] AND N. W. F. PHILLIPS[3]

Abstract

An investigation of the mercury photosensitized decomposition of ethane has been made, a continuous flow system being used. Under these circumstances, in the absence of secondary reactions, it is found that there is considerable production of hydrogen. It is therefore concluded that the primary step in the reaction is a C—H bond split.

The mechanism of the reaction is discussed in detail, and it is concluded that the processes occurring, both with and without added hydrogen, are:

$$C_2H_6 + Hg(^3P_1) = C_2H_5 + H + Hg(^1S_0)$$
$$H_2 + Hg(^3P_1) = 2H + Hg(^1S_0)$$
$$H + C_2H_6 = CH_4 + CH_3$$
$$H + C_2H_6 = C_2H_5 + H_2$$
$$2CH_3 = C_2H_6$$
$$CH_3 + C_2H_5 = C_3H_8$$
$$2C_2H_5 = C_4H_{10}$$
$$2H = H_2$$

It is also concluded from a discussion of the various steps that the reaction

$$H + C_2H_6 = CH_4 + CH_3$$

is somewhat faster than

$$H + C_2H_6 = C_2H_5 + H_2 .$$

This necessitates a revision upwards of Steacie and Phillips' estimate of the activation energy of the latter reaction to about 9 Kcal.

Introduction

The mercury photosensitized decomposition of ethane has been examined in a qualitative manner by Tolloczko (17), Taylor and Hill (15), and Kemula (2). A more detailed investigation of the reaction was made by Kemula, Mrazek, and Tolloczko (3). In their experiments the reaction mixture was circulated through a trap at $-80°$ C. in an attempt to remove the products of the reaction as fast as formed, and thus prevent secondary processes. This attempt was not very successful, since more than half of their products were of a molecular weight higher than that of butane, and hence could have resulted from secondary changes only. The analysis of their products was only roughly performed, and consequently the results of their experiments were not very significant.

A more thorough investigation in which the secondary decomposition of *higher* products was entirely eliminated has recently been made by Steacie and Phillips (13). The essential features of their technique were the employ-

ment of powerful light sources, low temperature distillation methods of analysis, and more efficient trapping methods for the removal of higher products.

By operating with a trap cooled to $-130°$ C., they found that the products of the reaction consisted entirely, within the experimental accuracy of 0.3%, of methane, propane, and butane, as expressed by the stoichiometric equation

$$1.00 \ C_2H_6 \ = \ 0.587 \ CH_4 + 0.239 \ C_3H_8 + 0.174 \ C_4H_{10} \ .$$

The quantum yield in terms of ethane disappearing was found to be about 0.2.

If the decomposition were carried out in the presence of added hydrogen, the yield of methane was increased and hydrogen was consumed, as indicated by the average stoichiometric equation

$$1.00 \ C_2H_6 + 0.347 \ H_2 \ = \ 1.12 \ CH_4 + 0.11 \ C_3H_8 + 0.12 \ C_4H_{10} \ .$$

In discussing the mechanism of the reaction, they considered the following steps:

Primary Reactions

$$\begin{align}
C_2H_6 + Hg(^3P_1) &= 2CH_3 + Hg(^1S_0) \tag{1} \\
C_2H_6 + Hg(^3P_1) &= C_2H_5 + H + Hg(^1S_0) \tag{2} \\
H_2 + Hg(^3P_1) &= 2H + Hg(^1S_0) \tag{3} \\
C_2H_6 + Hg(^3P_1) &= CH_2 + CH_4 + Hg(^1S_0) \tag{4}
\end{align}$$

Secondary Reactions of Radicals or Atoms with Ethane

$$\begin{align}
CH_3 + C_2H_6 &= CH_4 + C_2H_5 \tag{5} \\
H + C_2H_6 &= CH_4 + CH_3 \tag{6} \\
H + C_2H_6 &= C_2H_5 + H_2 \tag{7} \\
C_2H_5 + C_2H_6 &= C_4H_{10} + H \tag{8} \\
CH_3 + C_2H_6 &= C_3H_8 + H \tag{9}
\end{align}$$

Radical and Atom Recombination Reactions

$$\begin{align}
2CH_3 &= C_2H_6 \tag{10} \\
CH_3 + C_2H_5 &= C_3H_8 \tag{11} \\
CH_3 + H &= CH_4 \tag{12} \\
2H &= H_2 \tag{13} \\
H + C_2H_5 &= C_2H_6 \tag{14} \\
2C_2H_5 &= C_4H_{10} \tag{15}
\end{align}$$

Other Secondary Reactions of Radicals

$$\begin{align}
C_2H_5 + H_2 &= C_2H_6 + H \tag{16} \\
CH_3 + H_2 &= CH_4 + H \tag{17} \\
CH_3 + CH_4 &= C_2H_6 + H \tag{18} \\
C_2H_5 + CH_4 &= C_2H_6 + CH_3 \tag{19}
\end{align}$$

Reactions Involving the Methylidene Radical

$$CH_2 + C_2H_6 = C_3H_8 \tag{20}$$
$$CH_2 + C_3H_8 = C_4H_{10} \tag{21}$$
$$CH_2 + C_2H_6 = CH_3 + C_2H_5 \tag{22}$$
$$2CH_2 = C_2H_4 . \tag{23}$$

They thus considered three possible primary processes for the decomposition of the ethane molecule, *viz.*,

(a) the elimination of a methylidene radical;

(b) a C—H bond split to give an ethyl radical and a hydrogen atom;

(c) a C—C bond split to give two methyl radicals.

If Reaction (4) were the primary step, propane and butane formation would have occurred by Reactions (20) and (21), and thus at the lowest trapping temperatures the formation of butane should have ceased. As this was not the case, and for other reasons discussed at length in their paper, Steacie and Phillips considered Reaction (4) to be very unlikely as the primary step.

In considering Reaction (2) as the initial process, they assumed the subsequent steps to be Reactions (6), (5), (10), (11), (12), (14), and (15). They pointed out that the main difficulty to be overcome by any mechanism which assumes a primary C—H split would be to account for the absence of hydrogen in the products of the reaction. By assuming that hydrogen atoms, if formed, were consumed chiefly by Reaction (6), and that molecular hydrogen was formed by Reaction (13), *i.e.*, by diffusion to the wall, they calculated that the quantity of hydrogen formed on this basis during an experiment would be from 30 to 200 times the minimum detectable amount. They therefore concluded that a mechanism involving a C—H bond split was inconsistent with experiment, and that the initial step was a C—C bond split (Reaction (1)), followed by Reactions (5), (10), (11), and (15).

The Tenability of a Mechanism Involving a C—H Split

An examination of the reasoning which led to the discarding of the possibility of a C—H split for the primary process shows that re-dissociation of molecular hydrogen by Reaction (3) has been assumed to be negligible. In view of the large cross section of hydrogen relative to ethane for the quenching of $^3P_1$ mercury atoms, it was decided that it was possible that Reaction (3) might be of importance in reducing the concentration of molecular hydrogen in the system.

In order to evaluate the upper limit of the hydrogen concentration under these circumstances, let us consider the following reaction steps:

$$C_2H_6 + Hg(^3P_1) = C_2H_6 + Hg(^3P_0) \tag{1a}$$
$$C_2H_6 + Hg(^3P_1 \text{ or } ^3P_0) = C_2H_5 + H + Hg(^1S_0) \tag{2}$$
$$H + C_2H_6 = CH_4 + CH_3 \tag{6}$$
$$H + C_2H_6 = C_2H_5 + H_2 \tag{7}$$
$$2H = H_2 \text{ (gas)} \tag{13a}$$
$$2H = H_2 \text{ (wall)} \tag{13b}$$
$$H_2 + Hg(^3P_1) = 2H + Hg(^1S_0) \tag{3}$$

From this scheme a steady state concentration of hydrogen can be deduced. Hydrogen formation will occur by Reactions (7), (13a), and (13b), and its destruction by (3). Hence we have

$$\frac{d[H_2]}{dt} = 0$$

$$= \frac{[H_2]\sigma_1^2\mu_1^{\frac{1}{2}}I_{abs}}{[C_2H_6]\sigma_2^2\mu_2^{\frac{1}{2}} + [H_2]\sigma_1^2\mu_1^{\frac{1}{2}}}$$

$$- f\left(\frac{[C_2H_6]\sigma_2^2\mu_2^{\frac{1}{2}}eI_{abs}}{2([C_2H_6]\sigma_2^2\mu_2^{\frac{1}{2}} + [H_2]\sigma_1^2\mu_1^{\frac{1}{2}})} + \frac{[H_2]\sigma_1^2\mu_1^{\frac{1}{2}}I_{abs}}{[C_2H_6]\sigma_2^2\mu_2^{\frac{1}{2}} + [H_2]\sigma_1^2\mu_1^{\frac{1}{2}}}\right),$$

where σ_1 and σ_2 are the mean quenching diameters of excited mercury and hydrogen and excited mercury and ethane respectively; μ_1 and μ_2, their respective reduced masses; I_{abs} is the resonance radiation absorbed in einsteins per sec.; e is the efficiency of Reaction (2) relative to (1a) plus (2), *i.e.*,

$$e = \frac{k_2}{k_{1a} + k_2},$$

and f is the fraction of hydrogen atoms which react to form H_2. This last quantity is given by

$$f = \frac{k_7[H][C_2H_6] + k_{13a}[H]^2[C_2H_6] + \dfrac{k_{13b}[H]}{[C_2H_6]}}{k_7[H][C_2H_6] + k_{13a}[H]^2[C_2H_6] + \dfrac{k_{13b}[H]}{[C_2H_6]} + k_6[H][C_2H_6]}.$$

Whence we get

$$\frac{[H_2]}{[C_2H_6]} = \frac{ef}{2r(1 - f)},$$

where

$$r = \frac{\sigma_1^2\mu_1^{\frac{1}{2}}}{\sigma_2^2\mu_2^{\frac{1}{2}}} = 60.$$

Now in the experiments performed at the lower trapping temperatures, as in Runs 7 and 8 of Table II of the previous paper, the amount of ethane in the gas phase was only about one-tenth of the total amount present owing to condensation in the traps. Hence if we assume as an extreme case $e = 1$, = 0.9, then the percentage of hydrogen which should be found in the products of the reaction is 0.75, which is only two or three times the sensitivity of the analytical method used. If we make the more reasonable assumption that $e = 0.5$ and $f = 0.5$, then the amount of hydrogen which should be found in the products is 0.04%, which would have been quite undetectable by the analytical methods employed.

It is therefore possible that the decomposition occurs by an initial C—H bond split. Of course, although this analysis indicates that a C—H split is *possible*, it offers no proof that it actually occurs as the primary step in the reaction. It was to establish this point with certainty that the present experi-

ments were performed. A continuous (*i.e.*, single pass) flow system was employed. By this method the concentration of hydrogen, if formed, would be kept low, and hence the back reaction, (3), would be diminished; this would permit the hydrogen to accumulate in the products.

Experimental

The Reaction System

The main portion of the apparatus is shown in Fig. 1. The gas at constant pressure entered the system through a calibrated capillary flowmeter. It then flowed through the mercury saturator, S, a desaturating trap, D, and the light-source–reaction vessel. The saturator, S, provided a mercury surface of about 30 cm². and was electrically heated to 60 to 80° C. The trap, D, of about 100 cc. capacity, was packed with small iron pellets. Suitable tests showed that this completely removed the excess mercury picked up by the gas in S, and thus the mercury vapor pressure could be regulated by adjusting the temperature of the thermostat surrounding D.
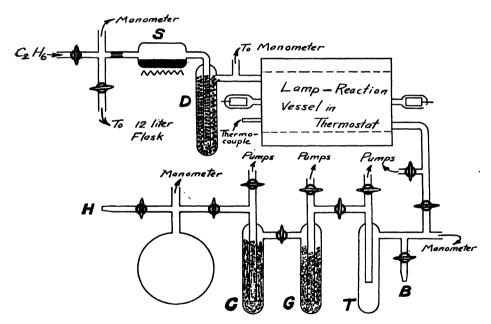
FIG. 1. *Apparatus.*

The light-source–reaction vessel arrangement has already been described (14). It made possible the utilization of the very high output of mercury resonance radiation of 1.5×10^{-5} einsteins per sec.

The pressure in the reaction vessel was regulated by controlling the outflow of the gases, a file-scratched stopcock being used as an adjustable leak. The gas flowed through this stopcock into three traps, T, G, and C, cooled to $-183°$ C. The first trap was initially empty, the second packed with

silica gel, and the third with activated charcoal. A 500 cc. expansion bulb and a manometer were connected to the charcoal trap. The first trap served to collect any higher products and all the ethane. The second and third took out methane and hydrogen. The total amount of these gases could be inferred by isolating the traps and the expansion bulb and warming the traps to room temperature.

The different parts of the apparatus could be separately evacuated as indicated, and ground joints *B* and *II* attached to the collecting traps made provision for the transfer of gases to the analytical system.

The Analytical System

The analytical system consisted of a low temperature fractional distillation apparatus of the Podbielniak type. The column was of small dimensions, and the apparatus could thus be used for the analysis of relatively small samples. With 500 to 600 cc. of gas an accuracy of about 0.3% could be attained. In the analysis the methane and hydrogen were taken off together, and their separate amounts determined by combustion. The method of carrying out the combustion analysis was somewhat novel, and is very convenient for use with a vacuum system. A diagram of the combustion apparatus is given in Fig. 2.
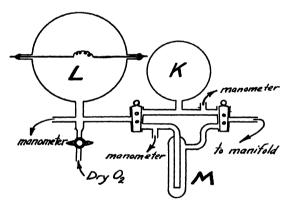
FIG. 2. *Combustion apparatus.*

The combustion pipette, *L*, has a volume of about two litres, and contains an electrically heated platinum spiral of the usual type. Oxygen, which has been dried by passage through a liquid air trap, can be led in as indicated. The gas sample is expanded from the manifold of the distillation apparatus into the bulb *K* of known volume, and its pressure is read on the manometer. The gas from *K* is then expanded into *L*, which has been previously evacuated. It is not necessary to read the pressure in *L*. Oxygen is then run in and the combustion carried out as usual. The gases from *L* are then pumped out through the trap *M*, which is immersed in liquid air. Carbon dioxide and water from the combustion are thus retained, and oxygen is pumped away. *M* is then allowed to warm up to room temperature. The pressure in *M*

minus the vapor pressure of water thus gives the amount of carbon dioxide formed. Whence, knowing the relative volumes of K, L, and M, we can calculate the percentage of methane in the sample.

Materials

Ethane was obtained in cylinders from the Ohio Chemical and Mfg. Co. It was stated to be 97% pure. Analysis showed it to contain 1.3% of ethylene, less than 0.3% of hydrogen plus methane, and less than 0.3% of higher hydrocarbons.

The cylinder gas was purified by passage through a 60 cm. tube containing copper oxide at 300° C., through saturated bromine water into a two-litre bottle illuminated by a Point-o-lite lamp, through a 40% solution of potassium hydroxide, and finally through a trap at −80° C. to remove water. The resultant ethane contained no impurities which could be detected with the analytical method used.

Light Intensity

The measurement of the light intensity, and the determination of the amount of resonance radiation absorbed have been previously described (14).

Experimental Procedure

In making an experiment, the lamp was first run for 30 min. to ensure that it had reached a steady state. The saturator was heated, the traps were cooled, and the ethane flow was then started and continued for a definite period of time. Blank experiments showed that only hydrogen and methane collected in the packed traps, and that no appreciable amount of hydrogen was dissolved in the ethane in the unpacked trap. After the experiment the hydrogen-methane fraction was transferred to the analytical system, and the hydrogen was determined by combustion.

Results

The results of a number of experiments are given in Table I.

TABLE I

THE PRODUCTION OF HYDROGEN IN THE MERCURY PHOTOSENSITIZED DECOMPOSITION OF ETHANE

Ethane flow, 3.0 cc. per sec. at N.T.P. Mercury vapor pressure, 1.3×10^{-3} mm. Resonance radiation absorbed, 1.2×10^{-5} einsteins per sec.

Run No.	Time, min.	Pressure, cm.	Temperature, °C.	Hydrogen formation, moles per sec. $\times 10^6$	Moles of hydrogen formed per quantum absorbed
1	30	4.3	90	0.96	0.080
2	30	4.3	67	1.03	0.086
3	30	4.3	67	0.94	0.078
4	61	4.8	65	0.95	0.079
5	30	4.3	–	0.00 }	Blank runs,
6	60	4.3	–	0.00 }	arc not on.
7	30	4.3	450	5.5	0.48

It may therefore be concluded that, in contrast to the results of the experiments in a circulatory system, hydrogen appears in large quantities when its partial pressure is kept down by the rapid removal of the products of the reaction. The quantum yield for its formation under these circumstances is about half as great as that based on the disappearance of ethane in the circulatory system. It will also be observed from Table I that the production of hydrogen rises rapidly with increasing temperature.

Discussion

It follows from the above results that it is no longer necessary to rule out a C—H bond split mechanism. In fact, it now appears certain that the primary step must involve such a split, *i.e.*, that it must be Reaction (2). The only other alternative would be a C—C split followed by some reactions of methyl or ethyl radicals which produce hydrogen. The only possible reactions of this type would appear to be (8), (9), or (18), and there is no doubt that these are too slow to account for the observed hydrogen production.

Accepting a C—H bond split as the primary step, we then have as alternatives the following schemes:

Scheme I

$$C_2H_6 + Hg(^3P_1) = C_2H_5 + H + Hg(^1S_0) \tag{2}$$
$$H + C_2H_6 = CH_3 + CH_4 \tag{6}$$
$$H + C_2H_6 = C_2H_5 + H_2 \tag{7}$$
$$2CH_3 = C_2H_6 \tag{10}$$
$$CH_3 + C_2H_5 = C_3H_8 \tag{11}$$
$$2C_2H_5 = C_4H_{10} \tag{15}$$
$$2H = H_2 \tag{13}$$

Scheme II

$$C_2H_6 + Hg(^3P_1) = C_2H_5 + H + Hg(^1S_0) \tag{2}$$
$$H + C_2H_6 = CH_3 + CH_4 \tag{6}$$
$$CH_3 + C_2H_6 = CH_4 + C_2H_5 \tag{5}$$
$$2CH_3 = C_2H_6 \tag{10}$$
$$CH_3 + C_2H_5 = C_3H_8 \tag{11}$$
$$2C_2H_5 = C_4H_{10} \tag{15}$$
$$2H = H_2 \tag{13}$$

These schemes assume the same primary step, and the same radical recombination reactions to produce the final products. They differ fundamentally, however, in the presence or absence of Reaction (5) as a means of production of ethyl radicals and of loss of methyl radicals.

With appropriate assumptions as to the relative rates of the various steps we can account stoichiometrically for the products of the reaction on either basis. However, general evidence from other investigations seems to indicate that Reaction (5) is slow compared to (6) and (7). Rice (9) assigned a value of 17 Kcal. to the activation energy of Reaction (5), and while this estimate is

perhaps high it is probably of the right order of magnitude. It may therefore be assumed with considerable plausibility that Reaction (5) is slow, and Scheme II is ruled out. This view is confirmed emphatically by recent work done at Princeton. Concerning this Prof. H. S. Taylor writes (16) ". . . . all the evidence we have had for methane producing processes, starting from methyl, seems to lead to the conclusion that such processes were slow. With methyl iodide and with metal alkyls it was necessary to assume activation energies of 10 Kcal. or more. Morikawa found 11 to 15 Kcal. for the interaction of methyl and deuteromethane. I have had some experiments made . . . . on the photodecomposition of mercury dimethyl, causing this to take place in the presence of ethane and determining at 35, 90, and 160° whether any methane was formed. There are negligible amounts at the two lower temperatures and very much less at 160° than we would have got with the hydrogen in place of ethane. This indicates that the activation energy must be more than 10 Kcal."

We may therefore consider Scheme I to be established. The low quantum yield may be ascribed partly to inefficiency in the primary process, perhaps by the occurrence of

$$C_2H_6 + Hg(^3P_1) = C_2H_6 + Hg(^3P_0) ,$$

and also partially by the occurrence of Reaction (10), leading to the reformation of ethane. This question will be discussed further in a communication dealing with the reaction in the presence of deuterium.

In discussing the results obtained at higher temperatures, it seems that the obvious explanation lies in an increase in the rate of Reaction (7) as compared with (6), as would be expected from its higher activation energy (see later). This is in accord with the results of Trenner, Morikawa, and Taylor (18), who found that at higher temperatures Reaction (7) became predominant. This process would also lead to an increased production of ethyl radicals, and the higher yields of butane relative to propane confirm this idea.

The Reaction in the Presence of Hydrogen

On account of the very high quenching efficiency of hydrogen, a simple calculation shows that in all the hydrogen-ethane mixtures used in the previous investigation the hydrogen was responsible for at least 99% of the quenching. Hence Reaction (3) is established with certainty as the primary step. In the circulatory system, as the reaction proceeds, a considerable quantity of methane is produced which remains in the gas phase. However, this methane, owing to its very small quenching cross section, will absorb only a negligible amount of the incident energy.

Since methane is formed and hydrogen consumed in the reaction, there seems to be no doubt that Reaction (6) is the predominating methane producing step. The only other ways of producing methane involve methyl radicals, and since Reaction (6) is the only reaction producing these in relatively large amount, it would seem to be established with certainty.

To explain the formation of butane it is necessary to have a step which produces ethyl radicals. The only possible reactions of this type appear to be (5) or (7), and as we have seen from the previous section Reaction (5) may be ruled out. The evidence available for Reaction (7) indicates an activation energy in the neighborhood of 9 Kcal. (12, 18), which would be sufficiently fast.

The next question to be answered is how satisfactorily will these reactions account for the results on a stoichiometric basis. First, we may consider the mode of disappearance of the atoms and radicals. Present evidence seems to be in favor of assigning rapid rates to recombination reactions such as (10), (11), and (15) (see, for example, (8)). Reactions producing hydrogen atoms such as (9), or

$$C_2H_6 + C_2H_5 = H + C_4H_{10} \tag{24}$$

are generally considered to have high activation energies, possibly of the order of 15 to 20 Kcal. (9). The occurrence of Reactions (16) and (17) presents some possibility because of the concentration factors in their favor. Leermakers (4) puts $E_{16} = 15$ Kcal. For E_{17} we have estimates (1, 6, 7, 10) from 8 to 23 Kcal., though the best evidence seems to be in favor of a value lower than 15 Kcal. The occurrence of Reactions (16) and (17) to any great extent, however, would lead to too high a value for the ratio

$$\frac{\text{hydrogen consumed}}{\text{methane produced}},$$

as well as suggesting chain characteristics which would not be in accord with the low quantum yield.

Recombination of hydrogen atoms, it would seem, could hardly compete with radical recombination reactions, since there are no reasons for assuming very different orders of concentration for the atoms and radicals, and as the reactions involving atoms are more inefficient owing to third body restrictions (see, for example (5)).

We therefore have as the mechanism of the reaction:

$$H_2 + Hg(^3P_1) = 2H + Hg(^1S_0) \tag{3}$$
$$H + C_2H_6 = CH_3 + CH_4 \tag{6}$$
$$H + C_2H_6 = C_2H_5 + H_2 \tag{7}$$
$$2CH_3 = C_2H_6 \tag{10}$$
$$CH_3 + C_2H_5 = C_3H_8 \tag{11}$$
$$2C_2H_5 = C_4H_{10} \tag{15}$$
$$2H = H_2 . \tag{13}$$

This mechanism accounts completely for the products of the reaction, provided that we assume that Reaction (6) is about four times as fast as (7).

The only way to avoid such an assumption would be to postulate some reaction of velocity comparable to that of (7) which consumes hydrogen and destroys ethyl radicals. The former requisite is necessary to account for the over-all hydrogen consumption, and the latter to account for the low yield

of propane and butane relative to methane. The only possible reactions seem to be

$$H + C_2H_5 = C_2H_6 \tag{14}$$

$$H_2 + C_2H_5 = C_2H_6 + H . \tag{16}$$

In view of the low concentrations of both colliding partners and the dreierstoss restrictions on (14), its occurrence with sufficient rapidity is impossible. The unlikelihood of the occurrence of Reaction (16) has already been mentioned, and results obtained on the reaction with deuterium, to be reported later, also rule it out*.

Apparently, then, it must be assumed that Reaction (6) is about four times as fast as (7). Steacie and Phillips (12) originally found an activation energy of 6.3 Kcal. for (7). This value, however, is now open to some question, since they did not take into account the possibility of the formation of methane in the reaction of hydrogen atoms with ethane. Trenner, Morikawa, and Taylor (18) estimated $E_6 = 7.2$ Kcal., $E_7 = 11.4$ Kcal. Steacie (11) in a further investigation reported $E_6 = 8.6$ Kcal. The present results, by requiring Reaction (6) to be four times as fast as (7) necessitate a revision upward of our previous estimate of E_7 to about 9 Kcal., which is approaching the value reported by Trenner, Morikawa, and Taylor.

References

1. v. HARTEL, H. and POLANYI, M. Z. physik. Chem. B. 11 : 97-138. 1930.
2. KEMULA, W. Roczniki Chem. 10 : 273-286. 1930.
3. KEMULA, W., MRAZEK, S., and TOLLOCZKO, S. Collection Czechoslov. Chem. Commun. 5 : 263-278. 1933.
4. LEERMAKERS, J. A. J. Am. Chem Soc. 56 : 1899-1904. 1934.
5. MORIKAWA, K. BENEDICT, W. S., and TAYLOR, H. S. J. Chem. Phys. 5 : 212-225. 1937.
6. PANETH, F. A., HOFEDITZ, W., and WUNSCH, A. J. Chem. Soc. (London), 372-379. 1935.
7. PATAT, F. Z. Physik. Chem. B. 32 : 274-293. 1936.
8. RICE, F. O. and HERZFELD, K. F. J. Am. Chem. Soc. 56 : 284-289. 1934.
9. RICE, F. O. and RICE, K. K. The aliphatic free radicals. Johns Hopkins Press, Baltimore. 1935.
10. SICKMAN, D. V. and RICE, O. K. J. Chem. Phys. 4 : 608-613. 1936.
11. STEACIE, E. W. R. J. Chem. Phys. 6 : 37-40. 1938.
12. STEACIE, E. W. R. and PHILLIPS, N. W. F. J. Chem. Phys. 4 : 461-468. 1936.
13. STEACIE, E. W. R. and PHILLIPS, N. W. F. J. Chem. Phys. 6 : 179-187. 1938.
14. STEACIE, E. W. R. and PHILLIPS, N. W. F. Can. J. Research. B, 16 : 219-221. 1938.
15. TAYLOR, H. S. and HILL, D. G. J. Am. Chem. Soc. 51 : 2922-2936. 1929.
16. TAYLOR, H. S. Private communication.
17. TOLLOCZKO, S. Przemysl Chem. 11 : 245-253. 1927.
18. TRENNER, N. R., MORIKAWA, K., and TAYLOR, H. S. J. Chem. Phys. 5 : 203-211. 1937.

*In a recent private communication, Professor Taylor suggests that it is possible that Reaction (7) is nevertheless faster than (6), if we assume that we have as an important reaction

followed by

$$H + C_2H_6 = 2CH_3 , \tag{25}$$

$$CH_3 + H = CH_4 . \tag{12}$$

The main trouble with such a mechanism from our point of view is that by requiring all the methyl radicals to be formed via ethyl, it is difficult to see how the butane formation can be suppressed sufficiently so that large amounts of methane are produced.

This suggestion would, however, give a very simple explanation of Trenner, Morikawa and Taylor's results, since assuming a low activation energy for Reaction (25), its rate would not increase as much as that of (7) as the temperature was raised. As a result the concentration of atomic hydrogen would decrease, that of ethyl would increase, and there would be less methane production at higher temperatures.

THE MERCURY PHOTOSENSITIZED DECOMPOSITION OF ETHANE

III. THE REACTION IN THE PRESENCE OF ADDED DEUTERIUM[1]

By E. W. R. Steacie[2], W. A. Alexander[3], and N. W. F. Phillips[4]

Abstract

The mercury photosensitized reactions of ethane-deuterium mixtures have been investigated. The products of the reaction were separated by low-temperature fractional distillation, and the deuterium content of each was determined. It was found that the methane produced was highly deuterized, while the residual ethane was only slightly deuterized. Propane and butane were also considerably deuterized. It is concluded:

(a) That rapid exchange of methyl radicals and deuterium atoms occurs, as previously suggested by Morikawa, Benedict, and Taylor;

(b) That ethyl radicals are rapidly exchanged in a similar way;

(c) That the reactions

$$C_2H_5 + H = C_2H_6,$$

and

$$C_2H_5 + H_2 = C_2H_6 + H$$

do not occur to any great extent, and hence the low quantum yield of the reaction cannot be ascribed to re-formation of ethane.

Introduction

The results of an investigation of the mercury photosensitized decomposition of ethane and a discussion of the mechanism of the reaction have been given in previous papers (5, 6, 7). Experiments have also been reported on the reaction in the presence of hydrogen. It was concluded that the processes occurring both in the presence and in the absence of added hydrogen can be adequately accounted for by the following reactions. (The numbering of these reactions is the same as that used in (7).)

$$C_2H_6 + Hg(^3P_1) = C_2H_5 + H + Hg(^1S_0) \tag{2}$$
$$H_2 + Hg(^3P_1) = 2H + Hg(^1S_0) \tag{3}$$
$$H + C_2H_6 = CH_4 + CH_3 \tag{6}$$
$$H + C_2H_6 = C_2H_5 + H_2 \tag{7}$$
$$2CH_3 = C_2H_6 \tag{10}$$
$$CH_3 + C_2H_5 = C_3H_8 \tag{11}$$
$$2C_2H_5 = C_4H_{10} \tag{15}$$

It is possible to obtain considerable information on certain points by the substitution of deuterium for hydrogen, and an examination of the distribution of deuterium among the products of the reaction. The present paper deals with experiments of this kind.

Experimental

Apparatus and Procedure

The apparatus has already been described (7). It consisted essentially of storage bulbs for the reactants, a circulation system, and a pumping system. Circulation was accomplished by means of a reciprocating pump and a series of mercury valves so arranged that the gases always flowed in one direction. The gases were saturated with mercury vapor by passing them over a heated mercury surface at 60 to 80° C., and then through a trap at 20° C. to remove the excess vapor. The gases then passed through the illuminated reaction vessel, through a trap at −130° C. to remove the reaction products of higher molecular weight, and thence back to the circulating pump. At the end of a definite time of reaction, the lamp was shut off, the pump stopped, and the cold trap allowed to warm up to room temperature.

The gases were then pumped by means of a Toepler pump into a portable mercury gas holder, and transferred to a low-temperature fractional distillation apparatus of the Podbielniak type. The separated fractions from the still were burned, the resulting water was decomposed on a heated tungsten filament, and the resulting hydrogen was analyzed for its deuterium content. The deuterium analysis apparatus was a modified high pressure, high temperature thermal conductivity apparatus similar to that used by Melville and Bolland (1, 3).

Materials

The ethane used was obtained from the Ohio Chemical and Mfg. Co., and was purified by distillation in a still of the Podbielniak type.

The deuterium used in the first run was obtained by the decomposition of 99.6% deuterium oxide by metallic magnesium at 480° C. (2). The deuterium used in Experiments 2 and 3 was obtained by the decomposition of deuterium oxide with metallic calcium. In both cases the gas was dried by passage through a liquid air trap before use.

Results

Three runs were made, different proportions of ethane and deuterium being used. The operating conditions, etc., are given in Table I. The total initial pressure given in the table was observed with the whole system at room temperature.

The analyses of the products are given in Table II. In the analysis the products were separated into five fractions, hydrogen + methane, methane, ethane, propane, and butane. No other products were detected. The percentages of methane and hydrogen in the first fraction were determined by combustion in the ordinary way.

The deuterium contents of the reactants and products, and the input and yield of the process with respect to hydrogen and deuterium are given in Table III. The total hydrogen value given in Column 4 in terms of mole-atoms includes the quantities of hydrogen and deuterium in the various substances, and is obtained by multiplying the mole percentage of each substance in the products, as given in Table II, by the number of hydrogen

atoms in the molecule. The total deuterium content of each substance given in Column 5 is obtained by multiplying the figures in Columns 3 and 4. It is evident from the deuterium balance shown in the final column that the losses of deuterium are very small, when the large number of operations through which the gases have gone are considered.

TABLE I

THE MERCURY PHOTOSENSITIZED DECOMPOSITION OF ETHANE IN THE PRESENCE OF DEUTERIUM

Volume of system, 2180 cc.
Mercury vapor pressure, 1.3×10^{-3} mm.
Circulation rate—
   3 litres per min. in Run 1
   6 litres per min. in Runs 2 and 3
Temperature of reaction vessel, 75° C.

Arc current, 0.100 amp.
Arc potential, 495 volts.
Resonance radiation absorbed, 1.5×10^{-6} einsteins per sec.
Trap temperature, $-130°$ C.
Ethane vapor pressure, about 4 cm.

Run No.	Time, min.	Initial ratio $\dfrac{D_2}{C_2H_6}$	Total initial pressure. cm.	Fraction of C_2H_6 decomposed	Rate of C_2H_6 decomposition, moles per sec. $\times 10^8$	Quantum yield	Products, moles per mole of ethane decomposed			
							D_2 (consumed)	CH_4 (formed)	C_3H_8 (formed)	C_4H_{10} (formed)
1	75	0.52	31.6	0.51	2.74	0.182	0.23	1.01	0.10	0.12
2	90	1.00	34.2	0.66	2.48	0.165	0.43	1.21	0.10	0.12
3	83	1.83	63.5	0.39	1.95	0.130	0.38	1.13	0.12	0.13

TABLE II

DETAILS OF THE ANALYSES

Run No.	Hydrogen-methane fraction		Final percentages of the products of reaction				
	CH_4	H_2	H_2	CH_4	C_2H_6	C_3H_8	C_4H_{10}
1	18.8	81.2	26.4	33.7	32.5	3.4	4.0
2	12.1	87.9	35.8	39.9	17.0	3.3	4.0
3	9.1	90.9	59.4	15.6	21.5	1.7	1.8

Discussion

The most noteworthy points in the above results are:

(a) The very high deuterization of methane;

(b) The low deuterization of ethane;

(c) The quite high deuterization of propane and butane.

On the basis of Steacie and Phillips' mechanism for the reaction, the main method of methane formation is

$$H + C_2H_6 = CH_4 + CH_3, \tag{6}$$

together with a certain amount by

$$CH_3 + H = CH_4. \tag{12}$$

Obviously if all the deuterization of methane occurred in this manner, the maximum possible deuterium content of the methane would be one-quarter

that of the hydrogen present. Actually, as shown in Table III, the D-content of the methane is from 50 to 85% that of the hydrogen at the end of the experiment, *i.e.*, it is approaching complete distribution of deuterium between methane and hydrogen, rather than one-quarter of such a distribution.

Similar behavior was found in the reaction between deuterium atoms and methane by Morikawa, Benedict, and Taylor (4). They suggested that the very high exchange of methane was due to exchange reactions of methyl radicals, probably through the formation and decomposition of a quasi-molecule

$$CH_3 + D = CH_3D^* = CH_2D + H.$$

They inferred an activation energy of about 5 Kcal. for this reaction. The present results are in agreement with this suggestion.

TABLE III

SUMMARY OF DEUTERIUM CONTENTS—DEUTERIUM BALANCE

Run No.	Substance	Deuterium content, mole %	Total H+D, mole-atoms	Total D, mole-atoms	Total deuterium content, mole-atom %
1	H_2	28.6	52.8	15.2	
	CH_4	23.3	134.8	31.4	
	C_2H_6	4.8	195.0	9.4	
	C_3H_8	17.2	27.2	4.7	
	C_4H_{10}	16.6	40.0	6.6	
	Total		449.8	67.3	15.0
	Initial D_2	100	68.2	68.2	
	Initial C_2H_6	0	395.4	0	
	Total		463.6	68.2	14.7
2	H_2	33.5	71.6	24.0	
	CH_4	21.4	159.6	34.2	
	C_2H_6	12.0	102.0	12.1	
	C_3H_8	15.9	26.4	4.6	
	C_4H_{10}	16.2	40.0	6.5	
	Total		399.6	81.0	20.2
	Initial D_2	83.3	100	83.3	
	Initial C_2H_6	0	300	0	
	Total		400	83.3	20.8
3	H_2	68.0	118.8	80.8	
	CH_4	34.1	62.4	21.3	
	C_2H_6	11.4	129.0	14.7	
	C_3H_8	23.5	13.6	4.0	
	C_4H_{10}	21.2	18.0	3.8	
	Total		341.8	124.6	36.4
	Initial D_2	89.6	129.4	116.0	
	Initial C_2H_6	0	211.8	0	
	Total		341.2	116.0	34.0

Further, on the basis of Steacie and Phillips' mechanism, the formation of propane occurs solely by

$$CH_3 + C_2H_5 = C_3H_8 ,$$
                                           (11)

and that of butane solely by

$$2C_2H_5 = C_4H_{10} .$$
                                           (15)

Also, the only reaction producing ethyl radicals in appreciable amount is

$$H + C_2H_6 = C_2H_5 + H_2 .$$
                                           (7)

It would therefore be expected that propane would be deuterized in virtue of the rapid exchange of methyl radicals. However, butane would be expected to be entirely light. Actually, however, propane and butane are both exchanged to about the same extent. This relatively high exchange of butane is presumably to be ascribed to the exchange of ethyl radicals by a mechanism similar to that referred to above for methyl radicals, *viz.*,

$$C_2H_5 + D = C_2H_5D^* = C_2H_4D + H, \text{ etc.}$$

In the previous paper it was pointed out that in order to account satisfactorily for the products of the reaction, it was necessary to assume that the reaction

$$H + C_2H_6 = CH_4 + CH_3$$
                                           (6)

was about four times as fast as

$$H + C_2H_6 = C_2H_5 + H_2 .$$
                                           (7)

The only way to avoid such a requirement is to postulate some reaction, with a velocity comparable to that of (7), which consumes hydrogen and destroys ethyl radicals. The main possibilities are

$$H + C_2H_5 = C_2H_6$$
                                           (14)
$$H_2 + C_2H_5 = C_2H_6 + H .$$
                                           (16)

However, if either of these reactions occurred rapidly, re-forming ethane from most of the ethyl radicals produced by Reaction (7), we would expect the residual ethane at the end of an experiment to be completely exchanged. Actually, the ethane is by no means largely exchanged, and we may therefore rule out the occurrence of Reaction (14) or (16) to an extent comparable with (7). Steacie and Phillips' conclusion that Reaction (6) is faster than (7) therefore receives additional support. The small amount of ethane deuterization which actually occurs is undoubtedly to be ascribed to the occurrence to some extent of the above reactions, and of Reaction (10)

$$2CH_3 = C_2H_6 .$$

Since the recombination reactions, (10) and (14), occur only to a comparatively small extent, the low quantum yield of the reaction (of the order of 0.1) cannot be ascribed to this cause. It is most likely due to inefficiency in the primary step.

References

1. BOLLAND, J. L. and MELVILLE, H. W. Trans. Faraday Soc. 33 : 1316-1329. 1937.
2. KNOWLTON, J. W. and ROSSINI, F. D. Bur. Standards J. Research, 19 : 605-612. 1937.
3. MELVILLE, H. W. and BOLLAND, J. L. Proc. Roy. Soc. London, A160 : 384-406. 1937.
4. MORIKAWA, K., BENEDICT, W. S., and TAYLOR, H. S. J. Chem. Phys. 5 : 212-225. 1937.
5. STEACIE, E. W. R. and PHILLIPS, N. W. F. J. Chem. Phys. 4 : 461-468. 1936.
6. STEACIE, E. W. R. and PHILLIPS, N. W. F. J. Chem. Phys. 6 : 179-187. 1938.
7. STEACIE, E. W. R. and PHILLIPS, N. W. F. Can. J. Research, B, 16 : 303-313. 1938.

EQUILIBRIA IN TWO-PHASE, GAS-LIQUID HYDROCARBON SYSTEMS

II. METHANE AND PENTANE[1]

By E. H. BOOMER[2], C. A. JOHNSON[3], AND A. G. A. PIERCEY[4]

Abstract

The densities and compositions of both phases in the *n*-pentane–methane solubility equilibrium have been determined at 25°, 55°, and 85° C. at total pressures from 35 to 190 atm. The critical pressures of complete miscibility were found. The properties of the system are discussed. Similar measurements at 25° C. and at pressures from 35 to 135 atm. were made on a system composed of a mixture of *n*-pentane and isopentane with methane.

Introduction

In the first paper (3) of this series the methods and apparatus required in the determination of the composition and properties of both phases in liquid-gas systems have been described. In this and subsequent papers the results obtained with a number of different hydrocarbon systems will be presented. A discussion of the results as a whole and the theoretical aspects of the subject will be reserved for a future report. In what follows, the results of measurements on two systems, *n*-pentane–methane and mixed-pentanes–methane, will be given.

Literature

The solubility of methane in *n*-pentane at 25° C. and at pressures as high as 100 atm. has been determined by Frolich *et al.* (5). The composition of the gas phase was not found. If solubilities are expressed as volume of gas at 25° C. and 1 atm. per volume of liquid, the results confirmed Henry's law at least for engineering purposes. The solubility of the gas did appear to increase somewhat more rapidly than the pressure, an effect that was found to be real and of considerable magnitude in the present work. The work of Hill and Lacey (6) on the solubility of methane in *n*-pentane and isopentane at 30° C. and one pressure, 20.4 atm., may be mentioned together with the more extensive work at three temperatures, 100°, 160° and 220° F. with *n*-pentane by Sage, Webster, and Lacey (9). A rapid increase in solubility of methane in pentane at high pressures and an approach to the critical pressure of complete miscibility is evident.

Materials

The preparation of the gas has been described (4). The composition of the particular sample used was: methane, 94.4; nitrogen, 5.6%. Traces of

other gases amounting to 0.1% may have been present. The pressure-volume-temperature behavior and density of this gas are shown in Table I. The data were obtained in the usual manner, one of the high pressure solubility pipettes and the gas measuring system described previously (3) being employed. If the data of Kvalnes and Gaddy (7) for pure methane are used as a standard, it may be stated that the gas used here approaches the ideal more closely than pure methane.

TABLE I

PRESSURE-VOLUME-DENSITY-TEMPERATURE BEHAVIOR OF THE GAS (94.4% OF METHANE, 5.6% OF NITROGEN)

Pressure, atm.	Temperature, °C.	Density, gm./cc.	Deviation, PV/P_1V_1	Pressure, atm.	Temperature, °C.	Density, gm./cc.	Deviation, PV/P_1V_1
1.0	25.0	0.0007005	1.0	1.0	35.0	0.0006776	1.0
35.5		0.02684	0.9266	67.9		0.05118	0.8991
67.9		0.05344	0.8900	134.8		0.1067	0.8563
101.8		0.08318	0.8572	274.6		0.2042	0.9114
134.8		0.1133	0.8332	341.8		0.2343	0.9870
167.9		0.1423	0.8266				
201.4		0.1689	0.8375	1.0	55.3	0.0006358	1.0
208.5		0.1735	0.8422	67.9		0.04686	0.9211
243.6		0.1955	0.8726	134.8		0.09605	0.8902
274.6		0.2130	0.9031	243.6		0.1678	0.9226
308.5		0.2300	0.9397	308.5		0.2008	0.9774
341.8		0.2438	0.9822	369.6		0.2270	1.035
369.6		0.2541	1.019				
				1.0	60.4	0.0006262	1.0
				369.6		0.2232	1.036

A relatively complete list of the properties of the gas is given here for record only. This gas was used throughout most of this work and the relation between its properties and the results will be discussed in future reports.

The *n*-pentane was a commercial product obtained from petroleum. This pentane was washed with a nitrating mixture to remove traces of sulphur and aromatic compounds. It was then washed with dilute alkali solution, and with water, and was finally dried over calcium chloride and distilled through a fractionating column. The fraction retained and used had the following properties: boiling range (700 mm. of mercury), 35.7 to 36.0° C.; density (23° C.), 0.624; refractive index (22° C.), 1.3563.

A small amount of a mixture of isopentane and *n*-pentane was prepared by the fractional distillation of naphtha from Turner Valley, Alberta. The fraction showed the following properties: boiling range (700 mm. of mercury), 27.7 to 35.1° C.; density (23° C.), 0.620; refractive index (22° C.), 1.3539.

The fractionating column was reasonably efficient under high reflux and gave a good separation of the pentanes from other hydrocarbons. In the illustrative figures following, this mixture is designated as *i*-pentane.

Results and Discussion

The experimental results are shown in Tables II and III.   Not all the results are included, approximately one-quarter having been discarded because of obvious errors due to leaks and failure to attain equilibrium.   In the tables, S_1'' gives the solubility of methane in pentane as the mole ratio, and S_2' gives the pentane content of the gas phase as the mole ratio of pentane to total gas.   Multiplying the first by 311 gives the solubility as cubic centimetres of methane at N.T.P. per gram of pentane.   Dividing the second by 311 gives the number of grams of pentane per cubic centimetre of expanded gas at N.T.P.   The mole fractions X, with subscripts 1 and 2 to designate methane and pentane and single primes and double primes to designate gas phase and liquid phase, are used to calculate the equilibrium constants.

TABLE II

METHANE–n-PENTANE SOLUBILITY EQUILIBRIUM

Pressure, atm.	gm. per cc.		Liquid			Gas					constant	
	Liquid	Gas	C₅H₁₂	CH₄	N₂	C₅H₁₂	CH₄	N₂	S_1''	S_2'	X_2'/X_2''	X_1'/X_1''
Temperature, 25° C.												
35.5	0.590	0.0366	83.9	15.6	0.5	8.3	84.8	6.9				
	0.592	0.0352	83.6	16.1	0.3	8.3	88.4	3.3	0.189	0.0905	0.099	5.46
68.1	0.564	0.0630	69.8	29.8	0.4	5.1	88.0	6.9	0.427	0.0537	0.073	2.95
101.4	0.520	0.0984	56.7	42.1	1.2	4.7	88.9	6.4				
	0.518	0.0975	56.7	42.6	0.7	5.2	89.2	5.6	0.746	0.0521	0.087	2.10
134	0.481	0.146	45.0	53.6	1.4	5.8	87.4	6.8	1.190	0.0615	0.129	1.63
167.6	0.380	0.233	28.1	68.3	3.6	12.2	83.1	4.7				
	0.380	0.236	28.2	67.7	4 1	12.2	82.0	5.8	2.415	0.139	0.434	1.21
188	0.350	0.348	22.5	72.9	4.6	22.5	73.4	4.1	3.240	0.290	1.00	1.01
Temperature, 55° C.												
35.5	0.563	0.0367	85.8	13.9	0.3	13.8	81.5	4.7	0.162	0.160	0.161	5.85
101.4	0.493	0.0972	60.3	38.6	1.1	8.1	86.2	5.7				
	0.495	0.0973	60.6	38.0	1.4	8.4	85.1	6.5	0.634	0.091	0.136	2.23
134	0.449	0.146	48.2	49.5	2.3	10.3	84.1	5.6	1.025	0.115	0.214	1.70
167.6	0.338	0.244	30.0	66.7	3.3	18.5	77.2	4.3				
	0.341	0.247	30.0	66.1	3.9	19.1	76.2	4.7	2.210	0 232	0 627	1.15
174.4	0.287	0.285	22.5	73.4	4.1	22.3	73.8	3.9	3.26	0.287	0.99	1.01
Temperature, 85° C.												
35.2	0.532	0.0367	87.6	12.1	0.3	19.0	77.0	4.0	0.138	0.234	0.217	6.36
100.7	0.464	0.105	63.3	35.3	1.4	14.5	79.1	6.4	0.558	0.170	0.229	2.24
133.7	0.404	0.161	49.7	47.8	2.5	17.7	77.3	5.0				
	0.404	0.160	49.4	48.5	2.0	17.7	76.6	5.7	0.972	0.216	0.357	1.60
147.2	0.368	–	42.8	54.3	2.9							
	0.368	0.194	43.1	53.8	3.1	20.8	74.5	4.7				
	0.370	0.194	43.0	54.2	2.8	21.2	74.8	4.0	1.26	0.250	0 488	1.38
160.1	0.211	0.210	20.8	75.0	4.2	20.6	75.0	4.4	3.60	0.262	0.99	1.00

These constants, the reciprocal of the Ostwald absorption coefficient for methane, are common in the literature (10) as a means of describing liquid-gas equilibria.

TABLE III

METHANE–MIXED-PENTANES SOLUBILITY EQUILIBRIUM (TEMPERATURE, 25° C.)

Pressure, atm.	Phase density, gm. per cc.		Phase composition, mole %						Solubility		Equilibrium constant	
			Liquid			Gas						
	Liquid	Gas	C_5H_{12}	CH_4	N_2	C_5H_{12}	CH_4	N_2	S_1''	S_2'	X_2'/X_2''	X_1'/X_1''
34.4	0.585	0.0386	82.3	17.0	0.7	10.4	84.8	4.8				
	–	0.0385	–	–	–	11.2	84.4	4.4	0.206	0.121	0.131	4.98
66.6	0.554	0.0613	68.9	30.6	0.5	4.7	89.5	5.8				
	0.556	0.0648	69.2	30.2	0.6	4.6	89.9	5.5	0.440	0.049	0.067	2.95
100.3	0.512	0.100	55.6	43.2	1.2	4.4	89.8	5.8				
	0.514	0.0971	57.2	42.2	0.6	4.2	88.0	7.8	0.757	,0.045	0.076	2.06
		0.1075				4.3	88.9	6.8				
133	0.440	0.1463	43.4	54.7	1.9	5.7	86.2	8.1				
	0.445	0.1500	41.1	56.4	2.5	6.4	86.7	6.9	1.313	0.064	0.142	1.56
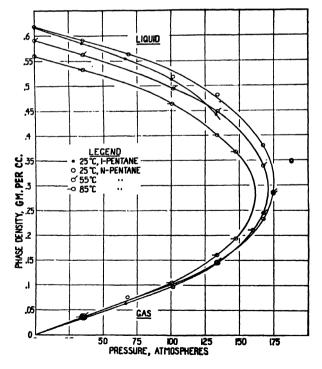
FIG. 1. *Relation between densities of gas and liquid phases at constant temperature and pressure.*

The results are shown in graphical form in Figs. 1 to 4. Figs. 1 and 2, showing respectively density and composition as functions of pressure at different temperatures, are fundamental in giving the directly measured quantities. Points in the single phase region for the n-pentane system are given in Table I at the highest pressure for each temperature. That these points are in the single phase region may be seen by reference to Figs. 1 and 2.

TABLE IV

CONDITIONS AT PRESSURE OF COMPLETE MISCIBILITY

Temperature, °C.	Pressure, atm.	Density, gm. per cc.	Pentane, mole %	S_1''	S_2'
25	175	0.307	19	4.02	0.234
55	171	0.293	25	2.91	0.333
85	162	0.285	31	2.75	0.450

n-Pentane

The properties of the system at the critical pressure of complete miscibility are given in Table IV. The data given in this table have been taken from enlarged copies of Figs. 1 and 2 and do not represent measured quantities.
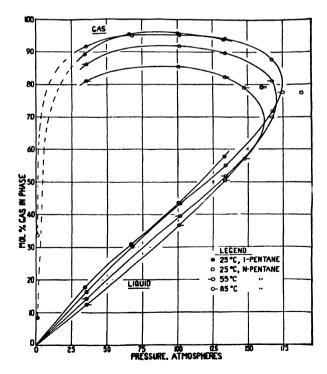
FIG. 2. *Relation between composition of gas phase and that of the liquid phase at constant temperature and pressure.*

The effects disclosed in Table IV are to be expected. With rising temperature, the critical pressure and density decrease, and the percentage of pentane in the system increases. Evidently the pressure of complete miscibility decreases more rapidly than the temperature increases and must approach the critical pressure of pentane.
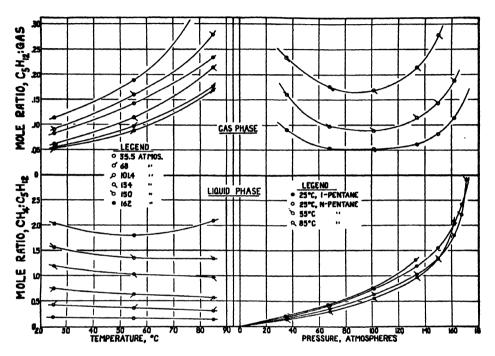
FIG. 3. Relation between solubilities, expressed as mole ratios of methane to pentane in liquid phase and pentane to gas in gas phase, and temperature and pressure.

The effect of increasing pressure of gas in the system upon the vapor pressure of pentane is shown in Fig. 2. Considerable vaporization of pentane into the gas phase occurs at relatively low pressures. The process becomes sufficiently important at 75 to 100 atm. to counteract the effect of increasing gas pressure, and the gas content of the gas phase reaches a maximum. The simple Poynting rule does not predict this maximum. In a future paper it will be shown that this maximum can be predicted, at least qualitatively. From the pressure corresponding to the minimum pentane-methane molecular ratio in the gas phase to the pressure of complete miscibility, under isothermal conditions, the concentration of pentane in the gas phase increases rapidly. The phenomenon may be described as one of increasing solubility of pentane in methane. The concentration of pentane in the gas phase is remarkably high and when expressed as partial vapor pressure, the ideal gas law being used, reaches meaningless values of several atmospheres.

The variation of the composition of the liquid phase is of interest in three particulars. At low pressures the gas content increases linearly with pressure. At pressures from 50 and 125 atm. there is a suggestion of concavity in the curves. (This effect has been found to be more pronounced in other systems, which will be discussed in subsequent papers.) It has been shown by Bassett and Dode (1) that with systems such as nitrogen-water, the liquid composition curves, plotted as in Fig. 2, go through a maximum and at no
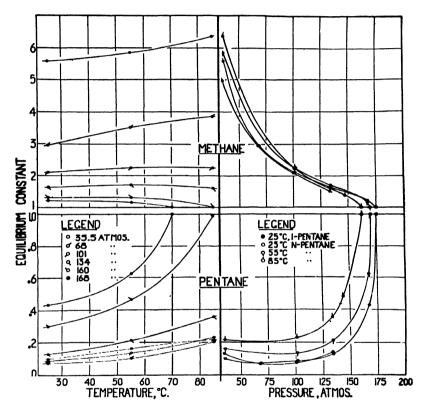
FIG. 4. Relation between equilibrium constants, the mole ratio of methane in gas phase to methane in liquid phase and similarly for pentane, and temperature and pressure.

pressure is there complete miscibility. In the present case, the great solubility of methane in pentane, compared to that of nitrogen in water, results in reversal of the trend of the curve and the existence of conditions of complete miscibility. Finally, at pressures below 150 atm. the effect of increasing temperature is to reduce the gas content of the liquid phase. In the region between 150 atm. and the critical pressures there is the phenomenon of retrograde gaseous solubility, the methane content of the liquid phase increasing with increasing temperature.

The work of Sage, Webster, and Lacey (9) on the *n*-pentane–methane system agrees very well with the present results. Their "bubble point" pressures and compositions may be compared with the present results by interpolation between the liquid phase data sh)wn in Fig. 2. A regular small discrepancy exists, the methane content given by Sage, Webster, and Lacey being greater than that found here. The discrepancy may be attributed to the presence of nitrogen in the gas used in the present investigation.

The data of Fig. 2 have been expressed in a different manner, and this is shown graphically in Fig. 3. The solubility of methane in pentane (liquid phase) is shown as a function of temperature and pressure. The minimum in solubility of methane with increasing temperature is shown clearly at 162 atm. It is interesting also to notice that at the lowest pressure used, 35.5 atm., the effect of temperature on the solubility is least. The variation of solubility with pressure at constant temperature shows clearly the limitations of Henry's law. Evidently deviations become appreciable at 40 to 50 atm., and above 150 atm. the solubility increases very rapidly with pressure.•

The effect of temperature and pressure on the solubility of pentane in the gas phase is shown more clearly in Fig. 3 than in Fig. 2. Under isobaric conditions, the pentane content of the gas phase increases with temperature, the increase being very great at high pressures. The minimum in pentane content with increasing pressure at constant temperature is shown very clearly. It is evident here, as in Fig. 2, that fixing the composition of the system and the temperature does not define the pressure except at the minimum point.

The use of equilibrium constants (10) to express and predict the behavior of gas-liquid systems makes their presentation here of some interest. Fig. 4 gives these constants for methane and for pentane as functions of temperature and pressure. In the range of conditions used, contrary to custom, it was not found necessary to use a semilogarithmic plot. Further, as found by Nederbragt (8), a semilogarithmic plot with temperature gave straight lines only at the lower pressures.

There is rough agreement between the equilibrium constants given here and those plotted by Souders, Selheimer, and Brown (10). The discrepancy is sufficiently great to make the use of their curves inadvisable except for approximate estimations. It does not appear that the equilibrium constants of one constituent are independent of the other constituent.

Isopentane

The few measurements on the mixed-pentane–methane system are, for comparison with the *n*-pentane system, shown in Table III and plotted in Figs. 1-4. Generally the differences between the two systems may be predicted on the basis that isopentane is more like methane in constitution than is *n*-pentane. Methane is definitely more soluble in the mixture of pentanes than in pentane alone. This has also been reported for isopentane at one pressure by Hill and Lacey (6). It is evident from Fig. 2 that the pressure of complete miscibility for the mixed pentanes and methane will be less than that for *n*-pentane and methane.

The equilibrium constant for methane in the mixed pentane system is slightly lower at all pressures used. This is due to the greater solubility of methane in isopentane and the slight difference in composition of the two gaseous phases. The equilibrium constants of the mixed pentanes have little meaning because the liquid is a mixture. They are shown, however, in Fig. 4 and it is evident that they differ barely by a significant amount from the equilibrium constant for *n*-pentane. The effect of isomerization of the solvent on the equilibrium constant of the solute is appreciable, but the equilibrium constants of the isomeric solvents are very nearly equal.

References

1. BASSETT, J. and DODE, M. Compt. rend. 203 : 775-777. 1936.
2. BOOMER, E. H. and JOHNSON, C. A. Can. J. Research, B, 15 : 363-366. 1937.
3. BOOMER, E. H., JOHNSON, C. A., and ARGUE, G. H. Can. J. Research, B, 15 : 367-374. 1937.
4. BOOMER, E. H., JOHNSON, C. A., and THOMAS, V. Can. J. Research, B, 15 : 360-362. 1937.
5. FROLICH, P. K., TAUCH, E. J., HOGAN, J. J., and PEER, A. A. Ind. Eng. Chem. 23 : 548-550. 1931.
6. HILL, E. S. and LACEY, W. N. Ind. Eng. Chem. 26 : 1324-1327. 1934.
7. KVALNES, H. M. and GADDY, V. L. J. Am. Chem. Soc. 53 : 394-399. 1931.
8. NEDERBRAGT, G. W. Ind. Eng. Chem. 30 : 587-588. 1938.
9. SAGE, B. H., WEBSTER, D. C. and LACEY, W. N. Ind. Eng. Chem. 28 : 1045-1047. 1936.
10. SOUDERS, M., SELHEIMER, C. W., and BROWN, G. Ind. Eng. Chem. 24 : 517-519. 1932.

EQUILIBRIA IN TWO-PHASE, GAS-LIQUID HYDROCARBON SYSTEMS

III. METHANE AND HEXANE[1]

BY E. H. BOOMER[2] AND C. A. JOHNSON[3]

Abstract

The densities and compositions of both phases in the *n*-hexane–methane solubility equilibrium have been determined at 25°, 55°, and 85° C., at total pressures from 35 to 230 atm. The critical pressures of complete miscibility were found. The properties of the system are discussed. Similar measurements were made on a system consisting of a liquid mixture, principally isomeric hexanes, and methane.

Introduction

In previous papers, methods and apparatus for the study of equilibria in two-phase, gas-liquid, hydrocarbon systems were described (1), and the results of the investigation of the pentane-methane solubility equilibrium were presented (2). The present paper gives results obtained with the next higher paraffin hydrocarbon, hexane, and the same gas. It is hoped that in a following paper reporting on results obtained with a third hydrocarbon, heptane, the relations between the three systems will be discussed.

Literature

Measurements of the type to be described are relatively rare. Frolich *et al.* (3) have measured the solubility of methane in *n*-hexane at 25° C. and at pressures as high as 90 atm. In this pressure range they found that the solubility followed Henry's law fairly closely. The agreement was better when the gas pressure was corrected to the ideal state. However, the solubility of the gas increased somewhat more rapidly than the pressure. The same phenomenon was found in the present work, the magnitude of the effect increasing greatly at higher pressures. Hill and Lacey (4) determined the solubility of methane at one pressure, 20.4 atm., and one temperature, 30° C. Similar measurements showed that the solubilities of methane in *n*-pentane, isopentane, and *n*-hexane increased in that order. More extensive measurements on the hexane-methane system have been carried out by Sage, Webster, and Lacey at 100°, 160°, and 220° F. (8). They give the "bubble point" pressures, *i.e.*, the pressure at which a gas phase just forms, in three different liquid solutions. In the region in which comparison is possible, the present results are in substantial agreement with those of Sage, Webster, and Lacey.

Apparatus and Materials

The apparatus and experimental methods have been described (1).

The gas used was the same as that described previously (2); its composition was methane, 94.4; nitrogen, 5.6%.

Pure *n*-hexane was synthesized from *n*-propyl bromide according to the Wurtz reaction. *n*-Propyl alchol was used as the original material. It was converted to *n*-propyl bromide in 80% yield by the hydrobromic-acid–sulphuric-acid method (7, p. 5). The directions of Lewis, Hendricks, and Yohe (6) for the similar synthesis of octane were followed, an anhydrous ether medium being used. The yield of *n*-hexane was not appreciable. It was found more satisfactory to carry out the reaction without the ether medium and to maintain careful temperature control. Briefly, the method was as follows: Anhydrous *n*-propyl bromide in a flask fitted with a reflux condenser was treated with a small portion of fresh, clean sodium wire. By means of a cooling bath the temperature was kept below 22° C. When reaction was complete, the sodium bromide was separated by filtration, and a second portion of sodium wire was added. This was repeated until the addition of sodium did not produce any reaction.

The liquid product was largely *n*-hexane containing some *n*-propyl bromide. It was fractionated carefully in an efficient vacuum jacketed, three foot column. The material retained and used as *n*-hexane had the following properties: boiling range (700 mm. of mercury), 68.8 to 69.1° C.; density (23° C.), 0.660 gm. per cc.; refractive index (21°), 1.3752.

A mixture, substantially isomeric hexanes, was prepared from naphtha from Turner Valley, Alberta. A five gallon lot was distilled through the column described and the fraction boiling at 60° to 70° C. retained. This material was treated exhaustively with a nitrating mixture, washed thoroughly with dilute alkali and water, and dried. Careful fractionation was carried out and a product having the following properties was retained: boiling range (700 mm. of mercury), 60.5 to 63.9° C.; density (20° C.), 0.664 gm. per cc.; refractive index (25° C.), 1.3739.

The properties suggest that the material consisted largely of β-methyl pentane and β-ethyl butane. The distillation curve shows that very little *n*-hexane was present.

Results and Discussion

The experimental results obtained with the *n*-hexane system are shown in Table I, and those with the mixed hexanes system in Table II. In the tables, S_1'' gives the solubility of methane in hexane as the mole ratio in the liquid phase, and S_2' gives the hexane content of the gas phase as the mole ratio of hexane to total gas. The quantity, 260.3 S_1'', gives the solubility of methane in hexane in cubic centimetres at N.T.P. per gram. The quantity, $S_1''/260.3$, gives the vapor content of the gas phase in grams of hexane per cubic centimetre of gas expanded to N.T.P. The mole fractions, X, with subscripts 1 and 2 to designate methane and hexane, and single prime and

double primes to designate gas phase and liquid phase, are used to calculate the equilibrium constants given in the last two columns of the tables.

The results are shown in graphical form in Figs. 1 to 4.   Figs. 1 and 2, showing density and composition as functions of pressure, are taken directly from the tables.   Figs. 3 and 4, showing solubilities and equilibrium constants, include data from the tables and some data calculated from an enlarged copy of Fig. 2.

TABLE I

PROPERTIES OF THE *n*-HEXANE–METHANE SOLUBILITY EQUILIBRIUM

Pressure, atm.	Phase density, gm. per cc.		Phase composition, mole %						Solubility		Equilibrium constant	
			Liquid			Gas						
	Liquid	Gas	C_6H_{14}	CH_4	N_2	C_6H_{14}	CH_4	N_2	S_1''	S_2'	X_2'/X_2''	X_1'/X_1''
Temperature, 25° C.												
1	0.655	–	–	–	–	19.6	80.4	–	–	–	–	–
36.2	0.635	0.0313	83.9	15.9	0.2	3.3	89.7	7.0				
	0.633	0.0292	83.5	16.2	0.3	2.6	92.0	5.4	0.192	0.0302	0.0350	5.66
68.4	0.609	0.0584	71.3	27.8	0.9	1.8	93.4	4.8	0.389	0.0188	0.0258	3.36
101.7	0.580	0.0909	59.6	39.2	1.2	2.1	90.9	7.0				
	0.579	0.0905	59.7	39.0	1.3	2.1	91.6	6.3	0.655	0.0204	0.0349	2.33
134.7	0.548	0.130	49.4	48.5	2.1	3.0	88.8	8.2	0.983	0.0305	0.0600	1.83
167.9	0.509	0.177	39.2	57.8	3.0	4.6	88.3	7.1				
	0.505	0.178	39.0	58.3	2.7	4.7	89.6	5.7	1.485	0.0488	0.1192	1.53
202.0	0.436	0.249	27.9	69.0	3.1	8.1	84.4	7.5				
	0.438	0.252	27.4	68.9	3.7	8.2	83.8	8.0	2.490	0.0888	0.2945	1.22
208.2	0.408	0.281	23.7	73.4	2.9	10.5	83.8	5.7				
	0.410	0.281	23.6	72.6	3.8	10.4	83.3	6.3	3.08	0.1168	0.442	1.145
229.3	0.371	0.367	18.0	77.1	4.9	17.5	77.9	4.6	4.27	0.212	0.968	1.01
Temperature, 55° C.												
1	0.627					63.15	36.85					
36.2	0.609	0.0297	85.5	14.2	0.3	4.9	87.3	7.8	0.166	0.0518	0.0576	6.14
101.7	0.556	0.084	62.8	35.5	1.7	3.4	89.9	6.7	0.565	0.0351	0.0540	2.53
167.9	0.484	0.163	42.1	55.3	2.6	5.7	88.2	6.0	1.315	0.0607	0.136	1.595
202.0	0.416	0.240	30.3	66.2	3.5	10.9	82.7	6.4				
	0.419	0.238	30.6	65.4	4.0	10.9	82.8	6.3	2.16	0.1225	0.369	1.257
208.2	0.373	0.277	24.9	71.0	4.1	14.6	80.8	4.6				
	0.373	0.275	25.0	71.5	3.5	14.5	80.8	4.7	2.86	0.170	0.583	1.133
219.1	0.319	0.323	18.9	76.8	4.3	18.6	76.8	4.6	4.06	0.229	0.986	1.00
Temperature, 85° C.												
1	0.597											
35.5	0.580	0.0301	87.1	12.6	0.3	11.3	82.9	5.8	0.145	0.1272	0.1296	6.56
101.4	0.530	0.0835	65.1	33.3	1.6	6.0	89.3	4.7	0.512	0.0641	0.0925	2.68
167.6	0.451	0.163	44.3	53.7	2.0	9.8	85.0	5.2	1.212	0.1088	0.2215	1.582
187.9	0.414	0.211	35.2	61.1	3.7	13.9	80.1	6.0				
	0.410	0.211	36.4	60.3	3.3	13.5	80.7	5.8	1.697	0.1588	0.383	1.33
201.0	0.324	0.321	25.0	71.4	3.6	25.0	70.3	4.7	2.85	0.334	1.00	0.985

TABLE II
PROPERTIES OF THE MIXED-HEXANES–METHANE SOLUBILITY EQUILIBRIUM
TEMPERATURE, 25° C.

Pressure, atm.	Phase density, gm. per cc.		Phase composition, mole %						Solubility		Equilibrium constant	
			Liquid			Gas						
	Liquid	Gas	C_6H_{14}	CH_4	N_2	C_6H_{14}	CH_4	N_2	S_1''	S_1'	X_1'/X_1''	X_1'/X_1''
1	0.659											
35.5	0.629	0.0306	84.1	15.6	0.3	4.1	89.0	6.9				
	0.631	0.0294	83.8	16.1	0.1	3.6	92.7	3.7	0.190	0.0401	0.0460	5.70
101.4	0.571	0.0892	59.1	39.8	1.1	2.0	91.4	6.6	0.674	0.020	0.0332	2.29
167.6	0.497	0.182	38.0	58.5	3.5	4.6	89.3	6.1	1.54	0.0476	0.1195	1.525
201.0	0.386	0.291	23.2	73.2	3.6	12.0	82.8	5.2				
	0.391	0.287	22.5	73.8	3.7	11.8	82.8	5.4	3.21	0.135	0.522	1.125
215.0	0.399	0.395	22.2	74.3	3.5	22.3	72.9	4.8	3.35	0.287	1.01	0.982
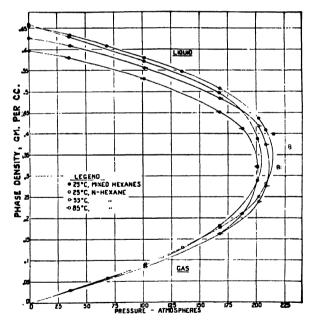
FIG. 1. *Relation between densities of gas and liquid phases and pressure at constant temperature.*

n-Hexane

At the lowest pressure used, 36 atm., methane dissolves to a greater extent in *n*-hexane than in *n*-pentane. This is in agreement with Hill and Lacey's (4) result at 20.4 atm. At higher pressures, however, methane is always more
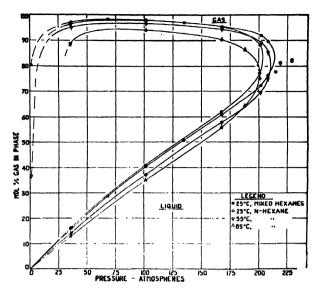
FIG. 2.   *Relation between composition of gas phase and that of the liquid phase and pressure at constant temperature.*
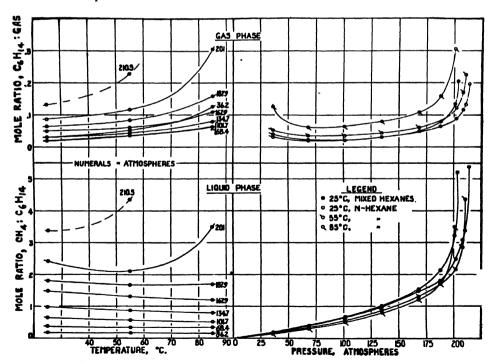
FIG. 3.   *Relation between solubilities, expressed as mole ratios of methane to hexane in liquid phase and hexane to gas in gas phase, and temperature and pressure.*

soluble in *n*-pentane than in *n*-hexane.   If solubility is expressed in cubic
centimetres per gram, methane is more soluble in pentane than in hexane
at all pressures up to the critical pressure for the pentane system.   However,
at pressures near the critical the solubility of methane in hexane is greater
than it is in pentane at the corresponding pressure.   The hexane content of
the gas phase is always less than the pentane content.   This is only to be
expected when the relative volatility of the two liquids is considered.   The
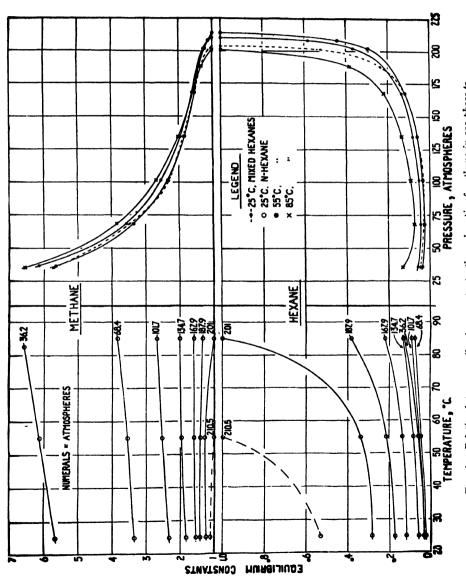
FIG. 4.   Relation between equilibrium constants, the mole ratio of methane in gas phase to
methane in liquid phase and similarly for hexane, and temperature and pressure.

pressure at which the vapor content of the gas phase is a minimum is about the same, 100 atm., in the two systems.

The agreement between the present results for the liquid phase and those of Sage, Webster, and Lacey is good, except at the highest pressures used by them, 165 to 170 atm. The agreement between these solubilities and those found by Frolich is excellent. A small regular difference exists, the present figures being the smaller; this may be attributed to the nitrogen content of the gas.

The limitations of Henry's law are shown clearly in Fig. 3. Deviations become appreciable at 40 to 50 atm. and a rapid increase in solubility with pressure becomes marked at pressures greater than 100 atm. The upper limit of the pressure in Frolich's work was 90 atm.

When the pentane and hexane systems are considered as a whole, it is seen that their behavior is essentially the same. The differences that exist are in the direction expected on the basis that hexane is denser and less volatile than pentane. For example, the hexane system shows a higher pressure of complete miscibility. Again, the pressure at which a solubility minimum becomes evident in the temperature range used is about 200 atm. for hexane and 160 atm. for pentane. The curve of composition-pressure for the liquid phase, Fig. 2, is slightly concave to the pressure ordinate, the inflexion leading to the critical region occurring at 150 to 175 atm. This effect is general (2) and more marked in the hexane system than in the pentane system.

The equilibrium constants, Fig. 4, change with temperature and pressure in a manner to be expected. The constant for hexane decreases to a minimum and increases rapidly to unity with increasing pressure. This has been found generally true by other investigators (5, 9). The constants for hexane are always less than those for pentane, in both cases of course approaching unity at the critical pressure. This might be expected to be a general rule for paraffins. The equilibrium constants of methane in the hexane system are greater than they are in the pentane system. The difference is small, about 5%, at the lowest pressure, but it increases as the critical pressure is approached. Evidently, the assumption that the equilibrium constant (9) for methane does not vary with the composition of the liquid holds only at relatively low pressures, where Henry's law is obeyed. Both equilibrium constants increase slowly with increasing temperature at low pressures. At high pressures, near the point of complete miscibility, the constants for hexane increase rapidly, and those for methane decrease slowly, with increasing pressure.

The properties of the system at the pressure of complete miscibility are given in Table III. The data have been taken from enlarged copies of Fig. 2 and are not the result of direct measurement. The shift in composition with increasing temperature is approximately linear with respect to the temperature. This is not true with regard to the two properties, pressure of complete miscibility and density. The pressure decreases to a greater extent and the density to a smaller extent in the interval from 55° to 85° C. than they do in the interval from 25° to 55° C.

Mixed Hexanes

The properties of the mixed-hexanes–methane system are given in Table II and shown in Figs. 1 to 4.   This system bears much the same relation to the *n*-hexane system that the mixed pentane system did to the *n*-pentane system (2).   The methane content of the liquid phase and the hexane content of the gas phase are greater in the systems containing mixed hexanes.   The pressure of complete miscibility is lower in the mixed hexanes systems, the lowering being equivalent to the effect of a 40° to 50° C. temperature rise. Such a result might be expected when branched and straight chain isomers are compared.   A molecule of the branch chain isomer resembles the methane molecule more closely than does a molecule of the straight isomer.   This resemblance is shown in the van der Waals forces, measured for example by freezing points or by internal pressure.   These forces increase in the order, methane (relatively small), branch chain isomer, straight chain isomer, so that the difference between the first two molecules is less than the difference between the first and third molecules.   The disturbance of intermolecular fields of force is less and consequently the mutual solubility is greater on mixing the former pair than is the case for the latter pair.

TABLE III

CONDITIONS AT PRESSURE OF COMPLETE MISCIBILITY

Temperature, °C.	Pressure, atm.	Density, gm. per cc.	Hexane, mole %	S_1''	S_2'
Hexane					
25	214	0.347	16.5	5.38	0.1975
55	210.5	0.325	19.7	4.36	0.246
85	201	0.310	23.5	3.50	0.307
Mixed hexanes					
25	203.5	0.340	17.0	5.21	0.205

References

1. BOOMER, E. H., JOHNSON, C. A., and ARGUE, G. H.   Can. J. Research, B, 15 : 367-374. 1937.
2. BOOMER, E. H., JOHNSON, C. A., and PIERCEY, A. G. A.   Can. J. Research, B, 16 : 319-327.   1938.
3. FROLICH, P. K., TAUCH, E. J., HOGAN, J. J., and PEER, A. A.   Ind. Eng. Chem. 23 : 548-550.   1931.
4. HILL, E. S. and LACEY, W. N.   Ind. Eng. Chem. 26 : 1324-1327.   1934.
5. KAY, W. B.   Ind. Eng. Chem. 30 : 459-465.   1938.
6. LEWIS, H. F., HENDRICKS, R., and YOHE, G. R.   J. Am. Chem. Soc. 50 : 1993-1998.   1928.
7. ORGANIC SYNTHESES.   Vol. I.   John Wiley and Sons, New York.   1921.
8. SAGE, B. H., WEBSTER, D. C., and LACEY, W. N.   Ind. Eng. Chem. 28 : 1045-1047.   1936.
9. SOUDERS, M., SELHEIMER, C. W., and BROWN, G.   Ind. Eng. Chem. 24 : 517-519.   1932.

A SOURCE OF CADMIUM RESONANCE RADIATION OF HIGH INTENSITY AND SOME PRELIMINARY RESULTS ON THE CADMIUM PHOTOSENSITIZED REACTION OF HYDROGEN AND ETHYLENE[1]

By E. W. R. STEACIE[2] AND ROGER POTVIN[3]

Abstract

An inexpensive and convenient source of cadmium resonance radiation (λ 3261) of high intensity has been developed. This should make possible more extended studies of cadmium photosensitized reactions. Some preliminary results on the reaction between hydrogen and ethylene are reported.

Introduction

The investigation of mercury photosensitized reactions has proved to be of great interest, since this method makes it possible to endow the reactant molecule with a very definite and reproducible amount of energy. In the case of the paraffin decompositions free radicals are usually produced in the process, and it therefore gives results of special interest in connection with the rates of elementary reactions. The great difficulty here, however, is that hydrogen has a much greater quenching efficiency than have the paraffins, roughly in the ratio of about 50 to 1. Now hydrogen is almost invariably a product of such decomposition reactions. As a result, as soon as a small quantity of hydrogen has built up, the reaction ceases to be the photosensitized decomposition and becomes the reaction of the paraffin with hydrogen atoms.

The $Hg(6^3P_1)$ excitation energy is 112 Kcal. The heat of dissociation of hydrogen into atoms is 102.5 Kcal. The energy required to rupture a C—H bond is about 80 to 90 Kcal., and that for a C—C bond is 70 to 80 Kcal. It follows that if we could obtain a substance with a resonance level about 90 Kcal. above the ground state, the excitation energy would probably be sufficient for the decomposition of the paraffins, but insufficient to dissociate hydrogen, and hence it would be possible to investigate decomposition reactions without complications due to hydrogen atom reactions. There are two metals which have sufficiently high vapor pressures at moderate temperatures, and which satisfy the energy requirements outlined above, viz., cadmium and zinc with $^3P_1$ levels 89 and 92 Kcal. above the ground state respectively.

No previous work has been done on zinc photosensitization, and only one brief investigation of cadmium photosensitization has been made. Bates and Taylor (1) showed that in ethylene-hydrogen-cadmium vapor mixtures illuminated with λ3261 no hydrogenation to ethane occurred, but that some of the ethylene was polymerized. They showed, however, that hydrogen quenched the resonance radiation, and suggested that it took up the energy of the excited cadmium atom as vibrational energy. (Hydrogen has a vibrational level very close to 89 Kcal.) Bender (2) has also investigated the quenching of cadmium resonance radiation by hydrogen.

Bender's results suggest possible complications in both cases, since the reactions

$$Cd + H_2 \longrightarrow CdH + H \ (-86 \ Kcal.)$$

and

$$Zn + H_2 \longrightarrow ZnH + H \ (-81 \ Kcal.)$$

are possible energetically, and in fact the band spectrum of CdH was detected by him. The extent to which these reactions occur is, however, open to question, and the investigation of cadmium and zinc photosensitized reactions appears to offer interesting possibilities in spite of this disturbing factor.

The above work was done nearly 10 years ago. In spite of its interesting nature it was not followed up, mainly because of the lack of a convenient source of reasonably high intensity in the cadmium resonance line at 3261 Å. As a matter of fact the development of the mercury photosensitization technique was also greatly retarded by the lack of suitable light sources. Recently, however, very convenient high voltage mercury arcs have been developed. These operate from a 5000 volt sign transformer, and employ about 10^{-3} mm. pressure of mercury vapor, with 10 to 15 mm. of neon or some other rare gas as a carrier. In such a lamp no reversal occurs, and the mercury resonance line at 2537 Å is very intense.

A number of lamps have been used in the past for the production of cadmium, or other metal, resonance radiation, neon or other inert gases being used as carriers (3–6, 9–11, 13). Most of these, however, are either weak or unsteady, or else are expensive and complicated and require too much attention to be convenient for photochemical purposes where long exposures are required.

Experimental

To obviate the above disadvantages a lamp has been constructed similar to the existing high voltage mercury lamps (7, 8, 12), the general technique used in neon sign manufacture being employed. A sketch is given in Fig. 1.
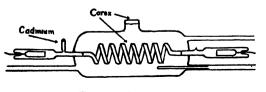
The emitting part of the lamp consisted of a spiral of 7 mm. internal diameter Corex D tubing. With the wall thickness

FIG. 1. *Apparatus.*

employed this has a transmission of about 95% at 3261 Å. Its transmission around 2300 is virtually zero, and it therefore filters out the lower cadmium resonance line. The ends of the Corex spiral were sealed directly to Pyrex tubing of the same diameter. The electrode chambers, also of Pyrex, were 15 mm. in diameter and 7 cm. long. The electrodes were standard neon sign "coated" electrodes 8 mm. in diameter and 3 cm. long. They were welded through nickel to tungsten wires which were sealed through the glass. A small side tube contained vacuum distilled cadmium.

The Pyrex reaction vessel was sealed on as shown. It contained a sealed-in Corex window to permit spectroscopic examination of the discharge. The lamp was filled with neon. The bombarding of the electrodes, filling, etc., were done by the usual technique by the Claude Neon Eastern Ltd.

The whole unit including the electrodes was placed in a furnace which was thermostatically controlled. It was operated at temperatures from 260 to 280° C. (corresponding to cadmium vapor pressures of from 7×10^{-3} to 2×10^{-2} mm.). In the first lamp used the neon pressure with the lamp cold was 15 mm. This gave good intensity but the lamp was very unstable in operation unless quite high cadmium pressures were used (corresponding to temperatures of 280° C. or higher). The lamp was therefore refilled with a neon pressure of 3 mm. This gave much steadier operation at lower temperatures.

The output of the lamp in the region of 3261 Å was measured with a thermopile, and suitable filters, and found to be about 5×10^{-7} einsteins per sec. when the lamp was operated on 80 ma. at about 500 volts. This is within one power of 10 of the output of the most intense commercial high voltage mercury arcs when operated under similar conditions.

A plate taken with a small Hilger quartz spectrograph is shown in Fig. 2. It will be seen that the resonance line at 3261 Å is strong, while the other lines in this part of the spectrum, 3404 Å, 3466 Å, and 3613 Å are relatively weaker. There is very little emission in the visible. The 2288 Å resonance line has been entirely filtered out by the Corex tubing. The lamp therefore

Fig. 2

seems to be entirely satisfactory for the investigation of cadmium photosensitized reactions.

An investigation of the cadmium photosensitized reaction between hydrogen and ethylene is in progress. Preliminary results indicate that:

(a) With pure ethylene little or no polymerization occurs.

(b) In ethylene-hydrogen mixtures polymerization of ethylene occurs, and in addition there is considerable hydrogenation.

(c) With mixtures high in ethylene the rate of reaction is nearly proportional to the partial pressure of the hydrogen.

The results suggest that either

(i) the reaction

$$Cd(^3P_1) + H_2 = CdH + H$$

occurs to a considerable extent, as has been suggested by Bender (2) so that hydrogen atoms are produced, or

(ii) that we have

$$Cd(^3P_1) + H_2 = H_2^*$$
$$H_2^* + C_2H_4 = C_2H_6, \text{ or } = H_2 + C_2H_4^* .$$

However, the question can be decided only by further work.

References

1. BATES, J. R. and TAYLOR, H. S.   J. Am. Chem. Soc. 50 : 771-773.   1928.
2. BENDER, P.   Phys. Rev. 36 : 1535-1542.   1930.
3. CARIO, G. and LOCHTE-HOLTGREVEN, W.   Z. Physik, 42 : 22-25.   1927.
4. ELLETT, A.   J. Optical Soc. Am. 10 : 427-437.   1925.
5. HOUTERMANS, F. G.   Z. Physik, 76 : 474-480.   1932.
6. KUNZE, P.   Ann. phys. (5)5 : 793-796.   1930.
7. MELVILLE, H. W.   Trans. Faraday Soc. 32 : 1525-1531.   1936.
8. MILLER, S. C. and FINK, D. G.   Neon signs.   McGraw-Hill Book Company, New York. 1935.
9. MITCHELL, A. C. G.   J. Franklin Inst. 212 : 305-316.   1931.
10. SCHÜLER, H.   Z. Physik, 35 : 323-337.   1926.
11. SCHÜLER, H.   Z. Physik, 59 : 149-153.   1930.
12. STEACIE, E. W. R. and PHILLIPS, N. W. F.   Can. J. Research, B, 16 : 219-221.   1938.
13. ZEHDEN, W.   Z. Physik, 86 : 555-582.   1933.

A SULPHUR-CONTAINING SUBSTANCE FROM THE SEED OF *CONRINGIA ORIENTALIS*[1]

By Clarence Yardley Hopkins[2]

Abstract

The seeds of *Conringia orientalis*, which contain a bitter principle, were crushed, freed from fat, and steeped in water. The chloroform extract of the aqueous liquor yielded a crystalline substance which was identified as 2-mercapto-5,5-dimethyl-oxazoline (I). It tastes bitter to some persons but is tasteless to others. The suggestion is made that the seeds contain β-methyl allyl isothiocyanate in the form of a glycoside, and that this substance is converted to (I) during the treatment described above.

Introduction

Conringia orientalis L. (Dumort) or hare's ear mustard is a common weed in the wheat fields of western Canada. Although a number of the Cruciferae have been subjected to chemical examination and have yielded mustard oil glycosides, the components of which are known, this species has not hitherto been studied. The seed has an intensely bitter taste, and is thus unlike the common white and black mustards which owe their burning taste to the isothiocyanate formed by hydrolysis of the sulphur-containing glycoside. It was of interest, therefore, to examine this seed and to determine if possible the nature of the bitter principle. A quantity of the seed became available during the course of another investigation and a study of its constituents was undertaken.

The seeds were crushed and freed from fat by extraction at low temperature with petroleum ether. Analysis of the defatted material showed a sulphur content of about 1%. It had a pronounced bitter taste. Extraction with alcohol in the manner commonly used for isolating glycosides left the residue free from bitterness. The extract yielded a concentrate of the bitter principle in the form of a brown amorphous solid which could not be induced to crystallize, even after varied treatments. Hydrolysis of this substance by acid and by alkali did not give any product that could be characterized.

Further quantities of the fat-free seed were treated with warm water so as to allow enzymic hydrolysis of the glycosides. Extraction of the aqueous liquor with chloroform yielded a crystalline sulphur compound. The quantity of substance obtained was equal to about 0.35% of the weight of the seed. After recrystallization it melted at 108.5 to 109.5° C.*, and analysis indicated the empirical formula C_5H_9ONS.

Preliminary examination of the substance showed that it had none of the reactions of an isothiocyanate. Its properties did not correspond with those of any known substance of the same formula. Experiments were begun to

* *Melting points are corrected.*

elucidate its structure and considerable progress was being made when notice of a new substance appeared in the literature, *viz.*, 2-mercapto-5,5-dimethyl-oxazoline (C_5H_9ONS) (1).   The melting point and degree of solubility in water, benzene, and petroleum ether were in agreement with those of the compound obtained in the present investigation.

A sample of the synthetic material (I) was obtained, and on examination the two proved to be identical.   A mixed melting point showed no depression.

$$(CH_3)_2 — C — O — C — SH$$
$$|\qquad\qquad ||$$
$$CH_2 — N$$

(I)

Further proof of their identity was obtained from measurements of ultra-violet absorption spectra.   As shown in Fig. 1 the absorption curves of the natural and the synthetic material virtually coincide.   Molecular extinction coefficients were calculated according to the method of Henri (3, pp. 359, 360).
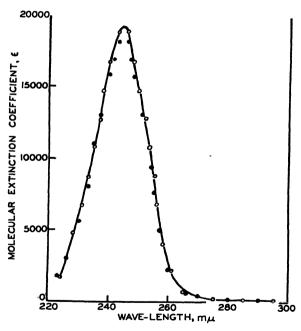
FIG. 1.   *Ultra-violet absorption curves:* O, *natural product;* ●, *synthetic 2-mercapto-5,5-dimethyl-oxazoline.*

Experimental

Material

The seed was obtained from a commercial sample of grain screenings from a terminal elevator at Fort William, Ontario.   After aspiration to remove chaff and straw, the mixture of seeds was separated into two fractions by immersion in ethylene dichloride.   The density of this liquid is such that the oil-bearing

seeds float while the starchy seeds sink. The oil-bearing seeds were passed over a machine that separates seeds according to their shape. This device was constructed in the laboratory. The hare's ear mustard being of ovoid shape was thereby separated from the round and flat seeds that accompanied it. After a final cleaning in the laboratory aspirator, the seed contained less than 2% of impurities. The material was ground in a small roller mill and extracted with petroleum ether to remove fat.

Isolation of Sulphur-containing Substance

One hundred grams of fat-free crushed seed was stirred into 400 cc. of water at 37° C. The mixture was agitated on a shaking machine for four hours. The pasty mass was centrifuged in bottles and the recovered liquor was extracted repeatedly with chloroform, separation being effected with the aid of the centrifuge. The chloroform extracts were dried over potassium carbonate.

On evaporation of the solvent there remained 0.5 gm. of crystalline solid, m.p. 99 to 101° C. After recrystallization from dry ether it melted at 104 to 105° C. Further recrystallization from benzene, by cooling to 0° C., gave crystals melting at 108.5 to 109.5° C.

Analysis of the substance indicated the formula C_6H_9ONS, as shown in Table I.

A molecular weight determination was inconclusive. Mol. wt. (Rast-Pregl.); found: 170,174. C_6H_9ONS requires: 131.

TABLE I

ELEMENTARY ANALYSIS

Element	Calc'd. for C_6H_9ONS	Found
C	45.80	46.01, 46.04
H	6.88	6.98, 7.09
N	10.7	10.9 (Kjeldahl)
S	24.4	24.3
O	12.2	11.7 (By difference)

Structure and Properties

A sample of the substance melting at 108.5 to 109.5° was mixed with synthetic 2-mercapto-5,5-dimethyl-oxazoline, which melted at the same temperature. The mixture showed no depression in melting point. 2-Mercapto-5,5-dimethyl-oxazoline crystallizes in white, prismatic needles. The substance is tasteless to some persons, including the author, while others find it intensely bitter*. It is readily soluble in alcohols, chloroform, acetone, and ethyl acetate; moderately soluble in water, ether, and benzene; but insoluble in hexane. The solubility in benzene at 0° C. is about 4.0 gm. in 100 cc.

It does not combine with methyl iodide under ordinary conditions, nor does it form a picrate. When heated at 95° C. with sodium plumbite solution the mixture darkens gradually, and a precipitate of lead sulphide is visible after 30 min. It is oxidized rapidly by concentrated nitric acid.

*References to taste throughout the text refer to the taste reaction of the author.

Attempted Isolation of the Bitter Principle

Quantities of the powdered, fat-free seed were extracted separately with methanol, 95% ethanol, dioxane, and ethyl acetate. In each case a bitter-tasting solid was recovered from the extract but none could be induced to crystallize. Methanol and ethanol were the best solvents, leaving the extracted residue devoid of bitterness. The bitter principle is insoluble in anhydrous acetone, ether, chloroform, and hexane.

Discussion

The sulphur-containing glycosides of Cruciferae species previously studied have yielded isothiocyanates of the general form RNCS. Thus sinigrin from *Brassica nigra* hydrolyzes as follows (2):

$$H_2O + CH_2 = CH . CH_2 . N = C \underset{OSO_3K}{\overset{S . C_6H_{11}O_5}{<}} \longrightarrow CH_2 = CH . CH_2NCS + C_6H_{12}O_6 + KHSO_4 .$$

The production of a cyclic compound from such a mustard oil could be explained by assuming that water adds to the $C≡S$ linkage and that ring closure then takes place with migration of one H atom.

$$\begin{array}{ccc} CH_2{=}CH & C{=}S \\ | & \| \\ CH_2{-}N \end{array} + H_2O \longrightarrow \begin{array}{ccc} CH_2{=}CH & HO{-}C{-}SH \\ | & \| \\ CH_2{-}\!\!-\!\!-\!\!N \end{array} \longrightarrow \begin{array}{ccc} CH_2{-}CH{-}O{-}C{-}SH \\ | & \| \\ CH_2{-}\!\!-\!\!-\!\!N \end{array}$$

This change has never been observed during the hydrolysis of sinigrin. It is known, however, that the presence of a tertiary carbon atom at the double bond facilitates ring closure of aliphatic isothiocyanates and thioureas (1).

It is not unlikely, therefore, that the substance 2-mercapto-5, 5-dimethyl-oxazoline is formed from the isothiocyanate $CH_2{=}C(CH_3){-}CH_2{-}NCS$ by addition of water and ring closure—

$$\begin{array}{ccc} & CH_2 \\ & \| \\ CH_3{-}C & HO . . CS . . H \\ | & \| \\ CH_2{-}\!\!-\!\!-\!\!N \end{array} \longrightarrow \begin{array}{ccc} (CH_3)_2{-}C{-}O{-}C{-}SH \\ | & \| \\ CH_2{-}\!\!-\!\!N \end{array}$$

Acknowledgments

Grateful acknowledgment is made to Dr. H. T. Clarke and Dr. H. Hirschmann, through whose kindness the absorption spectra determinations were carried out, and to Dr. H. A. Bruson, who supplied the synthetic material.

References

1. BRUSON, H. A. and EASTES, J. W. J. Am. Chem. Soc. 59 : 2011-2013. 1937.
2. GADAMER, J. Ber. 30 : 2322-2327. 1897.
3. INTERNATIONAL CRITICAL TABLES. Vol. 5. McGraw-Hill Book Company, New York. 1929.

THE PREPARATION AND SOME FLOW CHARACTERISTICS OF PLASTIC CASEIN[1]

By Wilfred Gallay[2] and James S. Tapp[2]

Abstract

The preparation of rennet casein has been studied on both a laboratory and plant scale, and the effect of the various factors in procedure on the quality of the casein produced is discussed. The details of preparation for a product of excellent quality are given. A simple heat resistance test showing the presence of impurities has been developed. The plasticity of a number of caseins has been measured by a direct method in a laboratory extruder, under pressure ranging up to 77,000 lb. per sq. in.; the maximum viscosity measured directly in this study was about one billion, seven hundred million poises. The flow-pressure curves obtained show no tendency towards a yield point, but show varying degrees of structural viscosity and may be fairly well represented by the relation $F = kP^n$, where F is the flow, P is the pressure, n and k are constants. Decrease in pH of the casein, decrease in ash, and increase in lactose content all lower the viscosity of plastic casein. Small increases in water content decrease the viscosity greatly. Up to 80° C. the temperature of drying has no appreciable effect on the viscosity. Moistening of casein plastic is discussed, as is also the distribution of water and vapor equilibria. Plastic casein is shown to exhibit streamline flow in extrusion, and plasticization is therefore more difficult to accomplish.

Plasticization of Casein

A casein plastic is prepared industrially by the homogenization of moistened casein granules and extrusion to the desired size, followed by either cutting directly to discs and hardening in formaldehyde, or by pressing the formed rods to sheets and hardening. The cured plastic is then machined to the desired size and form. The moistened casein is plasticized by means of a cylinder press fitted with a rotating screw which causes a rubbing and flowing of the casein over and into itself while transporting it forward to the extrusion orifice. The combination of the pressure and the heat developed brings about the desired homogenization. Facilities for cooling the casein during plasticization and gentle heating during extrusion are provided.

It is important to note that the speed of the screw and the clearances provided are fixed; the only variation possible in the operation of the extruder is the partial control of temperature afforded by the waterjacket around the screw. It is obvious therefore that the flow characteristics of the casein used must be such that within the limits of variation possible in the extruder plasticization will take place. If the viscosity of the casein is too low, the maximum rate of shear afforded by the extruder is insufficient to bring about a proper degree of plasticization, and the extruded material will consist merely of deformed casein particles adhering together in an irregular manner. If, on the other hand, the viscosity of the casein is too high, the rate of shear developed by the extruder produces excessive heating in the screw, and the material backs up through the feeding hopper as a result of the extremely high pressure developed.

Casein for plastics manufacture must therefore possess a viscosity within the range of the extruder. Uniformity of quality is important so that a standard manufacturing procedure may be adopted and relied upon to yield the desired results.

The purpose of the present work was to study the factors affecting the flow of rennet casein and methods of preparation to yield a uniform product of high quality.

A laboratory extruder was used for the measurement of the viscosity of rennet casein under varying rates of shear, pressures up to about 77,000 lb. per sq. in. being employed. The flow-pressure curves obtained were regular, and this direct method of measurement is more accurate and permits a greater range of experiment than one other indirect method previously described (1).

Preparation

The preparation of rennet casein has been described by a number of authors, but, generally speaking, insufficient correlation has been made between the various factors entering into the preparation and the properties of the resultant casein, particularly with regard to its suitability for plastic manufacture.

Rennet casein is prepared by the addition of rennet to skim milk, followed by pressing and drying of the coagulated curd. The skim milk should be fresh, since a high pH allows the combination of inorganic salts with the casein; this results in a casein of greater viscosity and a consequently greater ease of plasticization in an extruder or press. The coagulated curd is gummy and the particles tend to grow to large lumps. These lumps are not only rubbery and very difficult to grind in a curd mill, but they also occlude lactose and lactalbumen which cannot be removed by washing. . Shortly after coagulation and particularly when the curd suspension is heated, the coagulate begins to show marked syneresis with accompanied firming of the gel and loss of the sticky nature. This stickiness is probably due to albumen. It is obvious therefore that if the coagulate is not allowed to grow to larger lumps, but is kept in dispersed condition, then syneresis will occur with ready separation of water soluble constituents, which can then be removed by washing. It is to be noted that the particles formed by coagulation and syneresis retain their form through subsequent pressing and drying. If the particle size allowed is too small, however, the final grinding of the casein will produce a large proportion of fines. These fines have proved detrimental in the procedure now used in plastics manufacture, since on being moistened they occlude air and cake into lumps. Furthermore an appreciable proportion of the fines is lost during the separation of the casein curd from the whey by settling or screening.

It is therefore apparent that it is important to control the growth of the coagulate to optimum size. This may be effected by controlled agitation during coagulation and subsequent syneresis. The growth of the particles must be sufficiently slow so that time is available for this control. The amount of rennet used and the temperature for coagulation must be carefully chosen

so that a uniform means of control may be employed. Once the coagulate has grown to particles of a size greater than the optimum, powerful agitation is insufficient for dispersion. When syneresis is sufficiently advanced, the curd particles show no further tendency towards lumping. Syneresis is accelerated by slowly heating the curd suspension to about 60° C.

The water soluble impurities separated by syneresis may be removed by repeated washing of the curd. The washing efficiency is increased by the use of warm water; hot water causes an undue swelling of the curd. As much water as possible should be removed from the curd during pressing in order to shorten the time of drying. Prior to drying, the curd should be milled to shreds approximately twice the size desired in the final product; curd milling is necessary in order to avoid case hardening during drying. The drying temperature should be low with sufficient access of circulating air to ensure rapid removal of moisture.

These conditions for preparation were worked out in the laboratory, partly on a very small scale, but chiefly in batches of 80 lb. of skim milk. Additional experiments were carried out in casein plants on an industrial scale, from 4000 to 7000 lb. of skim milk being used in each experiment. In one plant engaged primarily in the production of acid caseins, no mechanical agitators were available. It was shown in several trials that it was impossible by hand-raking, even with four men working at a tank, to so control the particle size of the curd that large lumps could be avoided. In these experiments, the finished casein was of a very inferior quality. In a second plant, in which mechanical agitation was available but no variation in speed was possible, a very good product was obtained; the yield however was somewhat low owing to the production of fines which were lost in the removal of the whey.

The presence of lactose and albumen in the casein, if sufficient in amount, may cause a discoloration of the casein during drying even at a temperature of about 120° F. Smaller amounts, insufficient to discolor the casein powder, are readily detected however during the process of plasticization in the extruder. In the extruder a high temperature is attained for an appreciable period. The discoloration, particularly in an unpigmented plastic, is seen as dark streaks in the finished product. The effect of heating caseins to different temperatures for varying times was investigated, and a temperature of 150° C. for four hours was chosen as an arbitrary test for the heat resistance of the caseins. Under these conditions, available commercial caseins varied in color from ivory to deep brown. It was noted particularly that those caseins prepared in this study which had been carefully controlled during coagulation and therefore were well washed, showed excellent heat resistance. An obviously inferior grade of commercial casein was allowed to swell in water at 35° C., it was then thoroughly washed with warm water and dried at 50° C. The resultant casein had an appreciably increased heat resistance.

The effect of adding impurities artificially to a good casein was noted. Increasing amounts of lactose caused large increases in discoloration as a result of the heat test. Increasing amounts of albumen were much less

effective than lactose in this regard. Lactose alone was not affected by this heat treatment, and therefore it appeared that some combination of the protein and carbohydrate was responsible. Lactose treated with small amounts of acid and alkali and exposed to the heat test showed rapid darkening; therefore the effect may be due to the action of acidic or alkaline grouping in the protein on the sugar. The casein chosen for these experiments had been carefully prepared and washed, and had a pH of 6.9. Experiments showed that the lactose artificially added to the casein could be quite well removed by three washings with warm water.

In many instances, spotty effects were obtained by the heat resistance test, the color of the granules varying from ivory to deep red or brown. The explanation of this lies in the fact that during the coagulation and syneresis in preparation, both large and small particles were obtained. The small particles were well washed, and they therefore discolored very little as compared with the larger lumps which occluded lactose and albumen and discolored badly in the test.

Caseins prepared in the laboratory and on a plant scale under the conditions noted for high quality showed excellent results when used in a commercial screw extruder for plastics manufacture.

FIG. 1. *Effect of moisture content on flow of casein. Moisture contents—1, 27.10; 2, 27.35; 3, 28.00; 4, 28.30; 5, 28.55; 6, 29.25%.*

Effect of Moisture Content on Flow*

Casein swells in water and must be moistened prior to plasticization in order to provide sufficient medium for homogenization. Fig. 1 shows a series of flow-pressure curves for a rennet casein containing different amounts of water. The tremendous effect of small differences in moisture content is apparent. An increase of only 2.15% in moisture brings about an increase of 4700% in flow at a pressure of about 61,000 lb. per sq. in.

It is apparent from these results that the moisture content must be very carefully controlled. In commercial operation, the calculated amount of

---

* *All moisture contents have been calculated on the wet basis; e.g., 27% moisture content equals 38.89% moisture calculated on a bone-dry basis.*

water is added to the air-dry casein of known moisture content in an apparatus of the dough-mixer type. A reasonably good mixing is obtained and the amount of moisture lost by evaporation is small in comparison with the total mix. Such an apparatus is entirely inadequate for close control in laboratory work, and a closed roller mixer was developed for this purpose, by means of which in later experiments moisture contents could be so adjusted that the maximum error was less than 0.1%.

TABLE I

EFFECT OF MOISTURE CONTENT ON SPEED OF FLOW

Pressure, lb. per sq. in.	Flow (gm. per 5 min.) at moisture content of					
	27.10%	27.35%	28.00%	28.30%	28.55%	29.25%
23,060	–	–	–	–	–	0.0258
26,900	–	–	–	–	–	0.0415
30,740	–	–	–	0.0162	0.0169	0.0669
34,590	–	–	–	0.0209	0.0231	0.1046
38,430	0.0043	0.0093	0.0181	0.0305	0.0357	0.1555
42,270	0.0053	0.0099	0.0197	0.0440	0.0542	0.2204
46,120	0.0067	0.0117	0.0255	0.0598	0.0821	0.3165
49,960	0.0089	0.0158	0.0314	0.0788	0.1160	0.4075
53,800	0.0113	0.0188	0.0404	0.0970	0.1531	0.5490
57,650	–	0.0233	–	–	–	0.7195
61,490	0.0207	0.0301	0.0616	0.1510	0.2482	0.9670
65,330	–	–	–	–	–	1.3220
69,170	0.0265	0.0403	0.0878	–	0.3635	–
76,860	0.0338	0.0531	0.1080	–	0.5550	–

Casein granules vary greatly in size, and it was considered possible that the amount of moisture taken up varied with decreasing particle size. A sample of unscreened casein was moistened to 28% moisture content in the roller mixer according to the usual procedure. Then a separation into two fractions was made by inserting a cylindrical 30 mesh screen into the mixer and separating in the closed mixer. Determination of the moisture content of the −30 mesh, +30 mesh, and mixture of the two, however, showed no appreciable differences. In a further experiment equal amounts of +30 mesh casein with 10.30% water and −30 mesh casein with 0.45% water were mixed for the same length of time (15 hr.), and then moisture determination was made on the samples screened in the mixer. It was found that the +30 mesh casein then contained 7.35% moisture and the −30 mesh casein contained 3.95% moisture. The water content of the mixture was 5.70%. Casein therefore does not partake of the properties of an inelastic gel in the matter of equilibrium vapor pressure. It is important to note that a uniform mixture cannot be obtained by mixing two caseins of different moisture contents.

The heats of swelling of various caseins of different quality in water were measured, but the variations obtained were within the range of experimental error. Much more variation in results was obtained with varying degree of fineness of grinding of the caseins.

Effect of pH and Ash Content on Flow

The ash content of a rennet casein depends upon the pH of the milk from which it is prepared. Table II shows one series where the pH of the skim milk was allowed to fall by natural souring, and rennet caseins were prepared at intervals.

TABLE II
ASH CONTENT OF CASEINS FROM SKIM MILK AT VARYING pH

pH of skim milk	6.8 – 6.9*	6.2	5.9	4.6**
Ash content, %	8.9 – 9.1	7.76	5.74	0.56

* *Several samples.*   ** *Natural sour.*

The viscosities of solutions of acid caseins increase with increase in ash content, and the particularly high viscosity of rennet casein solutions is to be ascribed chiefly to high content of calcium phosphate. It is to be expected therefore that the speed of flow of a rennet casein will increase with decreasing pH of the skim milk from which it was prepared.
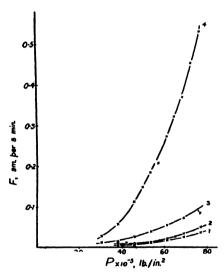
FIG. 2. *Effect of pH and ash content on flow of casein. Ash contents—1, 9.0; 2, 8.8; 3, 6.2; 4, 0.56%.*

The flow-pressure curves of four caseins differing appreciably in pH and in ash content owing to the pH of the milk are shown in Fig. 2. These four caseins after moistening and immediately prior to extrusion showed water contents of 27.20, 27.10, 27.15 and 27.15%.

Casein No. 4 of Fig. 2 was prepared from the same milk as the other caseins of this group but was allowed to reach the point of natural souring without rennet addition. This series shows the combined effect of ash content and pH of caseins on the speed of flow. All these caseins were coagulated to optimum particle size and thoroughly washed; the results showed that the pH of the caseins prepared from partly soured skim milk cannot be raised to a satisfactorily high value by washing.

The heat resistance of these caseins showed a low lactose and albumen content.

Effect of pH on Flow

In order to separate the effects of pH and ash of caseins on the flow, the following series of experiments were carried out. A rennet casein was prepared from fresh skim milk; it showed an ash content of 8.7% and pH of 7.1.

Portions of this casein were then agitated at room temperature for several hours with hydrochloric acid solutions of different concentrations; the caseins were then filtered, pressed, and dried. The acid treatment had little effect on the ash. The pH values of the treated caseins were measured and the flow-pressure curves determined after moistening. Fig. 3 shows the results obtained. It will be noted that there is some variation in the moisture content of these caseins prior to extrusion, causing some change in the speed of flow. Inspection of the figures show, however, that the curves are undoubtedly in the correct order, and that the error caused by varying moisture is a minor one.
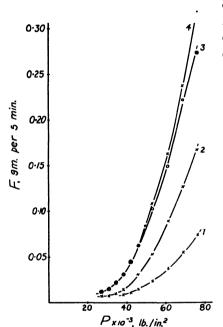
FIG. 3. *Effect of pH on flow of casein.* *pH values—1, 7.10; 2, 6.85; 3, 6.55, 4, 6.20. Moisture contents—1, 28.03; 2, 27.90; 3, 28.20; 4, 27.75%.*
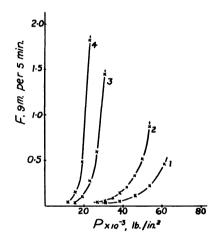
FIG. 4. *Effect of pH on flow of casein.* *pH values—1, 6.15; 2, 5.85; 3, 5.85; 4, 5.20%. Moisture contents—1, 25.55; 2, 25.63; 3, 28.35; 4, 28.10%.*

Further experimental data were available from another series in which portions of a commercial casein of inferior quality were treated with acid solutions of different concentrations, filtered, pressed, and dried. After moistening, the flow-pressure measurements were made. The results for two pairs of caseins, of different pH, each pair being at a different moisture level, are shown in Fig. 4. The marked increase in speed of flow with decreasing pH is well shown in this series also.

It is established therefore that a casein plastic with an absolute viscosity of some hundreds of millions of poises behaves as an ordinary lyophilic colloid with decreasing viscosity as the isoelectric point is approached.

Effect of Lactose on Flow

A rennet casein of excellent quality prepared in the laboratory and showing excellent heat resistance, high ash content and pH value, was treated at 65° C. for 20 min. with lactose solutions of varying concentrations. The caseins were then filtered, pressed, and dried. After moistening, flow measurements (Fig. 5) were made in the extruder. The variations in moisture content will account for the irregularities in the order with different pretreatments of lactose, but examination of the figures shows a definite increase in the speed of flow with increased lactose content.
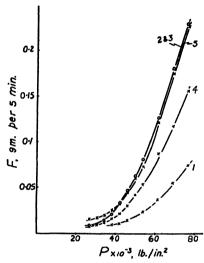
FIG. 5. *Effect of lactose on flow of casein. Lactose concentrations used in pretreatment—1, 0; 2, 0.4; 3, 1.5; 4, 3.0; 5, 6.0%. Moisture contents— 1, 28.03; 2, 28.25; 3, 28.15; 4, 27.80; 5, 27.70%.*
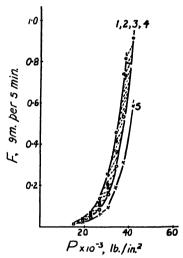
FIG. 6. *Effect of drying temperature on flow of casein. Drying temperature—1, 65°; 2, 50°; 3, 40°; 4, 40°; 5, 80° C. Moisture contents —1, 27.27; 2, 27.48; 3, 27.42; 4, 27.16; 5, 26.61%.*

Effect of Drying Temperature on Flow

Samples of a commercial casein were shaken for two hours with distilled water, then filtered, pressed, and dried for 24 hr. at temperatures ranging from 40° to 80° C. The caseins were then moistened, and the speed of flow measured in the extruder. Fig. 6 shows the results obtained.

It will be noted that there are no significant differences in flow; the casein dried at 80° C. is slightly more viscous than the others because of lower moisture content.

The flow-pressure curves are regular and show no tendency to a yield point on the pressure axis. The plastic casein exhibits structural viscosity, with the speed of flow increasing markedly with increased pressure; hence, the viscosity must be measured over a range of pressures in order that the plasticity may be characterized. The curves are of the exponential type

and are expressed fairly well by the equation $F = kP^n$, where F is the flow, P is the pressure, and k and n are constants. Fig. 7 shows some typical relations in logarithmic form.

Extent of Plasticization by Extrusion

Plasticization denotes a thorough homogenization of a material capable of plastic flow. The process is usually carried out by means of a combination of heat and pressure, and a variety of devices, depending on the properties of the material, are used to attain the plasticized state. In a rubber mill, tremendous pressures are attained in the nip between the rolls of the mill, and the rubber stock is rolled over and into itself and repeatedly subjected to the pressure. In a screw extruder, this action is attained to a much lesser degree, since different portions of a batch are not again mixed for further processing towards homogenization.
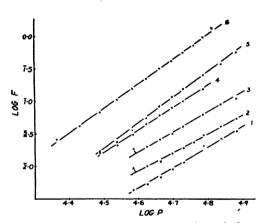
FIG. 7. *Logarithmic representation of flow-pressure curves. (See Fig. 1.)*
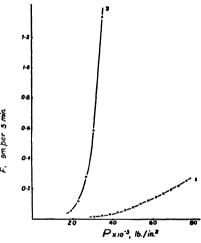
FIG. 8. *Effect of Baffle 1 on flow of casein. 1, with baffle; 2, without baffle. Moisture contents—1, 28.12; 2, 28.10%*

It was obvious that in the experimental extruder used in this study a much lesser degree of plasticization could be obtained than is possible in the commercial type of screw extruder, although the mode of action is some-what the same. No attempt was made to introduce a rotating screw, owing to the great experimental difficulties involved in applying and measuring accurately the pressures, and in maintaining constant the nip between screw and cylinder wall.

In view of the foregoing, it was considered advisable to gain an idea of the extent of homogenization attained in the experimental extruder (shown in Fig. 9). A commercial casein was dyed blue and then samples of the undyed and dyed caseins were moistened separately to the same standard moisture content in the roller mixer. After subsequent thorough mixing of the two caseins for 15 hr. no appreciable transfer of color was noted. The mixture was then extruded and a thin cross section of the extruded thread examined

under the microscope.   The result is shown somewhat diagrammatically in Fig. 11, *A*.   It was noted that the result obtained was merely an irregular pattern of blue and undyed casein, due to the deformation of the particles while under pressure in the cylinder of the extruder and during passage through the orifice. It was noted further that the extruded thread was weak and deeply pitted around the circumference.   It was then considered that insufficient plasticizing
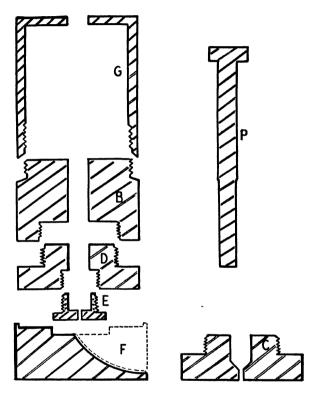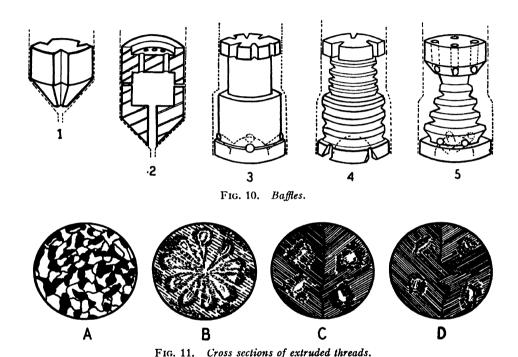
FIG. 9.   *Laboratory extruder.*

force was being applied, and Baffle 1 (Fig. 10) was inserted into the cylinder of the extruder to provide a greatly increased rate of shear.   The extrusion of the same mixture of dyed and undyed caseins described above was carried out with Baffle 1, and examination of the cross section of the thread obtained showed virtually no discontinuity of color.   A cross section taken from the casein plug in the main bore of the cylinder showed by the lack of uniformity of color that very little plasticization occurred as a result of direct pressure alone.   The extruded thread was much stronger than that obtained without the baffle and there was no appreciable pitting.   Fig. 8 shows the flow-pressure curves obtained in these two experiments.

The effect of the baffle is well illustrated in these curves. At a pressure of 34,000 lb. per sq. in. the flow is reduced to about 1.7% of the value obtained under the same conditions without the baffle.

A second baffle was then constructed (Fig. 10, 2) in which the casein was forced through 10 regularly spaced holes prior to entering a collecting chamber. A casein that had been moistened and dyed by a plastics manufacturer was used for extrusion. The thread obtained was strong and the surface free

FIG. 10. *Baffles.*

FIG. 11. *Cross sections of extruded threads.*

of pitting. Examination of the cross section, however, showed 10 regularly spaced areas that differed so greatly in intensity of color from the remainder of the total area as to appear almost colorless. The cross section is shown somewhat diagrammatically in Fig. 11, *B*. It was obvious that the 10-hole pattern of the baffle was reproduced in the extruded thread after the casein had passed through the collecting chamber and extrusion orifice.

Baffles 3, 4 and 5 (Fig. 10) were then constructed in attempts to improve still further the plasticization of the casein. Each of these contained a four-hole pattern immediately above the collecting chamber. Extrusions were made, each of these baffles being used, and in all cases four regularly spaced areas were obtained of very low color intensity.

In discussion with Dr. D. F. Stedman of these laboratories, it was suggested by him that the flow of rennet casein through such an extruder would

be of a streamline character and that non-uniform portions of the unplasticized casein might be separated during flow in this way. The following experiments were then carried out in order that the possibilities of streamline flow might be observed. Two samples of a commercial casein were dyed red and blue, and the two caseins separately moistened to the same standard water content. After insertion of Baffle 5 and assembly of the extruder, a strip of pasteboard of width equal to the diameter of the cylinder bore was inserted into the bore; this gave two separated portions. These were filled with the red and blue caseins respectively and the pasteboard was carefully removed. The extrusion was then carried out, and the cross section of the extruded thread examined under the microscope. The cross section is represented in Fig. 11*C*, The four nearly colorless areas were present as usual owing to the baffle, and the total area was quite sharply and distinctly divided into red and blue halves. To ordinary visual examination, also, the thread appeared to consist of two hemi-cylinders, one red and one blue, which had been caused to adhere. The experiment was repeated with the same caseins, Baffle 3 being used in place of No. 5. The result is shown in Fig. 11*D*. The result was virtually the same except that some of the blue casein had been displaced, probably during the filling of the cylinder.

Examination of dyed casein granules showed that most of the dye had been taken up by the outer portion of the granules, and that the intensity of color falls off quite sharply towards the interior. Attempts were made to ascertain the distribution of water in the granules after moistening, but no definite results were obtained. It would appear however that the intensity patterns shown in Fig. 11, *B*, *C*, and *D*, must be due to a separation of the dyed and undyed portions of the granules by virtue of their different susceptibility to plasticization under the applied pressure. The exterior dyed portion is apparently plasticized to a greater extent than the remainder, and the latter portion is forced through the holes, surrounded by the more plasticized material which flows more readily under the rate of shear brought about by the holes. Streamline flow of the separate threads then takes place through the mass of casein in the collecting chamber and the threads emerge through the final orifice and show the four-hole pattern as areas of low color intensity. It is quite possible that the distribution of water in the moistened granule is such that more ready plasticization of the outer portion of the granule takes place. This effect may act in addition to the greater shear suffered by this portion. It may be concluded from the appearance of such patterns that plasticization in such an extruder is far from complete.

Experimental

Preparation

In some instances three litre batches of skim milk were processed in four-litre beakers set in constant temperature baths. Most of the experimental runs were carried out, however, with 80 lb. batches of skim milk. The coagulation vessel was a cylindrical steam jacketed, metal tank, of about 12 gal. capacity, rounded at the bottom and fitted with a gate-valve at the bottom for drainage.

The inside was coated with a corrosion resistant lacquer. An automatic temperature regulator, by means of which the temperature could be controlled if necessary to $\pm 1°$ F., was fitted on the entrant steam line. The agitator was attached to the rim of the tank, and since the speed of the motor used was not adjustable, agitation was controlled by hand operation of an on-off switch. The curd, contained in cloth bags, was pressed between the plates of a multiple-leaf, laboratory model, horizontal filter press. The curd was ground in a small hand-driven disc mill and the casein was dried in thin layers on trays by means of air from a fan heated by a specially constructed electrically heated coil placed vertically in front of the fan. It was noted that the use of gas burners for this purpose resulted in a discoloration of the caseins. A roller mill such as that used for the grinding of grain was found to be excellently suited to the final grinding of casein, with good throughput and little production of fines. A large number of experimental batches were made, such factors as the temperature of coagulation, pH of the skim milk, amount of rennet, time interval between visible coagulation and heating of the curd, the number of washes and the temperature of the wash water, extent of curd grinding, drying temperature, and others being varied.

The procedure developed for a rennet casein of an excellent quality was as follows: 80 lb. of fresh skim milk was placed in the coagulation vessel and the temperature raised to 38° C. with continuous agitation. Then 250 cc. of Hansen's Standard Rennet which had been diluted 40 : 1 was added. This is equivalent to 2.8 oz. per 1000 lb. of skim milk. After two minutes agitation, the stirrer was stopped. Visible coagulation was noted in about 18 min. and the curd particles were allowed to grow to about 3 to 4 mm. diameter, the size being controlled by the extent of agitation. Five minutes after visible coagulation, the mixture was slowly heated to 55° C. over a period of 20 min. with constant agitation after a temperature of 45° C. was reached. Then the suspension was drained into a washing vessel, the curd was allowed to settle and the whey poured off. The curd was washed three times with water at 90 to 100° F., with three minutes' agitation each time in the coagulation vessel followed by drainage and thorough removal of the wash water. The final wash water was colorless and clear and the curd consisted of small discrete granules that had no tendency to adhere. The curd was then pressed for one hour and ground to particles 2 to 3 mm. in diameter. The curd contains about 60% moisture at this stage. Drying was carried out at about 45° C. with good circulation of air. The dried casein was again ground, it being necessary only to separate the granules formed by the grinding of the pressed curd. The final product consisted of white granules appearing translucent and sometimes transparent under magnification. The ash content was about 9%, the pH 6.9 to 7.0, and the heat resistance excellent. Preparations on a plant scale were carried out in a similar manner, except that the curd was washed either in the coagulation tank or in a movable tank fitted with filtering duck. Direct steam was used for heating the milk in 4000 to 7000 lb. batches. Pressing and curd milling were carried out in the usual commercial

apparatus, and drying was effected in a tunnel drier fitted with arrangements for a partial recirculation of air.

Analysis

Moistures were determined by heating to 105° C. for three hours. All pH measurements were made electrometrically, a glass electrode being used. Ash determinations were made by direct calcination in a muffle after charring at a low heat. Check determinations with added soluble calcium salts showed that sufficient calcium was present in the rennet casein to retain all the phosphorus.

Moistening Prior to Extrusion

It was found necessary for close control to moisten the casein in a closed vessel. The moist casein adheres to the walls of the mixing vessel, and ordinary shaking does not bring about the proper distribution of water. The method finally developed was as follows: 30 to 50 gm. of air-dry casein was placed in a cylindrical screw-top bottle of about 200 cc. capacity together with several glass alleys, and the calculated amount of water added. The total diameter of the glass spheres was somewhat greater than the height of the bottle. After a brief shaking by hand, the bottle was placed on its side on a rolling device, and the contents was thoroughly mixed by rolling, usually for an overnight period. There was virtually no sticking of the casein to the container.

Extrusion

1. *Apparatus*

The extrusion apparatus, Fig. 9, consisted essentially of a hardened and polished steel piston *P* and a corresponding cylinder with a small orifice at one end. The cylinder used in earlier experiments consisted of two threaded sections, *B* and *C*, which, after assembly, rested on the steel block *F*. In this position, the orifice opened into the milled slot (9 mm. wide) in *F*. Later, section *C* of the cylinder was divided into two parts, *D* and *E*, to facilitate the introduction and removal of baffles.

The piston guide *G* was turned from steel shafting. It had a wall thickness of 5 mm., an over-all diameter of 71.5 mm. and a height of 81.5 mm. The main cylinder, *B*, was 72.5 mm. in diameter, 51.5 mm. in height, and had a bore diameter of 10.345 mm. Cylinder section *D* had a height of 28.5 mm. and was otherwise of the same dimensions as *B*. The large bore of section *E* was 12 mm. and the extrusion orifice was 1 mm. in diameter. The piston *P* was 134.5 mm. in total length and had three different diameters as follows:— (*a*) the diameter of the section extending 74 mm. below the head was 11.090 mm., (*b*) that of the next section, 31 mm. long, was 10.285 mm., and (*c*) that of the remaining section, 20 mm. long, was 10.330 mm.

Baffle 1 was turned roughly from a piece of brass rod; it had an over-all height of 13.5 mm. and its other dimensions were such as would enable it to

fit snugly into the tapered inner bore of cylinder section C. Three grooves, $\frac{1}{16}$ in. deep, were cut on its outer surface. Baffle 2 was made in two parts from cold rolled steel shafting. The over-all length was 20.5 mm. The upper section had 10 holes, 1 mm. diam., drilled as indicated in Fig. 10. The lower part had one central hole 1.56 mm. in diameter. The entire unit fitted closely within the bore of section C. This baffle was used only once, as it expanded under operation and became jammed in the cylinder. It was for this reason that C was drilled out and replaced by D and E.

Baffles 3, 4, and 5 were each about 22 mm. in height. They fitted closely at top and bottom into sections D and E respectively. This arrangement ensured ready removal of the baffle from either D or E after an experiment. The dotted lines in Fig. 10 represent the cylinder bore and indicate the clearance at points along the baffle. Baffle 3 had 11 grooves at the top and four holes of 1.17 mm. diam. at the bottom leading to the small collecting chamber immediately above the orifice. In Baffle 4, there were three grooves at the top and three grooves at the bottom. Baffle 5 had four holes of 1.17 mm. diam. at the top and four holes of the same diameter at the bottom above the collecting chamber.

2. Procedure

Sections B and D were put together and the piston, lightly oiled, was worked back and forth in the bore two or three times, and was then wiped free of oil with a clean rag. Section E, together with the baffle to be used, was screwed into place. The bore was filled quickly with the moistened casein, the piston was inserted and pressed down by hand, then the piston was removed and more casein added and pressed down until the final level of casein was about $\frac{1}{4}$ in. from the open end of the cylinder. The guide G was set in place and the piston inserted. The assembled apparatus was set on the block F and the whole placed between the plattens of an Amsler hydraulic press. A $\frac{1}{4}$ in. disc of aluminium was placed between the head of the piston and the upper platten in order to equalize the pressure over the entire area of the head. The pressure was slowly increased to a high value and about 1 ft. of thread allowed to extrude before the pressure was dropped and actual measurements of flow were begun. The pressure was set at the lowest desired level and after several minutes the emerging thread was severed flush with the orifice by means of a specially constructed chisel, and at the same time a stop watch was started. The pressure was held steady without difficulty by manual control, the maximum deviation being ± 50 lb. gauge (about 380 lb. per sq. in.). After the desired time interval, the thread was cut off flush with the orifice and immediately transferred to a screw-top bottle. Samples were obtained in a similar manner at all the required pressures. The samples were weighed and the weight for five minutes extrusion used in plotting the flow-pressure curves. Extrusion was not continued in any experiment when the bottom of the piston came within $\frac{1}{4}$ in. of the top of the baffle. After a complete extrusion experiment under a range of pressure, the whole unit was

warmed with hot water or steam, the head of the piston was held in a vise, and the cylinder was pulled away with a twisting motion. There was no jamming of the piston, and it was found that no casein crept past the advancing piston during extrusion.

Acknowledgment

References

1. HALLER, W.   Kolloid Z. 57 : 197-203.   1931.

THE DETERMINATION OF TRYPTOPHANE BY A MODIFIED GLYOXYLIC ACID METHOD EMPLOYING PHOTOELECTRIC COLORIMETRY[1]

By J. L. D. Shaw[2] and W. D. McFarlane[3]

Abstract

An accurate and reliable method for the estimation of tryptophane is described. It is based on the glyoxylic acid reaction, and involves the use of the Evelyn photoelectric colorimeter. The technique makes it possible to ascertain readily whether the color being measured is due only to tryptophane.

The method has been applied to casein, of which, if necessary, only 25 mg. is required. The tryptophane determination is readily accomplished on a solution obtained by dissolving the casein in 10 or 20% sodium hydroxide or 5% formic acid by heating for a few minutes. With respect to alkali hydrolysis of casein under pressure, tryptophane is unstable in the sodium hydroxide hydrolysis, but is very stable in the baryta hydrolysis. The age and source of the casein are shown to be factors causing variations in the tryptophane content of different samples of casein, a variability which has been observed by a few previous workers.

Introduction

A thorough perusal of the literature reveals that although many methods have been proposed for the estimation of tryptophane there still remain unexplained a number of anomalies and discrepancies in the results. Lack of specificity of the reagent used in the colorimetric methods and failure to obtain a suitable standard for comparison have been the main reasons for questioning the results obtained by means of these methods. Before absolute confidence can be placed in a colorimetric method it must be shown that the color measured is due to tryptophane and to tryptophane alone. It is virtually impossible to demonstrate this by the ordinary methods of colorimetry, but, as will be shown later, this point can be checked when a photoelectric colorimeter is used.

Alkali hydrolysis is still widely used in the determination of the tryptophane content of proteins, although several workers have stated that tryptophane is unstable during this treatment. By use of the methods to be described in this paper, a critical study has been made of the determination of tryptophane in sodium hydroxide and barium hydroxide hydrolyzates of casein. Casein is the protein to which the methods of tryptophane estimation have been applied most frequently. Some 25 different values, ranging from 0.5 to 2.2%, for the tryptophane content of casein are given in the literature. However, as a few workers have noticed, different samples of casein may give different values for tryptophane when analyzed by the same method. Too frequently, nothing has been said about the source, mode of preparation, or the purity of the casein used. In no case has mention been made of the moisture content of the casein. As indicated later, this is variable and con-

siderable, and should be taken into account in the expression of the results of tryptophane determinations.

When the importance of tryptophane in animal and plant metabolism is considered, it is very surprising that these needs have not yet been met. This paper presents the results of what is believed to be a successful attempt to fulfil these needs in the estimation of tryptophane in proteins.

Experimental

I. Development of an Improved Method

The tryptophane used was the *l*-form*, and its purity was established by determining its total nitrogen content by means of the micro-Kjeldahl method, the digestion mixture of Campbell and Hanna (1) being used. Digesting for one hour or longer with this mixture gave results which were constant and of the theoretical value. Accurate results were not obtained with the following digestion mixtures:— (i) copper sulphate, potassium sulphate, and concentrated sulphuric acid; (ii) mercuric oxide, selenium oxide, and concentrated sulphuric acid; and (iii) precipitated red selenium and concentrated sulphuric acid.

The colorimeter used was of the single cell photoelectric type, designed by Evelyn (3); it was found to be admirably suited to this study.

Twelve published methods for the estimation of tryptophane were thoroughly examined and, for various reasons, discarded. We believe that the method offering the best possibilities was Winkler's (9) adaptation of the Hopkins-Cole reaction. Her method was carefully checked in every detail and modified in the following points:—

(1) The glyoxylic acid solution was prepared according to the method of Pesez (6), as follows: To 100 ml. of a 5% aqueous solution of oxalic acid in a 150 ml. beaker was added 3.0 ml. of a $N/5$ mercuric chloride solution and a few small pieces of aluminium wire. The beaker, covered with a watch glass, was placed on a boiling water bath and heated for five minutes after the first appearance of bubbles on the aluminium wire. After the mixture had been allowed to stand for a further five minutes at room temperature, it was filtered, and 2.0 ml. of concentrated sulphuric acid was added to the filtrate. The solution was stored in the ice box to be used as required. Prepared in this way, the glyoxylic acid was stable for two weeks or longer.

(2) Winkler placed particular stress on the importance of intense cooling during the addition of the sulphuric acid in the reaction. The writers found this to be unnecessary.

(3) All conditions and concentrations used in the reaction were examined to obtain maximum color development, *i.e.*, *(a) Strength of sulphuric acid*—the concentrated acid (sp. gr. 1.84) was found to be the only suitable strength; *(b) amount of concentrated sulphuric acid*—5 ml. proved to be the optimal amount (Fig. 1, a); *(c) time of standing between the addition of the concentrated*

* *Obtained from the Eastman Kodak Co., Ltd.*

acid and heating in boiling water—the length of time appeared immaterial, at least over the periods tested, *i.e.*, up to 20 min.; *(d) time of heating in boiling water*—five minutes was found satisfactory for the maximum development of the color (Fig. 2); *(e) amount of glyoxylic acid*—0.50 ml. of the glyoxylic acid solution was found to be the optimal amount (Fig. 1, *b*); *(f) amount of copper*
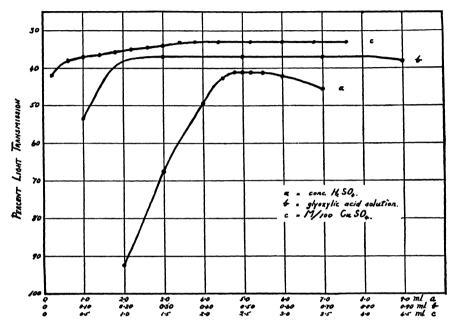
FIG. 1.   *Effect of (a) concentrated sulphuric acid, (b) glyoxylic acid, and (c) copper sulphate on the color intensity.   (Light filter = 540 mμ.)*

sulphate—0.50 ml. of a *M*/25 solution appeared to be perfectly satisfactory (Fig. 1, *c*); *(g) stability of the color*—found to be stable for at least three hours; *(h) reproducibility*—in this connection, it was ascertained that there was no necessity to standardize the glyoxylic acid, provided that it was prepared in the manner described above.
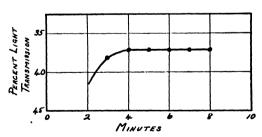
FIG. 2.   *Effect of the length of time of heating on the color intensity.   (Light filter = 540 mμ.)*

From the results obtained in the above-mentioned tests, the method finally adopted was as follows:—

From 0.10 to 2.00 ml. of an aqueous solution, containing 0.005 to 0.150 mg. of tryptophane, was placed in a 10 ml. glass-stoppered measuring cylinder, and 0.50 ml. of the glyoxylic acid solution and 0.50 ml. of a *M*/25 copper

sulphate solution were added. The volume was made up to 3.00 ml. with water. A total volume of 5.0 ml. of concentrated sulphuric acid was added from a burette in portions of 0.5, 1.0, 1.5, and 2.0 ml., the cylinder being well shaken under running cold tap water after the addition of each portion. After the addition of the acid, the cylinder was allowed to stand for about ten minutes in cold tap water and then placed in boiling water for five minutes. After the solution had been allowed to cool to room temperature, it was diluted to 10 ml. with a 5 : 3 (by volume) concentrated-sulphuric-acid–water mixture; this did not result in any heating. The solution was finally transferred to a clean, dry colorimeter tube. The reading was made after 15 min. The blank used was a colorless solution containing tryptophane in equal volume and concentration to the test solution and treated in the same way as the test solution, but to which no glyoxylic acid solution was added.

To prepare the calibration curves, 15 different amounts of a tryptophane solution were used, being equivalent in range to 0.007 to 0.141 mg. of tryptophane. Each solution was tested in duplicate in the manner described above. Two sets of readings were taken, a 540μ light filter being used, followed by a 520μ light filter; two calibration curves were thereby obtained. The choice of these two light filters was based on the absorption spectrum of the blue-violet color (Fig. 3). These two curves served, in the
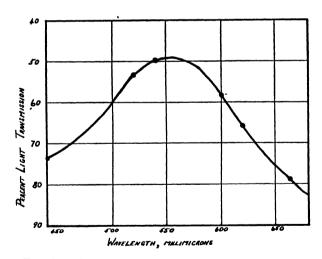
FIG. 3. *Absorption curve of color produced in the glyoxylic acid reaction.*

later work, to prove whether the color measured was due to tryptophane alone. With the exception of a few points where the highest concentrations of tryptophane were employed, the calibration curves obey Beer's law (Fig. 4), thus proving that the conditions and concentrations employed are optimal for the development of the color.

II. Application of the Method to the Determination of the Tryptophane Content of Casein

Casein was prepared from the winter milk of a herd of stall fed cows. The skim milk was used and the casein precipitated by the method of Moir (5) and purified according to the directions of Van Slyke and Baker (8, pp. 10, 11). The moisture content was determined by the technique of Snyder and Hansen (7) and found to be 8.41%. All results given below are expressed on the basis of the air-dried material, unless otherwise stated.
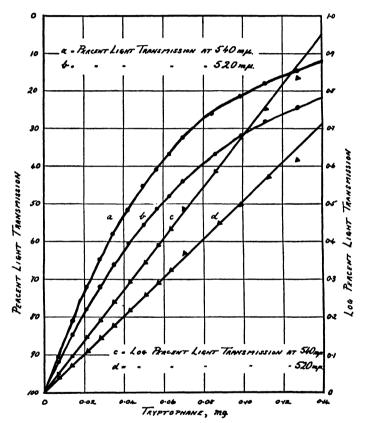
FIG. 4. Calibration curves and application of Beer's law.

One gram of the casein was dissolved in 20 ml. of a 20% solution of sodium hydroxide by heating on the boiling water bath for several minutes until a clear solution was obtained. The solution was transferred to a 200 ml. volumetric flask and made up to volume with water. Duplicate determinations of tryptophane in 1.00 ml. aliquots were made by the procedure described above. The blank also contained 1.00 ml. of the solution and was treated in exactly the same manner, but no glyoxylic acid solution was added. The readings with the two light filters corresponded to 1.16% of tryptophane. The deter-

mination was repeated several times and was also carried out with 20 ml. of a 10% solution of sodium hydroxide, or 20 ml. of a 5% formic acid solution, as the solvent for the casein. The same result was obtained in all determinations.

Although there was, most likely, a certain degree of hydrolysis, at least in the determinations in which sodium hydroxide was used as the solvent, it is doubtful whether the tryptophane was actually liberated from the protein combination. Hence, this method of examining the tryptophane content of casein will be referred to as simple solution in contradistinction to the far more drastic treatment of alkali hydrolysis under pressure.

III. *The Stability of Tryptophane during Alkali Hydrolysis under Pressure*

In the investigation of sodium hydroxide hydrolysis under pressure, 1 gm. of the casein was hydrolyzed with 20 ml. of a 20% solution of sodium hydroxide in the autoclave as recommended by von Deseö (2). The hydrolyzate was treated with sulphuric acid and kaolin as outlined by Folin and Marenzi (4). A new Pyrex Erlenmeyer flask was used for each hydrolysis, and it was also ascertained that no tryptophane was absorbed on the kaolin. Comparison of the results with those obtained as described above by simple solution of the casein shows that there was always a loss of about 10% of tryptophane under different conditions of temperature, pressure, and time of hydrolysis when a 10, 20, or 30% solution of sodium hydroxide was employed.

To examine baryta hydrolysis under pressure, 1 gm. portions of the same casein were hydrolyzed in the autoclave with 20-ml. aliquots of saturated baryta solution for different lengths of time (up to five hours), at different temperatures (120° and 150° C.), and pressures (2.0 and 4.5 atm.). The hydrolyzate in each case was immediately acidified with 20 ml. of $7N$ sulphuric acid and rapidly cooled. The barium sulphate was filtered off and thoroughly washed with water. The filtrate and washings were made up to 200 ml. with water, and 1.00-ml. aliquots were taken for the determination and for the blank.

The resultant color indicated about 1.3% of tryptophane in every case, but the disproportionality in the readings with the two light-filters showed that the color was not identical with that given by pure tryptophane. However, when the hydrolyzate was first extracted three times with ether, and the ether dissolved in the hydrolyzate was removed by evaporation *in vacuo* at room temperature, the determinations on 1.00-ml. aliquots of the solution gave the pure tryptophane color and corresponded in every case to 1.16% of tryptophane. The results, therefore, were in excellent agreement with those obtained when the casein had simply been dissolved in sodium hydroxide or formic acid. Obviously, baryta hydrolysis under pressure does not result in any loss of tryptophane.

The nature of the substance or substances removed by the ether extraction, and giving a color with glyoxylic acid, was not investigated. The results indicate, however, that the interfering substance, which may be indole or skatole, was not formed from tryptophane during hydrolysis in the autoclave.

IV. The Variation in the Tryptophane Content of Different Samples of Casein

Two other samples of casein, both several years old, were available. These had moisture contents of 10.08 and 7.80% respectively. In the determination of the tryptophane content by dissolving in a 5% solution of formic acid as described above, these samples gave less than 1% of tryptophane. Evidently, the age of the sample affects the tryptophane content of casein.

A fresh sample of casein was prepared from the milk of the same herd of cows, but after they had been on pasture for two months. The casein was obtained in exactly the same manner as before; it contained 10.87% of moisture. Repeated direct determinations of the tryptophane content of a sodium hydroxide solution of this sample of casein gave 1.19%.

The tryptophane content of the various samples of casein are given in Table I.

TABLE I

A COMPARISON OF THE TRYPTOPHANE CONTENT OF VARIOUS SAMPLES OF CASEIN

| Sample | Age | Moisture content, % | Tryptophane, gm. per 100 gm. moisture-free casein | | | |
| | | | Solution | | Hydrolysis | |
			NaOH, 10 or 20%	H·COOH 5%	NaOH, 20%	Ba(OH)₂, sat'd
Authors'—						
Sample from summer milk	Fresh	10.87	1.33	—	—	—
Sample from winter milk	Fresh	8.41	1.25	1.25	1.04	1.25
British Drug Houses "Light White Soluble"	8 years	10.08	—	1.09	—	—
Kahlbaum Co.	25 years	7.80	—	0.92	—	—

V. Amount of Protein Required for the Tryptophane Estimation

Although the above-mentioned tests were carried out with 1-gm. portions of the air-dried sample, it was evident that as small an amount as 25 mg. would be sufficient. On dissolving 25 mg. of casein in 1 ml. of a 10% solution of sodium hydroxide with the aid of heat, making up to 5.00 ml. with water, and using 1.00 ml. for the tryptophane determination, results were obtained which were comparable in accuracy and reproducibility with those of the tests in which larger amounts of the protein were used.

Note Added October 7

In making some tryptophane determinations recently we observed that when certain samples of concentrated sulphuric acid (c.p. grade) were employed, a yellowish-brown color developed in the blank determination. This leads to erroneous results even in determinations on aqueous solutions of pure tryptophane. The difficulty was overcome by distilling the acid.

Acknowledgment

References

1. CAMPBELL, W. R. and HANNA, M. I.   J. Biol. Chem. 119 : 1-7.   1937.

2. v. DESEÖ, D.   Biochem. Z. 271 : 142-145.   1934.

3. EVELYN, K. A.   J. Biol. Chem. 115 : 63-75.   1936.

4. FOLIN, O. and MARENZI, A. D.   J. Biol. Chem. 83 : 89-113.   1929.

5. MOIR, G. M.   Analyst, 56 : 147-149.   1931.

6. PESEZ, M.   Bull. soc. chim. (5) 3 : 676.   1936.

7. SNYDER, R. S. and HANSEN, H. C.   J. Ind. Eng. Chem. (An. ed.), 5 : 409-412.   1933.

8. VAN SLYKE, L. L. and BAKER, J. C.   N.Y. Agr. Exptl. Sta. Tech. Bull. 65.   1918.

9. WINKLER, S.   Z. physiol. Chem.   228 : 50-58.   1934.

TANNINS AND NON-TANNINS OF THE BARKS OF SOME EASTERN CANADIAN CONIFERS, PARTICULARLY WHITE SPRUCE[1]

BY W. E. GRAHAM[2] AND A. ROSE[3]

Abstract

The tannin content of the barks of several Eastern Canadian conifers has been determined by standard methods in an attempt to assess their value as sources of tanning extracts.

A more intensive study has been made of the extractable materials of white spruce bark. The chemical reactions of the extract from this bark show that the tannins therein are typical examples of the catechol or condensed group. Comparison of the ratio of tannin to non-tannins and the buffer index of this extract with the corresponding values for several commercial extracts indicates that the spruce extract would probably be fairly astringent. The titration curves of various fractions of the extract show some indications of the character of the non-tannin constituents.

The available literature on the subject of natural sources of tannin has been found to contain little or no quantitative information regarding the tannin content of the barks of the more abundant conifers of eastern and central Canada, with the exception, of course, of the well known Eastern hemlock *(Tsuga canadensis)*.

Large quantities of bark from the conifers cut for pulpwood in Eastern Canada (particularly white spruce, black spruce, and balsam) are wasted or destroyed annually. These barks, among others, have been examined in these laboratories during recent years as potential sources of tanning extracts.

A. General Analytical Results

Analytical Methods

The air-dried samples were ground in a Wiley mill. Extractions were carried out (i) according to the methods of the American Leather Chemists' Association (A.L.C.A.), suitably modified Pyrex Soxhlet extractors (43 mm. diameter) being used, or (ii) in some cases, according to the methods of the International Society of Leather Trades' Chemists (I.S.L.T.C.), a modified Koch extractor being used. In the first method the filtering medium used in the extractors was glass wool, washed with dilute hydrochloric acid, then with distilled water. The extracts were analyzed according to the respective official methods based on the two modes of extraction, rapid cooling being used in the A.L.C.A. method.

It is of interest to note at this point that the bark of the balsam *(Abies balsamea)*, which is the source of the Canada balsam of commerce, could not be extracted with hot water, even after removal of resinous material by means of ethyl ether, because of the presence of pectinous matter. Since balsam,

black spruce, and white spruce stands are closely intermingled in the principal pulpwood regions of Ontario and Quebec, this fact is of some importance in appraising the possibilities of one or all of these barks as sources of tanning extracts.

TABLE I

ANALYSIS OF BARKS

Bark of	Sample No.	Source	Method of extraction	Soluble solids, %	Soluble non-tannins, %	Tannin, %	Purity, %
Eastern cedar (*Thuja occidentalis* Linn.)	1	Ont.	A.L.C.A.	10.6	7.6	3.0	28
Red spruce (*Picea rubra*)	1	N.B.	A.L.C.A.	21.40	9.18	12.22	57.1
Black spruce (*Picea mariana*)	1	Ont.	A.L.C.A.	27.70	15.54	12.16	43.8
	2	N.B.	A.L.C.A.	24.00	13.97	10.03	41.7
	3	N.B.	A.L.C.A.	23.85	12.92	10.93	45.8
	4	N.B.	A.L.C.A.	21.48	11.97	9.51	44.2
	5	Ont.	A.L.C.A.	22.03	13.71	8.32	37.7
White spruce (*Picea canadensis*)	1	Que.	A.L.C.A.	40.5	18.5	22.0	54.3
	1	Que.	I.S.L.T.C.	32.3	11.5	20.8	64.4
	2	Que.	I.S.L.T.C.	33.0	12.8	20.2	61.2
	3	Que.	A.L.C.A.	42.2	21.1	21.1	50.0
	3	Que.	I.S.L.T.C.	32.3	13.0	19.3	59.6
	4	Ont.	A.L.C.A.	37.6	15.3	22.3	59.3

Analyses of the barks of three species of spruce and one of cedar are given in Table I. All results are reported on the moisture-free basis. "Purity" of the extract is defined as:

$$\frac{\text{Tannin}}{\text{Soluble solids}} \times 100\%.$$

B. White Spruce Bark: A Preliminary Investigation

The consistently high tannin content of bush-peeled white spruce bark, as shown in Table I, makes it a possible source of concentrated tanning extracts, provided that the economic obstacles involved in stripping, drying, sorting, and transporting the bark are not insuperable, and that the physico-chemical properties (color, purity, astringency, degree of fixation by hide fibre) of the extracts prepared from it are satisfactory. It is recognized that separation of white spruce bark from black spruce and balsam barks, either in the bush or at the point of shipment, might not be economically feasible even if practically possible. The tannins of all the eastern spruces are probably very similar chemically, and since white spruce bark is the most convenient of the three as a laboratory source of moderately concentrated extracts, it was selected for this exploratory study.

Only large-scale tests in the tannery are of real value in the assessment of the merits of a new extract; there are several factors, particularly in heavy leather manufacture, which are difficult to duplicate in the laboratory.

A study of some of the simpler chemical tests has been included in the present investigation for purposes of classification, more particularly because some Canadian tanners have expressed the opinion that the spruce barks contain a "pseudo-tannin" as opposed to a "true tannin". The formation of a precipitate on addition of bromine water, and also on refluxing with formaldehyde in hydrochloric acid solution, is a characteristic reaction of tannins of the catechol or condensed type. The "formaldehyde precipitation figure" of a tan liquor is the weight of the precipitate obtained on addition of formaldehyde expressed as a percentage of the weight of the tannin or the soluble solids content of the volume of liquor used. The ratio of these two figures is, of course, dependent on the purity of the extract. Because of the highly arbitrary nature of the official methods of tannin analysis, the formaldehyde figure (when expressed as a percentage of the tannin content) is of more importance as a means of classification and identification than as a possible basis for quantitative estimation of individual tannins.

The astringency of a tan liquor is probably its most important single characteristic; and it is found to be dependent on such subsidiary factors as concentration, pH, ratio of tannin to non-tannin, average molecular weight, and degree of dispersion, as well as on the chemical constitution of the tannins and non-tannins present.

While in general it is possible to predict the astringency of a tan liquor (under standard conditions) in rough fashion from a study of the tannin/non-tannin ratio, it has been found that the prediction is sounder if this ratio is considered in conjunction with the buffer index of the liquor.

The buffer index of a tannin infusion, tanning extract, or yard liquor is arbitrarily defined in the publications of the British Leather Manufacturers' Research Association (3, 6) as the number of millilitres of normal sodium hydroxide or hydrochloric acid solution required to change the pH of 100 ml. of liquor of 20° Barkometer strength (20° Bk. = specific gravity 1.020) by one unit within the limits pH = 3.0 to pH = 5.0, which is the range normally encountered in tannery practice. For a given extract, at a concentration equivalent to 20° Bk. strength, the buffer index is inversely proportional to the purity or the tannin/non-tannin ratio; and, as pointed out above, the astringency of a liquor is found to be a complex function of the pH, concentration, and tannin/non-tannin ratio. It is obvious that the astringency of an extract will be more greatly reduced, and the buffer index more greatly increased, if the non-tannin fraction consists of weakly acidic, polyphenolic compounds rather than of sugars or other materials of low buffering power.

For these reasons it was thought that a comparison of the buffer index of the white spruce extract with the corresponding values for commercial extracts of known characteristics would afford some indication of the astringency of the former, it being borne in mind that the spruce extract studied was representative neither of the total extractable matter of the raw bark nor of a potential commercial extract efficiently prepared.

For the determination of the buffer index values, glass electrode titrations and routine analyses (by the A.L.C.A. method, with slow cooling) were carried

out on the white spruce extract, diluted to 20° Bk., and on suitably diluted commercial samples of ordinary (unsulphited) solid quebracho, liquid hemlock, liquid oak bark, and paste gambier extracts.

The formaldehyde precipitation figures for all these extracts, as well as for white spruce, black spruce, and Western hemlock barks, were determined as part of the classification study.

It was originally intended that the scheme of Cameron and McLaughlin (2) be followed in the study of the titration curves of the spruce extract and of the various fractions obtained by steam distillation, ether extraction, and dialysis. However, the spruce extract was unlike the extracts investigated by Cameron and McLaughlin, in that the ether-extractable fractions were not large and their titration curves were not simple; hence the plan was not followed in detail.

Experimental

Extraction Characteristics

Tests were made on the efficiency of extraction at various temperatures, an extractor of the Koch (International) type being used, and the results were compared with extraction by the official methods.

Preparation of Concentrated Extract

A mixed sample of bush-peeled barks, analyzing 21.0% tannin and 16.4% soluble non-tannins (A.L.C.A. method, dry basis), was extracted in a small counter-current diffusion battery of nine 32-ounce bottles; eight were kept in a boiling water bath and one at room temperature.

In spite of the high temperature used, the extraction was slow and inefficient, principally because of the somewhat crude design of the apparatus, but a sufficient quantity of extract of 27° Bk. strength was obtained for the work in hand. This liquor had the following composition: insolubles, 1.92; soluble non-tannins, 29.18; tannin, 41.60 gm. per litre; total 72.70 gm. per litre. The purity was thus 58.8% as compared with 56.1% for the raw bark liquor.

The extract was stored in a refrigerator at 0° C. in order to check fermentation and bacterial action without resort to the use of antiseptics or fungicides; it was later noted that mold growth did not occur in liquors of 20° Bk. or greater strength. The liquor was brought to room temperature only as required for sampling.

Color of Extract

Several color tests on calfskin grain splits were made according to the (then) tentative method of the A.L.C.A. for skin color tests.

Formaldehyde Precipitation Test

In Lauffmann's method (4) the reagent consists of the following: water, 100; 40% formalin, 150; concentrated hydrochloric acid, 100 parts by volume. The reagent (25 ml.) was refluxed for 30 min. with 50 ml. of tannin solution of analytical strength (*i.e.*, containing 4.00 ± 0.25 gm. of tannin per litre). The flocculent precipitate was filtered off hot on a Gooch crucible with asbestos

mat, and washed with boiling water, then dried to constant weight at 105° C. The results are given in Table II.

Bromine Precipitation

On addition of 25 ml. of saturated bromine water to 50 ml. of spruce extract of analytical strength, a flocculent precipitate formed immediately. The precipitate was filtered off only with great difficulty and was redispersed on washing, hence the study was confined to an analysis for bromine content.

Steam Distillations

Steam distillation of 100 ml. portions of the original 27° Bk. extract and of the ether-extractable fraction was carried out, apparatus based on that of Cameron and McLaughlin (2) being used.

TABLE II

FORMALDEHYDE PRECIPITATION FIGURES FOR VARIOUS BARKS AND EXTRACTS

	Formaldehyde figure	
	As % of soluble solids	As % of tannin
Barks—		
White spruce	70.5	124.0
Black spruce	46.5	116.0
Western hemlock	73.9	142.0
Extracts—		
27° Bk. white spruce	72.2	111.0
Ordinary solid quebracho	98.7	114.5
Eastern hemlock	60.4	102.0
Liquid oak bark	6.9	10.6
Paste gambier	83.1	153.0

Ether Extraction

Extractions with ethyl ether were run for a minimum of 72 hr. in a 500 cc. continuous extractor* ((1), Fig. 1). The residual ether-extracted liquor was warmed gently and outgassed with hydrogen to remove traces of ether, then diluted to the original volume.

The ethereal extract separated into two layers because of the water carried over during the long extraction. The proportionately small amount of aqueous solution appeared to contain some tannin, hence it was shaken three times with dry ether; the ether layers were added to the original ether extract, and the aqueous layer to the residual ether-extracted liquor. The ethereal extract was then carefully concentrated on the steam bath to minimize loss of volatile constituents.

Concordant results in regard to the percentage of ether-extractable matter (other than volatile acids, such as acetic) were very difficult to obtain, principally because of retention of traces of solvent on drying at low temperatures and loss of volatile phenolic compounds at higher temperatures. For these reasons the concentrated ether extracts were redissolved in a minimum amount of methanol, then made up to volume with distilled water; portions equivalent to 100 ml. of the original 27° Bk. extract were pipetted out for the titrations or other operations. One such aliquot portion was titrated after steam distillation, others were titrated after drying at 25° and 105° C. and redissolving in water.

* As supplied by the Scientific Glass Apparatus Company of Bloomfield, N.J., U.S.A.

Titration Curves and Buffer Index Values

The circuit used in the glass electrode titrations was designed by V. G. Smith ((7), Fig. 1) and built by the senior author. It included the highly sensitive General Electric F.P.–54 Pliotron tube in conjunction with a Leeds and Northrup Type K2 potentiometer and Type 2420-D galvanometer.

The glass electrodes consisted of bulbs of Corning 015 glass blown on to stems of ordinary soda-lime tubing. The electrode system included a saturated solution of quinhydrone in $0.1N$ hydrochloric acid, a platinum wire being used as the internal electrode; this wire was sealed through the end of a smaller tube filled with mercury for the external connection.

The reference electrode was a small saturated calomel half-cell, so designed that it could be used with either the calibration or titration vessel. The bridge solution in both vessels was saturated-potassium-chloride–calomel.
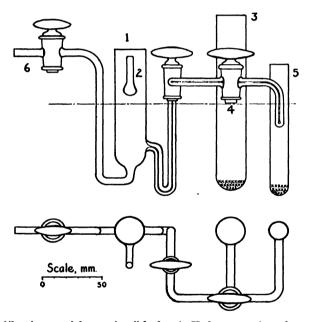
FIG. 1.   *Calibration vessel for use in oil bath.   1, Hydrogen or glass electrode cell; 2, hydrogen vent; 3, saturated potassium chloride reservoir; 4, three-way capillary stopcock; 5, calomel electrode cell; 6, suction tube for flushing out hydrogen electrode cell.*

The calibration vessel, Fig. 1, was designed for use in an oil bath, and could be adapted rapidly to hydrogen, quinhydrone, or glass electrode measurements. Despite the unorthodox arrangement of the liquid junction, measurements of potential with stable buffers were reproducible to within a few tenths of a millivolt. Because of the relatively high temperature coefficient of the saturated calomel half-cell, all calibrations and titrations were carried out at $20.0 \pm 0.1°$ C. in a well stirred kerosene bath, which was found to be quite

as convenient as a water bath, and was, of course, essential because of the characteristics of the electrometer circuit.

The titration vessel, Fig. 2, was constructed from an ordinary bottle (70 mm. inside diameter). The motor-driven Bakelite stirrer, the dipping arm of the calomel half-cell, the glass electrode, and a 10-ml. microburette passed through holes bored in the varnished stopper.

With the circuit and calibration vessel described it was possible to obtain calibration curves for the glass electrodes (buffers accurately standardized by means of the hydrogen electrode being used) which were nearly linear from pH = 1.5 to pH = 12.0; the slope of the curves was usually within 1 to 2% of the theoretical value, *i.e.*, 0.0001983 T, where T = temperature in °K. A group of typical calibration curves for the glass electrodes is shown in Fig. 3.

In the titrations, the standard, approximately normal, solutions of sodium hydroxide and hydrochloric acid were added in small portions from the microburette, sufficient time being allowed after each addition for the attainment of equilibrium conditions before the final potential measurement was taken.

Scale, mm.
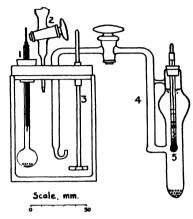
FIG. 2. *Titration vessel. 1, Glass electrode; 2, 10 ml. microburette; 3, Bakelite stirrer and glass bearing; 4, saturated potassium chloride bridge; 5, calomel electrode.*

The analyses, buffer index values, and other relevant data for the white spruce and commercial extracts of 20° Bk. strength are given in Table III, and the curves from which the buffer index values were calculated are plotted in Fig. 4. In each case the calculation involved merely reading off the total volume of 1.0N acid and alkali required to change the pH from 3.0 to 5.0; change in the slope of the curves within these limits was ignored.

TABLE III

ANALYSES AND BUFFER INDEX VALUES OF 20° BK. LIQUORS

	Quebracho	Spruce	Hemlock	Gambier	Oak bark
Analysis, gm. per litre —					
Insolubles	1.03	1.80	0.95	3.80	2.00
Soluble solids	49.80	51.00	49.30	48.70	45.30
Soluble non-tannins	6.93	20.15	20.08	23.20	15.60
Tannin	42.87	30.85	29.22	25.50	29.70
Purity, %	86.1	60.4	59.3	52.4	65.5
Tannins/non-tannins	6.19	1.52	1.46	1.10	1.90
Initial pH	4.32	4.00	3.71	4.32	2.75
Buffer index	0.55	1.09	1.72	1.78	2.15

In Fig. 5 are given the titration curves for the undiluted 27° Bk. spruce extract and the various fractions mentioned above: the steam distillate, aliquots of the ether-extractable material, and the ether-extracted liquor itself. The curves for the steam distillate and ether-extractable fractions are replotted on a larger scale in Fig. 6.
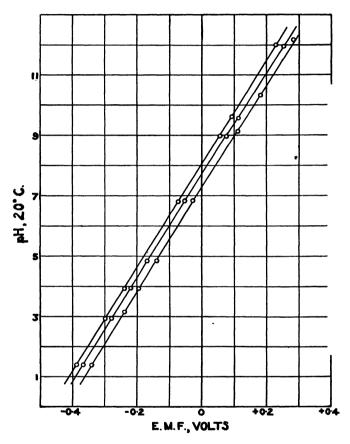
FIG. 3. *Typical calibration curves for Corning 015 glass electrodes, with 0.1 normal-hydrochloric-acid–saturated–quinhydrone filling, and saturated calomel half-cell, at 20° C.*

Fermentation

A portion of the original 27° Bk. spruce liquor was allowed to ferment freely at room temperature, since the fermentation of an extract is of importance to the tanner. Titrations of 100-ml. portions were carried out in the usual way.

Later, examination showed that the fermentation, which was marked by evolution of gas and formation of alcoholic materials, was due to two or more varieties of wild yeast, rather than to bacteria or molds.
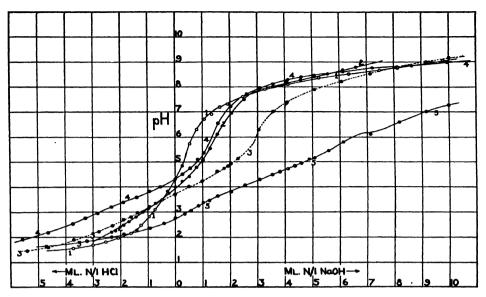
FIG. 4.   *Titration curves for 100-ml. portions of 20° Barkometer liquors.   1, Ordinary quebracho (solid extract), open circles, full line; 2, white spruce extract, solid circles, full line; 3, liquid hemlock extract, solid circles, dotted line; 4, paste gambier, half-black circles, full line; 5, liquid oak bark extract, half-black circles, full line.*
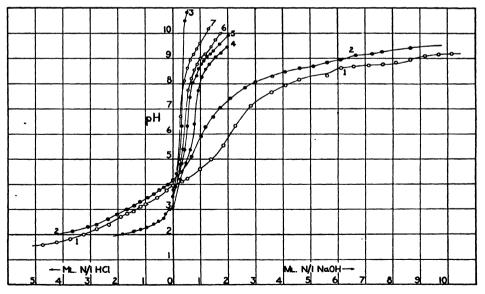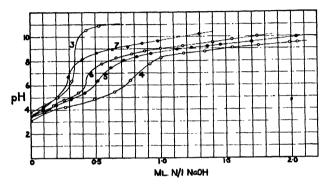
FIG. 5.   *Titration curves for original and ether-extracted 27° Barkometer spruce extract (100-ml. samples), and for steam distillate and ether-extractable fractions from 100-ml. samples of original liquor.   1, Original 27° Bk. extract; 2, same after ether extraction; 3, steam distillate; 4, total ether extract; 5, same after steam distillation; 6, ether extract after drying in vacuo at 25° C.; 7, same after drying at 105° C. (See Fig. 6).*

Discussion of Results

It is evident from the formaldehyde precipitation data that the tannins of white and black spruce bark are typical examples of the catechol or condensed group, in Freudenberg's classification. The bromine content of the bromo derivative of white spruce tannin is 52%, which is in agreement with values for other tannins of this group given by Perkin and Everest (5).

Tests on calfskin showed that the color was quite satisfactory; the samples had colors somewhat similar to those of samples tanned with sulphited quebracho extract.

FIG. 6. *Titration curves for steam distillate from 100 ml. of 27° Bk. liquor (Curve 3); total ether extract from 100 ml. (Curve 4), and same after steam distillation (Curve 5); ether extract from 100 ml. after drying in vacuo at 25° C. (Curve 6), and after drying in air at 105° C. (Curve 7).*

The buffer index and tannin/non-tannin ratio of the white spruce extract indicate that the liquor would probably be, in its general tanning properties, intermediate between the highly astringent extracts, such as ordinary quebracho and mimosa, on the one hand, and milder extracts such as hemlock, oak bark, and gambier, on the other. Certain chestnut wood extracts of French manufacture (3) show on examination both tannin/non-tannin ratios and buffer index values approaching those of the white spruce liquor, but information regarding their tanning properties is not available at the time of writing, hence it would be unwise to attempt any extensive predictions of the behavior of the spruce extract in the tannery.

The high buffer index of the oak bark extract examined is undoubtedly due in part to acidic fermentation products, since the pH of the undiluted liquor fell from 3.25 to 2.75 during the five months preceding this study. The pH of the hemlock extract fell from 4.20 to 3.71 during the same period. This acid-forming or "souring" tendency is of real importance in the rocker section of the heavy leather yard. The pH of a portion of the 27° Bk. spruce extract fell from 4.00 to 3.84 when it was allowed to ferment freely at room temperature for two months. It was found that the fermentation was due to two or more varieties of wild yeast and not to bacteria or molds. As expected, the titration curve of the fermented sample did not deviate greatly from that of the original material. The rapid fermentation caused by yeasts indicates

that the non-tannin fraction contains an appreciable proportion of sugars, which under tannery conditions might ferment to lactic, acetic, and other acids.

The titration curves for the steam distillate and the ether-extractable fractions (Figs. 5 and 6) suggest the presence of a number of weakly acidic (phenolic) materials in addition to volatile acids. The ether-extractable material not volatilized at 105° C. constitutes about 6.4% of the weight of soluble solids in the liquor, but its low buffering power (Curve 7, Fig. 6) indicates that it does not consist in large part of gallic acid or similar compounds. The volatile acids content of the unfermented 27° Bk. liquor was equivalent to about 0.18 gm. of acetic acid per litre.

A comparison of the curves for the original and ether-extracted 27° Bk. liquor shows that about 19% of the buffering power of the former (in the range pH = 3.0 to 5.0) is due to the ether-extractable material and the acids volatile with steam.

The ease of extraction of the tannins of white spruce bark is a matter of importance from several points of view. Tests made with an extractor of the Koch type at various temperatures showed that 76.2% of the tannin and 71.9% of the soluble non-tannins, these values being referred to the corresponding figures as found by means of the I.S.L.T.C. method of analysis as 100%, are ultimately extractable with water at 25° C. Accordingly, immersion in river water or leaching by rain or melting snow would cause serious losses of tannin. Thus, for example, analysis by the A.L.C.A. method of a sample of white spruce bark obtained from logs at a pulp mill revealed a tannin content of only 4.2%.

In conclusion it may be said that if concentrated tanning extracts can profitably be prepared from white spruce bark, then it is probable that these extracts could, because of their astringency, be used only in admixture with milder tanning materials in heavy leather manufacture, but might be used alone where straight quebracho extracts are now used, *e.g.*, in drum tannages of sheepskins, insole splits, and others.

Acknowledgments

References

1. Ashley, S. E. Q. and Murray, W. M.   Ind. Eng. Chem. (An. ed.) 10 (7) : 367-368. 1938.
2. Cameron, D. H. and McLaughlin, G. D.   J. Am. Leather Chem. Assoc. 25 : 325-328. 1930.
3. Jordan Lloyd, D. and Pleass, W. B.   J. Inter. Soc. Leather Trades Chemists, 17 : 352-358. 1933.
4. Lauffmann, R.   Collegium, No. 569 : 322-324.   1917.
5. Perkin, A. G. and Everest, A. E.   The natural organic colouring matters.   Longmans, Green and Company, London.   1918.
6. Pleass, W. B.   J. Inter. Soc. Leather Trades Chemists, 15 : 73-78.   1931.
7. Smith, V. G.   Can. J. Research, 10 : 479-481.   1934.

DICHLORINE HEXOXIDE[1]

BY M. H. KALINA[2] AND J. W. T. SPINKS[3]

Abstract

Some chemical and physical properties of dichlorine hexoxide are described and attention is drawn to its dangerous property of exploding violently on contact with organic substances.

The extinction coefficient of solutions of dichlorine hexoxide in carbon tetrachloride solution for a wave-length of 5460 Å has been measured and found to be 2.4, which is very much less than that of liquid dichlorine hexoxide for the same wave-length. A colorimetric method is described for the quantitative estimation of dichlorine hexoxide in solutions. The molecular weight of dichlorine hexoxide in carbon tetrachloride solution has been redetermined, and it confirms the formula Cl_2O_6.

Solutions of dichlorine hexoxide in carbon tetrachloride are decomposed photochemically by green light. Gaseous chlorine trioxide (ClO_3) is decomposed photochemically by λ3650. Its decomposition is photosensitized by chlorine and bromine, the quantum yield in the chlorine sensitized reaction being about 1.

Introduction

Dichlorine hexoxide was first observed in 1843 by Millon (11) who noticed the formation of a red liquid when chlorine dioxide was exposed to sunlight. Dichlorine hexoxide was mentioned again in the literature 80 years later by Bowen (3). In 1925, Bodenstein, Harteck, and Padelt (2) prepared the oxide in a relatively pure state and analyzed it. The analysis indicated that the ratio of chlorine to oxygen was 1 : 3. This fact together with the value for the molecular weight as determined in carbon tetrachloride solution led to the formula Cl_2O_6. The oxide was therefore named dichlorine hexoxide.

A short time later, while studying the kinetics of the thermal decomposition of ozone sensitized by chlorine, Schumacher and Stieger (14) came to the conclusion that chlorine dioxide and ozone, mixed at ordinary temperatures, should form chlorine trioxide or dichlorine hexoxide. This reaction does, in fact, take place very readily and is the basis of the method commonly used at present. The same method was developed by Allmand and Spinks (1) at about the same time from a study of the photochemical chlorine-ozone reaction.
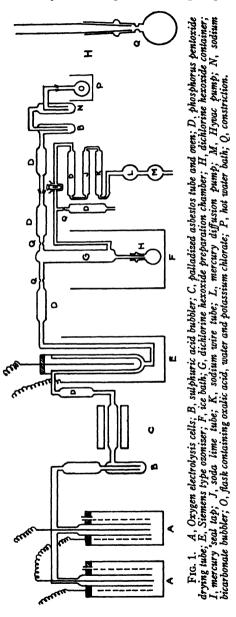
More recently, the compound has been purified and some of its physical properties measured (6). It has a melting point of $3.5 \pm 0.05°$ C., its color in the liquid state is like that of bromine, and it forms dark orange crystals

on freezing.   The crystals are of a light yellow color at −180° C.   The density of the liquid is 2.02 gm. per cc. at 3.5° C.

It is noteworthy that in the gas phase the oxide exists virtually entirely as chlorine trioxide (8). There is a small proportion of chlorine trioxide in the liquid hexoxide also, and the equilibrium, $Cl_2O_6 \rightleftharpoons 2ClO_3$, has been studied by the method of magnetic susceptibilities (4). The equilibrium constant was determined at various temperatures, and from these measurements the energy of dissociation in the liquid state was calculated to be −1730 ± 500 cal.

A short time after the present investigation was started the extinction coefficients of the gas and the liquid were published (7). The long wavelength absorption limit for the liquid hexoxide is at about 6400 Å, whereas the gaseous trioxide starts absorbing only at about 3600 Å.

The present work covers *(a)* experiments on some of the chemical and physical properties of dichlorine hexoxide, *(b)* the measurement of the extinction coefficient of dichlorine hexoxide in carbon tetrachloride solution, *(c)* preliminary experiments on the photodecomposition of dichlorine hexoxide and chlorine trioxide.

Preparation of Dichlorine Hexoxide

Essentially, the method of preparation of dichlorine hexoxide consists in mixing dry chlorine dioxide and ozonized oxygen in a suitable glass chamber at about 15° C. (14). The chlorine trioxide produced associates on the walls of the vessel, forming dichlorine hexoxide, which runs to the bottom (Fig. 1), and then into a small collecting bulb immersed in ice. Since dichlorine hexoxide has a great affinity for water, the gases must be thoroughly dried by means of phosphorus pentoxide, and moisture must be rigorously excluded from the apparatus. When it is necessary to transfer the dichlorine hexoxide

FIG. 1. *A, Oxygen electrolysis cells; B, sulphuric acid bubbler; C, palladized asbestos tube and oven; D, phosphorus pentoxide drying tube; E, Siemens type ozonizer; F, ice bath; G, dichlorine hexoxide preparation chamber; H, dichlorine hexoxide container; I, mercury seal tap; J, soda lime tube; K, sodium wire tube; L, mercury diffusion pump; M, Hyvac pump; N, sodium bicarbonate bubbler; O, flask containing oxalic acid, water and potassium chlorate; P, hot water bath; Q, constriction.*

to a special piece of apparatus such as a light-absorption cell, this piece of apparatus is connected to the collecting bulb through a glass septum which can be broken by means of a magnetic hammer.

The chlorine dioxide was prepared by mixing potassium chlorate, oxalic acid, and water in a small container, and heating to 60° C. The gases evolved were passed successively through a saturated sodium bicarbonate solution, concentrated sulphuric acid, and two phosphorus pentoxide tubes.

Ozone was prepared from oxygen in a Siemens type ozonizer operating on 60 cycles and 14,000 volts. The oxygen was prepared by the electrolysis of 20% sodium hydroxide between nickel electrodes. The oxygen was freed from traces of hydrogen, and was thoroughly dried before it passed to the ozonizer.

The dichlorine hexoxide is purified by keeping it at a temperature of 6° C. for about one hour under reduced pressure (Hyvac and mercury pump in series). This removes the more volatile impurities such as chlorine dioxide and leaves a relatively pure product melting at 3.5° C. Dichlorine hexoxide may also be purified by bubbling dry air through it. Another possible method would be to crystallize it from a 2 M solution of dichlorine hexoxide in carbon tetrachloride by cooling to about −23° C. The pure hexoxide crystallizes out in fine bright orange crystals.

Analysis

Thus far, there is no direct analytical method for determining dichlorine hexoxide other than the weighing of the pure substance. When dichlorine hexoxide or its solution in carbon tetrachloride is treated with water, the products of reaction are chlorine dioxide, chloric acid, and perchloric acid. These can be separated and determined by analysis (16); this gives a means of checking the total halogen present. Unfortunately, the ratio of the amounts of these products to the original dichlorine hexoxide is variable; consequently, this method of analysis is not applicable to mixtures of dichlorine hexoxide with the halogens or the halogen oxides. The latter might be formed, for example, by the decomposition of dichlorine hexoxide.

A colorimetric method was therefore developed for the determination of the amount of hexoxide present at any instant in a mixture containing dichlorine hexoxide, chlorine dioxide, and chlorine. It has been found experimentally that solutions of chlorine and chlorine dioxide in carbon tetrachloride do not appreciably absorb the mercury green line at 5460 Å, whereas a solution of dichlorine hexoxide in carbon tetrachloride absorbs 5460 Å strongly. (α_{5460} for chlorine is 0.02; α_{5460} for dichlorine hexoxide is 2.4.) Thus, if the extinction coefficient of dichlorine hexoxide in carbon tetrachloride solution for $\lambda 5460$ is determined by percentage transmission experiments with solutions of known concentration, it should be possible to use percentage transmission measurements of solutions of unknown concentration to determine their concentration. The percentage transmission can be measured either directly by use of a thermopile-galvanometer arrangement, or indirectly

by comparison in a colorimeter with an aqueous solution of potassium dichromate whose percentage transmission is known, monochromatic green light, λ5460 Å, being used.

Optical Arrangements

A mercury lamp taking 2 amp. at 140 volts was used as a light source. For accurate work a steady voltage was obtained by means of a voltage regulator*. The light filter for 5460 Å was a combination of Corning Nonex heat resisting yellow, 2.8 mm. thick; a Corning Didymium glass, 4.97 mm. thick; and a Corning Sextant green filter, 3.97 mm. thick, this serving to cut out the trace of red transmitted by the first two glasses. A Corning red-purple, ultra filter, 3.9 mm. thick, was used for 3650 Å. The light was measured by means of the usual Moll surface thermopile-galvanometer arrangement. In some experiments a monochromator was used to isolate 5460 Å from the light of the mercury lamp.

Chemical Properties

Dichlorine hexoxide has a great affinity for water, and it fumes in moist air, the reaction producing mainly chloric acid and perchloric acid. On the addition of the compound to water, dense white fumes are produced, together with some chlorine dioxide (16). When dichlorine hexoxide is added to an alkaline solution or to a solution of potassium iodide in water, there is a violent explosion which usually shatters the beaker. The substance explodes violently on coming into contact with a piece of wood. It also explodes when dropped on to vaseline or brominated grease. When it is spattered into a beaker containing alcohol, there are brilliant flashes and the alcohol ignites. It reacts with graphite and with iodine, but does not explode on coming into contact with them. A solution of dichlorine hexoxide in carbon tetrachloride is immediately decolorized by iodine, iodine tetroxide and iodine pentoxide being formed. No visible reaction takes place with bromine in carbon tetrachloride. Solutions of dichlorine hexoxide in carbon tetrachloride also oxidize sulphur and mercury (10).

When the hexoxide is mixed with sucrose a violent hissing occurs but no explosion—the sugar is presumably dehydrated. In one experiment a small preparation bulb was emptied except for the small amount of dichlorine hexoxide adhering to the walls, and illuminating gas was introduced. A violent explosion resulted, pulverizing the bulb. When bulbs containing liquid dichlorine hexoxide were thrown against a wall no explosion occurred. The vapor was not exploded by a spark from a Tesla coil or from an induction coil.

These experiments indicate that dichlorine hexoxide can give rise to violent explosions, and that particular care should be exercised to avoid contact of dichlorine hexoxide with organic materials. The experimenter should be adequately protected while preparing and handling the liquid hexoxide.

* *Suggested by Mr. B. G. Ballard of the National Research Laboratories, Ottawa.*

Extinction Coefficient of Dichlorine Hexoxide in Carbon Tetrachloride Solution

Liquid dichlorine hexoxide has a color like that of bromine, and, as already mentioned, its absorption curve has been determined by Goodeve (7). When carbon tetrachloride is added to dichlorine hexoxide the color becomes considerably lighter. Rough experiments with a colorimeter indicated that at 5460 Å the extinction coefficient for the liquid was much greater than that for the carbon tetrachloride solution. It was at first thought that this was due to a dissociation taking place in solution, just as in the gas phase, $Cl_2O_6 \rightleftarrows 2ClO_3$. However, a repetition of Bodenstein's determinations of the molecular weight in carbon tetrachloride gave a value of 167, very close to the theoretical for dichlorine hexoxide. (In a check on the method, the molecular weight of methyl oxalate was found to be 119; theoretical, 118.)

The first attempt to measure the extinction coefficient of solutions of dichlorine hexoxide in carbon tetrachloride, by matching the solutions in a colorimeter against standard solutions of potassium dichromate, failed. This was due to the introduction of small amounts of moisture, partly with supposedly dry carbon tetrachloride and partly from the air. This moisture could not be entirely excluded.

Consequently, apparatus was built in which dichlorine hexoxide could be dissolved in carbon tetrachloride in the absence of air and moisture (Fig. 2). A is a distilling flask containing pure dry carbon tetrachloride (16) and purified phosphorus pentoxide. This is connected to a Gerate glass cell
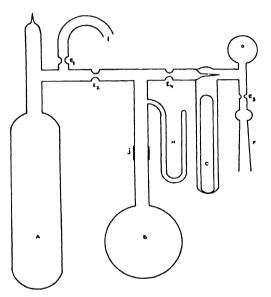
FIG. 2. A, distillation flask; B, cell; C, glass-enclosed hammer; D, hexoxide container; E, constriction; F, ground glass joint; H, U-tube for gas removal; I, carbon tetrachloride inlet and exhaust tube; J, graded glass seal.

by means of a graded seal J. The cell was 1.85 cm. long and 5 cm. in diameter, and had plane ends. After the bulb A had been partly filled, this part of the apparatus was evacuated and sealed off at E_1. Carbon tetrachloride was distilled back and forth six times from A to B, and then, after B had been filled, the cell was sealed off at E_2. The requisite amount of dichlorine hexoxide was made and purified in D. After evacuation, this was sealed off at E_3. The glass septum was then broken with the magnetic hammer and the dichlorine hexoxide dissolved in the carbon tetrachloride. The cell was then sealed at E_4, the free space above the carbon tetrachloride being quite small.

The temperature of the dichlorine hexoxide solution was maintained at 3° C. in a thermostat and the percentage transmission measured, the thermopile-galvanometer arrangement and wave-length 5460 Å being used. The molarity of the dichlorine hexoxide could be calculated from a knowledge of the weights of dichlorine hexoxide and carbon tetrachloride used. The weight of dichlorine hexoxide could be checked by analyzing for total halogen at the end of the experiment, the result agreeing well with the weight of dichlorine hexoxide taken.

TABLE I

RESULTS

Length of cell, 1.85 cm.

Molarity	0.0980	0.1075	0.0920	0.0259	0.0570
Per cent transmission	36.1	31.3	41.5	77.2	55.0
Extinction coefficient, α	2.44	2.53	2.24	2.33	2.24

It is seen that the extinction coefficient in carbon tetrachloride solution of molarity of about 0.1 is 2.4. The extinction coefficient for liquid dichlorine hexoxide is 80. In order to account for this difference solely by the dissociation

$$Cl_2O_6 \rightarrow 2ClO_3 ,$$

the dichlorine hexoxide would have to be virtually completely dissociated in solution. Molecular weight measurements indicate that in solution the hexoxide certainly does not dissociate to this extent. One might perhaps argue that the molecular weight measurements were made at −27° C., whereas the light absorption measurements were made at 3° C., and that the equilibrium might have been shifted by the temperature. However, such an explanation seems quite out of the question, as it would require a heat of dissociation of dichlorine hexoxide in solution of about 36,000 calories. (The corresponding heat of dissociation in the liquid phase is 1700 calories.)

The failure of the above chemical explanation leads to the suggestion that the difference between the extinction coefficients in the pure liquid and in carbon tetrachloride solution is due to a difference between the actual absorption of light by the molecules in solution and the absorption by molecules in the pure liquid state. This difference might be attributable either to *(a)* extensive solvation in carbon tetrachloride solution, or *(b)* to the fact that in the pure liquid the molecules are subject to strong fields which increase the transition probability between the normal and an excited state of the molecule, and thereby lead to an increase in the extinction coefficient. In view of the normal molecular weight in solution, this last explanation is favored.

While examples of a change in extinction coefficient due to a highly polar solvent, or compound formation, or hydration of ions are fairly common in the literature, only one other change similar to that observed in this work was found; namely, the change in the extinction coefficient of pure liquid bromine

when it is dissolved in an inert solvent (12). The absorption of light by bromine in the gaseous and liquid states and in solution has been investigated. The absorption curves show that for some wave-lengths the extinction coefficients in the three states are not very different. However, at 3080 Å, the extinction coefficients for liquid, solution, and gas are 630, 14.5, and 1.12, respectively. This is quite comparable to the effect with dichlorine hexoxide. The explanation given for the change in the extinction coefficient of bromine is that part of the absorption at 3080 Å is due to an intercombination transition $^1\Sigma - {}^3\Pi$. Electric fields favor the occurrence of such intercombinations, and it is suggested that the field of the surrounding molecules increases the probability of such a transition, thereby increasing the extinction coefficient. The effect is apparently stronger in pure liquid bromine than in a solution in carbon tetrachloride, where the bromine molecules are relatively far apart. A similar explanation might very well apply to the change in the coefficient of dichlorine hexoxide. However, thus far nothing is known of the potential curves for dichlorine hexoxide.

Measurements of extinction coefficients in the vapor phase and in solution for a given substance are rather more plentiful. Chlorine, for example, at 3300 Å, has a higher extinction coefficient in solution than in the gas phase (5, 9), whereas the extinction coefficients of iodine in the two phases are quite similar.

While the data are not sufficiently extensive to permit a detailed analysis, it does appear that in the transition from a gaseous phase to a solution, the validity of Beer's law is the exception rather than the rule (13). In this transition and in that from liquid to solution, a change in extinction coefficient might reasonably be expected if the two species of molecules did not have identical external fields. It is supposed for the moment, of course, that the solvent is inert and non-polar.

Photodecomposition of Dichlorine Hexoxide in Carbon Tetrachloride Solution

The extinction coefficient of dichlorine hexoxide at 5460 Å having been determined, it is obviously possible to follow changes in concentration by measuring the percentage transmission of 5460 Å from time to time. In this way, it is found that a 0.1 M solution of dichlorine hexoxide in carbon tetrachloride decomposes thermally quite rapidly at 2° C. The reaction is accelerated by green light, and rough measurements indicate a quantum yield of about 10 under our conditions.

Photodecomposition of Chlorine Trioxide in the Gaseous Phase

As we have already mentioned, dichlorine hexoxide exists mainly as chlorine trioxide in the gaseous phase, and it begins to absorb light strongly only at 3600 Å. Preliminary experiments in the photodecomposition have been carried out with the apparatus illustrated in Fig. 3. The over-all equation for the total decomposition of chlorine trioxide is $2ClO_3 \rightarrow Cl_2 + 3O_2$. Consequently, in a constant volume system, the reaction can be followed by

the change in pressure.   This was measured by means of a calibrated glass spoon gauge.   The tip of the pointer attached to the gauge moved 0.709 mm. for a change in pressure of 1 mm. of mercury.   The dichlorine hexoxide was made in a small bulb as described previously and sealed on to the apparatus at A. B is an outlet tube enabling this to be done. B was then sealed off and the pressure in the cell and both sides of the gauge was reduced to a very low value by means of a mercury pump.   The outside of the gauge was isolated by closing tap H.   The septum D was then broken and dichlorine hexoxide pumped through the apparatus, after which constrictions I and C were sealed off, in the order mentioned.   The cell was then illuminated and the reaction followed by the change of pressure shown by the spoon gauge.
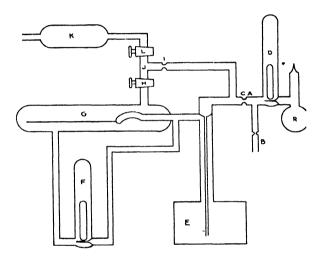
FIG. 3.   *A, straight line seal; B, side tube and constriction; C and I, constrictions; D and F, hammers and septa; E, cell; G, spoon gauge; H and L, taps; K, sodium wire tube; R, dichlorine hexoxide container.*

Preliminary experiments indicate that chlorine trioxide is relatively stable thermally (as compared to dichlorine hexoxide in solution) at 15° C., and is photodecomposed by 3650 Å.

Chlorine trioxide also undergoes a chlorine sensitized decomposition at $\lambda 3650$ Å, the quantum yield being approximately unity.   (Details of these experiments will be found in Reference (10).)

A bromine sensitized decomposition of chlorine trioxide has also been reported in the literature (15).

Since an exact investigation of the photokinetics of these reactions is obviously beset with considerable difficulties, it is being postponed until a more detailed study of the chemical and thermochemical properties of dichlorine hexoxide has been made.

References

1. ALLMAND, A. J. and SPINKS, J. W. T.   Nature, 124 : 651.   1929.
2. BODENSTEIN, M., HARTECK, P. and PADELT, E.   Z. anorg. Chem. 147 : 233-244.   1925.
3. BOWEN, E. J.   J. Chem. Soc. 123 : 2328-2330.   1923.
4. FARQUHARSON, J., GOODEVE, C. F. and RICHARDSON, F. D.   Trans. Faraday Soc. 32 : 790-795.   1936.
5. GILLAM, A. E. and MORTON, R. A.   Proc. Roy. Soc. (London), 124A : 604-616.   1929.
6. GOODEVE, C. F. and RICHARDSON, F. D.   J. Chem. Soc. 294-300.   1937.
7. GOODEVE, C. F. and RICHARDSON, F. D.   Trans. Faraday Soc. 33 : 453-457.   1937.
8. GOODEVE, C. F. and TODD, F. A.   Nature, 132 : 514-515.   1933.
9. HALBAN, H. v. and SEIDENTOPF, K.   Z. physik. Chem. 103 : 71-90.   1923.
10. KALINA, M.   Master's thesis.   University of Saskatchewan.   1938.
11. MILLON, E.   Ann. 46 : 281-319.   1843.
12. PORRET, D.   Proc. Roy. Soc. (London), 162A : 414-419.   1937.
13. RABINOWITCH, E. and WOOD, W. C.   Trans. Faraday Soc. 32 : 540-546.   1936.
14. SCHUMACHER, H. J. and STIEGER, G.   Z. anorg. Chem. 184 : 272-278.   1929.
15. SPINKS, J. W. T. and PORTER, J. M.   J. Am. Chem. Soc. 56 : 264-270.   1934.
16. SPINKS, J. W. T. and TAUBE, H.   Can. J. Research, B, 15 : 499-524.   1937.

THE EFFECT OF POLYHYDRIC ALCOHOLS ON THE TIME OF SET OF ALKALINE SILICA GELS[1]

By L. A. Munro[2] and J. A. Pearce[3]

Abstract

The behavior of glycerol in increasing the time of set of alkaline silica gels is not anomalous. There is a regular and further increase in time of set when the higher members of a series of polyhydric alcohols are added to the gels. The rate of change in the effect produced by increasing concentration of the addition agent varies with the concentration and pH. With the 2.23% gel, at pH 8.2, glycol showed a reversal of its effect on the time of set. The implications of this change are discussed.

In a previous study (4) on the effect of addition agents on the time of set of alkaline silica gels it was noted that glycerol showed anomalous behavior. Instead of the regular decrease in time of set caused by increasing amounts of the homologous series of soluble aliphatic alcohols, a marked increase in the setting time was caused by glycerol. Furthermore, although glycol decreased the time of set, the effect was much less than that obtained with the monohydric alcohols. It seemed of interest to extend the investigation to higher polyhydric alcohols. These have been studied over a range of pH and at two concentrations of silica.

Experimental

The silicate used was Baker's best grade of "Crystalline Sodium Silicate, $Na_2SiO_3 . 9H_2O$". Analysis of this gave the molar ratio of Na_2O to SiO_2 as 1.00 : 1.02. The water employed for making up solutions was redistilled and boiled before use. The stock sodium silicate solution was made up to a solution of specific gravity of 1.1569 (Westphal balance) in 1.5 to 2 litre batches. Larger volumes were avoided because it was observed that on prolonged standing a precipitate gradually formed. This aged silicate gave a slightly longer time of set (*e.g.*, from 210 to 225 sec.). The silicate solution was found to contain 6.7% of SiO_2. The solution was kept in a waxed Pyrex flask, as coatings of collodion, vaseline, and bakelite varnish had proved to be unsatisfactory.

The acetic acid was prepared by diluting 50 cc. of glacial acetic with 500 cc. of water. The addition agents were Eastman's best grade.

The time of set was determined by the tilted rod method of Hurd and Letteron (2).

The procedure of mixing was the same as that previously described (4). The liquids were added in 1.0, 2.0, and 3.0 cc. portions to the acid and made up to 25 cc. with water. The solids were added to the acid in 0.5, 2.0, and 4.0 gm. portions, and the whole was made up to volume.

The total weight of the largest amount of the difficultly soluble mannitol was added in a blank experiment to the mixed acid and silicate. This gave the volume of water necessary to bring the final volume to 50 cc. In the determination of the time of set for this particular addition agent the total quantity of agent was added to the acid plus the determined amount of water, and the silicate was then added, with rapid stirring. Complete and rapid solution was obtained.

Hurd, Raymond, and Miller (3) observed in their experiments a rise of 1.5°C. due to heat of neutralization. The present authors noted that with rapid-setting gels and high concentrations of addition substances there was a rise in temperature of four degrees on the addition of the silicate to the acid and addition agent. If the reagents were cooled and mixed in the beaker in a 16.0 ± 0.1° C. thermostat the temperature rose in a few seconds to 20°; at this point the beaker was transferred to a 20.00 ± 0.01° C. thermostat where setting proceeded at this temperature.

Owing to the slight solubility of dulcitol, with accompanying experimental difficulties, only one run was made. However, it appears that this alcohol is similar to mannitol in its effect.

Results*

The results are shown graphically in Figs. 1 to 5. In Figs. 1 to 4 the time of set is plotted against the molar concentration of addition agent. Fig. 5 shows the induced change in setting time as percentage of the original time
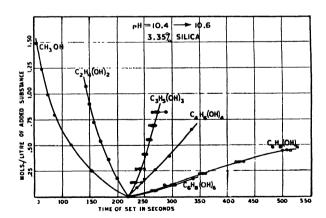
FIG. 1. *Silica gels, pH 10.4–10.6; prepared by adding 25 cc. Na₂SiO₃ solution (3.35% SiO₂) to 25 cc. acid mixture (16 cc. dilute acetic + addition agent + water).*
Curve 5—C₆H₈(OH)₆, mannitol. Curve 6—C₆H₈(OH)₆, dulcitol.

of set for different molar concentrations of added substance. These curves are the mean of several determinations made at different times, with different batches of silicate and addition agents. The greatest variation observed

* *Since the data are shown graphically, the tables of data have been omitted.*

in the setting time of a gel of pH 10.4 was ±7 sec. Curves 3 and 5, Fig. 1, show the typical relation of the curves to the divergent values. In no case is there any doubt as to the order in which the addition agents affect the time of set.
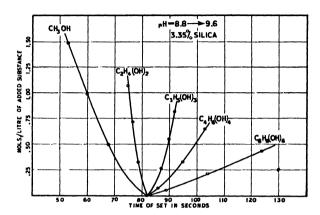
FIG. 2. *Silica gels, pH 8.8–9.6; 25 cc. Na$_2$SiO$_3$ solution (3.35% SiO$_2$) + 25 cc. acid mixture (18.5 cc. dilute acid + addition agent + water).*
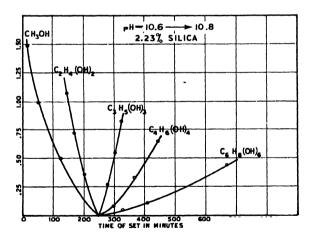
FIG. 3. *Silica gels, pH 10.6–10.8; 25 cc. Na$_2$SiO$_3$ solution (2.23% SiO$_2$) + 25 cc. acid mixture (10 cc. dilute acid + addition agent + water).*

As was noted previously, the pH, observed colorimetrically, increased on setting of the gel and with increased amounts of addition agents. With methanol the shift is greater; with glycol it is less; while with glycerol, erythritol, and mannitol the pH was the same as that of the original gel. In the case of methyl alcohol, for instance, 3 cc. of the addition agent gives a gel of pH 10.6, changing to 10.9, whereas the pH of the original gel without addition agent is initially

10.4, increasing to 10.6. The addition of 4 gm. of mannitol gave a pH of 10.4 to 10.6. The graphs, with the exception of No. 5, show a change in pH of the original gel on setting. In Fig. 5 the pH given represents the initial pH of the original gel.
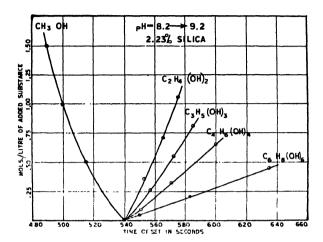
FIG. 4. *Silica gels, pH 8.2–9.2; 25 cc. Na₂SiO₃ solution (2.23% SiO₂) + 25 cc. acid mixture (12.5 cc. dilute acid + addition agent + water).*

Discussion

These experiments show conclusively that the previously observed behavior of glycerol is not anomalous, but is a regular step that progresses as the number of >CHOH groups increases (Figs. 1 to 4). The lengthening of the time of set of glycerol gels increases with the pH. This is in sharp contrast to the rapidly decreasing time of set with increasing pH for gels containing the monohydric alcohols such as methanol.

When the results are expressed as percentage change in time of set, a series of curves is obtained for each addition agent. It will be seen that slope changes with pH and concentration. Further it may be noted that the change in slope with change in pH is more pronounced with the gels of lower concentration. The effect of concentration and pH on the slope of the curves is most pronounced with the members at the extremes of the series, *viz.*, methanol and mannitol.

It will be observed that the curve obtained with glycol and the dilute gel at pH of 8.2 shows a reversal of slope (Figs. 4 and 5). This addition agent now behaves as glycerol, *i.e.*, it increases the time of set. Since it is known that the effect of an addition agent on acid gels is opposite to that on alkaline gels (6), one would expect a definite pH at which this reversal takes place— at first thought, the isoelectric point of silica sol, the pH of minimum set, which has been stated by Prasad and Hattiangadi (5) tó be 7.6. The fact

that the glycol effect changes between pH 8.2 and 10.6 indicates that this is not the case.

The pH at which the alcohols change from retarding to accelerating agents probably varies with the addition agent. Coehn (1) states that differences in the dielectric constants of the addition agents cause differences in charge
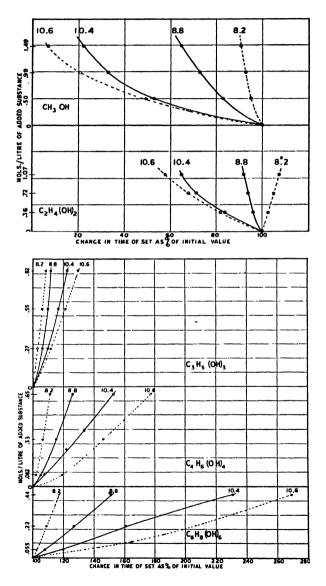
FIG. 5. *Solid curves—gels from "3.35%" silicate, pH 8.8 and 10.4; broken curves—gels from "2.23%" silicate, pH 8.2 and 10.6.*

on the colloidal particle. This implies a specific effect on the stability of the silica sol with consequent influence on the time of set. Differences in the concentration of the gel and its attendant electrolytes play important roles. Other factors will also be operative.

It is proposed to investigate this shift in behavior in relation to the pH of the gels of minimum setting time, the concentration of silica, and the dielectric constants of the addition agents.

Acknowledgment

References

1. COEHN, A. Ann. Physik, 64 : 217-232. 1898.
2. HURD, C. B. and LETTERON, H. A. J. Phys. Chem. 36 : 604-615. 1932.
3. HURD, C. B., RAYMOND, C. L. and MILLER, P. S. J. Phys. Chem. 38 : 663-674. 1934.
4. MUNRO, L. A. and ALVES, C. A. Can. J. Research, B, 15 : 353-359. 1937.
5. PRASAD, M. and HATTIANGADI, R. R. J. Indian Chem. Soc. 6 : 893-902. 1929.
6. PRASAD, M. and HATTIANGADI, R. R. J. Indian Chem. Soc. 6 : 991-1000. 1929.

EQUILIBRIA IN TWO-PHASE, GAS-LIQUID HYDROCARBON SYSTEMS

IV. METHANE AND HEPTANE[1]

By E. H. Boomer[2], C. A. Johnson[3], and A. G. A. Piercey[4]

Abstract

The densities and compositions of both phases in the methane–*n*-heptane solubility equilibrium have been determined at 25°, 55°, and 85° C. at total pressures from 35 to 250 atm. The critical pressures of complete miscibility were found, and the properties of the system are discussed. The nitrogen–*n*-heptane system was investigated similarly at 100.9 atm. and temperatures from 25° to 115° C. The system composed of Viking natural gas and impure heptanes was also investigated at 25° C. The three systems, methane-pentane, -hexane, and -heptane are compared and discussed.

Introduction

In previous investigations (2, 3) the methane-pentane and methane-hexane systems have been examined. The properties of both phases in equilibrium were determined at three temperatures and pressures up to the point of complete miscibility. In the present paper are presented the results obtained with the system *n*-heptane–methane, together with measurements on a system composed of *n*-heptane and a gas that is virtually pure methane, and those on the system *n*-heptane–nitrogen. The last-mentioned measurements were made in an effort to determine the effect of 5.6% of nitrogen in the gas used generally in this work. It may be said that the effect of the nitrogen is barely noticeable. In addition some measurements, preliminary to those outlined above, were made with impure heptane and a dry, high-methane natural gas from the Viking field.

This paper completes the publication of a series of measurements in which the normal paraffin hydrocarbons, pentane, hexane, and heptane have been used; it will be followed by reports on systems composed of naphthenic and aromatic hydrocarbons. In view of this, it is felt that the present paper should include a review of the three paraffin systems investigated, and discuss the relation between them. Consequently some of the data reported previously (2, 3) will appear again in this paper in one table and in one figure.

Materials

The gas used in the principal measurements has been described in previous reports (3). It had the composition: methane, 94.4; nitrogen 5.6%. Natural gas from the Viking field, Alberta, was also used in preliminary work on the

heptane system. This gas was taken from the supply mains, scrubbed with concentrated sulphuric acid to decompose odorant sulphur compounds added to the gas, and then passed over solid potassium hydroxide. The gas was dry and had the following composition on conventional analysis and combustion by means of the Orsat apparatus (Burrell): methane, 90.8; ethane, 3.5; nitrogen, 5.7%; density (N.T.P.), 0.000773 gm. per cc.

The gas contained some propane, possibly 1%, and traces of butane. The pressure-volume-density relations of this gas at 25° C. are given in Table I.

TABLE I

PRESSURE-VOLUME-DENSITY RELATIONS OF VIKING NATURAL GAS AT 25° C.
Methane, 90.8; ethane, 3.5; nitrogen, 5.7%

Pressure, atm.	Density, gm. per cc.	Deviation PV/P_1V_1	Pressure, atm.	Density, gm. per cc.	Deviation PV/P_1V_1
1	0.0007085	1.0	202.7	0.1730	0.8302
36.7	0.02727	0.9535	237.2	0.1969	0.8534
68.9	0.05446	0.8963	245.4	0.2021	0.8602
102.3	0.08504	0.8522	277.4	0.2193	0.8963
134.8	0.1164	0.8218	312.6	0.2358	0.9390
168.7	0.1458	0.8196			

The gas is slightly less ideal than the other gas used, as might be expected from its content of higher hydrocarbons.

In order to determine the influence of the nitrogen in the above-mentioned gases on the results, a third gas, virtually pure methane, was prepared. Viking natural gas was liquefied at atmospheric pressure by means of liquid air. The condenser was fitted with a small electric heater and a short, wire-packed distilling column. The condensed natural gas was distilled through this column. The composition of the overhead gas was followed continuously by means of a thermal conductivity, gas analysis apparatus. While nitrogen was distilling, the gas was vented to the atmosphere. The methane fraction was collected in gas-holders and compressed in storage cylinders. The residue, ethane, propane, water, etc., were discarded. A single run required 3.5 hr. and yielded about 60 litres of gas. It was not found possible to prepare pure methane with the apparatus. The gas produced always contained some nitrogen, from 0.3 to 0.5%, as impurity.

In the experiments with pure nitrogen, the commercial product supplied in steel cylinders under pressure was used. It was freed from oxygen by passage over hot copper, and dried under pressure.

Three different liquids were used in this work. Material of boiling range 90 to 95° C. was obtained by the fractional distillation of a light petroleum distillate. This material was nitrated thoroughly, washed, and dried. It was then distilled through a 38 in. vacuum-jacketed, packed column, and the fraction boiling over the range 90 to 93° C. (679 mm. of mercury) was retained. The density of the product was 0.704 at 20° C., this high value suggesting the presence of cycloparaffins.

An attempt was made to obtain *n*-heptane from Turner Valley naphtha. The 80 to 100° C. fraction was washed with sulphuric acid until no discoloration was observed. This material was washed, dried, and fractionated. The 75° to 94° C. fraction was nitrated thoroughly and then sulphonated by refluxing with fuming sulphuric acid for 48 hr. The 83 to 95° C. fraction was retained. The density, 0.707, and refractive index, 1.3961, at 21° C. indicated the presence of cycloparaffins.

Jeffery Pine Oil was the source of the *n*-heptane. This *n*-heptane was carefully distilled with high reflux through the column mentioned above. The physical constants of the middle portion remained unchanged on fractionation and this portion was used as *n*-heptane. The properties were: density, 20° C., 0.6834 (0.684, I.C.T.); refractive index, 22.5° C., 1.3863 (1.3867, I.C.T.).

Results and Discussion

The results and comparisons with other systems are presented in Tables II to VII inclusive, and in Figs. 1 to 7. The symbols have the same significance as those used previously (2, 3). Single primes refer to the gas phase, double primes to the liquid phase; the subscript 1 refers to the gas, usually methane, and subscript 2 refers to the liquid, heptane. The mole has been used to express quantities except in the results obtained with the impure heptanes and Viking gas; in these the mass fraction is used.

TABLE II

VIKING-NATURAL-GAS–IMPURE-HEPTANES SOLUBILITY
EQUILIBRIA AT 25° C.

Pressure, atm.	Phase density, gm. per cc.		Phase composition, weight % heptane	
	Liquid	Gas	Liquid	Gas
Heptane from petroleum				
136.8	0.6045	0.1265	86.1	6.6
172.4	0.561	0.172	80.0	11.5
204.6	0.517	0.223	73.4	19.0
237.9	0.440	0.309	61.1	36.3
238.1	0.444	0.311	61.0	36.5
Heptane from Turner Valley naphtha				
237.9	0.457	0.301	62.5	32.8

Impure Heptanes

The data obtained in experiments with impure heptanes and Viking gas are shown in Table II. These results are shown graphically in Fig. 1 together with the corresponding data for the *n*-heptane–methane (5.6% of nitrogen) system. Compositions are expressed in weight per cent because of uncertainty as to the nature of the impure heptanes. It is interesting to compare Fig. 1 (weight per cent ordinate) with Fig. 3 (mole per cent ordinate). The curves in the former are very useful in magnifying the changes in vapor content of the gas phase.

As a general rule, the mutual solubility of gas and liquid pairs will increase as the gas and liquid become more nearly alike in physical and chemical properties. The *n*-heptane–ethane system, investigated by Kay (5), shows

greater mutual solubility and a much lower pressure of complete miscibility than were found in the present work with gases consisting substantially of methane.   Hence, it might be predicted that Viking gas, in virtue of its content of higher gaseous hydrocarbons, would be more soluble than methane containing 5.6% of nitrogen in the same liquid hydrocarbon.   Reference to Fig. 1 shows that this is the case.

It is probable that the nature of the liquids used with Viking gas accounts in part for the results.   Both impure heptanes are mixtures containing branch chain, and straight chain, paraffin hydrocarbons and possibly cycloparaffins in small amounts.   The influence of the branch chain paraffins will be predominant and this influence, compared with that of the straight chain, *n*-heptane, will be one of increased mutual solubility between gas and liquid.

Thus, the differences between the results with the impure-heptanes–Viking-gas systems and the *n*-heptane–methane (5.6% of nitrogen) system are in the direction expected, and may be accounted for by both the composition of the impure heptanes and the composition of Viking gas.

Normal-heptane–Methane (5.6% of Nitrogen)

The data for the *n*-heptane–methane
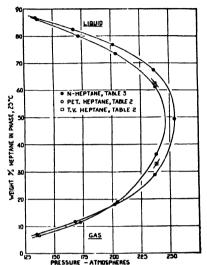
FIG. 1.   *Composition in weight per cent of gas and liquid phases at 25° C. as a function of pressure for n-heptane–methane (5.6% of nitrogen) and impure-heptanes–Viking-gas systems.*

system are given in Table III, and the properties of the system are illustrated in Fig. 2, showing phase density, in Fig. 3 showing phase composition, in Fig. 4 showing solubilities as mole ratios, and in Fig. 5 showing the equilibrium constants for methane and *n*-heptane.   Because of the great variation of the equilibrium constants in this system, the constants have been plotted on a semilogarithmic graph.   The general shape of the curves is not altered greatly by this procedure.   The properties of the system at the pressure of complete miscibility for each temperature, together with the same data for the systems pentane- and hexane-methane are given in Table VII.

This system behaves in all respects much as expected in the light of previous results with pentane (3) and hexane (2).   The lower volatility and higher molecular weight of *n*-heptane may be used to give a qualitative account of the differences between the three systems.

The *n*-heptane system obeys Henry's law with reasonable accuracy up to pressures of almost 100 atm.   Deviations are appreciable at lower pressures but become marked only at higher pressures.   The liquid composition curves,

TABLE III

METHANE (5.6% N₂)–n-HEPTANE SOLUBILITY EQUILIBRIUM

Pressure, atm.	Phase density, gm. per cc.		Phase composition, mole %						Solubility		Equilibrium constant	
			Liquid			Gas						
	Liquid	Gas	C_7H_{16}	CH_4	N_2	C_7H_{16}	CH_4	N_2	S_1''	S_1'	X_1'/X_1''	X_1'/X_1''
Temperature, 25° C.												
1	0.679					4.5	94.5					
36.2	0.661	0.0298	83.5	16.3	0.2	1.75	92.85	5.4				
	0.659	0.0280	83.8	15.9	0.3	–	–	–	0.192	0.0178	0.0209	5.76
68.4	0.637	0.0538	71.6	27.6	0.8	1.01	93.2	5.79				
	0.634	0.0554	–	–	–	1.29	92.8	5.91	0.385	0.0116	0.0161	3.47
101.7	0.610	0.0873	61.5	37.6	0.9	1.09	92.5	6.41				
	0.610	0.0859	60.8	38.7	0.5	1.09	93.6	5.31	0.624	0.0110	0.0178	2.44
135	0.585	0.122	51.8	47.0	1.2	1.33	90.8	7.87				
	0.584	0.121	–	–	–	1.19	91.0	7.81	0.907	0.0128	0.0244	1.93
167.9	0.556	0.161	43.5	53.9	2.6	2.20	91.0	6.8				
	0.555	0.160	43.8	54.0	2.2	2.15	91.0	6.85	1.235	0.0222	0.0498	1.685
202.2	0.521	0.208	35.4	62.2	2.4	3.7	89.4	6.9				
	0.521	0.206	35.4	61.9	2.7	3.5	89.9	6.6	1.752	0.0373	0.1017	1.47
236.0	0.466	0.267	26.0	70.5	3.5	–	–	–	2.71			
236.8	0.457	0.269	25.5	70.5	4.0	6.4	87.1	6.5	2.76	0.0684	0.251	1.236
243.6	0.444	0.293	22.6	73.1	4.3	8.3	85.8	7.9	3.23	0.0905	0.367	1.174
250.0	0.414	0.324	19.2	76.1	4.7	9.6	84.9	5.5	3.96	0.106	0.500	1.115
253.3	0.395	0.390	–	–	–	–	–	–				
Temperature, 55° C.												
1	0.653					23.1	76.9					
34.8	0.628	0.0267				3.2	90.4	6.4				
	0.634	0.0254	85.5	14.1	0.4	–	–	–	0.165	0.0331	0.0374	6.41
100.9	0.594	0.0765	63.9	35.2	0.9	2.1	92.8	5.1	0.551	0.0215	0.0329	2.63
167.2	0.540	0.141	46.8	51.3	1.9	3.2	90.6	6.2	1.096	0.0331	0.0684	1.765
236	0.446	0.250	28.4	68.5	3.1	7.9	86.0	6.1				
	0.449	0.246	28.4	68.3	3.3	7.8	86.4	5.8	2.41	0.0852	0.276	1.26
249.3	0.393	0.303	21.6	74.7	3.7	12.3	82.2	5.5				
	0.398	0.299	21.6	74.3	4.1	11.7	81.8	6.5	3.45	0.1364	0.555	1.10
252.8	0.385	–·	19.8	75.9	4.3	–	–	–				
	0.382	0.380	–	–	–	18.8	76.8	4.4	3.83	0.2315	0.95	1.01
Temperature, 85° C.												
1	0.628					67.7	32.3					
34.8	0.602	0.0241	86.5	13.0	0.5	4.0	91.8	4.2	0.1503	0.0417	0.0462	7.06
100 9	0.572	0.0735	65.1	33.9	1.0	3.1	91.1	5.8	0.521	0.0320	0.0476	2.68
167.2	0.521	0.1370	48.6	49.4	2.0	5.2	88.7	6.1	1.016	0.0549	0.107	1.79
236	0.389	0.264	–	–	–	12.7	81.9	5.4				
	0.395	0.262	26.4	69.5	4.1	13.0	82.1	4.9	2.63	0.1473	0.486	1.18
242.5	0.363	0.342	22.8	73.5	3.7	20.7	75.2	4.1	3.22	0.261	0.908	1.023
249.3	0.343	0.341	20.1	76.3	3.6	19.9	76.2	3.9	3.79	0.248	0.99	1.0

Fig. 3, show a marked concavity with a reversal in trend occurring over the pressure range 150 to 200 atm. This tendency of the composition curves to approach a maximum in respect to gas content of the liquid phase is more

marked here than it is in the pentane or hexane systems. This phenomenon, observed by Bassett and Dode (1) in the nitrogen-water system in such degree that no single phase region is exhibited, depends apparently on the mutual solubility of the components of the system.

Hill and Lacey (4) have given the composition at one point, 20.4 atm. and 30° C. for the liquid phase, as 9.6 mole per cent methane. Extrapolation
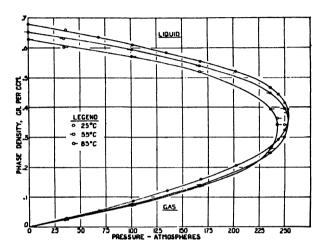
FIG. 2. *Density of gas and liquid phases at constant temperatures as a function of pressure for n-heptane–methane (5.6% of nitrogen) system.*
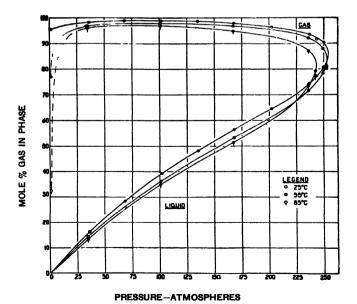
FIG. 3. *Composition in mole percentage of gas and liquid phases at constant temperatures as a function of pressure for n-heptane–methane (5.6% of nitrogen) system.*
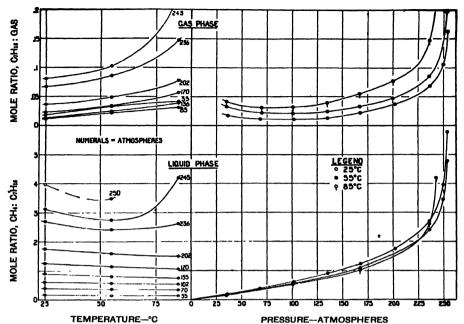
FIG. 4.   *Solubilities, as mole ratios of methane to n-heptane in liquid phase and n-heptane to gas in gas phase, as functions of temperature and pressure.*
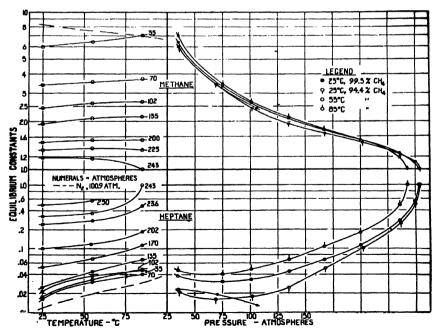
FIG. 5.   *Equilibrium constants, K_1 for methane and K_2 for n-heptane, as functions of temperature and pressure, including data on nitrogen and pure methane systems.*

of the present data to 20.4 atm. and interpolation to 30° C. gives a result, 9.4%, in good agreement with that of Hill and Lacey.

It is of interest to compare the present results with those of Kay (5) on the n-heptane–ethane system. The great influence of the gas may be illustrated best by the difference in pressure of complete miscibility. Replacing methane by ethane results in a drop of more than half in this pressure. A consideration of the equilibrium constants in the two systems indicates that the systems behave in much the same manner with changing temperature and pressure. The magnitude of the constant for methane is, however, roughly five times that for ethane. The greater solubility of ethane compared to methane accounts for this. The constant for heptane, K_2, is not independent of the gas. At low pressures and temperatures, the constant is smaller in the presence of ethane than it is in the presence of methane. This result can be attributed only to the influence exerted by the liquid phase on the composition of the gas phase. Although heptane should move into a gas phase composed of ethane more readily than into a gas phase composed of methane, the concentration of heptane in the liquid phase is so low that the opposite is true. Stated in another way, the more soluble ethane reduces the concentration of heptane in the liquid phase, with the result that the concentration of heptane in the gas phase is reduced, relatively, a greater amount than it is in the methane-heptane system.

At pressures greater than about 70 atm. the constant for heptane in the ethane-heptane system becomes greater than the constant in the methane-heptane system. This is, of course, to be expected since the constant approaches 1 at the pressure of complete miscibility, less than 100 atm. in the first system and more than 250 atm. in the second. It is characteristic of K_2 that at low pressures it changes only slowly, and at pressures about 75% of those at the point of miscibility it increases very rapidly. This change in trend occurs at about 70 atm. in the ethane-heptane system and at 200 atm. in the methane-heptane system. Finally, it is to be noted that both equilibrium constants in the ethane-heptane system change more rapidly with temperature than they do in the methane-heptane system.

The Influence of Nitrogen

The properties of the system, n-heptane–nitrogen at a pressure of 100.9 atm. and at different temperatures from 25° to 115° C. are given in Table IV. The system is shown graphically in Fig. 6, together with the comparable data from Table III on the n-heptane–methane (5.6% of nitrogen) system. Further, the essential data on the nitrogen system and the corresponding data on nitrogen in the n-heptane–methane (5.6% of nitrogen) system are given in Table V. The equilibrium constants for nitrogen are shown graphically as dotted lines in Fig. 5.

The solubility of nitrogen in n-heptane is approximately only one-third that of methane. Further, n-heptane vaporizes into methane to a greater extent than it does into nitrogen. The behavior of the methane system at 35 atm. is about the same as that of the nitrogen system at 100.9 atm. The

TABLE IV

NITROGEN–n-HEPTANE SOLUBILITY EQUILIBRIUM AT 100.9 ATM. PRESSURE

Temper-ature, °C.	Phase density, gm. per cc.		Phase composition, mole %				Solubility		Equilibrium constant	
			Liquid		Gas					
	Liquid	Gas	C_7H_{16}	N_2	C_7H_{16}	N_2	S_1''	S_2'	X_1'/X_1''	X_1'/X_1''
25	0.673	0.0993	88.0	12.0	1.04	98.96	0.136	0.0105	0.0118	8.24
55	0.653	0.109	87.2	12.8	1.76	98.24	0.147	0.0179	0.0202	7.54
	0.653	0.109	86.7	13.3	1.75	98.25				
85	0.625	0.101	86.04	13.96	2.44	97.56	0.162	0.0256	0.0289	6.99
	0.624	0.101	86.04	13.96	2.54	97.46				
115	0.593	0.098	85.02	14.98	5.05	94.95	0.177	0.0526	0.0594	6.34

effect of temperature changes on the two systems is very different. It may be seen in Fig. 6 that the solubility of nitrogen in n-heptane increases with increasing temperature, while the normal reverse behavior holds for methane under the same conditions. The solubility of methane in n-heptane increases
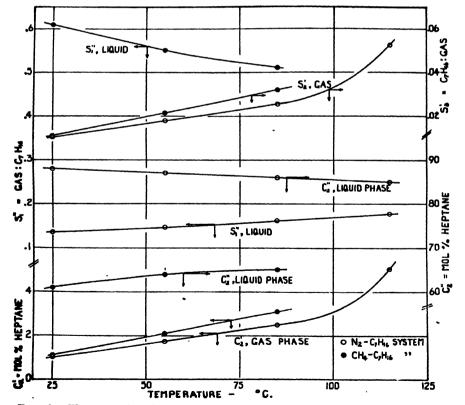
FIG. 6.   *The properties of the n-heptane–nitrogen system and the n-heptane–methane (5.6% of nitrogen) system at 100.9 atm. as a function of temperature.*

with increasing temperature only at pressures above 225 atm. and in the temperature range above 50° C.   Presumably nitrogen would behave like methane at some pressure range below 100.9 atm. and at lower temperatures.

TABLE V

COMPARISON OF HEPTANE-METHANE (5.6% OF NITROGEN) AND HEPTANE-NITROGEN SYSTEM
AT 100.9 ATM.

Temperature, °C.	Nitrogen, mole %				Equilibrium constant, N_2		Equilibrium constant, C_7H_{16}		Solubility N_2 in liquid		Solubility, calculated
	Liquid phase		Gas phase								
	1	2	1	2	1	2	1	2	1	2	
25	0.7	12.0	5.9	98.95	8.4	8.24	.018	.0118	.0115	.136	.0081
55	0.9	13.1	5.1	98.24	5.7	7.54	.0329	.0202	.0141	.147	.0073
85	1.0	14.0	5.8	97.5	5.8	7.0	.0476	.0289	.0154	.162	.0097

NOTE: 1—*refers to heptane-methane (5.6% of nitrogen) system, Table III.*
       2—*refers to heptane-nitrogen system, Table IV.*

The distribution of nitrogen between the gas and liquid phases of the n-heptane–methane (5.6% of nitrogen) system as given in Table III has been used to calculate solubilities and equilibrium constants given in Table V. The results are only approximate because of the small concentrations of nitrogen involved.   In addition, the solubility of nitrogen in n-heptane at pressures corresponding to the partial pressures of nitrogen in the n-heptane–methane (5.6% of nitrogen) system has been calculated from the data on the n-heptane–nitrogen system.   Henry's law and identical liquid phases have been assumed.   The calculated values are a little lower in all cases than the observed values.   The discrepancy is in the right direction when it is considered that the two liquid phases are not identical.   The liquid phase in the methane system is much less dense than the liquid phase in the nitrogen system, and contains much methane.   Nitrogen would be more soluble in the n-heptane–methane mixture than in n-heptane alone.   The error involved in the assumption of Henry's law is, probably, not significant.   The data of Table V suggest the conclusion that, for practical purposes, the behavior of the nitrogen in the n-heptane–methane (5.6% of nitrogen) system may be determined on the basis of Henry's law.   In other words, nitrogen at low partial pressures behaves ideally in the n-heptane–methane (5.6% of nitrogen) system.

A study of the equilibrium constants for nitrogen confirms the previous conclusion.   It is roughly true that the constants for nitrogen given in Table V are much the same in the two systems.   As would be expected, the constant for nitrogen is several times as great as that for methane, and, further, while the constants for methane increase with temperature, the constants for nitrogen decrease with increase in temperature.   This result follows from the nature of the solubility changes with temperature.

The constants for *n*-heptane given in Table V for the two systems are different by significant amounts but change with temperature in the same manner. The constant for *n*-heptane is less in the nitrogen system than it is in the methane system. This result follows from a low concentration of *n*-heptane in the gas phase and a high concentration in the liquid phase of the nitrogen system. The low concentration of *n*-heptane in the gas phase occurs in spite of the high concentration of *n*-heptane in the liquid phase, and must be attributed to the lack of any molecular similarity between *n*-heptane and nitrogen. The statement that compressed gaseous nitrogen is a poorer solvent than methane for *n*-heptane, while unconventional, expresses the conditions fairly well. Previously, in a discussion of the relations between the *n*-heptane–methane and *n*-heptane–ethane systems, the concentration of *n*-heptane in the liquid phase was considered to control the gas phase composition. Molecular similarity is the more important variable in the comparison of the *n*-heptane–nitrogen and *n*-heptane–methane systems.

TABLE VI

METHANE (0.5% OF NITROGEN)–*n*-HEPTANE SOLUBILITY EQUILIBRIUM AT 25° C.

Pressure, atm.	Phase density, gm. per cc.		Phase composition, mole %						Solubility		Equilibrium constant	
			Liquid			Gas						
	Liquid	Gas	C_7H_{16}	CH_4	N_2	C_7H_{16}	CH_4	N_2	S_1''	S_1'	X_1'/X_1''	X_1'/X_1''
35	0.658	0.0275	83.8	16.2	0.0	1.95	97.33	0.72	0.1945	0.0199	0.0233	5.98
	0.658	–	83.7	16.3	0.0	–	–	–				
70.4	0.634	0.0521	71.2	28.8	0.0	1.70	98.30	0.0	0.4065	0.0139	0.0193	3.42
	0.633	0.0532	70.9	28.9	0.2	1.04	98.96	0.0				
106	0.605	0.0852	59.3	40.7	0.0	0.71	99.26	0.03	0.685	0.00785	0.0130	2.43
	0.607	0.0855	59.3	40.6	0.1	0.83	98.67	0.50				

In order to have further information on the influence of nitrogen on the systems involving methane, the data of Table VI were obtained. The methane used in these experiments contained only 0.5% of nitrogen. The liquid phases in the two series of experiments, Tables III and VI, are identical for all practical purposes. Evidently the presence of 5.6% of nitrogen in the methane used does not change the composition of the liquid phase by any great amount. The data have not been plotted in Fig. 3 because they lie so close to the curve for 25° C. but are shown as equilibrium constants in Fig. 5. There is a small difference between the composition of the two liquid phases which is in the correct direction of higher gas content when 0.5% of nitrogen is present. The compositions of the gas phases in the two cases are not in agreement. The deviations are erratic and are due, probably, to experimental error. In conclusion, for practical purposes nitrogen in methane to the extent of 5.6% at least can be ignored as far as its influence

on the composition of the liquid phase is concerned. The behavior of the nitrogen can be predicted on the assumption that it is an ideal gas and obeys Henry's law. If desired, its presence may be corrected for by considering the pressure on the system as that measured, less the Dalton partial pressure of nitrogen, and calculating compositions on the basis of hydrocarbons only.
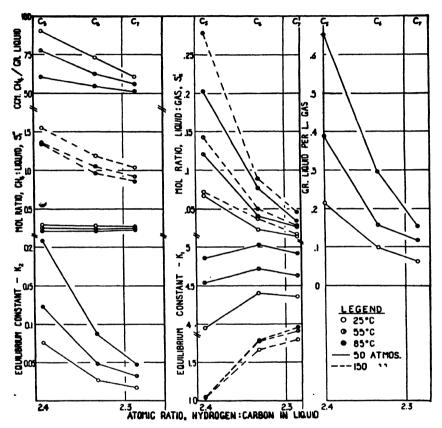
FIG. 7. *Comparison of the properties of n-pentane-, n-hexane-, n-heptane-methane (5.6% of nitrogen) systems on the basis of hydrogen–carbon atom ratio in liquid hydrocarbon.*

Comparison of the Pentane-, Hexane-, Heptane-methane Systems

Some of the data of Table III and corresponding data from previous papers (2, 3) are shown graphically in Fig. 7. The atomic ratio of hydrogen to carbon has been used as the distinguishing characteristic for the hydrocarbons and appears as abscissa. Many other properties of the molecule as, for example, molecular weight, volume, boiling point, freezing point, and refraction, were investigated, but no regularities such as straight lines were found. In Table VII are given the properties of the three systems, methane-pentane, -hexane, and -heptane at the pressure of complete miscibility.

TABLE VII

Conditions at pressure of complete miscibility for three systems, methane-pentane, -hexane, -heptane

Carbon number	Temperature, °C.	Pressure, atm.	Density, gm. per cc.	Liquid, mole %	S_1''	S_2''
5	25	175	0.307	19	4.02	0.234
6	25	214	0.347	16.5	5.38	0.1975
7	25	254	0.370	14	5.78	0.163
5	55	171	0.293	25	2.91	0.333
6	55	210.5	0.325	19.7	4.36	0.246
7	55	253	0.350	16.5	4.79	0.198
5	85	162	0.285	31	2.75	0.450
6	85	201	0.310	23.5	3.50	0.307
7	85	243	0.330	18.5	4.20	0.227

In their general behavior, the properties of the three systems change regularly. The curvature of the liquid phase composition line, Fig. 3, is most pronounced for the heptane system and least for the pentane system. Again, in the neighborhood of the pressure of complete miscibility, the peak of the curve is sharpest for the heptane system and flattest for the pentane system. According to the gas phase composition curves, the minimum of vapor content occurs at about the same pressure, 75 to 100 atm., irrespective of compound or temperature. The vapor content of the gas phase varies with the compound, however, and is roughly proportional to the normal vapor pressure of the compound. This is illustrated by the solubility, S_2', and number of grams of liquid per litre of gas, in Fig. 7. The effect of rising temperature on the vapor content of the gas phase is the same for all; the vapor content increases. The effect is most marked for pentane and least for heptane.

The solubility of gas in liquid, S_1'', expressed as a mole ratio, changes only slightly with the hydrogen-carbon ratio at low pressures. At high pressures, however, as shown by the 150 atm. lines of Fig. 7, the solubility decreases with decreasing hydrogen-carbon ratio; that is, in going from pentane to heptane. This is the behavior to be expected. When solubilities are expressed as cubic centimetres of gas per gram of liquid, the solubility decreases from pentane to heptane at all pressures and nearly linearly. A rise in temperature results generally in a decrease in S_1'' and the effect is most marked with pentane. However, at high pressures or high temperatures or both, the solubility will increase with increasing temperature. In the range of temperature studied, this effect becomes observable at 150 atm. for pentane, 187 atm. for hexane, and 227 atm. for heptane. It is of interest to remember that in the nitrogen-heptane system, S_1'' increased linearly with temperature in the range studied at 100.9 atm. (Fig. 6).

The magnitude of S_1'' may be very great as the pressure of complete miscibility is approached. The highest values are shown by the heptane system. However, at equal pressures, below the pressure of miscibility for all the

systems being compared, S_1'' is always greatest for pentane and least for heptane.

The behavior of the equilibrium constants is very similar for the three systems, with a regular variation from compound to compound. At all comparable pressures, K_2 decreases in going from pentane to heptane, and changes most with temperature in the case of pentane. At the pressure of minimum K_2, about 100 atm., the effect of temperature is most pronounced. The data of Nederbragt (6) on butane fit in well with the present work, the equilibrium constant for butane being greater than that for pentane at the same temperature and pressure.

The equilibrium constant for methane, K_1, at pressures above 50 atm., increases in going from pentane to heptane. At low pressures and high temperatures, K_1 is, roughly, constant for all compounds and is sensitive to temperature. A maximum is shown for hexane at 50 atm. which is characteristic at low pressures. The data of Nederbragt (6) for methane in the methane-butane system fit these results. K_1 in the methane-butane system is less than K_1 in the methane-pentane system at the same temperature and pressure.

The change in the equilibrium constant for methane, K_1, with the liquid component is not very great under any conditions, but is real. Only if the systems were ideal, would a constant K_1, independent of the liquid component, be found. It might be predicted that K_1 will approach a constant limiting value for paraffin hydrocarbons higher than those used here. The change in equilibrium constant for the liquid, K_2, with change in the liquid component, is relatively very great at the higher hydrogen-carbon ratio and higher temperatures. However, there is a suggestion that with the higher paraffin hydrocarbons, K_2 changes only slightly and may approach a minimum limiting value.

In Table VII, describing the systems at the pressure of complete miscibility, the change shown in properties with change in liquid component is just what might be expected. The change in the pressures is very regular. Upon increase of the carbon number by one, the pressure of complete miscibility increases by 40.5 atm. with a maximum deviation of 2 atm. in this series at all three temperatures used. Interpolation of the results obtained by Sage, Lacey and Schaafsma (7) with the propane-methane system gives a value of 39 atm. per carbon atom difference between propane and pentane at 25° C. The rule does not hold at higher temperatures, the figures being 44.5 and 52.5 atm. at 55° and 85° C.

The region of retrograde condensation, that is, the region between the pressure of complete miscibility and the point of minimum vapor content of the gas phase, is largest for heptane and least for pentane. This region in the methane-propane system (7) is still more restricted than in the pentane system. Further, as might be predicted, the region of retrograde condensation is reduced by rising temperature.

The changes in the other properties, such as density and composition, (Table VII) with the compounds are in the direction expected. Generally, the shift, such as the increase in density or decrease in liquid content of the system, is greater in the interval, pentane-hexane, than in the interval, hexane-heptane. There is a very great change in composition of about 100% increase in liquid content in going from the pentane system to the propane system (7).

References

1. BASSETT, J. and DODE, M.   Compt. rend. 203 : 775-777.   1936.
2. BOOMER, E. H. and JOHNSON, C. A.   Can. J. Research, B, 16 : 328-335.   1938.
3. BOOMER, E. H., JOHNSON, C. A., and PIERCEY, A. G. A.   Can. J. Research, B, 16 : 319-327.   1938.
4. HILL, E. S. and LACEY, W. N.   Ind. Eng. Chem. 16 : 1324-1327.   1934.
5. KAY, W. B.   Ind. Eng. Chem. 30 : 459-465.   1938.
6. NEDERBRAGT, G. W.   Ind. Eng. Chem. 30 : 587-588.   1938.
7. SAGE, B. H., LACEY, W. N., and SCHAAFSMA, J. G.   Ind. Eng. Chem. 26 : 214-217.   1934.

THE KINETICS OF THE DECOMPOSITION REACTIONS OF THE LOWER PARAFFINS

III. PROPANE[1]

By E. W. R. Steacie[2] and I. E. Puddington[3]

Abstract

The kinetics of the thermal decomposition of propane has been investigated over a temperature range from 551° to 602° C. The limiting high pressure first order rate constants are given by

$$\log_{10}k = 13.46 - \frac{63300}{2.3RT} \text{ sec.}^{-1}$$

The first order rate constants fall off strongly with increasing percentage decomposition, and the rate decreases with decreasing pressure in a manner similar to the rate decrease in the decomposition of the butanes.

Analyses of the products of reaction at various stages show them to be independent of temperature over the range examined, but to be affected by the initial pressure. This effect is undoubtedly due to the secondary hydrogenation of some of the initial products. The analytical results are in excellent agreement with those of Frey and Hepp.

Introduction

Recent papers from this laboratory (15, 16, 17) have pointed out the need for further work on the kinetics of the thermal decomposition reactions of the simple paraffin hydrocarbons. Investigations of the kinetics of the decomposition of *n*-butane (16) and isobutane (17) have already been reported. The present paper deals with propane.

Early work with propane (4, 7, 11, 12, 13) showed the decomposition to be fundamentally homogeneous and first order, the main reactions being

$$C_3H_8 = C_3H_6 + H_2$$
$$C_3H_8 = C_2H_4 + CH_4 .$$

Ethane and butane have also been reported as primary products, but in relatively small amounts.

Marek and McCluer (8), using a flow method, found the products to be as indicated by the above equations, in approximately equal amounts. They reported that the rate, after correction for the back reactions, is given by

$$\log_{10}k = 13.44 - \frac{62100}{2.3RT} \text{ sec.}^{-1}$$

Later Paul and Marek (10) examined the reaction more thoroughly, using low conversions to eliminate secondary processes. Change of the surface and of the surface/volume ratio were found to be without effect on the rate. The temperature coefficient was found to differ greatly from that indicated by the previous equation, being given by

$$\log_{10}k = 16.60 - \frac{74850}{2.3RT} \text{ sec.}^{-1}$$

Frey and Hepp (6) investigated the reaction at one temperature only, using a flow system. Their absolute rates were in good agreement with those obtained by other workers. Thorough analyses of the products of the reaction were made by low temperature distillation. These will be discussed later.

Dintzes and Frost (1, 2, 3) examined the reaction at temperatures from 619° to 666° C., and at initial pressures from 1 to 78 mm., using a static system. They found that the unimolecular constants fell off very strongly during an individual run. The addition of hydrogen, methane, or ethylene had no apparent effect on the reaction rate.

In view of the widely different values reported for the activation energy of the reaction, re-investigation with particular attention to the temperature coefficient seemed to be desirable.

Experimental

A static method, which has been previously described (16), was used. The products of the reaction were analyzed by low temperature fractional distillation in a still of the Podbielniak type. In the analyses considerable difficulty was experienced in obtaining a sharp cut between propane and propylene. To obviate this difficulty propane and propylene were taken off as a single fraction, and the propylene in this fraction was determined by absorption in fuming sulphuric acid in a Burrell gas analysis apparatus. Analyses were made on samples withdrawn from the reaction system at 6, 12.5, 25, and 50% pressure increase.

Propane of 99.9% purity was obtained in cylinders from the Ohio Chemical and Mfg. Co., and was used without further purification.

Results
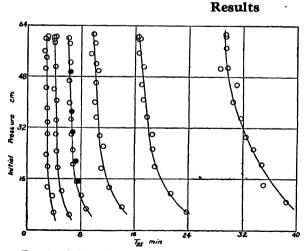
FIG. 1. *Effect of pressure and temperature on the reaction rate. The curves from left to right represent respectively 602°, 592°, 582°, 572°, 562°, 551°, C. Black circles are the results of experiments in a packed reaction vessel.*

The Rate of the Reaction

The reaction rate was followed by observing the pressure increase in a system of constant volume, as before. The results of rate experiments are given in Table I, in which $T_{12.5}$ and T_{25} correspond to the times for a 12.5 and a 25% pressure increase, respectively. The data are shown graphically in Fig. 1.

Limiting high pressure rates were found in the usual way by plotting T_s

TABLE I
The effect of temperature and pressure on the reaction rate

Initial pressure, cm.	$T_{12.5}$, min.	T_{25}, min.	Initial pressure, cm.	$T_{12.5}$, min.	T_{25}, min.
Temperature, 602° C.					
60.5	0.9	2.7	33.8	1.0	3.0
59.5	1.0	2.9	30.0	1.0	3.0
56.0	0.8	2.5	23.8	1.0	2.9
54.0	0.9	2.8	19.8	1.0	3.1
50.5	0.9	2.7	13.5	1.0	3.1
44.2	0.9	2.8	10.5	1.3	3.8
38.0	1.0	3.0	5.25	1.5	4.0
Temperature, 592° C.					
60.6	1.4	4.2	40.2	1.4	4.3
60.1	1.4	4.0	34.5	1.5	4.3
59.8	1.4	4.0	30.0	1.5	4.3
59.5	1.3	4.0	24.5	1.5	4.4
58.5	1.4	4.0	19.5	1.5	4.6
51.3	1.4	4.1	12.10	1.6	5.2
44.3	1.3	3.9	4.40	2.0	6.3
Temperature, 582° C.					
60.0	2.1	6.1	30.10	2.2	6.6
58.5	2.0	6.2	25.10	2.3	6.9
52.4	2.2	6.4	20.30	2.3	6.9
46.5	2.1	6.2	15.50	2.4	7.4
39.80	2.1	6.3	10.95	2.9	8.1
34.65	2.2	6.5	6.45	3.0	8.8
Temperature, 582° C. Packed reaction vessel					
48.8	–	6.4	21.1	2.4	7.3
36.4	2.2	6.5	15.0	2.5	7.6
30.8	–	6.8			
Temperature, 572° C.					
61.7	3.5	9.8	35.1	3.4	10.3
58.3	3.4	10.0	29.7	3.5	10.8
55.4	3.2	9.5	25.95	3.9	11.4
51.9	3.5	10.2	19.50	3.7	11.1
49.8	3.6	10.5	13.42	4.2	12.3
46.5	3.4	10.1	6.76	5.0	14.1
39.9	3.3	10.0			
Temperature, 562° C.					
60.45	5.8	16.5	35.10	6.1	17.8
60.00	5.8	16.8	30.00	6.3	18.5
59.90	5.6	16.5	25.30	6.2	18.4
55.45	5.7	16.5	19.90	6.2	19.0
50.65	5.6	17.2	11.25	7.0	21.4
45.30	5.9	17.0	5.87	7.5	23.8
40.70	–	17.3			

TABLE I—*Concluded*

THE EFFECT OF TEMPERATURE AND PRESSURE ON THE REACTION RATE—*Concluded*

Initial pressure, cm.	$T_{12.5}$, min.	T_{25}, min.	Initial pressure, cm.	$T_{12.5}$, min.	T_{25}, min.
Temperature, 551° C.					
57.15	10.1	29.4	29.20	11.2	32.4
51.00	10.3	29.6	25.40	11.4	33.6
50.65	9.8	28.6	20.23	11.4	34.8
45.30	10.8	31.0	14.15	11.6	35.1
40.35	10.8	30.5	8.72	12.2	38.5
34.80	10.8	31.7			
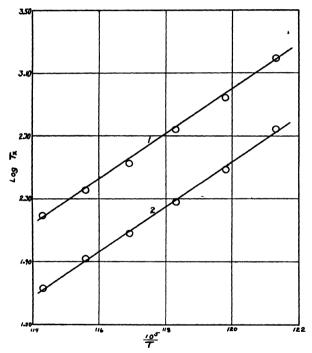
FIG. 2.   *The effect of temperature on the rate of the reaction.*

against the reciprocal of the initial pressure, and extrapolating to infinite pressure. The values thus obtained are given in Table II.

The temperature coefficient of the reaction is shown graphically in Fig. 2, in which Curve 1 represents the values of T_{25}, and Curve 2 those of $T_{12.5}$. These curves lead to values of the activation energy of 63,600 and 62,900 cal. per mole, respectively. Since the ratio $T_{25}/T_{12.5}$ is independent of the temperature, and of the initial pressure, it is justifiable to infer the activation

TABLE II
LIMITING HIGH PRESSURE RATES

Temperature, °C.	$T_{12.5}$, min.	T_{25}, min.	$\dfrac{T_{25}}{T_{12.5}}$	Limiting high pressure rate constant, sec.$^{-1}$ (calculated from T_{25})
602	0.91	2.60	2.86	18.5 $\times$ 10^{-4}
592	1.35	3.75	2.78	12.8 $\times$ 10^{-4}
582	2.00	5.55	2.78	8.65 $\times$ 10^{-4}
572	3.16	9.15	2.89	5.24 $\times$ 10^{-4}
562	5.10	14.50	2.85	3.31 $\times$ 10^{-4}
551	9.30	26.00	2.80	1.84 $\times$ 10^{-4}

energy from values of T_{25} or $T_{12.5}$. The high pressure rate constants calculated from values of T_{25} are also given in Table II. From these values we obtain for the high pressure rate at any temperature (as calculated from T_{25})

$$\log_{10}k = 13.16 - \frac{63300}{2.3RT} \text{ sec.}^{-1}$$

Table III gives complete data for two typical runs at 582° C. The falling off in the rate constants as the reaction progresses is noteworthy. Similar behavior has been found by Dintzes and his collaborators (1, 2, 3). The rate

TABLE III
COMPLETE DATA FOR TYPICAL RUNS

Initial pressure, 39.80 cm. Temperature, °C., 582			Initial pressure, 46.5 cm. Temperature, °C., 582		
Time, min.	ΔP, cm.	k, sec.$^{-1}$	Time, min.	ΔP, cm.	k, sec.$^{-1}$
0.0	–	–	0.0	–	–
0.5	1.75	15.3 $\times$ 10^{-4}	0.5	2.1	15.4 $\times$ 10^{-4}
1.0	2.80	12.3	1.0	3.4	12.6
1.5	3.90	11.5	1.5	4.6	11.8
2.0	4.95	11.1	2.0	5.8	11.3
3.0	6.20	9.48	3.0	7.3	9.44
4.0	7.48	8.74	4.0	8.8	8.70
5.0	8.58	8.05	5.0	10.2	8.20
6.0	9.59	7.67	6.0	11.4	7.80
6.3	9.95	7.63	6.2	11.6	7.73

constants in Table III are calculated on the assumption that 100% pressure increase corresponds to completion. Analytical results given later show that up to 25% decomposition the pressure change is an accurate measure of the percentage decomposition, and hence justify the method of calculating the rate constants. At higher percentage decompositions, however, considerable polymerization, hydrogenation, and other secondary reactions occur, and the pressure increase is therefore a somewhat unreliable measure of the extent of reaction. It appears from Table III, and from similar calculations for other runs, that the initial rate constants are approximately 100% higher than those

at 25% decomposition.   We may therefore correct the above equation, and obtain for the initial high pressure rate constants

$$\log_{10}k = 13.46 - \frac{63300}{2.3RT} \text{ sec.}^{-1}$$

In Fig. 1 the filled circles represent runs made in a reaction vessel filled with broken quartz, so as to increase the surface/volume ratio by a factor of about 15.   It is evident that no appreciable increase in rate occurs with increased surface, and hence the reaction is completely homogeneous.
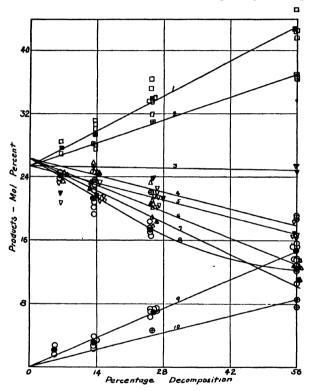
FIG. 3.   *Extrapolation to determine initial products of the reaction.   Open symbols represent actual analyses; black symbols represent mean values.   From top to bottom the curves represent successively CH_4, CH_4 at low pressure, C_2H_4 at low pressure, H_2 at low pressure, C_2H_4, C_3H_6, C_2H_6 at low pressure, H_2, C_2H_6, and C_3H_6 at low pressure.*

The Products of the Reaction

Analyses of the products of the reaction were made over the temperature range from 551° to 602° C., and at initial pressures of 60 and 20 cm.   Products were withdrawn for analysis at times corresponding to pressure increases of 6, 12.5, 25, and 50%.   The results of these analyses are given in Table IV, and are shown graphically in Fig. 3.

TABLE IV

The products of the reaction

Products, mole per cent	Temperature, °C.						
	551	562	572	582	592	602	Mean

Initial pressure, 60 cm. Sample withdrawn at T_{50}

H_2	—	—	10.6	12.3	13.3	13.5	12.4
CH_4	—	—	44.8	42.6	42.5	41.5	42.8
C_2H_4	—	—	16.1	16.2	18.5	16.7	16.9
C_2H_6	—	—	15.8	15.4	12.8	15.3	14.8
C_3H_6	—	—	12.4	13.5	12.8	13.0	12.9
% Decomposition	—	—	58.6	55.0	57.3	52.6	56.1

Initial pressure, 60 cm. Sample withdrawn at T_{25}

H_2	17.0	17.4	16.6	17.2	18.5	15.5	17.0
CH_4	36.5	33.9	33.6	31.8	33.5	35.3	34.1
C_2H_4	22.0	22.4	21.6	20.3	20.2	21.5	21.3
C_2H_6	6.5	7.4	7.1	7.3	7.2	7.4	7.1
C_3H_6	18.0	19.0	21.1	23.4	20.5	20.2	20.8
% Decomposition	24.4	25.0	25.4	26.2	25.0	24.6	25.1

Initial pressure, 60 cm. Sample withdrawn at $T_{12.5}$

H_2	20.2	19.4	20.8	23.0	22.5	—	21.2
CH_4	30.6	31.1	29.8	28.0	27.6	—	29.4
C_2H_4	21.5	23.5	20.8	21.0	21.3	—	21.6
C_2H_6	3.1	2.4	2.6	3.2	3.9	—	3.1
C_3H_6	24.7	23.5	25.9	24.8	24.7	—	24.7
% Decomposition	12.6	12.8	12.4	14.2	14.2	—	13.6

Initial pressure, 60 cm. Sample withdrawn at T_6

H_2	24.3	24.2	—	—	– –	—	24.2
CH_4	27.0	28.4	—	—	—	—	27.7
C_2H_4	23.4	20.8	---	—	—	—	22.1
C_2H_6	1.8	2.8	—	– –	---	—	2.3
C_3H_6	23.4	24.5	—	---	—	—	23.9
% Decomposition	6.0	6.1	—	– –	—	—	6.05

Initial pressure, 20 cm.

Temperature	582	592	592	592
Sampled at	T_{50}	T_{50}	T_{25}	$T_{12.5}$
H_2	18.7	18.8	22.1	23.6
CH_4	37.0	36.6	31.0	28.3
C_2H_4	25.5	25.0	23.8	25.4
C_2H_6	7.7	8.5	4.8	0.0
C_3H_6	11.1	11.2	18.4	22.6
% Decomposition	54.0	52.8	25.5	13.1

The products are not appreciably affected by the temperature over the range examined, but vary considerably with the initial pressure, especially at high percentage decompositions. This difference appears to be due entirely to the hydrogenation of ethylene, since in both cases extrapolation to zero decomposition leads to a convergence of the curves for ethylene, ethane, and hydrogen. Ethane therefore appears to be definitely not an important initial product of the reaction.

In addition to the products listed in Table IV, a small amount of some polymer was also formed, and a visible deposit of carbon appeared on the quartz surface after a few runs. A very small amount of some higher boiling product was also observable in the still after all the gaseous products had been taken off in analyses at 50% decomposition. The amounts of carbon and polymers formed per run were, however, so small that they introduce no appreciable error into the analyses.

Discussion

The Rate of the Reaction

A comparison of the initial high pressure rates obtained in this work with the rates reported by others is given in Table V.

TABLE V

COMPARISON OF RESULTS

Observers	E, Kcal.	$\log_{10}A$	k_{575}, sec.$^{-1}$
Pease and Durgan (12)	(65.0)	—	—
Frey and Hepp (6)	—	—	1.5×10^{-3}
Marek and McCluer (8)	62.1	13.44	2.6×10^{-3}
Paul and Marek (10)	74.9	16.60	1.9×10^{-3}
This investigation	63.3	13.46	1.1×10^{-3}

The absolute rates are thus in comparatively good agreement. There seems to be no doubt, however, that the values of E and A reported by Paul and Marek are very much too high.

As the products of the reaction have been shown to be independent of temperature over the range investigated, the energies of activation of the two main reactions

$$C_3H_8 = C_3H_6 + H_2 \tag{1}$$

$$C_3H_8 = C_2H_4 + CH_4 \tag{2}$$

are identical, and equal to 63.3 Kcal. Also, as discussed in the next section, the two reactions appear to occur to the same extent in the initial stages of the decomposition. We can therefore apportion the rate constants equally between them, and we have for the separate reactions

$$\log_{10}k_1 = \log_{10}k_2 = 13.16 - \frac{63300}{2.3RT} \text{ sec.}^{-1}$$

The Products of the Reaction

As may be seen from Fig. 3, the initial products of the reaction appear to be those indicated by the above equations, in equal amount, *i.e.* 25% each of propylene, ethylene, methane, and hydrogen. This is in accord with the findings of Marek and McCluer.

As the products change greatly as the reaction proceeds, it is of course necessary to make comparisons at the same percentage decomposition, and roughly at the same pressure. Frey and Hepp reported the products at 739 mm. and 10% decomposition at 575° C. to be: H_2, 23.0; CH_4, 26.1; C_2H_4, 22.7; C_2H_6, 2.7; C_3H_6, 25.3%. Under similar conditions, the results from this investigation are H_2, 22.4; CH_4, 28.0; C_2H_4, 23.2; C_2H_6, 2.8; C_3H_6, 23.6%. The agreement is excellent.

The products are in only fair agreement with those predicted by the Rice free radical mechanism. On this basis the ratio $\dfrac{C_2H_4 + CH_4}{C_3H_6 + H_2}$ should have a value of 1.5, whereas in fact it is 1.0. In any case, the work of Patat (9) has definitely shown that in its present form the Rice-Herzfeld mechanism is untenable for propane.

The Effect of Pressure on the Reaction Rate

It will be seen from Fig. 1 that the rate of reaction falls off rapidly with diminishing pressure, and that this effect is noticeable at quite high pressures. This behavior is similar to that of the butanes. As with the butanes, in order to fit the results to the Kassel theory it is necessary to consider part of the molecule to be frozen, and to reduce the number of oscillators, s, from the theoretical value of 19 to 7. With $s = 7$, the theory fits the results excellently if we assign to the other parameters the values $\nu = 1000$ cm.$^{-1}$, $m = 22$, $\sigma = 4 \times 10^{-8}$ cm.

In the case of the butanes, the rapid falling off in rate for such complex molecules was tentatively assumed to be due to some sort of chain process initiated by radicals. With propane, the work of Patat rules out the Rice-Herzfeld mechanism, but does not exclude the possibility of a radical chain mechanism, provided that the chains are very short. Actually, the work of Echols and Pease (5), and of Sickman and Rice (14), shows that very short chains can be initiated by the introduction of radicals into propane. Hence the effect of pressure on the rate has perhaps the same explanation for propane as for the butanes.

References

1. DINTZES, A. I. and FROST, A. V. J. Gen. Chem. U.S.S.R. 3 : 747-758. 1933.
2. DINTZES, A. I. and FROST, A. V. Compt. rend. acad. sci. U.R.S.S. 4 : 153-157. 1933.
3. DINTZES, A. I. and FROST, A. V. Compt. rend. acad. sci. U.R.S.S. 5 : 513-515. 1934.
4. EBREY, G. O. and ENGELDER, C. J. Ind. Eng. Chem. 23 : 1033-1035. 1931.
5. ECHOLS, L. S. and PEASE, R. N. J. Am. Chem. Soc. 58 : 1317. 1936.
6. FREY, F. E. and HEPP, H. J. Ind. Eng. Chem. 25 : 441-449. 1933.
7. FREY, F E. and SMITH, D. F. Ind. Eng. Chem. 20 : 948-951. 1928.
8. MAREK, L. F. and McCLUER, W. B. Ind. Eng. Chem. 23 : 878-881. 1931.
9. PATAT, F. Z. physik. Chem. B, 32 : 294-304. 1936.
10. PAUL, R. E. and MAREK, L. F. Ind. Eng. Chem. 26 : 454-457. 1934.
11. PEASE, R. N. J. Am. Chem. Soc. 50 : 1779-1785. 1928.
12. PEASE, R. N. and DURGAN, E. S. J. Am. Chem. Soc. 52 : 1262-1267. 1930.
13. SCHNEIDER, V. and FROLICH, P. K. Ind. Eng. Chem. 23 : 1405-1410. 1931.
14. SICKMAN, D. V. and RICE, O. K. J. Chem. Phys. 4 : 608-613. 1936.
15. STEACIE, E. W. R. Chem. Rev. 22 : 311-402. 1938.
16. STEACIE E. W. R. and PUDDINGTON, I. E. Can. J. Research, B, 16 : 176-193. 1938.
17. STEACIE, E. W. R. and PUDDINGTON, I. E. Can. J. Research, B, 16 : 260-272. 1938.

A STUDY OF THE DETERMINATION OF VITAMIN A BY SPECTROPHOTOMETRY AND BY PHOTOELECTRIC COLORIMETRY[1]

By W. D. McFarlane[2] AND A. J. Sutherland[3]

Abstract

A comparison has been made of the determination of vitamin A in cod-liver oils and concentrates of vitamin A by means of (a) extinction coefficient measurements at 3280 Å, and (b) photoelectric colorimetry. Both methods are shown to yield results of equal accuracy, but with cod-liver oils special precautions have to be taken in the preparation and purification of the unsaponifiable fraction. No significant difference was found between the means of the quotients, blue value/E value, for low potency cod-liver oils and those for concentrates.

The estimation of vitamin A by direct spectrophotometric measurements before and after its destruction by intense ultra-violet irradiation has been investigated. The conditions are described which permitted the complete destruction of vitamin A in a concentrate with apparently no significant effect on the other absorbing constituents of the oil except carotene. The residual absorption after irradiation amounted to about 5% of the initial absorption. With cod-liver oils the values obtained by this method are 20 to 30% lower than those obtained by absorption measurements on the unsaponifiable fraction. The results obtained with the concentrate indicate that a correction may be applied which reduces the discrepancy to about 10 to 15%.

Part I. A Comparison of the Spectrophotometric Method and the Photoelectric Colorimetric Method of Determining Vitamin A

Two methods have been proposed as satisfactory alternatives for the biological assay of vitamin A, namely: (a) colorimetric determination—measurement of the intensity of the blue color produced when antimony trichloride dissolved in chloroform is added to a chloroform solution of the unsaponifiable portion of the oil (blue value); and (b) spectrophotometric determination—measurement of the intensity of absorption of ultra-violet -radiations of wave-length 3280 Å by an alcohol or cyclohexane solution of the unsaponifiable portion of the oil (E value).

Crews and Cox (5) applied these two methods simultaneously to a series of oils and concentrates. They found that the ratio, blue value/E value, for the unsaponifiable portion of cod-liver oils is about 30, but for concentrates the value is approximately 50. Similar results have been recorded by several workers, notably Morgan et al. (14), who conclude that the principal sources of

error are *(a)* the presence in the unsaponifiable fraction of substances other than vitamin A which absorb in the near ultra-violet or inhibit the blue color reaction, and *(b)* the inefficiency of the tintometer as an instrument for measuring the transient blue color.   Haines and Drummond (8) analyzed halibut-liver oils by the two methods and obtained results that were in good agreement.   Josephy (12) concluded that the two measurements agree with a mean error of less than 5%, and Black *et al.* (2) arrived at a similar conclusion with regard to colorimetric and vitameter measurements.

Since 1934, when the International Committee (11) approved only the ultra-violet absorption measurement as an alternate to biological assay, this method has found particular favor.   The physical method was adopted in preference to the colorimetric solely because the absorption at 3280 Å could be measured with greater accuracy.   Dann and Evelyn (6) recently reported that when the Evelyn photoelectric colorimeter is employed the extinction coefficient of the blue solution at 6200 Å is a linear function of the concentration of vitamin A.   They clearly define the conditions that permit measurements of the blue color being made with an error of only 0.85% as compared with an acknowledged error of 10 to 15% in the Lovibond tintometer readings. It would appear therefore that the principal objection to the acceptance of the blue value as a measure of vitamin A has been removed.   They have also determined the photoelectric blue value and the *E* value of 21 oils and 18 concentrates, and they find a much greater disagreement between the two values than was recorded by earlier workers.   It must therefore be concluded that there may arise in either method, or in both, errors that are of much more significance than those eliminated by refinement in colorimetric technique. The method of saponification employed by Dann and Evelyn required three washings of the ether extract containing the unsaponifiable fraction with water only, whereas the British Pharmacopoeia recommends that the ether extract be washed twice with $N/2$ potassium hydroxide and three times with water. It has been our experience that the unsaponifiable fraction of some oils may be difficult to purify, hence the use of a standard saponification process for all samples may lead to errors of such magnitude that the true relation between the blue value and the *E* value will be obscured.   Wilkie (16) points out that if reproducible blue values or *E* values are to be obtained the ethereal extract containing the unsaponifiable material must be washed, alternately, with dilute alkali and water until the washings fail to show any trace of precipitate when acidified with dilute hydrochloric acid.

Experimental

In this study the photoelectric blue values and the *E* values of 16 cod-liver oils and 15 concentrates which include 6 halibut-liver oils, 4 high-potency fish oils, and one sample of vitamin distillate have been determined.   In the analyses of the concentrates about 100 mg. of the oil was weighed directly into a 25 ml. volumetric flask and dissolved in a mixture of 90 parts of absolute ethyl alcohol and 10 parts of cyclohexane, and the solution was diluted to

volume with this solvent. The blue reaction was carried out according to the method of Dann and Evelyn (6), an aliquot portion of the solution (or of a more dilute solution in the same solvent) being transferred to the colorimeter tube and evaporated to dryness *in vacuo*, and the residue taken up in 1 ml. of pure anhydrous chloroform for the colorimetric determination.

The spectrographic measurements were made with a large quartz spectrograph, Littrow mounting, with 30° quartz prism and lens of 1800 mm. focal length. The dispersion was approximately 2.5 Å per mm. at λ2500 and 25.0 Å per mm. at λ5500. The spectrograph was fitted with a Bellingham and Stanley single-disc rotating sector photometer (1936 design). Illumination was effected by a condensed spark between tungsten-steel electrodes 4 mm. apart. The spectrograms were recorded on Eastman No. 40 (8 by 10 in.) plates. The plate was examined visually with the aid of a magnifying glass, and the exposure on which the points of equal density became coincident was marked. The reading was checked by re-examining the image of the spectrogram projected on a lantern screen. It was found that no greater accuracy in reading was to be obtained by using a photoelectric densitometer. From the blue-color readings obtained with the Evelyn photoelectric colorimeter it was possible to determine the dilution of the original solution with which the matching density at 3280 Å would come on a plate covering density settings of the photometer from 0 to 0.15 by steps of 0.01. Thus the total duration of exposure of the oil to ultra-violet radiations was the same for each sample and was reduced to a minimum. The error in reading a single plate did not exceed 3%. After preparation of the solution of the oil the two estimations were carried out without delay.

The first determinations on cod-liver oil were made with a fresh sample of the "standard-of-reference oil" of the U.S. Pharmacopoeia. Saponification was carried by the procedure recommended by Wilkie (16) with the exception that petrol ether was used instead of ethyl ether. Less difficulty was experienced with the formation of emulsions when petrol ether was used to extract the unsaponifiable fraction. Occasionally a precipitate formed at the interface and prevented a complete separation of the two phases. This difficulty can be overcome by adding a few drops of 95% ethyl alcohol to the ether layer. Vaseline contains ingredients that absorb strongly at 3280 Å; consequently it should not be used to lubricate the stopcock of the separatory funnel. A paste of cane-sugar and glycerol was found to be a safe and efficient lubricant. The thoroughly washed ether extract was distilled *in vacuo* in an all-glass distilling apparatus that permitted the solvent (absolute-alcohol–cyclohexane mixture) being introduced through a side-arm before the vacuum was released. After examination of the contents of the flask in a good light to ascertain that all the residue was dissolved, the solution was transferred to a volumetric flask and made up to volume. Blue-value and *E*-value determinations were carried out in the same manner as with concentrates. The

following is a summary of the results of the determinations on the unsaponifiable fraction of the U.S.P. Reference Oil:—

I. *Blue value*
> (*a*) Nine determinations on solutions of different concentrations of the same unsaponifiable fraction.
> Range of galvanometer readings 15 to 69, 57.4 ± 0.48.
> (*b*) Four determinations on different samples of the oil, 55.9 ± 0.87.

II. *E value* (E 1%, 1 cm., 3280 Å)
> Eight determinations with different samples of the oil, 1.36 ± 0.0072.
> Ratio, blue value/E value = 41.1.

The results of the antimony trichloride test were actually calculated as the L value of the oil [See Dann and Evelyn (6)] and multiplied by 20 to give the blue value. It may be concluded from these results that the determinations can be carried out on different samples of the same oil with a high degree of precision. Our E value for the reference oil is virtually identical with the value 1.35 ± 0.0053 (10 observations) recently recorded by Barthen and Leonard (1).

Table I shows our results obtained with oils and concentrates, together with those of other workers which have been recalculated for purposes of comparison. It will be noted that our results, in contrast to the others, show no significant difference between the means of the ratios B.V./E for low

TABLE I

RESULTS OF SPECTROPHOTOMETRIC AND COLORIMETRIC DETERMINATIONS OF VITAMIN A
IN COD-LIVER OILS AND CONCENTRATES

	Nature and number of samples	Range of blue values	Ratio $\frac{B.V.}{E}$	
			Range	Mean
Cod-liver oils				
Crews and Cox	10	12 – 46	19 – 30	27.2 ± 1.26
Authors	16	22 – 70	34.4 – 42.3	39.4 ± 0.47
Concentrates				
Crews and Cox	32	530 – 80,000	39.0 – 66.7	51.6 ± 0.79
Authors	15	1002 – 7,150	39.2 – 41.4	40.5 ± 0.12
Haines and Drummond	5	600 – 3,440	52.0 – 55.7	53.2 ± 0.47
Cod-liver oils and concentrates				
Crews and Cox	42	12 – 80,000	19 – 66.7	45.8 ± 1.28
Authors	31	22 – 7,150	34.4 – 42.3	39.9 ± 0.25
Dann and Evelyn	39	—	—	48.8 ± 5.95

potency cod-liver oils as compared to concentrates. The absolute value of the mean, but not its probable error, depends on the factor employed to convert L values to blue values. However the average value of approximately 40 for the ratio B.V./E is very close to that obtained for pure vitamin A if its blue value is taken as 80,000 (3) and its E value as 2100 (10). The correlation between the results of the two methods as applied to concentrates is excellent, the average error of a single determination being only about $\pm 1\%$. It would appear, therefore, that the same entity is being measured quantitatively in both methods. To convert their L values to E values, Dann and Evelyn recommend multiplying by 0.41 $\pm$ 0.05. The factor obtained by us was 0.50 $\pm$ 0.01.

With cod-liver oils the relation is not quite so good, the average error of a single estimation being about $\pm 6\%$. An error of this magnitude indicates, however, a decided improvement in technique over that available to Crews and Cox, which gave an error of $\pm 19\%$.

With several oils, and with two in particular, a low value for the ratio B.V./E was first obtained when the saponification had been carried out by the British Pharmacopoeia procedure. The determinations were repeated with more thorough washing of the unsaponifiable fraction, the result being that the E value was now decidedly lower, whereas the blue value was not appreciably altered. With the two most refractory oils as many as 14 alternate washings with 15 ml. portions of $N/6$ potassium hydroxide and 100 ml. portions of water were required before the ratio B.V./E approximated that for concentrates.

The general conclusion is that vitamin A can be determined with equal accuracy either by photoelectric colorimetry or by ultra-violet spectrophotometry, the main source of error being inherent in the saponification process.

Part II. The Estimation of Vitamin A from Spectrophotometric Measurements before and after its Destruction by Irradiation

It is well known that a significant part of the total absorption by an oil is due to substances other than vitamin A. Even when the absorption due to unsaturated fatty acids is eliminated by employing the unsaponifiable fraction of the oil for the absorption measurement, the error due to foreign absorbents may still be considerable, particularly if the unsaponifiable fraction has not been adequately purified. The magnitude of the irrelevant absorption was pointed out by Macwalter (13) who found that approximately 40% of the absorption by a cod-liver oil was due to impurities which, unlike vitamin A, were not destroyed by oxidation for five hours at 100° C.

Obviously, quantitative estimation of vitamin A by absorption spectroscopy is possible only when the amount of the irrelevant absorption can be accurately determined. If the absorption by vitamin A could be eliminated without affecting the absorption by other substances, it would be possible to estimate the absorption due to vitamin A alone. The vitamin A content of an oil

could thus be determined directly without resort to saponification and the laborious and time-consuming purification of the unsaponifiable fraction. A simpler and more reliable measurement that would be free from the errors inherent in the saponification process would be obtained.

Several attempts have been made to make the spectrophotometric method more accurate by correcting for the irrelevant absorption. Notevarp (15) first suggested that it might be possible to destroy vitamin A quantitatively by intense irradiation of an alcoholic solution of the oil. He found oxidation and heating to be an uncertain method of removing vitamin A, and stated that when fat was present, an actual increase in absorption resulted from this treatment. In his experiments vitamin A was destroyed by irradiation with a 500 watt Orsam "Vitalux" lamp, the solution being placed about 4 cm. from the surface of the lamp for about six hours. No reference was made to the effect of this treatment on the other absorbing constituents of the oil. It was not shown that the residual absorption after irradiation was equivalent to the absorption by constituents of the oil other than vitamin A. The subject was to be treated in more detail at a later date.

More recently Chevallier (4) found that vitamin A could be accurately determined by dissolving the oil in alcohol, measuring the light absorption, irradiating with a mercury-vapor lamp fitted with a Wood's filter, again measuring the absorption, and multiplying by 3, the diminution of intensity of the absorption at 3280 Å. In support of the method it was stated that when a solution of pure vitamin A in ethyl alcohol had been subjected to intense irradiation the remaining absorption amounts to two-thirds of the initial absorption. The exact procedure used in irradiation and the details of the experiments were not given.

In our experience the destruction of vitamin A is a very slow process when alcohol is used as the solvent and when fat is present in the solution. It is well known that the vitamin is much less stable in chloroform solution (7), and for this reason alcohol or cyclohexane is now always used as the solvent for absorption measurements. It would appear therefore that the photo-chemical decomposition of vitamin A would be more rapid and complete if chloroform were used as the solvent.

Selective absorption of ultra-violet radiations is a characteristic property of unsaturated compounds and particularly of a molecule with a conjugated system of double bonds. Compounds of this nature that are present in liver oils are various phenanthrene derivatives, unsaturated fatty acids, carotene, and vitamin A. The unsaturated fatty acids and sterols show maximum absorption at wave-lengths less than 3000 Å; carotene, at 4500 Å. All these compounds, however, show a small end-absorption at 3280 Å. It should be possible to determine whether vitamin A alone is being oxidized, by following simultaneously the changes during irradiation in the absorption coefficient; in the blue color given by antimony trichloride; the iodine absorption value; and the carotene content of the oil. In the experiments described below, this has been done, a concentrate of the unsaponifiable material of a fish-liver

oil being used. It is shown that, under certain conditions of irradiation when a light-filter is employed that transmits ultra-violet rays of 3000 to 4000 Å only, vitamin A alone is oxidized to any significant extent, and that after the complete destruction of vitamin A the residual absorption does not exceed 10% of the original absorption. Some preliminary experiments on the destruction of vitamin A in cod-liver oils by irradiation are also discussed.

Experimental

Irradiation was carried out with a Hanovia quartz mercury-vapor arc, which was covered by a reflector and set horizontally at a height of 10 cm. above a small cylindrical tin can (6 by 6 cm.) in which was placed a 50 ml. beaker containing the solution to be irradiated. The can was covered with a Corning red-purple-ultra No. 597 light filter (8 by 8 cm.). This filter has a light transmission of 90% at 3650 Å and 30% at 3300 Å. It is not transparent below 3000 Å or above 4000 Å but transmits again in the region of 7200 Å. It has a high thermal coefficient of expansion and is easily broken by heat. Throughout the irradiation the filter was kept cool by means of a stream of running water. Strips of adhesive tape around the filter caused the water to drain off without wetting the interior of the can.

Solutions of vitamin A were prepared by weighing about 30 mg. of the concentrate into the beaker and dissolving in 5 ml. of anhydrous chloroform. The solutions were irradiated for varying lengths of time, the lamp current being maintained at 3.5 amp., 220 d.c. Each solution was finally transferred to a 25 ml. volumetric flask and made up to volume with chloroform. The following determinations were carried out, without delay, on aliquots of each solution.

1. *Extinction Coefficient.* A 5 ml. aliquot of the solution was evaporated *in vacuo* to dryness. The residue was taken up in absolute-ethyl-alcohol–cyclohexane mixture (90 : 10) and diluted to the required volume with this solvent. The value $E_{1\ cm.}^{1\ \%}$ at 3280 Å was determined by the procedure already described in Part I. The residue from 5 ml. of chloroform alone showed a small absorption at 3280 Å for which a correction was made.

2. *Antimony Trichloride Reaction.* The blue reaction and the colorimetric determination of the intensity of the blue color were carried out by the procedure of Dann and Evelyn (6). A 2 ml. aliquot of the solution was diluted to 10 ml. with chloroform, and 1 ml. of this solution was taken for the determination.

3. *Iodine Absorption.* The determination was made by the Hanus method, a 5 ml. aliqout of the solution, a 30 min. absorption period, and $N/50$ iodine and sodium thiosulphate solutions, being used.

4. *Carotene Content.* The yellow color of the solutions was assumed to be due entirely to carotene. Readings of the intensity of the yellow color were made with an Evelyn photoelectric colorimeter, and the carotene equivalent was obtained by reference to a calibration curve that had been previously prepared by use of standard solutions of β carotene.

Following the investigation of the effect of irradiating solutions of the concentrate, the procedure was applied to four cod-liver oils. In each determination 0.1 gm. of the oil was dissolved in 5 ml. of anhydrous chloroform and the solution irradiated for one hour in the manner described above. Determinations were made of the extinction coefficient of the oil at 3280 Å before and after irradiation and also on the non-saponifiable fraction of the oil. Measurements of blue-color reactions and iodine absorption were also made at varying intervals during the irradiation of one oil.

In Fig. 1 are plotted the absorption curves obtained before and after irradiation of the concentrate. The results of irradiation for two hours were virtually identical with those of 1½ hours' irradiation. It may be concluded, therefore, that after irradiation for one hour the absorption at 3280 Å had virtually reached a minimum value and underwent a further reduction of only about 3% after irradiation for an additional hour. Also shown in Fig. 1 is the curve obtained after subtraction from the value for the initial absorption the absorption due to carotene plus the residual absorption after 90 min. irradiation. This curve fits, extremely well, the curve obtained when the absorption curve of pure vitamin A, as given by Holmes and Corbet (10), is reduced to the same absorption maximum. The values for the absorption of carotene between 3000 and 4000 Å were calculated from the ultra-violet absorption

FIG. 1. *Effect of irradiation on the ultra-violet absorption of a concentrate of vitamin A.*

curve of carotene as given by Heierle (9). Prior to irradiation the carotene content of the solution was 0.76 mg., and after one hour irradiation it was reduced to 0.30 mg. per gm. of concentrate.

The results indicate that irradiating for one hour results in a complete destruction of vitamin A without affecting to any significant extent the other absorbing constituents with the exception of carotene. This is further substantiated by the results presented in Fig. 2 which show that the blue-color reaction of the concentrate is destroyed by irradiation for one hour and that, in general, during irradiation the changes in the blue value and absorption value parallel each other. A slight lag in the destruction of vitamin A during

the initial period of irradiation is observed. It will be noted further that, although the results given in Figs. 1 and 2 were obtained with the same concentrate, the absorption by the two solutions before irradiation is not the same. A period of several months intervened between the two experiments, and during this time the small amount of concentrate underwent considerable oxidation.
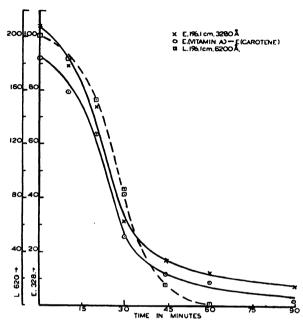
FIG. 2. *Effect of irradiation on the blue-color reaction (L value) and ultra-violet absorption (E value) of a concentrate of vitamin A.*

Though the iodine absorption value of the concentrate (Fig. 3) undoubtedly diminished most rapidly during the first hour of irradiation, when vitamin A was undergoing rapid photo-chemical oxidation, it still continued to decrease after a negative blue-color reaction was obtained. The decrease in iodine absorption due to the oxidation of carotene is not known, but it is believed to be negligible.

In Table II are summarized the results of the absorption measurements carried out with cod-liver oils before and after their irradiation. Those referred to as being obtained by a "modified photometry" were made with the irradiated solution in the tube on the variable-aperture side of the sector photometer (which ordinarily contains the solvent only) and a solution of the untreated oil in the tube on the fixed-aperture side of the photometer. This procedure was first introduced by De (7). The results obtained by this method, as is to be expected on theoretical grounds, are in good agreement with those obtained by taking the difference between two separate absorption

TABLE II

RESULTS OF EXTINCTION COEFFICIENT MEASUREMENTS ON COD-LIVER OILS BEFORE AND
AFTER ULTRA-VIOLET IRRADIATION

Sample No.		$E_{1\,cm.}^{1\,\%}$, 3280 Å				
		Before irradiation	After irradiation	By difference	By modified photometry	Unsaponifiable fraction
38–279		1.39	0.54	0.85	0.85	1.24
38–280		1.41	0.46	0.95	0.91	1.26
37–556		1.42	0.40	1.02	1.06	1.30
38–305	{ 3280	1.50	0.45	1.05	1.02	1.34
	{ 3198	1.59	0.45	1.14	—	—

measurements before and after irradiation. It will be noted further that these values are about 20 to 30% lower than those obtained by direct measurement on the unsaponifiable fraction. Sample No. 38/305 is the U.S.P. reference oil, which officially contains 3000 International Units of vitamin A. An E value of 1.02 would give a conversion factor of 2900 which, judged by present standards, would appear to be too high. During the one-hour irradiation no change in the iodine absorption number of the oil could be detected, the blue-color reaction was negative after 30 min. irradiation, and the extinction coefficient at 3280 Å had reached a minimum value after irradiation for one hour. If it is assumed that photochemical decomposition products of vitamin A are responsible for the residual absorption after irradiation of the concentrate for one hour (see Fig. 1), and if this correction of 8.5% is applied to the measurement with the reference oil,

FIG. 3. *Effect of irradiation on the iodine absorption by a concentrate of vitamin A.*

its E value (by difference) would now become 1.18, which is still 12% less than the value for the unsaponifiable fraction. From the results obtained with the concentrate it was expected that the E value (by difference) would have tended to be higher than that of the unsaponifiable fraction; no explanation is forthcoming for the fact that it is lower.

When absorption measurements are made directly with oils the head of the absorption band is usually displaced towards the shorter wave-lengths. This was found to be the case with all these oils; the reference oil, for example, showed maximum absorption at 3198 Å. Two values are recorded in Table II for the direct E value of the reference oil. It will be seen that

reading the plate at 3280 Å and not at the head of the absorption band gives a corrected E value of 1.05, which is in better agreement with the E value obtained by modified photometry. The plates obtained by modified photometry always showed the maximum absorption to be very close to 3280 Å.

Acknowledgments

The authors are indebted to Dr. A. S. Cook of the Ayerst, McKenna and Harrison Company, Montreal, for supplying the samples and for carrying out some of the blue-value determinations, and to Dr. D. K. Froman of the Department of Physics, Macdonald College, for many helpful suggestions.

References

1. BARTHEN, C. L. and LEONARD, C. S. J. Am. Pharm. Assoc. 26 : 515-524. 1937.
2. BLACK, A., GREENE, R. D., SASSAMAN, H. L., and SABO, C. J. Am. Pharm. Assoc. 27 : 199-205. 1938.
3. CARR, F. H. and JEWELL, W. Nature, 131 : 92. 1933.
4. CHEVALLIER, A. Z. Vitaminforsch. 7 : 10-16. 1938.
5. CREWS, S. K. and COX, S. J. Analyst, 59 : 85-90. 1934.
6. DANN, W. J. and EVELYN, K. A. Biochem. J. 32 : 1008-1017. 1938.
7. DE, N. K. Indian J. Med. Research, 24 : 737-749. 1937.
8. HAINES, R. T. M. and DRUMMOND, J. C. Brit. Med. J. I : 559-561. 1933.
9. HEIERLE, E. Ber. Schweizerischen botan. Ges. 44 : 18-87. 1935.
10. HOLMES, H. N. and CORBET, R. E. J. Am. Chem. Soc. 59 : 2042-2047. 1937.
11. HUME, E. M. and CHICK, H. Med. Research Council, Special Rept., Ser. No. 202, IV. 1935.
12. JOSEPHY, B. Acta Brevia Neerland. Physiol., Pharmacol., Microbiol. 3 : 133-135. 1933.
13. MACWALTER, R. J. Biochem. J. 28 : 472-475. 1934.
14. MORGAN, R. S., EDISBURY, J. R., and MORTON, R. A. Biochem. J. 29 : 1645-1660. 1935.
15. NOTEVARP, O. Biochem. J. 29 : 1227-1235. 1935.
16. WILKIE, J. B. J. Assoc. Official Agr. Chem. 20 : 206-208. 1937.

CALYCANTHINE

III. SOME DEGRADATION EXPERIMENTS[1]

BY LÉO MARION[2] AND RICHARD H. F. MANSKE[2]

Abstract

The identification of 4-carboline amongst the degradation products obtained by the action of selenium on calycanthine makes it possible to account for 12 of the 22 carbon atoms of calycanthine. The fusion of calycanthine with phthalic anhydride yielded 12 : 13-benzcanthin-11-one, which was also obtained from tryptamine and phthalic anhydride. On the basis of these observations a partial formula for calycanthine is suggested. The oxidation of calycanthine with mercuric acetate eliminated two hydrogen atoms, giving rise to a base which can be reduced again to calycanthine. Reduction of calycanthine with hydriodic acid and red phosphorus yielded quinoline, and methylation in the presence of air gave rise to oxygenated products containing three nitrogen atoms, and to methylamine. The phenylcarbamyl derivative of calycanthine has the same ultimate composition as, but differs from, that of N-methyltryptamine.

Calycanthine ($C_{22}H_{28}N_4$) is the main alkaloid present in the seeds of *Calycanthus floridus* L. The formation of benzoyl-N-methyltryptamine in the oxidative degradation of calycanthine (4) accounts for one-half of the molecule only. The authors have made numerous attempts to elucidate the molecule further, and some of these are now placed on record.

Dehydrogenation with selenium yielded two basic fragments. One of these, melting at 307° C.,* is also a product of the distillation of calycanthine with zinc dust. The analytical figures indicate the formula $C_{16}H_{10}N_2$ which probably includes the tryptamine portion of the calycanthine molecule plus six carbon atoms belonging to the remaining fragment. It gives a negative test with Ehrlich's reagent indicating that the α- and β-positions of the indole nucleus are substituted. Its further investigation has been left in abeyance pending the accumulation of a larger supply.

The second basic fragment obtained in the dehydrogenation, first isolated as the picrate, $C_{17}H_{11}O_7N_5$, m.p. 263° C., was eventually obtained as a well crystallized base, m.p. 186° C. Its solutions were fluorescent, and the analyses of both the base and its picrate indicated the formula $C_{11}H_8N_2$, which is that of a carboline. It has been identified as 4-carboline (I), and admixture of the picrate with that of synthetic 4-carboline failed to depress the melting point. If taken in conjunction with the production of benzoyl-N-methyltryptamine,

I.

II.

the isolation of 4-carboline as a dehydrogenation product supports the partial structure II, previously suggested by one of us (4), which accounts for 12 of the 22 carbon atoms of calycanthine.

The elimination of the N-methyl of the methylcarboline portion of the molecule, in reactions involving the dehydrogenation of the tetrahydropyridine ring, illustrated by the production of 4-carboline, also occurs in the fusion of calycanthine with phthalic anhydride which yielded a basic substance, $C_{18}H_{10}ON_2$, m.p. 227° C. (The action of organic acids in eliminating an N-methyl from a base is a reaction discovered by von Braun and Weissbach (1), who obtained impure and partly racemised *l*-nornicotine on heating *l*-nicotine with hydrocinnamic acid.) This substance ($C_{18}H_{10}ON_2$) gives a negative test with Ehrlich's reagent. From its ultimate composition and its mode of formation, the most probable structure seemed to be that of 12 : 13-benzcanthin-11-one (III), in which one mole of phthalic anhydride is involved. This compound (III) is named as a derivative of the hypothetical substance IV for which the generic name *canthine* is now proposed.

III. IV. V.

A substance probably having formula (III) has been synthesized from tryptamine and phthalic anhydride, and the synthetic product, m.p. 227° C., did not depress the melting point of the base obtained from calycanthine when mixed with it.

In the hope of preparing a base similar to (III), but without the benzene ring which base (III) owed to phthalic anhydride, tryptamine was fused with succinic anhydride. The product, $C_{14}H_{14}O_2N_2$, m.p. 172° C., however, contained two atoms of oxygen and reacted positively with Ehrlich's reagent, so that the α- or β-position of the pyrrole nucleus in the product must be free or potentially so. Furthermore, the product behaved as a phenolic base and the two methylene groups originally attached to the indole nucleus in tryptamine have not been dehydrogenated. It is, possibly, 3,4,5,6,12,13-hexahydro-3-hydroxycanthin-11-one (V).

The reduction of calycanthine with hydriodic acid and red phosphorus yields quinoline. It is doubtful, however, whether this grouping exists as such in calycanthine, and its formation is possibly due to a rearrangement.

When calycanthine is oxidized with mercuric acetate according to the method of Gadamer (2), two hydrogen atoms are eliminated. This gives rise to a new base which forms an amorphous picrate. The base is easily converted back to calycanthine by reduction. The readiness with which

calycanthine is oxidized may explain the formation, on methylation, of products containing oxygen. Späth and Stroh (7) have methylated calycanthine in an evacuated tube and obtained a methiodide, $C_{22}H_{26}N_4(CH_3)_2 . 2CH_3I$. Gordin (3), however, had found that if the methylation was conducted in the presence of air, one nitrogen atom was lost, and the product contained oxygen. It is not considered proved that the entry of oxygen into the molecule is due to the oxidation of calycanthine or of a derivative by atmospheric oxygen. The results obtained by the authors confirm those of Gordin, and the methylation of calycanthine gave rise to oxygenated derivatives containing three atoms of nitrogen only. With methyl iodide as methylating agent, products were obtained containing one, two, and three atoms of oxygen. The nitrogen atom which is lost during methylation is eliminated in the form of methylamine, which has been isolated from the mother liquors as the chloroplatinate.

Calycanthine forms a phenylcarbamyl derivative, $C_{36}H_{38}O_2N_6$, m.p. 252° C., which corresponds to one mole of calycanthine and two moles of phenylisocyanate. The phenylcarbamyl derivative of N-methyltryptamine, $C_{18}H_{19}ON_3$, which has the same ultimate composition as, but is not identical with, the calycanthine derivative, melts at 153° C. (5). Both derivatives, however, yield an orange color in Ehrlich's test.

Experimental

Dehydrogenation with Selenium

Anhydrous calycanthine (5.7 gm.) was heated in a metal bath with 5.7 gm. of selenium, in a stream of nitrogen. The temperature was gradually brought up to 300° C., where it was kept for one-half hour. The flask and the melt, which had set to a hard resin, were crushed together in a mortar and extracted in a Soxhlet with petroleum ether and with ether. Both extracts yielded a base which, after recrystallization from methanol, melted at 306 to 307° C. This base, owing to the small quantity obtained, may be still slightly impure. Calcd. for $C_{16}H_{10}N_2$: C, 83.3; H, 4.34; N, 12.16%. Found: C, 82.52, 82.55; H, 4.62, 4.45; N, 12.20, 12.07%. The combined mother liquors from the crystallization of the latter base were treated with picric acid. From the mixed product, fractional crystallization yielded a picrate, m.p. 263° C., as fine yellow needles. Calcd. for $C_{17}H_{11}O_7N_5$: C, 51.4; H, 2.77; N, 17.65%. Found: C, 51.50, 51.46; H, 3.02, 2.99; N, 16.22, 16.26%. When this substance was mixed with the picrate of 4-carboline (m.p. 264° C.) the melting point was not depressed. The base liberated from the picrate was crystallized from absolute ether, from which it separated as short, colorless needles, m.p. 186° C. Calcd. for $C_{11}H_8N_2$: C, 78.57; H, 4.76; N, 16.66%. Found: C, 78.66; H, 5.11; N, 16.53%.

Zinc Dust Distillation

A mixture of calycanthine and zinc dust was heated, ultimately to dull redness in a tube through which a stream of hydrogen was being passed. The distillate contained indoles in abundance together with a small amount of

crystalline material. The latter was washed with cold ethanol and recrystallized once from a large volume of the same solvent. It then consisted of fine almost colorless needles which melt at 305 to 306° C. In admixture with the substance prepared by the selenium dehydrogenation there was no depression in melting point.

Synthesis of 4-Carboline

3,4,5,6-Tetrahydro-4-carboline was prepared from tryptamine as described by Späth and Lederer (6) and dehydrogenated by heating with selenium at 300° C. for one-half hour in a stream of nitrogen. The base was extracted with ether and crystallized from the same solvent. It was then sublimed at 200° (2 mm.), and converted to the picrate which was recrystallized from methanol, m.p. 264° C.

Reduction of Calycanthine

A mixture of calycanthine (6 gm.), red phosphorus (6 gm.), and 50% hydriodic acid (45 cc.) was refluxed gently for 90 hr. and evaporated to about one-third of its volume. This was filtered, the filtrate basified, and the precipitated base collected on a filter, and dried. Distillation of this base at 200 to 260° C. (1 mm.), yielded an oil which appeared to be a mixture. It was distilled in steam and the distillate, on treatment with picric acid, yielded a picrate melting at 202 to 203° C. before and after admixture with an authentic specimen of quinoline picrate.

Oxidation of Calycanthine

To a solution of 0.3192 gm. of calycanthine in 1.5 cc. of glacial acetic acid was added 2 gm. of mercuric acetate dissolved in 15 cc. of water containing a few drops of acetic acid, according to the method of Gadamer (2). The solution was allowed to stand at room temperature for 40 hr. during which a precipitate of short needles separated. Water was added, and the mixture warmed on the steam-bath for 20 min. and allowed to stand at room temperature a further 22 hr. The precipitated mercurous acetate was filtered on a tared alundum crucible, washed with a little water, dried at 105° C., and weighed: 0.4545 gm. The elimination of two hydrogen atoms corresponds to 0.4761 gm. of mercurous acetate. Yield, 95.4%. The filtrate was acidified with hydrochloric acid and the mercury removed with hydrogen sulphide. The base recovered was oily and could not be crystallized. It yielded an amorphous picrate melting indefinitely between 105° and 135° C. All attempts to crystallize this picrate have been unsuccessful. Calycanthine picrate crystallizes from methanol in fine, silky needles, m.p. 186 to 187° C. The oxidized base is readily converted back to calycanthine by reduction with zinc and acetic acid.

Treatment of Calycanthine with Phthalic Anhydride

A mixture of calycanthine (1 gm.) and phthalic anhydride (10 gm.) was heated in an oil bath for four hours at 200° C. and five hours at 225 to 230°. After cooling, the melt was repeatedly digested with boiling water containing some hydrochloric acid. From the combined and filtered acid extracts a

base was isolated which, after several recrystallizations from acetone-methanol, was obtained as slender colorless needles, m.p. 227° C. Wt. 0.043 gm. Calcd. for $C_{18}H_{10}ON_2$: C, 80.0; H, 3.74; N, 10.37%. Found: C, 79.56, 79.41; H, 3.69, 3.79; N, 10.67, 10.60%.

Synthesis of 12 : 13-benzcanthin-11-one

A mixture of tryptamine (4 gm.) and phthalic anhydride (11 gm.) was heated in an oil bath, four hours at 200° C. and five hours at 230° C. The product was worked up as in the above case. It yielded a relatively large quantity of a neutral product, m.p. 165° C., identified by melting point and mixed melting point as 3-(β-phthalimido-ethyl)-indole, and 0.029 gm. of a base which separated from acetone-methanol as fine, soft needles, m.p. 227 to 228°. Calcd. for $C_{18}H_{10}ON_2$: N, 10.37%; found: N, 10.51%. A mixture of this substance with the base obtained from calycanthine and phthalic anhydride melted at 227 to 228° C.

Treatment of Tryptamine with Succinic Anhydride

Tryptamine (4 gm.) and succinic anhydride (10 gm.) were heated together in an oil bath for four hours at 200° C. and five hours at 225 to 230°. The cooled melt was digested with cold dilute hydrochloric acid and the acid extract basified with ammonia. When potassium hydroxide is used instead of ammonia, the precipitated base redissolves in the basic solution. The basic product (0.142 gm.), crystallized several times from acetone-methanol, was obtained as fine, colorless needles, m.p. 172° C. Calcd. for $C_{14}H_{14}O_2N_2$: C, 69.42; H, 5.78; N, 11.57%. Found: C, 69.39; 69.32; H, 5.99, 5.98; N, 11.46, 11.34%.

Reaction of Calycanthine with Phenylisocyanate

The phenylcarbamyl derivative of calycanthine was obtained by heating the base in chloroform with phenylisocyanate and evaporating to dryness. The residue was digested repeatedly with cold dilute hydrochloric acid and the combined acid extracts were basified. The filtered and dried basic product separated from chloroform-methanol as colorless prisms, m.p. 252° C. Calcd. for $C_{36}H_{38}O_2N_6$: C, 73.72; H, 6.49; N, 14.34%. Found: C, 73.65, 73.67; H, 6.46, 6.27; N, 14.30, 14.25%.

Methylation of Calycanthine

The products obtained in the methylation of calycanthine were difficult to isolate and purify. Although the samples analyzed have been purified as carefully as possible it is not certain that they were entirely homogeneous. The analyses are reported below simply to show the constancy of the presence of oxygen and the loss of one nitrogen atom in all the methylated products. A solution of anhydrous calycanthine in chloroform when treated with methyl iodide gradually deposits a crystalline product which can be separated by difference in solubility in methanol into a methiodide, m.p. 249° C., and a second product, m.p. 235 to 237° C., also containing iodine. The latter gave the following analytical figures. Calcd. for $C_{26}H_{32}ON_3I$: C, 58.95; H, 6.02;

N, 7.94; I, 24.00%. Found: C, 55.47, 55.57; H, 6.01, 6.11; N, 7.97, 7.84; I, 22.77%. When hydrolyzed with aqueous-methanolic potassium hydroxide it gave rise to a compound soluble in chloroform and crystallizable from chloroform-methanol as small, white, lustrous plates, m.p. 216 to 218° C. (calcd. for $C_{26}H_{34}O_3N_3I$: C, 55.2; H, 6.02; N, 7.44; I, 22.5%—found: C, 55.47, 55.57; H, 6.01, 6.11; N, 7.97, 7.84; I, 22.77%), and a second compound, m.p. 243° C., insoluble in chloroform. This was crystallized from methanol. Calcd. for $C_{26}H_{34}O_2N_3I$: C, 57.05; H, 6.22; N, 7.68; I, 23.20%. Found: C, 55.20, 55.34; H, 6.26, 6.15; N, 7.44, 7.43; I, 24.46%.

The collected mother liquors from the methylated calycanthine were mixed with methanolic potassium hydroxide and distilled. The distillate was collected in dilute hydrochloric acid, and evaporated on the steam bath in a stream of air. It left a crystalline residue which was recrystallized from methanol-acetone and then converted into a chloroplatinate, m.p. 223 to 225° C. A mixture of this substance with methylamine chloroplatinate (m.p. 225 to 227° C.) melted at 227° C. Calcd. for $CH_3 . NH_2 . H_2PtCl_6$: Pt, 41.3%. Found: Pt, 40.4%.

When calycanthine is methylated with dimethyl sulphate in the presence of potassium carbonate, a methylated base is obtained which melts at 219° C. Calcd. for $C_{25}H_{35}O_5N_3S$: C, 61.33; H, 7.16; N, 8.58; S, 6.54%. Found: C, 60.72, 61.00; H, 6.88, 6.75; N, 8.54, 8.34; S, 6.52%. This base is not precipitated by potassium hydroxide from its solution in dilute acid. If, however, this solution is heated with ammonium chloride a base containing no sulphur is precipitated. Crystallized from absolute alcohol and from acetone-ether, as clusters of prismatic needles, it melted at 214 to 216° C., after sintering somewhat at 205° C. Calcd. for $C_{24}H_{32}O_5N_3$: C, 64.9; H, 7.44; N, 9.47%. Found: C, 63.94, 63.85; H, 7.09, 7.02; N, 9.42, 9.65%.

References

1. BRAUN J. v. and WEISSBACH, K. Ber. 63 : 2018-2026. 1930.
2. GADAMER, J. Arch. Pharm. 253 : 274-289. 1915.
3. GORDIN, H. M. J. Am. Chem. Soc. 33 : 1626-1632. 1911.
4. MANSKE, R. H. F. Can. J. Research, 4 : 275-282. 1931.
5. MANSKE, R. H. F. Can. J. Research, 5 : 592-600. 1931.
6. SPÄTH, E. and LEDERER, E. Ber. 63 : 2102-2111. 1930.
7. SPÄTH, E. and STROH, W. Ber. 58 : 2131-2132. 1925.

THE ALKALOIDS OF FUMARIACEOUS PLANTS

XVIII. *FUMARIA OFFICINALIS* L.[1]

By Richard H. F. Manske[2]

Abstract

An examination of *Fumaria officinalis* has disclosed the presence of seven alkaloids. Of these, only protopine (0.05%) had been previously reported. In this plant other known alkaloids are *dl*-tetrahydro-coptisine (2.5 p.p.m.), cryptocavine (20 p.p.m.), aurotensine (0.4 p.p.m.), and possibly sinactine (22 p.p.m.) which, however, was not conclusively identified and is referred to as alkaloid F36. The remaining two alkaloids are apparently new; F37 (26 p.p.m.), $C_{21}H_{23}O_5N$, is non-phenolic and contains two methoxyl groups; F38 (3 p.p.m.) $C_{20}H_{19}O_6N$, is phenolic and is probably a phthalide isoquinoline alkaloid. A neutral substance, $C_{11}H_{16}O_3$, was also isolated.

Attention is directed to the significance of alkaloid structure in an evolutionary series of plants, and some preliminary generalizations are adumbrated.

If the nature of the chemical constituents of plants, and here reference is restricted to alkaloids, is a criterion of relationship, the inclusion of Fumariaceae as a sub-family in Papaveraceae is amply justified. Protopine has been isolated from no fewer than 35 species inclusive of 14 genera, but only from plants in the Papaveraceae family (11). No other alkaloid is known to have such a wide distribution, and there is ample ground for the belief that it will be found in most of the genera in this family. In fact, its complete absence in a particular species would call for more than passing comment. Other alkaloids, but noticeably cryptopine, allocryptopine, glaucine, and the proto-berberine bases, are known to occur in several genera, and even in related families. Furthermore, virtually all the Papaveraceous alkaloids can be regarded as derivatives of benzyl-isoquinoline. Such a relation cannot be regarded as fortuitous and definitely suggests a common origin for all members of the Family.

On the basis of the morphology and anatomy of the vegetative organs, Leger (3) concluded that the genus *Fumaria* is phylogenetically the oldest and *Papaver* the most recent. His classification is shown schematically on the following page.
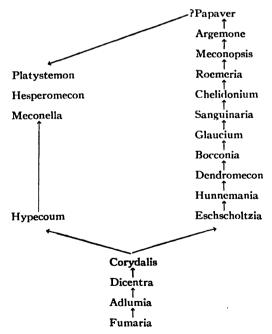
On the other hand, Fedde (1) regards the sub-family Fumarioideae as the most recent. Although the order suggested by Leger is retained, the temporal sequence is reversed. On this basis the genus *Fumaria* is to be regarded as the most recent. Such a hypothesis is consistent with the fact that no species of *Fumaria* is native to America. On this continent the endemic genus *Adlumia* was presumably evolved from *Dicentra* or a common ancestor. In Asia the corresponding scandent genus is *Dactylicapnos*.

The hypothesis that progress in evolution is accompanied by an increased complexity of chemical constituents has been suggested at various times, and McNair (10) has applied such a criterion in an attempt to place the

Angiosperms in an evolutionary sequence with reference to alkaloids. In the author's opinion it is questionable whether an acceptable criterion of complexity can be formulated. McNair suggested the average molecular weight as such a criterion, although obvious disadvantages are at once apparent. It seems more probable that taxonomic similarities and differences will be reflected in the chemical constitution of the contained alkaloids. The possibilities of testing this hypothesis by means of data accumulated in studies of the alkaloids of Fumariaceous plants, reported in this series of papers, have been kept in mind, and it now seems advisable to mention some of the conclusions which may be drawn. Dicentrine, glaucine, and glaucentrine are found together only in the Eucapnos section of *Dicentra*, namely in *D. eximia*, *D. formosa*, and *D. oregana* (5, 9). In *Corydalis* the protoberberine alkaloids are widely distributed. They are rarer in *Dicentra* and virtually absent in *Papaver*. Bicuculline and corlumine appear to be more specific and their limited occurrence may well form the basis for a reclassification. Nevertheless no satisfactory chemical criteria are available as yet which would serve to indicate the progress of evolution in Papaveraceae. Many more data are necessary and the examination of some species of *Fumaria* was deemed essential.

Fumaria officinalis L., with which the present paper deals, is the common fumitory of European origin, although it is now widely distributed in temperate regions. It is the type species of a genus which includes some fifty species and numerous varieties. They are native to northwestern and Central

Europe, to the region from the Mediterranean to the extra-tropical Himalaya, and to Western and Central Asia.

The plant was examined chemically shortly after the recognition of organic bases as a class of natural compounds. A number of authors have isolated an alkaloid (fumarine) which Schmidt (11) proved to be identical with protopine, although it is now doubtful whether this alkaloid was obtained in a state of purity from the plant in question.

The present investigation has disclosed that protopine, while definitely present, constitutes only a portion of the total alkaloid content, which in any case is less than 0.2%. No fewer than six other alkaloids have been isolated, and, of these, three may be new. Cryptocavine (9) and aurotensine (9) were obtained in small amounts and compared with authentic specimens from previous sources. A third alkaloid almost certainly is *dl*-tetrahydro-coptisine. Analytical data, color reactions, and the lack of optical activity are in agreement with this supposition, although direct comparison with an authentic specimen has not been made. The same alkaloid has alsô been isolated from *Corydalis cheilanthifolia*.

Closely associated with the *dl*-tetrahydro-coptisine is an alkaloid which resembles sinactine. Analytical data are in fair agreement with the formula $C_{20}H_{21}O_4N$ and two methoxyl groups are indicated. It melts at 177° C.* as does sinactine, but the optical rotation of $-78.9°$ is not comparable to a value of about 300° for the latter. In view of the frequent occurrence of racemic alkaloids in the tetrahydro-protoberberine group the alkaloid in question may represent a largely racemized specimen of sinactine. Nevertheless, reduction of the quaternary iodide, formed by oxidation with iodine in ethanol, yielded a base that melted at 163° C., and repeated recrystallization did not alter this value. Späth and Mosettig (12) state that *dl*-sinactine melts at 171° C., presumably uncorrected. An observation that is relevant here, and which may ultimately have more significance, is that the phenolic alkaloid F13 (9) first isolated from *Corydalis scouleri* (6) and later from *C. sibirica* (7) on methylation with diazomethane yields a base identical with this alkaloid. In fact the necessary formula, $C_{19}H_{19}O_4N$, is in better agreement with the analytical figures than the formulae ($C_{16}H_{17}O_3N$ and $C_{17(18)}H_{19}O_4N$) previously considered. Since, therefore, the base has not been definitely identified, it will be provisionally referred to as alkaloid F36.

The remaining two alkaloids appear to be new. F37, melting at 177° C., yields analytical figures in fair agreement with $C_{21}H_{23}O_5N$ containing two methoxyl groups. This formùla is homologous with that for cryptocavine. The latter is optically inactive and the remote possibility that it is the racemic form of F37 has been considered, although the color reactions are not identical. Cryptocavine is undoubtedly of the protopine type. In the case of corycavamine racemization is effected by heating with acetic anhydride. Alkaloid F37, however, did not yield cryptocavine under these conditions.

* *All melting points are corrected.*

Alkaloid F38, melting at 255° C., is phenolic, contains one methoxyl group, and is best represented by $C_{20}H_{19}O_6N$. This formula is isomeric with that of corlumidine (6). On methylation it may be expected to yield either corlumine or adlumine, but owing to the small amount available this possibility has not been tested experimentally.

Experimental

A preliminary investigation of *F. officinalis* was carried out with 2.4 kg. of material collected in Switzerland. This was made available to the author by Dr. Richard Ruedy of these laboratories, to whom thanks are due. The main lot of material was obtained from the New York Chemical Corporation, New York. It weighed 49 kg. Cryptocavine, aurotensine, and alkaloid F38 were not isolated from the smaller lot, although there is no reason to assume that they were absent. In any case they were found only in traces in the main lot and their isolation in a pure form is tedious. The following account refers only to the 49 kg. of material. The procedure detailed in an earlier communication (4) has been followed and the same designations of the various fractions are employed. The results are summarized in the following outline:

Base hydrochlorides extracted from aqueous solution by means of chloroform—

BC —Non-phenolic bases, —*dl*-tetrahydro-coptisine, F36, F37.·
EC —Phenolic bases extracted from alkaline solution by means of ether,—F37 (in part).
BCE—Phenolic bases precipitated by carbon dioxide,—uncrystallized.

Base hydrochlorides not extracted from aqueous solution by means of chloroform—

BS —Non-phenolic bases,—protopine, cryptocavine.
BSE—Phenolic bases precipitated by carbon dioxide,—aurotensine, F38.
EES—Phenolic bases extracted from the bicarbonate solution by means of ether,—aurotensine, F38.

dl-Tetrahydro-coptisine and Alkaloid F36

·The non-phenolic fraction (BC) was dissolved in hot dilute hydrochloric acid and filtered. On cooling, a crop of pale yellow, fine needles separated. This, on recrystallization from much hot water was almost colorless and after drying melted at 252 to 253°C., with only slight previous sintering or darkening. Goto and Kitasato (2) record the melting point of sinactine hydrochloride as 272° C. In this property, therefore, the differences are also appreciable. The free base was regenerated by shaking an aqueous suspension of the hydrochloride with ammonia and ether, and washing the resultant ether extract. Removal of the solvent from the latter yielded a crystalline residue which was washed with cold methanol and then recrystallized from chloroform-methanol. As thus obtained *alkaloid F36* consists of well developed, stout, colorless prisms and melts sharply at 177° C. The yield was about 1.1 gm. (22 p.p.m.). Further recrystallization did not raise the melting point. With Gaebel's reagent it gives a positive test for the methylenedioxy group. $[\alpha]_D^{23°} = -78.9°$ ($c = 0.4$ in chloroform). Found:. C, 70.25, 70.40; H,

6.21, 6.44; N, 4.87; 4.99; OMe, 18.86, 18.54%.   Calcd. for $C_{20}H_{21}O_4N$; C, 70.80; H, 6.20; N, 4.38; OMe, 18.20%.

A small portion of the alkaloid, dissolved in boiling ethanol containing some potassium acetate, was treated with iodine until the color due to the latter was permanent.   Some water was added and the ethanol boiled off.   The dark brown iodide as thus obtained was washed with cold water and its brown solution in hot glacial acetic acid was treated with zinc dust until it was colorless.   The base was regenerated from the filtered solution by means of ammonia and extracted with ether.   Evaporation of the extract yielded an almost colorless resin which readily crystallized in contact with methanol. It melted at 163° C. and this value was not changed after three further recrystallizations from methanol.   Determination of the melting point in an evacuated tube gave the same value.

The mother liquor from which the hydrochloride of alkaloid F36 had been crystallized was basified with ammonia, and the liberated bases were extracted with a large volume of ether.   Evaporation of the extract yielded a resinous residue, which crystallized in contact with methanol.   The base was dissolved in chloroform and the solution evaporated to a thin syrup.   The addition of methanol yielded fine silky needles which melted at 217° C.   When recrystallized again in the same manner the *dl-tetrahydro-coptisine* melted at 222 to 223° C. and yielded with sulphuric acid a colorless solution which, on heating, only turned brown.   The optical activity in chloroform ($c = 0.4$) was −5.5° for the crude base and virtually zero for the purified specimen.   The total amount obtained including that recovered from the mother liquor was 0.12 gm. (2.5 p.p.m.).   Found: C, 70.20, 70.31; H, 5.31, 5.37; N, 4.64, 4.53%; OMe, negative.   Calcd. for $C_{19}H_{17}O_4N$: C, 70.59; H, 5.26; N, 4.33%.

Alkaloid F37

A small amount of this alkaloid was obtained from the mother liquors from which *dl*-tetrahydro-coptisine and alkaloid F36 had been obtained.   The greater portion remained in the alkaline filtrate from fraction BC and was obtained from this by ether extraction (fraction EC).   It is, however, not phenolic.   The residue from the latter, after the removal of the ether, crystallized readily from methanol in which it is moderately soluble.   It was obtained in colorless, well defined prisms which melt sharply at 177° C.   Dissolved in cold sulphuric acid, it gradually developed a blue color.   Gentle heating of the solution greatly intensified the blue color and further heating produces a transient pink which changes to dirty olive.   The yield was 1.3 gm. (26 p.p.m.). Found: C, 68.06, 68.32; H, 6.27, 6.23; N, 4.45, 3.72; OMe, 16.62; 16.06%. Calcd. for $C_{21}H_{23}O_5N$: C, 68.29; H, 6.23; N, 3.79; 2OMe, 16.80%.

Protopine

The isolation of protopine from the fraction (BS) has been repeatedly described.   It is therefore considered unnecessary to give details except to state that in this case it was purified as the hydrochloride.   The base, liberated from the salt and recrystallized, melted at 210° C. and admixture with an

authentic specimen did not lower the melting point. The yield was 24 gm. (0.05%).

Cryptocavine

The mother liquor from the protopine hydrochloride was basified with potassium hydroxide, and the regenerated bases were converted to hydrobromides in dry methanol. A mixture of salts separated. This was extracted with hot methanol until only the protopine salt remained. The combined extract was evaporated somewhat and on cooling deposited another small crop of protopine hydrobromide. Further evaporation and cooling of the filtrate yielded the not quite pure hydrobromide of *cryptocavine*. It was recrystallized from hot water, from which it first separates as a gelatinous mass which, on gentle warming, changes to a mass of fine needles. The free base regenerated from the hydrobromide was recrystallized from chloroform-methanol. Colorless stout prisms melting sharply at 223° C. were thus obtained. Dissolved in a drop of acetic acid, it yields on the addition of sulphuric acid, a pink solution which gradually becomes blue. Admixture with cryptopine or with corycavine lowered the melting point at least 20° C. However, in admixture with a specimen of cryptocavine from *Corydalis ochotensis* (8) there was no depression in melting point. The alkaloid is optically inactive in chloroform solution ($c = 0.4$). The yield was 1.0 gm. (20 p.p.m.). Found: C, 68.17, 68.38; H, 6.43, 6.57; N, 3.85, 3.90; OMe, 17.37, 16.88, 15.32%. Calcd. for $C_{21}H_{23}O_5N$: C, 68.29; H, 6.23; N, 3.79; 2OMe, 16.80%. Calcd. for $C_{22}H_{25}O_5N$: C, 68.93; H, 6.53; N, 3.66; 2OMe, 16.19%.

Alkaloid F38

The fraction (EES) in contact with methanol deposited a sparingly soluble base. This was dissolved in boiling chloroform of which about 800 cc. was necessary. The filtered solution (charcoal) was evaporated to a small volume and crystallization brought to completion by the addition of methanol. The base then melted not quite sharply at 255° C. It was redissolved in hot dioxane in which it is moderately soluble, and the filtered solution evaporated somewhat. The addition of hot methanol induced rapid crystallization of colorless, fine, stout prisms, which melted to a dark tar at 256° C., some shrinking taking place at 240 to 245° C. The yield was about 0.15 gm. (3 p.p.m.). Found: C, 64.46, 64.41; H, 5.38, 5.28; N, 3.88, 3.81; OMe, 8.99, 8.87%. Calcd. for $C_{20}H_{19}O_6N$; C, 65.04; H, 5.15; N, 3.79; 1OMe, 8.40%.

Aurotensine

The mother liquors from which alkaloid F38 had been isolated as well as fraction (BSE) were separately neutralized with hydrogen chloride in small volumes of methanol. Dry ethyl acetate was added until the incipient turbidity just disappeared on mixing. In both cases a small yield of a mixture of hydrochlorides was obtained. They were combined and dissolved in hot water. The rapidly cooled solution was basified with ammonia and extracted with ether. The residue from the ether extract was a mixture. It was

extracted with hot methanol, which left a residue of alkaloid F38 weighing about 20 mg. The methanol extract was evaporated to a small volume and cooled. A mixture of colorless prisms and pink plates separated. The former consisted of F38 and remained undissolved on gentle heating, whereas the pink plates dissolved and recrystallized from the filtered solution. As thus obtained, the bases melted at 128° C. The base was redissolved in hot methanol and the solution evaporated to a small volume. Crystallization was immediately induced by seeding with a crystal of aurotensine and the crystals thus obtained consisted of pale pink, well developed rhombic plates melting at 128° C. Admixture with an authentic specimen of aurotensine did not lower the melting point. The yield was 20 mg. (0.4 p.p.m.).

Isolation of a Neutral Substance

The fraction (LC) consisted largely of fumaric acid. This was removed by washing the ether solution with aqueous sodium bicarbonate. The dried ether solution was evaporated to a small volume. The residual pale yellow oil deposited a small amount of crystalline material in the course of several days. Adhering oil was largely removed by pressing between layers of filter paper. The crystalline material was recrystallized four times from hot benzene, in which it is moderately soluble. Colorless stout prisms melting sharply at 152° C. were thus obtained. This substance is sparingly soluble in cold benzene and virtually insoluble in hexane. It is insoluble in water but dissolves in hot aqueous potassium hydroxide. Found: C, 67.50, 67.50; H, 8.29, 8.19%. Calcd. for $C_{11}H_{16}O_3$: C, 67.35; H, 8.16%. Methoxyl is absent.

References

1. FEDDE, F. Die Natürlichen Pflanzenfamilien, Engler-Prantl. Wilhelm Engelmann, Leipzig. 1936.
2. GOTO, K. and KITASATO, Z. J. Chem. Soc. 1234-1237. 1930.
3. LEGER. Mem. Soc. Linn. Normandie, 18 : 195-623. 1894–1895.
4. MANSKE, R. H. F. Can. J. Research, 8 : 210-216. 1933.
5. MANSKE, R. H. F. Can. J. Research, 10 : 765-770. 1934.
6. MANSKE, R. H. F. Can. J. Research, B, 14 : 347-353. 1936.
7. MANSKE, R. H. F. Can. J. Research, B, 14 : 354-359. 1936.
8. MANSKE, R. H. F. Can. J. Research, B, 15 : 274-277. 1937.
9. MANSKE, R. H. F. Can. J. Research, B, 16 : 81-90. 1938.
10. McNAIR, J. B. Bull. Torrey Botan. Club, 62 : 515-532. 1935.
11. SCHMIDT, E. Arch. Pharm. 239 : 395-408. 1901.
12. SPÄTH, E. and MOSETTIG, E. Ber. 64 : 2048-2050. 1931.

LOBINALINE, AN ALKALOID FROM *LOBELIA CARDINALIS* L.[1]

By Richard H. F. Manske[2]

Abstract

Lobelia cardinalis L. was found to contain essentially only one alkaloid, which has been named *lobinaline*. Its empirical formula probably is $C_{28}H_{38}ON_2$, and this bears no obvious relation to the alkaloids of *L. inflata*. It does, however, yield benzoic acid on oxidation with alkaline permanganate, but only one mono-substituted benzene nucleus is present. Lobinaline mono-hydrochloride is virtually insoluble in cold water but dissolves readily in dilute acids.

The chemical constituents of closely related plant species within a genus frequently display striking similarities. Occasionally an alkaloid is a constituent of all species within a family. More frequently closely related alkaloids are widely distributed in a family, but it is becoming increasingly evident that specific differences are generally accompanied by definite differences in the elaborated alkaloids. Examples are too numerous to quote in detail but such genera as *Lupinus*, *Aconitum*, and *Senecio* may serve as examples, in each of which the alkaloids of different species display an obvious similarity but, as a rule, not complete identity. *Lobelia cardinalis* L., the chemistry of which forms the subject of this paper, contains an alkaloid which bears no obvious relation to the many alkaloids of *L. inflata* L. All of the latter are derivatives of piperidine and contain only one nitrogen atom (2, 3, 4, 5, 6). The main, and perhaps only, alkaloid from *L. cardinalis*, for which the name *lobinaline* is now proposed, contains two nitrogen atoms. Furthermore, it cannot be formed by the condensation of two molecules of an alkaloid from *L. inflata*. The empirical formula, $C_{28}H_{38}ON_2$, is not consonant with such a hypothesis. Nevertheless, there appears to be one point of similarity, and that is in the occurrence of a C-benzoyl group (or the corresponding carbinol) in both types of alkaloids, one such group being present in lobinaline.* It has not been possible to prepare an oxime, although the presence of a ketonic oxygen is still assumed in view of the fact that oxidation with chromic acid results only in deep seated changes. Oxidation with potassium permanganate yields benzoic acid in amount insufficient for the presence of two mono-substituted benzene nuclei.

Further than this, no insight into the constitution of the alkaloid has been obtained. Nevertheless, the properties of the mono-hydrochloride are unique

* *In a recent study of Eastern North American species of Lobelia, Rogers McVaugh (Rhodora, 38 : 241-263. 1936) has concluded that L. cardinalis has probably existed unchanged since Tertiary times. The same may be said for L. siphilitica which is the closest relative to L. cardinalis. A preliminary examination of the former has shown that lobinaline, however, is definitely absent. One point of similarity of the two species was found in the occurrence of a mixture of resinols, α- and β-viscol, in both plants. Whether or not these substances are characteristic of the genus, remains to be determined. L. inflata is regarded as of more recent origin with no certain affinities, but obviously only very distantly related to L. cardinalis.*

and point to a profound difference between the nature of the two nitrogen atoms. The salt is virtually insoluble in water and its suspension in boiling water yields the insoluble base and the soluble dihydrochloride. The free base, lobinaline, was obtained in crystalline condition only after three to four years of intermittent work and the dihydrochloride has not yet been crystallized.

Dr. Klaus Unna of the Merck Institute of Therapeutic Research, Rahway, N.J., has kindly undertaken to study the pharmacology of lobinaline, and the author takes this opportunity to acknowledge his indebtedness.

The following summary of his findings was submitted by Dr. Unna:

LOBINALINE MONO-HYDROCHLORIDE

Lobinaline mono-hydrochloride was tested for its toxicity and its effect on respiration and blood pressure. In all cases the results were compared with those obtained with lobeline sulphate Merck.

The toxicity was determined in mice. Following subcutaneous injection, death occurred first at 800 mg. per kg., whereas the minimal lethal dose for lobeline was found at 300 mg. per kg.

The normal respiration of rabbits and cats—anesthetized with urethane or urethane and chloralose- -was not influenced by lobinaline in doses of 0.25 to 3 mg. per kg. intravenously. Even when the respiration had been depressed by intravenous injection of 4 mg. per kg. of morphine hydrochloride, no increase of the rate and depth resulted from the intravenous injection of lobinaline in doses up to 3 mg. per kg.; lobeline, on the other hand, produced marked effects on the respiration in doses of 0.25 to 1 mg. per kg.

Lobinaline was found to depress the blood pressure. The extent of the fall in blood pressure was proportional to the dose administered. It was very slight after 0.25 mg. per kg., but very marked, and in two cases fatal, after 2 mg. per kg. intravenously. The heart rate was unaltered or slightly increased. No symptoms of vagus stimulation were observed. The effect on the blood pressure remained unchanged after atropine. Lobeline on the other hand, caused a fall in blood pressure owing to the very marked stimulation of the vagi. This effect was completely abolished by atropine.

The foregoing data demonstrate that lobinaline is devoid of the characteristic actions of lobeline, that is, stimulation of the respiratory, vasomotor, and vagus centres. It depresses the blood pressure markedly, but in contrast to the effect of lobeline this fall remains unchanged after atropine. In mice lobinaline is less toxic than lobeline.

Experimental

The plant, *Lobelia cardinalis*, commonly known as the cardinal flower, was collected during several years as it became available and the alkaloid isolated shortly after drying. From a total of 47.3 kilos there was obtained 180 gm. of crude total alkaloid.

For this purpose the dried and ground material was extracted with methanol and the evaporated extract acidified with hydrochloric acid and diluted with hot water. The remaining methanol was boiled off and the cooled solution filtered through a layer of charcoal. It was then extracted with ether until no appreciable extract was obtained. The solution was then basified with excess ammonia and exhausted again with ether. The crude base obtained from the ether extract consisted of a pale brown viscous resin. Further extraction of the alkaline aqueous solution with chloroform yielded a dark resinous product which, however, was not soluble in dilute acid.

Lobinaline Mono-hydrochloride

Direct efforts to crystallize the crude alkaloid as well as attempts to obtain crystalline salts proved unavailing. The following procedure, discovered in the course of attempts to separate the total base into fractions of varying

basicity, is direct and yields a pure product. A clarified (charcoal) ether solution of the resinous base is shaken in a separatory funnel with successive portions of dilute hydrochloric acid until crystals make their appearance. At this point the addition of dilute hydrochloric acid is continued until no more solid hydrochloride is obtained. The mixture is filtered and the solid washed alternately with water and with ether. As thus obtained lobinaline mono-hydrochloride is not quite pure. Further purification is effected by shaking with aqueous sodium hydroxide and ether, and repeating the above procedure with the washed ether solution. The air-dried salt is extremely soluble in methanol but does not crystallize satisfactorily when its solution in this solvent is diluted with water, ether, or acetone. It may be recrystallized by dissolving it in chloroform, in which it is moderately soluble, and adding acetone to the somewhat concentrated solution. Fine, colorless needles melting at 220° C.* are thus obtained. The salt is readily soluble in dilute acids including acetic acid, but is decomposed by boiling with water into the readily soluble dihydrochloride and the resinous base, from both of which the mono-hydrochloride can be regenerated by appropriate treatment. A certain amount of water of crystallization is tenaciously retained and analyses are in best agreement with the sesquihydrate. Found: C, 70.16, 70.19; H, 8.67, 8.72; N, 5.83, 5.78 (Dumas), 5.76, 5.68 (Kjeldahl); Cl, 7.35%. Calcd. for $C_{28}H_{38}ON_2 . HCl . 1\frac{1}{2}H_2O$; C, 69.82; H, 8.73; N, 5.82; Cl, 7.37%.

Lobinaline

The first crystals of lobinaline were obtained only from the repeatedly purified mono-hydrochloride. When these were available for inoculation the crude mono-hydrochloride sufficed equally well.

The former was dissolved in dilute hydrochloric acid and the solution basified with sodium hydroxide, and the liberated base extracted with ether which had been freed from alcohol and peroxides. The washed solution was dried over potassium carbonate and evaporated to a small volume. Several such solutions were prepared and in one of them a crystal nucleus appeared after several days. Inoculation of the others induced immediate crystallization, which was somewhat hastened by the cautious addition of purified hexane. After washing with ether-hexane the alkaloid was recrystallized from dry ether in which it is moderately soluble. Fine colorless prisms, melting at 94 to 95° C. were thus obtained. $[\alpha]_D^{24°} = +22.3°$ ($c = 0.8$ in chloroform). Found: C, 80.79, 80.81; H, 9.02, 9.16; N, 6.62, 6.68%. Calcd. for $C_{28}H_{38}ON_2$; C, 80.38; H, 9.09; N, 6.70%. A methoxyl determination gave 2.36 and 2.26%. This value is much too low for one such group and is probably due to the partial elimination of methyl from an N-methyl group. The mono-hydrochloride was prepared from the purified lobinaline and was identical with the purified salt obtained in the first instance. The various mother liquors were combined and yielded appreciable quantities of the mono-hydrochloride, and it is improbable that alkaloids other than lobinaline will be found in more than traces.

* *All melting points are corrected.*

Oxidation with Permanganate

A solution of 1.75 gm. of pure lobinaline in 100 cc. of acetone-water (60 : 40) was treated with finely powdered potassium permanganate (10.1 gm.) until the pink color remained for two hours. The mixture was then diluted with much water and the acetone boiled off. A stream of sulphur dioxide was passed in to dissolve the precipitated manganese dioxide, and then a slight excess of hydrochloric acid was introduced to liberate most of the combined sulphur dioxide. An amorphous precipitate was filtered off and the filtrate repeatedly exhausted with ether, the recovered solvent being used for each successive extraction. The residue from the ether was freed of acetic acid and moisture *in vacuo* at room temperature, and then repeatedly extracted with purified hexane-ether (70 : 30). This treatment decreased the weight of the residue by 0.296 gm., and the extract after evaporation and drying weighed 0.289 gm. The product was almost pure benzoic acid. It was recrystallized from hexane; it then melted either alone or in admixture with benzoic acid at 121° C. The yield of benzoic acid was only 56% of that required for one mono-substituted phenyl group in the alkaloid. The amorphous by-products are largely soluble in alkali and presumably represent oxidation products, but their further oxidation with permanganate is extremely slow. It is nevertheless unlikely that two phenyl groups are present because the amount of benzoic acid which should then have been produced is 1.022 gm. No special significance is attached to the presence of acetic acid in the oxidation product. It is highly probable that it might have arisen from the oxidation of some of the acetone.

Oxidation with chromic acid in dilute sulphuric acid at steam bath temperatures was slow, and a substantial amount of the lobinaline used was recovered as the mono-hydrochloride.

Oxidation with Mercuric Acetate

The procedure of Gadamer (1) was followed in detail. A solution of the mono-hydrochloride (1.000 gm.) in 5 cc. of acetic acid was treated with a solution of 6 gm. of mercuric acetate in 30 cc. of water containing 1 cc. of acetic acid. A small amount of mercurous acetate was deposited at room temperature in the course of 12 hr. The mixture was then heated for three hours on a steam bath, cooled, and the crystalline precipitate filtered off and washed with a little cold water. After drying to constant weight at 110° C. it weighed 1.6434 gm. The oxidation of four hydrogen atoms requires 2.1664 gm. The yield was therefore 76% of the theoretical on such a supposition.

References

1. GADAMER, J.   Arch. Pharm. 253 : 274-289.   1915.
2. WIELAND, H.   Ber. 54 : 1784-1788.   1921.
3. WIELAND, H. and DRAGENDORFF, O.   Ann. 473 : 83-101.   1929.
4. WIELAND, H. and DRISHAUS, I.   Ann. 473 : 102-118.   1929.
5. WIELAND, H., KOSCHARA, W., and DANE, E.   Ann. 473 : 118-126.   1929.
6. WIELAND, H., SCHÖPF, C., and HERMSEN, W.   Ann. 444 : 40-68.   1925.

HEAT CAPACITY OF ETHYLENE IN THE CRITICAL RANGE[1]

By D. B. Pall[2] and O. Maass[3]

Abstract

Some of the data of a previous publication on this subject have been experimentally verified. The calorimeter has been improved so as to increase the accuracy of the new results by a factor of four. The ethylene was purified by means of a new still giving very sharp separations. Good agreement between the present results and those found previously is shown.

Introduction

In a previous paper, values for the heat capacity of ethylene over a range of temperatures near the critical region were reported (1). In particular, it was found that the heat capacity of the system just above the critical temperature is a function of the thermal history. It seemed desirable to check this result with that obtained with a sample of ethylene purified in a different manner, and in an apparatus showing improved accuracy.

The New Calorimeter

The method inherent in the use of the new calorimeter was, like that of the calorimeter used previously, an adiabatic electrical method for measuring heat capacity at constant volume.

The essential change lay in the use of a new type of container for the ethylene. Instead of a cylindrical steel bomb immersed in a mercury bath, there was used a spherical brass bomb, whose surface was uniformly wound with a single length of wire, which served the purpose of a heating coil (Fig. 1). Thus the temperature everywhere on the surface was the same during heating.

The method of sealing after introduction of the medium was not altered; as before, the new bomb was fitted with a gooseneck into which solder was melted under vacuum, in order to effect closure.
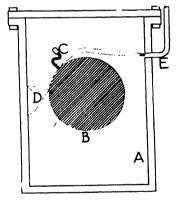
Fig. 1. *The calorimeter. A, Steel outer container. B, Spherical brass bomb, whole surface wound with No. 28 copper wire. C, Gooseneck, cutoff after filling and sealing under vacuum. D, Two of the seven thermocouples connected in series. E. Outlet for the bomb-heater leads. There are two other outlets, one for the thermocouple leads, and the other for evacuation of the calorimeter.*

The new bomb was $2\frac{5}{8}$ in. in diameter; it had a volume of 150 ml. and weighed 115 gm. Uniformly wound with No. 28 enamelled copper wire, the electrical resistance was 18 ohms, and the heat capacity 14 cal. per °C. The ratio of heat capacity to volume was so improved over that of the old container, that heat capacity measurements on ethylene at a density of 0.2255 and a temperature of 10° C. could be made with one-fourth of the previous error.

An additional change made was the conversion of the thermocouples from the radiation to the contact type. Actually, less heat is conducted between the inner and outer parts of the apparatus by contact than by radiation thermels; the amount is in any case negligible in comparison with conduction by air. Seven contact thermels gave a greater sensitivity than twelve radiation thermels.

The manner of operation was the same as that described for the previous apparatus.

Purification of the Ethylene

An absolute check on the purity of the material used in the new bomb appeared to be desirable. For this reason a low temperature still was constructed, designed after the Podbielniak stills (2), with modifications making it suitable for the purification of large quantities of gases. The still had a vacuum jacketed column 100 cm. long and 3.8 mm. in diameter. Boiling temperatures were measured by means of a copper-constantan thermocouple to better than 1° C. The separations effected by this apparatus are very sharp. The stock was tank material, about 99.7% pure, supplied by the Ohio Chemical Company. Ten per cent first and last fractions were discarded, and no change could be detected in the boiling point of the middle fraction.

Results

The bomb was so filled that the average density was the same as that used in the previous work, namely 0.2255.

Three sets of data were experimentally determined:

(1) Dependence of heat capacity of ethylene on the thermal history. The maximum difference due to extreme variation of thermal history of the heat capacity of the whole system at constant volume between 9.36 and 10.36°C. was found to be 3.1%. The separate results are listed in Table I. In the first paper on this subject (1) the value 2.6% was reported for this same quantity. However, it was thought that there might be an error as great as ±1% in this figure. The new value of 3.1% is probably good to about 0.3%, so that the existence of this thermal history effect in heat capacity is definitely placed outside of the limit of experimental error.

In the range 9.36° to 10.36° the two fillings give as absolute values of the heat capacity of the heterogeneous system, 0.609_5 and 0.603_2, again in good agreement.

TABLE I

DEPENDENCE OF THE HEAT CAPACITY OF ETHYLENE ON THE THERMAL HISTORY.
9.36 TO 10.36° C. AVERAGE DENSITY, 0.2255

Type of system	C_v, cal./°C./gm.	Mean C_v, cal./°C./gm.
Heterogeneous (brought to initial temp. from below 8° C.)	0.6040 0.6040 0.6017	0.6032
Homogeneous (brought to initial temp. from above 13° C.)	0.5846 0.5818 0.5866	0.5843

(2) Heat capacities below the critical temperature (Table II). In this case, the absolute agreement with the previous results is not as good. However, the position of the maximum in the heat capacity curve at 9.0° C. is verified, and the same sharp drop between 9.2° C. and 9.4° C. is noted. The results are listed in Table II.

TABLE II

HEAT CAPACITY OF THE SYSTEM ETHYLENE BELOW THE CRITICAL TEMPERATURE
AVERAGE DENSITY, 0.2255

Range, °C.	8.72 – 8.84	8.84 – 9.01	9.01 – 9.21	9.21 – 9.35
Average heat capacity, cal./°C./gm.	1.483	1.529	1.524	0.993

(3) Time lag results. These appear in Table III. The mathematical background of the functions used is described in the article on the previous part of this work (1). Owing to the great change in the ratio of the heat capacity of ethylene to the heat capacity of the container, comparison of these results

TABLE III

UNIMOLECULAR RATES, AND ΔT_o VALUES, FOR TIME LAGS

Range, °C.	Temperature interval, °C.	Time of heating, sec.	$\Delta T_o \times 10^3$, °C.	$\Delta T_o \times 10^3$, corrected to a 0.2° range	k, sec.$^{-1} \times 10^4$
8.72 – 8.84	0.122	550	82	134	5.1
8.84 – 9.01	0.172	800	109	127	3.55
9.01 – 9.21	0.196	910	118	120	1.75
9.21 – 9.35	0.142	475	41.5	58	1.9

with those previously obtained is difficult. However, at least approximate agreement can be demonstrated. At 8.84° C., k for the first bomb is 6.1 × 10^{-4} sec.$^{-1}$; for the second it is 5.1 × 10^{-4} sec.$^{-1}$. Similarly the results for the heat absorbed after heating through the interval 9.01° to 9.21° C. are

respectively 0.14 and 0.23 cal. per gm., corresponding to the widely different ΔT_0 values of 0.029° C. and 0.120° C.

In this same region no time lags were observed on lowering the temperature through an interval.

Conclusions

It may be stated that there is good agreement between these results and those obtained previously (1) with a different gas sample and a different apparatus. The new apparatus appears to function in a very satisfactory manner. The smaller limit of error places the difference in heat capacity due to thermal history definitely beyond the limit of experimental error. Thus the theoretical conclusions drawn in the previous work are placed on a more solid experimental groundwork.

References

1. PALL, D. B., BROUGHTON, J. W., and MAASS, O.　Can. J. Research, B, 16 : 230-241.　1938.
2. PODBIELNIAK, W. J.　J. Ind. Eng. Chem., Anal. ed. 5 : 119-135.　1933.

AN INVESTIGATION OF THE HYDROGEN-CHLORIDE–PROPYLENE REACTION IN THE REGION OF THE CRITICAL TEMPERATURE[1]

By C. H. Holder[2] and O. Maass[3]

Abstract

The reaction between hydrogen chloride and propylene has been studied in the gaseous state above the critical temperature and in the liquid state just below the critical temperature. Pressures were used such that the density of the gaseous mixtures could be made as great as the density of the liquid mixture at some temperature.

The rate of reaction above the critical temperature increases slowly with increasing pressure until a certain critical density is attained, after which the rate inceases rapidly. In the liquid state the reaction has a positive temperature coefficient except for a 25° temperature range just below the critical temperature. In this region there is a rapid decrease in density of the medium with rise in temperature and a negative temperature coefficient occurs.

The density of the liquid reactants at a number of temperatures just below the critical temperature (here defined as the temperature where the visible meniscus disappears) has been reproduced above the critical temperature for a small temperature range. The reaction velocity data obtained under these conditions show a minimum in passing through the critical temperature region.

The above results have been interpreted on the basis of a "structure" characteristic of the liquid state which favors higher reaction velocity and which may exist above the critical temperature at sufficiently high densities.

Introduction

A survey of the literature has revealed very few reaction velocity measurements in the liquid phase which can be compared to the rate in the gaseous phase. This is not surprising in view of the experimental difficulties involved and the necessity of obtaining a set of reactants that must meet a number of requirements.

Trautz (11, 12) studied the reaction between nitric oxide and chlorine and report that it takes place via the intermediate compound $NOCl_2$. The value for the termolecular constant in the liquid phase at $-58°$ is 10 (gram molecules per litre)$^{-2}$ sec. $^{-1}$ as compared with the corresponding value of 0.7 found by extrapolation of the data for the gaseous system. In the condensed state, therefore, the rate is about 14 times as fast as that in the gaseous state.

The racemization of pinene has been studied in the gas phase at low pressure and in the liquid phase, where the concentration is 1000 times greater (7). The reaction is homogeneous and monomolecular at both concentrations, so that in both phases the rate constant is virtually the same.

The object of the present work was to ascertain whether there is a property of the liquid state other than concentration that is responsible for chemical reaction, and whether this property manifests itself in a negative temperature

coefficient for reaction velocity measurements as the system passes through the critical temperature from the liquid to the gaseous states at equal density. It has been suggested that the temperature coefficient is governed not solely by activation phenomena but also by the destruction, with rise in temperature, of orientated groups of molecules within the body of the liquid. The view has been taken that the liquid state is characterized by a "dynamic structure" due to the formation of these groups. Increase in concentration and lowering of temperature tends to promote the formation of "dynamic structure". Increase in concentration has the more marked influence particularly when a "critical concentration" is passed. Thus "structure" formation is possible above the so-called critical temperature provided the concentration is above a "critical concentration". If the presence of a "structure" promotes the velocity of a chemical reaction the rate of reaction will diminish above the critical temperature if this is the temperature at which the liquid "structure" is destroyed.

The reaction between propylene and hydrogen chloride has been studied previously in this laboratory by Sutherland and Maass' (8). They found that the reaction rate above the critical temperature falls off to a value that is virtually zero. The present authors have found it necessary to use gaseous mixtures of a somewhat greater density as a basis of comparison with rates of reaction in the liquid mixtures, and that under such conditions the reaction does take place in the gaseous state to a greater extent than was expected from the conclusions of Sutherland and Maass.

Experimental

The apparatus is essentially the same as that used by Sutherland and Maass (8) and later described by Holder and Maass (4).

In view of the results obtained in a study of the effect of small amounts of water on the reaction in the liquid state (1), great care was taken to have the gases free from all impurities, especially water vapor. A distillation of a sample of propylene in a Podbielniak column showed that the fraction used was a pure product.

Propylene and hydrogen chloride were prepared as described by Maass and co-workers (2, 6).

Results

Propylene–hydrogen-chloride system

It was desired in this research to compare the rate of reaction in the liquid state with that in the gaseous state at the same density. An ideal system for such an investigation must meet a number of requirements. The critical temperatures of both the reactants and the reaction products should be within a fairly narrow temperature range so that condensation will not take place at the higher pressures. The compressibility of the mixture should be such that densities equal to those in the liquid state may be obtained at pressures that do not involve too great a risk to the experimenter. The hydrogen-chloride–propylene system fulfils most of these requirements. The

critical temperatures of the reactants are in a convenient temperature range (52° and 92° C.). However, the critical temperature of the main reaction product, isopropyl chloride, is probably quite high, judging by analogy with the critical temperature of normal propyl chloride, which has a boiling point of 46.5° and a critical temperature of 230° (b.p. of isopropyl chloride is 36.5°). Consequently, for runs at high pressures there will be a tendency for condensation to take place during the reaction owing to the increase of the critical temperature of the mixture above the temperature of the experiment. The compressibility of a 2HCl : 1C_3H_6 mixture is such that densities equivalent to those in the liquid state may be obtained from 70° (critical temperature of the mixture) up to 100°. For a 1HCl : 1C_3H_6 mixture, liquid densities may be obtained from 75° (critical temperature of the mixture) up to 105°. Both systems have been investigated. Owing to the catalytic effect of the excess hydrogen chloride (5) the reaction that occurs in the 2 : 1 mixture does so to an easily measurable extent in a few hours, and for this reason this system has been investigated most thoroughly.

It is well to note in passing that the term "critical temperature" when applied to two-component systems does not have the same meaning as for a pure substance (13, p. 269). In fact the term critical region is more appropriate in reference to a mixture of two substances. This is the temperature region from the "plait-point temperature" to the "critical temperature of contact". It is in this region that retrograde condensation occurs. The term critical temperature as used in this paper is the highest temperature at which a liquid phase was present at a pressure somewhat greater than the critical pressure, as observed by Sutherland and Maass (8).

Homogeneity or Heterogeneity of the Propylene–hydrogen-chloride Reaction

When a mixture of hydrogen chloride and propylene in the molecular ratio 2 : 1 is compressed at 100 atm. and 105° a reaction rate of 0.40 to 0.45% per hr. has been observed, and this can be detected with an accuracy of about 15% for a run of five hours using a reaction cell having a capacity of 0.35 cc. For runs at slightly lower pressures or for shorter periods the rate is less than the experimental error, and it therefore may be considered a zero reaction. This zero reaction for hydrogen chloride and propylene above the critical temperature has been previously observed in this laboratory (8), and was found to hold true even for a 10 hr. run under the above conditions. The writers, on the contrary, have found repeatedly a slow reaction of the order of magnitude indicated above.

The initial runs in new reaction bulbs have been found to vary in such a way as to indicate that the reaction is at least partially heterogeneous, since it appears to depend on the condition of the glass walls of the individual reaction bulb. A large number of runs were made in order to investigate this behavior. The conclusions arrived at may be explained however by considering a few typical cases.

The reaction cells were blown from heavy wall Pyrex tubing (1 cm. internal diameter, 3 mm. wall). Eleven of these, which ranged in capacity from 0.170

to 0.414 cc., were used. For convenience of comparison, in these experiments on catalysis, runs were always made at 105° C., 100 atm. pressure and density 0.265. Under such conditions most of these reaction cells gave an initial rate of the order of 3.5% per hour for the first run. On the other hand, four cells were used which gave initial rates of 0.50, 0.30, 0.35, 0.68% (average of 0.45%) per hour for the first run. The former are then about eight times as fast as the latter. The initial rate in "fast" cells was not a steady state, as shown by subsequent runs. In such cases the rate invariably decreased. It was at first found that the reactions in all "fast" bulbs after a number of runs came to a steady state that was of the same order of magnitude as that in the originally "slow" bulbs. However a number of cells have since been prepared which reach a steady state at twice this rate. In one case runs were made that gave a total reaction time of 215 hr. but this failed to reduce the rate below 1.0% per hour.

The effect of reheating the bulb till molten and blowing a partially conditioned bulb is interesting. In such cases the activity is partly but not fully restored. This behavior indicates that the high initial runs in new bulbs cannot be explained fully as due to the presence of moisture which might be present from the operation of sealing in the bulb. It is suggested that the large variation of the activity of the reaction cells, out of all proportion to their variation in size, may be explained on the basis of Taylor's theory (9, 10) of heterogeneous catalysis due to active centres. The existence of "fast" bulbs is due to a large number of active centres on a cell wall, possibly in the form of humps or projections, and vice versa. It is possible that in subsequent reactions these active spots lose their activity owing to an accumulation of reaction products as an adsorbed layer. Thus, on reheating and blowing the walls of such a conditioned bulb the fresh surface will reappear, but the new surface will now be smoother and have fewer active centres, so that the reaction rate is not as high as the original rate.

Since this catalysis found in new reaction bulbs appeared to be due to a condition of the wall rather than to the presence of moisture, it was decided to investigate whether changing the surface area in a bulb that had reached a steady state would increase the amount of reaction in proportion to the increase in surface. As it was desired to avoid the heterogeneous reaction in the experiments to be undertaken later on, this investigation was made with a bulb that had reached a steady state of low reaction rate.

The method employed was to use a reaction cell unit in which the cell proper was spheroidal in shape and was joined at the lower extremity to about 3 cm. of 1.4 mm. bore capillary tubing. The diameter of this capillary was determined by calibration with mercury. The length of the tube occupied by the gases was measured by means of a glass millimetre scale placed behind the tube. From the geometry of spheroids and cylinders it is obvious that allowing the gases to react in one case in the spheroid and in the next case in the spheroid plus about 2 cm. of the cylindrical section introduces an increase in surface per unit volume.

The cell used in these determinations had a volume of 0.171 cc., and if one assumes it to be a sphere the surface area was 1.45 sq. cm. A 2 cm. length of the capillary had a volume of 0.031 cc. and a surface area of 0.88 sq. cm. Thus the change in surface per unit volume when 2 cm. of capillary is exposed is an increase of 35% over that for the spheroid alone.

Measurements were made at 105° and 75° C. and are presented in Table I. The time of reaction was in each case made sufficiently long that an increase in rate proportional to the increase in surface would easily be made evident. From the results of Table I it is obvious that the small variations in the rates are within the limit of experimental accuracy, and therefore it may be concluded that if a heterogeneous reaction that is proportional to the surface area does occur, then the proportion of the heterogeneous reaction to the homogeneous reaction must be such that an increase of 38% in the heterogeneous reaction gives less than 0.5% reaction (as this amount would have been easily measurable).

TABLE I

EFFECT OF SURFACE ON THE RATE OF REACTION IN A CONDITIONED BULB

	Run no.	Surface	Reaction, %
105° C. 10 hr. Dens., 265	187	Bulb only	7.0
	188	Bulb only	7.5 Av. 7.2%
	183	38% increase	6.8
	189	38% increase	7.5
	170	23% increase	7.1 Av. 7.1%
75° C. 4 hr. Dens., 352	Curve 162	Bulb only	7.5
		30% increase	7.2
75° C. 4 hr. Dens., 294	165	Bulb only	6.8
	166	30% increase	6.8

It follows then that the maximum that can be allotted to the heterogeneous reaction is 19% of the total reaction under these conditions.

On the other hand, it does seem probable that a certain heterogeneity of reaction is present even in these "slow" cells. As mentioned above, all the reaction cells used did not in their steady state exhibit the same rate of reaction. An examination of the rates and relative sizes of the cells readily showed that no relation existed between rate and surface area (a large cell would of course possess a smaller surface per unit volume than a small one). Rather, the speed of a particular cell appeared to be a unique property of that cell. For example, a bulb with a volume of 0.414 cc. gave a rate almost 60% greater than a bulb of 0.171 cc.

It has been found that with bulbs which varied in speed measurably under the conditions of comparison, the results at densities of 0.32 or greater gave rates in very close agreement. Hence, although a small amount of heterogeneous reaction may occur in "slow" bulbs at low densities, this effect is so small a part of the total reaction at high densities that it may be neglected.

Mercury was shown to affect the reaction to a very slight extent. The effect was examined by exposing increasing amounts of mercury surface to

the reactants.   An estimated increase of surface of 32 times gave an increase in rate from 1.64 to 2.65% in four hours.

Reaction Velocity of Propylene–hydrogen-chloride above the Critical Temperature

The data recorded in the following pages were obtained with conditioned cells that gave reaction rates of about 0.50% per hour at 105° C. with the reaction mixture under a pressure of 100 atm.   In one case, 91 runs were made in a single cell, and a test run after this time indicated that the cell had been in an equilibrium condition during this period.
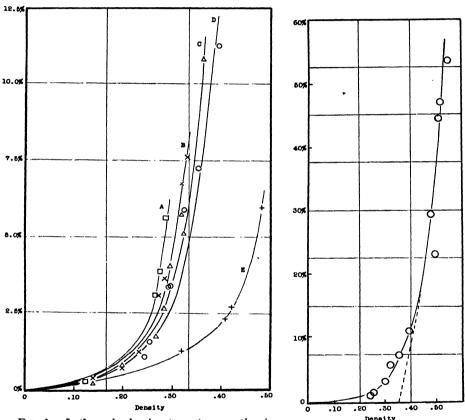
FIG. 1.   *Isothermals showing percentage reaction in four hours plotted against density.   A. 2HCl : 1C₃H₆ at 105°.   B. 2HCl : 1C₃H₆ at 95°.   C. 2HCl : 1C₃H₆ at 85°.   D. 2HCl : 1C₃H₆ at 75°.   E. 1HCl : 1C₃H₆ at 85° C.*

FIG. 2.   *Isothermal at 75° showing percentage reaction in four hours plotted against density.*

The reaction in the gaseous phase has been studied over a wide density range and at temperatures of 75°, 85°, 95°, and 105° C. for a 2 : 1 mixture, and at 85° for a 1 : 1 mixture.   These data are tabulated in Table II and are shown graphically in Figs. 1 and 2.   The density measurements have been

corrected for a small dead space in the apparatus and for the thermal coefficient of expansion of the reaction cell (Pyrex). The pressure coefficient of expansion has been estimated and found to be negligible. The density of the reactants was measured during each reaction velocity determination as described by Holder and Maass (4). The amount of reaction is expressed, for comparison, in terms of a four hour run, but in practice the time chosen was that which would give sufficient reaction to be easily measurable, but not long enough for large amounts of reaction product to form. This assumption, that the reaction is linear with time, has been found to be true for a temperature of 105°, and from the curve for 75° in Fig. 6 it is seen to be true for rates of reaction up to about 15%. A curve showing the rate of reaction with increasing density for a 1HCl : 1C₃H₆ system at a temperature of 85° has been included. In view of what has already been said in regard to the formation of a reaction product with a high critical temperature, it is

TABLE II

RATE OF PROPYLENE–HYDROGEN-CHLORIDE REACTION ABOVE THE CRITICAL TEMPERATURE

Reaction Cell No. 7B			Reaction Cell. No. 10B		
Run No.	Density	Per cent reaction in 4 hours	Run No.	Density	Per cent reaction in 4 hours
105°			85° (cont'd)		
111	0.125	.28	155	0.316	5.7
112	.203	.74	154	.361	10.8
113	.264	3.1	153	.445	22.3
114	.273	3.9	222	.491	33.5
115	.287	5.6	232	.542	60.9
95°			75°		
104	0.138	.42	163	0.241	1.1
99	.199	.74	167	.254	1.6
102	.233	1.3	165	.294	3.4
116	.271	3.1	156	.321	5.9
117	.285	3.6	162	.353	7.2
100	.317	6.7	157	.393	11.2
101	.329	7.6	158	.437	16.5
229	.484	42.5	161	.480	29.4
			159	.496	23.3
			185	.513	44.4
			160	.520	47.0
			233	.544	53.4
85°			1HCl : 1C₃H₆, 85°		
105	0.138	.21			
106	.200	.83			
107	.266	1.8	207	0.318	1.3
108	.286	2.7	208	.408	2.4
110	.294	4.1	220	.422	2.7
109	.315	5.1	209	.485	6.0

very likely that the reactions at 75° at high densities are accompanied by the formation of a liquid phase as the reaction proceeds.

The curves of Figs 1 and 2 show a number of interesting features. The curve for 75°, Fig. 1, which is just 5° above the critical temperature, rises very slowly at first until a density of about 0.27 is reached, at which the slope increases more rapidly. At higher densities the curve becomes very nearly a straight line. If this portion of the curve is extrapolated to zero reaction we find that it cuts the density ordinate at about 0.35, which, as shown later, is the value of the critical density of the mixture. The conclusion that arises from such a result then is that the reaction above the critical temperature depends essentially on the attainment of a concentration comparable to that in the liquid state.

If the data at 85° for the 2 : 1 and 1 : 1 mixtures· are now plotted, as percentage reaction *versus* partial density of hydrogen

FIG. 3. *Percentage reaction in four hours plotted against partial density of hydrogen chloride for mixtures at 85° C. Curve A is for 2 : 1 mixture. Curve B is for 1 : 1 mixture.*

TABLE III

DENSTIY OF LIQUID MIXTURES

Temp., °C.	Density 2 : 1	Density 1 : 1
25	0.675	
35	0.659	
45	0.628	
50	0.600	0.526
60	0.544	0.510
65	0.480	
70	0.350 (calcd.)	0.457
75		0.320 (calcd.)

chloride, as in Fig. 3, it is observed that the two curves are very close together.

Measurement of the Density of Liquid Mixtures

The densities of $2HCl : 1C_3H_6$ mixtures have been measured at temperatures from 25° to 65° C. inclusive, and those for a $1HCl : 1C_3H_6$ mixture at temperatures from 50° to 70° inclusive. These data are recorded in Table III and shown graphically in Fig. 4. These measurements were made by calculating the mass of reactants (measured out in calibrated volumes) that was necessary to fill completely the reaction cell of known volume with liquid. Each curve has been extended to a density at its critical temperature that is the mean of the critical density of hydrogen chloride and that of propylene. These points fit on curves that can be obtained by extrapolation of the observed densities at lower temperatures.

Reaction Velocity of Propylene–hydrogen-chloride below the Critical Temperature

The temperature coefficient of the reaction in the liquid state below the critical temperature has been determined. These runs were made by starting with a cell in which just sufficient pressure had been applied to condense the liquid completely. However, since the reaction takes place with a contraction in volume a vapor phase soon reappears.

hers (5) have found that the reaction has a positive temperature coefficient from −78° to 45° C. The writers have investigated the rate from 25° up to the critical temperature. The data are recorded in Table IV and are plotted together with
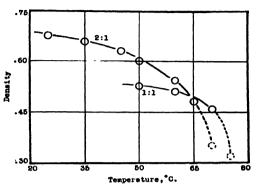
FIG. 4. *Density plotted against temperature for 2 : 1 and 1 : 1 liquid mixtures.*

other data in Fig. 5. The results for both 2 : 1 and 1 : 1 mixtures give the same type of curves although the latter are not plotted in Fig. 5. For both mixtures there is a positive temperature coefficient up to about 45°, over which range the density varies only slightly. Between 45° and the critical temperature, through which region the density is changing greatly, the temperature coefficient becomes negative. This will later on be ascribed to a
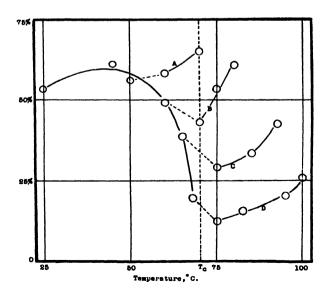
FIG. 5. *Percentage reaction in four hours plotted against temperature, showing the negative temperature coefficient in the liquid state and the discontinuity in rate in passing through the T_c at identical densities.*

partial destruction of regional orientation caused by a rapidly diminishing density in this particular temperature range. The probability that this is the cause is made apparent when rates above and below the critical temperature are compared.

TABLE IV

REACTION IN LIQUID STATE

Temp., °C.	2 : 1 Density	Per cent reaction in 4 hours	Temp., °C.	1 : 1 Density	Per cent reaction in 4 hours
25	0.675	53.6	50	0.526	4.5
45	0.628	61.1	60	0.510	3.6
50	0.600	56.1	70	0.457	3.1
60	0.544	49.2			
65	0.480	39.9			
68	0.404	19.6			

Comparison of Rates of the Propylene–hydrogen-chloride Reaction for Equal Densities above and below the Critical Temperature

As the basis of comparison for these experiments, measurements have been made below the critical temperature at a certain temperature with just sufficient pressure to give 100% liquid in the cell at the beginning of the run. The density at this temperature has then been reproduced at a higher temperature by applying sufficient pressure, and the rate has been measured. The results are given in Table V. The first column is a list of densities of the liquid medium as given in Table IV, and the number in parentheses is the temperature at which the liquid mixture has this density. The second column gives the temperatures at which this density was reproduced, and the third column, the percentage reaction in four hours observed at this temperature and density. These results for the 2 : 1 mixtures have been plotted in Fig. 5. The 1 : 1 mixtures show the same effect but to a less pronounced degree and are not plotted.

TABLE V

RATE OF PROPYLENE–HYDROGEN-CHLORIDE REACTION ABOVE AND BELOW THE CRITICAL TEMPERATURE (70°)

Density	Temperature, °C.	Per cent reaction in 4 hours
0.600 (50°)	50	56.1
	60	58.2
	70	65.3
0.544 (60°)	60	49.2
	70	43.1
	75	53.4
	80	60.9
0.480 (65°)	65	39.9
	75	29.4
	85	33.5
	95	42.6
0.404 (68°)	68	19.6
	75	12.8
	85	15.5
	95	20.0
	100	26.0

The curves *B, C, D* in Fig. 5 show a definite decrease in reaction velocity in the critical temperature region which it is suggested may be explained by the change in properties of the medium in passing from below to above the critical temperature. The continuous nature of Curve *A*, Fig. 5, seems to justify this explanation. In this case the density at 50° was reproduced at two higher temperatures which are still below the critical. This curve indicates a positive temperature coefficient with no dip in the curve for reactions at constant density. However, when a constant density is maintained through the critical temperature one finds a minimum in the curve. For instance, it is seen from the 0.480 density curve that the rate for 65° is 39.9%, and at 75° this has dropped to 29.4%, a decrease of about 25% of the higher rate.
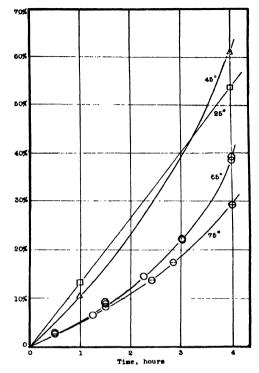
FIG. 6. *Percentage reaction plotted against time in hours at 25°, 45°, 65°, and 75° C.*

It is necessary to raise the temperature to about 93° before the rate at 65° is equaled.

The rate *vs.* time curve for the reaction at 75°, with a density equal to that of the liquid mixture at 65°, has been plotted in Fig. 6. Similar curves for the reaction in the liquid phase at 25°, 45°, and 65°, starting with 100% liquid phase, are included for comparison. The results are listed in Table VI. The reaction at 25° has been studied extensively by Brown (1), using a somewhat different technique whereby the re-

TABLE VI

RATE *vs.* TIME DATA AT 25°, 45°, 65°, AND 75° C.

No. of hours	Reaction, %	No. of hours	Reaction, %
65° C., Dens., 0.480		75° C., Dens., 0.480	
0.5	2.9	0 5	2.7
1.25	6.4	1.5	8.8
1.50	9.1	2 42	13.8
1.50	8.1	2 83	17.4
2.25	14.7	4.0	29.4
3.0	22.3		
3.0	22.2	25° C. Dens., 0.675	
4.0	39.2	1.0	13.1
4.0	38.6	4.0	53.6
		45° C. Dens., 0.628	
		1.0	10.6
		4.0	61.1

actants were condensed into heavy walled reaction cells, which were then sealed off at liquid air temperatures. The amount of reaction was followed by titration methods. The results obtained by this method agree very well with those observed by the writers.

The reaction at 25° is linear with time up to four hours, and this has been confirmed by Brown, who made more detailed measurements, whereas those at 45°, 65°, and 75° give rates that increase with time more rapidly than for a linear relation. The contraction of the liquid phase as a reaction proceeds has been observed to be greater for a run at 45° or 65° than at 25°.

If now the rate *vs.* time curves for the reaction at 75° and 65° (above and below the critical temperature respectively) be considered, it will be observed that the curves are close together for the first 1.5 hr., but that after this they separate more and more. When the reaction at 75° has proceeded for about two hours the first appearance of a vapor phase can be noticed. This is attributed to the formation of a reaction product with a high critical temperature in the highly compressed gaseous system. The introduction of this third compound causes the critical temperature of the system to increase, and, when it reaches 75°, liquefaction, as evidenced by meniscus formation at the top, will take place. This would not be observed immediately.

Discussion

At the time when the rates of reaction between hydrogen chloride and propylene in the liquid state and at low temperatures were first investigated in this laboratory (5), it was observed that no reaction took place in the gaseous state even at relatively high temperatures. A mixture of hydrogen chloride and propylene was kept under observation for a period of a year without any measurable reaction taking place, although this mixture when condensed and sealed off in a bulb reacted to a measurable extent within a few minutes. An experimental technique was then devised for mixing the reactants above the critical temperature and then compressing them to a high degree of density, and the result found was that no measurable reaction occurred until the temperature was lowered below the critical temperature. It was suggested at the time that an explanation might be found in the assumption that the liquid state of aggregation had a "structure", which greatly enhanced the reaction velocity.

A whole series of investigations was then undertaken to determine whether a liquid possessed a "structure" and whether the critical temperature phenomena were due to the rapid disappearance of "structure" in the critical temperature region. Considerable evidence for this was discovered but a slightly different point of view was gradually acquired. Although rise of temperature should undoubtedly tend to destroy "structure", the decrease in density of the liquid in equilibrium with its vapor does the same, and eventually a critical density is approached where a "structure" is destroyed by leaps and bounds. Conversely, a medium at a temperature above its critical temperature and compressed to a pressure greater than its critical pressure such that its

density actually is greater than that of the liquid at its critical temperature should develop a "structure". The investigation of Geddes and Maass (3) seems, particularly, to confirm this conclusion.

With this point of view in mind, the reaction between hydrogen chloride and propylene was reinvestigated, as it was felt that if the foregoing reasoning were correct a liquid "structure" would form even above the critical temperature, provided that the concentration were high enough, and that then if "structure" increases the rate of reaction, measurable rates of reaction should be found even above the critical temperature. In other words, it was expected that an increase in density, once a critical density had been passed, would have a far greater influence on the rate of reaction than increase of temperature in the critical temperature region.

The original apparatus (8) was rebuilt to permit measurements at higher pressures than those used by Sutherland and Maass. Furthermore, since it was realized that densities were the all-important consideration means were devised for more accurate measurements of density than those carried out by the above-named investigators.

It was discovered that in the work of Sutherland and Maass the critical density had not quite been reached, but otherwise their results were in principle confirmed. It was also discovered that the walls of the reaction vessel used by the present writers had a slight catalytic effect which, as was brought out in the discussion of these measurements, was small compared with the measurements of reaction velocity at densities above the critical density. What remains uncertain is whether the catalytic activity can be reduced to an extent such that the reaction velocity is zero at the lower densities.

The critical density at the critical temperature of the $2HCl : 1C_3H_6$ mixture was estimated to be 0.35. From the results shown in Fig. 1, it is seen that once a density of 0.25 is passed the rate of reaction increases by leaps and bounds with rise in density. In Fig. 2, drawn so as to make possible the inclusion of results at densities where the reaction proceeds up to 55% completion in four hours, it is seen that at 75° the reaction-rate–density relation tends to become linear, and on extrapolation to zero reaction rate gives a density value corresponding to the critical density of the medium at 5° below the temperature of the experiment, namely, the critical temperature of this system.

From Fig. 1 it is also apparent that, as would be expected, activation increases with rise in temperature, for at equal densities the rate of reaction increases. Unfortunately, at the higher temperatures it was not possible to carry out measurements at densities higher than those given because the pressure limit of the equipment had been reached.

In Fig. 1 is shown Curve E representing a reaction of a $1HCl : 1C_3H_6$ mixture at 85°, the same temperature for which data in Curve C for a $2HCl : 1C_3H_6$ mixture were obtained. As mentioned before, plotting both these curves on the basis of the partial density of the hydrogen chloride brings the curves close together. This indicates that for equal concentrations of hydro-

gen chloride, irrespective of the concentration of the propylene, the rate of the reaction is nearly the same. This point is to be investigated further. It is apparent however that the change in rate with hydrogen chloride concentration in no way follows a simple relation. As can be seen from the curve in Fig. 2, in which the abscissae are a measure of the concentration of the hydrogen chloride, the rate above a concentration corresponding to a density of 0.4 for the mixture increases approximately according to the 5th power of the concentration of the hydrogen chloride. This shows that the mechanism of the reaction is influenced in the high density region, i.e., the region where presumably the "liquid state" exists, by some factor that does not involve the order of the reaction.

The reason why the rate of the reaction of the liquid mixtures, under pressures corresponding to their vapor pressure, passes through a maximum with change in temperature is now made apparent. As was pointed out before, the rate of the reaction increases with rise in temperature owing to increased activation, but once 45° is passed, the density of the liquid decreases so rapidly (see Fig. 4) that this more than compensates for the influence of increased thermal energy. This is brought out rather well in Fig. 7, in which the percentage reaction for equal times is plotted against density of the liquid, indicating as seen, that at the critical density the reaction rate would be zero. A possible reason why the rate in the compressed gas at densities below this is still appreciable is that a certain amount of "structure" still exists in the highly compressed gas.

FIG. 7. *Density of the liquid medium at various temperatures from 25° to 68° inclusive, plotted against percentage reaction in four hours.*

The data presented in Fig. 5 give rise to interesting speculations, which the authors, however, at this time do not wish to suggest as other than a tentative explanation. As rise in temperature should tend to destroy the "structure", it may be that at the critical temperature the heat energy of the molecules may reach a critical value where, with further rise in temperature within the neighborhood of the critical density, more rapid destruction of "structure" takes place than at other temperatures. In that case where the concentration is kept constant with rise in temperature, owing to

this effect the rate of reaction is actually decreased and a large increase in temperature is required to bring it back. Thus for curve A, where the medium still has a density considerably above the critical density, the temperature coefficient is positive, although it is probably not as large as it would be at lower temperatures. With the mixtures at lower densities the temperature coefficient actually becomes negative. It may be argued that the data are presented for reactions carried out over a four-hour period, and that for a two-hour period the decrease in reaction rate at the critical temperature is less. However, when the time–reaction-rate curves at 65° and 75° in Fig. 6 are examined, it is seen that there is still a negative temperature coefficient at two hours and no indication of a positive temperature coefficient at any shorter time. The ideas advanced concerning the reason for the apparent negative temperature coefficient at the critical temperature are put forward as suggesting further investigation to be undertaken to determine whether they are correct.

From a consideration of the solubility measurements carried out by various workers in the region of the critical temperature, it is felt that an accurate determination of solubility in this region would reveal a curve very similar to that obtained in Fig. 5 for reaction velocity. The expected result is that the solubility found a few degrees above, would be somewhat less than that found a few degrees below, the critical temperature at the critical density. However, at densities greater than the critical density the solubility just above the critical temperature will then be of the same order of magnitude as the solubility in the liquid state at the same density. An apparatus is now being constructed to investigate this problem. The solubility of substances in highly compressed gases is of particular interest to geologists.

References

1. BROWN, A. G. Ph.D. Thesis, McGill University. 1938.
2. COFFIN, C. C. and MAASS, O. J. Am. Chem. Soc. 50 : 1427-1437. 1928.
3. GEDDES, A. L. and MAASS, O. Phil. Trans. Roy. Soc. A, 236 : 303-332. 1937.
4. HOLDER, C. H. and MAASS, O. Can. J. Research, B, 15 : 345-351. 1937.
5. MAASS, O. and SIVERTZ, C. J. Am. Chem. Soc. 47 : 2883-2891. 1925.
6. MAASS, O. and WRIGHT, C. H. J. Am. Chem. Soc. 46 : 2664-2673. 1924.
7. SMITH, D. F. J. Am. Chem. Soc. 49 : 43-50. 1927.
8. SUTHERLAND, H. S. and MAASS, O. Can. J. Research, 5 : 48-63. 1931.
9. TAYLOR, H. S. Z. Elektrochem. 35 : 542-548. 1929.
10. TAYLOR, H. S. and SHERMAN, A. Trans. Faraday Soc. 28 : 247-253. 1932.
11. TRAUTZ, M. and GERWIG, W. Z. anorg. allgem. Chem. 146 : 1-41. 1925.
12. TRAUTZ, M. and SCHLUETER, H. Z. anorg. allgem. Chem. 136 : 1-47. 1924.
13. YOUNG, S. Stoichiometry. Longmans, Green and Company, London. 1918.

Section B

INDEX TO VOLUME XVI

Authors

Section B

INDEX TO VOLUME XVI

Subjects

ERRATA

Pages 76–79, inclusive. The empirical formulae for anolobine and all derivitives should contain two hydrogen atoms less than the number given.

Page 437, line 16, for "CH$_3$. NH$_2$. H$_2$PtCl$_6$" read "(CH$_3$. NH$_2$)$_2$. H$_2$PtCl$_6$".